

NASA Conference Publication 2278

NASA
CP
2278
c.1



Failure Analysis and Mechanisms of Failure of Fibrous Composite Structures

LOAN COPY: RETURN TO
AFWL TECHNICAL LIBRARY
KIRTLAND AFB, N.M. 87117

*Proceedings of a workshop held at
NASA Langley Research Center
Hampton, Virginia
March 23-25, 1982*



25th Anniversary
1958-1983

NASA



Failure Analysis and Mechanisms of Failure of Fibrous Composite Structures

Compiled by
Ahmed K. Noor
The George Washington University
Joint Institute for Advancement of Flight Sciences
NASA Langley Research Center

Mark J. Shuart
James H. Starnes, Jr.
and Jerry G. Williams
NASA Langley Research Center

Proceedings of a workshop sponsored by
NASA Langley Research Center and
The George Washington University Joint Institute
for Advancement of Flight Sciences and held at
Langley Research Center
Hampton, Virginia
March 23-25, 1982



National Aeronautics
and Space Administration

Scientific and Technical
Information Branch

1983

PREFACE

This document contains the proceedings of the joint NASA/George Washington University Workshop on Failure Analysis and Mechanisms of Failure of Fibrous Composite Structures. The workshop was held March 23-25, 1982, at Langley Research Center and was attended by over 80 researchers from government agencies, aircraft manufacturers, and universities. The objectives of the workshop were to assess the present state of the art of failure analysis and current design practices, to identify deficiencies in these technologies, and to identify directions for future research leading to a verified failure analysis capability for fibrous composite structures.

The workshop was organized into the following six sessions:

1. Design Technology I
2. Design Technology II
3. Failure Mechanisms and Failure Criteria
4. Delaminations and Stress Concentrations
5. Compression Failure and Transverse Strength
6. Effects of Defects and Experimental Methods

* Certain materials are identified in this publication in order to specify adequately which materials were investigated in the research effort. In no case does such identification imply recommendation or endorsement of the product by NASA, nor does it imply that the materials are necessarily the only ones or the best ones available for the purpose. In many cases equivalent materials are available and would probably produce equivalent results.

Ahmed K. Noor
Mark J. Shuart
James H. Starnes, Jr.
Jerry G. Williams
Workshop Coordinators

CONTENTS

PREFACE	111
INTRODUCTION	1

SESSION I - DESIGN TECHNOLOGY I

Moderator: Jerry G. Williams

COMMERCIAL TRANSPORT AIRCRAFT COMPOSITE STRUCTURES	7
John E. McCarty	
A PRELIMINARY DAMAGE TOLERANCE METHODOLOGY FOR COMPOSITE STRUCTURES	67
D. J. Wilkins	

SESSION 2 - DESIGN TECHNOLOGY II

Moderator: James H. Starnes, Jr.

DESIGN AND ANALYSIS OF COMPOSITE STRUCTURES WITH STRESS CONCENTRATIONS	95
S. P. Garbo	
SAFE-LIFE AND DAMAGE-TOLERANT DESIGN APPROACHES FOR HELICOPTER STRUCTURES	129
Harold K. Reddick	

SESSION 3 - FAILURE MECHANISMS AND FAILURE CRITERIA

Moderator: Ahmed K. Noor

FAILURE MECHANISMS	153
H. Thomas Hahn	
STRENGTH THEORIES OF COMPOSITES: STATUS AND ISSUES	173
Edward M. Wu	

SESSION 4 - DELAMINATION AND STRESS CONCENTRATIONS

Moderator: T. Kevin O'Brien

ANALYSIS OF DELAMINATION	191
Frank W. Crossman	
NOTCH STRENGTH OF COMPOSITES	241
James M. Whitney	

SESSION 5 - COMPRESSION FAILURE AND
TRANSVERSE STRENGTH
Moderator: Mark J. Stuart

COMPRESSION FAILURE OF COMPOSITE LAMINATES	265
R. B. Pipes	
THE IN SITU TRANSVERSE LAMINA STRENGTH OF COMPOSITE LAMINATES	293
Donald L. Flaggs	

SESSION 6 - EFFECTS OF DEFECTS AND
EXPERIMENTAL METHODS
Moderator: John R. Davidson

EFFECTS OF DEFECTS IN COMPOSITE STRUCTURES	305
G. P. Sendeckyj	
EXPERIMENTAL METHODS FOR IDENTIFYING FAILURE MECHANISMS	313
I. M. Daniel	

GENERAL DISCUSSION

DISCUSSION OF MATRIX CRACKING IN GRAPHITE/EPOXY COMPOSITE MATERIALS	342
Walter L. Bradley	
DISCUSSION OF COMPOSITE STRUCTURES	343
John N. Dickson	
ANALYSIS EXPLAINS VARIABLE RATE OF INSTABILITY-RELATED DELAMINATION GROWTH. . .	348
John D. Whitcomb	
THE APPROACH TO FAILURE ANALYSIS OF COMPOSITES	349
Kenneth Reifsnider	
DISCUSSION OF INTERLAMINAR STRENGTH EFFECTS ON AIRCRAFT DESIGN	351
D. J. Watts	
BIBLIOGRAPHY	353

INTRODUCTION

Over the past several years, considerable effort has been made by the research, development, and design communities to understand the mechanisms of failure of fibrous composite materials and the effect of these mechanisms on the performance of structural components made from these materials. Experience has shown that the use of fibrous composite materials for new design applications requires a better understanding of their failure mechanisms so that safe, reliable structural designs can be developed. The full weight-saving potential of composite structures can only be realized by understanding their failure mechanisms, developing the capability to predict accurately the effect of these mechanisms on structural performance, and transferring this knowledge to designers of composite structures.

The joint NASA/George Washington University Workshop on Failure Analysis and Mechanisms of Failure of Fibrous Composite Structures was held at NASA Langley Research Center, March 23-25, 1982, to assess the current state of the art of failure analysis for composite structures and of current design practices, to identify deficiencies in these technologies, and to identify directions for future research leading to a verified failure analysis capability for composite structures. This document contains copies of the workshop presentations and includes some of the subsequent discussions. An extensive bibliography on various aspects of the failure of composite materials and structures is also included. Some general comments on topics discussed during the workshop are presented in this introduction.

Local Damage and Its Effect on Design

The strength of composite structures has been shown to be reduced significantly by local damage and discontinuities. Traditionally, the concern for durability of metal structures has focused on tension-fatigue behavior. However, for composite structures, both tension- and compression-loading responses are important, and a large percentage of the reduction in strength due to damage can be measured in static tests. Experience has shown that defects and local damage can exist in a laminate prior to their visual detection. An assessment of the effect on strength of such damage is important to the structural designer.

Nondestructive damage assessment methods are commonly used to monitor damage growth. Surface inspection techniques include the use of edge replicates and moire fringe patterns. Ultrasonic attenuation, vibrothermography, and radiography also are used when damage measurements more definitive than surface inspection are desired. Test and analysis studies are used by structural designers to ensure that the structural strengths and stiffnesses are not reduced to unacceptable levels due to damage propagation between inspection periods.

Damage Growth and Failure Criteria

Because of their importance to practical applications of composites, damage growth and failure criteria are current research topics. Damage growth in composite laminates can result from either matrix- or fiber-dominated failure mechanisms. Matrix-dominated failure mechanisms include ply delamination and matrix cracking. Failure mechanisms for fibers include fiber fracture and fiber microbuckling. Damage

growth that results from matrix-dominated failures has received considerable attention. By contrast, limited work has been done on damage growth resulting from fiber failures. For matrix-cracking and fiber fracture mechanisms, fracture mechanics has been used to establish a criterion for damage growth based on the strain energy release rate for a laminate. Using this criterion, the damage grows when the strain energy release rate reaches a critical value calculated from the various fracture mode contributions.

Failure criteria for composite structures are being studied widely. Failure criteria for composite materials subjected to multiaxial states of stress have traditionally been operational rather than mechanistic. These criteria are not derived from mechanics principles but are empirical statements of the material failure process. Nevertheless, composite failure criteria are useful tools for material characterization and for estimating the load-carrying capacity of composite structures. Initially, familiar and easy-to-use failure criteria for isotropic materials were generalized for anisotropic composite materials. Examples of these criteria are: maximum stress criteria, maximum strain criteria, and distortional energy criterion (e.g., Tsai-Hill, Hoffman). Later, tensor polynomial criteria for composites were proposed. The maximum stress and strain criteria are popular because they are operationally simple. For multiaxial states of stress, these criteria are, in effect, curve-fitting schemes and have no analytic foundation. The distortional energy and tensor polynomial criteria have built-in generality and mathematical consistency. Most of the existing failure criteria agree with one another when used to predict uniaxial and pure shear strength data along material symmetry axes. However, the failure criteria do not always agree when applied to combined stress states. Better correlation between the analytical predictions using failure criteria and experiments have been observed when the failure criteria are applied to the entire laminate rather than to the unidirectional constituent layers. As the understanding of specific failure mechanisms for composite structures increases and as new mechanisms are identified, new failure models and criteria may be required.

Delamination

Delamination is a common failure mode in composite structures because interlaminar strength is the lowest strength in a laminated material. Interlaminar stresses can be caused by out-of-plane loads, surface impact, or interlaminar defects. These stresses are also induced near any free edge (including notches and through-the-thickness discontinuities) of a laminate subjected to inplane loading.

Delamination is a design consideration for composites in the same manner as tensile strength, compressive strength, and fatigue life. Therefore, the analysis and control of delamination are being widely studied. Analytical and computational models have been developed for the accurate determination of interlaminar stresses near free edges prior to delamination. These models are based on the use of perturbation techniques, approximate three-dimensional elasticity solutions, finite differences, and more recently, finite elements. Classical techniques of linear elastic fracture mechanics have been used for predicting the onset and growth rates of delamination.

The number of techniques to control delamination is limited, but the following three procedures are being used:

1. Proper choice of the laminate construction (e.g., modifying the stacking sequence) to reduce the interlaminar stresses
2. Material selection (e.g., resins with improved fracture toughness)
3. Reinforcement through the laminate thickness (e.g., stitching)

Also, good quality assurance programs can eliminate large voids as sources of delamination. The use of the aforementioned suppression techniques can result in changing the mode of failure from delamination to another type.

Global Instabilities and Component Failure

The failure characteristics of structural components are generally more complex than those of the relatively simple coupon specimens often used for material characterization. Structural components can be subjected to combined loading conditions with both in-plane and out-of-plane loading components and can respond to the applied loads by structural response phenomena, such as component buckling. Extrapolating coupon data to large-scale structural components may be inadequate. Local damage or a local failure can cause the load distribution in a structural component to change significantly. The loading conditions and response phenomena of structural components can cause large interlaminar stresses in the component which cause failure to occur by mechanisms not observed in simpler coupon tests.

The differences between the failure analyses for coupons and for structural components are also being examined. Heuristic failure analyses developed from coupon data may be useful for estimating failure of a structural component subjected to the same loading conditions as the coupon tests, but these analyses may need reevaluation when other loading conditions or failure mechanisms are likely to occur. Heuristic analyses based on uniaxial in-plane loading conditions may not be adequate for more complex loading conditions. A simple analysis for predicting delamination-related failures may not be accurate for other failure modes (e.g., shear crippling) if delamination is suppressed. No reliable failure analysis has yet been developed for combined in-plane and out-of-plane failures such as the skin-stiffener separation failure mode observed for stiffened panels with buckled skins. Research is currently under way to develop failure analyses suitable for large-scale structural components, but additional experience with large components and with more complex responses and loading conditions is needed before reliable, verified failure analyses are readily available.

Analysis Methodology for Predicting Progressive Failure

Although methods are currently available for predicting the strength of composite laminates subjected to unidirectional loading, analysis methodology is still evolving for predicting the progressive failure of composite structures subjected to multidirectional loading. Failure of a laminated composite structure may start at a local defect that is characterized on the micromechanics level and may grow to the sublaminar, laminate, and subcomponent levels. Analysis methodology for predicting the progressive failure of composite structures could start at the micromechanics

level and trace the failure through the aforementioned levels. Different analytical models would be needed at each level. At the first level the model might include (a) distribution of local damage and defects, (b) consequent local states of stress and deformation and (c) nonlinear material response. At the sublaminate and laminate levels, the analytical model should be capable of predicting interlaminar stresses. At all levels, simple models are needed which capture the major response characteristics. However, a reliable verified failure analysis for a composite component can only be achieved if the sensitivity to damage in the various regions of the structure is known.

Damage-Tolerant Design Technology

Most high-strength graphite-epoxy composite laminates lack the ductile behavior at high strains which is characteristic of metals. Composite structures respond to local strain concentrations (such as those that exist in the vicinity of holes and impact damaged regions) by localized failure. This local failure reduces the local stiffnesses and transfers high strain concentrations into adjacent regions, which may cause the local damage to propagate. Recent studies indicate that residual strength of impact-damaged laminates can be improved by increasing the fracture toughness of the matrix material, and some investigators anticipate that a high-failure-strain fiber could also improve damage tolerance characteristics.

Specific matrix properties that constitute toughness are not well established; however, a high failure strain (greater than 4 percent) for the matrix with nonlinear stress-strain response at high strains may be a necessary but not a sufficient condition. Resin materials with high fracture toughness (referred to herein as tough resins) may improve the impact damage tolerance characteristics of brittle composites by suppressing the delamination mode of failure. For brittle composites, delamination growth is the dominant failure mechanism observed in tests. The performance of tough-resin composites under cyclic loading is not yet well established. Local shear crippling appears to be the dominant failure mechanism for tough-resin laminates with damage or discontinuities such as holes.

Achievement of damage tolerance for heavily loaded composite aircraft structures can be addressed at several levels of structural complexity. At the material level, tough resins and high-failure-strain fibers are being developed. Improved damage tolerance can also be achieved through the use of innovative structural configurations designed to arrest and contain the damage within a region of acceptable size. There have been recent advancements in damage containment for both tension- and compression-loaded applications. Finally, damage tolerance can be addressed at the global structural level by designing efficient structures capable of carrying the redistributed loads following local, regional failure. In summary, a combination of advancements including material improvements, damage containment configuration development, and global-local redistribution design methods are needed to meet the stringent damage tolerance requirements typical of heavily loaded aircraft components such as a wing.

Future Directions of Research

This workshop emphasized the need for a systematic study to understand the failure mechanisms of composite structures from the micromechanics to the component levels and to develop a reliable and verifiable capability for predicting progressive

failure. As new resins and fibers are developed, the effect of material nonlinearity on damage onset and propagation needs to be assessed. For design purposes, simple computational models that capture the multilevel aspects of failure are needed. Different models may be needed at each level.

**COMMERCIAL TRANSPORT AIRCRAFT
COMPOSITE STRUCTURES**

**John E. McCarty
Boeing Commercial Airplane Company
Seattle, Washington**

This presentation will take a look at the role that analysis plays in the development, production, and substantiation of aircraft structures; the types, elements, and applications of failure that are used and needed; the current application of analysis methods to commercial aircraft advanced composite structures, along with a projection of future needs; and some personal thoughts on analysis development goals and the elements of an approach to analysis development.

INTRODUCTION

ANALYSIS ROLE

ANALYSIS ELEMENTS

COMPONENT ANALYSIS

ANALYSIS DEVELOPMENT

SUMMARY

The analysis of structure is the only truly feasible means of substantiating the strength, fatigue life, and damage tolerance of a majority of commercial aircraft structures. This is true simply because only a minimum number of critical locations on the aircraft can be validated by full-scale testing. Test data at the coupon, detail, structural element, and subcomponent levels provide half of the information required to establish the critical margin of safety. The other half is obtained by structural analysis. Therefore, the confidence and credibility of the analysis tools used are very critical to the acceptance of analysis as the prime means of structural substantiation of commercial aircraft structure.

AREAS OF DISCUSSION

FAILURE ANALYSIS

FAILURE MECHANISMS

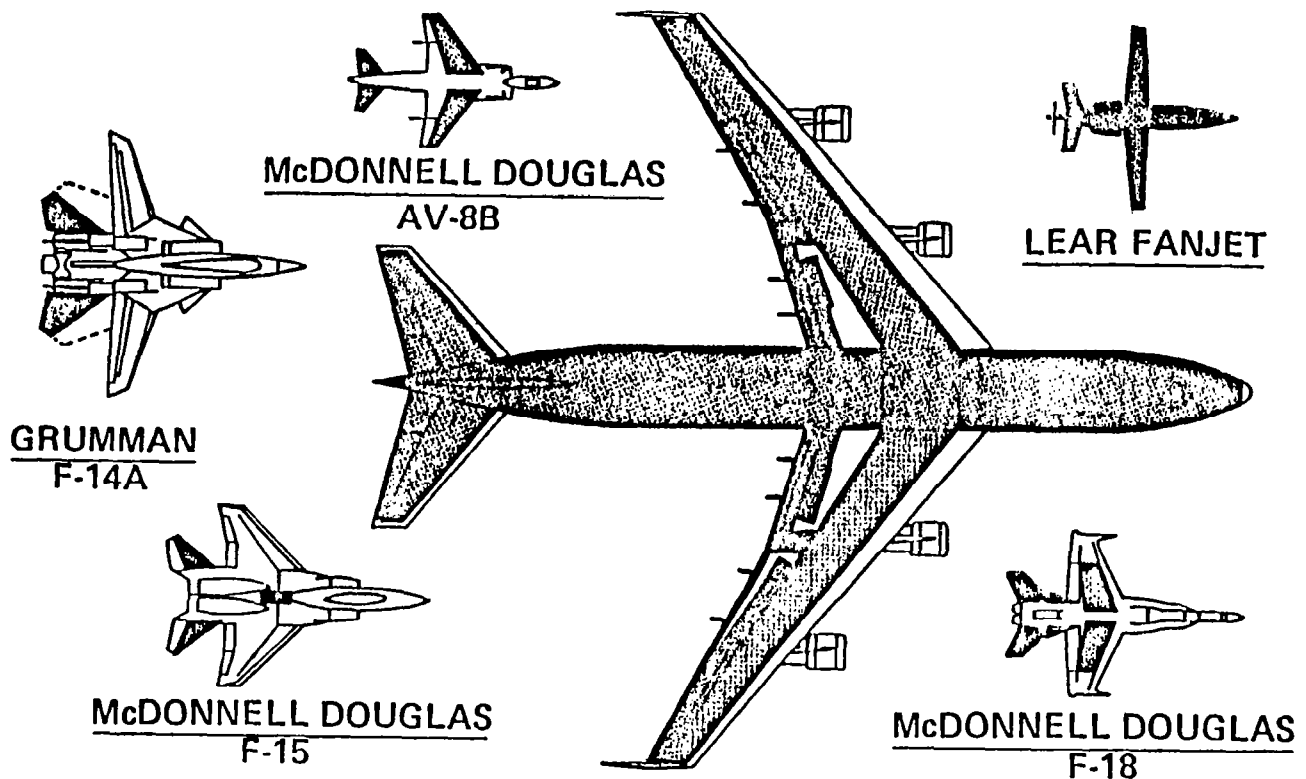
ANALYSIS ROLE FOR COMMERCIAL AIRCRAFT:

"THE PRIMARY MEANS OF STRUCTURAL SUBSTANTIATION FOR CERTIFICATION OF COMMERCIAL AIRCRAFT IS BY ANALYSIS. IT IS EXPECTED THAT THE ANALYSIS WILL BE SUPPORTED BY THE APPROPRIATE TEST EVIDENCE"

This figure dramatizes the idea of why the analysis is really the only means of fully substantiating the structure of large aircraft. This in no way implies that the same is not true for small aircraft. The large number of structural details that must be reviewed in producing any aircraft requires that all information required by both halves of the margins of safety equations be available.

Transport Aircraft Composite Structures

- Large primary structure composite development



The Federal Aviation Regulations (FAR 25) (ref. 1) established the requirements for structural certification of commercial aircraft. The list of numbered paragraphs shows those most pertinent to this discussion on advanced composite applications. In addition to the FAR 25, the FAA has issued an advisory circular for composite structure (ref. 2). The advisory circular provides guidance to both industry and the FAA as to the acceptable means of compliance with the FAR 25 for advanced composites.

CURRENT REGULATIONS
INVOLVED IN COMPOSITE
CERTIFICATION

MATERIAL AND PROCESS SPECIFICATIONS	{ 25.603 25.605	MATERIALS FABRICATION METHODS
MATERIAL PROPERTIES	{ 25.613 25.615 25.619	MATERIAL STRENGTH PROPERTIES AND DESIGN VALUES DESIGN PROPERTIES SPECIAL FACTORS
PROOF STRENGTH	{ 25.305 25.307	STRENGTH AND DEFORMATION PROOF OF STRUCTURE
DAMAGE TOLERANCE	25.571	FATIGUE EVALUATION OF FLIGHT STRUCTURE

ADVISORY CIRCULAR AC NO. 20-107 DATED 7/10/78
SUBJECT: COMPOSITE AIRCRAFT STRUCTURE

These lines selected from FAR 25 (ref. 1) and the advanced composite advisory circular (ref. 2) illustrate FAA's recognition of the major role that structural analysis plays in the substantiation of the strength and damage tolerance of a commercial aircraft structure. Both the regulations and the guidelines recognize the relationship of the types of material, experience with material, and structural configuration and concepts, as well as the supportive contribution of test data.

FAR 25 & ANALYSIS

FAR 25.307..."STRUCTURAL ANALYSIS MAY BE USED ONLY IF THE STRUCTURE CONFORMS TO THOSE FOR WHICH EXPERIENCE HAS SHOWN THIS METHOD TO BE RELIABLE..."

FAR 25.571(b) DAMAGE-TOLERANCE (FAIL-SAFE) EVALUATION...
"THE DETERMINATION MUST BE BY ANALYSIS SUPPORTED BY TEST EVIDENCE AND (IF AVAILABLE) SERVICE EXPERIENCE..."

ADVISORY CIRCULAR & ANALYSIS

AC NO. 20-107

3b..."THE EXTENT OF TESTING AND/OR ANALYSIS AND THE DEGREE OF ENVIRONMENTAL ACCOUNTABILITY REQUIRED WILL DIFFER FOR EACH STRUCTURE DEPENDING UPON THE EXPECTED SERVICE USAGE, THE MATERIAL SELECTED, THE DESIGN MARGINS, THE DATA BASE AND EXPERIENCE WITH SIMILAR STRUCTURE AND ON OTHER FACTORS AFFECTING A PARTICULAR STRUCTURE."

5..."THE STATIC STRENGTH OF COMPOSITE DESIGN SHOULD BE DEMONSTRATED THROUGH A PROGRAM OF COMPONENT ULTIMATE LOAD TESTS IN THE APPROPRIATE ENVIRONMENT, UNLESS EXPERIENCE WITH SIMILAR DESIGNS, MATERIAL SYSTEMS AND LOADINGS IS AVAILABLE TO DEMONSTRATE THE ADEQUACY OF THE ANALYSIS SUPPORTED BY SUBCOMPONENT TEST."

This particular statement should be of interest to the workshop attendees since several of the presentations relate to the idea of material system allowables.

ADVISORY CIRCULAR & ANALYSIS

4b. "THE MATERIAL SYSTEM ALLOWABLES SHOULD BE ESTABLISHED ON THE LAMINATE LEVEL BY EITHER TEST OF THE LAMINATE OR BY TEST OF THE LAMINA IN CONJUNCTION WITH A TEST VALIDATED ANALYTICAL METHOD"

An understanding of which analysis tools relate to commercial aircraft safety and which to lifecycle economics is required to form a proper perspective of the analysis substantiation requirements. This chart attempts to provide a view of this idea. The confidence required for safety is attained by conservative application of simple analysis methods supported by extensive testing, or realistic application of a variety of analysis tools of varying sophistication supported by appropriate levels of test evidence.

DESIGN/ANALYSIS AND CERTIFICATION ELEMENTS

SAFETY	{	STATIC STRENGTH	EXTERNAL LOADS ANALYSIS <u>MAT'L & STR. ALLOWABLES</u> <u>FAILURE CRITERIA & ANALYSIS</u>
		DAMAGE TOLERANCE	<u>FLAW GROWTH ANALYSIS</u> <u>RESIDUAL STRENGTH ANALYSIS</u> INSPECTION REQUIREMENTS
		FLUTTER MARGIN	STIFFNESS REQUIREMENTS FLUTTER ANALYSIS
ECONOMICS	{	MAINTENANCE COST	<u>DURABILITY - FATIGUE ANALYSIS</u> INSPECTION COST REPAIR COST
		PRODUCTION COST	MAT'L COST DESIGNED-IN COST MANUFACTURING METHODS & COST INSPECTION METHODS & COST

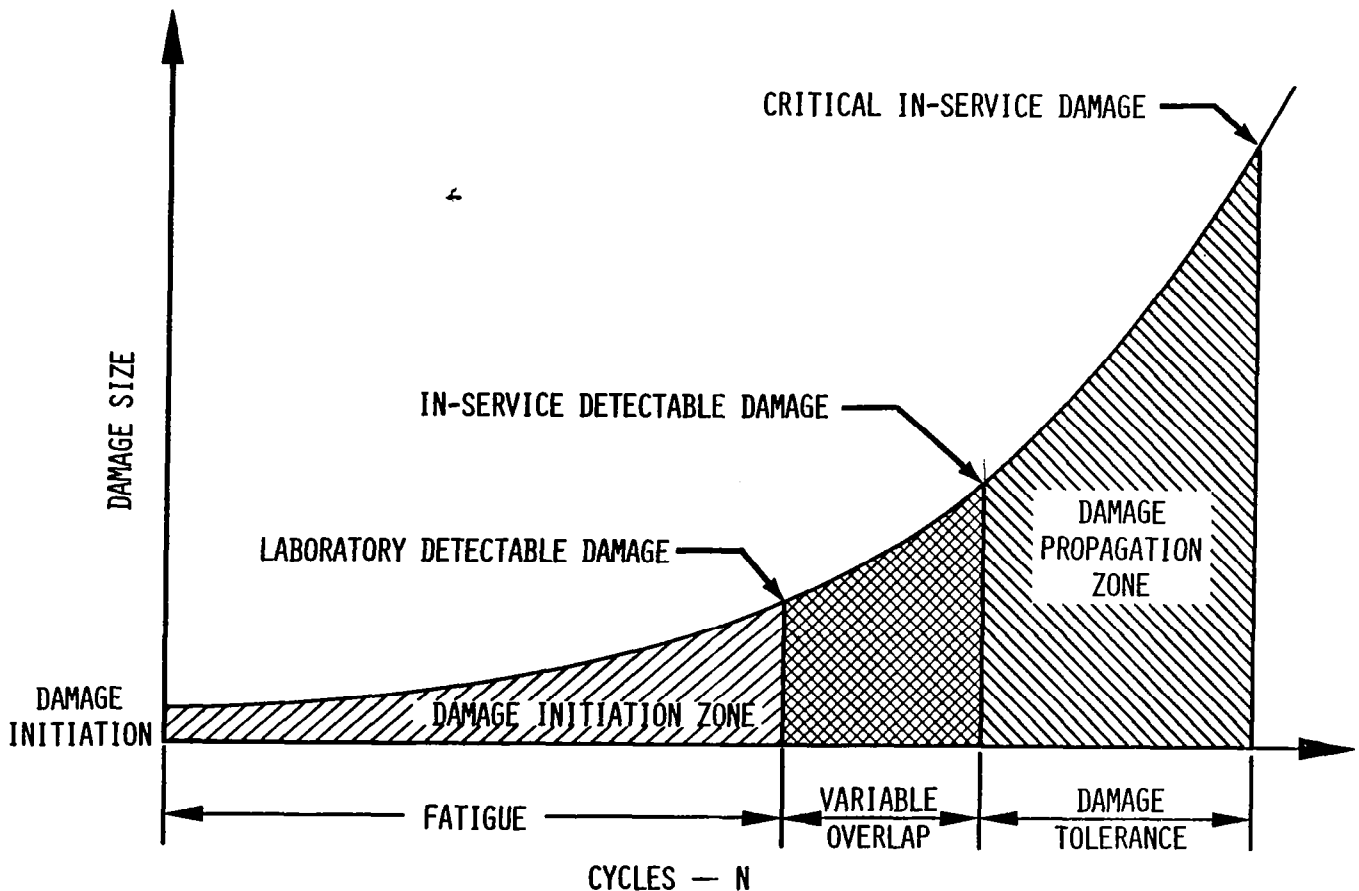
To better describe the requirements of damage-tolerant concepts, two charts are presented with the following statements. (1) The anticipated damage that may arise from normal aircraft operations can include fatigue damage, manufacturing and/or maintenance flaws, or errors in undetected accidental damage. (2) The damage tolerance design structure must also provide a very substantial means of protecting against accidental damage sustained in flight as a result of such things as engine breakup, hail, and bird or other types of impact damage. In these particular cases it is expected that the damage will be found upon completion of the flight.

DAMAGE TOLERANCE

"THE STRUCTURE MUST BE DESIGNED IN SUCH A WAY
THAT ANY DAMAGE INCURRED FROM NORMAL OPERATION
IS DETECTABLE BEFORE THE STRENGTH OR STIFFNESS
OF THE STRUCTURE FALLS TO AN UNACCEPTABLE LEVEL."

In order to establish for this discussion the separation of the fatigue aspect of analysis from that of damage tolerance analysis, this chart gives a graphical representation of this separation. Simply stated, damage-tolerant considerations must include the idea of damage detectability. Therefore, the idea acts to provide a real design and application separation. Once detectable, the time to grow to critical is the area needing the damage tolerance growth analysis.

DISCIPLINED ANALYSIS APPROACH TO DURABILITY/DAMAGE GROWTH DESIGN CONSIDERATIONS



This chart presents a breakdown by category of some of the detailed aspects of the requirements of damage tolerance analysis. Categories 2 and 3 are the analysis areas of concern in this discussion. However, Category 1 was the means of meeting the damage tolerance requirements for the Boeing 727 advanced composite elevator.

DAMAGE TOLERANCE ANALYSIS REQUIREMENTS

STRUCTURAL CATEGORY			TECHNIQUE OF ASSURING SAFETY	TECHNOLOGY CONTROL METHOD
SECONDARY STRUCTURE	DAMAGE TOLERANCE DESIGN	① SECONDARY STRUCTURE	DESIGN FOR LOSS OF COMPONENT OR SAFE SEPARATION	● CONTINUED SAFE FLIGHT
PRIMARY STRUCTURE		② DAMAGE OBVIOUS OR MALFUNCTION EVIDENT	ADEQUATE RESIDUAL STRENGTH WITH EXTENSIVE DAMAGE THAT IS OBVIOUS	● RESIDUAL STRENGTH
		③ DAMAGE DETECTION BY PLANNED INSPECTION PROGRAM	INSPECTION PROGRAM MATCHED TO STRUCTURAL CHARACTERISTICS	● RESIDUAL STRENGTH ● CRACK GROWTH ● INSPECTION PROGRAM
	SAFE-LIFE DESIGN	④ SAFE-LIFE	CONSERVATIVE FATIGUE LIFE	● FATIGUE

The ability to configure a new aircraft is based on the state of the art of the available analysis tools. The structure configuration, structural concept, and material selection are all evaluated analytically. The payoff of this analytical effort is the future successful production and operation of new aircraft. The ability to change and improve the aircraft is reduced with this advancement through the development, production, and operational cycle. The state of the art and the ease of application of the analysis of tools applied early in the design cycle are significant factors in developing a successful aircraft.

DESIGN/ANALYSIS ROLE IN STRUCTURAL AIRFRAME DEVELOPMENT

- RESEARCH & DEVELOPMENT

IDENTIFY NEW STRUCTURAL PAYOFFS
EVALUATE MATERIALS & STRUCTURAL CONCEPTS
GUIDE THE TEST PLANNING & DATA ANALYSIS

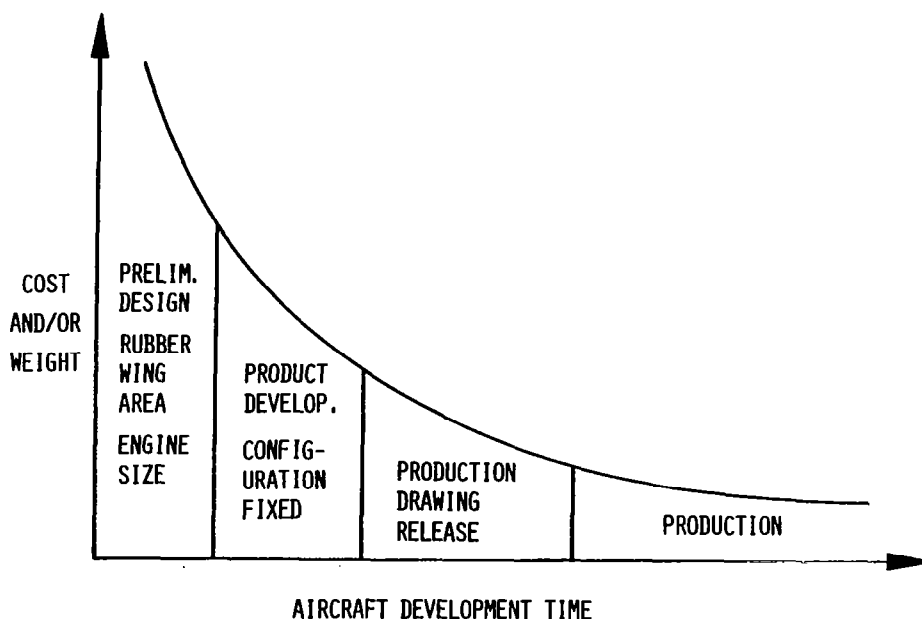
- PRELIMINARY DESIGN & PRODUCT DEVELOPMENT

TRADES - WEIGHT & COST
CONFIGURATION & CONCEPTS

- AIRCRAFT PROGRAM

STRUCTURAL SIZING
DRAWING RELEASE
FORMAL ANALYSIS - FOR CERTIFICATION
MARGINS OF SAFETY
TEST/ANALYSIS CORRELATION

ANALYSIS SUPPORTED DECISION EFFECT ON COST AND/OR WEIGHT



An element in utilizing any analytical capability is the fact that in a large design program there must be a discipline to the tools used. Each company publishes design manuals, stress manuals, and analysis programs in various forms to ensure some uniformity in analysis procedures. The key then is the disciplined procedures that provide the benefits shown on this chart.

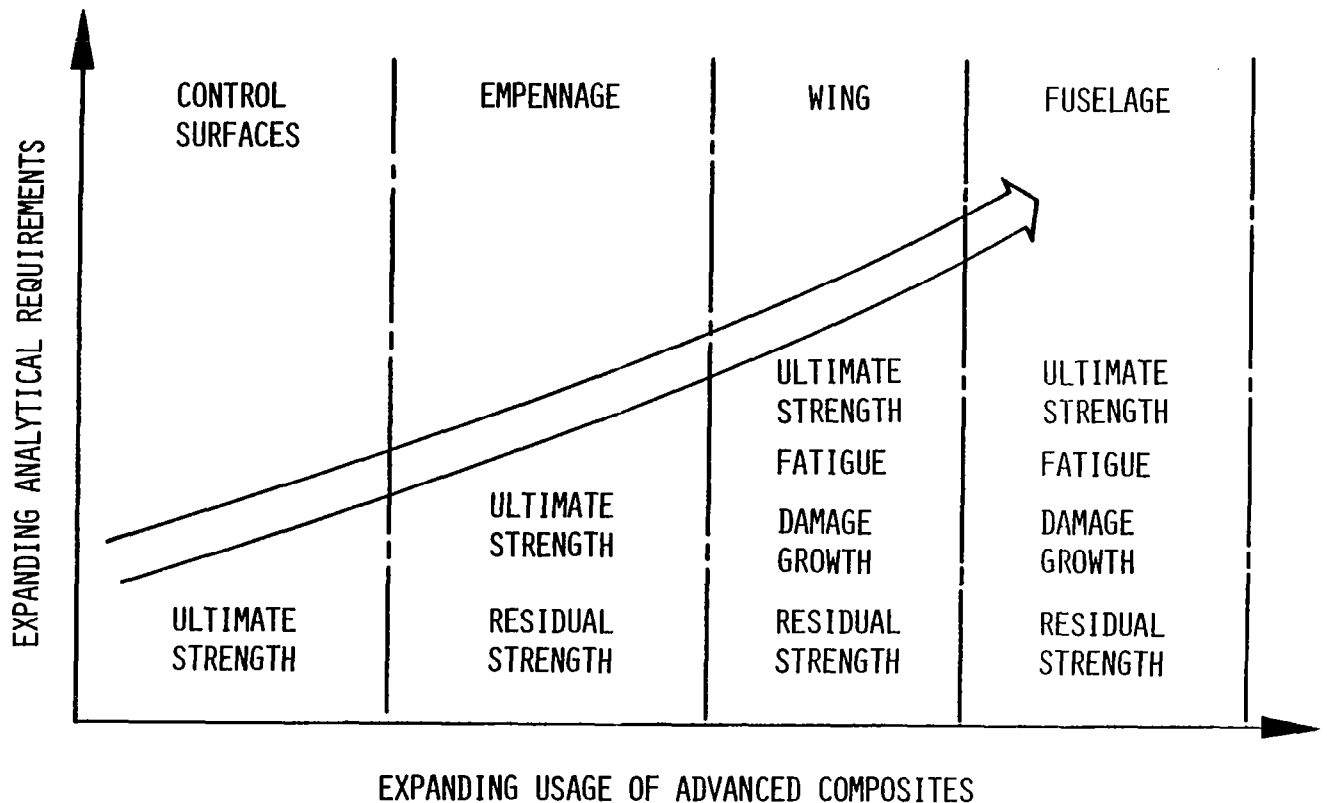
ANALYSIS SUPPORT OF AIRCRAFT PROGRAMS

KEY - DISCIPLINED PROCEDURES

PROVIDES ACCEPTABLE TOOLS AT ALL LEVELS
USABLE BY LARGE NUMBERS OF NON-SPECIALISTS
CAUSES ATTENTION TO BE FOCUSED ON CRITICAL PARAMETERS
PROVIDES COMMON QUANTIFIABLE BASE FOR DECISION MAKING
CORRELATES FLEET AND TEST EXPERIENCE
ESTABLISHES BASE FOR AIRFRAME SUSTAINING

This list will be familiar to all those in the structures technical community. The application of analysis of tools in each of these levels of structural significance will be discussed. These analysis classifications have been separated for discussion purposes into the areas of requirements analysis and capability analysis. The idea is that the structure is required to perform a set of structural functions or requirements, and the structure has been designed to provide a level of capability to meet those performance requirements.

ANALYSIS PROCEDURE NEEDS



A collection of analytical tools across all the analysis disciplines (strength, fatigue, and damage tolerance) provides a means of quantifying the structures capability margin (margins of safety) in each area. This and the following charts are aimed to illustrate the disciplined approach in production analysis of structures.

DESIGNED & REQUIRED STRUCTURAL PERFORMANCE

PERFORMANCE EVALUATION:

$$\text{MARGIN OF SAFETY} = \frac{\text{CAPABILITY OF STRUCTURE}}{\text{STRUCTURAL REQUIREMENTS}} - 1 = \underline{\hspace{1cm}}\%$$

A discipline analysis procedure can be used not only to establish the margins of safety but also as a means of quantifying structural performance against weight and cost. The analytical tools should end up clearly defining both the requirements of the structure and the capability of the structure being designed.

COMMON APPROACH TO STATIC, FATIGUE, DAMAGE GROWTH AND RESIDUAL STRENGTH DESIGN

ANALYSIS	ULTIMATE STRENGTH	FATIGUE STRENGTH	DAMAGE GROWTH	RESIDUAL STRENGTH
REQUIREMENT	f_{tu}	FQ_{REQUIRED}	DTR_{REQUIRED}	f_{RS}
CAPABILITY	F_{tu}	FQ_{DETAIL}	DTR_{DETAIL}	F_{RS}
MARGIN	$\frac{F_{tu}}{f_{tu}} - 1$	$\frac{FQ_{\text{DETAIL}}}{FQ_{\text{REQUIRED}}} - 1$	$\frac{DTR_{\text{DETAIL}}}{DTR_{\text{REQUIRED}}} - 1$	$\frac{F_{RS}}{f_{RS}} - 1$

The idea of an analysis model being part of the requirements analysis does not imply a single model, but refers rather to all the analysis tools required to establish the requirements half of the margins of safety equation. The analysis model for structure can include the following: finite element, interlaminar stresses, laminate stress analysis at the detailed stress analysis level, fatigue damage model, damage growth model, and fracture mechanics analysis.

ANALYSIS PROCEDURE

REQUIREMENTS ANALYSIS	ULTIMATE STRENGTH	FATIGUE DURABILITY	FLAW GROWTH	RESIDUAL STRENGTH
● AIRCRAFT	FLIGHT ENVELOPE	SERVICE LIFE	INSPECTION INTERVALS	FLAW DETECTABILITY
● LOADING	STATIC 1.5 x LIMIT	REPEATED SPECTRUM	REPEATED SPECTRUM	STATIC LIMIT
● ENVIRONMENT	MAX CRITICAL	NORMAL USAGE	NORMAL USAGE	MAX. CRITICAL
● ANALYSIS MODEL	MAX STRAIN (ETC.)	ACCUMULATIVE DAMAGE	FLAW GROWTH	STRESS INTENSITY (ETC)
● REQUIRED CAPABILITY	CRITICAL STRAIN	MAX CYCLIC STRAIN	GROWTH INTERVAL REG.	CRITICAL FLAW SIZE

The capabilities analysis recognizes that the structural form, the type of applied load, the material used, and the expected failure mechanism or mechanisms must be part of any evaluation. The material properties can be as simple as test data to develop the properties, i.e., tension, compression, or shear, or they can be established by analysis procedures, such as in a simple column analysis. Because of the intrinsic variability of material properties, a reliability analysis of the test data must be part of any procedure. These forms of capability analysis and the requirement analysis are only an example.

ANALYSIS PROCEDURE

CAPABILITY ANALYSIS	ULTIMATE STRENGTH	FATIGUE DURABILITY	FLAW GROWTH	RESIDUAL STRENGTH
• GROSS CONFIGURATION	_____ TYPE OF STRUCTURE _____			
• DETAIL CONFIGURATION	_____ TYPE OF STRUCTURAL ELEMENT _____			
• MATERIAL PROPERTIES	STATIC ALLOWABLE	FATIGUE DATA	FLAW GROWTH DATA	FRACTURE TOUGHNESS
— RELIABILITY 1	•	•	•	•
— ENVIRONMENT 2 FACTORS	•	•	•	•
• DETAIL CAPABILITY	ALLOWABLE STRAIN	MAX FATIGUE STRAIN	$\frac{dA}{dN}$ RATE	K_I ALLOWABLE

1 25.613 (a) & (b) (ref. 1)

2 25.613 (c) (ref. 1)

This section of the discussion will look at where we are in the development cycle of commercial aircraft advanced composite structure. I will try to express two ideas: (1) the application of the appropriate analysis tools to the component and recognition of the background that has been established to date, and (2) a projection of future needs.

COMMERCIAL AIRCRAFT DEVELOPMENT OF COMPOSITE STRUCTURE

CURRENT

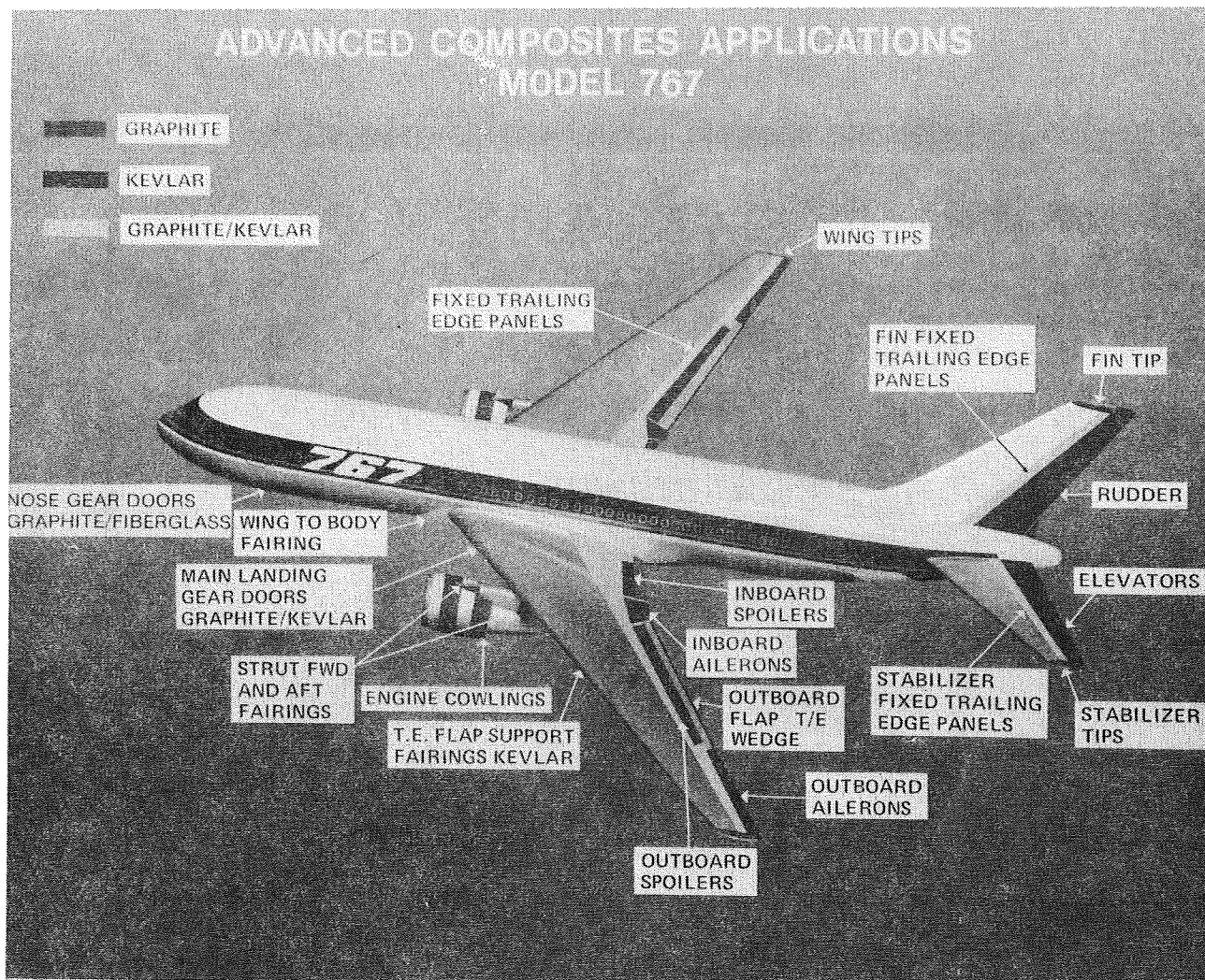
- CONTROL SURFACES
- EMPENNAGES

FUTURE

WINGS

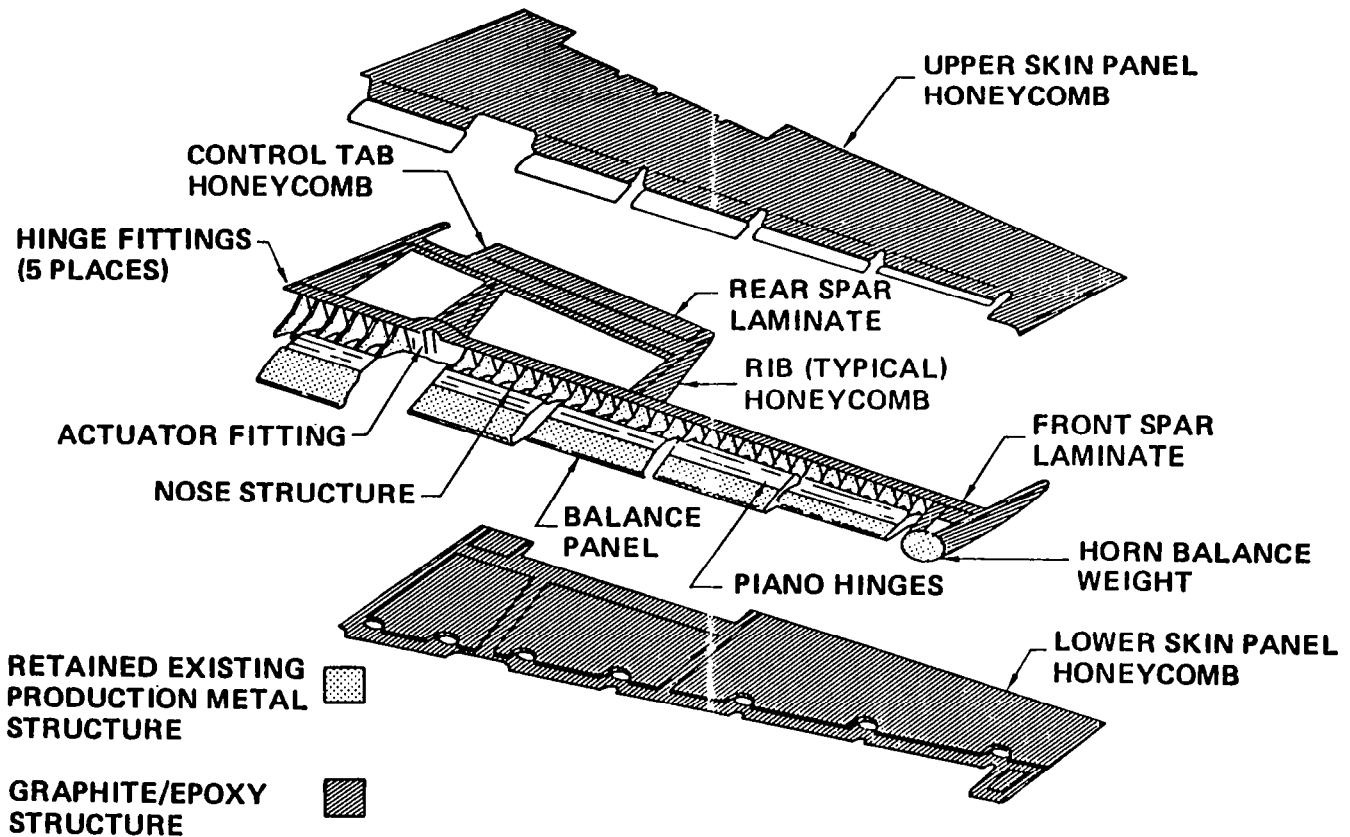
BODY

This figure is shown here to establish the current production status of advanced composites on commercial aircraft. The primary control surfaces, of graphite/epoxy, have been designed and certified using analysis tools available to date. An example of the level of this analysis is illustrated in the discussion that follows on the 727 advanced composite elevator.



The 727 elevator, which is illustrated in the figure, shows an upper and lower skin of honeycomb design consisting of one ply of cloth at $\pm 45^\circ$ and a chordwise 0° tape direction. The spars are laminate with $\pm 45^\circ$ dominant webs and with 0° dominant in the chords. The few ribs noted are primarily $\pm 45^\circ$ with some 0° in the chords and honeycomb webs. This design has been fully certified by the FAA.

Elevator Structural Arrangement



The following lists of analysis considerations are to direct attention not to the detailed analysis but to those facts that were considered in the interplay between this structure and current analysis capability or the analysis capability available at the time of the development and certification of the 727 elevator. The analysis used was just at the level required to meet those certification and design requirements. Since, as noted on the chart, only ultimate strength certification requirements were needed, this is all that is addressed by the analysis tools available.

727 ELEVATOR - ANALYSIS CONSIDERATIONS

DESIGN CRITERIA

SIMILAR STIFFNESS TO ALUMINUM ELEVATOR

DAMAGE TOLERANCE CATEGORY #1

TEMPERATURE RANGE -75°F TO 180°F

MOISTURE CONTENT 1% \pm .1% BY WEIGHT

RESULTS OF CRITERIA ON DESIGN

LOW ULTIMATE DESIGN STRAIN

NO FATIGUE CONSIDERATIONS

NO DAMAGE TOLERANCE REQUIREMENTS

CERTIFICATION CONSIDERATIONS

1ST OF A TYPE MUST TEST TO ULTIMATE

WITH ACCOUNTABILITY FOR MOISTURE & TEMPERATURE

ULTIMATE STRENGTH ONLY

The tools used in the analysis of the 727 elevator were those that have been used in the past on some large control surfaces, i.e., on the Boeing 747. Most Boeing control surfaces are currently analyzed by hand. The 727, being the first generic of its type at Boeing, incorporated the use of the finite element method. The Boeing 767 control surfaces were primarily analyzed by hand. For the reasons noted, other than the first generic, the finite element method was used on this 727 elevator. The other analysis concerned the stability and the ultimate strength of both the surface panels and the web of the front spar. Simplified analysis was used to adequately establish the buckling capability of these honeycomb panels. The ultimate strains were simply the strains associated with the maximum strain in the most critical direction compared to point design allowables of the specific layup developed by test.

727 ELEVATOR ANALYSIS REQUIREMENTS

FINITE ELEMENT ANALYSIS

- NO RIBS BACKING UP HINGE FITTINGS
- METHOD OF ACCOUNTING FOR MOISTURE/TEMPERATURE
- CHECK STIFFNESS SIMILARITY

DETAIL ELEMENT ANALYSIS (STRENGTH CHECK)

SURFACE PANELS

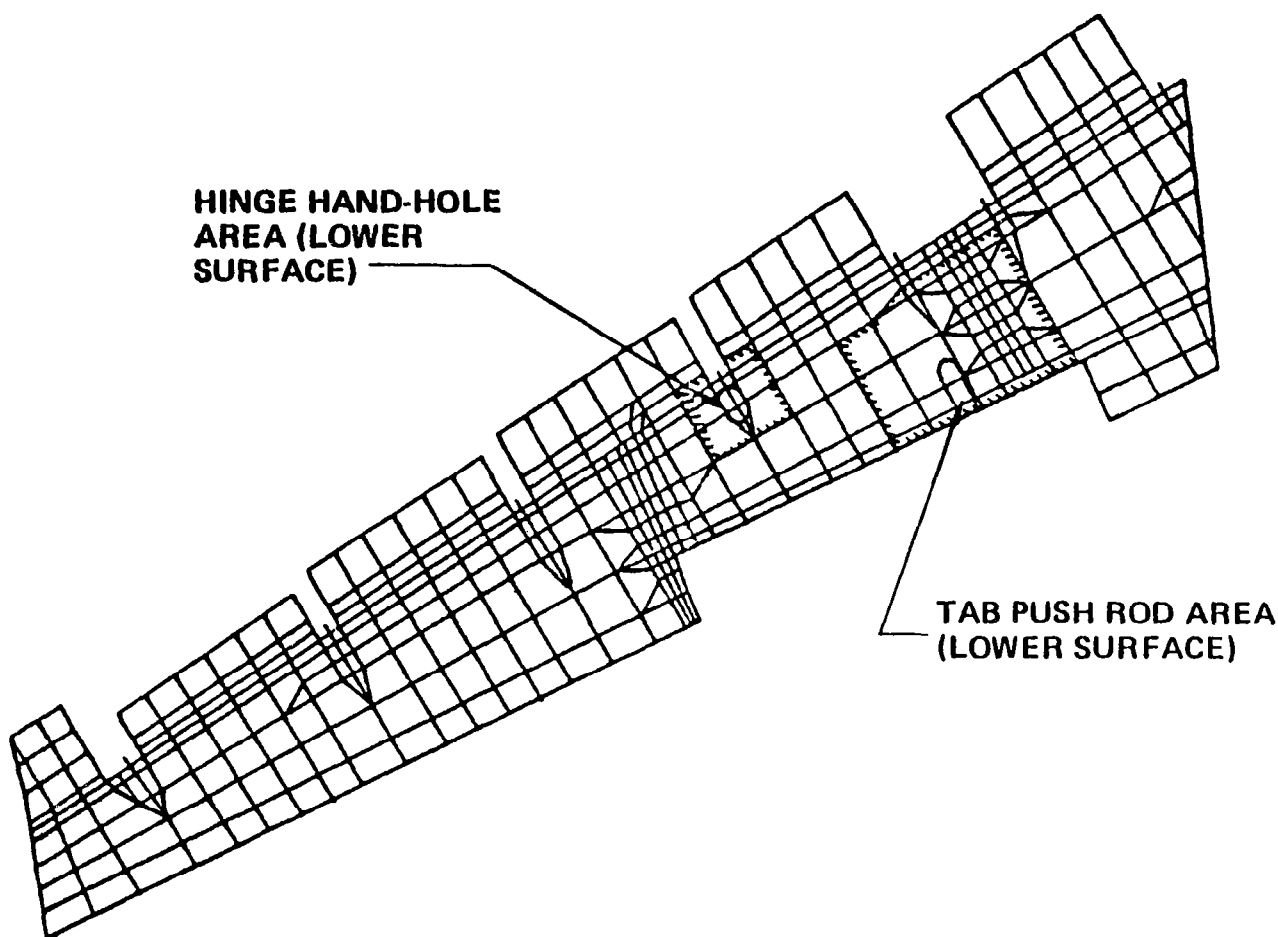
- STABILITY - MODIFIED ALUMINUM METHOD
- ULTIMATE STRAIN - MAX. PRINCIPAL

FRONT SPAR

- WEB SHEAR STABILITY - MODIFIED AL. METHOD
- ULTIMATE STRAIN IN SHEAR
- CHORD STRAINS - ULTIMATE STRAINS T & C
- JOINT STRENGTH BEARING, TENSION

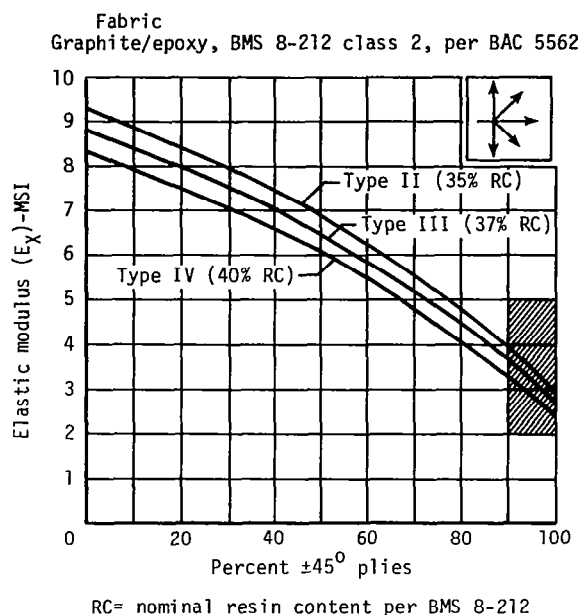
This figure simply illustrates the finite element model used. Note the grid refinement aft of the hinge locations. The extra attention in this area was due to the fact that this was the first Boeing design that did not use a backup rib at each hinge location. The local load redistribution from the hinges was of particular interest.

Elevator Finite Element Model



This figure and the next one illustrate the simplicity of the data available for basic analysis. These strain cutoffs and modulus charts, along with some bearing allowables and the laminate testing that was part of the ancillary test program of the 727 elevator, are all that was provided for both the preliminary design as well as the formal analysis.

ELASTIC MODULUS AND ALLOWABLE STRAINS



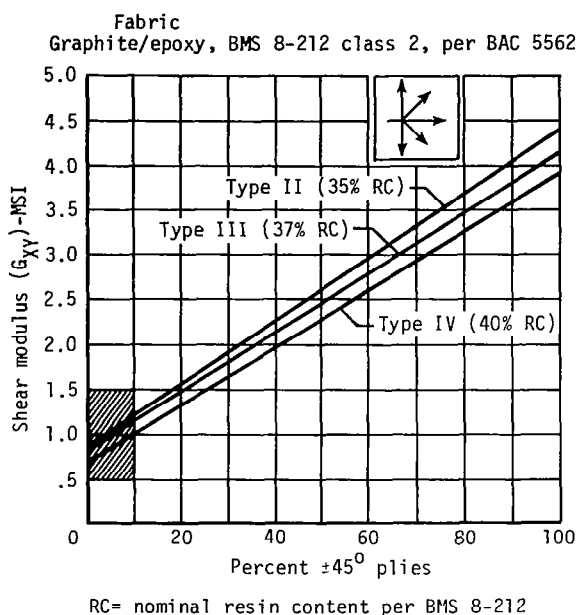
Limit and ultimate
strain (in/in)

	Limit strain	Ultimate strain	
		"A" basis	"B" basis
Laminate tension ϵ_t	.0035	.0059	.0064
Laminate compression ϵ_c	.0027	.0054	.0059
Sandwich tension ϵ_t	①	.0043	.0046
Sandwich compression ϵ_c	①	.0035	.0038

① Ultimate strain $\div 1.5$

Caution: Properties in the cross-hatched region
may be adversely affected by temperature
and humidity

IN-PLANE SHEAR MODULUS AND ALLOWABLE STRAINS



Limit and ultimate
strain (in/in)

	Limit strain	Ultimate strain	
		"A" basis	"B" basis
Laminate shear ϵ_{xy}	.0053	.0108	.0117
Sandwich shear ϵ_{xy}	①	.0070	.0076

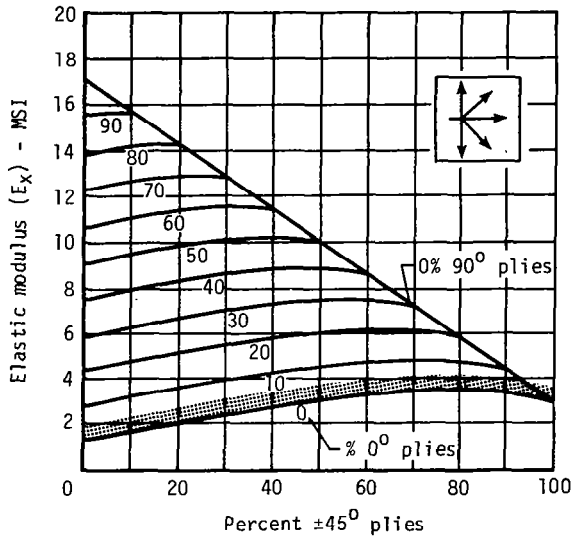
① Ultimate strain $\div 1.5$

Caution: Properties in the cross-hatched region
may be adversely affected by temperature
and humidity.

ELASTIC MODULUS AND ALLOWABLE STRAINS

Tape

Graphite/epoxy, BMS 8-212 Type III Class 1, per BAC 5562



Limit & ultimate strain
(in/in)

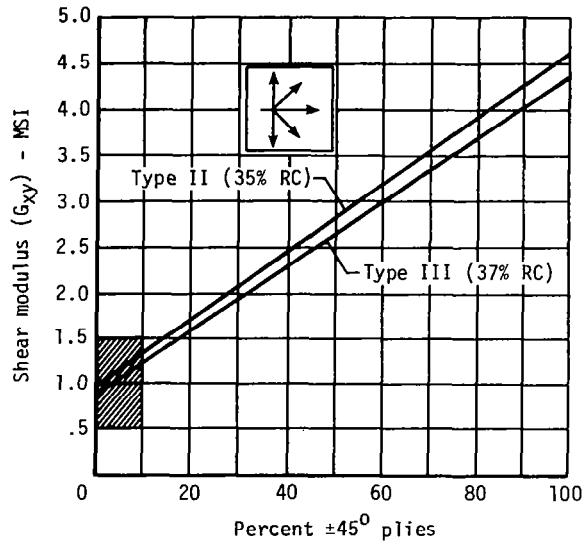
	Limit strain	Ultimate strain	
		"A" basis	"B" basis
Tension ϵ_t	.0035	.0082	.0090
Compression ϵ_c	.0027	.0067	.0072

Caution: Properties in the cross-hatched region may be adversely affected by temperature and humidity.

IN-PLANE SHEAR MODULUS AND ALLOWABLE STRAINS

Tape

Graphite/epoxy, BMS 8-212 Class 1, per BAC 5562



RC-nominal resin content per BMS 8-212

Limit & ultimate strain
(in/in)

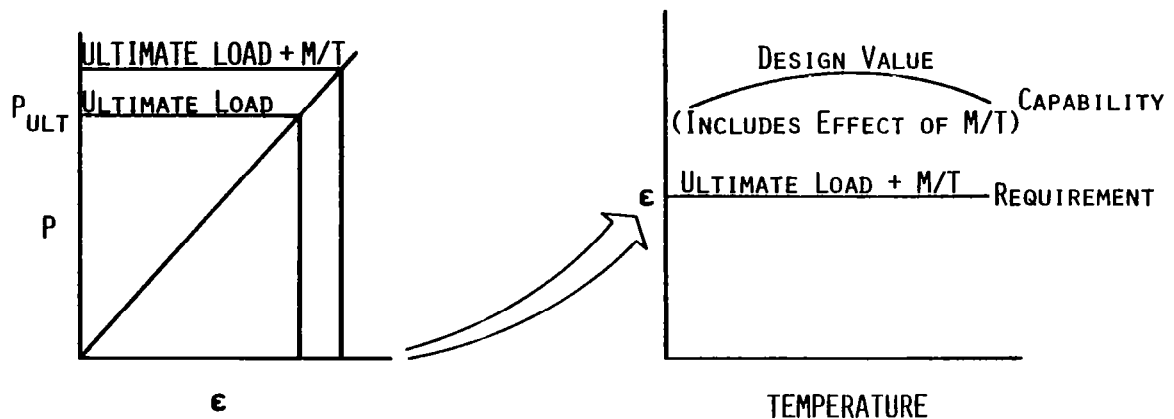
	Limit strain	Ultimate strain	
		"A" basis	"B" basis
Shear ϵ_{xy}	.0053	.0133	.0144

Caution: Properties in the cross-hatched region may be adversely affected by temperature and humidity.

One of the unique considerations of the analysis model was the use of the characteristics of the material, the finite element analysis, and the validation by full-scale ultimate load test of the strain distribution to establish a means of analytically accounting for the effects of moisture and temperature in the ultimate load test results. Since material acts in a linear manner and the response to both load-induced strains and moisture- and temperature-induced strains is also linear in response in fiber-dominated structure, the two can algebraically be added to establish accurate strain in the material at all locations by analysis. The distribution for the loads analysis is verified by the full-scale test. By comparing this analysis strain level to those established by laminate level testing, a margin of safety can be adequately described.

727 ELEVATOR ANALYSIS CONSIDERATION ULTIMATE LOAD TEST MOISTURE AND TEMPERATURE ACCOUNTABILITY

- MATERIAL RESPONSE
- FINITE ELEMENT ANALYSIS
- STRAIN DISTRIBUTION VALIDATION
- LINEAR STRAIN RESPONSE
- FIBER DOMINATED AND MAJOR LOAD PATH DESIGN



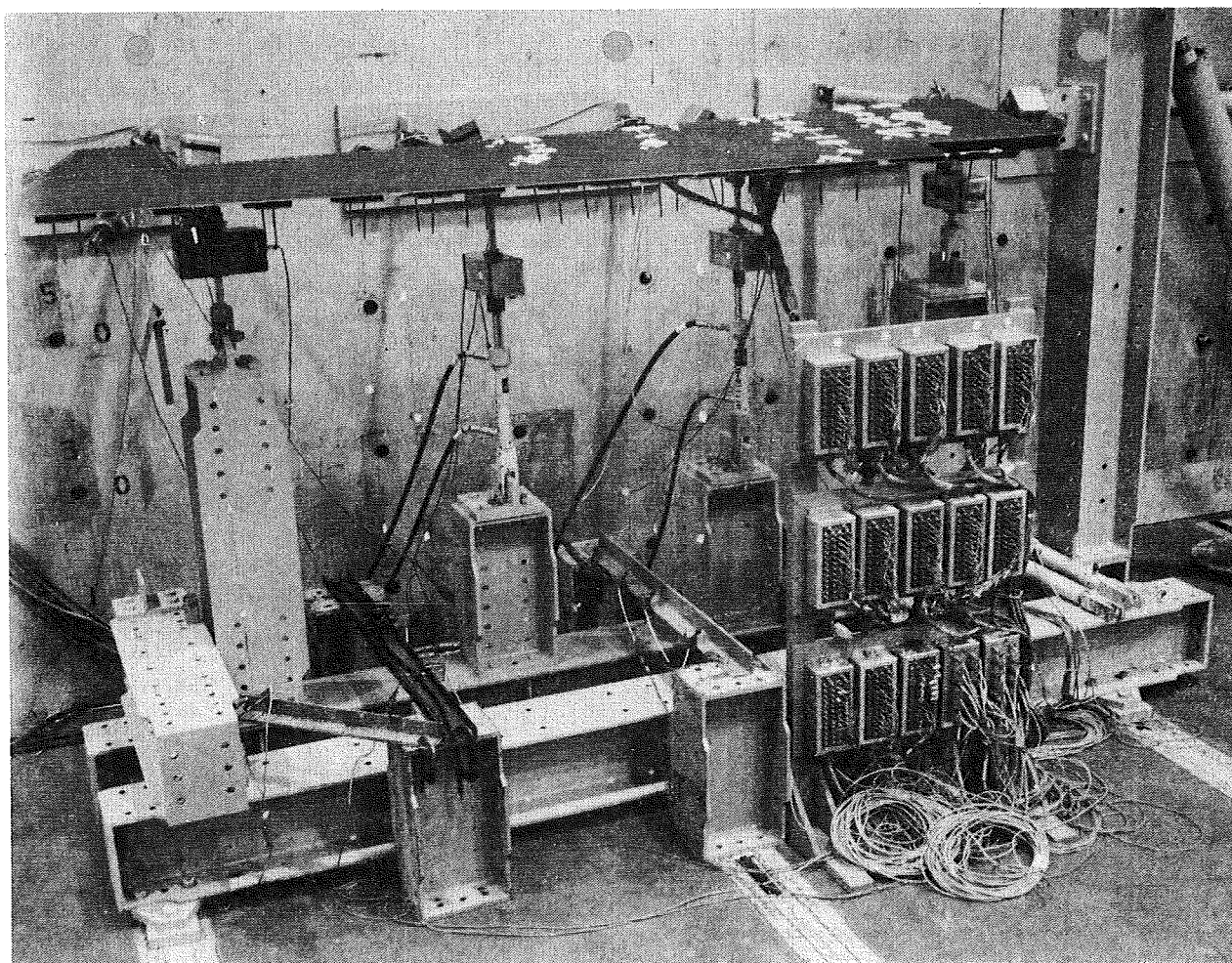
This table illustrates the result of including the effects of moisture and temperature in the requirements part of the margin of safety calculation.

PRINCIPAL STRAINS, ALLOWABLES, AND MARGINS OF SAFETY - ATLAS PANEL 1135, LOAD CASE 125

PANEL SURFACE	ENVIRONMENTAL CONDITION	PRINCIPAL STRAINS*			ALLOWABLE PRINC. STRAINS*			MARGINS OF SAFETY		
		ϵ_{MAX}	ϵ_{MIN}	γ_{MAX}	ϵ_{MAX}	ϵ_{MIN}	γ_{MAX}	ϵ_{MAX}	ϵ_{MIN}	γ_{MAX}
EXTERIOR	70° DRY	1989	-2404	4393	5310	-4930	8499	1.67	1.05	.93
	70° WET	1545	-2294	3840	4260	-4410	6690	1.76	.92	.74
	-75° DRY	1754	-2073	3826	7060	-5670	8156	3.03	1.74	1.13
	-75° WET	1463	-2116	3579	5850	-5790	6422	3.00	1.74	.79
	140° DRY	2406	-2833	5239	4450	-4600	8800	.85	.62	.68
	140° WET	1938	-2700	4638	3600	-3900	6755	.86	.44	.46
	180° DRY	2693	-3127	5821	3980	-4400	8608	.48	.41	.48
	180° WET	2221	-2990	5211	3260	-3650	6770	.47	.22	.30
INTERIOR	70° DRY	1502	-1629	3132	4930	-5310	8499	2.28	2.26	1.71
	70° WET	1006	-1451	2456	4410	-4260	6690	3.38	1.94	1.72
	-75° DRY	560	-1098	1657	5670	-7060	8156	9.13	5.43	3.92
	-75° WET	327	-1183	1509	5790	-5850	6422	16.71	3.95	3.26
	140° DRY	2185	-2087	4273	4600	-4450	8800	1.11	1.13	1.06
	140° WET	1679	-1898	3577	3900	-3600	6755	1.32	.90	.89
	180° DRY	2591	-2364	4956	4400	-3980	8608	.70	.68	.74
	180° WET	2084	-2175	4259	3650	-3260	6770	.75	.50	.59

* MICROSTRAIN

The following figures represent two of the test articles that were used (1) to demonstrate the analysis of the structure for the load strains and for the thermal and moisture strains and (2) to show that the analysis gave good correlation in fiber-dominated structure. The results of these two tests are illustrated on the three graphs. In addition to the 727 and the 737 tests, I have shown the similar compatibility of the linear strain effect previously discussed. These tests, along with the test data at the coupon structural element and subcomponent levels, which included the effects of moisture and temperature, formed the basis both for demonstrating the requirements of capability analysis validity and for providing the capability data to form the margins of safety used in the certification of both the 727 and 737 advanced composite components.



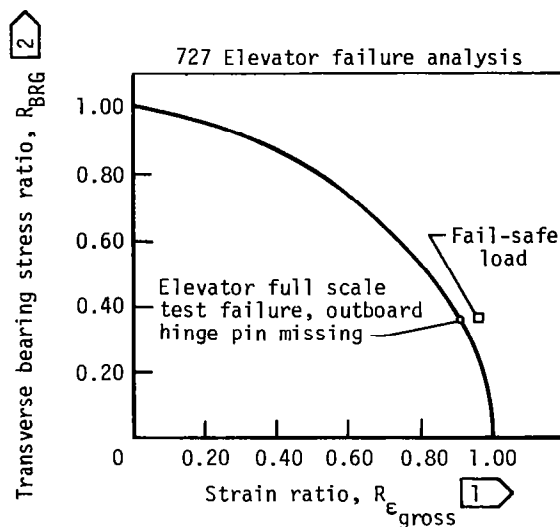
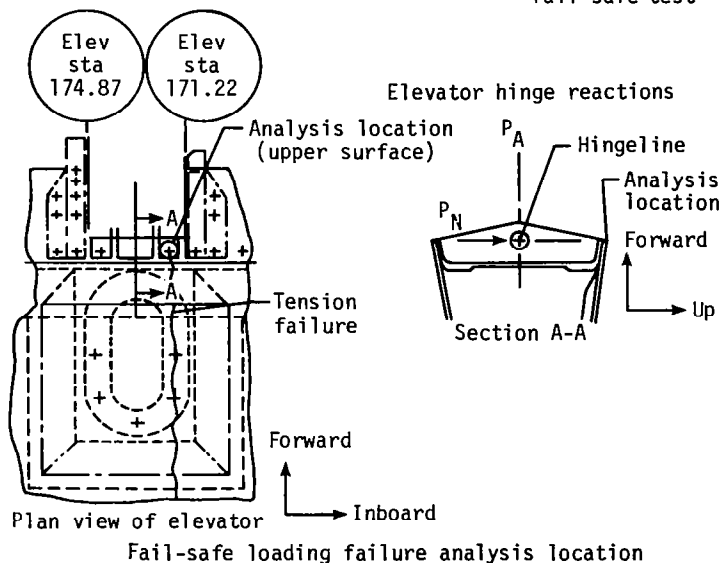


The failure of the front spar of the 727 elevator during test was for a Boeing design condition, not an FAA required condition. The failure occurred in a combined load area of the upper chord of the spar at the hinge fitting. The combined load in the fastener area was demonstrated to be the reason for this failure. A simple interaction curve showed that the failure should have occurred. Good correlation between (1) the stress analysis at both the finite element level and the detailed hand analysis level and (2) the test data and interaction curve shown gave a very good correlation with the failure noted.

727 Elevator Failure Analysis

Combined load on front spar chord
hinge fitting attachment

Failure of front spar in a Boeing
fail-safe test

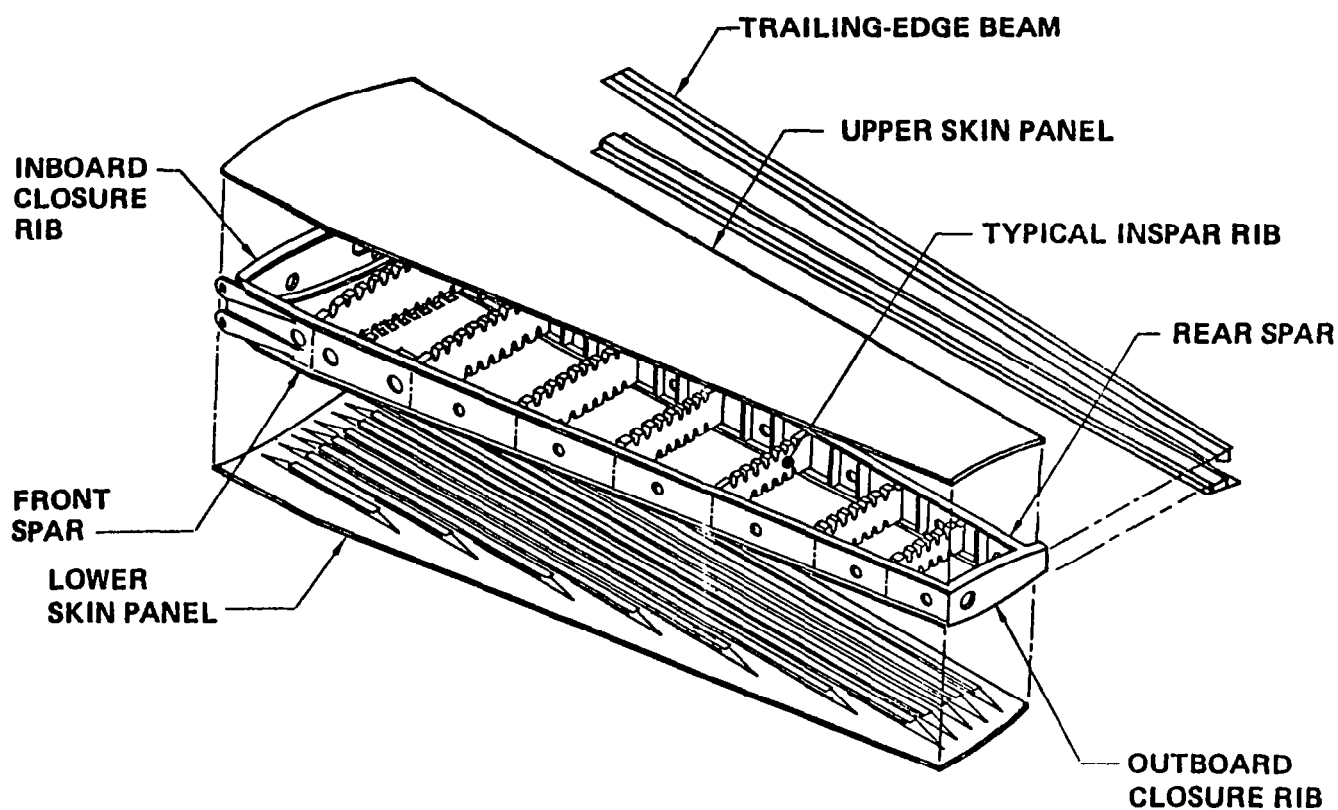


- ① $R_{\epsilon_{gross}}$ of 1.00 based on $\epsilon_{gross} = 0.0046 \text{ mm/mm, (in/in)}$, from room temperature, dry test specimens (fig 71)
- ② R_{BRG} of 1.00 based on $f_{BRG} = 709 \text{ MPa (102 800 lbf/in}^2\text{)}$ from room temperature, dry test specimens (fig 68)

Interaction Curve Bearing versus Tension Bypass Strain

A look at the 737 structure will give some insight into the levels of information and analysis capability that were required for this structure. Again, simple tools could be used since the structure is primarily designed by stiffness. This shows a breakdown of the structural elements of the 737 horizontal stabilizer, which consists of cover panels (co-cured I-stiffened panels), laminate front and rear spars, and honeycomb composite ribs.

Stabilizer Inspar Structural Arrangement



The 737 analysis considerations look at the design criteria impact, and here again stiffness design dominated and therefore produced low strain levels. The damage tolerance requirements are shown to be category 2. This requires that the horizontal stabilizer be designed for large detectable damage with no growth. The same moisture/temperature characteristics and analysis procedure were established as were used for the elevator. Therefore, the 737 requires certification for both damage tolerance and ultimate strain. Again, a finite element analysis was applied to the horizontal stabilizer primarily because of the design, which carries only the two spars through the center section. Therefore, a very significant shear lag and load distribution problem needs careful analysis. Also, by using finite elements and cutting or removing structure to simulate damage tolerance requirements, the analysis procedure was easier to perform.

737 STABILIZER - ANALYSIS CONSIDERATIONS

DESIGN CRITERIA

- SIMILAR STIFFNESS TO AL. STABILIZER
- DAMAGE TOLERANCE CATEGORY #2
- CONTROL STRAIN TO ELIMINATE DAMAGE GROWTH
(I.E., CATEGORY #3)
- TEMPERATURE/MOISTURE (SAME AS ELEVATOR)

RESULTS OF CRITERIA ON DESIGN

- LOW ULTIMATE DESIGN STRAINS
- NO FATIGUE CONSIDERATIONS
- NO FLAW GROWTH CONSIDERATIONS
- TOLERANT TO DISCRETE DAMAGE

CERTIFICATION CONSIDERATION

- 1ST OF A TYPE MUST BE TESTED ULTIMATE
WITH ACCOUNTABILITY FOR MOISTURE & TEMPERATURE
- ULTIMATE STRENGTH
- DAMAGE TOLERANCE (CATEGORY #2)

737 HORIZONTAL ANALYSIS REQUIREMENTS

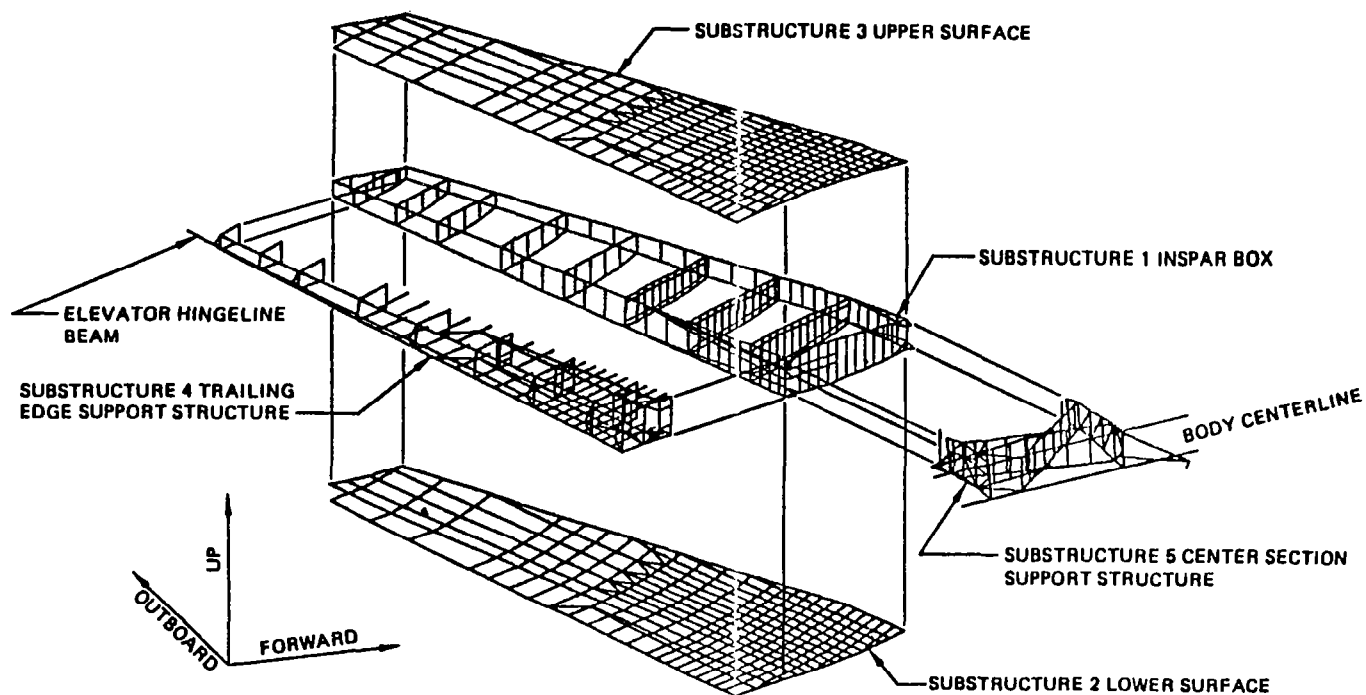
FINITE ELEMENT ANALYSIS

- SPAR CARRY THROUGH TO CENTER SECTION ONLY
- METHOD OF ACCOUNTING FOR MOISTURE/TEMPERATURE
- CHECK STIFFNESS SIMILARITY
- DAMAGE TOLERANCE ANALYSIS
- MAJOR DAMAGE/FAIL SAFE

DETAIL ELEMENT ANALYSIS (STRENGTH CHECK)

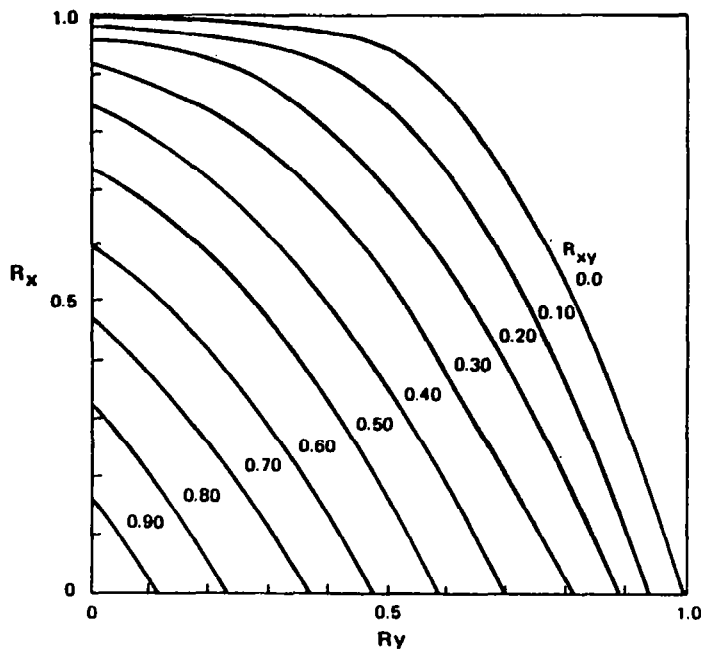
- SURFACE PANEL ANALYSIS
- STABILITY, STRENGTH & DAMAGE TOLERANCE
- SPARS
- WEB - STABILITY, STRENGTH & DAMAGE TOLERANCE
- CHORDS - STABILITY, STRENGTH & DAMAGE TOLERANCE
- JOINT - STRENGTH
- RIBS
- STRENGTH & SKIN ATTACHMENT

The breakdown of the finite element model is shown below. Notice the finer grid in the shear lag load distribution region toward the inboard end.

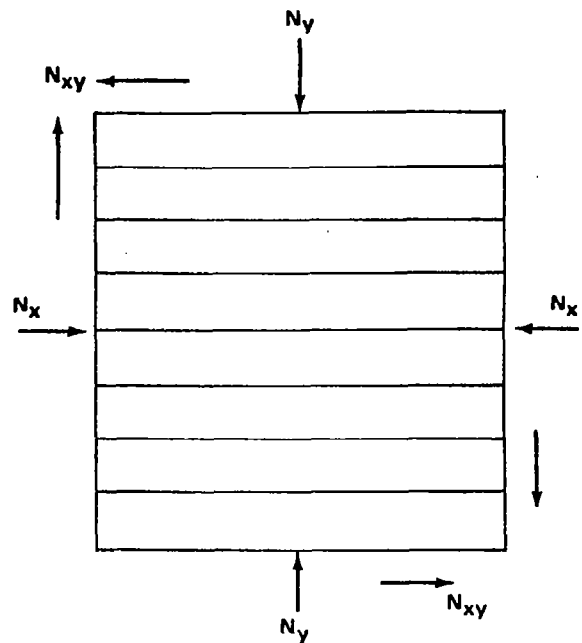


737 Composite Horizontal Stabilizer Finite Element Model Substructure Definition

Buckling Analysis



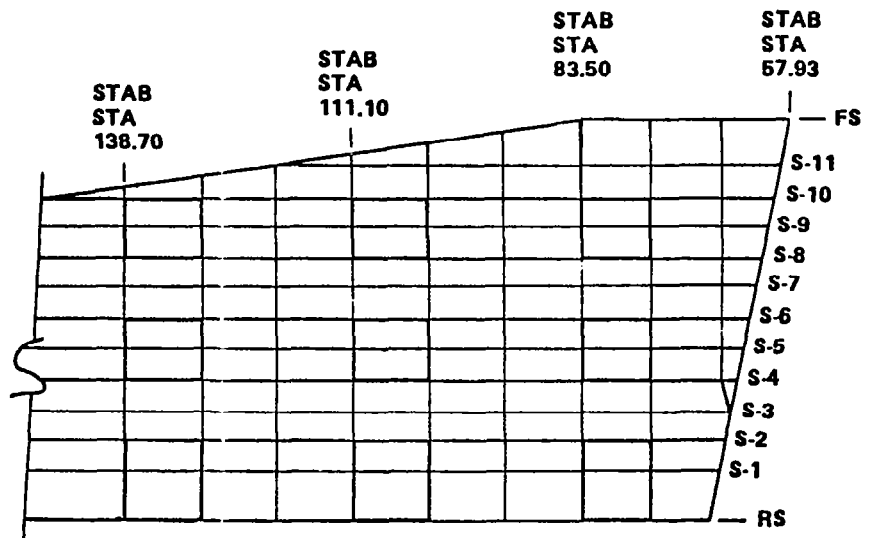
BUCKLING INTERACTION-VIPASA



PANEL 69.9 cm (27.5 in) x 8
STRINGER BAYS

Analysis Approach

- Skin panels buckle at 42% ultimate load
- At ultimate
 - Bending carried by stringers and spar chords
 - Shear carried by skin
- Stiffness matching constraints
- Strain cutoffs



INBOARD SKIN PANEL

The pin removal in the lug in the rear spar simulated a fatigue failure in the aluminum inboard of the graphite structure. The center section is an arrangement of a truss network which carries the torsional loads in the diagonals of the truss and the bending in the front and rear spars of the truss. A failure in this inboard section, particularly at the adjacent lug, would cause a significant load redistribution in the rear spar of the composite structure. This test, therefore, was felt to simulate adequately this type of possible failure mechanism.

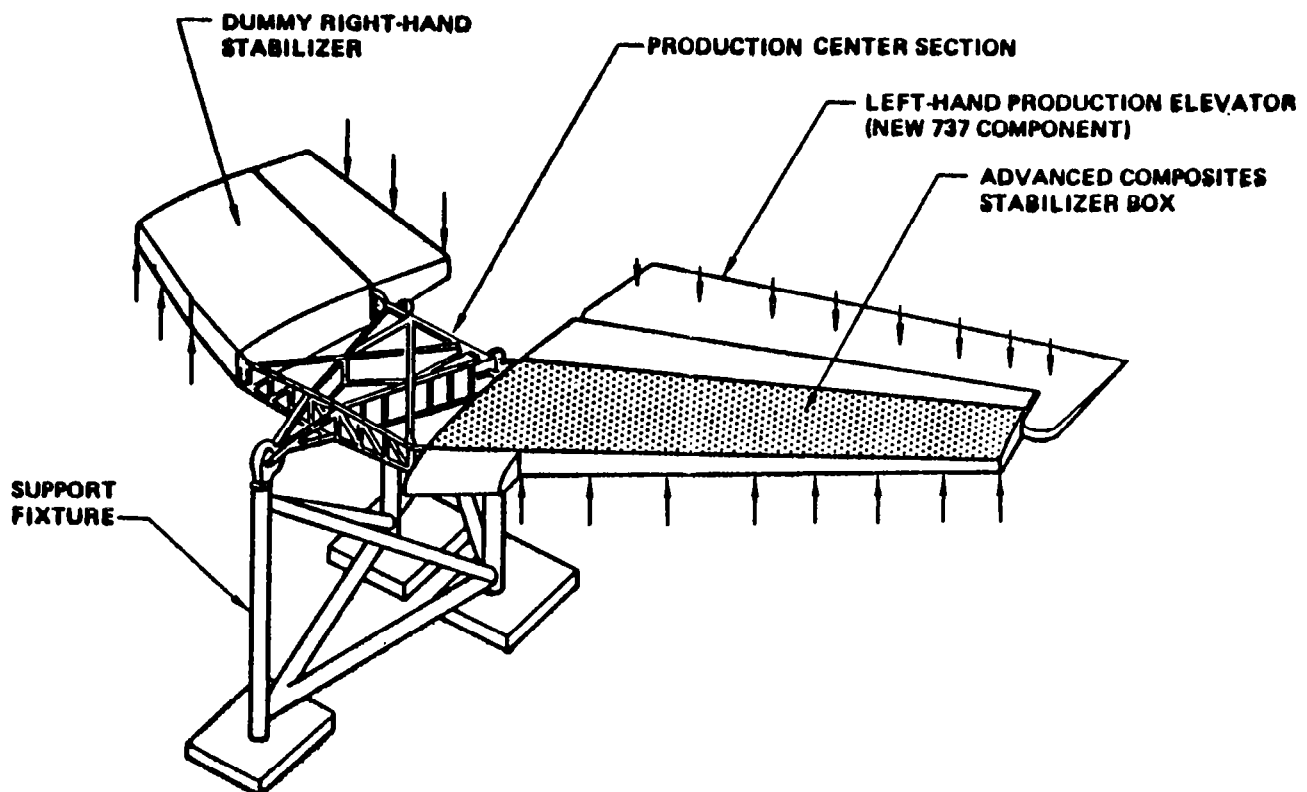
- Maximum positive bending
 - Rear spar lower pin removed
 - Front spar lower pin removed
- Maximum negative bending
 - Front spar upper pin removed
 - Rear spar upper pin removed

Damage Tolerance Test

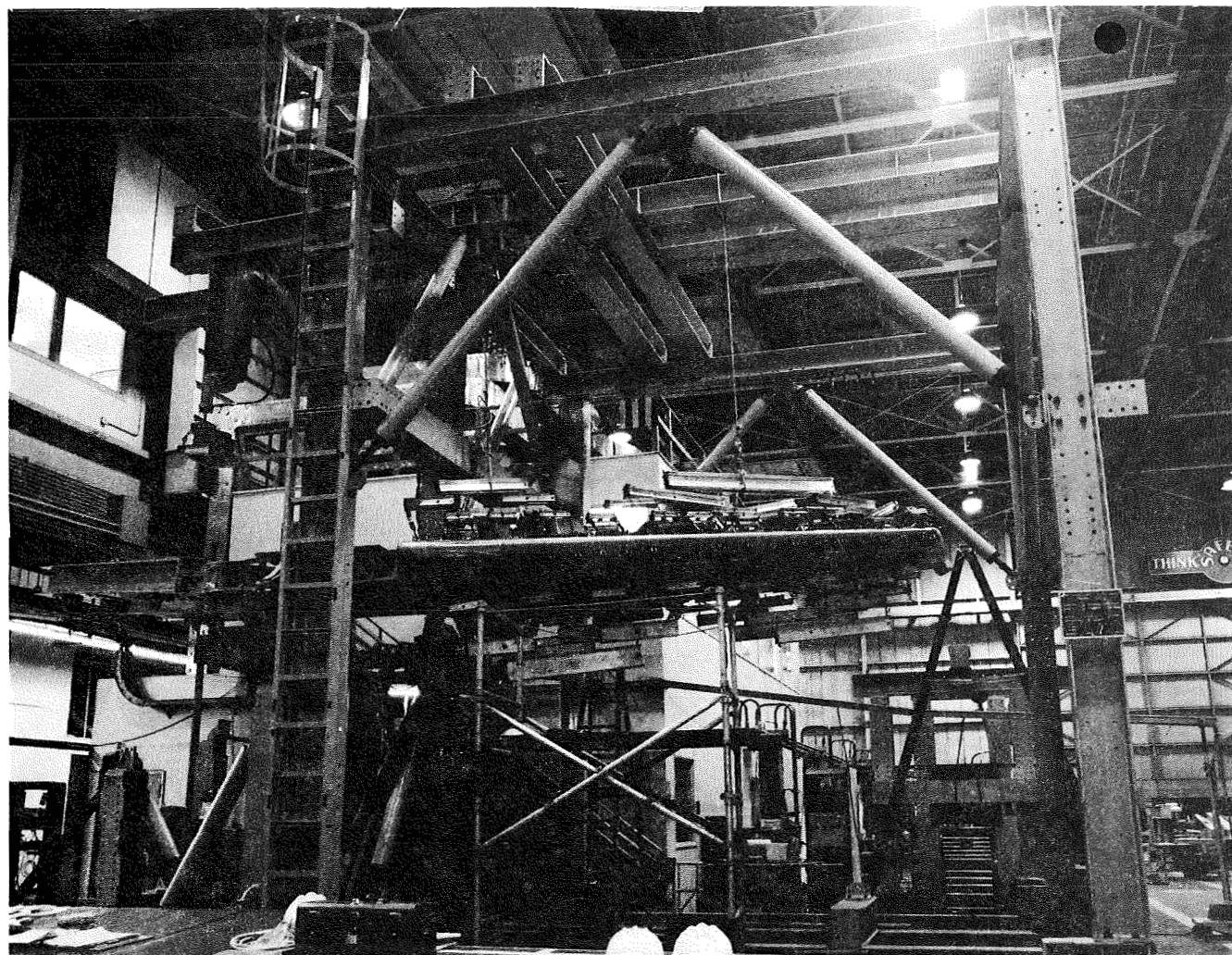
The test set-up for the full-scale ground test is shown. Strain surveys to limit load were performed for four load cases. Thermal linkage functional tests at high and low temperatures were performed to verify the thermal compensating linkage. The lateral stiffness of the elevator attachments was determined.

The test box was spectrum loaded for one-half lifetime to verify no intrinsic damage growth. Small cuts, impact damage, and damaged fastener holes were introduced into the test box. The box was spectrum loaded for one full lifetime to demonstrate that visible damage will not propagate during one lifetime of spectrum loading. Four ultimate load conditions were applied to the test box. Following these tests, a sequence of tests were performed in which the lug pins were removed to simulate center section lug failures. The lightning protection system was verified by subjecting an outboard tip section to a lightning test.

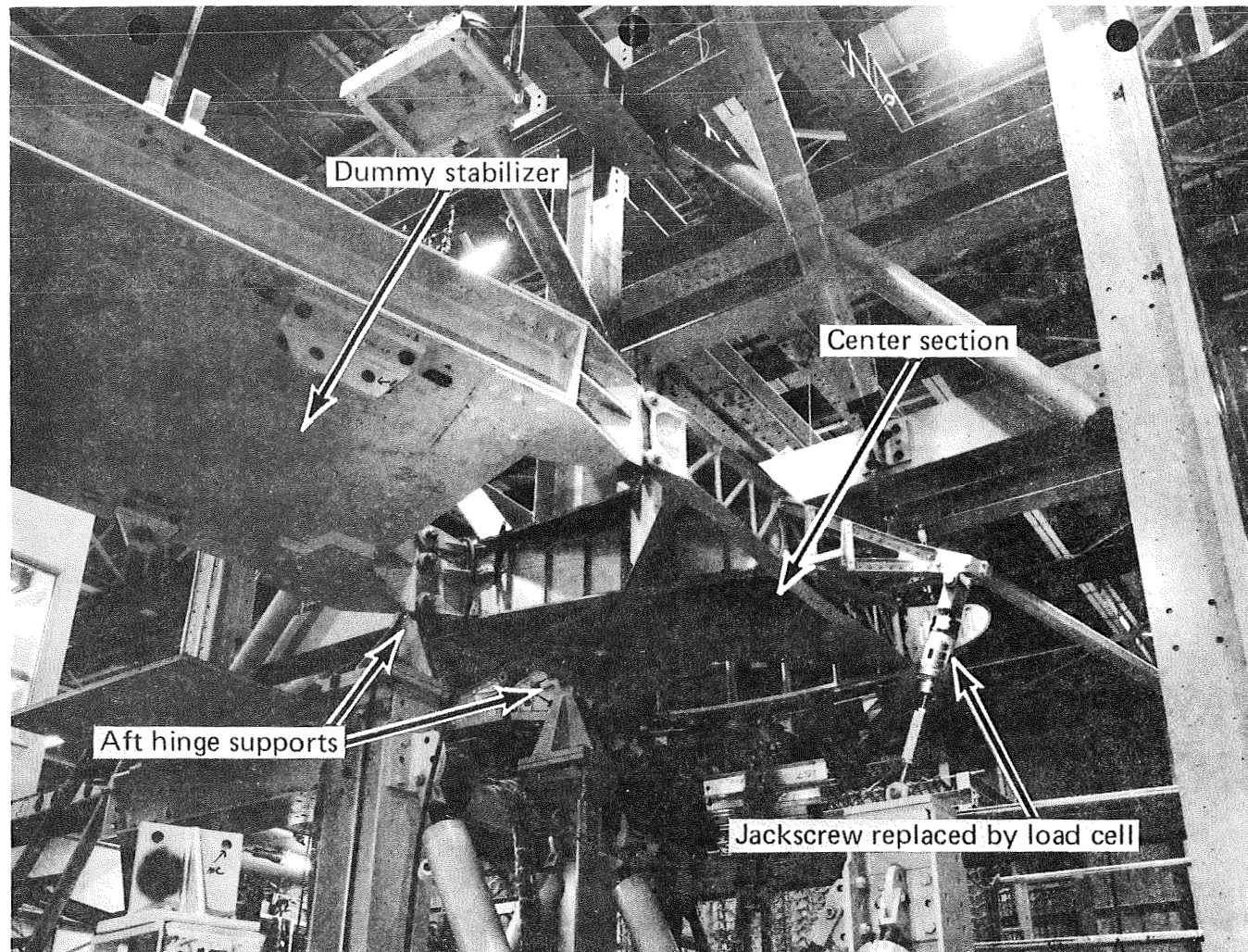
Full-Scale Ground Test



This photograph shows the full-scale test specimen mounted in the support jigs. Loads were applied by a system of pads to simulate spanwise and streamwise load distribution.



This photograph shows the stabilizer's center section interface. Attachment of the stabilizer is made with five bolts, three at the rear spar and two at the front spar.

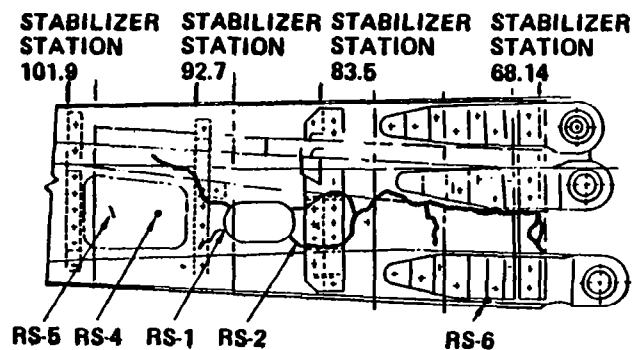


Test Configuration–Failure

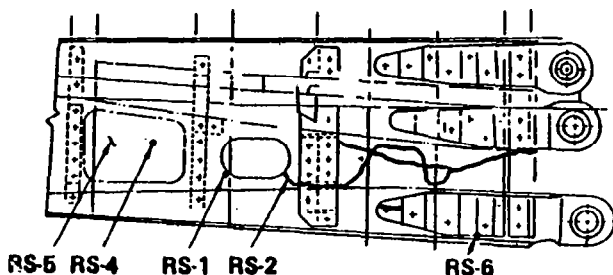
- Removed pin in upper lug rear spar
 - Simulated center section failure
- Applied load case 4010 (down bending)
 - 67% DUL required
- Failure occurred at 61% DUL

It can be seen from these illustrations of the failure of the rear spar that the crack extension modes varied from a tension failure at the most inboard end, which went completely through the surface and through the thickness of the web, to the beginning of a shear failure, some of which initiated interlaminarly. The propagation of the flaws from the most inboard to the most outboard cracks shown was verified by the strain gage data, which showed the inboard gages going nonlinear earlier than the outboard gages.

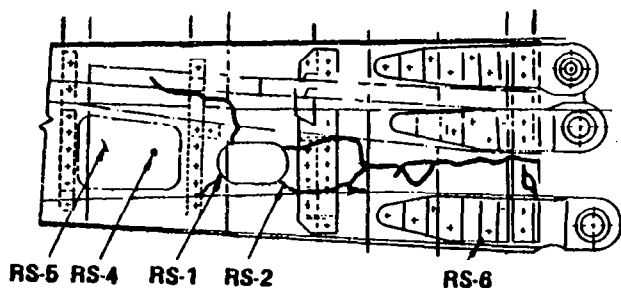
Failure Description



- WEB CRACKS,
FORWARD FACE

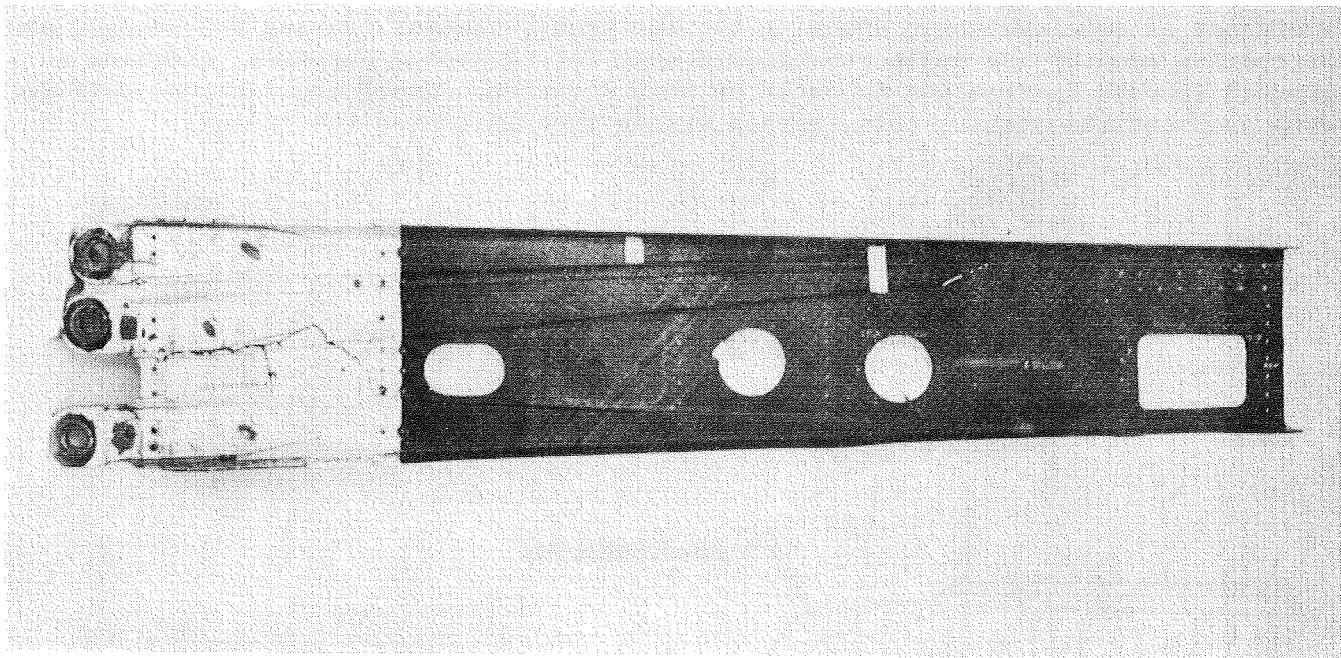


- THROUGH THICKNESS
CRACK

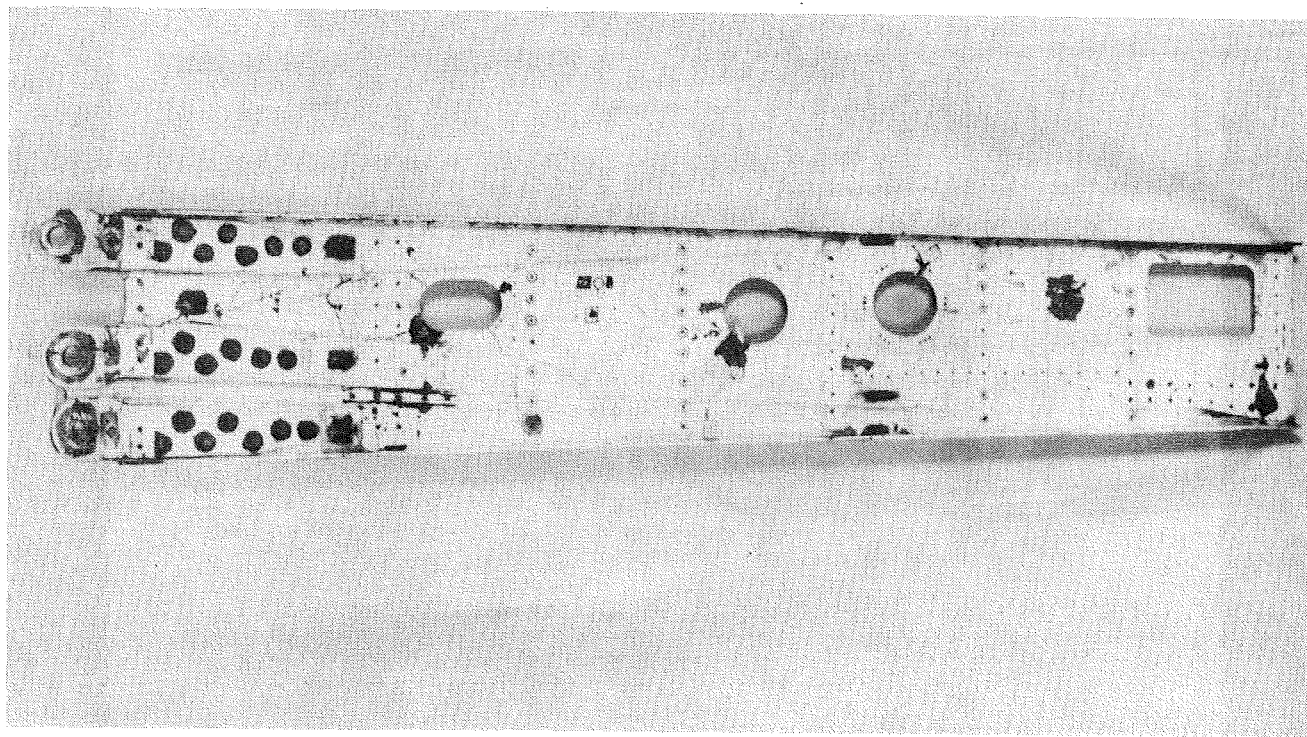


- WEB CRACKS,
AFT FACE

These photographs show the spar after it had been removed from the horizontal stabilizer for a closer examination.



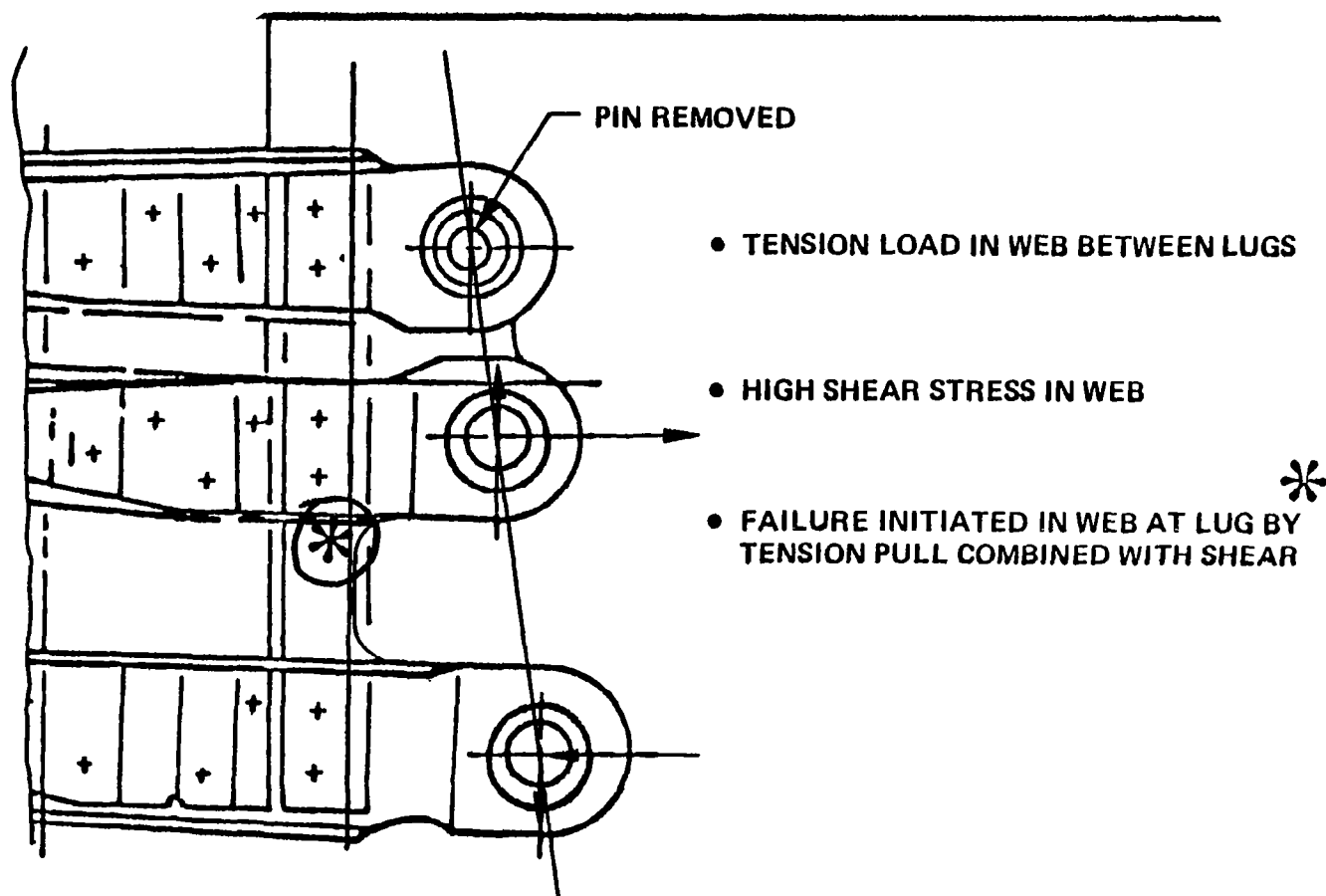
WEB CRACKS, FORWARD FACE



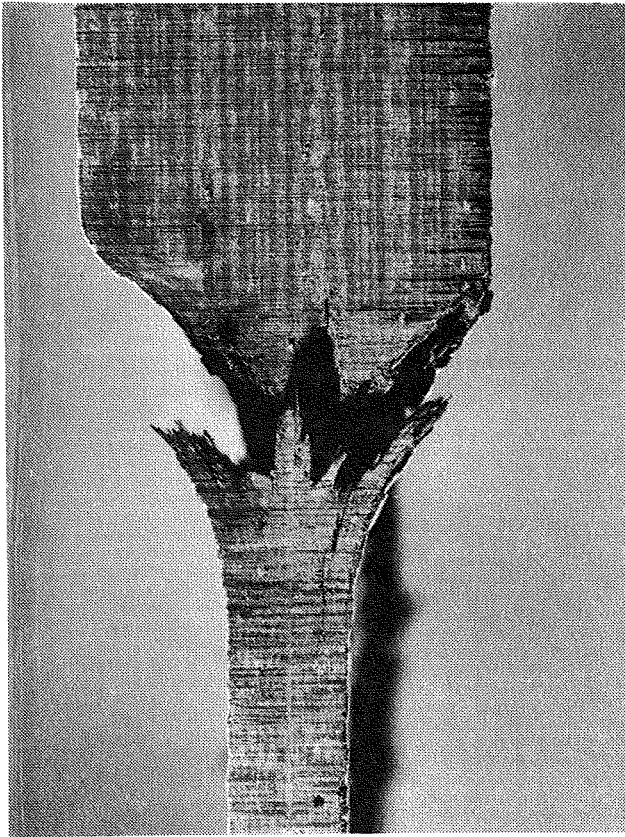
WEB CRACKS, AFT FACE

This figure indicates the loading which initiated the failure just below the fail-safe lug at the most inboard location. This failure propagated aft, creating a shear concentration in the web which then propagated in a shear mode, causing the damage seen in the previous photographs. This tension load between the fail-safe lug and the lower lug is caused by the dihedral change at the side of the body. There was an aluminum angle spanning the lug areas; however, during the design, some of the lug area of the angle was trimmed away for clearance purposes, allowing a greater imposed deformation to occur at this location. Since the web must perform with a compatible strain, this tension strain then initiated the failure.

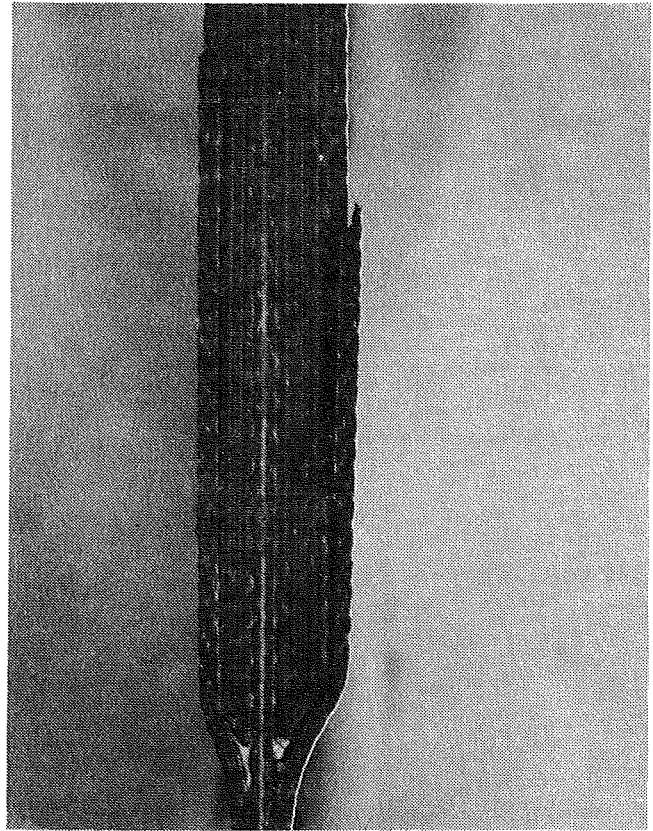
Damage Tolerance Failure Sequence



This photograph illustrates the detail of the tension failure. The lug areas are made of co-cured highly uniaxially oriented fiber slabs which are then wrapped in two channel halves with cloth to form the "I" section of the spar. The two halves and the cap strip are then bonded together in a single envelope bagging operation. The failure occurred where the wrapped plies of cloth turned the corner and therefore took the tension load in the resin direction, as previously described. Only XX plies were continuous straight up the center of the web. Therefore, this compatible deformation initiated the failure.



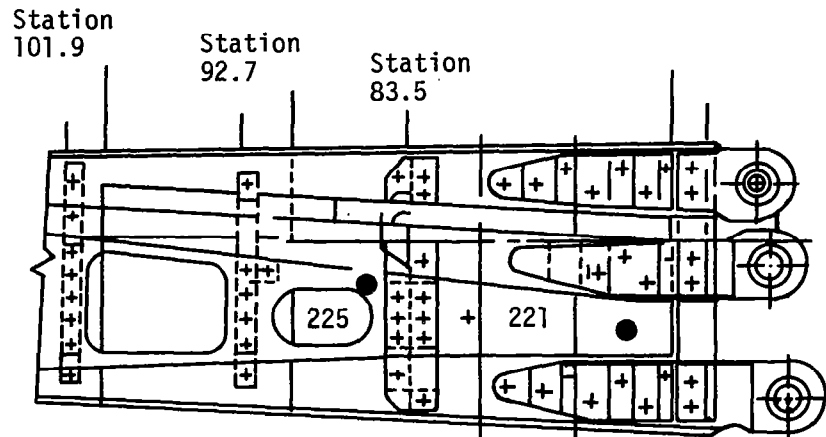
TENSILE FAILURE OF INBOARD WEB



DELAMINATION OF FACE PLYS

It can be seen, as was previously mentioned, that the most inboard gage was nonlinear at a load below which the outboard gage was still linear, indicating that the failure was beginning to propagate from the inboard to the outboard direction.

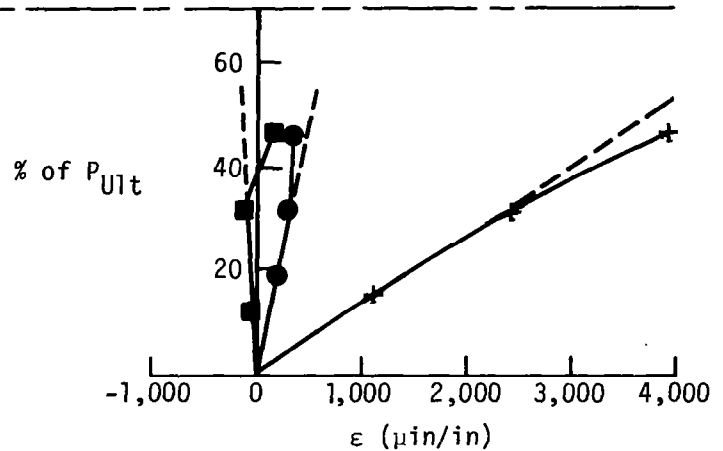
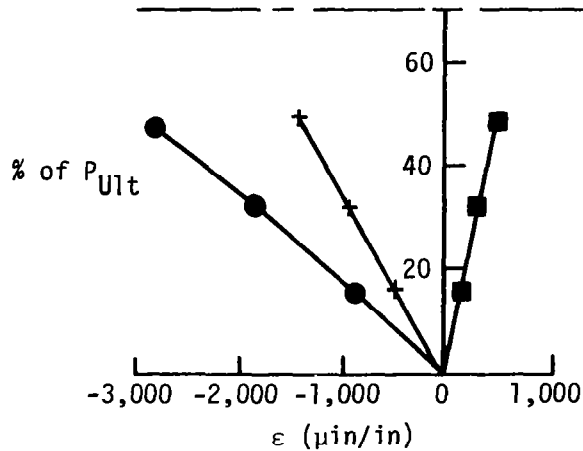
DAMAGE TOLERANCE- TEST FAILURE STRAIN GAGE READINGS



Gage	225		
Channel	A ●	B +	C ■
	622	623	624

Limit load

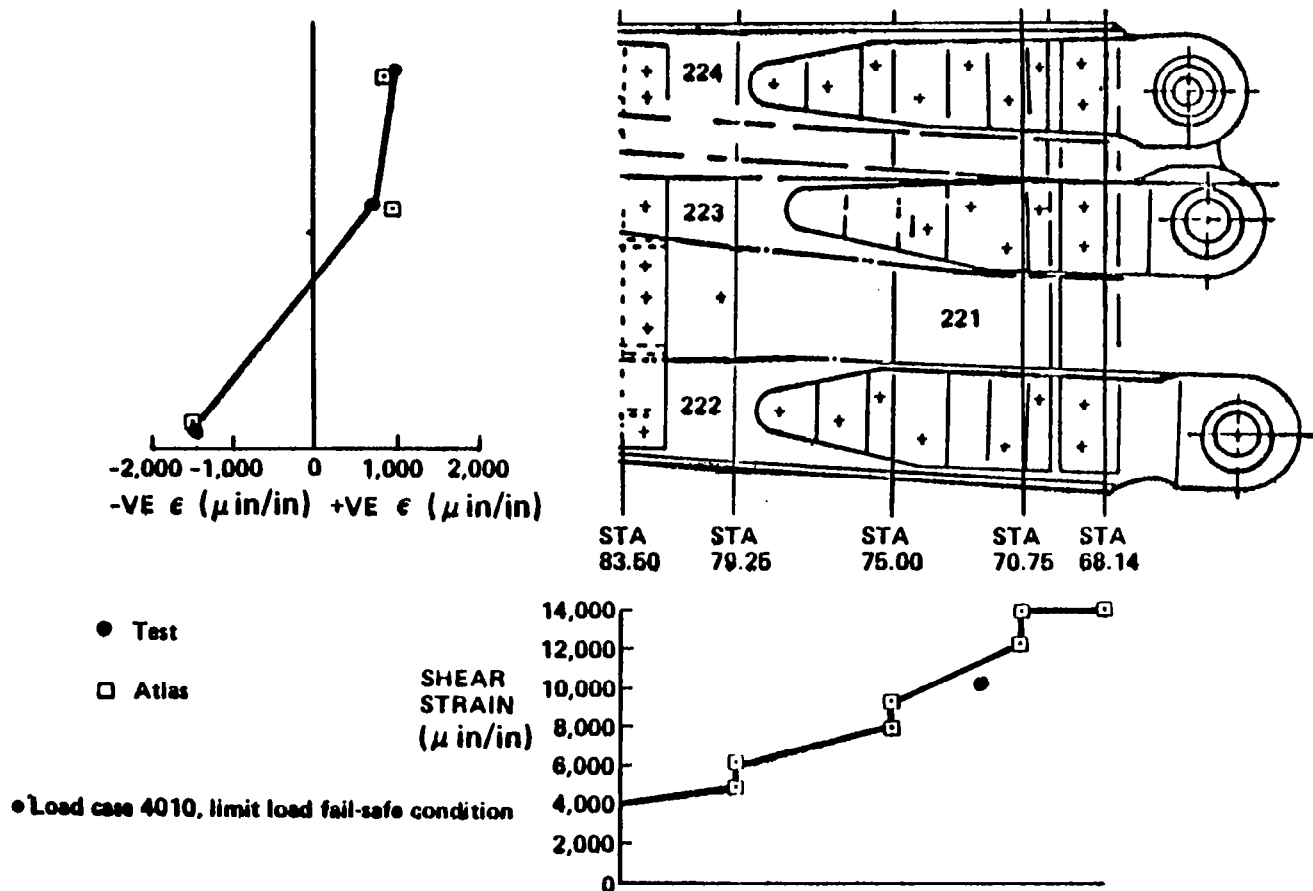
Gage	221		
Channel	A ●	B +	C ■
	619	620	621



The accuracy of the finite element analysis as compared to strain gage data is shown in this figure. The extremely high shear strains that occurred during this test are illustrated. The additional shear strain induced by the tension failure would raise the local shear strain in the web above the capability established from test data.

Damage Tolerance

Finite Element and Strain Gage Comparison



After establishing the failure mechanism, a plan for repair and avoidance of this failure mode was established. The conclusions shown here played a critical role in establishing the repair process.

Damage Tolerance

Conclusions

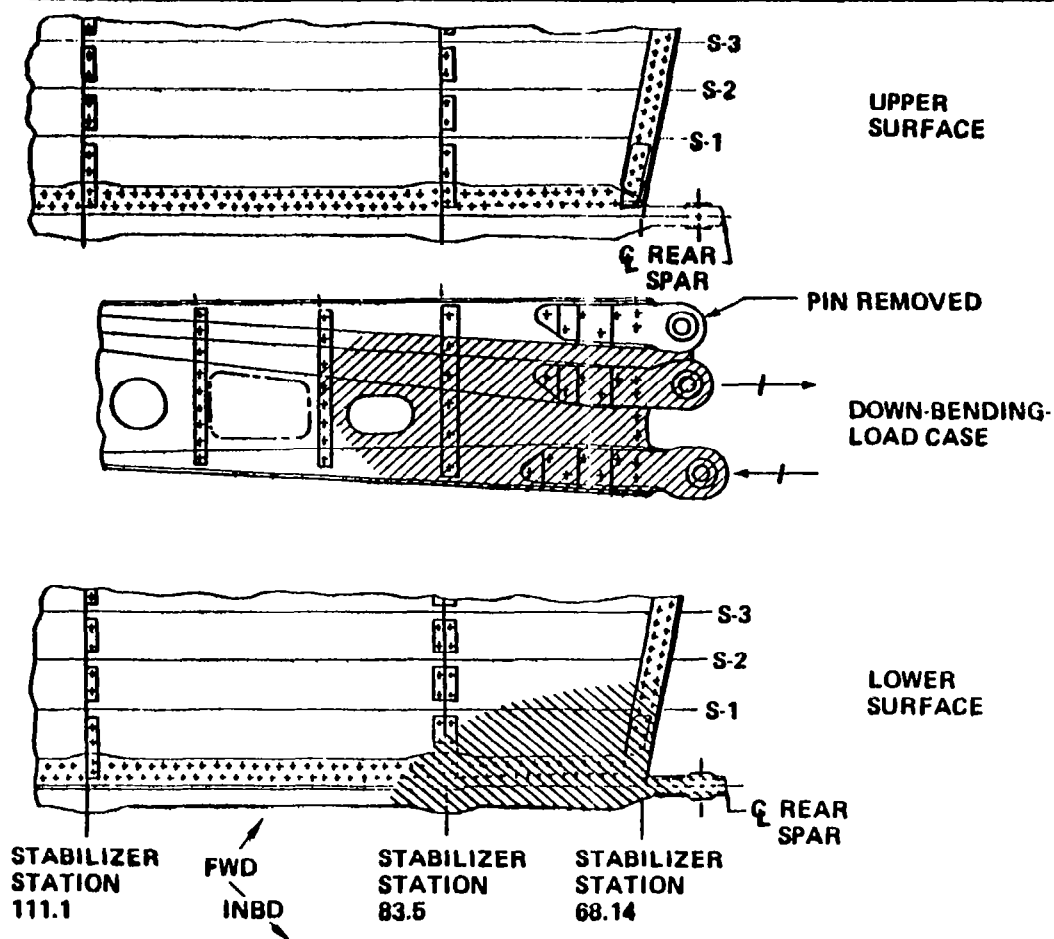
- **Load level**
 - **61% as tested**
 - **67% required**

- **Rear-spar web detail insufficient for fail-safe loading**

- **This area only critical area of stabilizer for this condition**

Only the areas of the horizontal stabilizer that are critical for this condition are shaded in this figure.

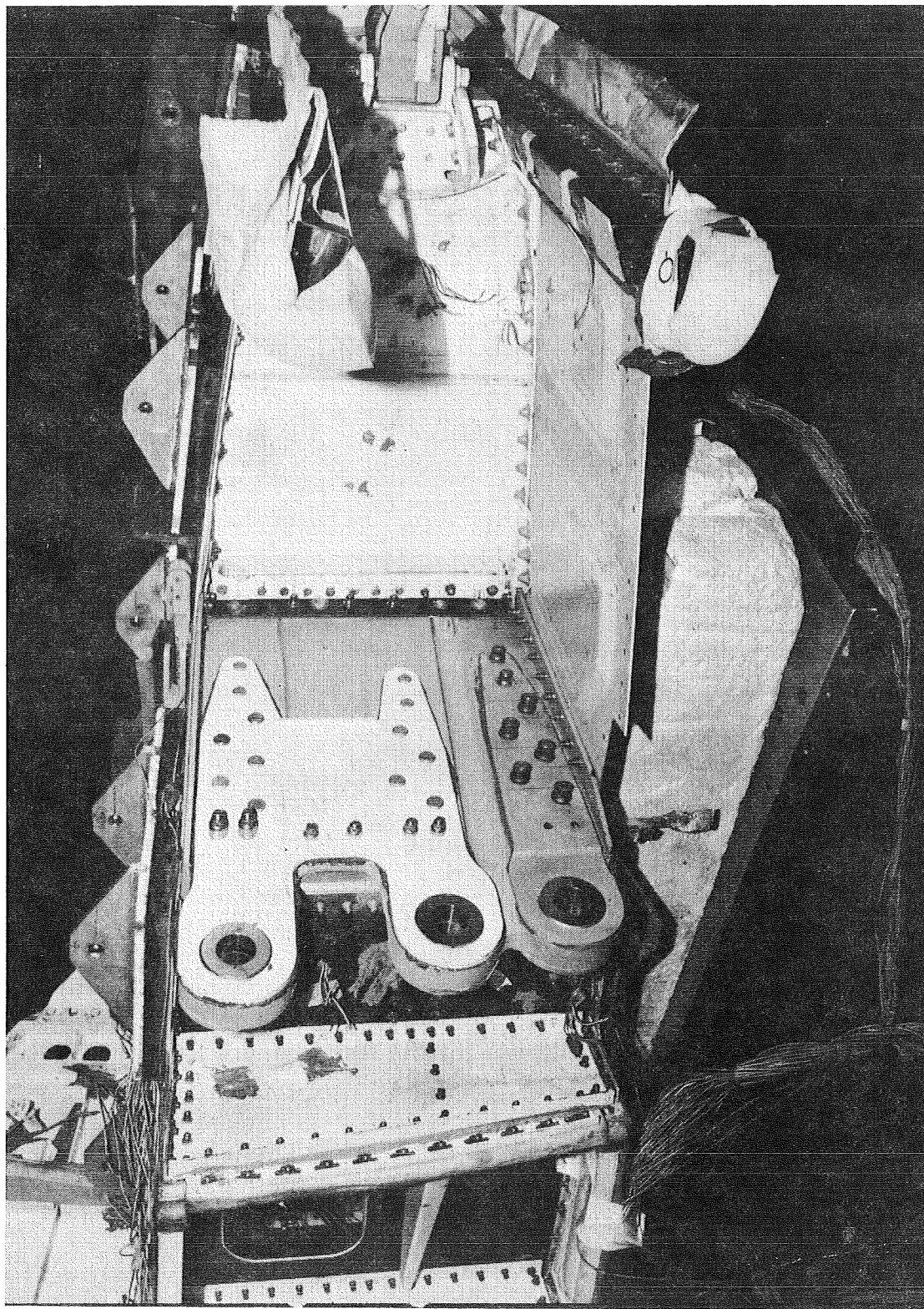
Only Area of Structure Critical for Upper-Pin-Removed Fail-Safe Case



Repair Plan

- Design a reinforcement for the rear-spar web area
- Verify adequacy of rear spar by analysis
- Apply modification to all five shipsets

This photograph shows the steel repair plate on the rear spar. The steel was used to assure minimum tension elongation and to minimize the thickness in the fit-up areas.



In considering what is needed in the future to support the analysis and design of composite wings and bodies for commercial transports, we must consider the possible criteria requirements as well as the design goals. To improve the weight savings and to sustain the kind of damage that can be expected in service, it is believed that an increased design strain capability is needed, both in design and in material application. We will have to fulfill category #2 and possibly category #3 of the damage tolerance requirements if the raising of the strain level causes flaw growth. Obviously, in moving to the wing, high end loads will be encountered. As an example, these high end loads will require careful design at the side of the body in order to remove the high concentrated loads from the stringers. This design analysis and test matrix will be particularly critical in the success of wing design. Similarly, diffusion into large fuselage structural shells of concentrated loads (e.g., the keel beams) will be extremely important, and careful analysis will be required. The determination of buckling criteria is essential to establishing a good weight savings capability for composites in fuselage shells. Good criteria and test data, as well as validating analysis, are particularly important. We must also consider the possibility that new uses will require a wider range of environmental conditions. Finally, raising the strain level in these critical structure components may again require us to consider fatigue damage. We need to have a matrix fatigue damage rule.

WING & BODY - FUTURE ANALYSIS CONSIDERATIONS

POSSIBLE CRITERIA, REQUIREMENTS OR DESIGN GOALS THAT WILL INFLUENCE ANALYSIS NEEDS

INCREASE IN DESIGN STRAINS

DAMAGE TOLERANCE REQUIREMENTS

CATEGORIES #2 & #3

HIGH LOAD TRANSFER JOINTS

SIDE OF BODY JOINTS
KEEL BEAM

BUCKLING CRITERIA (AT OR BELOW LIMIT?)

HIGHER TEMPERATURE (/MOISTURE) REQUIREMENTS
BODY (WITH INSULATION)

FATIGUE CONSIDERATIONS
MATRIX DAMAGE RULE

There are three or four areas that need to be considered in developing the analytical capabilities to be used in these major components of primary structure. They sound fairly simple, particularly the ones associated with strength, but since we will be asked to design closer to the capability of the material, the ability to predict both the ultimate strength and the residual strength requirements accurately in the design is much more important for both the static and damage tolerance conditions. Therefore, high competence in both aspects of the analysis and in validation by test is of extreme importance. Interlaminar effects, working the material in its weak direction, are of extreme concern to everyone. We must be able to predict interlaminar flaw growth, first of all from a grow-no-grow criteria and then under cyclic load. Those loads which induce these normal load stresses or strains are often secondary kick loads induced by eccentricities or secondary load paths. In metal structures these loads are often not a major concern, except possibly in fatigue. The secondary load calculations must improve in accuracy since they will most likely be the initiating phenomena for interlaminar flaw growth and failure.

WING & BODY - ANALYSIS DEVELOPMENT AREAS

DEVELOPMENT MUST CONSIDER REQUIREMENTS OF BOTH THE REQUIREMENT ANALYSIS AND CAPABILITIES ANALYSIS

1. STRENGTH PREDICTION

ULTIMATE STRENGTH

RESIDUAL STRENGTH

HIGH CONFIDENCE

2. INTERLAMINAR EFFECT

STATIC STRENGTH

GROWTH PREDICTION

3. SECONDARY LOADING

NORMAL TO LAMINATE

BUCKLING INDUCED

PRESSURE INDUCED

ECCENTRICITY OR KICK LOADS INDUCED

It is important to remember that we must bring these analytical tools along as early as possible, not necessarily in the most perfected form, but in a form that can be used as we begin to make these early configuration trade-offs, material selections, and manufacturing decisions. Once a company has begun to change from those pieces of equipment currently available for machining and assembling aluminum to those required for fabricating and assembling advanced composite structure, a major commitment will have been made. Therefore, it is important that we consider the development of methods that will support us in the near-term development of these components prior to production commitment. Development and validation of these methods must go hand in hand, and test techniques and procedures must be able to produce consistent and valid results. In addition, those test results must be validated, along with the analysis on structures simulating real aircraft loading.

WING & BODY - ANALYSIS DEVELOPMENT CONSIDERATIONS

TIMING

ROLE IN EARLY CONFIGURATION SELECTION

IMPACT ON MATERIAL DEVELOPMENT & SELECTION

PLANNING OF DEVELOPMENT PROGRAMS & TESTING

VALIDATION

SUPPORT METHOD WITH ADEQUATE TESTING

TESTING INCLUDES REAL STRUCTURE APPLICATIONS

Here some thoughts are presented on what structural analytical goals should be in terms of the type of tools needed.

STRUCTURAL ANALYTICAL TOOLS GOALS

- ESTABLISH A LEVEL OF CONFIDENCE IN THE ANALYTICAL PROCESS SUCH THAT IT IS THE PRIME TOOL FOR STRUCTURAL VALIDATION
 - QUALITY SUCH THAT ANY REQUIRED FULL-SCALE TESTING WOULD ONLY BE USED TO PROVIDE FOR AIRCRAFT GROWTH OR TO UNCOVER GROSS HUMAN ERROR IN APPLICATION OF THE ANALYSIS OR MANUFACTURING METHODS
 - CAPABILITY OF BEING IMPLEMENTED IN A SIMPLE AND ECONOMIC MANNER BY A LARGE GROUP OF ENGINEERS
 - USABLE WITHIN THE CONSTRAINTS IMPOSED BY AVAILABLE DATA AND FLEXIBLE ENOUGH TO IMPROVE WITH THE EXPANSION OF AVAILABLE DATA
 - CAPABLE OF IMPACTING THE DESIGN AS WELL AS BEING USED TO ANALYZE THE DESIGN
 - VALIDATABLE BY TEST EVIDENCE

Here are some thoughts on the analysis development aspects, whether related to advanced composites or to other types of structures. For successful development, I believe that those people involved in research need a group working environment, and that working environment includes enthusiastic management backing, adequate but not excessive budgets, facilities available for developing the analytical tools in terms of computer access, test facilities, and, of course, supporting organizations. But one of the key elements for success is easy interface with production analysts and design people to ensure that the methods are going to be truly usable by the production engineers.

Making a good initial choice of which development areas to start is extremely difficult. In making prioritized lists we must make sure that we are looking for real needs and that we plan our program to meet those needs when they are required at the right depth. Let's not produce a program of perfection that is too late to support some of the earlier decisions in the development of advanced composite structure. We must be aware that our development should show true progress, not rehash over and over again the methods already available. On the other hand, let's not be afraid to adapt current methodology and carry that information from past experience.

Whether the method is used in a timely manner will depend on how familiar it is in form to something the current production stress analyst is familiar with. This takes an honest and realistic evaluation of what is available so as not to produce a replacement for something that is adequate today. Are all the items that are needed to peripherally support the analytical method well defined? Finally, take the time to establish a well-developed method specification and review this specification with the potential users, so the end product will be adequately suited to the job.

ANALYSIS DEVELOPMENT

ITEMS NEEDED FOR SUCCESSFUL DEVELOPMENT

- GOOD WORKING ENVIRONMENT
 - ENTHUSIASTIC BACKING
 - ADEQUATE BUDGET
 - FACILITIES
 - SUPPORTIVE ORGANIZATION
 - EASY INTERFACE WITH METHODS USER
- GOOD INITIAL CHOICE OF DEVELOPMENT AREA
 - REAL NEED CLEARLY IDENTIFIED
 - PLAN TO MEET NEED (APPROPRIATELY)
 - WHEN NEEDED
 - RIGHT DEPTH
 - UTILIZES CARRY-OVER FROM PAST EXPERIENCE
 - TRUE DEVELOPMENT PROGRESS
 - OR
 - MODIFICATION TO CURRENT METHODS
 - ALTERNATE METHODS EVALUATED - (HONESTLY)
 - REPLACEMENT
 - INFORMATION AVAILABLE TO SUPPORT SOLUTION
 - ESTABLISHED AND WELL DEVELOPED METHOD SPECIFICATION
- END PRODUCT QUALITY SUITED TO JOB

In order to produce methods of high quality, keep the process simple. In concept and in method, this produces a tremendous payoff in terms of development time, cost, and ease of utilization, and certainly helps assure the early success of both development and application. Many who are in research for a long period of time tend to become perfectionists in method development. Let's be careful of this trap while making sure that each item we add to the method is a true improvement and expands the information produced by the analysis procedure.

The key to a manager's good over-all development and management of method development is the balance of the budget he makes available relative to the quality level of the method developed. To expand on the idea of a method's usability and simplicity, it also should show adaptability to being part of other methods, in order to be available for future expansion.

ANALYSIS DEVELOPMENT

CONSIDERATION DEVELOPING QUALITY METHOD

- SIMPLE IN CONCEPT & METHOD

 - MINIMAL DEVELOPMENT TIME & COST

 - USAGE & APPLICATION EASIER

 - INHERENT SIMPLICITY - HELPS ASSURE EASY SUCCESS

- REFINEMENT OF METHOD

 - PERFECTIONISM

 - TRUE IMPROVEMENT

 - EXPANDS INFORMATION

 - BUDGET VS. QUALITY LEVEL

- ADAPTABILITY

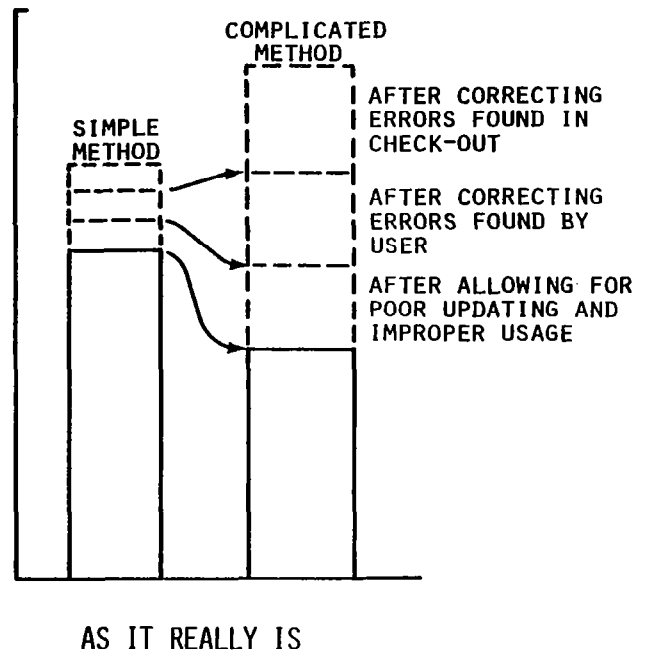
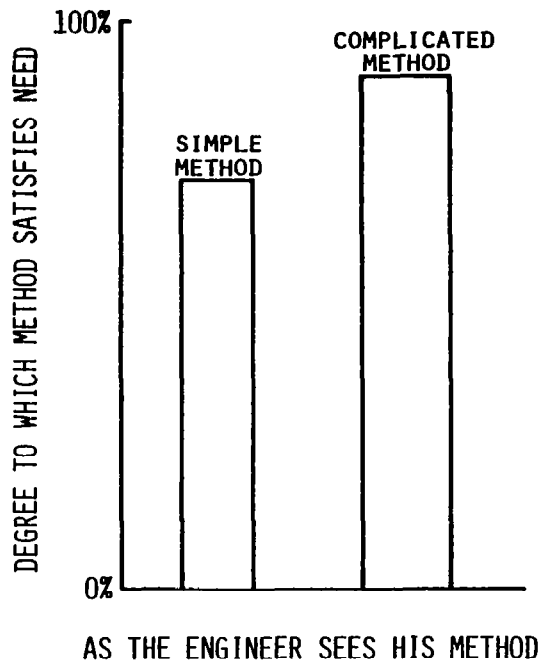
 - USABLE AS PART OF OTHER METHOD

 - BALANCED FOR CURRENT USAGE

 - &

 - FUTURE EXPANDED APPLICATION

COMPROMISE BETWEEN SIMPLICITY AND THEORETICAL PERFECTION



Accuracy in method development is very important, and this accuracy should be validated by tests. To produce analytical tools for which there is no test validation in the real world is useless, and one or two data points are not sufficient if you expect production stress analysis personnel to accept your methodology. Testing should be repeated again and again and should be validated with test data. In establishing a method, be sure that there are no additional unnecessary additions to the solution which really do not improve the accuracy or produce more information, as previously noted. Don't join in analysis fads; make a good, unbiased judgement of the need for the method. Consider design handbook methods for end products to be as important as a computer method. The majority of detail stress analysis is still performed by hand today. Finally, keep in mind that the production analyst is your final user. If analysis methods of similar nature can be joined to form a single standard procedure, do it. Provide the flexibility for all uses and users. Can it be used in a disciplined manner by large organizations? This is critical.

ANALYSIS DEVELOPMENT

- ACCURACY
 - IMPROVED SOLUTION (OVER CURRENT)
 - NO UNNECESSARY ADDITION
- FADS
 - METHOD OF IMPLEMENTATION
 - COMPUTER VS. DESIGN MANUAL (FORMATS)
 - NEW LOOK TO OLD SOLUTION
 - PREJUDGEMENT OR PREJUDICED APPROACH
 - POOR PROGRESSIVE JUDGEMENT
 - EMOTION & SNAP JUDGEMENT
 - (PRESSURE - TIMING)
- PRODUCTION ANALYSIS & STANDARDIZATION
 - FLEXIBILITY FOR ALL USES & USERS
 - AVAILABLE TO ALL PROJECTS
 - DISCIPLINED USE BY LARGE ORGANIZATION

Proper and timely application requires a follow-up; this means provide support when it is needed, keep the user up to date on any modifications, listen to his inputs, don't be defensive. Think about expanding the method's usage and adaptability to new applications, and continue to evaluate it against new methods and recognize when it must be replaced. Then, when it must be replaced, proceed with a new development as needed.

ANALYSIS DEVELOPMENT

PROVIDE ADEQUATE FOLLOW-UP

CONTINUE INTERFACE WITH USER

PROVIDE SUPPORT WHEN NEEDED

KEEP USER UP TO DATE ON ANY MODIFICATION
USER MANUAL (REVISIONS)

LISTEN TO USER INPUTS (ACCEPT INPUTS)

EXPANDED USAGE (SCOPE & TIME)

CONTINUOUS REVIEW FOR ADAPTABILITY
OR

NEW APPLICATION

CONTINUE EVALUATION AGAINST NEW METHOD
(RECOGNIZE REPLACEMENT)

PROCEED WITH NEW DEVELOPMENT WHEN NEW REAL NEED IDENTIFIED

Finally, here are some rules for success in the analysis development:

- (1) Coordinate carefully between the researcher and user; be sure that there are no other alternate methods before you start the development, and have alternate methods available and assessed should your development not produce results.
- (2) Allow time for corrections and updates, particularly after you expose the method to the user; be sure, as you plan your development, that you plan the means of validation, since you want to have high confidence in its results.
- (3) It is a good idea not only to have those specifications developed and reviewed by the user, but to have him on board in frequent discussions during the development.

This will give the program timely evaluation, build confidence in its usage, and also ensure that it is used correctly so that you are not blamed for its error or inaccuracy. Remember, many methods operate in a production environment for a long period of time. They must be effective over this total period of time.

ANALYSIS DEVELOPMENT

DEVELOPMENT RULES FOR SUCCESS

- COORDINATION BETWEEN
DEVELOPER & USER
- BACKUP OR ALTERNATE METHOD
AVAILABILITY ASSESSED
- TIME ALLOWED FOR CORRECTION & UPDATE
AFTER USER EXPOSURE
- ESTABLISH OR ESTABLISHED MEANS OF VALIDATION
INSURANCE OF HIGH CONFIDENCE IN METHOD
- DEVELOPER/USER BOTH RETAIN PESSIMISM
- USER ON BOARD FROM START OF DEVELOPMENT
TIMELY EVALUATION
BUILDS CONFIDENCE IN USAGE
ASSURE CORRECT USAGE

METHOD OPERATES EFFECTIVELY IN PRODUCTION ENVIRONMENT
FOR A LONG PERIOD OF TIME

SUMMARY

- **ANALYSIS PLAYS A MAJOR ROLE
IN CERTIFICATION & DEVELOPMENT**
- **ANALYSIS APPLICATION NEED TO BE
APPROPRIATE TO JOB**
- **ANALYSIS METHODS NEED TO BE
TEST VALIDATED**
- **ANALYSIS FUTURE NEEDS ARE:
PREDICTION ACCURACY
INTERLAMINAR STRESSES
SECONDARY LOADS**
- **ANALYSIS DEVELOPMENT MUST RECOGNIZE:
REAL NEEDS
ADVANTAGES OF SIMPLICITY**

REFERENCES

1. Airworthiness Standards: Transport Category, Airplanes. FAR Pt. 25, FAA, June 1974.
2. Composite Aircraft Structures. Report No. AC 20-107, FAA, July 1978.

**A PRELIMINARY DAMAGE TOLERANCE METHODOLOGY
FOR COMPOSITE STRUCTURES**

**D. J. Wilkins
General Dynamics
Fort Worth, Texas**

PREVIEW

The work described in this presentation was supported by the F-16 Airplane System Program Office, Aeronautical Systems Division, United States Air Force, as part of the F-16 Production Fleet Management Program. As indicated in Figure 1, the presentation will briefly explore General Dynamics' certification experience for the primary, safety-of-flight composite structure applications on the F-16, will describe the rationale for the selection of delamination as the major issue for damage tolerance, and will outline the modeling approach selected. The development of the necessary coupon-level data base will be referred to and briefly summarized. The major emphasis will be the description of a full-scale test where delamination growth was obtained with which to demonstrate the validity of the selected approach. A summary will be used to review the generic features of the methodology.

- CERTIFICATION EXPERIENCE
- DELAMINATION RATIONALE
- MODELING APPROACH
- DATA BASE DEVELOPMENT
- FULL-SCALE VERIFICATION
- SUMMARY

Figure 1

DEFINE THE WORDS

The Air Force, in MIL-STD-1530A, Airplane Structural Integrity Program, sets forth specific definitions of the words "durability" and "damage tolerance." For the purpose of this presentation, the definitions are given in Figure 2.

<i>DURABILITY</i>	THE ABILITY OF THE AIRFRAME TO RESIST CRACKING, CORROSION, THERMAL DEGRADATION, DELAMINATION, WEAR, AND THE EFFECTS OF FOREIGN OBJECT DAMAGE FOR A SPECIFIED PERIOD OF TIME
<i>DAMAGE TOLERANCE</i>	THE ABILITY OF THE AIRFRAME TO RESIST FAILURE DUE TO THE PRESENCE OF FLAWS, CRACKS, OR OTHER DAMAGE FOR A SPECIFIED PERIOD OF TIME

Figure 2

CERTIFY COMPOSITES BY TEST

In contrast to the combined analysis/test procedures used to certify metallic parts on the F-16, the composite primary structure parts had to be certified completely by test (Figure 3). Full-scale room temperature, dry static and fatigue tests of the vertical tail and the horizontal tail were supplemented with beam tests representing critical load paths. Beams were tested statically at environmental conditions ranging from cold, dry to hot, wet. Coupled load/environment fatigue tests were also performed. All of these tests were necessarily defined only in terms of the contractually specified "design usage."

For reference, the vertical tail employs thick graphite-epoxy skins bolted to aluminum spars and ribs, and the horizontal tail uses graphite-epoxy skins bonded to full-depth aluminum honeycomb core and bolted to a titanium hub/spar sub-structure.

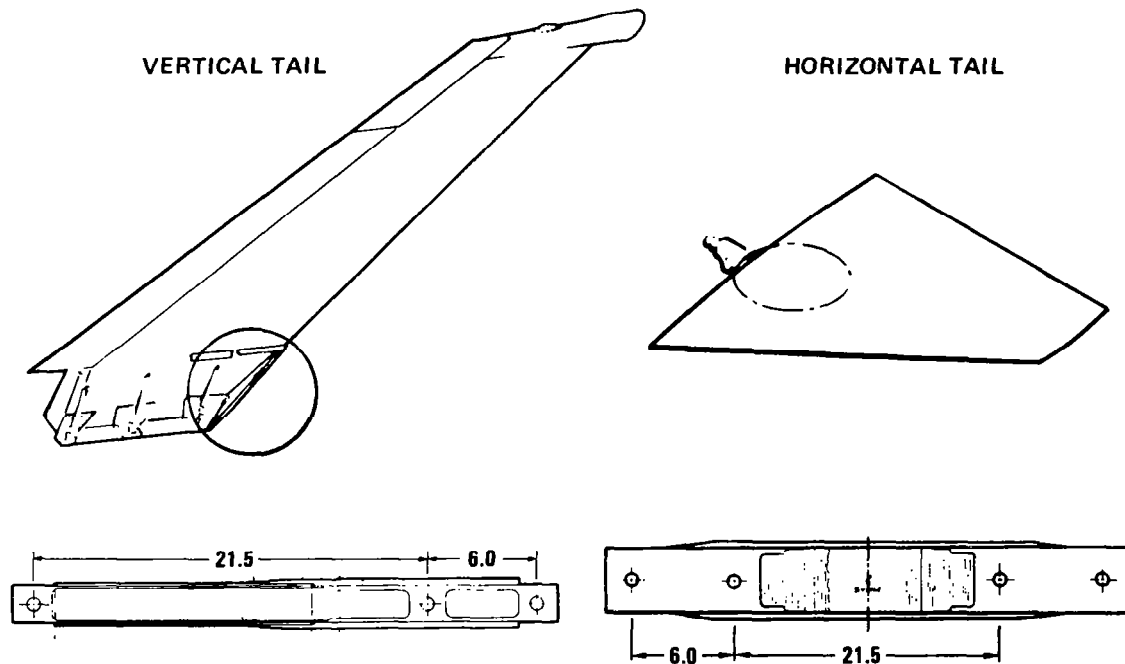


Figure 3

COMPOSITES ANALYSIS IS NECESSARY FOR TRACKING USAGE CHANGES

As we moved into Fleet Management activities, it became apparent that the design-usage-related test program was less than adequate for meeting the needs of the Air Force Logistics Command in terms of making maintenance decisions. And tests of each individual airplane/damage situation were out of the question. It was quickly concluded that composites analysis was necessary for tracking fleet and individual aircraft usage changes and to make repair decisions (Figure 4). Because few "zero-defect" parts are really built, the analysis must be able to relate defect size to time in service. The analysis should address the typical flaws occurring in manufacturing (durability flaws), those resulting from unusually bad manufacturing errors (damage tolerance flaws), and large damages occurring as a result of service usage. The issue is how these various flaws behave as a function of severe, normal, or mild usage of the airplane. The indicated relationship of flaw size to a buckling limit is illustrated in the following figure.

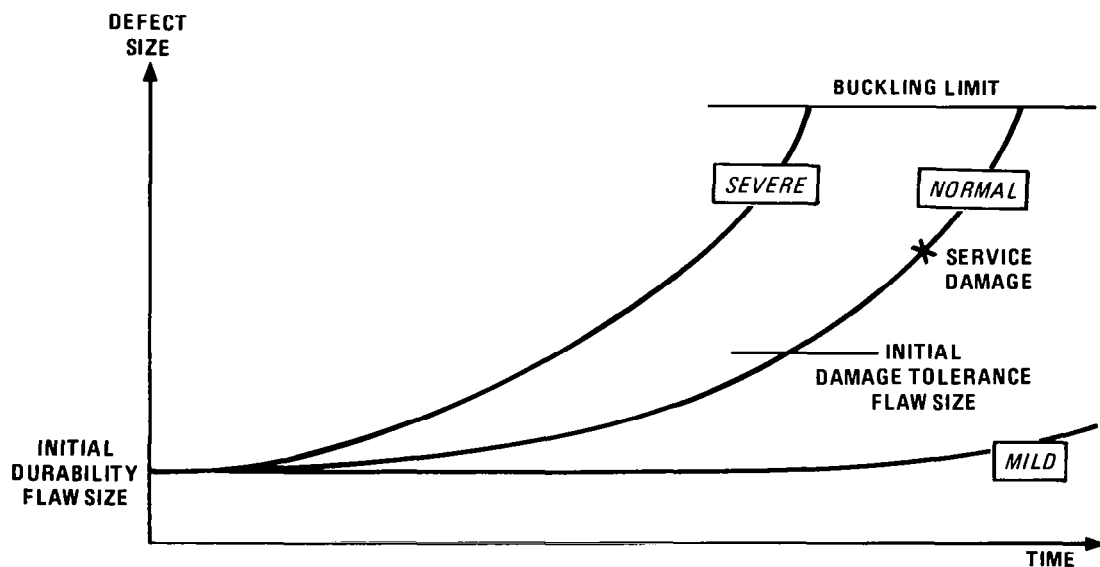


Figure 4

DELAMINATION IS MOST PREVALENT GROWTH MODE

In research work previously performed for the Air Force (Reference 1), we discovered that if any life-limiting, growth-related failure mode was likely to happen in a composite structure, it is probably delamination. Figure 5 shows about 15 inches of the overall 88-inch length of a box beam tested with a severe combination of bending and torsion. A delamination propagated in the compression surface skin until the surface finally buckled and caused the beam to fail. Some insight into the nature of delamination in graphite-epoxy can be obtained by exploring the toughness of some typical laminates in each of the three directions, as is outlined on the next chart.

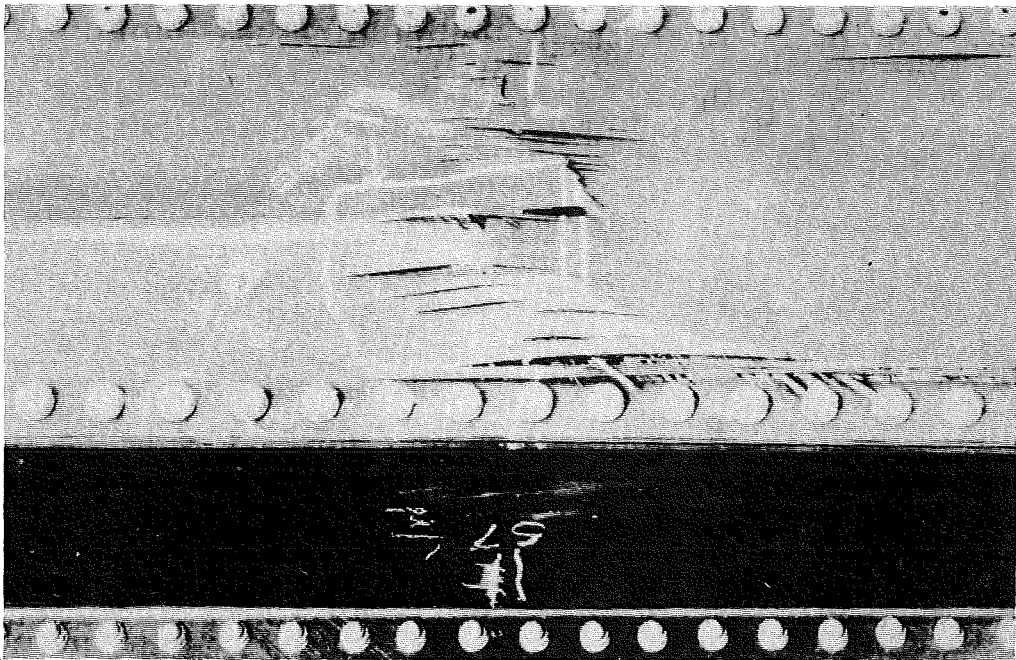


Figure 5

GRAPHITE-EPOXY FRACTURE TOUGHNESS

Figure 6, adapted from the results of Reference 2, plots fracture toughness (K_{IC} as measured by edge-notched beams or center-notched tensile coupons) as a function of the percentage of 0° plies in a balanced, symmetric laminate containing only 0° and $\pm 45^\circ$ plies of unidirectional tape. The trends are typical of the Thornel 300/Narmco 5208 class of graphite-epoxy, but the absolute numbers are not strictly valid because no ASTM standards have been developed for fracture toughness of composites. Nevertheless, we would agree that a $\pm 45^\circ$ laminate has a reasonable toughness slightly less than aluminum. As 45° plies are replaced by 0° plies, the toughness would be expected to increase until it was about doubled. On the other hand, as 45° plies are replaced by 90° plies, the toughness is expected to decrease until it reaches a minimum represented by a crack running completely in the resin between the fibers. The real point is that in the interlaminar mode, the toughness is always at the minimum.

These low values of interlaminar toughness are only significant as they relate to the out-of-plane loads discussed in the next chart.

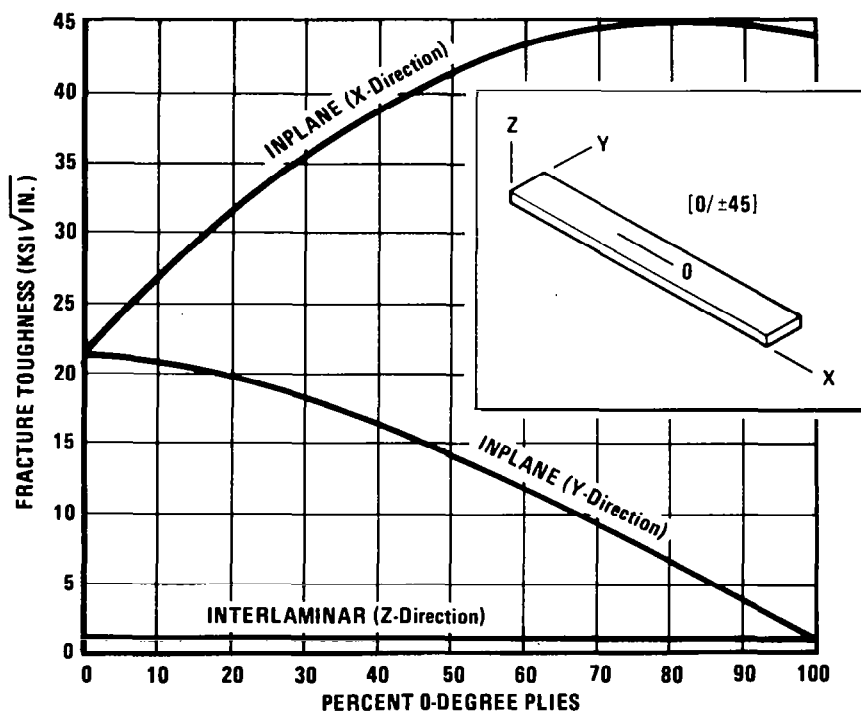


Figure 6

SOURCES OF OUT-OF-PLANE LOADS

Shown schematically in Figure 7 are five of the most common design details from which real hardware is constructed. Each of these details, even under in-plane loading, gives rise to interlaminar normal and shear forces. The interlaminar forces act directly on the plane of minimum toughness. As a result, delaminations may form, and if the in-plane forces are compressive, buckling becomes a pertinent issue.

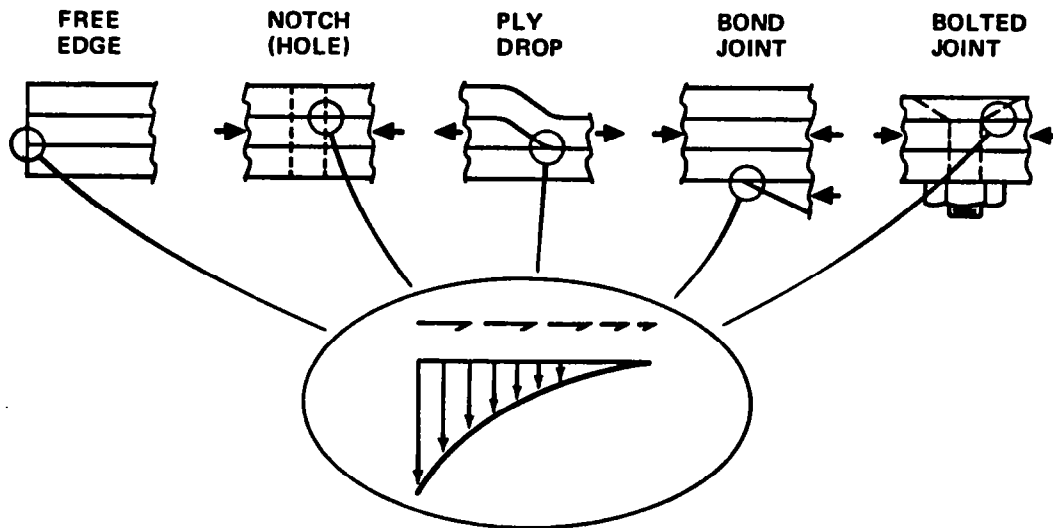


Figure 7

TRANSFORM THE PROBLEM

Creation of a compression coupon data base is impractical because interlaminar tension and shear interact with local and overall buckling so that specimen size, end conditions, and lateral support make scaleup difficult. A simpler, more direct approach (Figure 8) is to use an analysis to define the transfer function between applied loads and local rupture forces. Then the experimental effort can focus on tension and shear failure mechanisms.

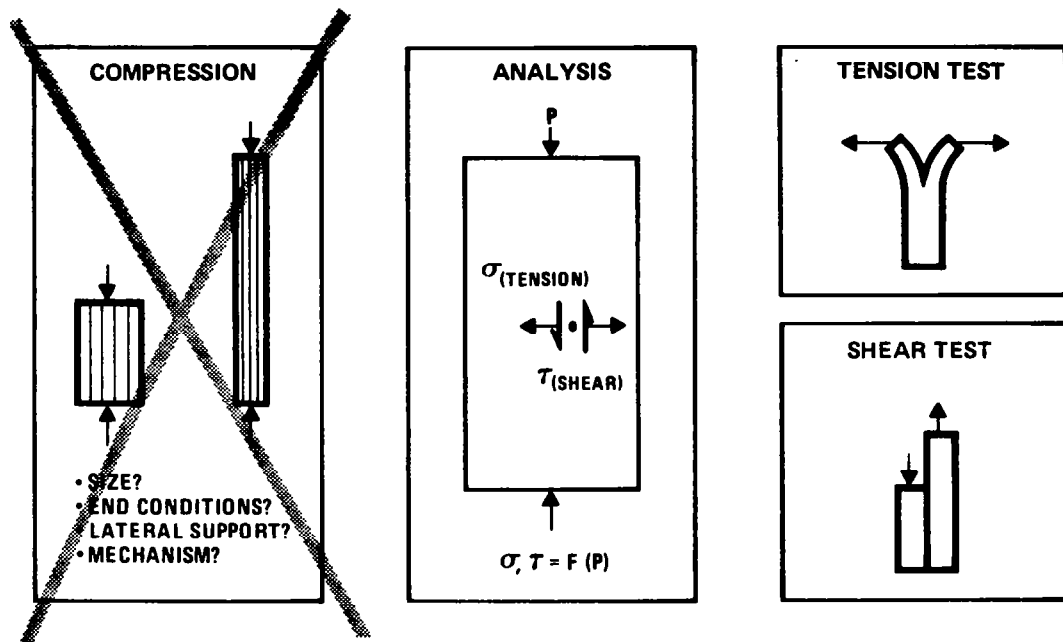


Figure 8

DELAMINATION ANALYSIS USES FRACTURE MECHANICS APPROACH

The capability is available from adhesive fracture technology (Reference 3) for computing the profiles of strain-energy release rate around a delamination in a laminated plate under general loading. As schematically depicted by Figure 9, the profiles can be broken into three components for use in a fracture-mechanics-based failure theory (such as Reference 4). The calculations can be performed with finite element methods coupled with the virtual crack closure technique (Reference 5).

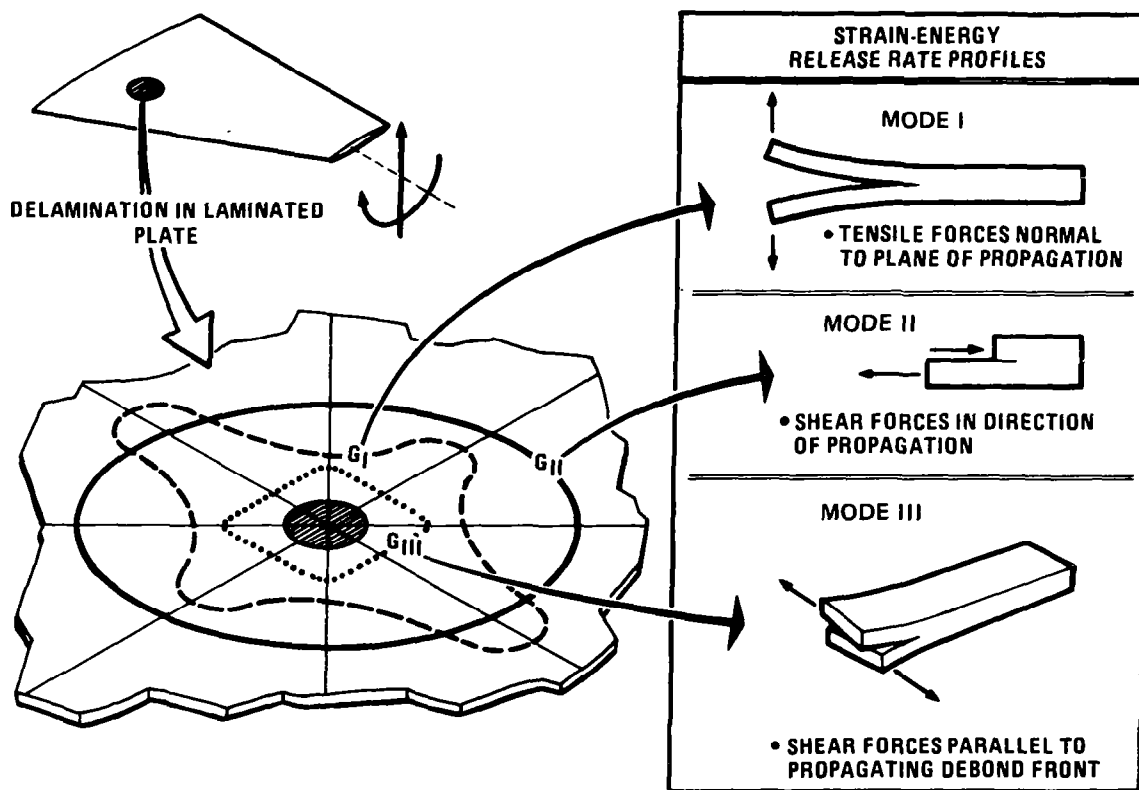


Figure 9

COMPOSITES DAMAGE TOLERANCE APPROACH

With this background, an approach (Figure 10) was taken for damage tolerance of composites on the F-16. Achievable goals were carefully set for this study by emphasizing manufacturing defects (such as planar voids) rather than service defects, concentrating on delamination as the major mechanism, developing a fracture-mechanics-based model, and doing it in five increasingly complex phases. The first three phases defined acceptable coupon test specimens, checked the influence of environmental effects, and sought a method for predicting unidirectional delamination growth under spectrum loads. The fourth phase was intended to extend the test base to limited two-dimensional growth in beam specimens representing thin and thick areas of the horizontal tail. Its results are not included in this presentation. Correlating delamination growth in a full-scale horizontal tail to that predicted by the coupons was the goal of the final phase.

- EMPHASIZE MANUFACTURING DEFECTS
- CONCENTRATE ON DELAMINATION
- DEVELOP A FRACTURE MECHANICS-BASED MODEL
- COMPLETE A 5-PHASE PROGRAM

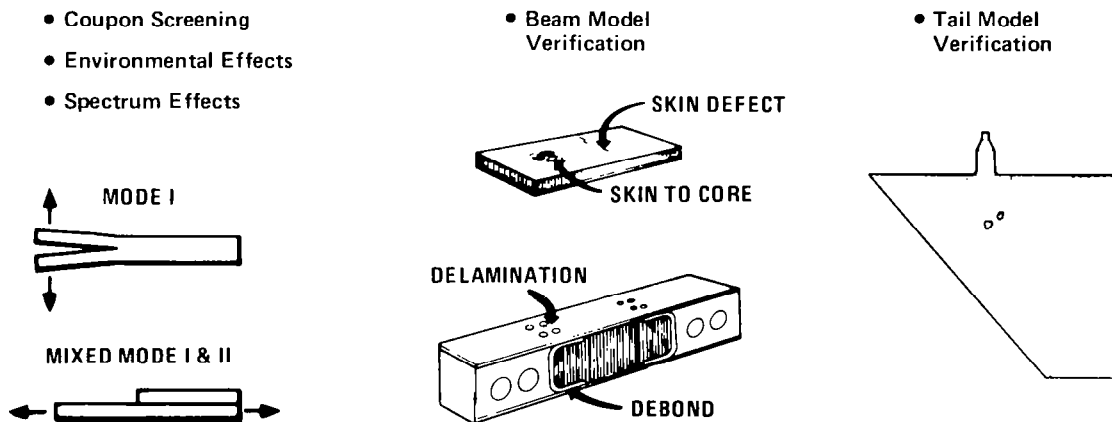


Figure 10

COUPON TESTS

The coupon test phases (Figure 11) were performed with a Mode I coupon and a mixed mode coupon with about 75% Mode II response. As reported in Reference 6, static tests produced the critical strain-energy release rates and their environmental behavior, and fatigue tests measured the delamination growth rates for constant amplitude and spectrum loading.

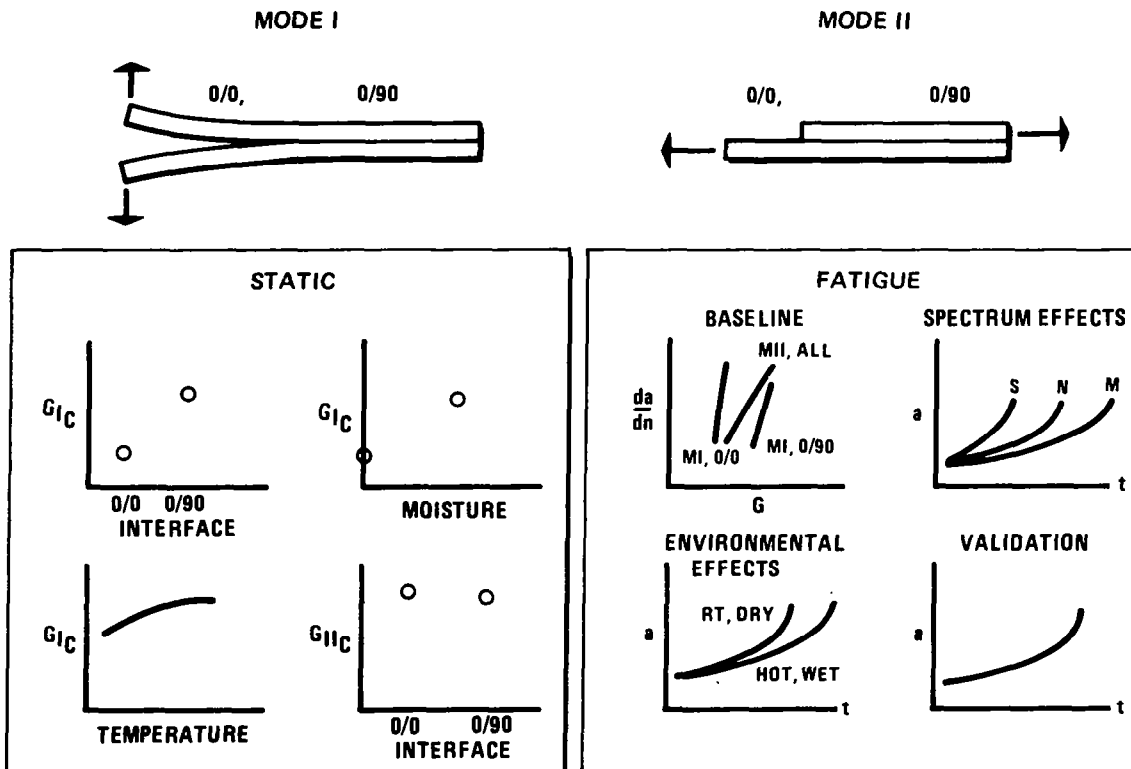


Figure 11

COUPON SUMMARY

Figure 12 outlines some of the important results of the coupon phases. These results have since been supplemented by the research reported in Reference 7.

- DEVELOPED UNIQUE TEST SPECIMENS AND METHODS
- MEASURED CRITICAL STRAIN-ENERGY RELEASE RATES
- FOUND GROWTH BEHAVIOR TO OBEY SIMPLE POWER LAWS
- CHECKED ENVIRONMENTAL EFFECTS
- PREDICTED SPECTRUM GROWTH ACCURATELY

Figure 12

TAIL MODEL VERIFICATION

An introduction for the final demonstration phase of the program is presented in Figure 13.

- OBTAIN A TAIL WITH KNOWN DEFECTS
- PERFORM FATIGUE TEST USING TRUNCATED SPECTRUM
- DO FRACTURE ANALYSIS
- CORRELATE MODEL TO GROWTH OBSERVATIONS

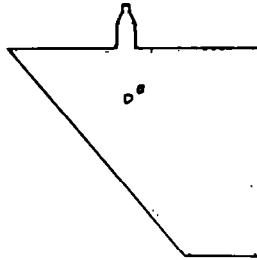


Figure 13

DEFECT LOCATIONS

Horizontal tail unit number 110 was selected for test and was brought back after 144 flight hours of normal service. One reason for its selection was that it contained a "corner defect," a 2.1-inch long by 0.3-inch wide delamination between the 51st and 52nd plies of the 52-ply graphite-epoxy skin, that had been repaired by injection of resin. Figure 14 shows the locations of the corner defect, the titanium hub-spar substructure, and the boundary of a ply termination separating the 12- and 10-ply thicknesses in the skin. In an area of high stress coinciding with the ply termination, two additional defects were introduced. One was an impact damage produced by dropping a 3.25-pound steel dart with a 1-inch-diameter hemispherical nose from a height of 2 feet. The other was a routed 3-inch hole in the skin down to the aluminum core, representing the clean-up hole around a typical skin repair that never got a patch bonded over it.

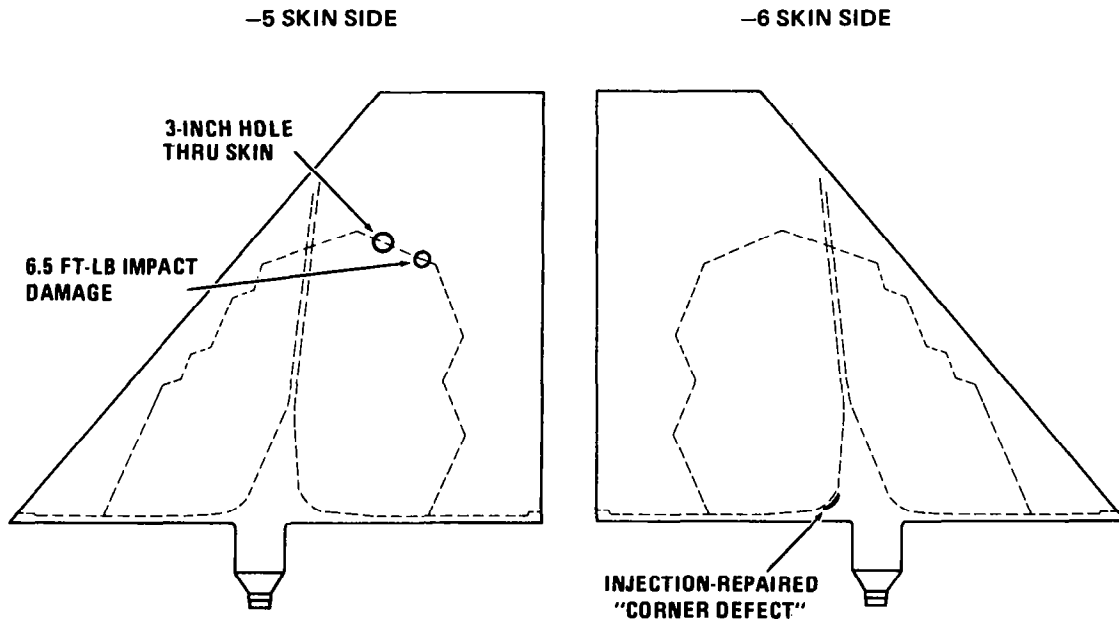


Figure 14

TAIL TEST HISTORY

The tail was tested in an air-conditioned lab environment. Figure 15 outlines the testing sequence.

- 1 LIFETIME OF DESIGN USAGE SPECTRUM LOADING
- 2 SPECTRUM REPETITIONS WITH LOADS MAGNIFIED BY 1.3
- 4162 FULLY REVERSED CYCLES OF 1.3 TIMES MAXIMUM SPECTRUM LOAD
- RESIDUAL STRENGTH TEST TO 246% DESIGN LIMIT LOAD

Figure 15

TAIL FLAW GROWTH

The overall views of both tail surfaces (Figure 16) show the outlines of delaminations created by the testing. The impact damage grew only slightly during the first few loads and exhibited no further growth. Delaminations grew from the 3-inch hole during the constant amplitude cycling. Large delaminations were produced in the root area of both surfaces. The first large increment of delamination at the 3-inch hole and at the root occurred during the first 2235 cycles of the constant amplitude cycling during which no inspections were made.

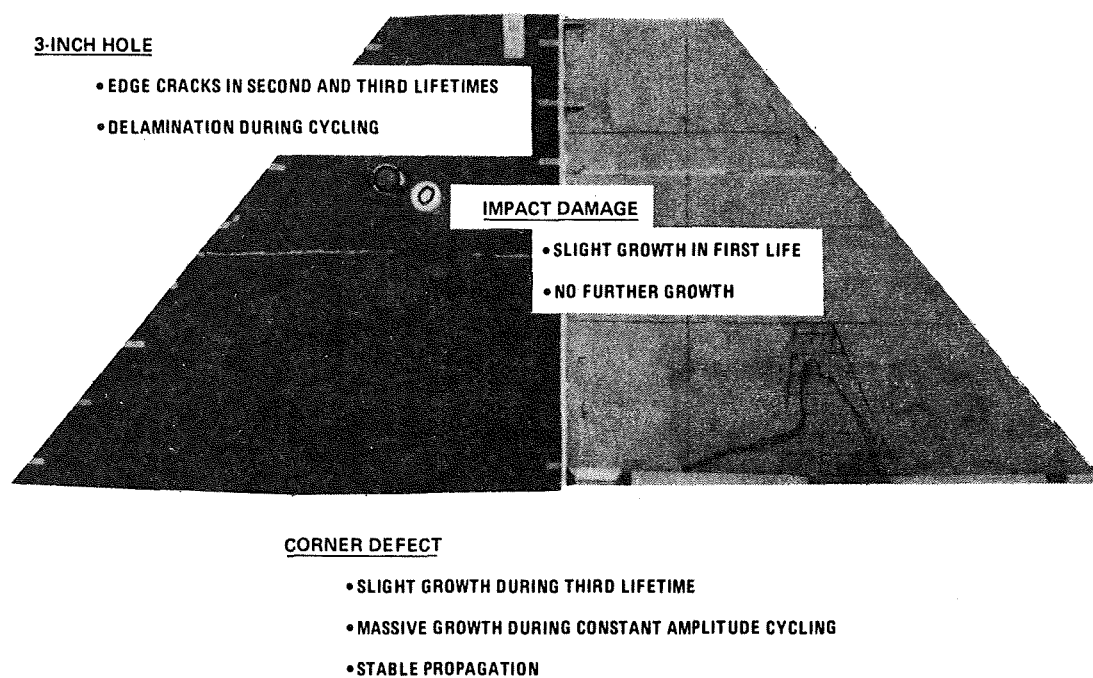


Figure 16

ROOT AREA MATH MODELS

The finite-element based fracture analysis used the "zoom-in" technique shown in Figure 17. Each succeeding detailed model was loaded with deflections from the previous model using MSC NASTRAN.

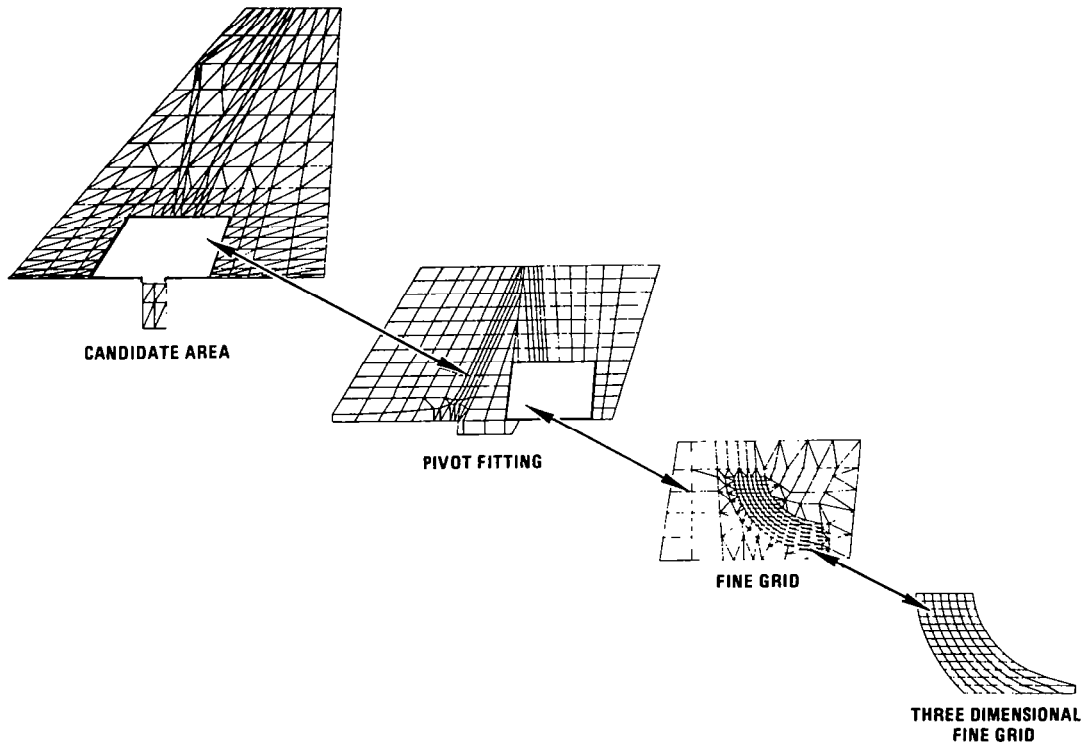


Figure 17

PLY CRACKING APPARENTLY TRIGGERED DELAMINATION

Figure 18 shows the 3-D brick model of the skin, substructure, and core in the local area of the "corner defect," as well as its top view and an internal view of the local geometry. The model showed a strong through-the-thickness stress concentration associated with the bonding of the skin to the titanium spar. Transverse stresses in the bottom +45° ply were much higher than the ply could carry, so its stiffnesses were modified to represent a cracked ply. Introduction of a delamination by releasing nodes as indicated gave a strain-energy release rate that was 90% of the critical static strain-energy release rate and thus was near the upper end of the delamination growth curve referred to in Figure 11.

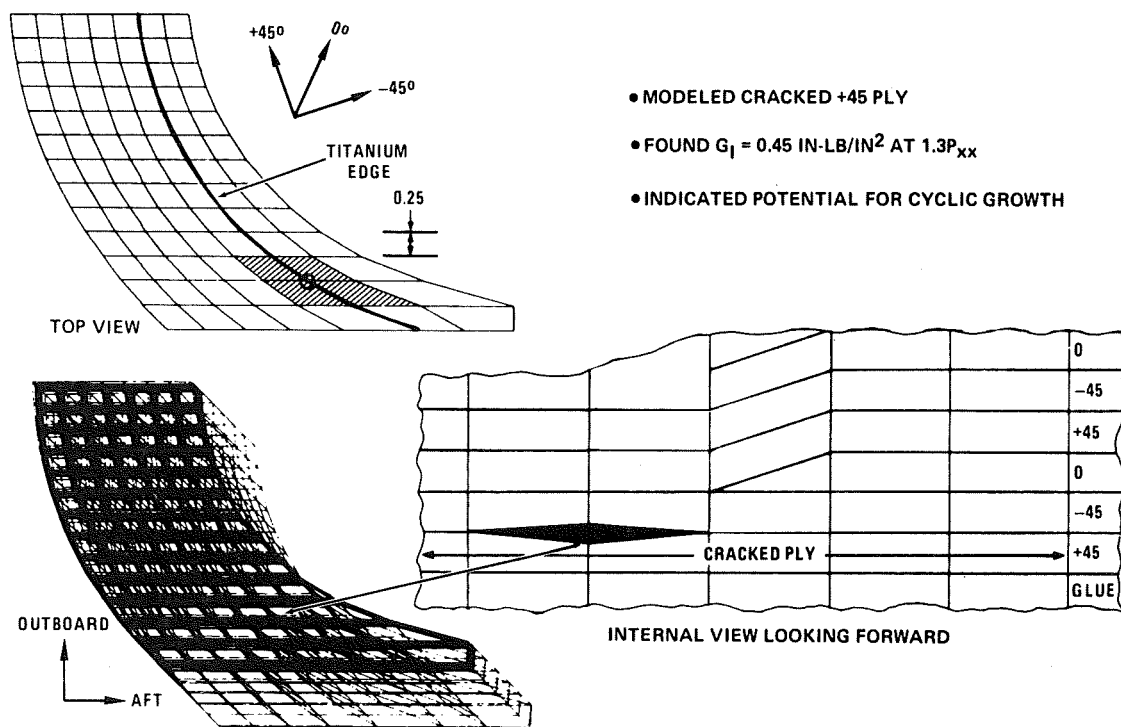


Figure 18

DELAMINATION GREW FROM 3-INCH HOLE

A closer view of the impact damage and 3-inch hole growth indications is presented in Figure 19, along with the number of fully reversed constant amplitude cycles associated with them.

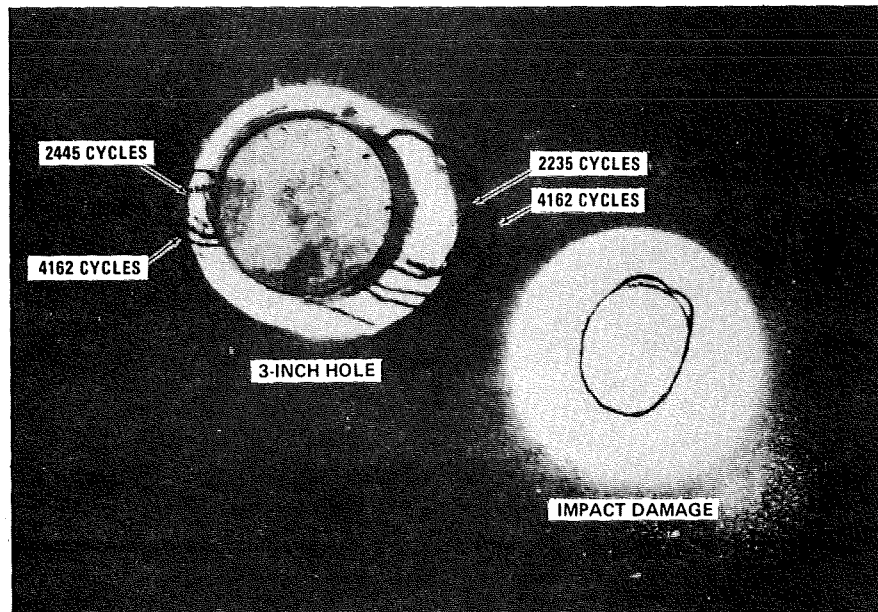


Figure 19

3-INCH HOLE MATH MODELS

Figure 20 depicts the "zoom-in" technique used for the 3-inch hole math models.

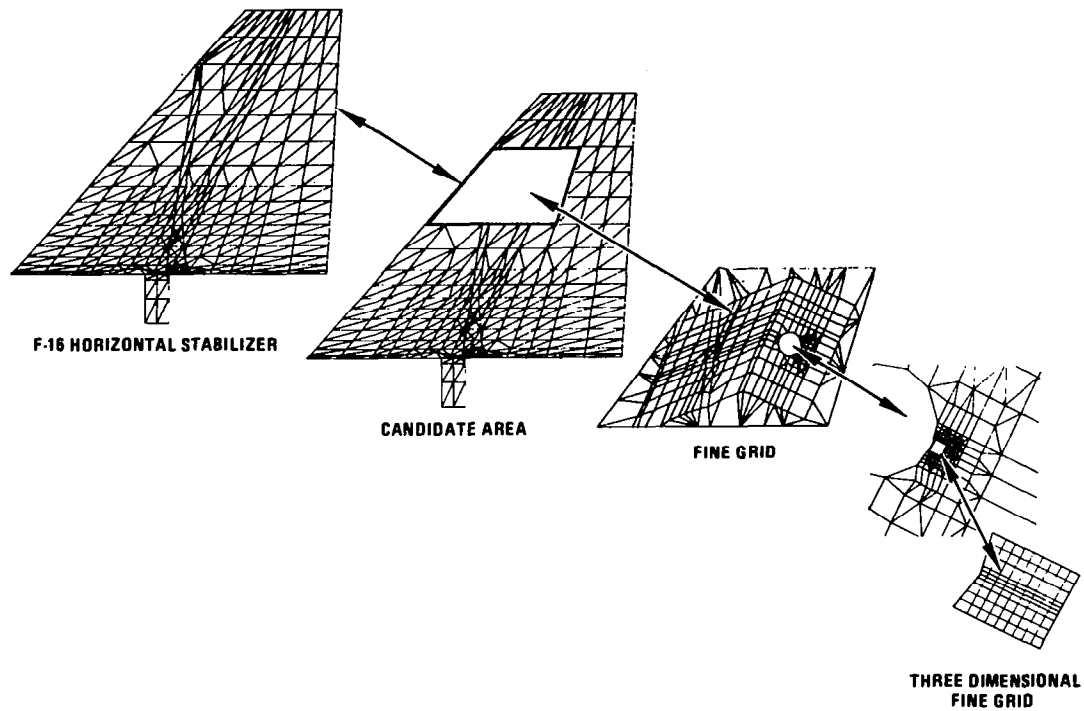


Figure 20

SEQUENCE OF CRACK ANALYSIS

The edge of the 3-inch hole is shown in Figure 21, along with the stacking sequence of the plies, all of which were modeled individually in the 3-D brick model. The model delamination was located between a -45° ply and a 0° ply. A node was released from the edge, then in all three possible directions, to indicate the preferred growth direction, which was along the ply termination. Succeeding nodes were released to "grow" the delamination.

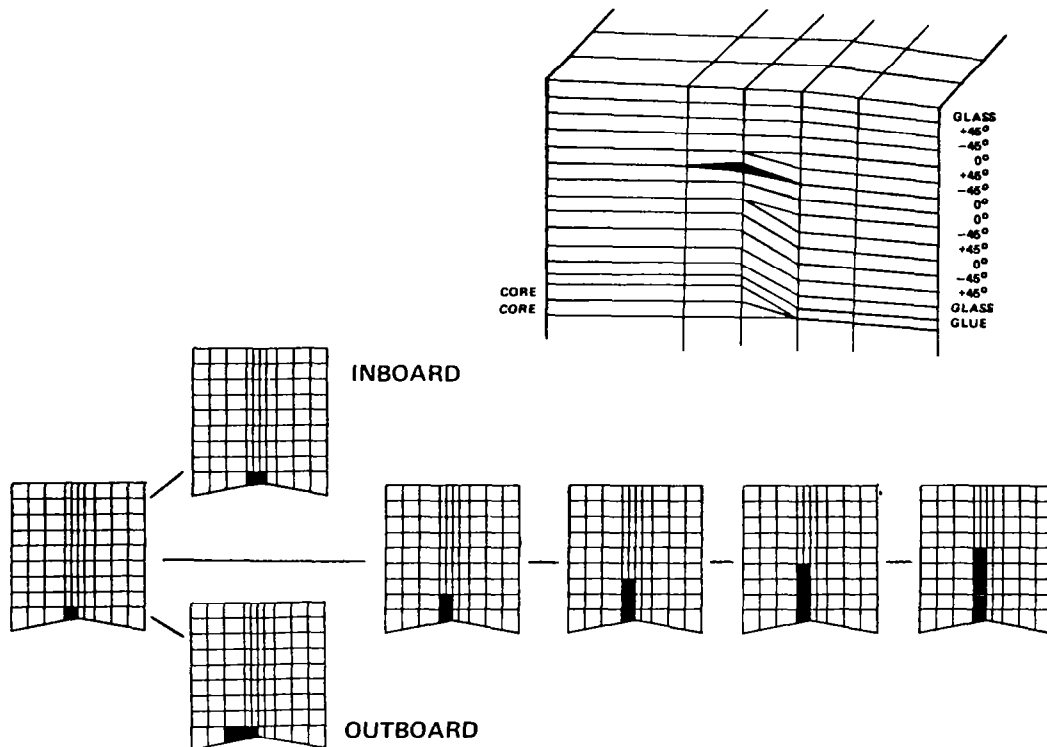


Figure 21

FRACTURE ANALYSIS AT P_{XX} LOAD

Results of the models, scaled to the peak load in the original design usage spectrum, are plotted in Figure 22. The analysis showed that a delamination of 0.085 inches should have resulted from that load. The plot of strain-energy release rate as a function of crack length was scaled to the square of the applied load and combined with the coupon static fracture and delamination growth rate data to produce the results shown in Figure 23.

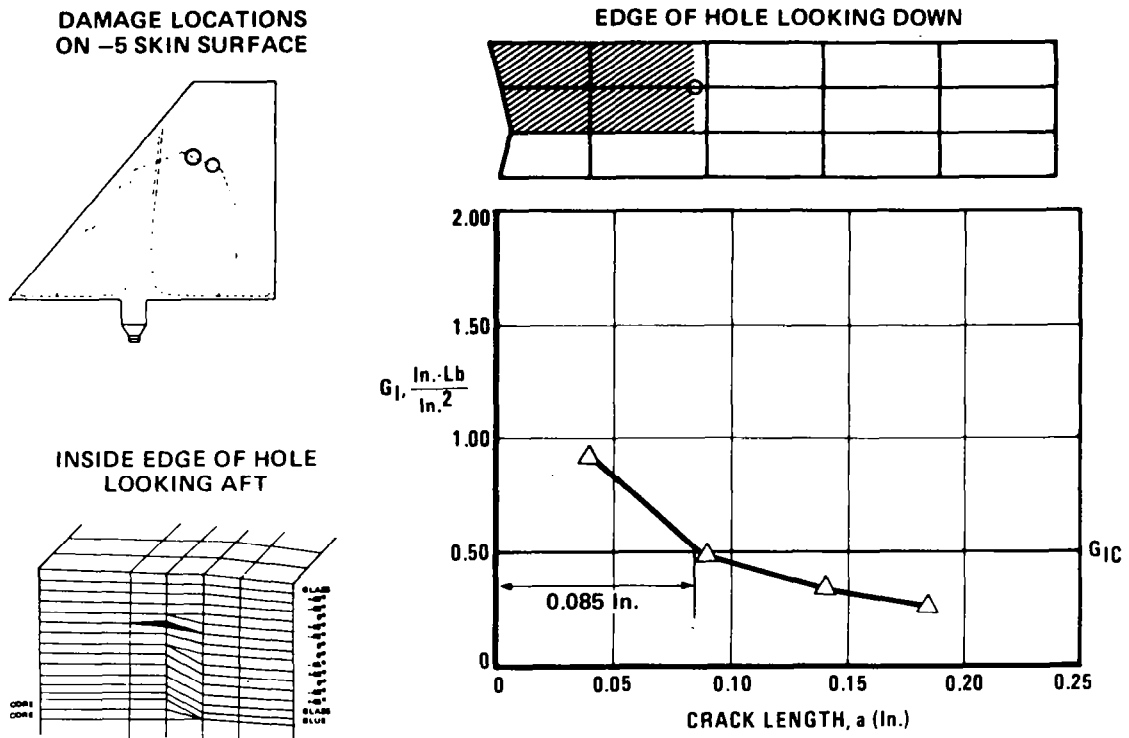


Figure 22

ANALYSIS AGREES WITH OBSERVED GROWTH

Figure 23 summarizes and correlates the growth calculations and observations. The resolution of the hand-held ultrasonic inspection technique at the edge of the hole was not good enough to locate the small delaminations predicted by the analysis. However, edge cracks were observed by surface replication of the cut surface of the hole. The agreement between calculations and measurements for the larger delaminations is quite satisfactory.

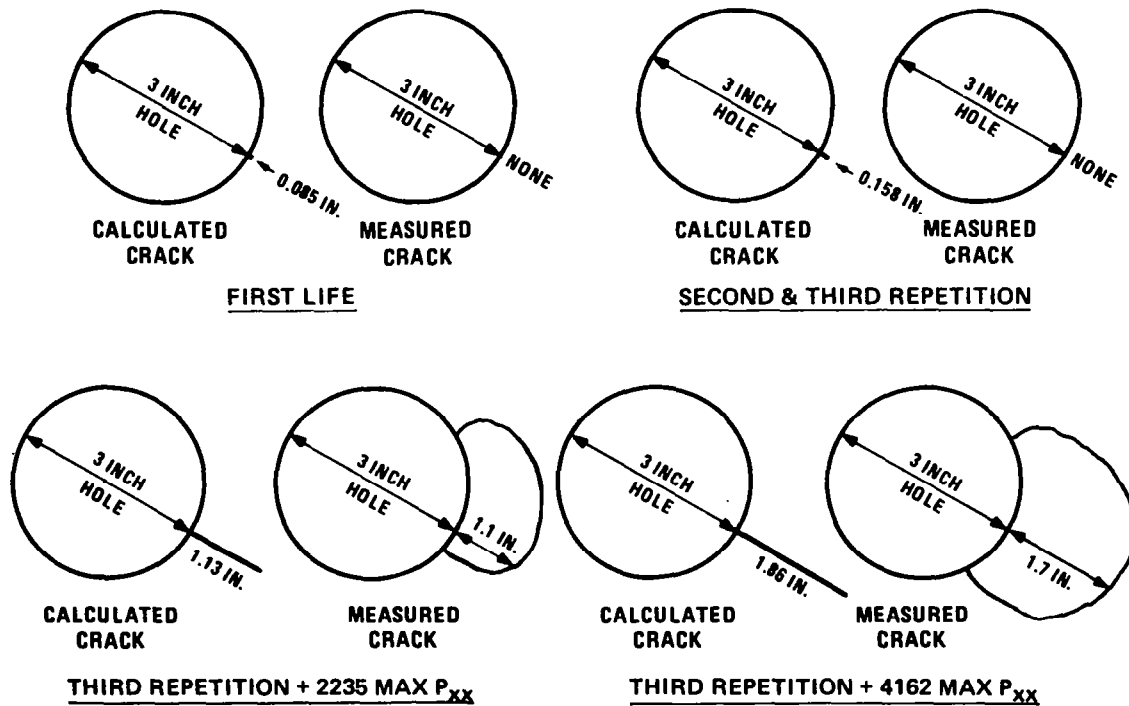


Figure 23

SUMMARY

The highlights of the program are reviewed and summarized in Figure 24.

COUPONS

- **DEVELOPED UNIQUE TEST METHODS**
- **FOUND SIGNIFICANT DIFFERENCES BETWEEN PEEL & SHEAR**
- **PREDICTED SPECTRUM GROWTH**

TAIL

- **OBTAINED GROWTH ONLY UNDER EXTREME CONDITIONS**
- **DEMONSTRATED HIGH DAMAGE TOLERANCE**
- **SHOWED STABLE GROWTH IN REAL HARDWARE**
- **DEVELOPED MODELING PROCEDURE**

Figure 24

COMPOSITES DURABILITY AND DAMAGE TOLERANCE ANALYSIS

The methodology, which General Dynamics believes to be equally applicable to both durability and damage tolerance analyses, is outlined in Figure 25. Its input is a flight-by-flight load history that is coupled to the fracture analysis to produce a sequence to strain-energy release rate/delamination size relationships. The coupon data base can then be entered to judge the potential for static or cyclic growth including the influence of moisture and temperature. A simple load-by-load growth model produces predictions of delamination size as a function of flight hours. This methodology has many attractive features, but the most important one is that it should be applicable to virtually any laminated composite structure.

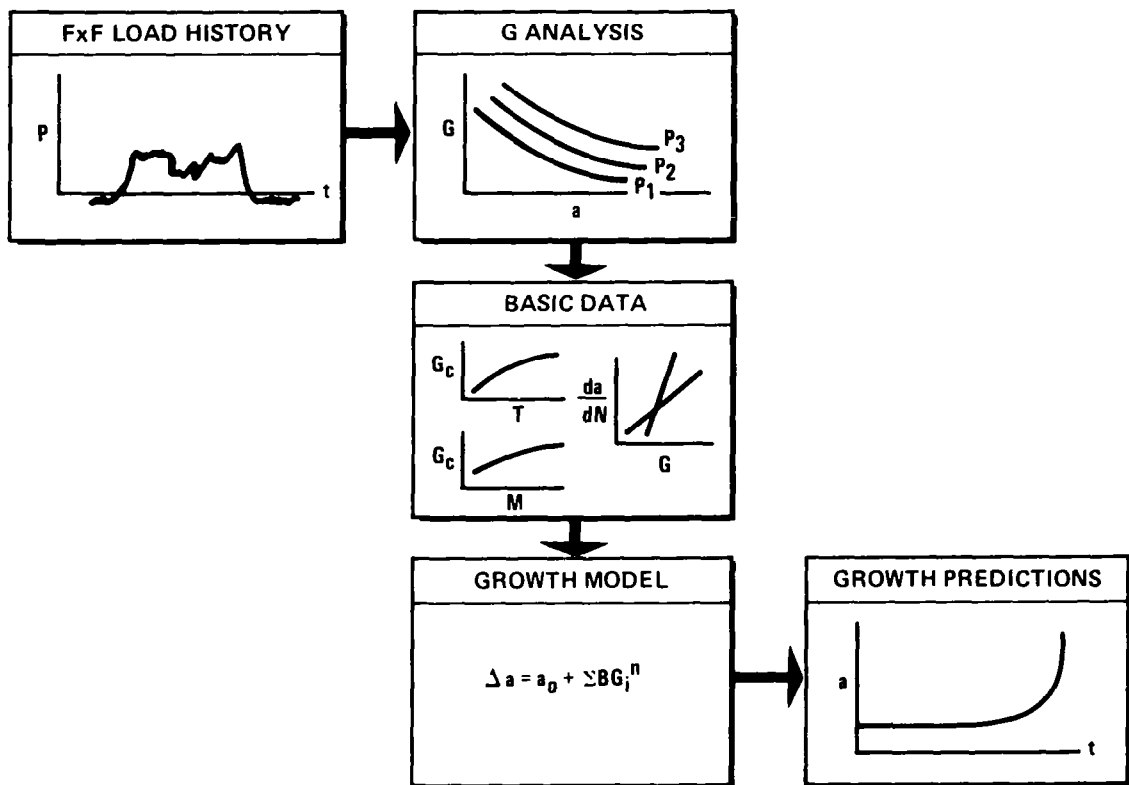


Figure 25

REFERENCES

1. Wolff, R. V. and Wilkins, D. J., "Durability Evaluation of Highly Stressed Wing Box Structure," Fourth Conference on Fibrous Composites in Structural Design, (San Diego, California, November 14-17, 1978), Plenum Press, 1980, pp. 761-770.
2. Konish, H. J., Swedlow, J. L., and Cruse, T. A., "Fracture Phenomena in Advanced Fiber Composite Materials," AIAA Journal, Vol. 11, 1973, p. 40.
3. Anderson, G. P., Bennett, S. J., and DeVries, K. L., Analysis and Testing of Adhesive Bonds, Academic Press, New York, 1977.
4. Wu, E. M., "Application of Fracture Mechanics to Anisotropic Plates," Journal of Applied Mechanics, Vol. 34, 1967, pp. 967-975.
5. Rybicki, E. F. and Kanninen, M. F., "A Finite Element Calculation of Stress Intensity Factors by a Modified Crack Closure Integral," Engineering Fracture Mechanics, Vol. 9, 1977, pp. 931-938.
6. Wilkins, D. J., Eisenmann, J. R., Camin, R. A., Margolis, W. S., and Benson, R. A., "Characterizing Delamination Growth in Graphite-Epoxy," Damage in Composite Materials: Basic Mechanisms, Accumulation, Tolerance, and Characterization, ASTM STP 775, American Society for Testing and Materials, 1982.
7. Wilkins, D. J., A Comparison of the Delamination and Environmental Resistance of a Graphite-Epoxy and a Graphite-Bismaleimide, Naval Air Systems Command Report NAV-GD-0037, September 15, 1981.

DESIGN AND ANALYSIS OF COMPOSITE STRUCTURES
WITH STRESS CONCENTRATIONS

S. P. Garbo
McDonnell Aircraft Co., McDonnell Douglas Corporation
St. Louis, Missouri

INTRODUCTION

This presentation provides an overview of an analytic procedure which can be used to provide comprehensive stress and strength analysis of composite structures with stress concentrations. The methodology provides designer/analysts with a user-oriented procedure which, within acceptable engineering accuracy, accounts for the effects of a wide range of application design variables. The procedure permits the strength of arbitrary laminate constructions under general bearing/bypass load conditions to be predicted with only unnotched unidirectional strength and stiffness input data required.

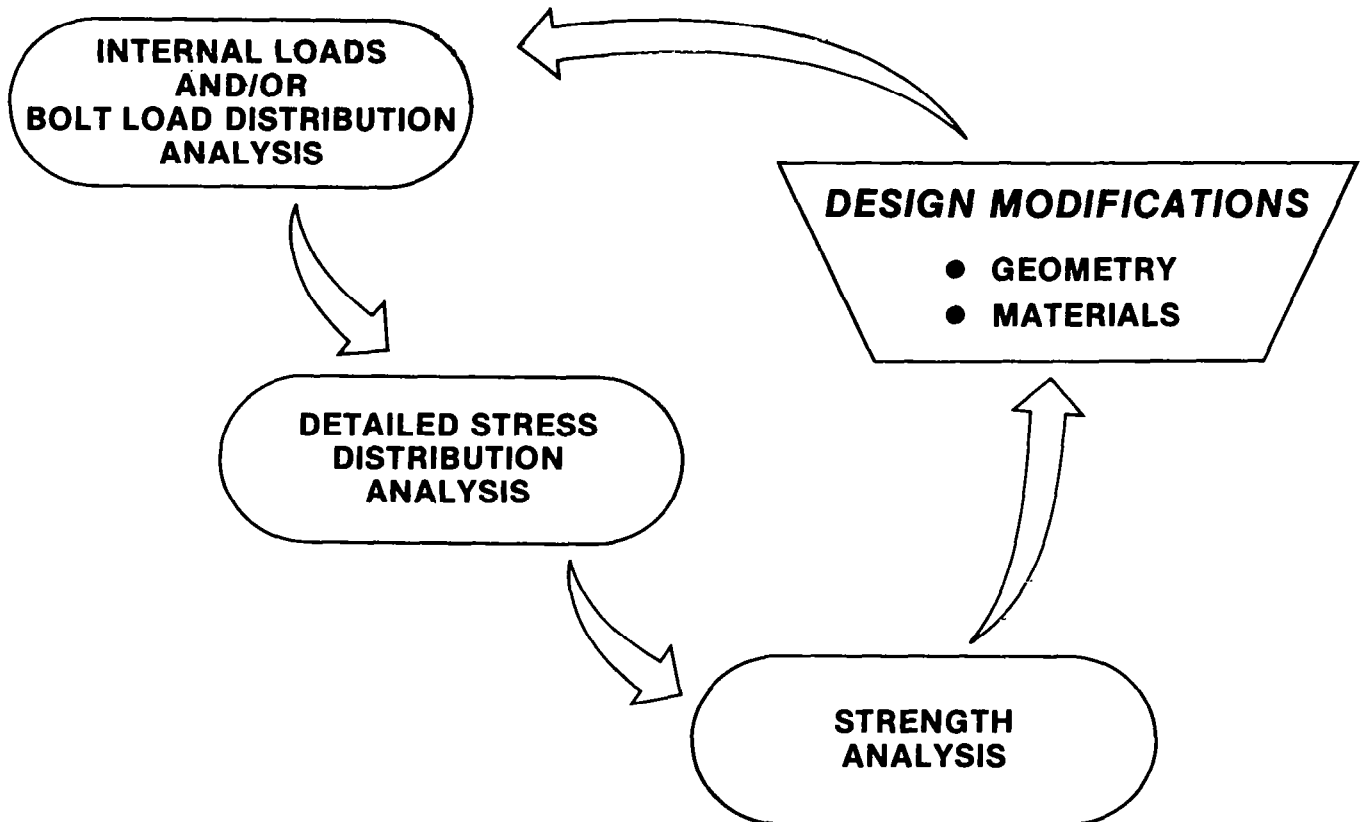
In particular, the presentation includes:

- (1) A brief discussion of the relevancy of this analysis to the design of primary aircraft structure
- (2) An overview of the analytic procedure with theory/test correlations
- (3) An example of the use and interaction of this strength analysis relative to the design of high-load transfer bolted composite joints

Many of the results presented were taken from two recently completed MCAIR programs funded by the U.S. Air Force and the U.S. Navy (refs. 1 and 2).

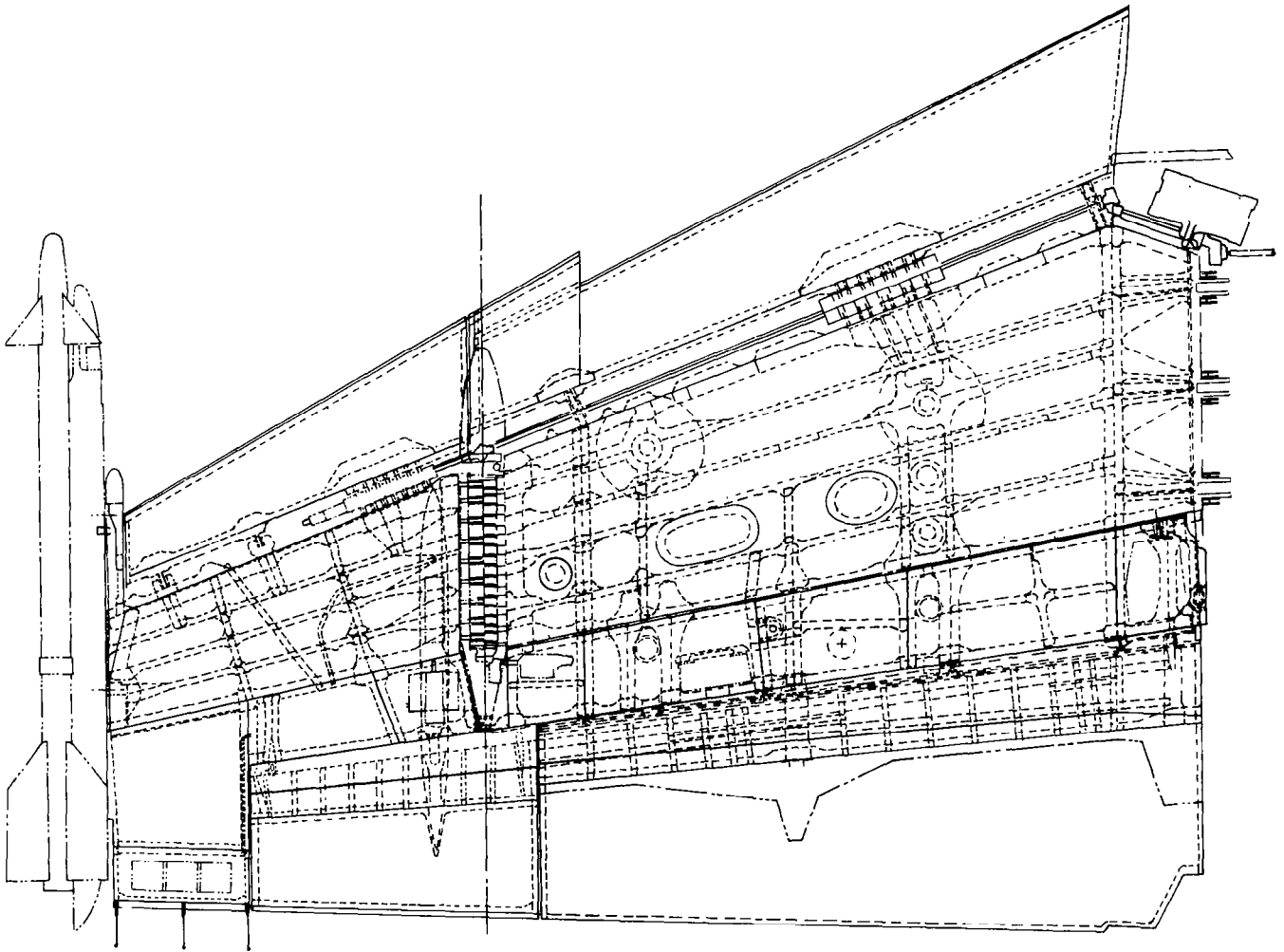
DESIGN/ANALYSIS ITERATIONS

The usual project sequence of design/analysis iterations is illustrated. The emphasis of methodology discussed in this presentation is in the areas of (1) detailed stress analysis about a structural discontinuity or stress riser which results in local stress concentrations and (2) strength analysis performed on the stress (strain) solutions to determine load capability.



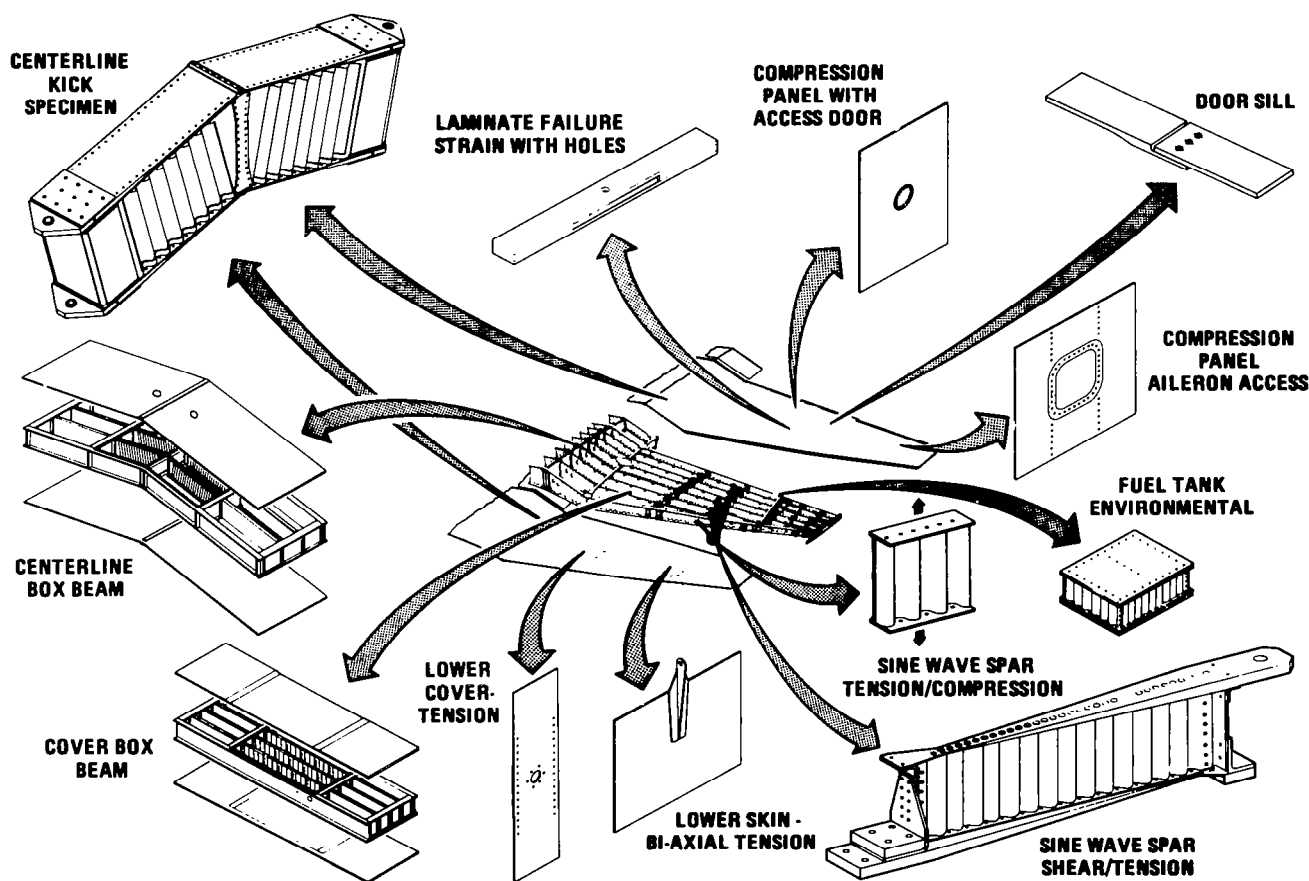
F/A-18A WING STRUCTURE

The planview of the F/A-18A wing structure is presented to illustrate the prevalence of stress risers in typical primary aircraft structure. This production structure is comprised of monolithic composite skins mechanically fastened to aluminum spar and rib substructure. Evident are numerous stress risers due to required access doors, cutouts, and pylon post holes required for attachment of external equipment. Additionally, fastener holes are required along all spars and ribs to mechanically attach wingskins to substructure, and local load introductions (e.g., leading- and trailing-edge flap attachments) and major structural splices (e.g., wingfold) result in many required high-load transfer joints. The point to be made is that for current and near-term aircraft, accurate analysis of the effects of stress risers on structural efficiency is of prime importance.



AV-8B COMPOSITE WING TEST PROGRAM

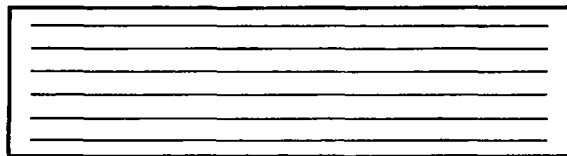
A visual overview of typical coupon, element, and subcomponent specimens tested during the Harrier composite wing development program illustrates again the concern of structural designer/analysts with the effects of stress risers on structural integrity. In almost all structural tests depicted, the presence of a stress riser is evident. For composite materials which possess little of the ductility (forgiveness) of metals, the presence of these geometric details results in structure designed to static strength requirements. This emphasizes the need and importance of comprehensive, accurate, and detailed internal load, stress, and static strength analyses. Without such analysis, costly and extensive test programs are required which are often repeated when changes in load conditions, stress riser geometry, and layup occur. The result is a project dependence on empirically derived allowables which significantly limit full utilization of laminate tailoring design options.



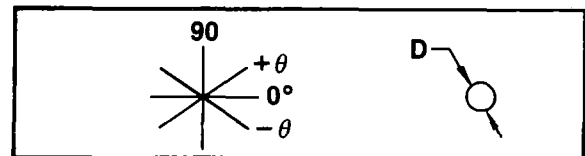
STIFFNESS AND STRENGTH DESIGN DATA

The items listed under lamina (unidirectional ply) and laminate indicate variables which affect stiffness and strength. Fundamental differences between the mechanical behavior of metals and composites are due to the composite stiffness and strength anisotropy and its material inhomogeneity. These factors complicate considerably the complete characterization of lamina mechanical properties relative to metals and introduce the necessity of additional strength characterization requirements at the laminate level for each layup variation. The objective of our analysis development has been to provide a comprehensive and general laminate strength analysis based primarily on lamina stiffness and strength data, thus minimizing the level of laminate testing currently required for applications.

LAMINA



LAMINATE



- IN-PLANE LOADINGS ... { TENSION
COMPRESSION
SHEAR

- INTERLAMINAR LOADINGS

- ENVIRONMENT

- NONLINEARITIES

- IN-PLANE LOADINGS ... { BI-AXIAL
OFF-AXIS } ... { TENSION
COMPRESSION
SHEAR
BEARING

- INTERLAMINAR LOADINGS { PRESSURE
BENDING

- MATERIAL TAILORING { LAYUP
STACKING SEQUENCE
ANISOTROPY

- GEOMETRY { HOLE SIZE
HOLE TOLERANCE
FASTENER TYPE

- ENVIRONMENT

- NONLINEARITIES

AS/3501-6 GRAPHITE-EPOXY LAMINA PROPERTIES

This table summarizes stiffness and strength data along the principal material axes of the AS/3501-6 graphite-epoxy material system. These data are usually generated by testing unnotched specimens and most data are routinely obtained during material quality assurance testing performed by companies at the time material shipments are received. These data are the basis upon which general laminate stiffness, stress, and strength analyses are performed using the procedures discussed in this presentation.

MECHANICAL PROPERTY	RTD ¹	RTW ²	ETW ³
E_1^t (MSI)	18.85	18.85	18.54
E_1^c (MSI)	18.20	18.20	17.80
E_2 (MSI)	1.90	1.63	0.74
G_{12} (MSI)	0.85	0.85	0.38
ν_{12}	0.30	0.30	0.30
F_1^{tu} (KSI)	230	230	236
F_1^{cu} (KSI)	321	179	111
F_2^{tu} (KSI)	9.5	5.6	4.3
F_2^{cu} (KSI)	38.9	33.4	12.4
F_{12} (KSI)	17.3	19.8	11.9

- ¹ Room temperature dry (as manufactured)
- ² Room temperature with 1.05% moisture
- ³ Elevated temperature ~ 250°F and 1.05% moisture

INTERNAL LOADS ANALYSIS

While this is not the main subject of this presentation, it is important to realize that the needed detailed stress and strength analyses, especially for bolted composite joints, are directly related to internal load distribution analysis. Should local laminate failures occur due to fastener loadings, joint-member and fastener-to-joint-member flexibilities (spring rates) will be altered and internal load paths will change. The variables listed are important to accurate internal load analysis and have direct effects on laminate point strength analysis.

- **GEOMETRY...** { **IN-PLANE**
 THRU-THE-THICKNESS
- **MEMBER STIFFNESSES**
- **FASTENER STIFFNESSES (SPRING RATES)**
- **MANUFACTURING TOLERANCES**
- **MULTIPLE FASTENERS**
- **LOADING COMPLEXITIES**
 - TENSION**
 - COMPRESSION**
 - SHEAR**
 - VARIATIONS**
- **MATERIAL NONLINEARITIES**

DETAILED STRESS DISTRIBUTION ANALYSIS

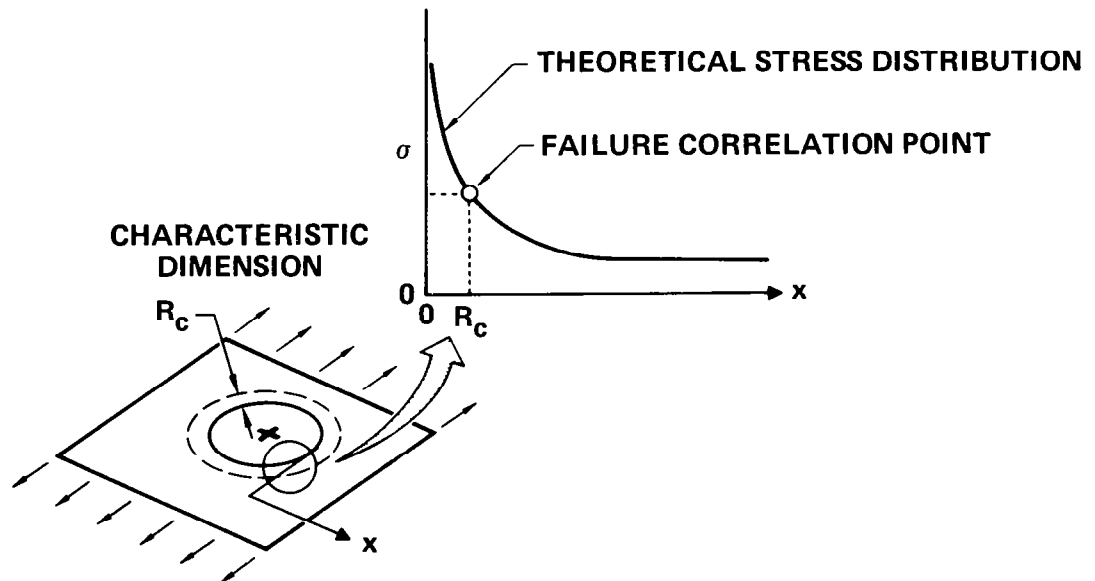
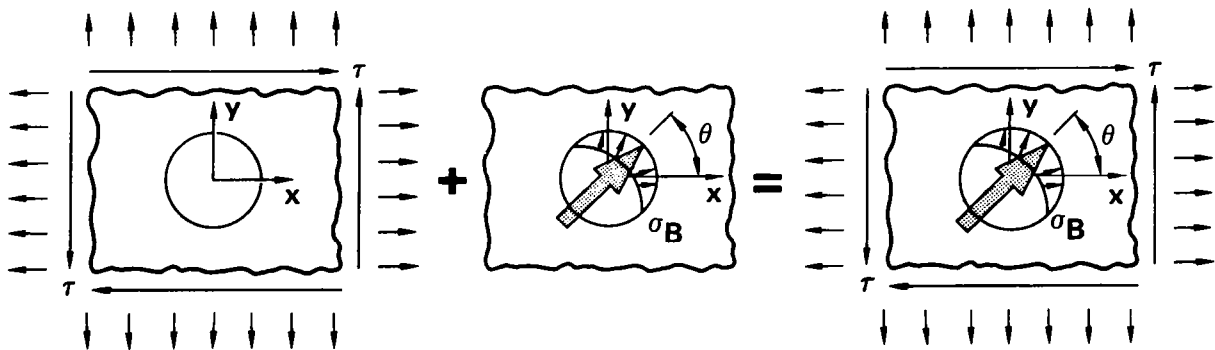
This list represents some of the more important variables typical of general aircraft structure. The initial thrust of our strength analysis development was to provide a user-oriented procedure which would account for the effects of fastener holes on laminate strength for arbitrary laminates under general biaxial and fastener bearing loads. Currently we are extending these procedures to account for the general class of stress risers, through-the-thickness variables, and finite-geometry effects.

- GENERAL LOADINGS {
 - BIAXIAL
 - BEARING/BYPASS
 - BENDING/PRESSURE
- GEOMETRY {
 - HOLE SIZE
 - CUTOUT SHAPE
 - WIDTH (EXTERNAL BOUNDARIES)
 - MULTIPLE STRESS RISERS
 - HOLE TOLERANCES
- THROUGH-THE-THICKNESS {
 - STACKING SEQUENCES
 - CLAMP-UP (TORQUE-UP)
 - JOINT ECCENTRICITY
 - FASTENER TYPES (CSK)
 - FOUNDATION STIFFNESS
 - ORTHOTROPY
- MATERIAL NONLINEARITIES
- ENVIRONMENT

FAILURE PREDICTION OF BOLTED COMPOSITE JOINTS

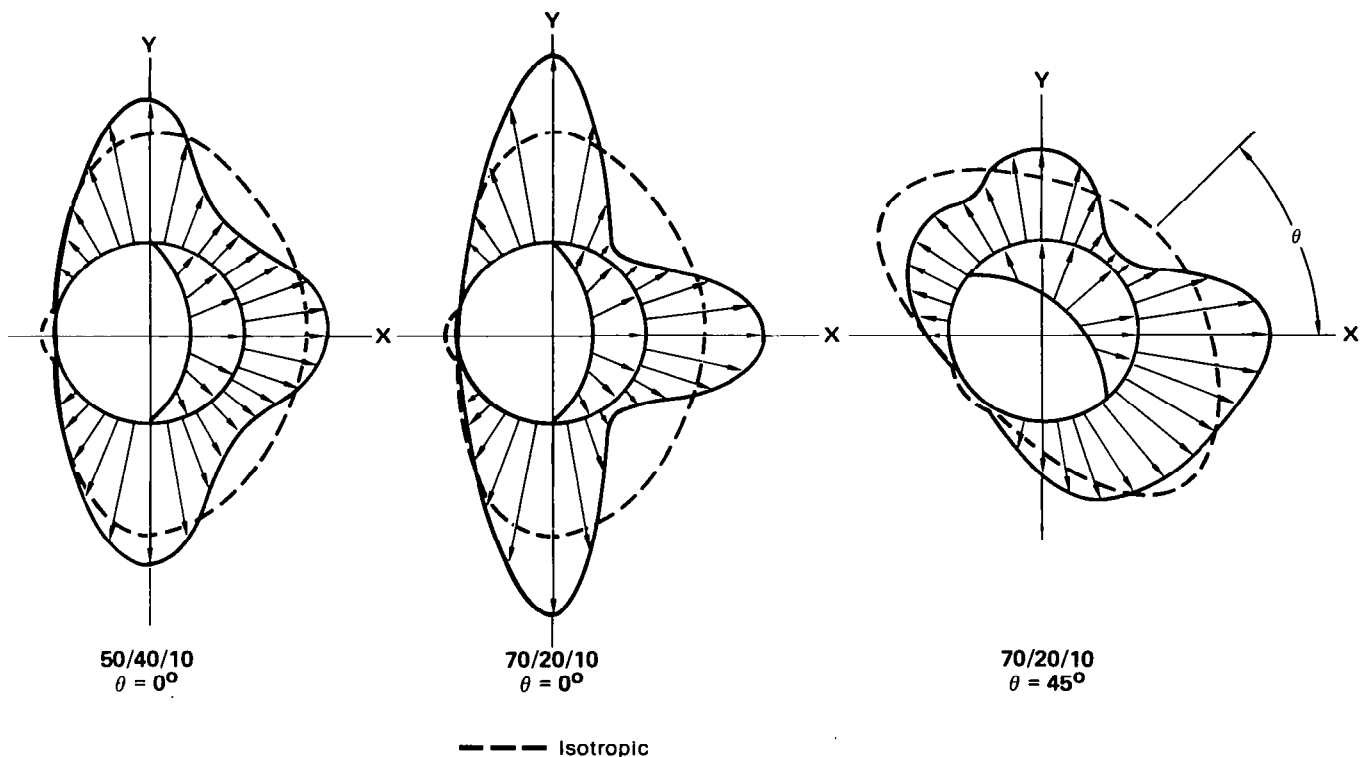
An overview of the MCAIR analytic approach is idealized in this illustration. The principle of superposition is used to obtain laminate stress and strain distributions due to combined bearing and bypass loads. Once laminate stresses and strains are known, failure analysis is performed at a characteristic dimension (R_c) away from the hole. This bolted joint stress field model (BJSFM) generalizes Whitney and Nuismer's postulated characteristic dimension concept to apply to anisotropic laminates under general biaxial loadings (ref. 3). Failure predictions are made on a ply-by-ply basis by comparing material lamina allowables with elastic point stresses calculated for each ply at a characteristic dimension from the edge of the hole. Various material failure criteria (Tsai-Hill, maximum stress, etc.) available for user selection can then be used to compare stresses with lamina allowables.

This program is available to the industry through the Air Force Flight Dynamics Laboratory and is detailed in reference 1. This user-oriented program can be used to generate complete stress (strain) solutions at or about the hole, or just the failure load, critical ply, and failure location.



CIRCUMFERENTIAL STRESS SOLUTIONS UNDER PURE BEARING LOAD

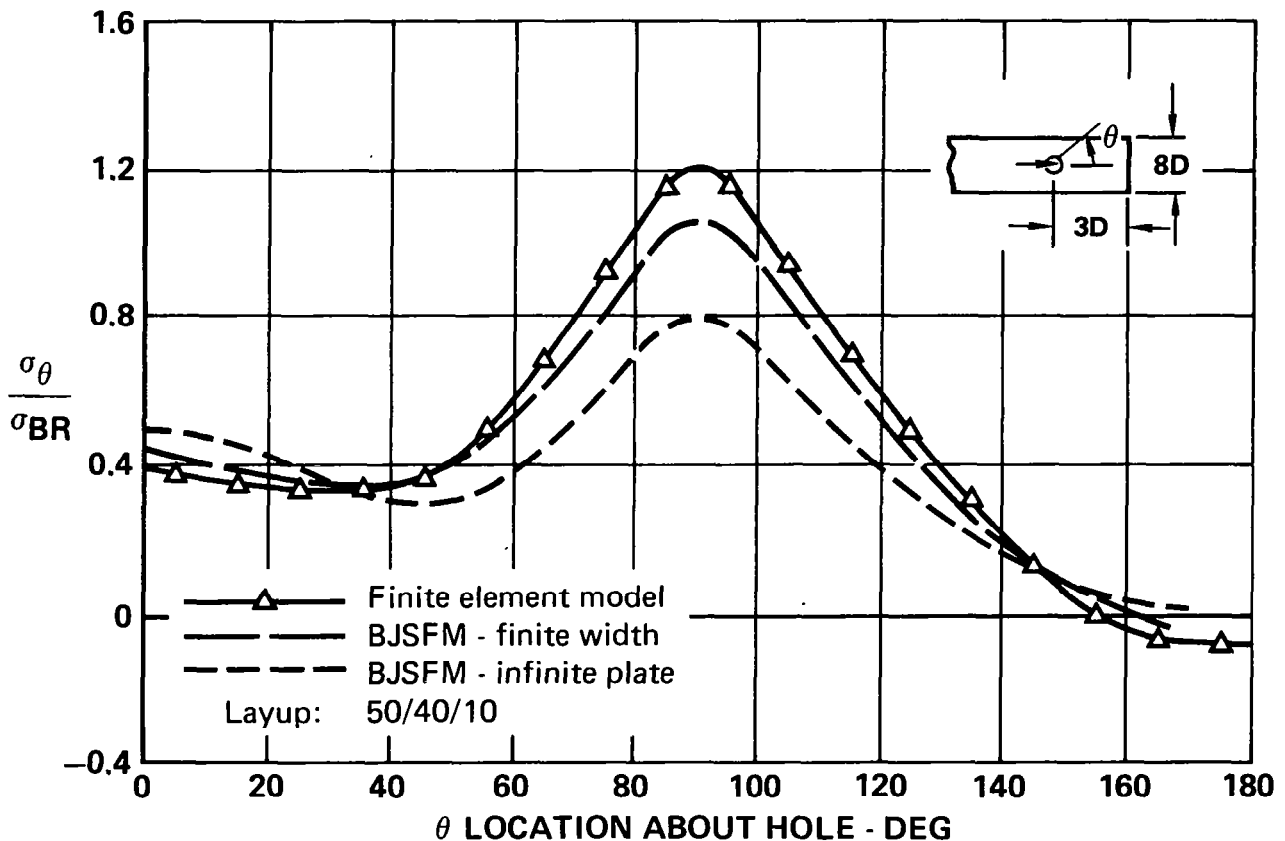
The need for detailed distributions in orthotropic laminates is illustrated by using the BJSFM program to determine circumferential stress distributions about a fastener hole loaded by pure bearing. A 50/40/10 layup and a 70/20/10 layup from the 0° , $\pm 45^\circ$, and 90° family of ply orientations were analyzed. Solutions for both of these layups are compared with solutions obtained for an isotropic material. In the first two comparisons, bolt bearing was directed along the 0° ply orientation (principal material axis). In comparison with the dashed line representing isotropic material stress solutions, orthotropy in the two composite layups causes a marked change in maximum stress and locations. This directional dependence increases with the degree of orthotropy (higher percentage of 0° plies relative to load direction), as can be observed by comparing the solutions of the 70/20/10 layup with the 50/40/10 layup. Additionally, if bolt bearing is directed off the principal material axis, the circumferential stresses change markedly. The dashed line illustrates the fact that solutions for an isotropic (metal) material are unaffected by change in bolt bearing direction.



EFFECTS OF FINITE GEOMETRY

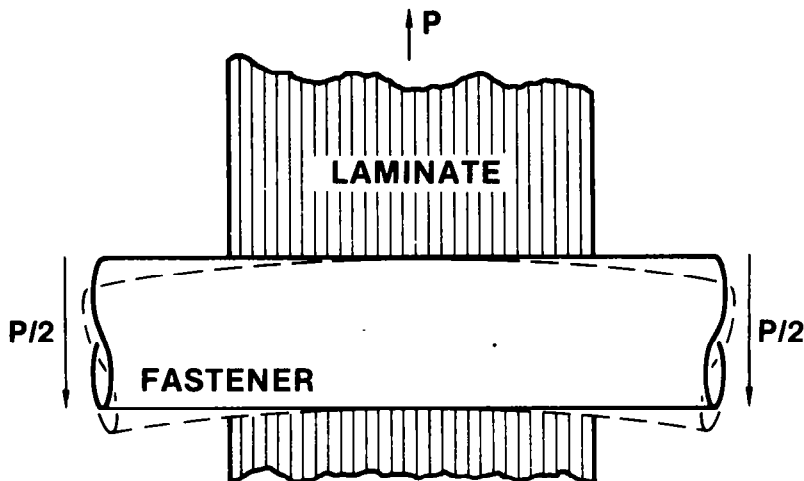
To evaluate the effects of finite geometry on stress solutions and establish limits on the accuracy of infinite plate solutions, a comparison of BJSFM solutions with finite element solutions was performed. In this illustration, circumferential stresses normalized to the average bolt bearing stress are plotted about the half-circle from directly in front of the neat-fit bolt (0°) to directly behind the bolt (180°). The dashed line indicates the infinite plate BJSFM solutions, the solid line represents the BJSFM solution corrected using the DeJong finite-width approximation method, and the triangular symbols represent the finite element solution. Results indicated that for an e/D of 9, the BJSFM solutions, corrected for finite width, correlate extremely well with finite element solutions where W/D ratios were greater than 4. However, as indicated in this graph, at an e/D value of 3, BJSFM infinite-plate solutions that were approximately corrected for finite widths (long-dash line), while significantly improved over the original BJSFM infinite-plate solution (short-dash line), still differ from the correct finite geometry solution (triangle symbol line). Full correction for finite geometry is anticipated using boundary collocation procedures currently under development at MCAIR.

SMALL EDGE DISTANCE

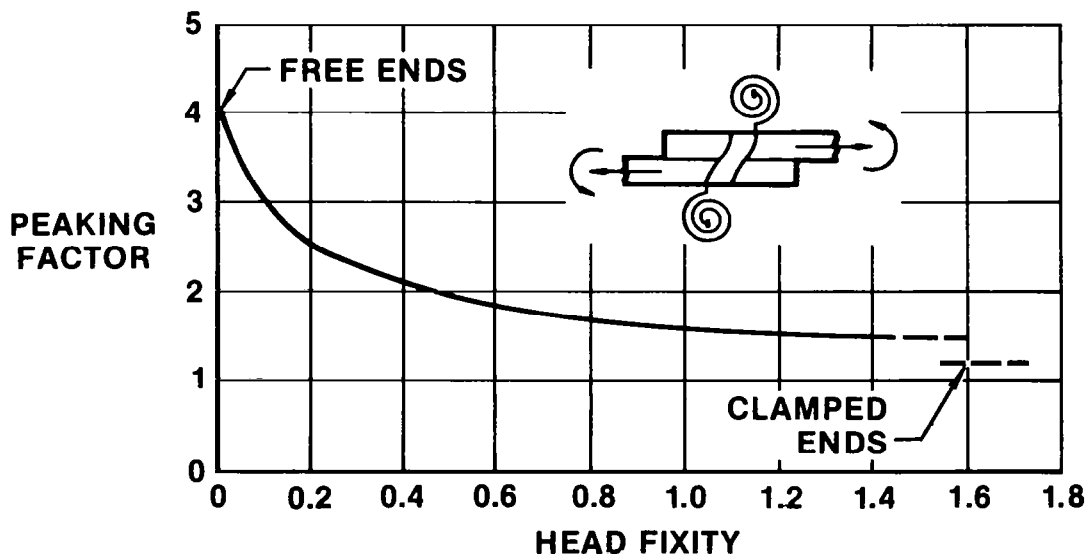


THROUGH-THE-THICKNESS ANALYSIS

The previous results ignore thickness-direction variables. These variables can be important and additional procedures are required to account for their effects. Some of the related through-the-thickness variables are listed here. New procedures using beam-on-elastic foundation theory are currently being developed at MCAIR to examine the effect of these design variables on fastener-to-joint-member spring rates and on bearing stress distributions in the thickness direction. Preliminary results of one parametric study are shown that relate the peaking of bearing stresses (relative to an average bearing distribution) to fastener head fixity.

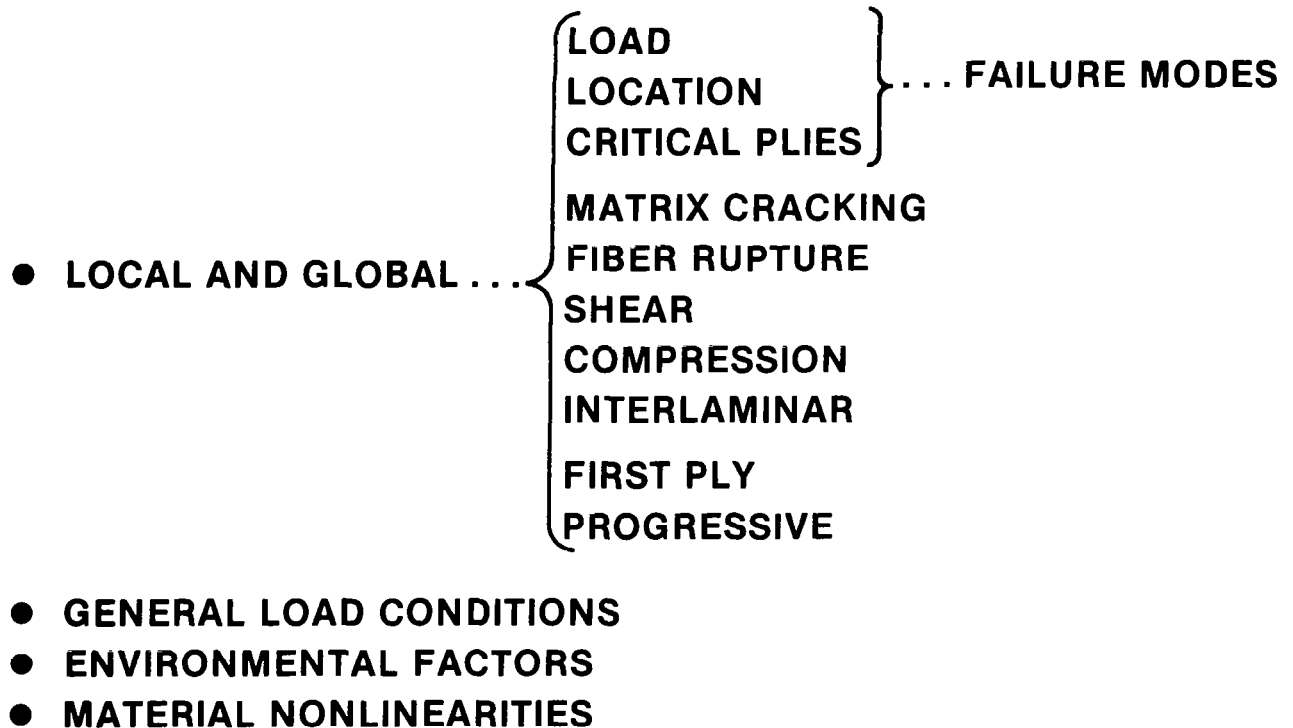


- JOINT ECCENTRICITY
- INTERLAMINAR STRESSES
- STACKING EFFECTS
- THICKNESS EFFECTS
- ORTHOTROPY EFFECTS
- FASTENER FIT
- INTER-PLY REINFORCEMENTS



STRENGTH ANALYSIS

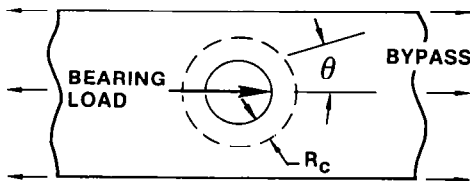
Given a detailed ply-by-ply stress analysis, strength predictions using the characteristic dimension failure hypothesis can be made. Point material failure criteria (Tsai-Hill, maximum strain, etc.) are used to predict ply matrix, fiber, or shear failure about the fastener hole at a distance R_C away from the hole boundary. This is automatically performed by the BJSFM program by comparing the complete stress (strain) solution about the fastener hole boundary with user-selected material failure criteria. Critical plies, failure loads, and locations are identified. However, in addition to failure at a point, the "patterns" of failure must be evaluated to predict overall joint modes of failure such as bearing, shearout, or net section. Examples of these predictions and correlations with data are presented in the following illustrations.



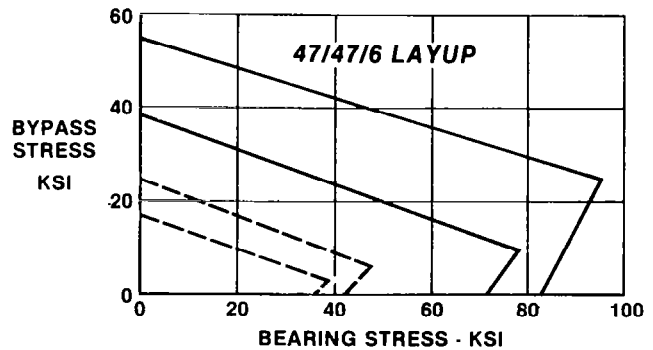
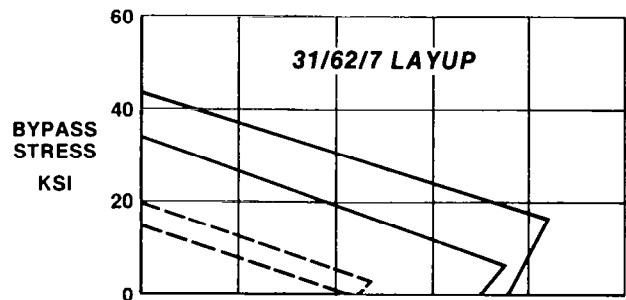
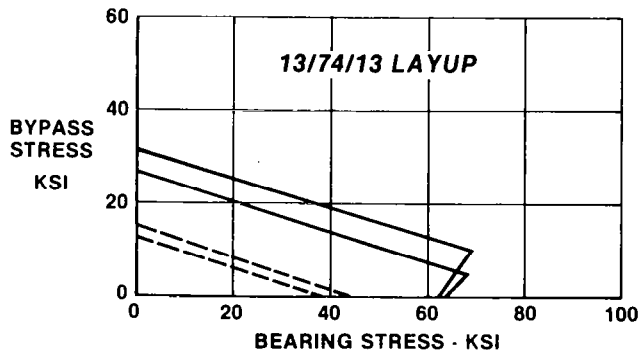
BEARING/BYPASS STRENGTH PREDICTIONS

Examples of laminate strength predictions under general bearing and bypass loadings are presented for a wide range of layups. The higher stress predictions of each of the solid and dashed line sets represent predictions at the characteristic dimension away from the hole boundary. The solid line represents predicted ply fiber or shear failure and correlates within ± 10 percent with the test data for this wide range of layups. The dashed lines represent predicted matrix failure (i.e., matrix cracking due to tensile load transverse to fibers) but no correlation of this predicted failure with changes in mechanical properties was observed, and this type of ply failure was ignored in all subsequent analyses. The lower strength predictions of each of the solid and dashed line sets represent application of failure criteria on the hole boundary. The difference between predictions on the hole boundary ($R_c = 0.0$ inch) or away from the hole boundary ($R_c = 0.02$ inch) correlates with the conservatism inherent in strictly using elastic stress concentration factors to predict strength.

PREDICTED PLY MATRIX, FIBER, AND SHEAR FAILURES

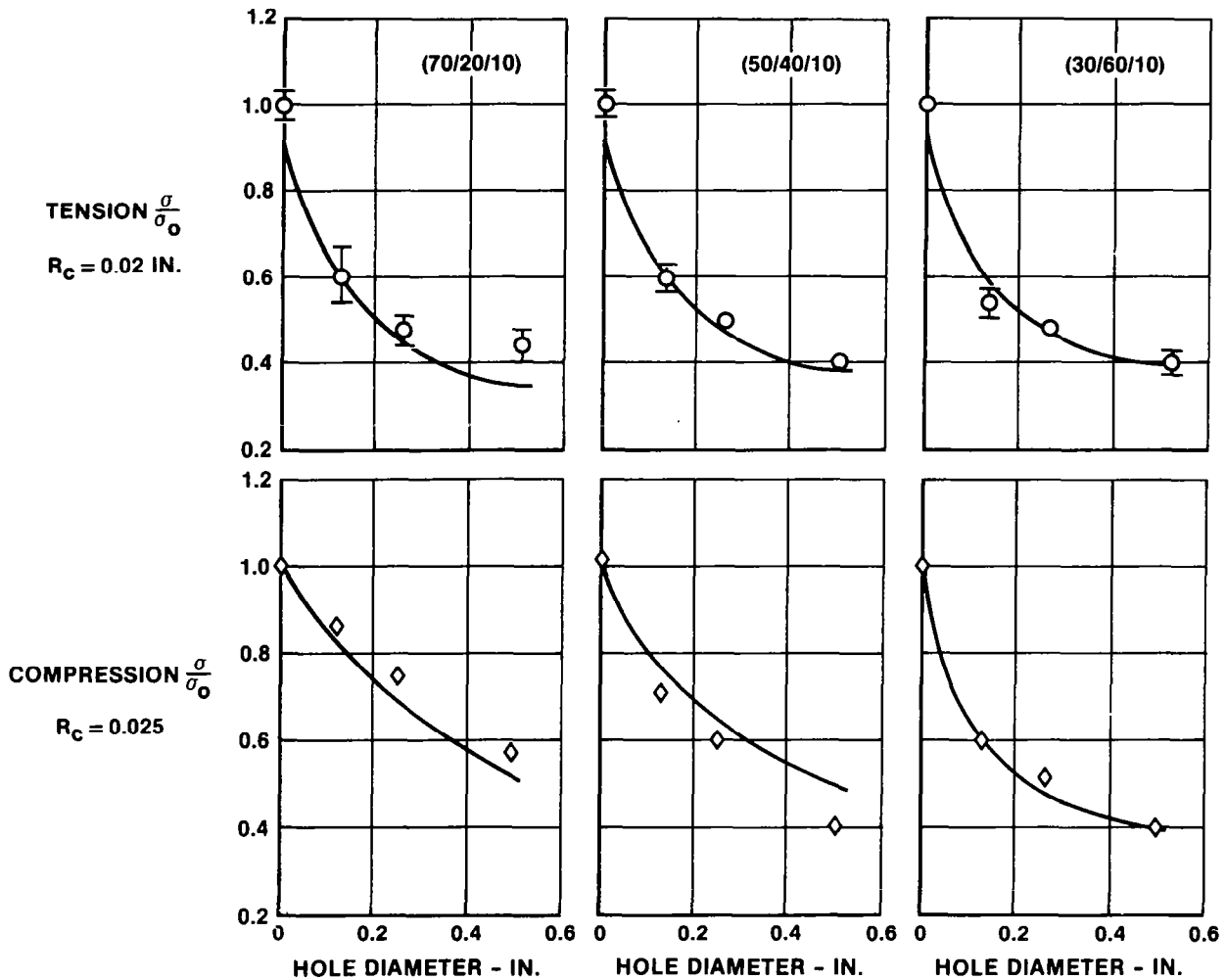


— Ply fiber or shear failure
 - - - Ply matrix failure



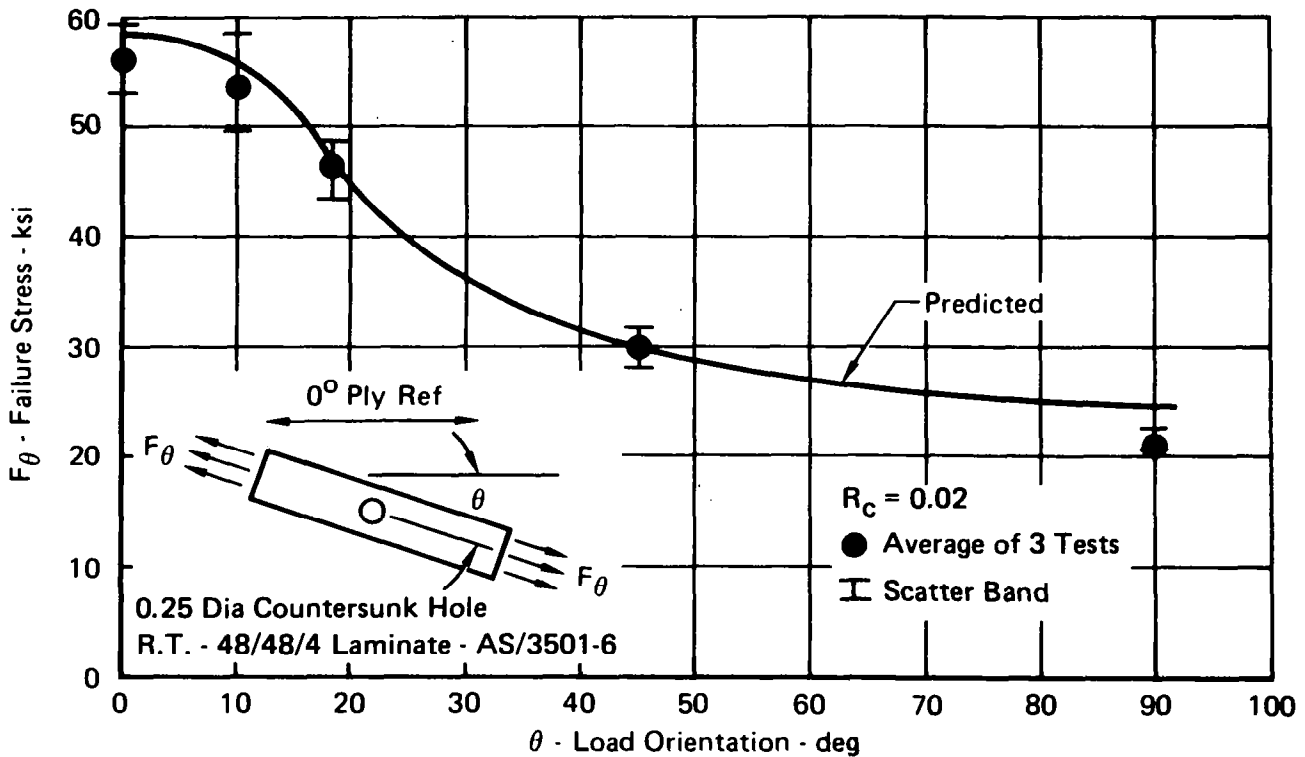
HOLE SIZE AND LAYUP EFFECTS

Hole size effects are accounted for analytically. Stress gradients at the edge of the hole vary with hole size and laminate orientation. Smaller diameter holes produce steeper stress gradients which decay rapidly as the distance from the hole is increased. This confines maximum stress to a smaller area in the laminate; thus a laminate has greater load-carrying capability with a small hole than with a larger hole. Analytical correlation is shown with strength data for various hole sizes and laminates loaded in tension and compression.



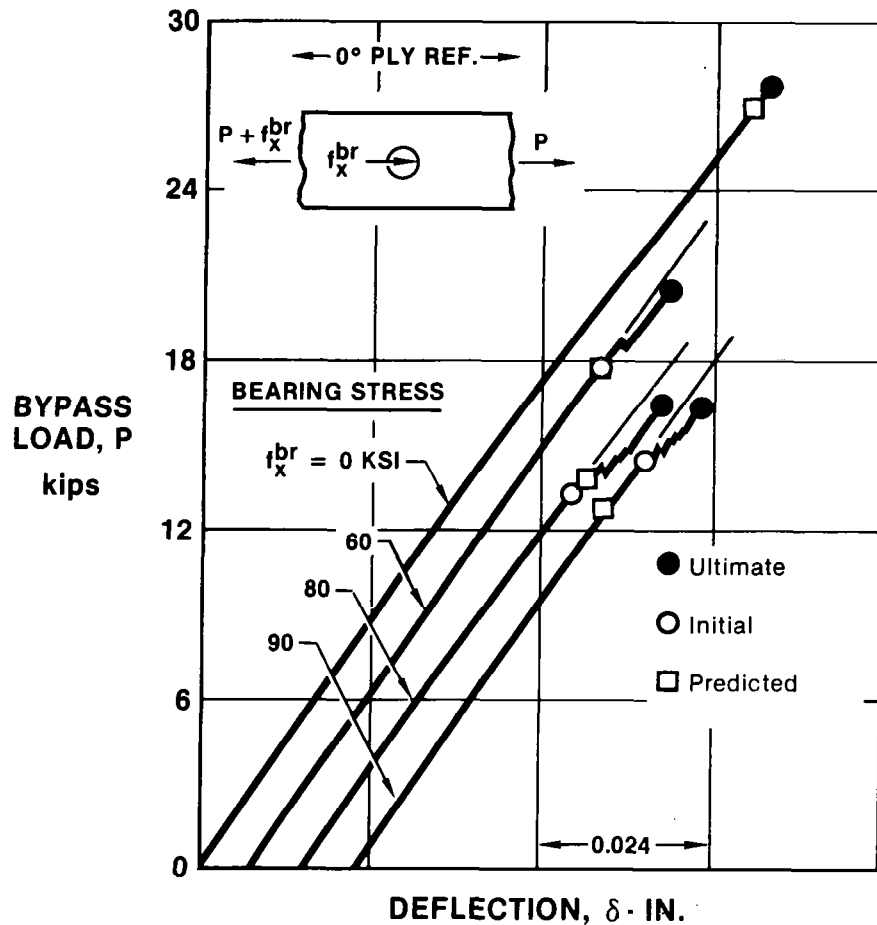
OFF-AXIS TESTING

Test data are compared with predictions for a laminate with a countersunk hole that is loaded to failure uniaxially at various angles relative to the principal material axis. Countersunk fastener holes were analyzed as being equivalent in diameter to a constant-diameter hole which displaces the same volume of material as the countersunk hole. The correlation shows that the BJSFM procedure can account for countersunk hole configurations, strength anisotropy, and off-axis loadings while using a constant characteristic dimension (R_C).



REPRESENTATIVE LOAD-DEFLECTION DATA FOR 50/40/10 LAYUP

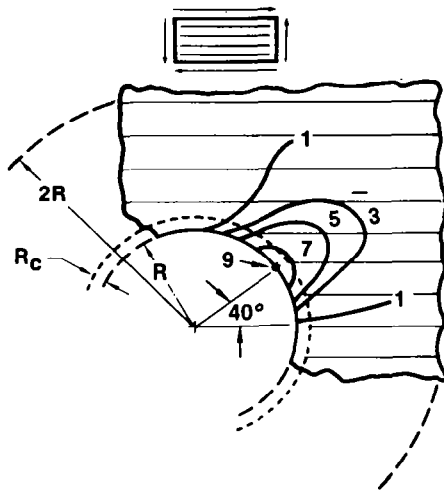
The previous theory-test correlations presented strength data for laminates with an unloaded hole. As bearing stresses are applied to the hole boundary, bypass strength decreases and noncontinuous or nonlinear load-deflection behavior is observed prior to specimen ultimate failure. At low bearing stress conditions, strength predictions based on first-ply fiber failure correlate very closely with the ultimate specimen strength. However, as bearing loads increase, first-ply fiber and shear failures correlate with the occurrence of initial nonlinear or discontinuous load-deflection behavior.



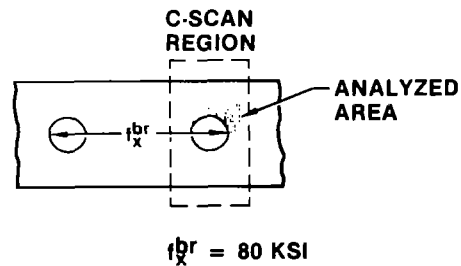
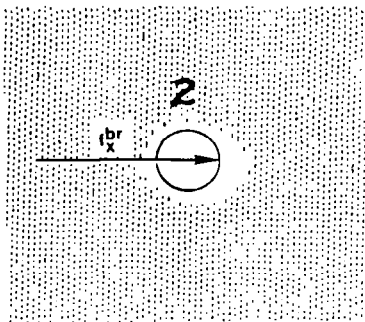
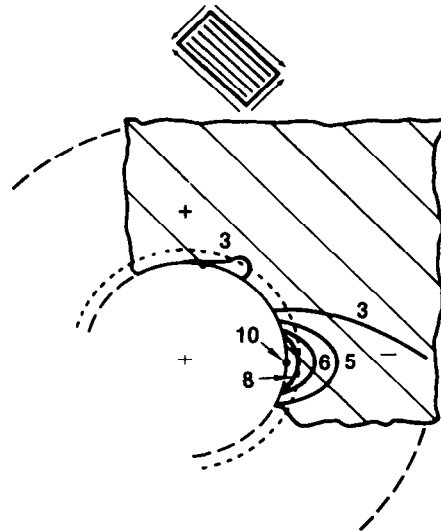
BEARING-ONLY LOAD CONDITION

The local nature of failure due to pure bearing loads is examined analytically using the BJSFM procedure. The results shown indicate the critical plies and contours of equal strain levels for an 80-ksi bearing load when first ply failure is predicted. Ply failures occur at 0° and 45° due to excessive shear. The contours indicate where failure patterns in specimens would likely occur. The C-scan documents the occurrence of local damage at this bearing stress level, and qualitatively agrees with predicted failure contours.

SHEAR-CRITICAL 0° PLY



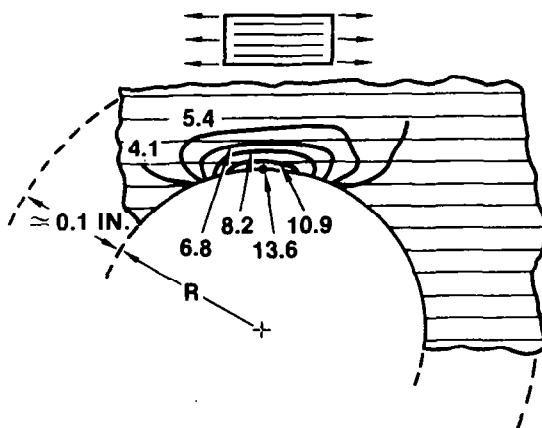
SHEAR-CRITICAL -45° PLY



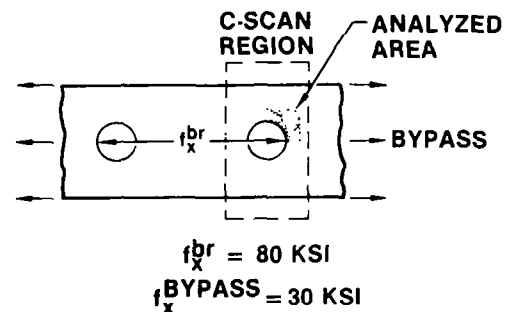
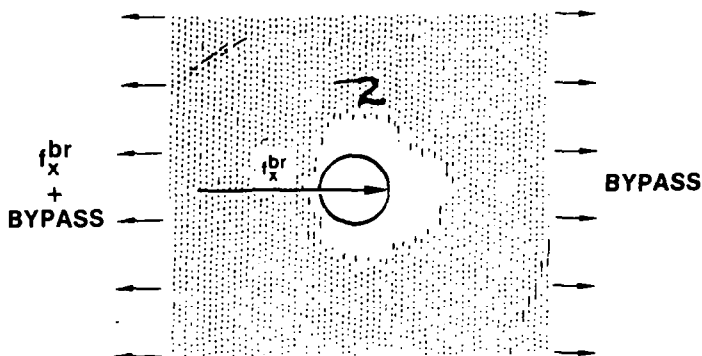
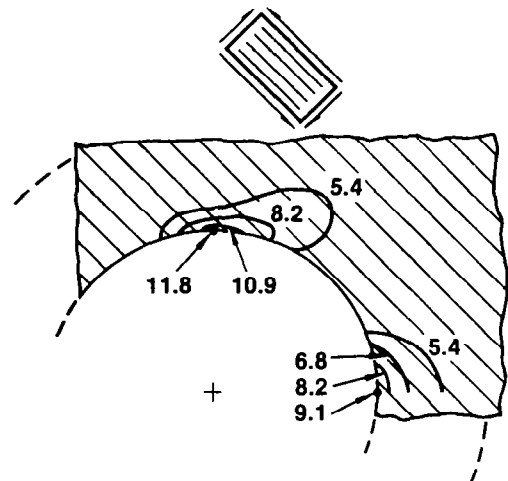
BEARING-PLUS-BYPASS LOAD CONDITION

The analysis of the previous pure bearing case was extended to include the added effect of a bypass load equivalent to a stress of 30 ksi. The critical plies and contours are indicated. The patterns have shifted to the net section and now the 0° ply has become fiber critical (before it was shear critical); the 45° ply is still shear critical, but this is now at the net-section region as well as in front of the bolt. The same specimen previously loaded to 80 ksi of bearing only was loaded to that same bearing load and then further loaded to a bypass stress of 30 ksi. The C-scan again qualitatively verified predicted failure patterns.

FIBER-CRITICAL 0° PLY



SHEAR-CRITICAL - 45° PLY

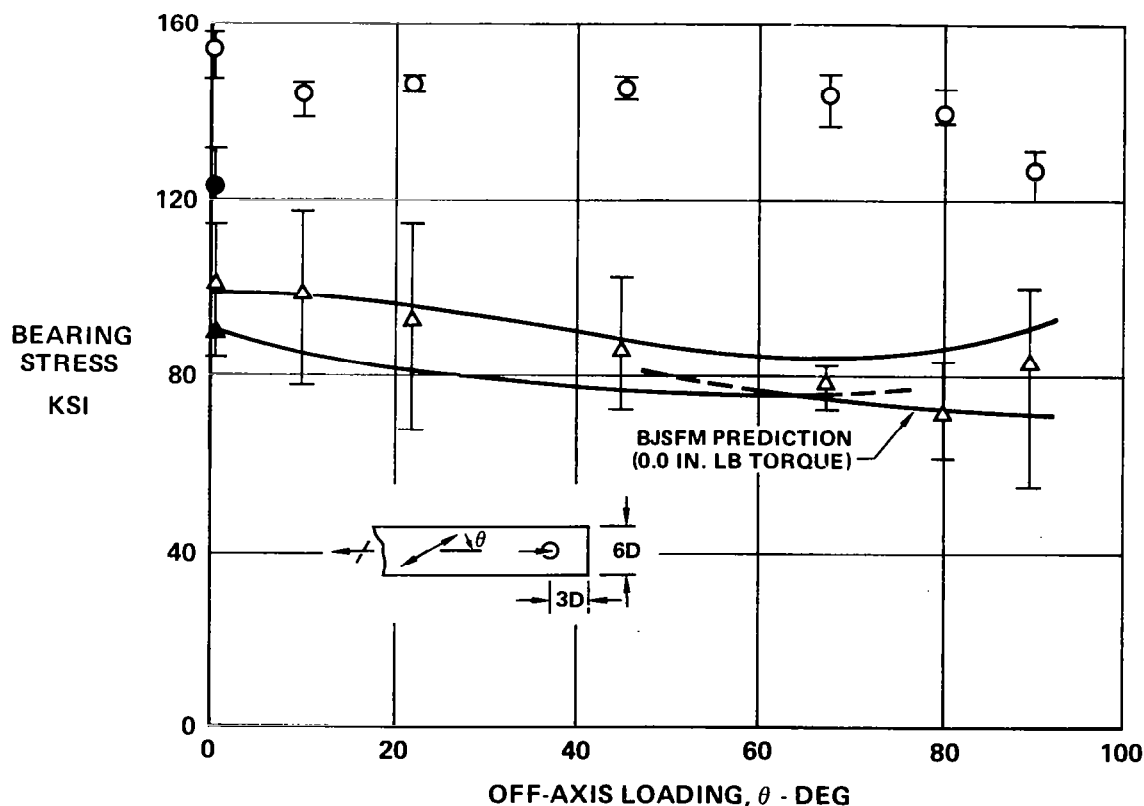


OFF-AXIS BEARING TEST DATA

In the off-the-principal-material-axis study, the BJSFM procedure was used to examine the directional dependence of pure bearing strength in a 50/40/10 laminate. Test data with scatter bands are compared with predictions. Onset of joint nonlinear load deflection behavior is indicated by open triangle symbols. Specimen ultimate bearing strengths are indicated by open circles and occurred at approximately 50 percent higher loads. Specimens failed predominantly in bearing shearout at off-axis load directions ranging from 0° to $22\frac{1}{2}^\circ$, tension-cleavage at the 45° off-axis load direction, and net-section failures at the $67\frac{1}{2}^\circ$ to 90° off-axis load directions. Solid symbols indicate specimens tested with no fastener torque-up; all others were torqued to 50 in.-lb. Strengths were predicted based on ply fiber or shear failure using the 0.02-in. characteristic dimension and the maximum strain failure criterion. Compared to off-axis loading of unloaded hole specimens, two important characteristics are predicted: (1) laminate strength is relatively constant over the entire range of off-axis load directions, and (2) $\pm 45^\circ$ and 90° plies are equally critical within 10 percent. This is in contrast to the unloaded hole case in which a pronounced sensitivity to off-axis bypass loading was observed and singular ply orientations were usually critical.

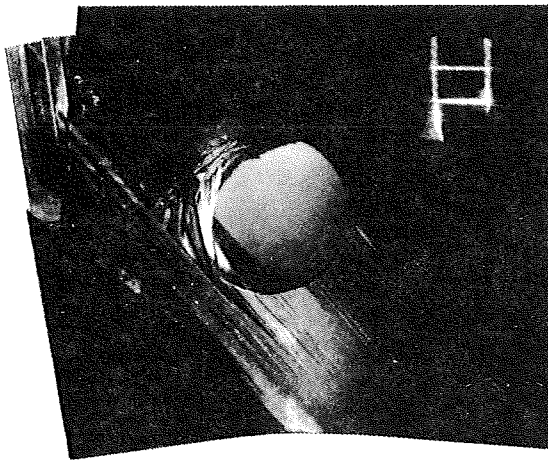
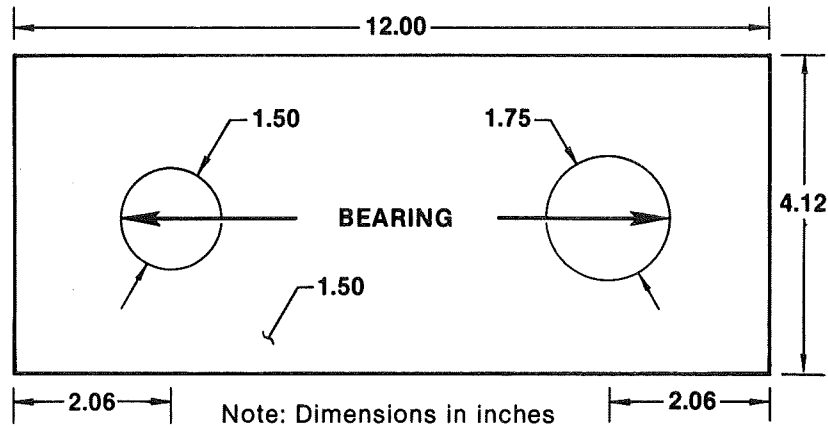
Unlike loads at onset of nonlinear joint load deflection behavior, test results indicate that ultimate bearing strengths are insensitive to off-axis loading effects at all but the 0° and 90° loading directions. In all cases, specimen failures occurred after permanent hole elongations had developed. The onset of the associated transition from linear to nonlinear failure modes was predictable using the linear-elastic BJSFM procedure.

(50/40/10 LAYUP)

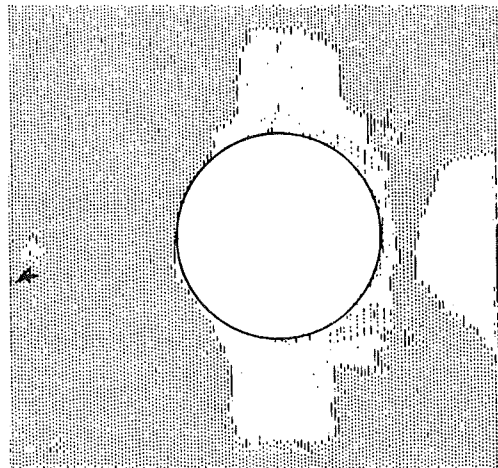


HIGH-LOAD LUG

A further verification of the BJSFM strength procedure was performed using a boundary collocation procedure to account for finite geometry effects. The 1.50-in.-thick specimen was designed to contain two different lug sizes that would be loaded in pure bearing. The lower left photograph indicates the failed left end, and the lower right C-scan documents the close-to-failure damage of the right end of the specimen. Failure modes of both ends were as predicted.



**PREDICTED
SHEAR FAILURE
154 kips**

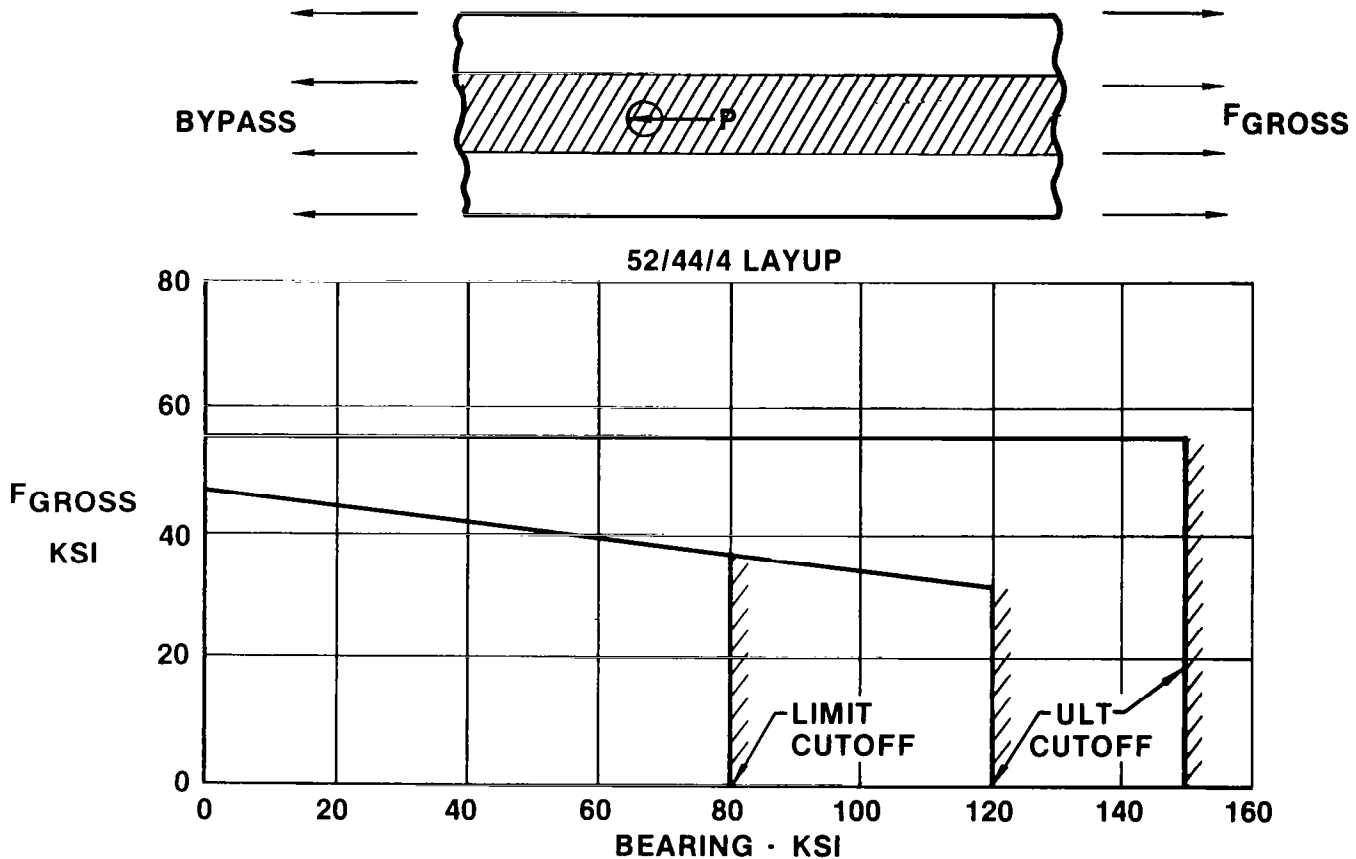


**PREDICTED
NET-SECTION
159 kips**

$P_{TEST} = 150$ kips

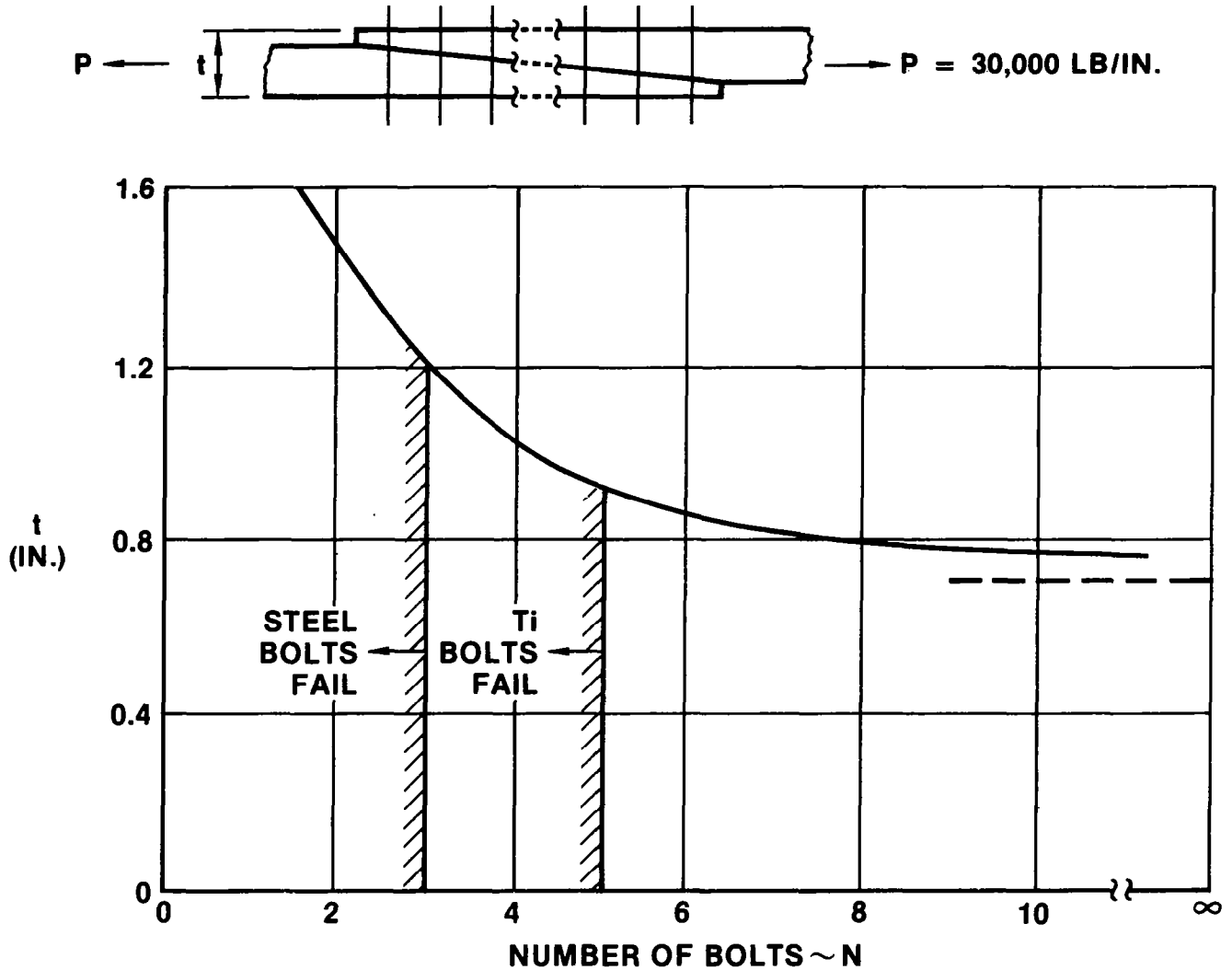
STRENGTH ENVELOPES FOR APPLICATIONS

The utility of the previous analytic procedures was recently demonstrated in a MCAIR/NADC-funded program (ref. 2) to design high-load-transfer metal-to-composite bolted joints applicable to a fighter wing root area. This graph indicates predicted strength envelopes used to design the required joint for either a monolithic 55/44/4 laminate (lower curve) or a locally softened 52/44/4 laminate (horizontal, upper curve) where 0° plies were replaced by $\pm 45^\circ$ plies local to fastener hole areas. For the monolithic case, the limit cutoff represents the predicted first-ply shear failures under pure bearing loads.



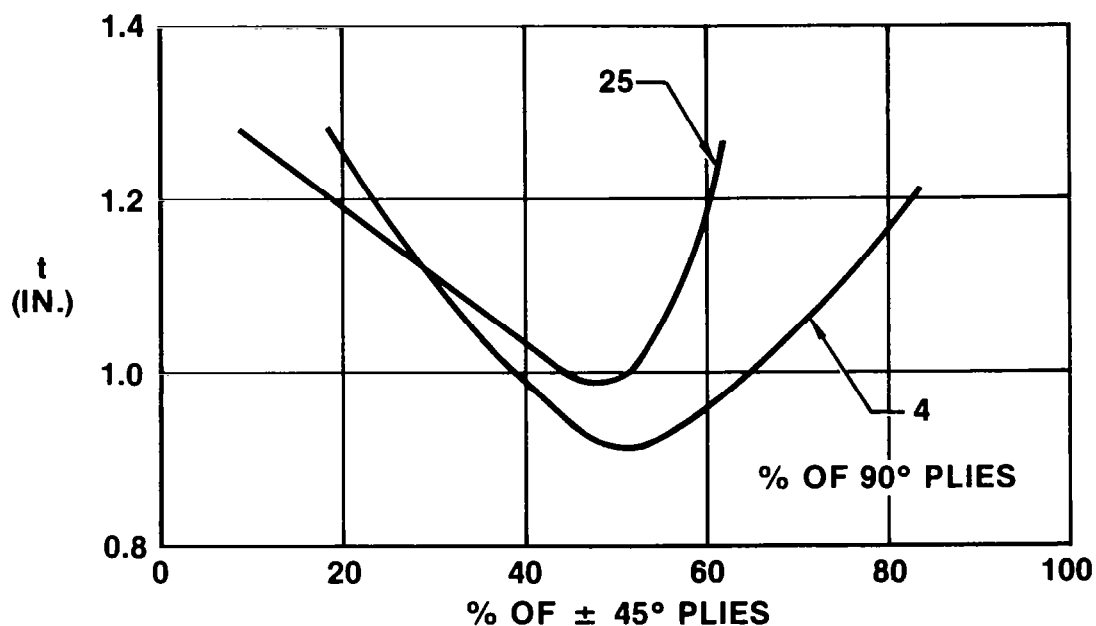
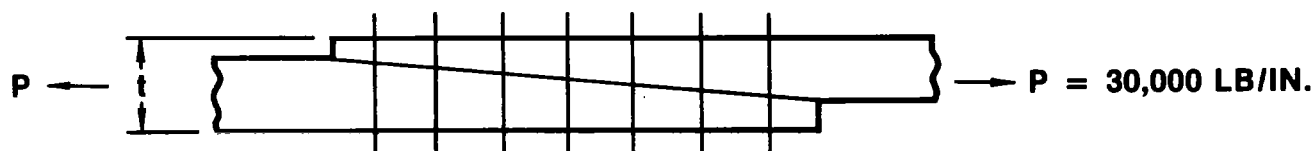
JOINT THICKNESS VERSUS NUMBER OF BOLTS

Based on a design ultimate load requirement of 30,000 lb/in., the previous strength envelope for the monolithic laminate was used to predict the number of in-line bolts required versus overall joint thickness. Cutoffs based on fastener shear strength are also indicated.



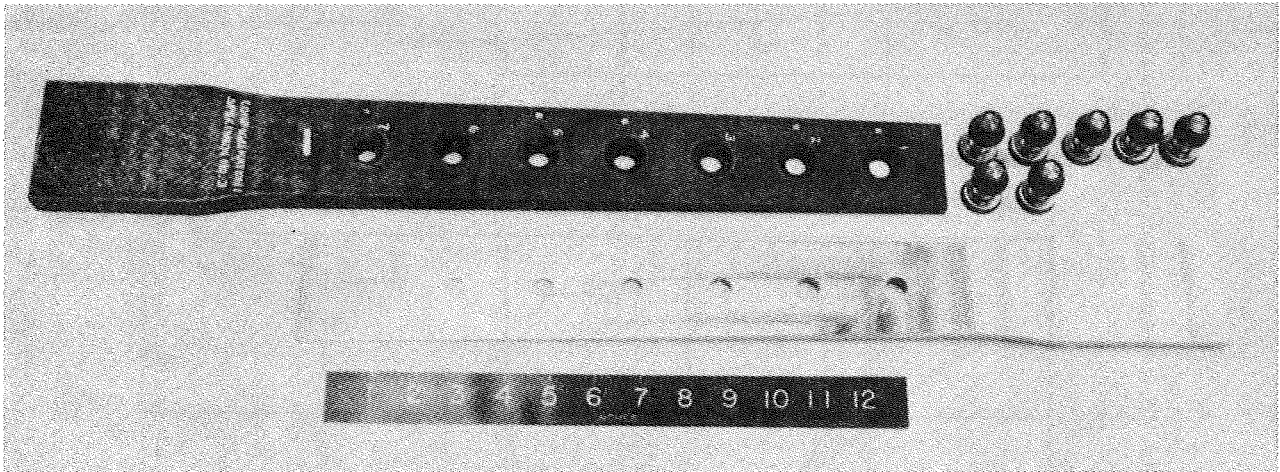
LAYUP VERSUS OVERALL JOINT THICKNESS

Based on a seven-bolt-in-tandem joint configuration, the BJSFM laminate strength procedure was used to efficiently evaluate the effect of layup variations on joint thickness. The results of this study are plotted for layups having 4 to 25 percent of their 90° plies aligned with the chord direction of the baseline wing; the remaining plies were oriented in the spanwise (0°) direction.



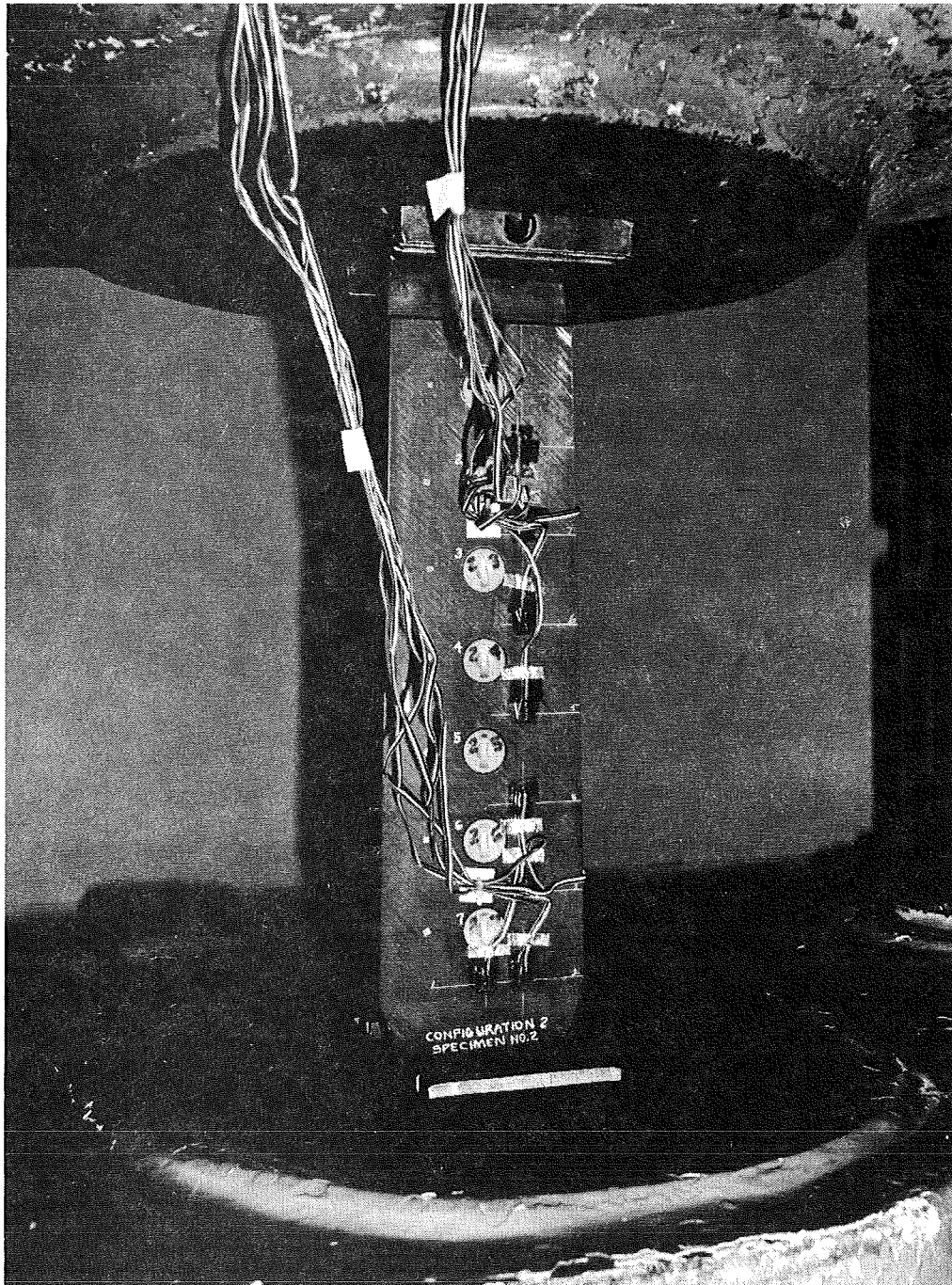
SCARFED MONOLITHIC-LAMINATE TEST SPECIMEN

Based on the results of the previous two analytic studies, scarfed monolithic-laminate and scarfed softened-laminate specimens were fabricated to verify predictions. The graphite-epoxy and titanium members are shown with the 0.50-in.-diameter fasteners used in the monolithic-laminate design. The specimen is representative of a single column of a wing root splice that would be spaced every 2.50 in. across the chord of the wing root.



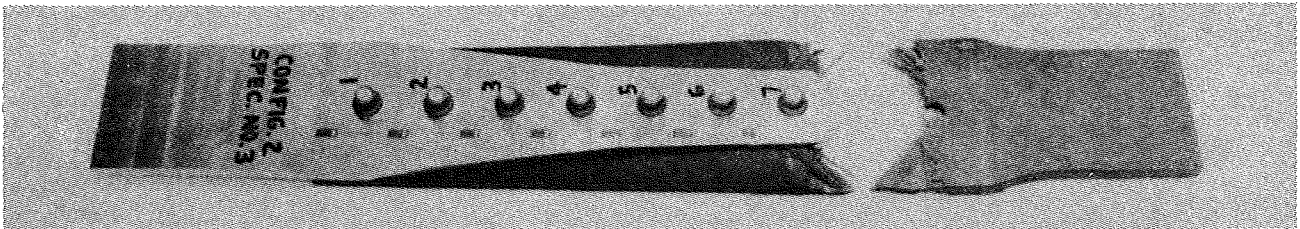
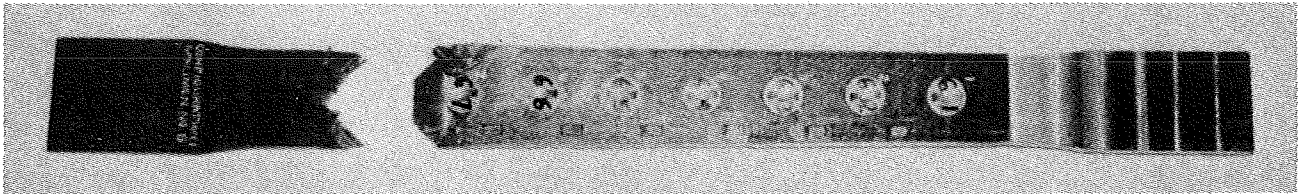
SCARFED SOFTENED-LAMINATE TEST SPECIMEN

The scarfed softened-laminate splice is shown assembled and strain gaged prior to test. The softened-laminate splice test specimen represents a single spanwise column of the wing root design which would be repeated approximately every 10 in. across the chord of the baseline wing root area. The taper of the planform was designed to simulate the gradual increase of spanwise loading due to increased wing bending moments encountered closer to the root area.



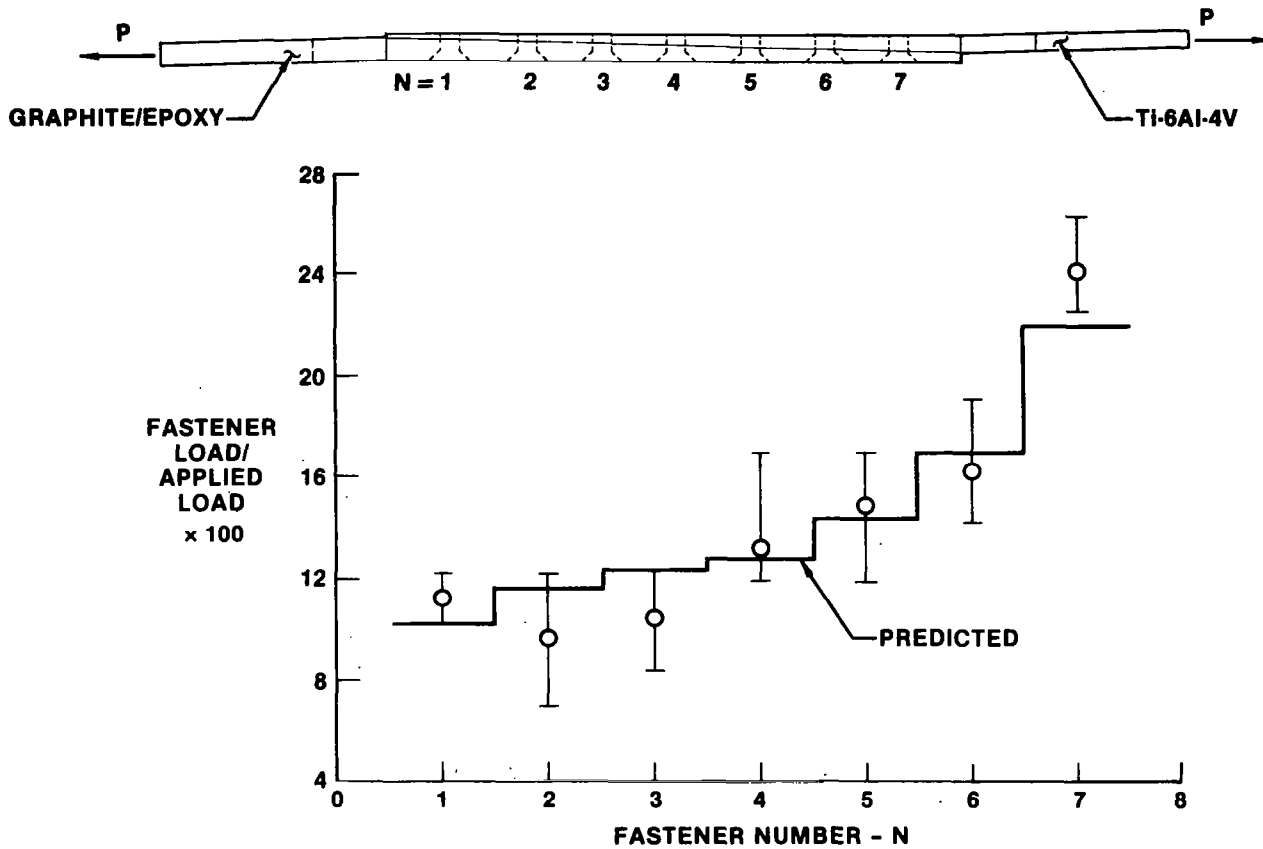
REPRESENTATIVE STATIC FAILURES

The scarfed monolithic-laminate splice (upper photo) and softened-laminate splice (lower photo) are pictured after static failure. As predicted, both specimens failed in the net-section area of that fastener location having the highest bypass load. The static joint failure load for the monolithic-laminate was 68 kips; the softened-laminate failed at 125 kips. Both loads were within 10 percent of prediction.



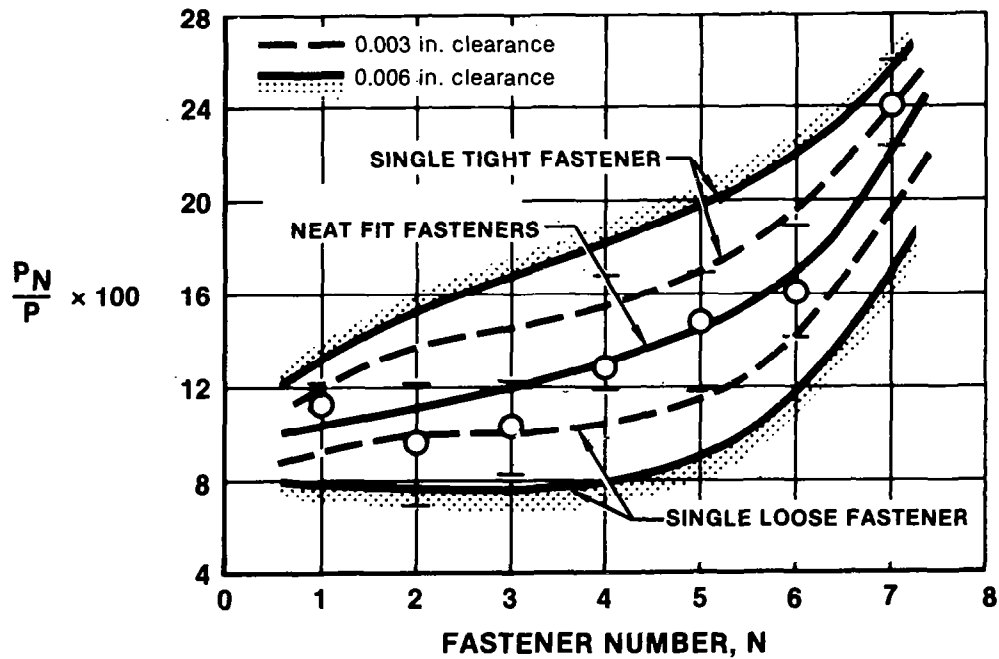
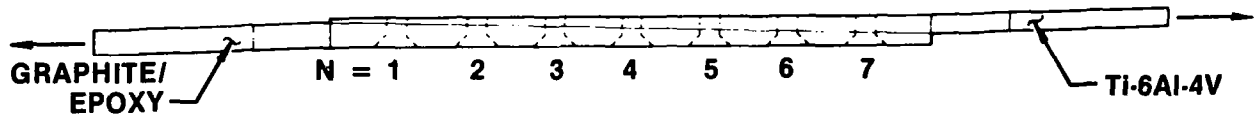
BOLT LOAD DISTRIBUTIONS

Correlations between predicted bolt load distributions and test are indicated for the scarfed monolithic-laminate splice. The predicted distribution is based on neat-fit fasteners with member and fastener flexibilities accounted for.



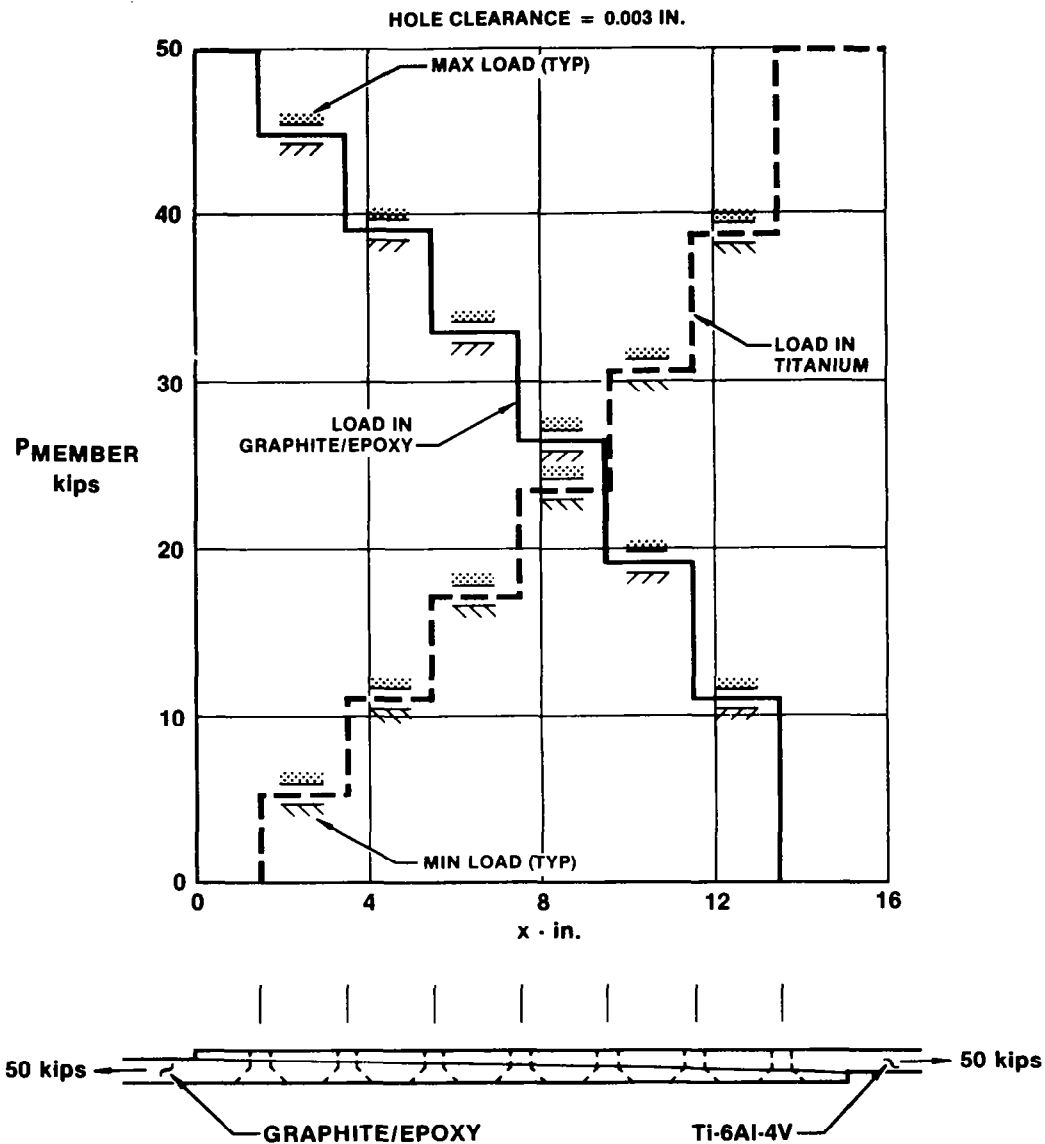
EFFECT OF HOLE CLEARANCES ON BOLT LOADS

To investigate the cause of scatter in bolt load distributions, the effect of a 0.003-in. and 0.006-in. clearance at each of the fasteners was analyzed. The results illustrated in this figure offer a possible explanation of the scatter and indicate the importance of this variable.



EFFECT OF HOLE CLEARANCE ON LOCAL MEMBER LOADS

The occurrence of a 0.003-in. clearance on each of the fasteners was evaluated relative to its effect on joint member loads. Unlike its effect on bolt loadings, when the area of the joint members is taken into account, the effect of clearance on joint member loading is relatively small.



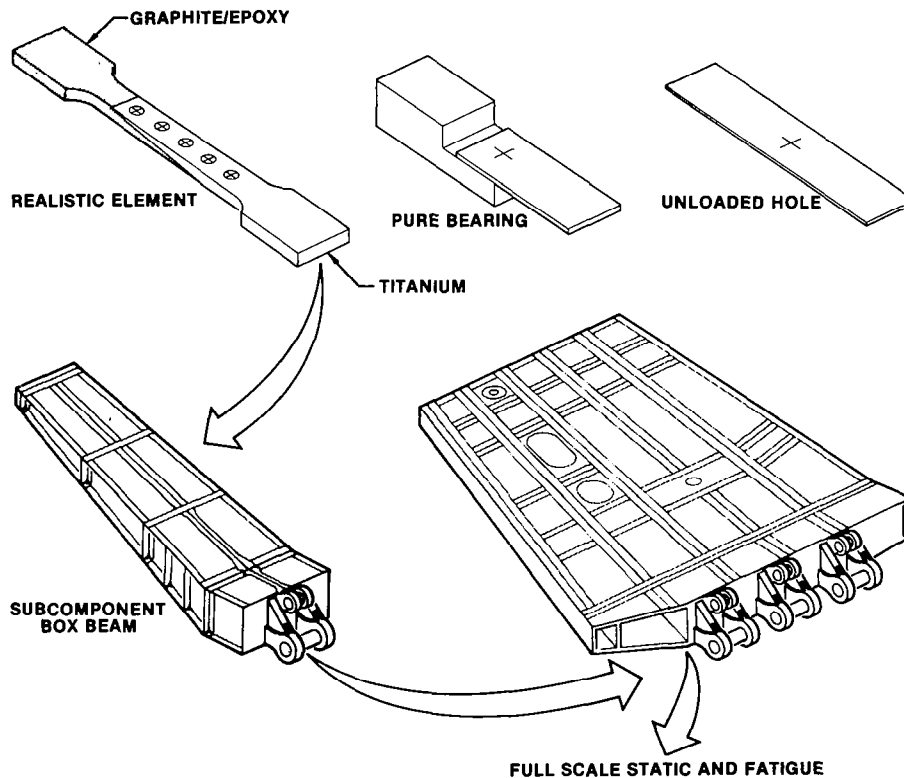
CONCLUSIONS

As a backdrop for conclusions, this sketch idealizes the evolution of structural testing typical of project hardware development programs. Usually testing proceeds from simple coupon specimens to more structurally detailed element specimens, then to subcomponent box beams, and finally to full-scale static and fatigue-test articles. For the application of composites the testing requirements are extensive and costly, especially for establishing material allowables, because of loading possibilities and geometry effects which change for each laminate variation.

The BJSFM analysis procedure should considerably reduce the need for coupon testing relative to laminate variations, hole size, general bearing/bypass load interactions, and environmental test conditions.

Analysis and experimental data were compared to verify that the BJSFM procedure accurately predicts laminate strength under general tension and compression bearing/bypass loadings. Theoretical studies were reported which demonstrated method utility and the need for detailed stress solutions. Correlations between the closed-form BJSFM stress solutions and finite element solutions were reported which defined current program finite geometry limitations.

Three benefits are provided by using the BJSFM procedure. (1) Test data requirements are minimized, requiring only knowledge of mechanical properties for the unidirectional-ply and one-laminate configuration. (2) Design conservatism and unconservatisms can be reduced through this accurate, comprehensive, and inexpensive analysis. (3) parametric evaluations of failure mechanisms can easily be conducted to provide guidance for the design of efficient bolted composite joints.



REFERENCES

1. Garbo, S. P.; and Ogonowski, J. M.: Effect of Variances and Manufacturing Tolerances on the Design Strength and Life of Mechanically Fastened Composite Joints. AFWAL-TR-81-3041, Air Force Wright Aeronautical Laboratories, 1981.
2. Buchanan, David L.; and Garbo, S. P.: Design of Highly Loaded Composite Joints and Attachments for Wing Structures. NADC-81194-60, Naval Air Development Center, 1981.
3. Whitney, J. M.; and Nuismer, R. J.: Stress Fracture Criteria for Laminated Composites Containing Stress Concentrations. J. Composite Mater., vol. 8, 1974, pp. 253-265.

**SAFE-LIFE AND DAMAGE-TOLERANT DESIGN
APPROACHES FOR HELICOPTER STRUCTURES**

Harold K. Reddick, Jr.
Applied Technology Laboratory
US Army Research and Technology Laboratories (AVRADCOM)
Ft Eustis, Virginia

INTRODUCTION

The safe-life and damage-tolerant design approaches presented herein apply to both metallic and fibrous composite helicopter structures. However, to maintain the theme of this workshop, this presentation will emphasize the application of these design approaches to fibrous composite structures.

In the current generation of Army helicopters, such as the UH-60 Black Hawk shown in Figure 1, composite materials make up as high as 17 percent of the airframe and rotor weight. With the advent of major helicopter composite structures R&D projects, such as the Advanced Composite Airframe Program (ACAP), and Manufacturing Methods and Technology (MM&T) projects, such as UH-60 Low Cost Composite Blade Program, it is estimated that within a few years composite materials could be applied to as much as 80% of the airframe and rotor weight of a helicopter in a production program. Along with this application is the essential requirement that sound, definitive design criteria be developed in order that the composite structures possess high fatigue lives for economy of ownership and good damage tolerance for flight safety.

Safe-life and damage-tolerant criteria are applied to all helicopter flight critical components, which are generally categorized as follows:

- Dynamic components - main and tail rotor system, which includes blades, hub and rotating controls, and drive train which includes transmission, and main and interconnecting rotor shafts.
- Airframe - fuselage, aerodynamic surfaces and landing gear.



Figure 1

TYPICAL STRESS SPECTRA FOR A HELICOPTER BLADE ROOT END AND TRANSPORT AIRPLANE ROOT END

The dynamic components previously described tend to be fatigue critical. Although fatigue problems have been known to occur within the helicopter airframe, it for the most part is designed by strength and minimum gage.

Figure 2 shows a typical comparison of the stress history for a transport helicopter blade root end and that for a typical commercial transport wing root. The helicopter dynamic components tend to be loaded at frequencies that are a multiple of rotor speed - typically 2 to 20 Hz. This loading rate represents 7 million to 70 million cycles per 1000 operating hours. Thus these components experience a much higher frequency of cyclic loading but with a narrower spread of the loading than the fixed wing aircraft component.

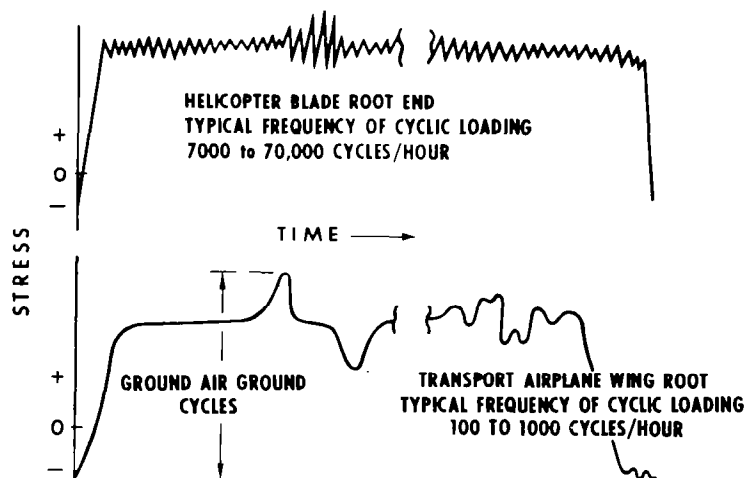


Figure 2

SAFE LIFE PHILOSOPHY

The safe-life design approach is stated in Figure 3. It applies to statistically predictable failures which are those occurring from the random combination of fatigue strength and applied fatigue loads.

**ALL FATIGUE CRITICAL COMPONENTS OF
THE HELICOPTER ARE DESIGNED TO A
SPECIFIC SERVICE LIFE, IN OPERATIONAL
HOURS, AND ARE REMOVED FROM SERVICE
AT OR BEFORE THIS ELAPSED TIME SO
THAT THE PROBABILITY OF A FATIGUE
FAILURE IS REMOTE**

Figure 3

SAFE-LIFE METHODOLOGY

The methodology for the fatigue design of primary structural components is schematically outlined in Figure 4. The three basic elements of safe-life design include:

- Working Fatigue S-N Curve -- developed based upon coupon tests to determine curve shapes, full-scale specimen tests to provide data points for constructing a mean curve, and then a statistical reduction of the mean curve to a "working" curve upon which the damage calculations are based. A minimum of six full-scale test specimens are generally required to establish the mean curve. The statistical reduction is made on the stress (and not cycles) for it is the high cycles region of the S-N curve at which fatigue loading occurs.

- Design Loading Spectra - developed from the mission profile which is a prediction of how the aircraft shall be used, and the flight loads which are developed for the various maneuvers and flight conditions of the helicopter's mission profile. Obviously in the development of a new helicopter system, these loads must initially be either predicted or empirically derived from measured loads on similar helicopters.

- Cumulative Damage Theory - the combination of loads and fatigue strength by means of a cumulative damage theory results in the component fatigue life.

The safe-life methodology outlined herein typifies that used by most US and European helicopter manufacturers (references 1 through 3) although specific approaches for analysis of the loads and the material fatigue data vary with the manufacturers.

For the UH-60 Black Hawk and the YAH-64 Apache, the Army's more recent helicopter development programs, the minimum required fatigue life for all dynamic components has been 5,000 and 4,500 flight hours, respectively. Many of the components on these aircraft have exceeded their minimum fatigue life requirement.

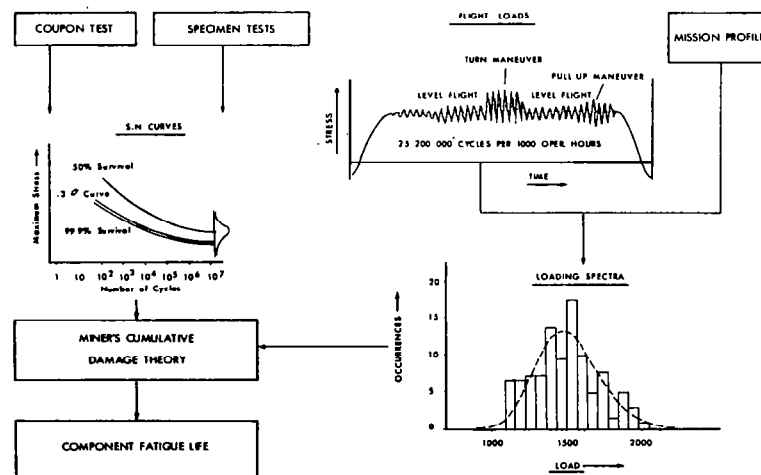


Figure 4

FAILURE RATE VS FLIGHT HOURS

The safe-life design approach, when properly executed, places statistically predictable failures at an extremely remote probability of occurrence. This approach does, however, assume the structure to be flaw free. Over the years operational experience has shown (references 4 through 6) that the safe-life approach by itself is not adequate because of unpredictable failures resulting from such sources as manufacturing defects and service-induced damage (see Figure 5). Furthermore, review of this operational experience has shown these unpredictable failures to far outnumber the predictable ones.

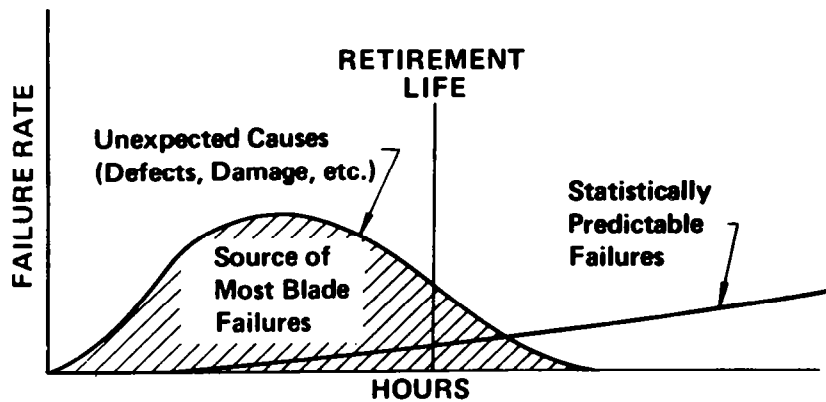


Figure 5

DAMAGE SOURCES

The statistically nonpredictable failures discussed in the previous figure result from one of three categories of damage - initial, as originating from material defects or manufacturing-induced anomalies, service-induced or ballistic. Examples for each of the damages are presented in Figure 6. Ballistic damage is certainly an in-service occurrence; however, because of the extreme nature of this damage and its associated short residual life requirement (30 minutes to roughly 5 hours), is generally addressed separately from the other damage types, and shall not be discussed herein.

- DESIGN ERRORS
- MATERIAL—AND MANUFACTURING—INDUCED DEFECTS
 - IMPROPER LAYUP
 - INCORRECT/INCOMPLETE CURING
 - MACHINING ERRORS
 - HANDLING/ASSEMBLING AREAS
- SERVICE INDUCED DAMAGE
 - FOREIGN OBJECT DAMAGE (FOD)
 - MAINTENANCE ERRORS
 - GROUND HANDLING
- BALLISTIC DAMAGE
 - SMALL ARMS PROJECTILES (7.62mm & 12.7mm)
 - HIGH EXPLOSIVE INCINDIARY (23mm HEI-T)

Figure 6

EARLY DAMAGE TOLERANCE REQUIREMENTS

Although damage tolerance as we know it today is a relatively new technology, its importance was recognized as long as four centuries ago. Near the end of the fifteenth century, technical notes were written on what must have been one of the first requirements for damage-tolerant design. They were in the notebook of Leonardo da Vinci in which he discussed the physics of flight and the design of "flying machines," and are shown in Figure 7 (reference 7).

In the early 60's a fail-safe design philosophy began to evolve within the rotary wing industry and has been used in numerous applications for both metallic and fibrous composite structures (references 8 through 10). The safeguard in the fail-safe approach is that damage, induced or fatigue, will be detected by inspection procedures before it grows to such an extent that the residual strength of the structure is reduced below a safe level.

In the early 70's a third design philosophy - damage tolerance - began to evolve. It is similar to the fail-safe approach but further considers the growth of damage resulting during manufacture or service usage. Therefore, fundamental to the damage-tolerant approach is an understanding of structural performance in the presence of defects or damage.

"IN CONSTRUCTING WINGS ONE SHOULD MAKE ONE CORD TO BEAR THE
STRAIN AND A LOOSER ONE IN THE SAME POSITION SO THAT IF ONE
BREAKS UNDER STRAIN THE OTHER IS IN POSITION TO SERVE THE SAME
FUNCTION"

FROM LEONARDO DA VINCI'S NOTEBOOK
ON DESIGN OF "FLYING MACHINES"
15TH CENTURY

Figure 7

DAMAGE TOLERANCE PHILOSOPHY

Damage tolerance is a safety requirement and equates to the fail-safe design approach employed for flight critical components by the rotary wing industry since the early 60's. Damage tolerance is the ability of the structure to resist failure due to the presence of defects, cracks, or other damage for a time period sufficient to enable their detection.

The essential elements of damage tolerance are presented in Figure 8. In designing to this philosophy, the criteria must address both the static residual strength and damage propagation for the structure under consideration.

The fail-safe and damage tolerance design philosophies each have the common objective of providing structural integrity at a reasonable level of assurance for all safety-of-flight structures, that is structure whose failure could cause direct loss of the aircraft. Reference 5 points out an important distinction between fail safety and damage tolerance. Fail safety as it was defined prior to the evolution of damage tolerance is based upon the premise that one cannot be certain that cracks (or damage) will not initiate at some time during the aircraft life and these cracks must be detected before the strength drops below a certain level. Damage tolerance, on the other hand, assumes the existence of initial flaws in the structure and the structure is designed to retain adequate residual strength until damage is detected and corrective actions taken.

Although the damage-tolerant approach has begun to see a more widespread usage within the Army, there is still considerable work to be accomplished in developing specific requirements and procedures for this design approach.

The basic philosophy of damage tolerant design is based upon:

- **THE ACCEPTANCE THAT DAMAGE WILL OCCUR**
- **AN ADEQUATE SYSTEM OF INSPECTION SO THE DAMAGE MAY BE DETECTED**
- **AN ADEQUATE STRENGTH MAINTAINED IN THE DAMAGED STRUCTURE**

Figure 8

RESIDUAL STRENGTH AND DAMAGE GROWTH

The damage-tolerant requirement, which is illustrated schematically in Figure 9, addresses both the residual strength and the damage propagation for the structure under consideration.

The residual strength is the amount of static strength available at any time during the service exposure with damage present. Safety is ensured by designing to requirements wherein damage is never allowed to grow and reduce the residual static strength of the structure below a specified value, such as that corresponding to the maximum load to be experienced in service.

The damage growth curve presents damage size as a function of time. The period of time required for damage to grow from a minimum detectable size, such as by in-service inspection, to a critical size is the detection period. The critical size generally corresponds to the maximum service load residual strength, although for composites this value could be dictated by stiffness loss to a critical value.

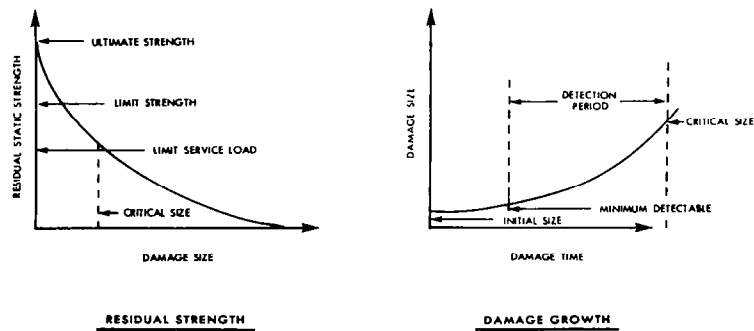


Figure 9

DAMAGE TOLERANCE APPROACHES

Damage tolerance may be achieved in one of two different methods as shown in Figure 10. In fail-safe structures, damage tolerance (and their safety) is assured by the allowance of partial structural failure, the ability to detect this failure prior to total loss of the structure, the ability to operate safely with the partial failure prior to inspection and the maintenance of specified static strength throughout the period. Fail-safe structures are usually comprised of multiple elements or load paths such that damage can be safely contained by failing a load path or by arresting a rapidly running crack. In safe crack growth structures, damage tolerance is achieved by sizing the structure, using fracture mechanics or empirical data, such that initial damage will grow at a stable, slow rate and not achieve a size large enough to fail the structure prior to detection. A special case within this category is nonpropagating-defect structures wherein the structure is designed to sufficiently low stress levels for virtually no propagation of the largest defect that would not be detected during a production inspection or that could be incurred in service.

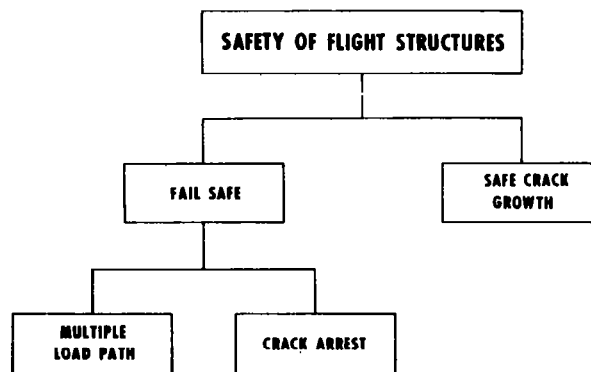


Figure 10

SAFE-LIFE AND DAMAGE TOLERANCE REQUIREMENTS FOR ARMY HELICOPTERS

The structural design specification for helicopter MIL-S-8698 imposes requirements for safe-life fatigue design of flight critical structures but not for fail-safe or damage tolerance design (Figure 11). In the more recent major helicopter system procurements, the Army has required fail safety or damage tolerance for the helicopter primary structure. These requirements have been stated in general terms as follows:

"The primary structure shall incorporate materials, stress levels, and structural configurations that will minimize the probability of loss of the aircraft due to damage of a single structural element (including control system or dynamic components), or due to propagation of undetected flaws, cracks, or other damage. Slow crack growth, crack arrestment, alternate load paths and systems, and other available design principles shall be used to achieve this capability.---"

Because of the general nature of these requirements, they were successfully applied to both metallic and fibrous composite structures (reference 11). It has been left up to the helicopter manufacturer to define the specifics such as damage or flaw sizes, inspection intervals, etc., subject, of course, to Government approval.

- MIL-S-8698, STRUCTURAL DESIGN REQUIREMENTS, HELICOPTERS
 - SAFE LIFE DESIGN REQUIREMENTS
 - NO FAIL SAFE/DAMAGE TOLERANCE DESIGN REQUIREMENTS
- SYSTEM DEVELOPMENT SPECIFICATIONS (UH-60, YAH-64)
 - FAIL SAFE/DAMAGE TOLERANCE DESIGN REQTS
 - REQUIREMENTS ARE GENERAL
 - TAILORED TO METALLIC STRUCTURES

Figure 11

COMPOSITE MAIN ROTOR BLADES

The Army's work in composite main rotor blades has spanned well over a decade. Composite blades are either in production or at various stages of planned implementation for nearly all inventory helicopters.

Four composite blade designs are shown in Figures 12 through 15, and although they were each developed by a different helicopter manufacturer, there is a certain degree of commonality in the fail-safe and damage-tolerant structural design approaches. Two blades are in production - the CH-47D blade (Figure 12) manufactured by Boeing Vertol and the K-747 blade (Figure 13) manufactured by Kaman Aerospace. The Hughes Helicopters AH-64 composite blade (Figure 14) and the Sikorsky UH-60 composite blade (Figure 15) are currently under manufacturing development in MM&T programs and are planned for future production implementation.

All blades are of damage-tolerant, high fracture toughness materials - either fiberglass or Kevlar. The UH-60 blade spar will be approximately 50% graphite; this is necessitated by the desire to maintain the same $9\frac{1}{2}\%$ blade airfoil thickness as the titanium spar blade that it is to replace, and at the same time to match flap, torsion, and chord stiffnesses. To accomplish this with fiberglass would necessitate increasing the inboard airfoil thickness to 14.5%.

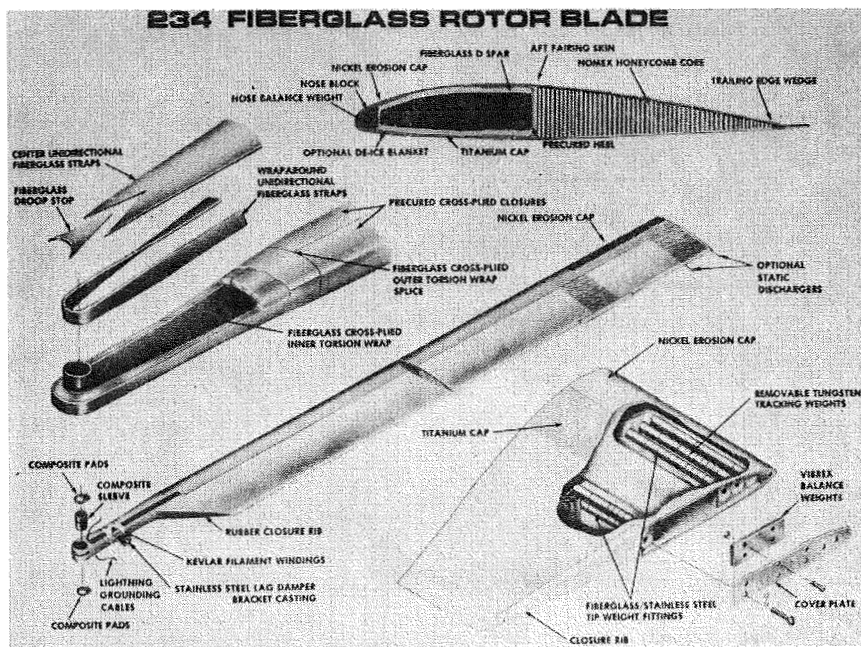


Figure 12

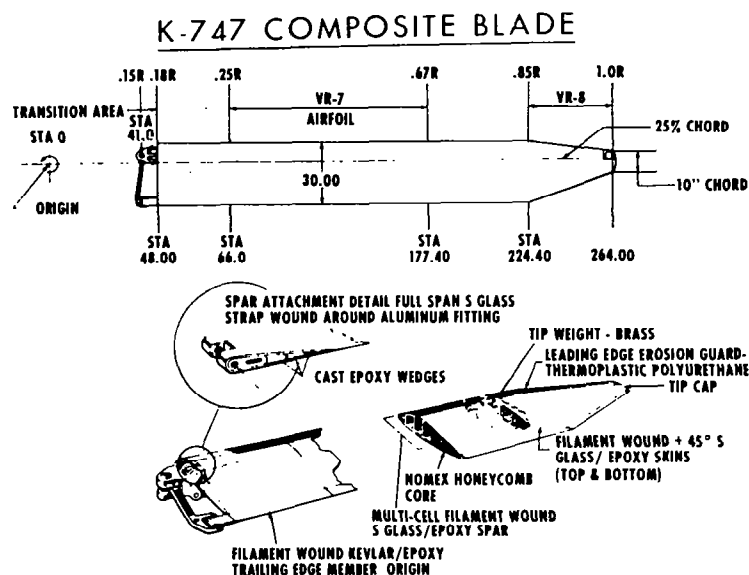


Figure 13

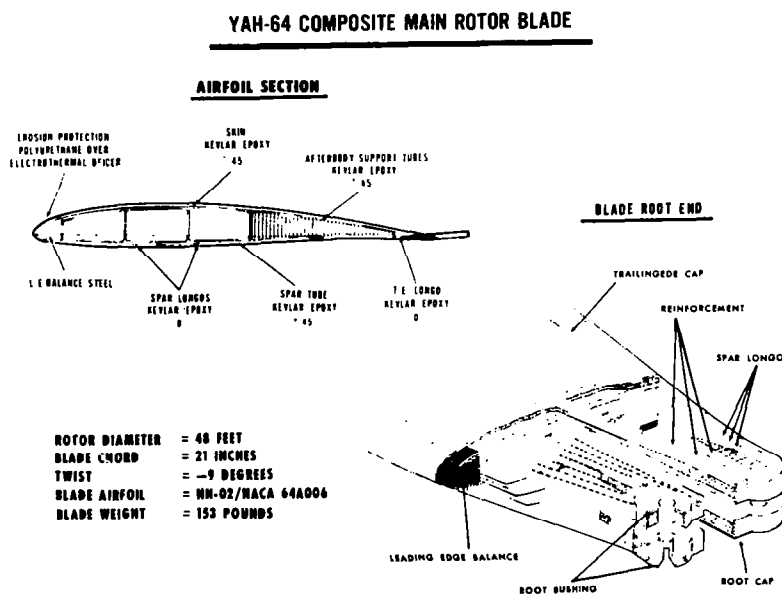


Figure 14

COMPOSITE MAIN ROTOR BLADES (CONTINUED)

All blades have a redundant load path root end except for the CH-47D blade; its single lug root end configuration was dictated by hub interface requirements. Hence fail safety in the root end has generally been achieved through redundancy.

For the constant airfoil section, damage tolerance is achieved with the material selection and relatively low design operating strain levels, typically 1500 $\mu\text{in./in.}$ to 1800 $\mu\text{in./in.}$

Two of the blade concepts - the K-747 and AH-64 - also contain structural redundancy of the spar in the airfoil region through a multi-tubular (or cell) concept; this is to a large degree for ballistic tolerance.

In general, the damage tolerance of these blades was developed and demonstrated through subcomponent and full-scale testing. Analysis was generally by classical techniques, with fail safety or damage tolerance assessed by assuming loss of a certain portion of the structure.

UH-60 COMPOSITE MAIN ROTOR BLADE

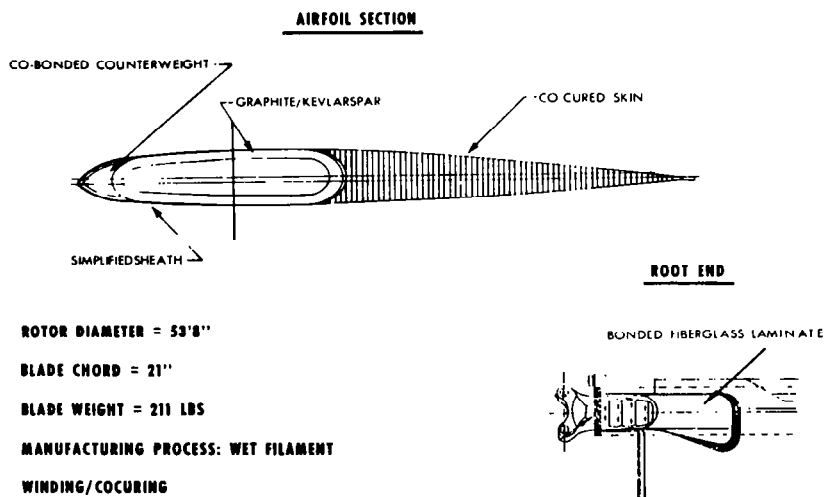
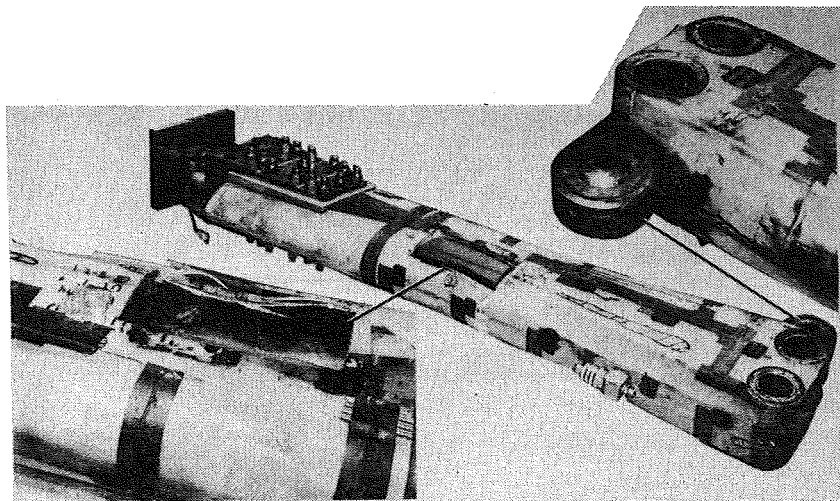


Figure 15

COMPOSITE ROTOR BLADE DAMAGE TOLERANCE DEMONSTRATED BY HLH ROOT END TEST

Some of the early R&D emphasis on composite blades centered on the root end, for the success of composite applications to the rotor blade hinged to a large degree on the development of a root end that was structurally efficient, fail safe, and at the same time producible. Results from damage tolerance testing on the root end of the HLH blade which was fiberglass construction and weighed 780 lbs are summarized in Figure 16. After testing this specimen for 490 hours to demonstrate safe life, the specimen was damaged to varying degrees, from severing one of the four root end lugs to removing a 6" x 12" section, and again tested as shown in the figure to demonstrate its fail-safe properties. At the cutout section the axial, flap, and chord stiffness were reduced by approximately 50 percent, and torsion was reduced by 85 percent.



- UNDAMAGED AFTER
240 HOURS AT 100% OF DESIGN LOADS
250 HOURS AT 300% OF DESIGN LOADS
- SUCCESSFULLY WITHSTOOD 100% OF DESIGN LOADS
40 HOURS WITH LUG CUT
130 HOURS WITH LUG CUT AND FORWARD UPPER STRAPS SLOTTED (1/8 IN. SPANWISE BY 6 IN. CHORDWISE) AND THEN
SUSTAINED LIMIT LOAD WITH NO DAMAGE PROPAGATION
30 HOURS WITH LUG CUT AND FORWARD UPPER AND LOWER STRAPS CUT (12 IN. SPANWISE BY 6 IN. CHORDWISE)

Figure 16

COMPOSITE ROTOR BLADE DAMAGE TOLERANCE
DEMONSTRATED BY UTTAS ROOT END TEST

Investigations have shown that initial deterioration of composites under repeated loading is manifested in a gradual loss of stiffness which is attributable initially to failure or breakdown within the resin. This factor, combined with another important feature that this loss in stiffness can occur, depending upon the stress level, many thousand cycles before static failure, yields the possibility of inherent damage tolerance for many composite structures.

This detection method of stiffness loss has been demonstrated in full-scale fatigue testing of fiberglass rotor blades. Reference 8 reports that during fail-safe testing of the Boeing Vertol UTTAS rotor blade root end, which was fiberglass/epoxy construction, there was a noticeable decrease in torsional stiffness after approximately 2×10^6 cycles at elevated test loads. This testing is summarized in Figure 17. Although the blade still retained its full structural integrity, the change in stiffness was deemed a failure. The loads were dropped to high-speed level-flight values and the equivalent of 30 flight hours was run, with no further measured degradation. Test loads were then increased to the original high level and testing continued until blade deflections exceeded machine capability. Even here there was no structural failure. Dynamic analyses, based upon reduced stiffness values, showed that the vibrational levels would have risen to a level noticeable to the pilot, but would still have been within a safe operating range. Additionally, regions of surface delamination became visible along with the stiffness loss. A key issue that must be addressed with this detection procedure is tying the indication, such as increased vibration level, to the correct source.

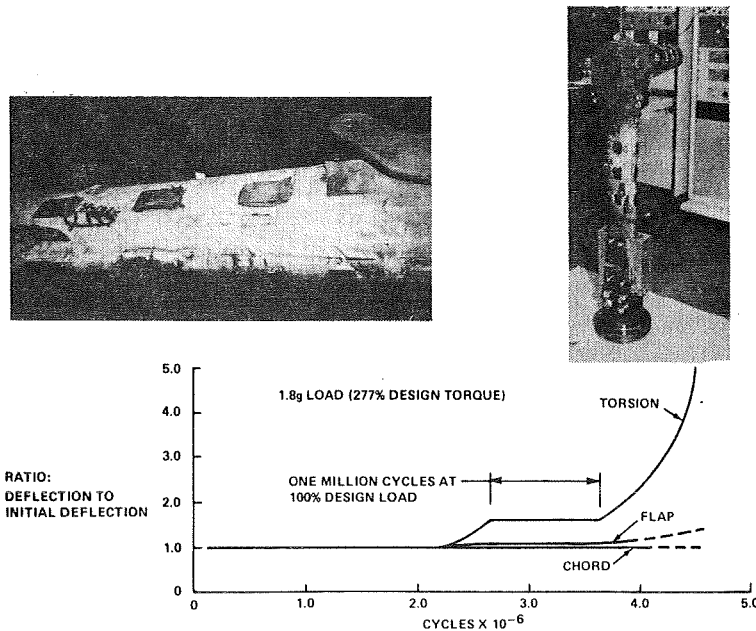


Figure 17

UH-60 COMPOSITE TAIL ROTOR SPAR

The UH-60 composite tail rotor spar provides a good example of the need for damage tolerance criteria for composites. This component is in production on the UH-60. It is graphite/epoxy and is highly complex in configuration, being made up of more than 300 individual detailed plies in order to satisfy strength and stiffness distribution requirements. Because of this complexity and the manufacturing process used, the rejection rate of this component during early production was quite high. Because the effect of manufacturing defects (See Figure 18) had not been quantified for this component, the acceptance criteria was stringent.

Three steps were taken to reduce this unacceptably high rejection rate:

1. Alternate layup
2. Press grade graphite
3. Inspection and acceptance criteria

Out of the three corrective steps, implementation of improved inspection techniques and an improved acceptance criterion, based upon actual testing of specimens with known defects (voids, porosity and inclusions), had the most significant impact in significantly lowering the rejection rate.

QUAL TEST SPEC #3

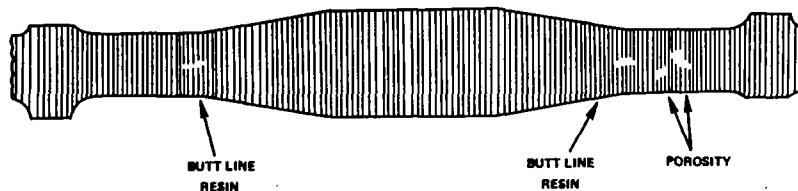
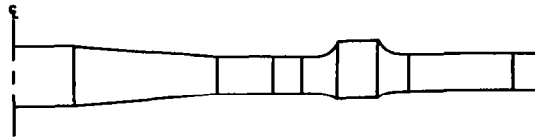


Figure 18

UH-60 COMPOSITE TAIL ROTOR SPAR - NDI

Typical ultrasonic indications in spars that were fatigue tested to determine acceptance criteria are shown in Figure 19.

SPAR NDI INDICATIONS TESTED



TESTED									
● POROSITY	YES		YES		YES				YES
● BUTT LINE RESIN		YES	YES						
● PLY ENDING RESIN									
TO BE TESTED									
● POROSITY	YES		YES	YES					
● BUTT LINE RESIN									
● PLY ENDING RESIN									
● EDGE POROSITY	YES	YES	YES						
● FILLER PLY POROSITY/RESIN									

Figure 19

UH-60 COMPOSITE TAIL ROTOR SPAR FATIGUE TEST

Fatigue testing of a tail rotor spar is shown in Figure 20.

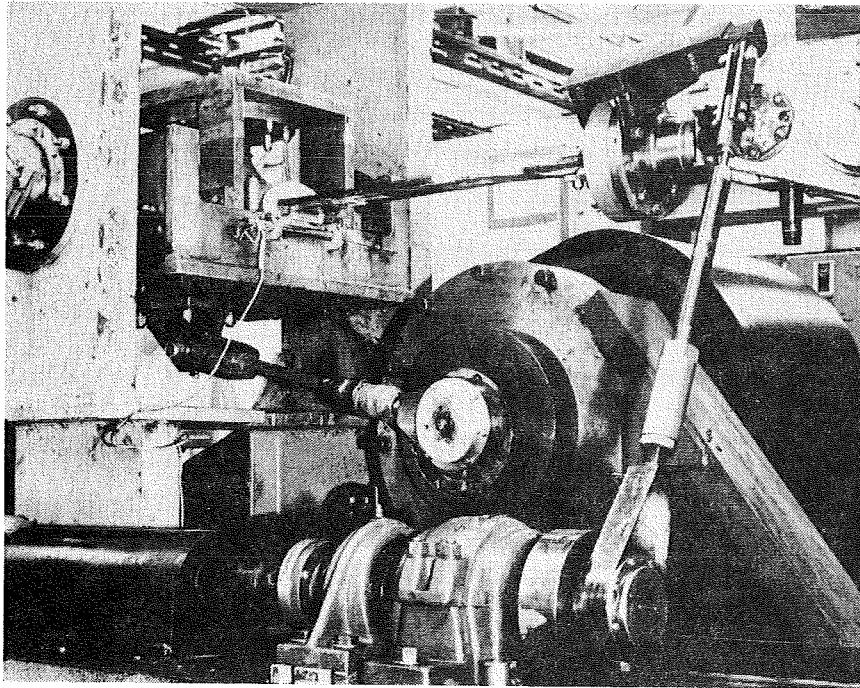


Figure 20

UH-60 COMPOSITE TAIL ROTOR SPAR FATIGUE TEST RESULTS

Figure 21 shows that spars with various defects fell within the scatter of spars that were void-free; this enabled establishment of a new acceptance criteria.

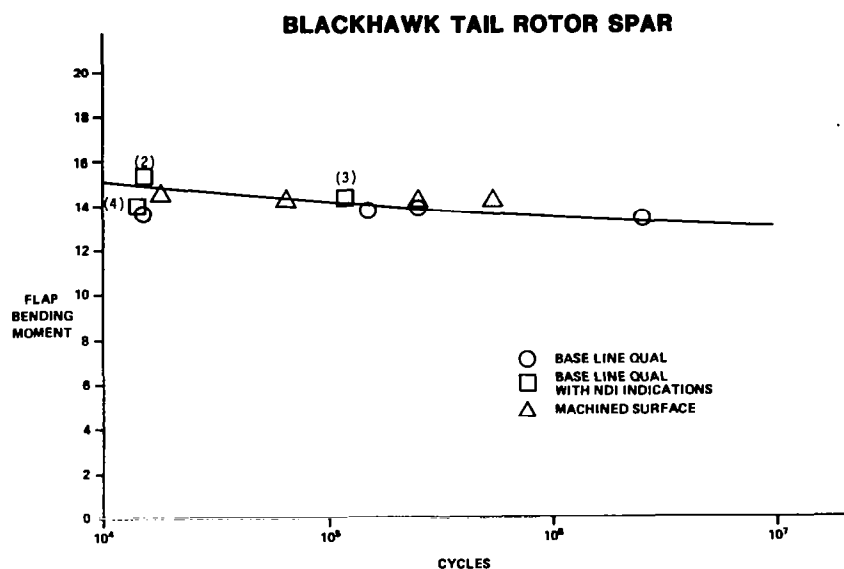


Figure 21

SUMMARY/CONCLUSIONS

Helicopter flight-critical structures, although limited primarily to rotor blades, have been successfully designed for damage tolerance. This has been accomplished through redundancy, use of damage-tolerant materials and sizing to low operating stress levels. Design and demonstration have been based on laboratory testing.

The increased application of composites to more complexly loaded structures, such as bearingless rotor hubs which inherently will operate at higher strain levels, further amplifies the need for a sound damage-tolerant criterion. Development of the criterion must address those items listed in the last bullet of Figure 22.

- o LABORATORY TESTING THE BASIS FOR DESIGN AND DEVELOPMENT OF DAMAGE TOLERANT COMPOSITE STRUCTURES
- o DAMAGE TOLERANT CRITERIA FOR COMPOSITES NEEDED, ESPECIALLY IN LIGHT OF
 - COMPOSITES APPLICATION TO MORE COMPLEXLY LOADED COMPONENTS
 - INCREASED STRAIN LEVELS
- o DAMAGE TOLERANT CRITERIA DEVELOPMENT MUST INCLUDE
 - PREDICTIVE CAPABILITY
 - DAMAGE SIZE REQUIREMENTS
 - NDT CAPABILITY/DAMAGE DETECTABILITY
 - DESIGN REQUIREMENTS
 - ENVIRONMENTAL EFFECTS
 - TEST/QUAL REQUIREMENTS

Figure 22

REFERENCES

1. Helicopter Fatigue - A Review of Current Requirements and Substantiating Procedures. AGARD Report No. 674, Feb. 1979.
2. Proceedings of the AHS Midwest Region Helicopter Fatigue Methodology Meeting (St. Louis, MO), March 23-25, 1980.
3. Nobak, R.: State of the Art and Statistical Aspects of Helicopter Fatigue Substantiation Procedures. Helicopter Fatigue Life Assessment, AGARD Conference Proceedings No. 297, March 1981.
4. Immen, F. H.: Failsafe vs Safe Life Philosophy in V/STOL Design. J. Am. Helicopter Soc., vol. 14, no. 4, Oct. 1969.
5. Cansdale, R.: An Evaluation of Fatigue Procedures for UK Military Helicopters. Helicopter Fatigue Life Assessment, AGARD Conference Proceedings No. 297, March 1981.
6. Polley, I. M.: Damage Tolerance Design for Helicopter Structural Integrity. Paper presented at Second European Rotorcraft and Power Lift Aircraft Forum (Buckeburg, Germany), September 1976.
7. Toor, P. M.; and Payne, B. M.: Damage Tolerance Design and Analysis of a Typical Aircraft Wing Structure (New or Existing). Case Studies in Fracture Mechanics, T. P. Rich and D. J. Cartwright, eds., AMMRC-MS-77-5, Army Materials and Mechanics Research Center, June 1977.
8. Field, D. M.; Finney, R. H.; and Stratton, W. K.: Achieving Fail Safe Design in Rotors. Paper presented at 28th Annual AHS Forum (Washington, D.C.), May 17-19, 1972.
9. McCall, C. D.; Field, D. M.; and Reddick, H. K.: Advanced Technology as Applied to the Design of the HLH Rotor Hub. Paper presented at 29th Annual AHS Forum (Washington, D.C.), May 9-11, 1973.
10. Smith, H. G.: Fail Safe Structural Features of the Hughes OH-6A. Paper presented at Second European Rotorcraft and Power Lift Forum (Buckeburg, Germany), September 1976.
11. Weiss, W. L.; and Zola, D. C.: The Application of Fracture Mechanics to the Design of Damage Tolerant Components for the UTTAS Helicopter. Paper presented at 30th Annual AHS Forum (Washington, D.C.), May 7-9, 1974.

FAILURE MECHANISMS

H. Thomas Hahn
Washington University
St. Louis, Missouri

LONGITUDINAL TENSION

• FAILURE MODES



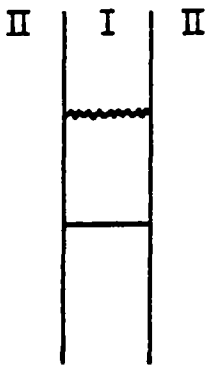
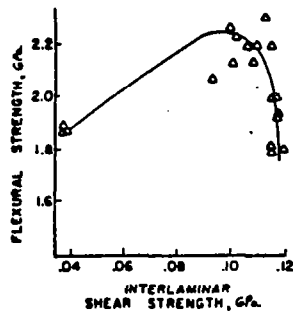
WEAK MATRIX
WEAK INTERFACE



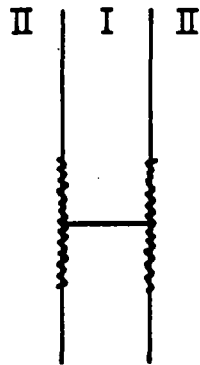
OPTIMUM



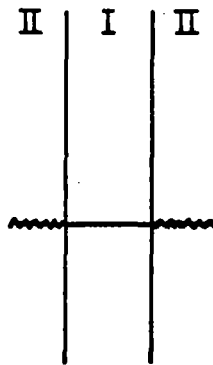
STRONG MATRIX
STRONG INTERFACE



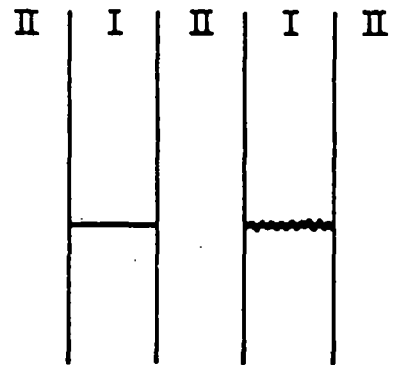
(a)



(b)



(c)

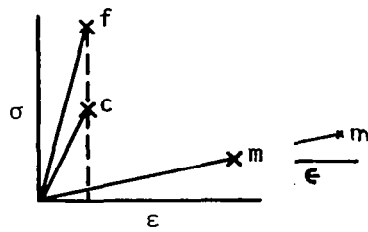


(d)

CRACK GROWTH MODES IN UNIDIRECTIONAL COMPOSITES

• PREDICTION OF STRENGTH

RULE OF MIXTURES



BRITTLE MATRIX

$$X_L = (v_f + v_m E_m / E_f) X_f$$

MINIMUM FIBER VOLUME FRACTION

$$v_f = \frac{E_f}{E_f - E_m} \left(\frac{X_m}{X_f} - \frac{E_m}{E_f} \right)$$

• BUNDLE STRENGTH

FIBER STRENGTH DISTRIBUTION

$$R(X_f) = \exp [-L(X_f/X_{f0})^\alpha]$$

$$R(Y_f) = \exp [-L(Y_f/Y_{f0})^\alpha]$$

$$X_{f0} = E_f Y_{f0}$$

AVERAGE FIBER STRENGTH

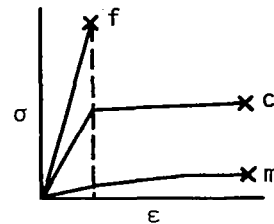
$$\bar{X}_f = X_{f0} L^{-1/\alpha} \Gamma(1 + 1/\alpha)$$

BUNDLE STRENGTH

$$X_b = X_{f0} (L\alpha e)^{-1/\alpha}$$

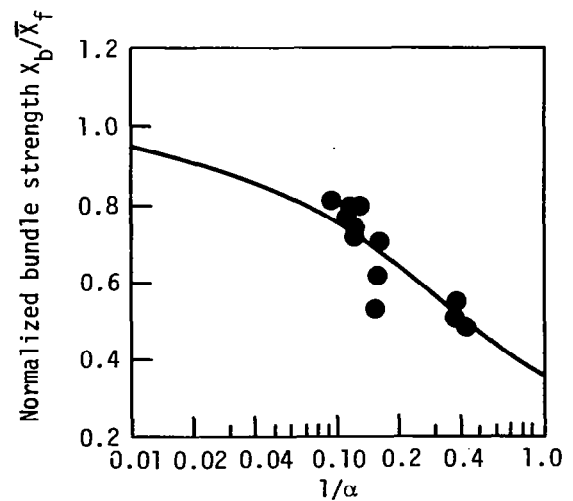
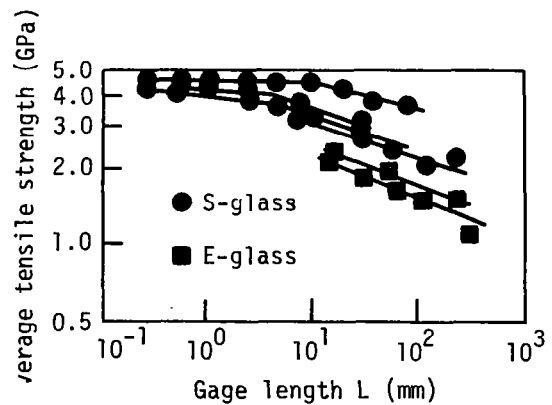
BUNDLE-TO-FIBER STRENGTH RATIO

$$\frac{X_b}{\bar{X}_f} = \frac{1}{(\alpha e)^{1/\alpha} \Gamma(1 + 1/\alpha)}$$



DUCTILE MATRIX

$$X_L = v_f X_f + v_m X_m$$



• OPTIMUM STRENGTH

$$\chi_L = v_f \chi_b(\delta) + v_m \bar{\sigma}_m^*$$

$$\frac{\chi_b(\delta)}{\bar{\chi}_f(L)} = \frac{1}{(\alpha e)^{1/\alpha} \Gamma(1 + 1/\alpha)} \left(\frac{L}{\delta}\right)^{1/\alpha}$$

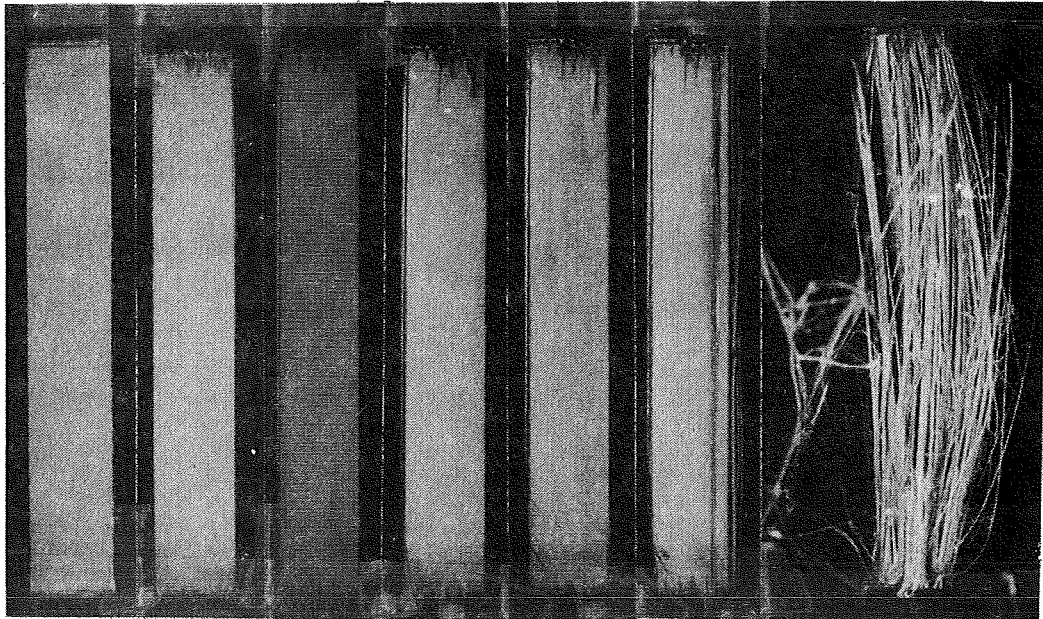
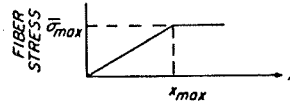
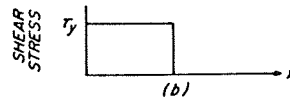
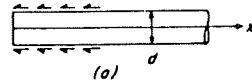
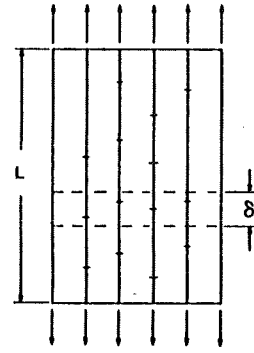
INEFFECTIVE LENGTH OR
LENGTH OF FAILURE INTERACTION ZONE

$$\frac{\delta}{d} = 2 \left(\frac{\bar{\chi}_f}{4\tau_y} \right)^{\alpha/(\alpha+1)} [(\alpha+1)L/d]^{1/(\alpha+1)}$$

IF $\alpha \gg 1$, RULE OF MIXTURES

$$\frac{\delta}{d} = \frac{\bar{\chi}_f}{2\tau_y}$$

$$\chi_L = (v_f + v_m E_m/E_f) \bar{\chi}_f$$



Stress, %UTS 0 45 72 86 94 99 100
Static failure sequence for Kevlar 49/epoxy

LONGITUDINAL COMPRESSION

• MICROBUCKLING OF FIBERS

INITIAL DEFLECTION

$$v_0 = f_0 \sin \frac{\pi X}{\ell}$$

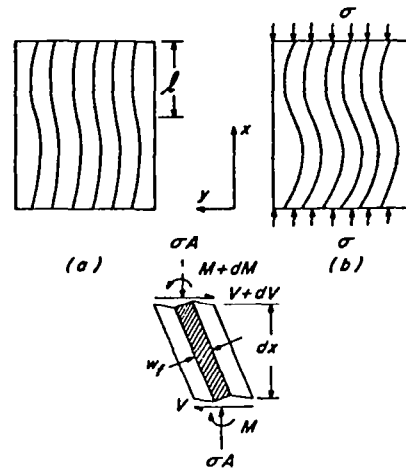
FINAL DEFLECTION

$$v = f \sin \frac{\pi X}{\ell}$$

COMPRESSIVE STRESS

$$\sigma = \left[G_L + \frac{\pi^2}{12} v_f E_f \left(\frac{w_f}{\ell} \right)^2 \right] \left(1 - \frac{f_0}{f} \right)$$

$$\approx G_L \left(1 - \frac{f_0}{f} \right)$$



• COMPRESSIVE STRENGTH

$$X'_L = G_L \left(1 - \frac{f_0}{f_c} \right)$$

LOCAL SHEAR FAILURE

$$f_c = f_0 + \frac{\ell}{\pi} \frac{X_S}{G_L}$$

FLEXURAL FAILURE OF FIBER

$$f_c = f_0 + \frac{2\ell}{w_f} \frac{\ell}{\pi^2} \frac{X_f}{E_f}$$

FINAL STRENGTH

$$X'_L = G_L \frac{1}{1 + (\pi f_0 / \ell) / (X_S / G_L)}$$



Shear type

Buckling type

Compression failure mode for G_I/E_p

TRANSVERSE TENSION

• ELASTIC PREDICTION

$$(\sigma_m)_{\max} = (\text{SCF}) \bar{\sigma}_2$$

$$X_m = (\text{SCF}) X_T$$

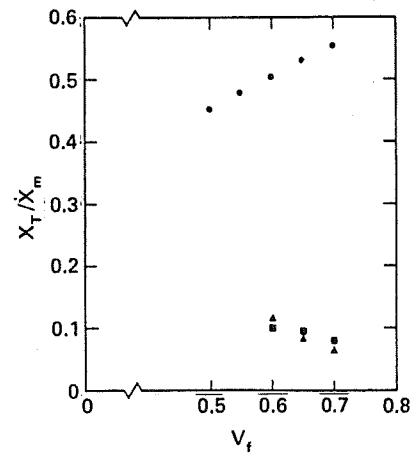
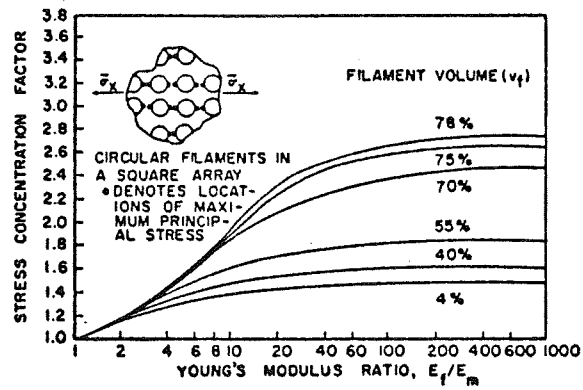
$$\frac{X_T}{X_m} = \frac{1}{\text{SCF}}$$

$$\text{SCF} \uparrow \text{ AS } \frac{E_f}{E_m} \uparrow$$

$$\text{SCF} \uparrow \text{ AS } X_m \downarrow$$

$$\frac{X_T}{X_m} \downarrow \text{ AS } X_m \downarrow$$

USE X_{int} IF INTERFACIAL FAILURE



MATRIX DUCTILITY

$$X_T = v_f \bar{\sigma}_{f2}^* + v_m \bar{\sigma}_{m2}^*$$

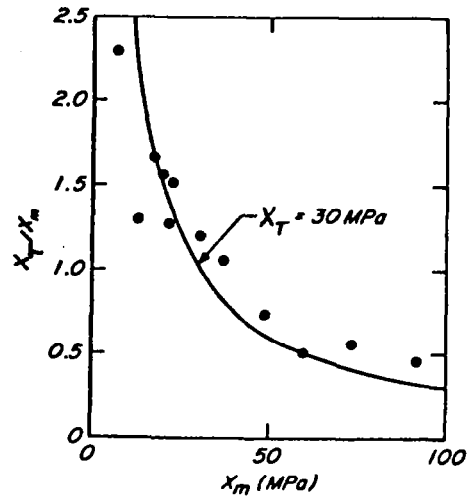
$$= (v_f/\eta_2 + v_m) \bar{\sigma}_{m2}^*$$

$$K_{m2} = (\sigma_m)_{\max} / \bar{\sigma}_{m2}^*$$

$$\frac{X_T}{X_m} = \frac{1 + v_f (1/\eta_2 - 1)}{K_{m2}}$$

$$K_{m2} \uparrow \text{ AS } X_m \uparrow$$

$$\frac{X_T}{X_m} \downarrow \text{ AS } X_m \uparrow$$



TRANSVERSE COMPRESSION

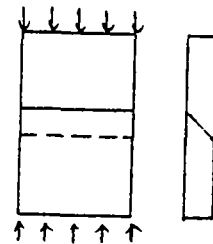
FAILURE PLANE

~ 45° INCLINED

$$X'_T/X_T$$

$$4 \sim 7$$

$$\sim X'_m$$



LONGITUDINAL SHEAR

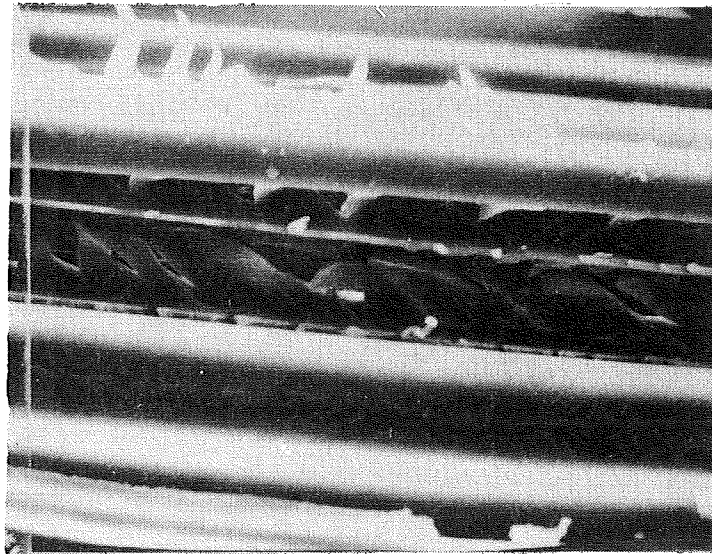
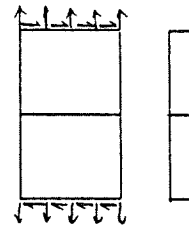
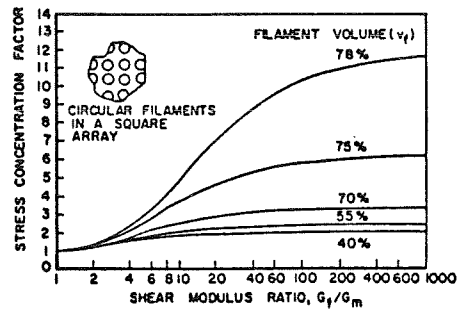
ELASTIC PREDICTION

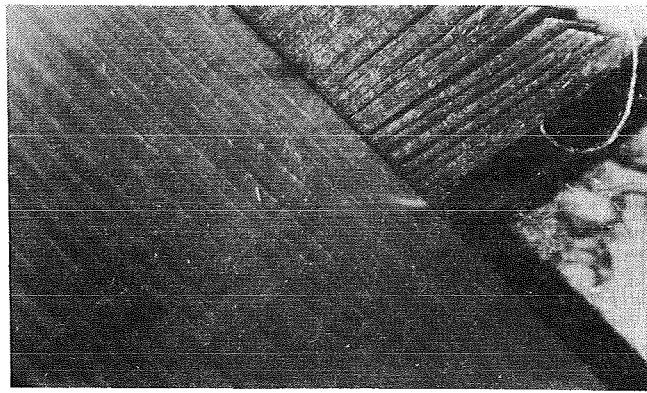
SAME AS X_T

$$\frac{X_S}{S_m} = \frac{1}{SCF}$$

MATRIX DUCTILITY

$$\frac{X_S}{S_m} = \frac{1 + v_f(1/\eta_6 - 1)}{K_{m6}}$$





macroscopic

Shear failure for Kevlar 49/Ep

LAMINA FATIGUE

LONGITUDINAL TENSION

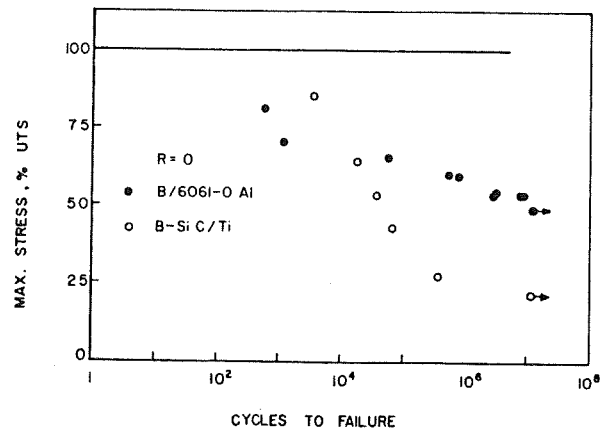
MATRIX-CONTROLLED FAILURE LIKELY

FATIGUE LIMIT STRAIN OF MATRIX \approx
FATIGUE LIMIT STRAIN OF COMPOSITE

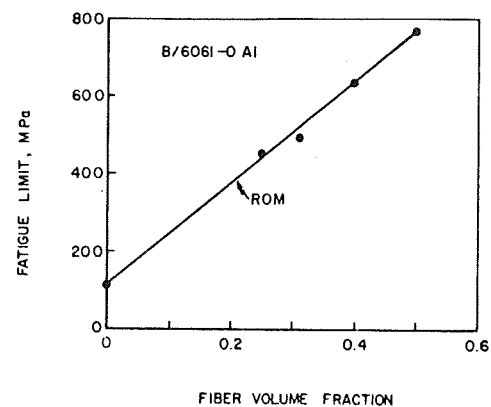
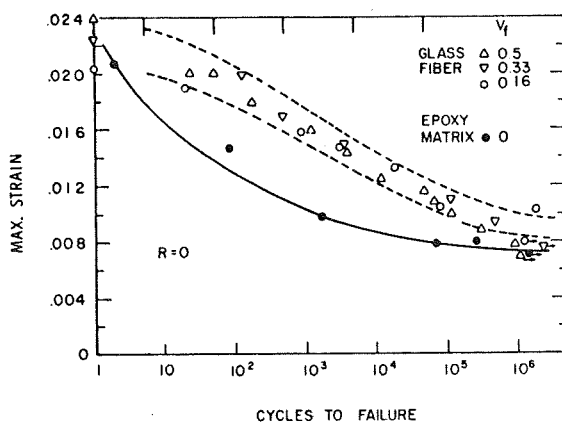
FATIGUE LIMIT STRESS

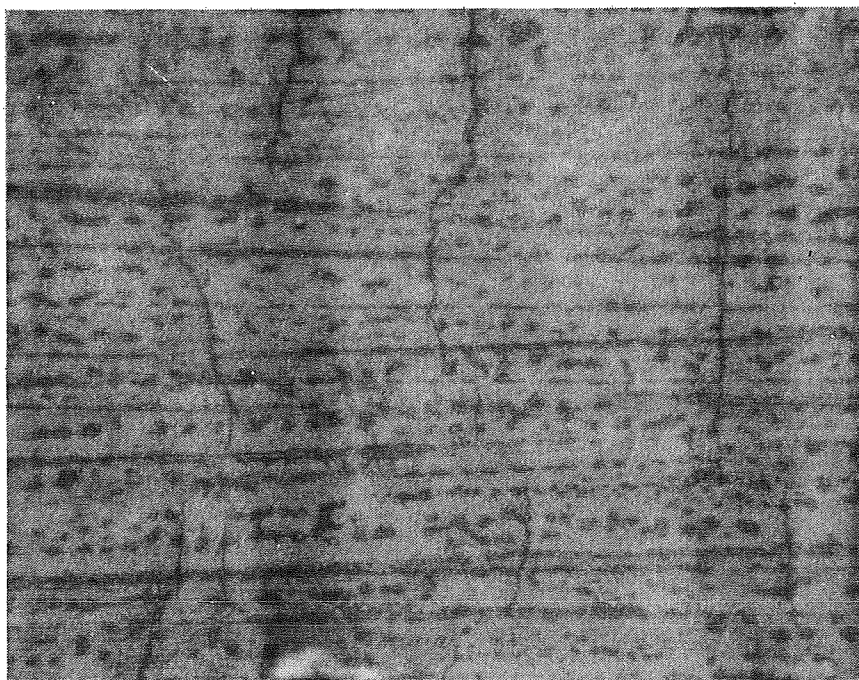
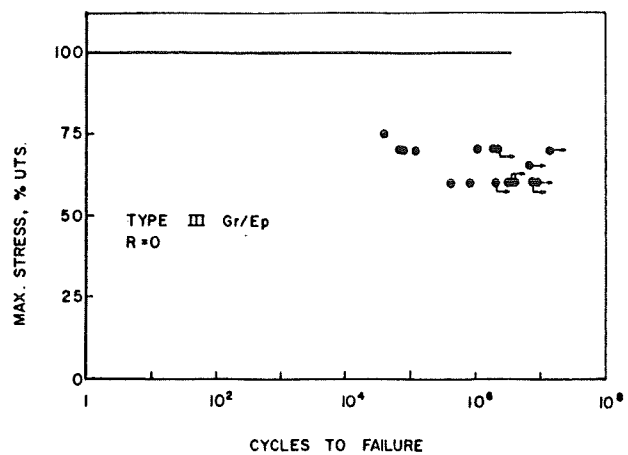
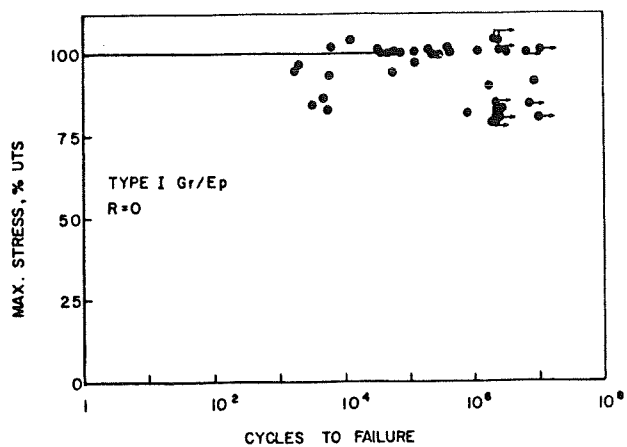
$$S_{FL} = S_{mFL} + v_f(E_f/E_m - 1) E_m \epsilon_{FL}$$

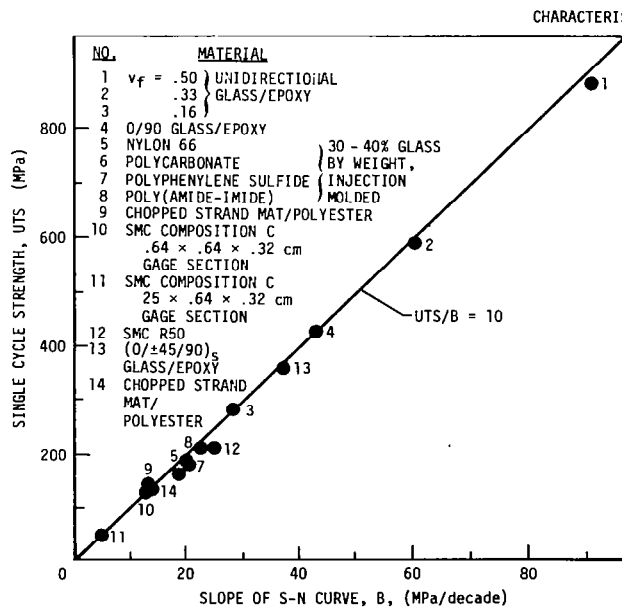
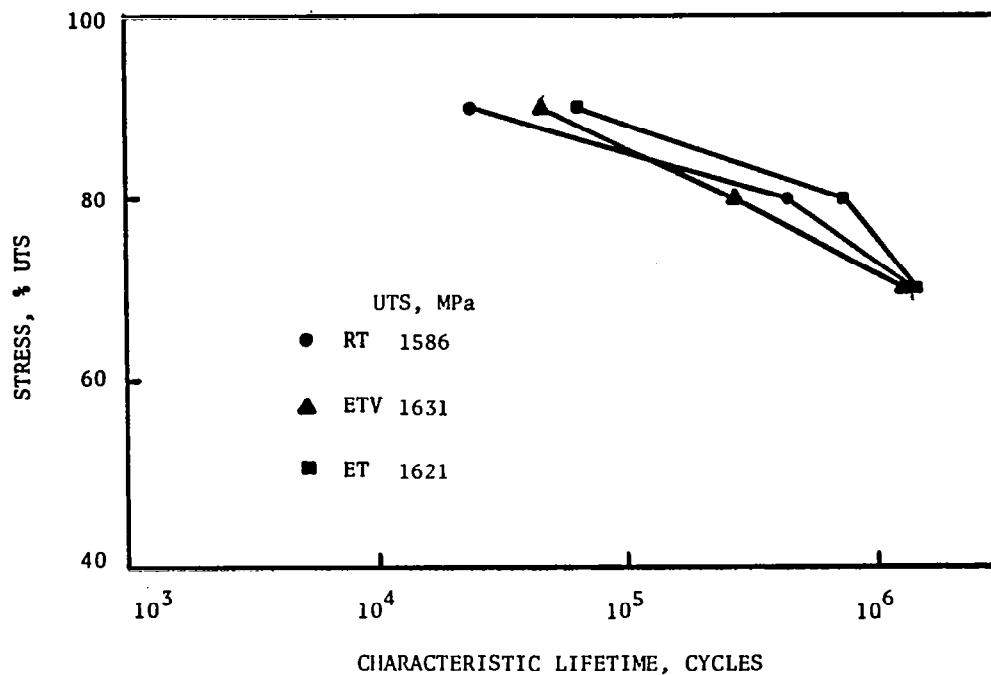
LOW FATIGUE SENSITIVITY IF FATIGUE
LIMIT STRAIN > STATIC FAILURE STRAIN
OF FIBER



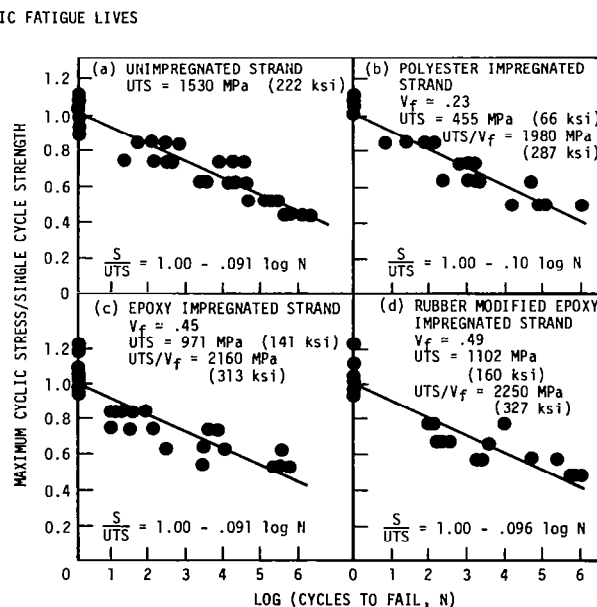
Longitudinal S-N data for B/Al and B-SiC/Ti
(Ultimate tensile strength - 1698 MPa for B/Al
and 1296 MPa for B-SiC/Ti)



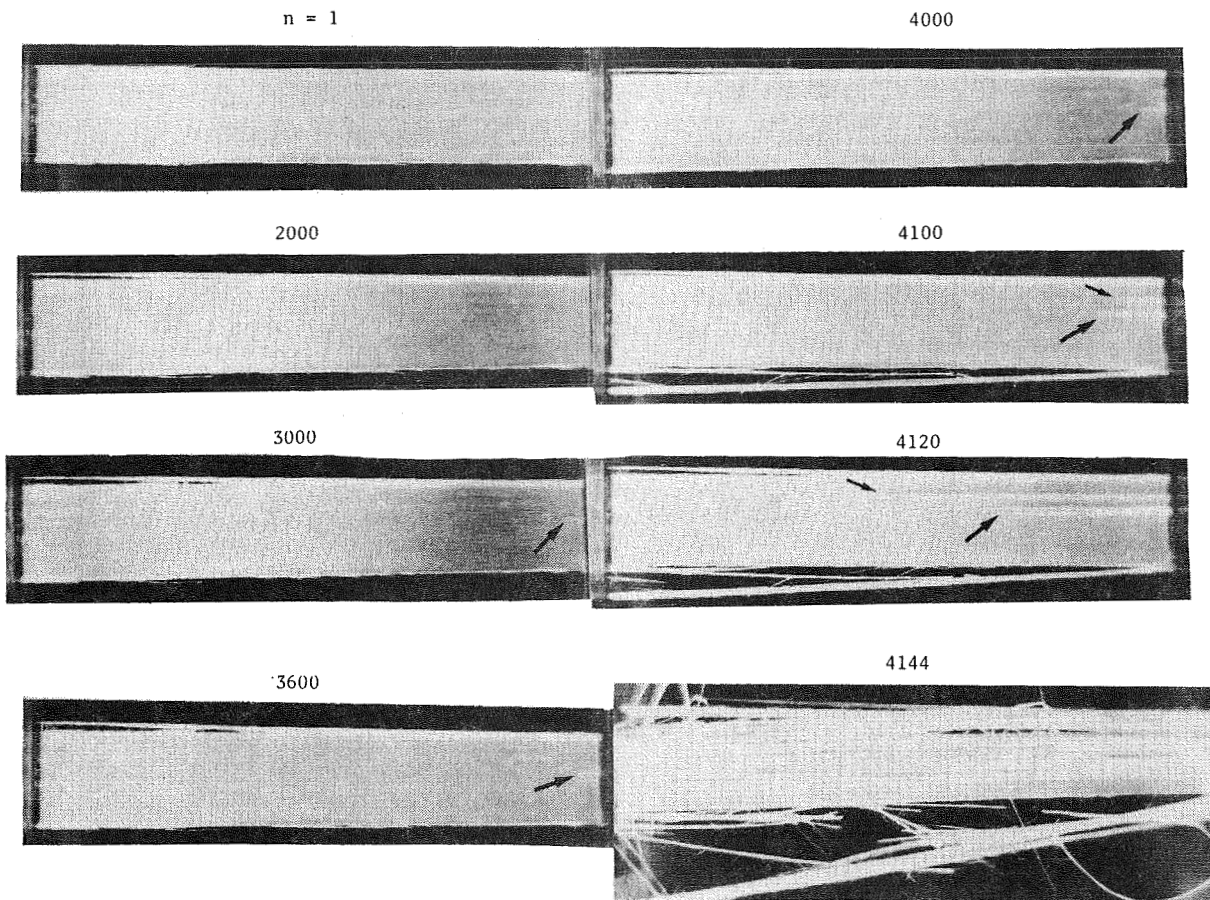




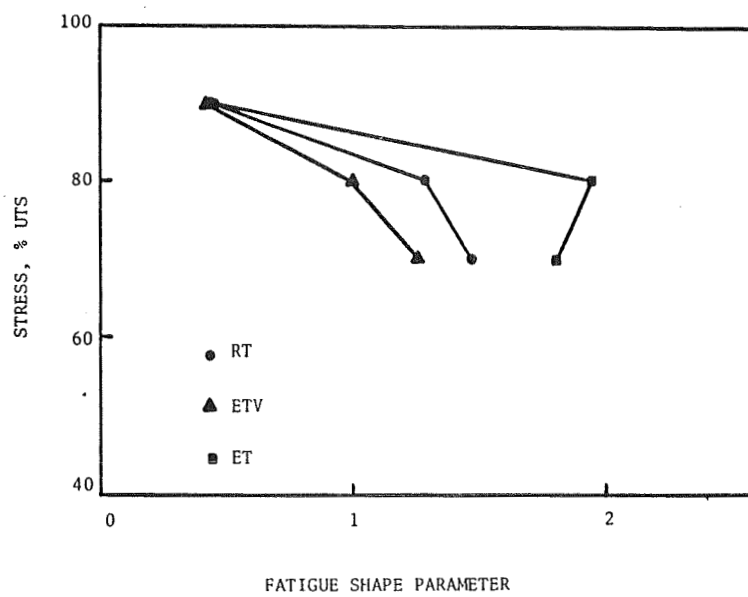
Single cycle strength versus slope of S-N curve, nonwoven glass fiber composites, tension-tension fatigue at $R = 0$ to 0.1



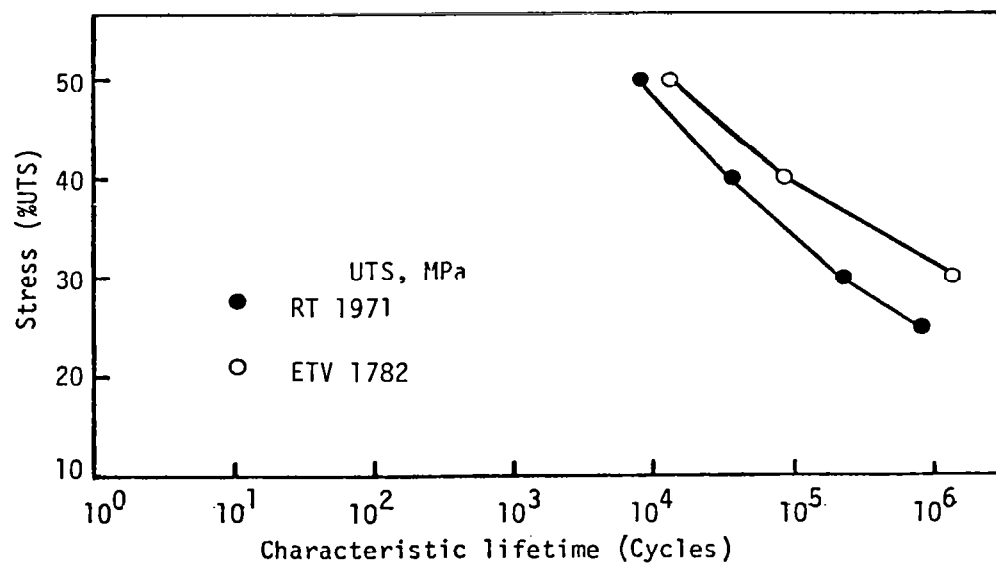
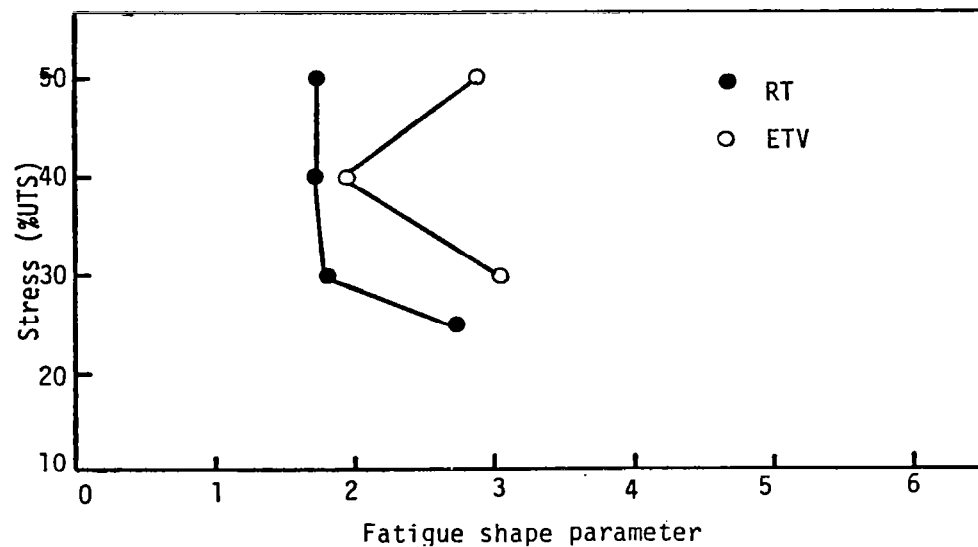
Normalized tensile fatigue life curves for E-glass strand without matrix and with several matrices (5 Hz, $R = 0.10$).



Fatigue failure process at 60 percent UTS, RT, G1/Ep



Fatigue shape parameters



Weibull parameters for fatigue life distributions

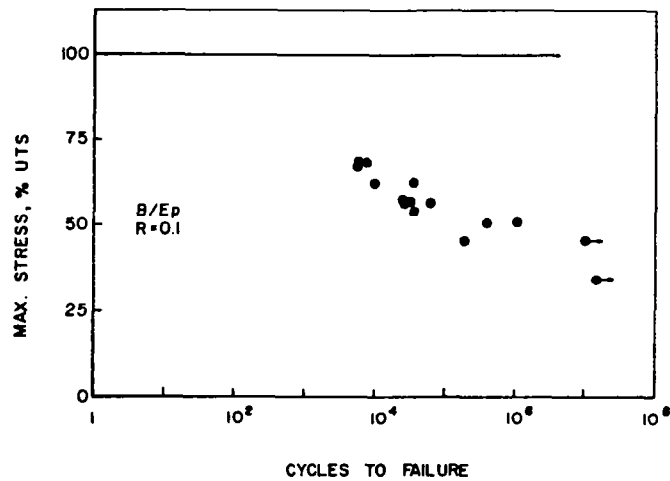
• TRANSVERSE TENSION AND LONGITUDINAL SHEAR

HIGHLY FATIGUE SENSITIVE

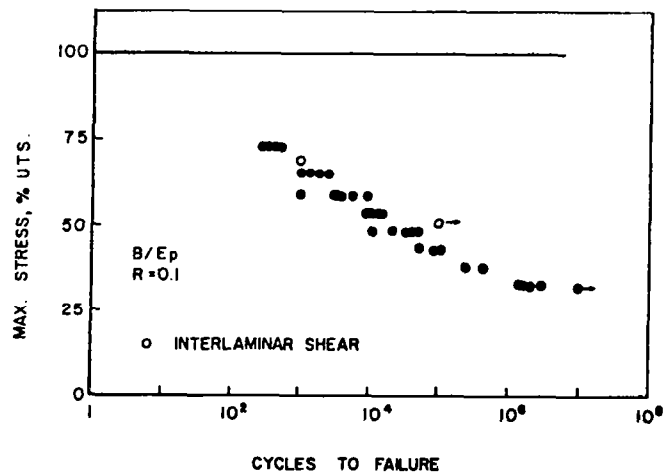
MORE THAN 60% REDUCTION IN STRENGTH
AT 10^6 CYCLES

FAILURE RESULTING FROM FAST CRACK
PROPAGATION

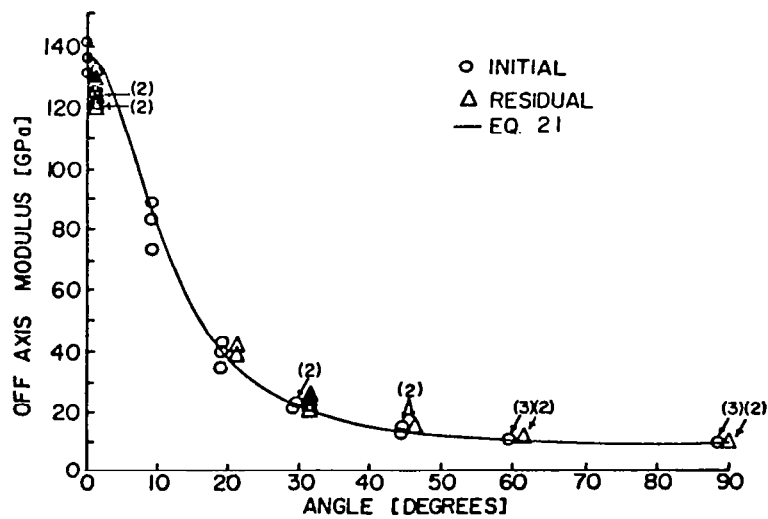
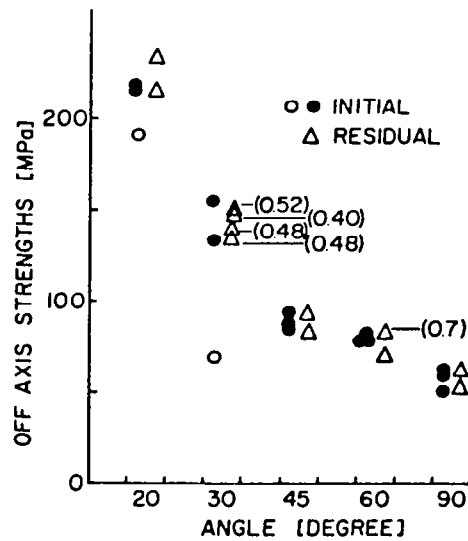
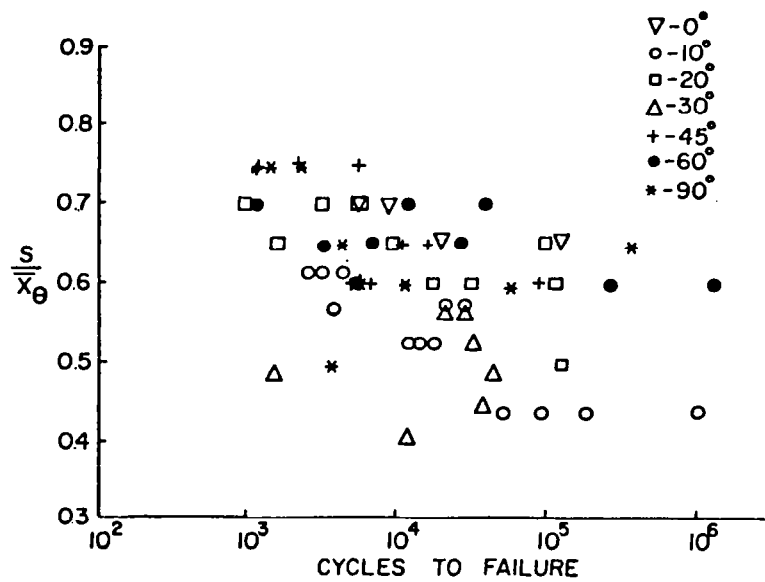
NO INDICATION OF GRADUAL CHANGES IN
MODULUS AND STRENGTH

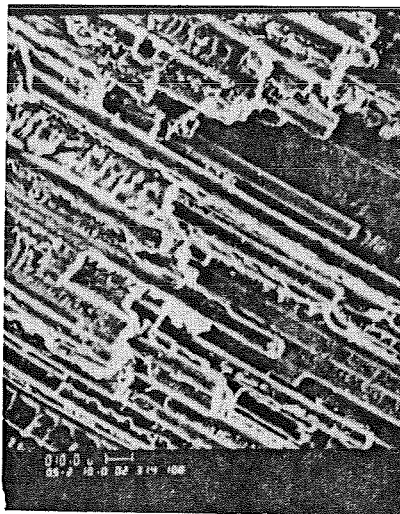


Transverse S-N data for B/Ep (Ultimate tensile strength = 60.9 MPa)

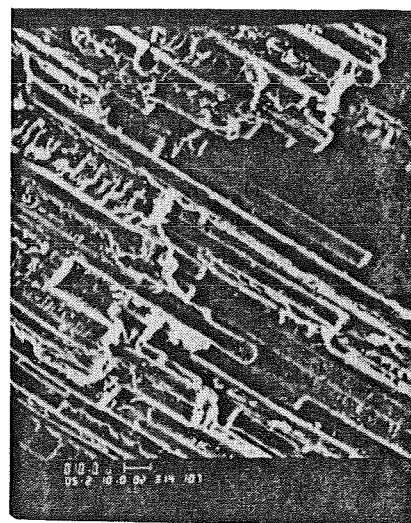


Shear S-N data for B/Ep. (Longitudinal shear strength = 66.7 MPa, interlaminar shear strength = 81.4 MPa)



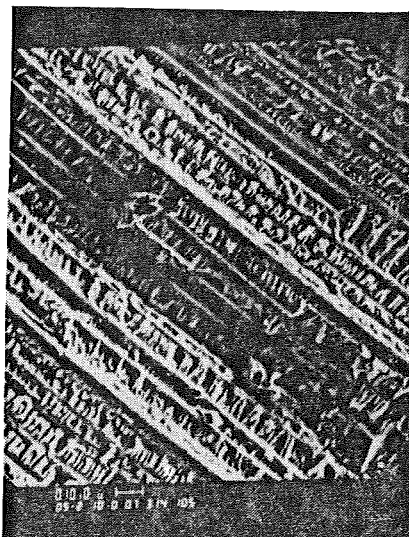


LEFT

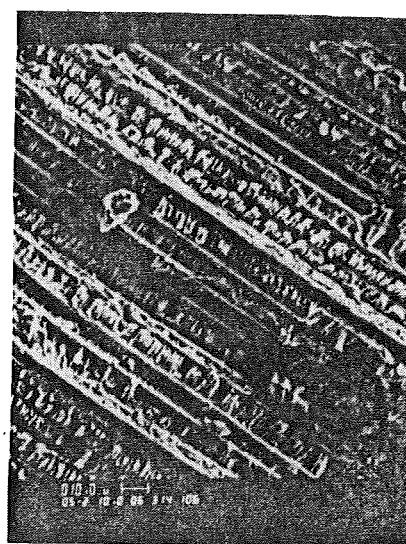


RIGHT

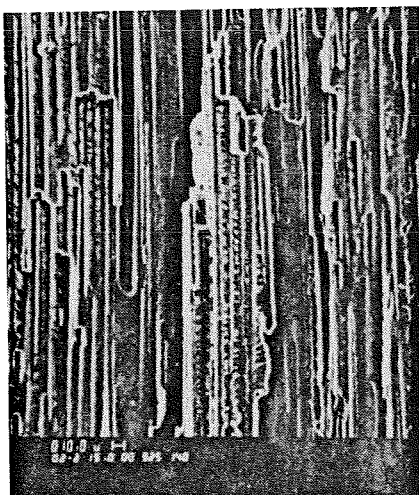
30°



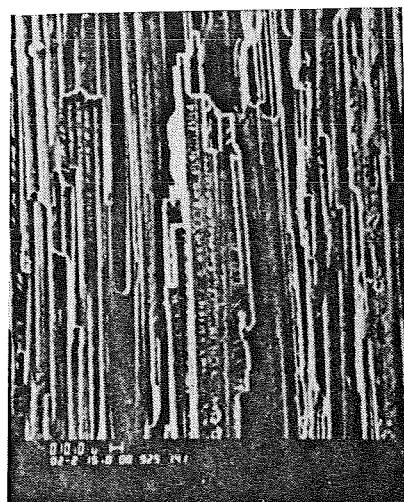
LEFT



RIGHT

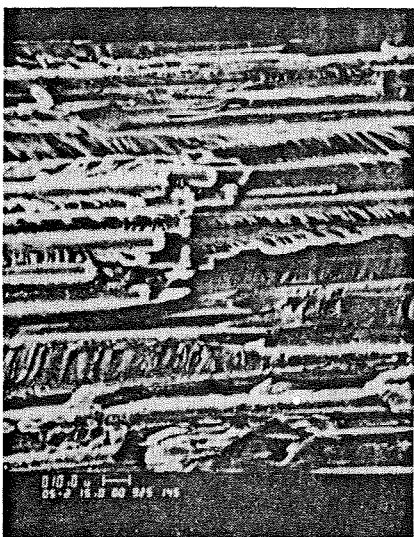


LEFT

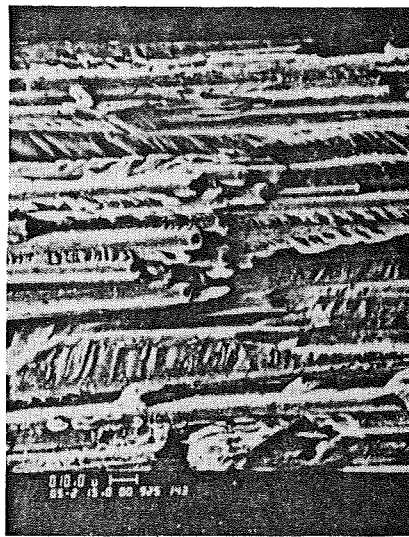


RIGHT

90°



LEFT



RIGHT

LAMINATE FATIGUE

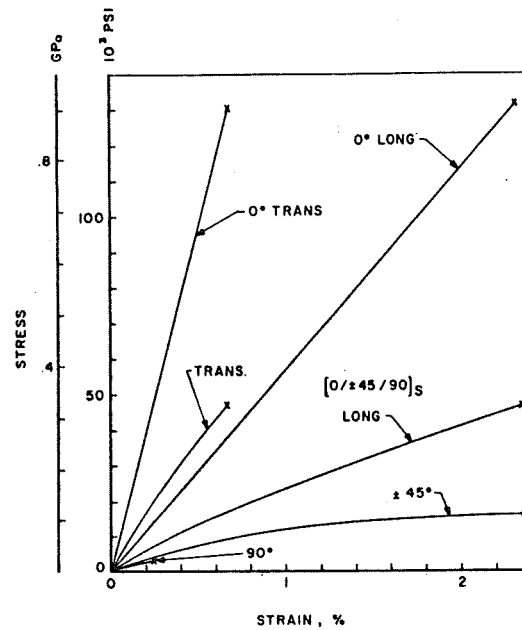
FAILURE PROCESSES

FIRST PLY-FAILURE

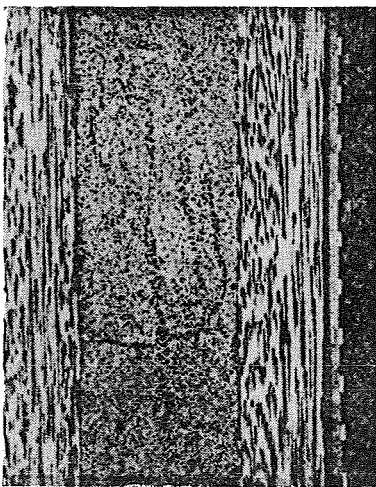
ASYMPTOTIC INCREASE IN CRACK DENSITY IN PLIES

DELAMINATION

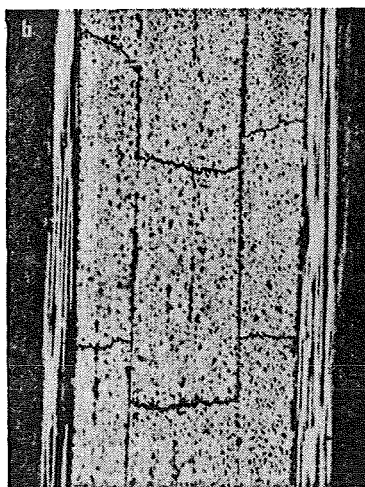
LAMINATE FRACTURE



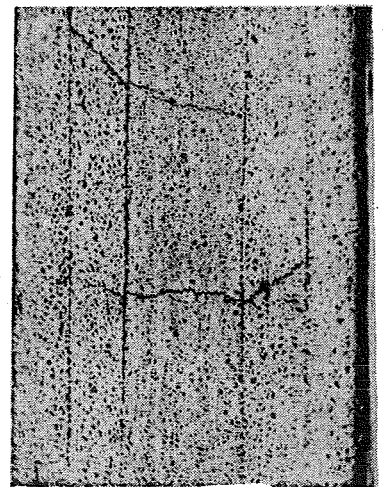
Stress-strain relations of $[0/\pm 45/90]_s$ G1/Ep and of constituent plies



$[0/90]_s$



$[0/\pm 45]_s$

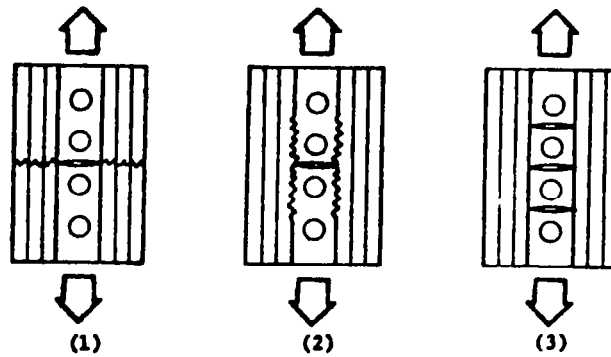


$[0/\pm 45/90]_s$

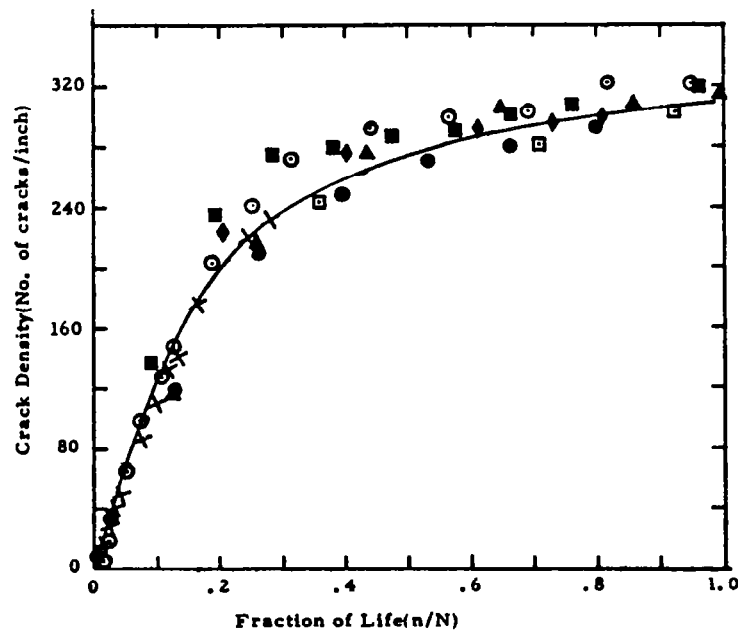
Failure modes at free edge

Graphite/Epoxy T300/5208 [0/90/±45]_s

Symbol	Maximum Stress ksi	Life N
□	50	793,340
○	50	704,870
●	60	37,560
■	60	52,360
▲	60	23,090
◆	60	24,570
X	40	



Typical failure mechanisms of composite laminates - Mode (1) is the most catastrophic and mode (3) the most desirable



STRENGTH THEORIES OF COMPOSITES:

STATUS AND ISSUES

Edward M. Wu
Lawrence Livermore National Laboratory
University of California
Livermore, California

Central Issues

Under Uniaxial Stress

Fiber controlled? or Fiber dominated? 

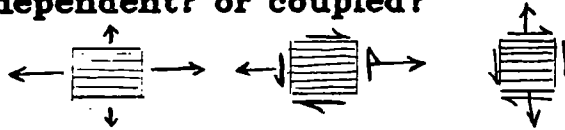
Matrix controlled? or Matrix dominated? 

Should tensile & compressive strength be related?



Under Combined Stress

Are longitudinal & transverse strength independent? or coupled?



How to measure strength coupling?

ROLE OF MATRIX BINDER IN LONGITUDINAL STRENGTH (REFS.1 AND 2)

MATRIX BINDER PROVIDES LOCAL REDUNDANCY



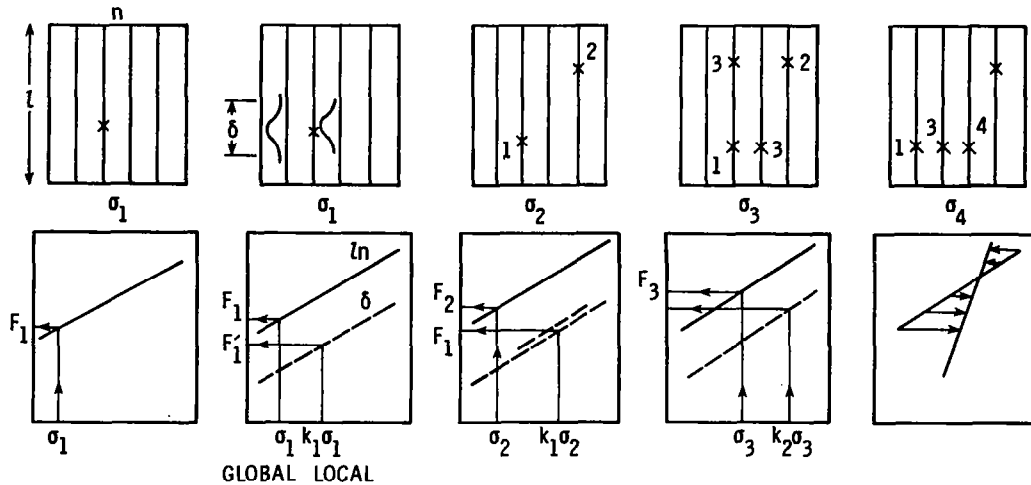
δ = INEFFECTIVE LENGTH
~ 10 d

FIBER BREAK	WITHOUT MATRIX NO. OF LOAD CARRYING FIBERS		WITH MATRIX NO. OF LOAD CARRYING FIBERS	
0	3	P/3	3	P/3
1	2	P/2	3-8	~ P/3-

LONGITUDINAL STRENGTH DEPENDS ON MATRIX EFFECTIVENESS

PARAMETER $\delta \left(E_m/E_f, \sigma_{m,ult}, \sigma_{INTERFACE} \right)$

LONGITUDINAL COMPOSITE FAILS SEQUENTIALLY (REF. 3)



LONG. COMPOSITE
FAILURE IS SEQUENTIAL

$$\frac{\sigma_1}{\sigma_{ult}} \sim .2$$

SMALL δ MORE
UNSTABLE
BUT STRONGER

LARGE α MORE
UNSTABLE
WEAKER

MATRIX
INCREASES
 α

- LONG COMPOSITE FAILURE IS SEQUENTIAL, NO WELL-DEFINED PLANE OF FAILURE

LONGITUDINAL STRENGTH: FIBER-DOMINATED OR FIBER-CONTROLLED

HIGH LONGITUDINAL STRENGTH OF FIBER IS DUE TO:

DEFECTS ARE MINIMIZED BY SMALL FIBER DIAMETER

$$\sigma_{ult} \sim 600 \text{ ksi} \quad (\text{STEEL} \sim 200 \text{ ksi})$$

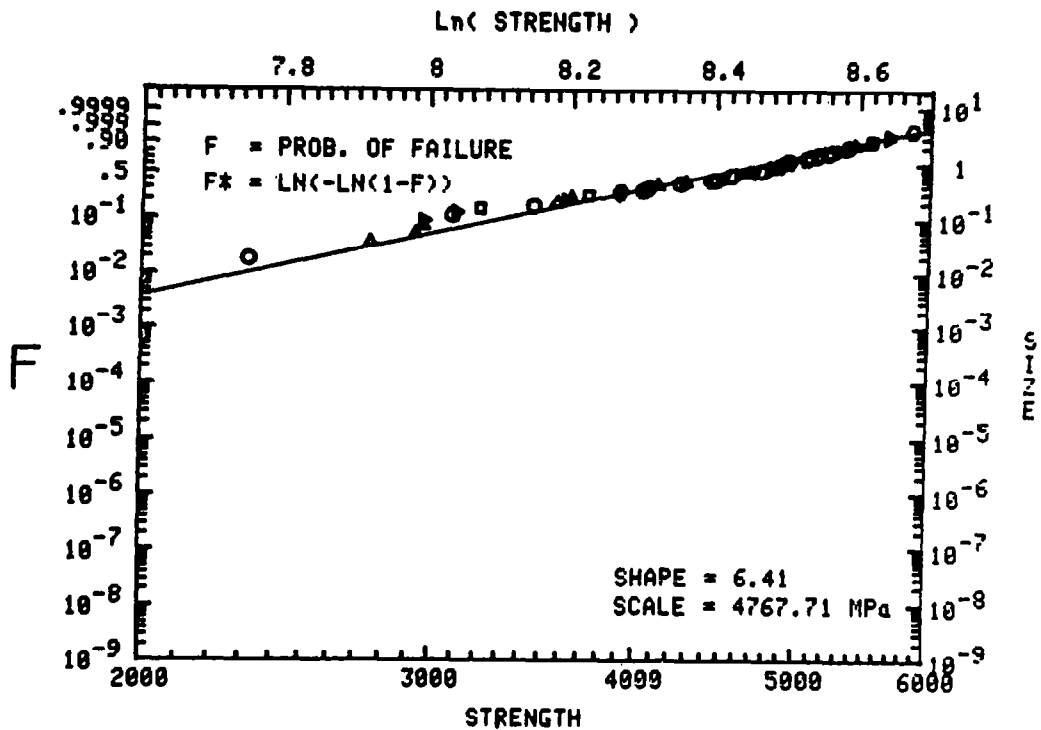
BUT EXISTENCE OF A SINGLE FLAW LEADS TO FAILURE
(WEAKEST LINK OF CHAIN)

• • LARGE SCATTER

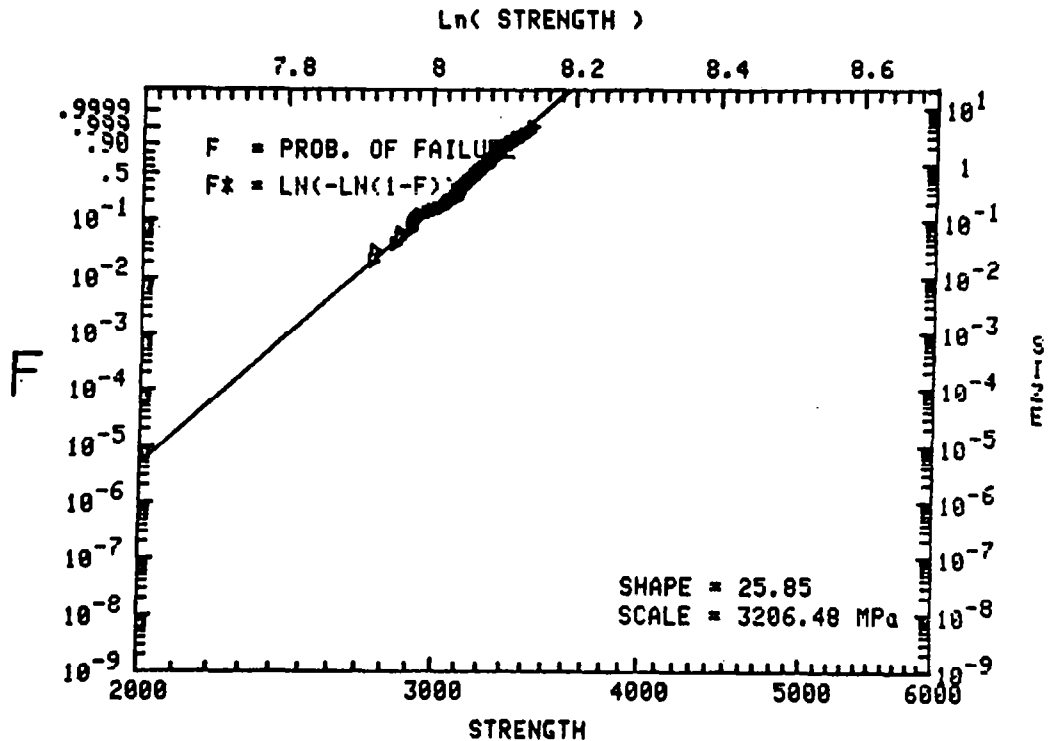
	COEFF. OF VAR.	SHAPE
FIBER	20%	6-8
STEEL	3-5%	25-50

	WITH MATRIX	WITHOUT MATRIX
BUNDLE STRENGTH	550 ksi	350 ksi
BUNDLE SCATTER	4-5%	20-25%

- LONGITUDINAL COMPOSITE STRENGTH IS FIBER-DOMINATED
WITH SUBSTANTIAL MATRIX INFLUENCE

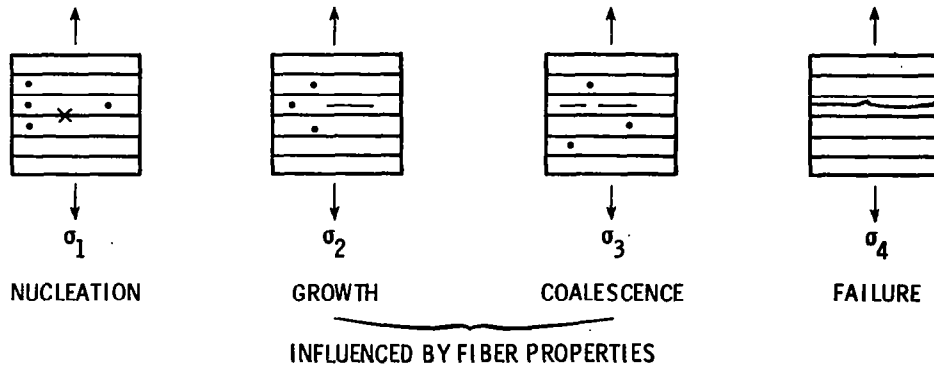


KEVLAR 49 FILAMENT (5CM)
 INTRINSIC STRENGTH (.02CM/MIN, 23C), N=54



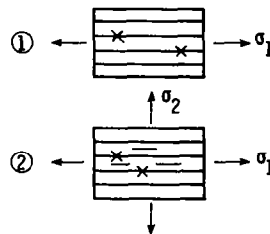
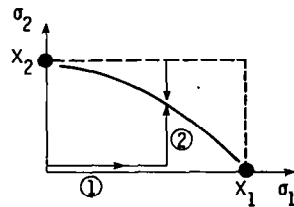
KELVAR 49-332/T403 STRAND
 INTRINSIC STRENGTH (1CM/MIN), N=100

TRANSVERSE STRENGTH: MATRIX-DOMINATED OR MATRIX-CONTROLLED (REF. 4)

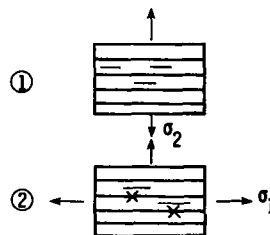
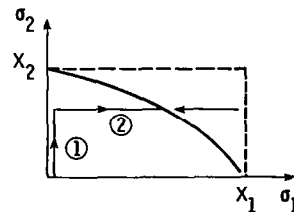


TRANSVERSE STRENGTH IS MATRIX-DOMINATED,
INFLUENCED BY FIBER AND PACKING, NOT WELL-DEFINED PLANE OF FAILURE

STRENGTH COUPLING UNDER COMBINED STRESS



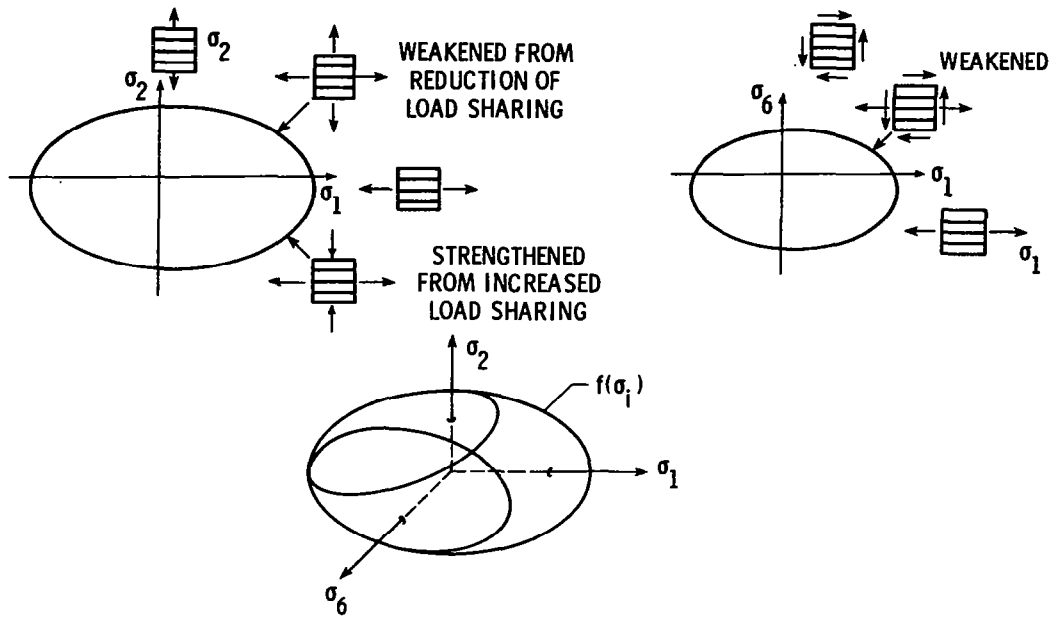
- BROKEN FIBER INITIATES TRANSVERSE CRACK, THEREFORE REDUCES TRANSVERSE STRENGTH



- STRENGTH COUPLING IS EXPECTED FROM PHYSICS OF FAILURE

- TRANSVERSE CRACK REDUCES LOAD TRANSFER, INCREASES δ , REDUCES LONGITUDINAL STRENGTH

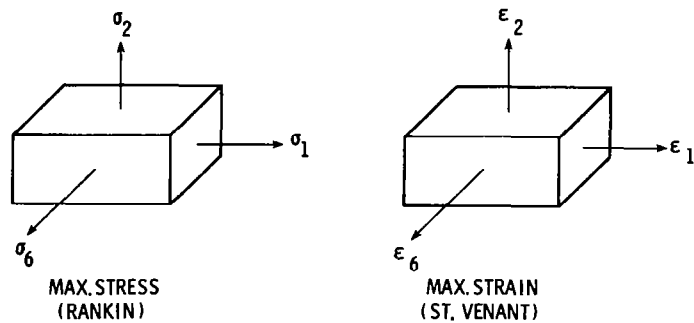
FAILURE SURFACE FOR STRENGTH COUPLING (REFS. 5 AND 6)



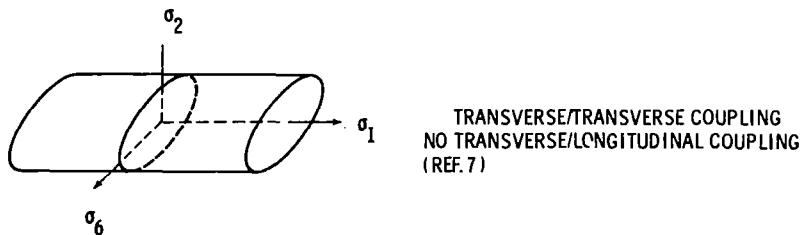
$$f(\sigma_i) = \sigma_i F_i + F_{ij} \sigma_i \sigma_j + F_{ijk} \sigma_i \sigma_j \sigma_k + \dots \leq 1$$

TENSOR POLYNOMIAL EXPANSION OF SURFACE

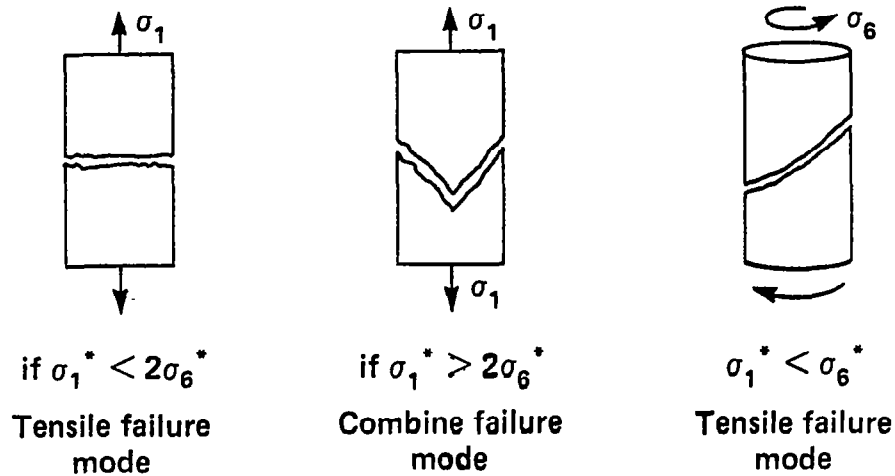
NONCOUPLING STRENGTH CRITERIA



BOTH CAN BE EXPRESSED AS TENSOR POLYNOMIALS (REF. 5)



FAILURE TESTS REQUIRES WELL-DEFINED FAILURE MODES



Plane of Failure does not necessarily correspond to applied stress

Plane of Failure of composites are seldom well defined

Failure Criterion based on applied stress is NOT Mechanistic; it is Operational

CONSISTENCY IN STRENGTH THEORY FORMULATION

	Output		Mtl constant	Input
Deformation	ϵ_{ij}	=	S_{ijkl}	σ_{kl}
	ϵ_{ij}	=	α_{ij}	ΔT
Strength	σ_{ij}^*	=	()	σ_{ij}
			$\sigma_{ij} < \sigma_{ij}^*$ uniaxial	
			$\sigma_{ij} < f(\sigma_{ij}^*)$ combined	

$$f(\sigma_{ij}) = F_{ij} \sigma_{ij} + F_{ijkl} \sigma_{ij} \sigma_{kl} + F_{ijklmn} \sigma_{ij} \sigma_{kl} \sigma_{mn} + \dots$$

F_{ij} etc material constants dimensions $\left[\frac{1}{\text{stress}} \right], \left[\frac{1}{\text{stress}^2} \right], \dots$

- Independent of mtl's coordinates
- Allow mathematical operations

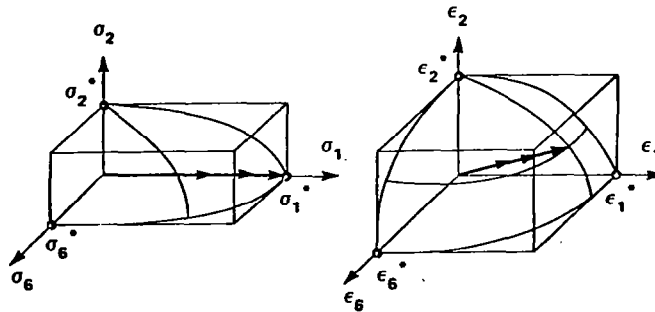
FAILURE STRENGTH MEASUREMENTS

Design loading conditions (direction of stress vector) which is capable of discriminating failure criteria

		Stimuli		
		σ_1	σ_2	σ_6
Failure strains	ϵ_1	S_{11}	S_{12}	S_{16}
	ϵ_2	S_{12}	S_{22}	S_{26}
	ϵ_6	S_{16}	S_{26}	S_{66}
		σ_1	σ_2	σ_6
		Failure stresses		

$$F_i \sigma_i + F_{ij} \sigma_i \sigma_j + \dots = 1$$

Material response constants



One dimensional stress give rise to 3D strain

One dimensional strain give rise to 3D stress

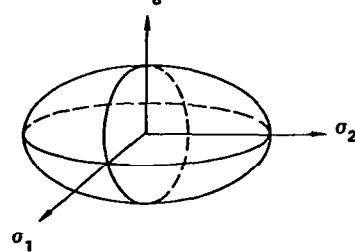
Consistent characterization desirable

THREE-DIMENSIONAL FAILURE CRITERION

Tensor-polynomial Failure Criterion:

$$F_i \sigma_i + F_{ij} \sigma_i \sigma_j + \dots = 1 \quad i, j = 1, 2, 3, 4, 5, 6$$

$$F_i = \begin{bmatrix} F_1 \\ F_2 \\ F_3 \\ 0 \\ 0 \\ 0 \end{bmatrix} \quad F_{ij} = \begin{bmatrix} F_{11} & F_{12} & F_{13} & 0 & 0 & 0 \\ & F_{22} & F_{23} & 0 & 0 & 0 \\ & & F_{33} & 0 & 0 & 0 \\ & & & F_{44} & 0 & 0 \\ & & & & F_{55} & 0 \\ & & & & & F_{66} \end{bmatrix}$$



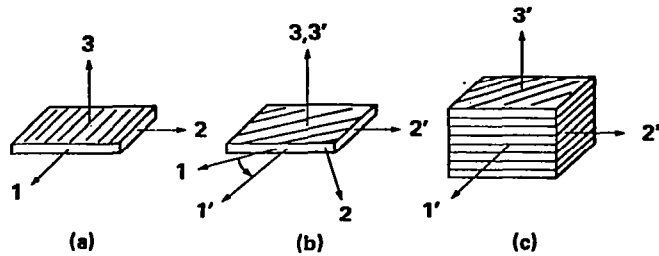
2-D a failure surface

3-D a hyper-surface (6)

- How many independent tests? (12)
- What are the tests?

NO. OF INDEPENDENT TESTS

Failure tensor F_i, F_{ij} follow tensor transformation rules



- 3-D failure criterion for lamina (a) only

Symmetry condition of orthotropic lamina $2 = 3$

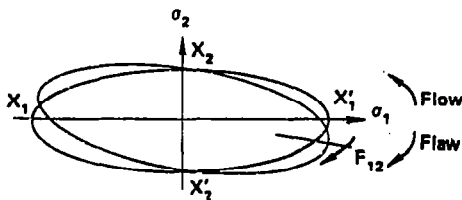
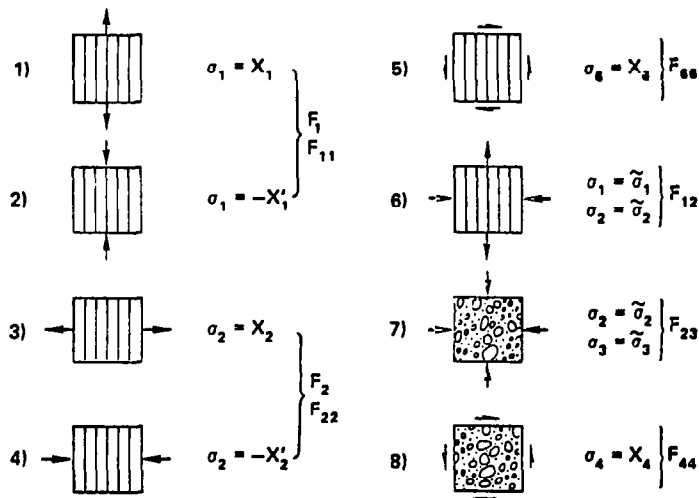
Tensor Notation	Contracted Notation	12 - 4 = 8
$F_{22} = F_{33}$	$F_2 = F_3$	
$F_{1122} = F_{1133}$	$F_{12} = F_{13}$	
$F_{2222} = F_{3333}$	$F_{22} = F_{33}$	
$F_{1313} = F_{1212}$	$F_{55} = F_{66}$	

Component not associate with planer properties

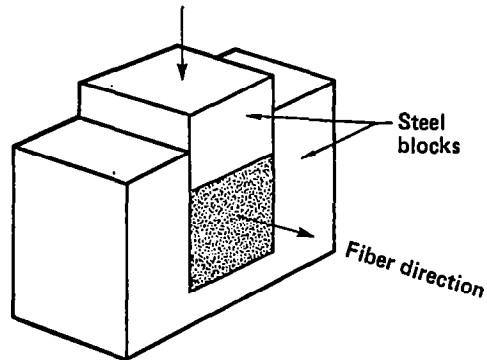
F_{2233} (F_{23}) Transverse strength coupling

F_{2323} (F_4) Shear

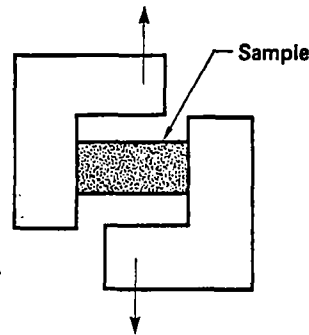
INDEPENDENT EXPERIMENTS



EXPERIMENTS ASSOCIATE WITH THICKNESS DIRECTION



Experiment No. 7
Biaxial compression



Experiment No. 8
Shear test

SHOULD TENSILE AND COMPRESSIVE STRENGTH BE RELATED?

FOR UNIAXIAL TENSION: $\sigma_i \neq 0, \sigma_i = 0, i \neq 1$

$$F_{11} \sigma_1^2 + F_1 \sigma_1 = 1 \Rightarrow F_1 = \frac{1}{X_1} - \frac{1}{X_1'}, F_{11} = \frac{1}{X_1 X_1'}$$

$$\sigma_1 (F_{11}, F_1) = \sigma_1 (X_1, X_1') \quad \begin{array}{l} X_1 \text{ TENSILE STRENGTH} \\ X_1' \text{ COMPRESSIVE STRENGTH} \end{array}$$

$$F_1 = \frac{1}{X_1} -$$

ALTERNATE EQUIVALENT FORM:

$$\tilde{F}_{11} (\sigma_1 - \tilde{\sigma}_1)^2 = 1$$

$$\tilde{F}_{11} \sigma_1^2 - (2\tilde{\sigma}_1 \tilde{F}_{11}) \sigma_1 = 1 - \tilde{\sigma}_1^2 \tilde{F}_{11}$$

NOW, INTERPRET $\tilde{\sigma}_1$ AS INTERNAL STRESS (A MATERIAL CONSTANT).

STRESS ANALYSIS MUST OPERATE ON $(\sigma_1 - \tilde{\sigma}_1)$,

WHICH IS AN OPERATIONAL INCONVENIENCE

Top Diagram (Tension and Shear Failure):

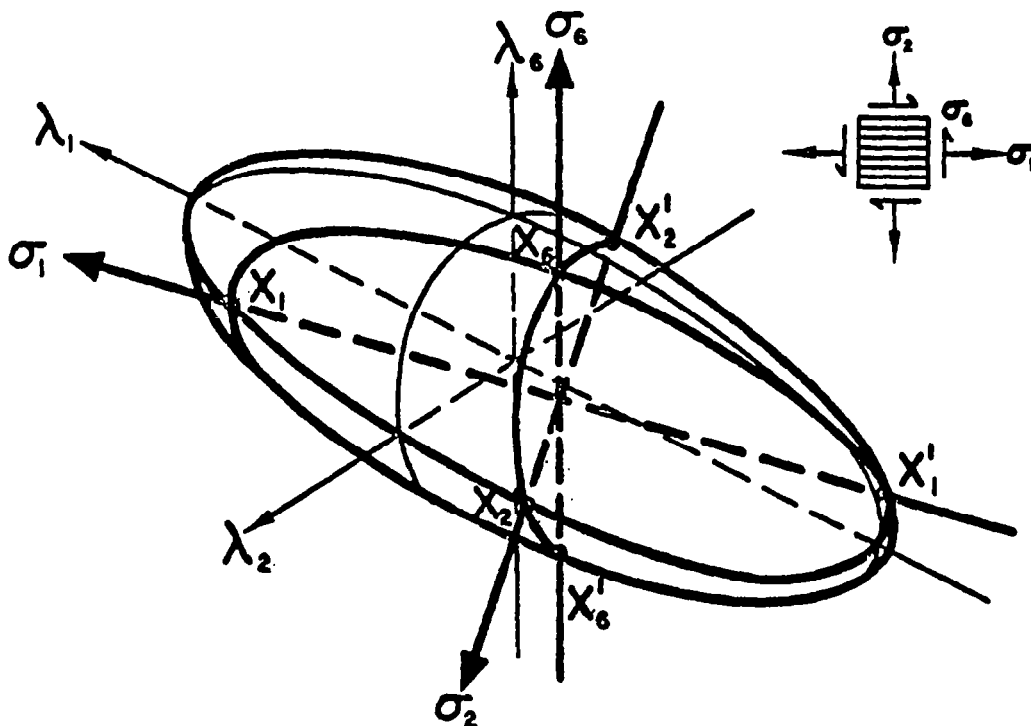
- Block: Tension σ_1 applied vertically.
- Element: Principal stress σ_1 and shear stress τ at 45° .
- Mohr's Circle: Circle in the first quadrant with center on the σ_1 axis. Failure point is at $(\sigma_1/2, \tau)$.
- Equations: $\frac{\sigma_1}{\tau} = 1$, $\frac{\sigma_2}{\sigma_6} \approx 1$.
- Label: **Combine failure mode**

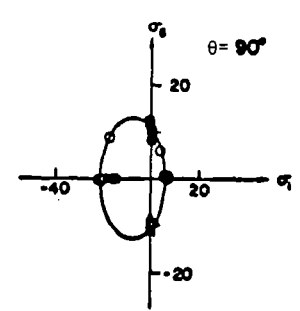
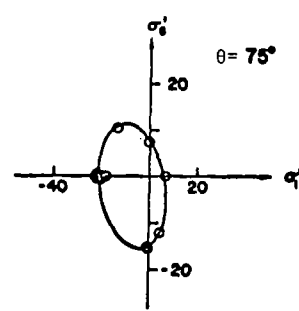
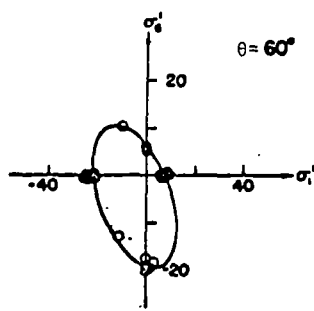
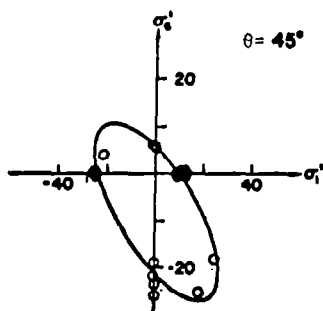
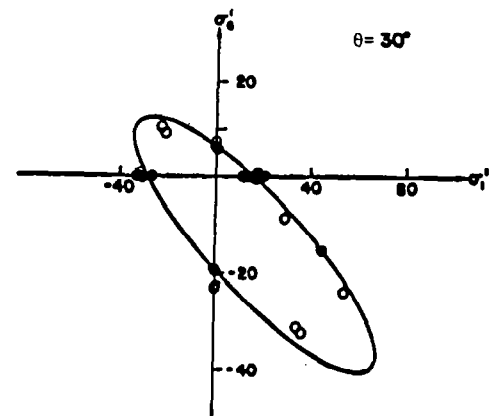
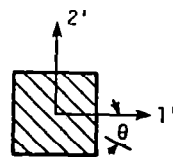
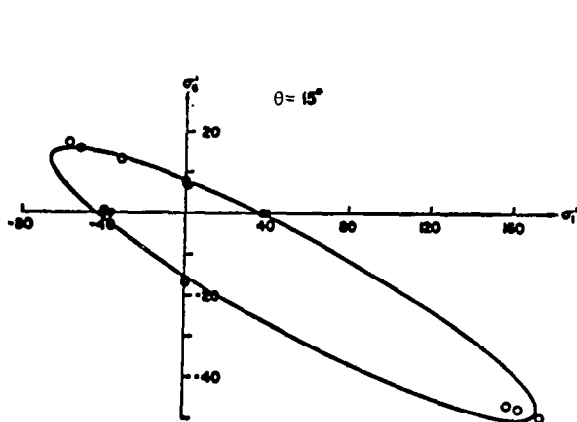
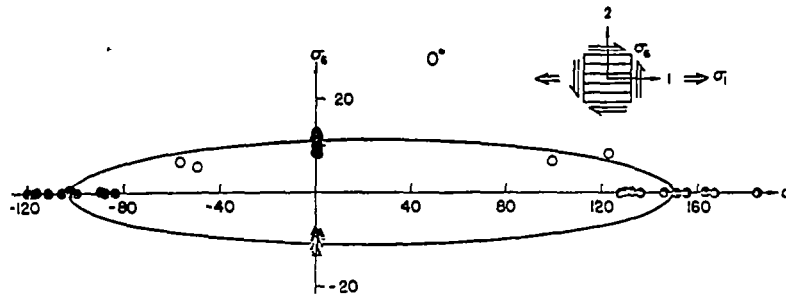
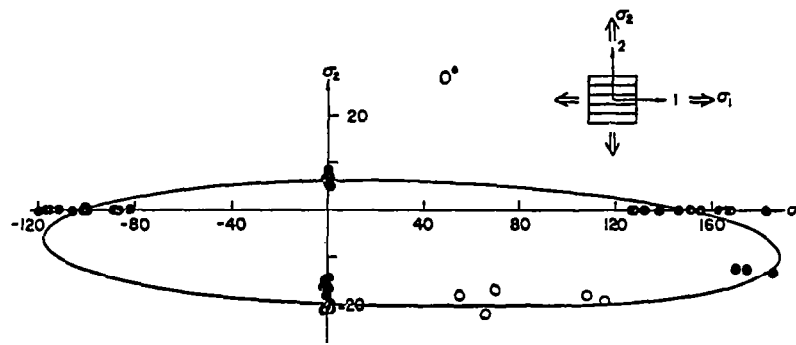
Middle Diagram (Compression and Shear Failure):

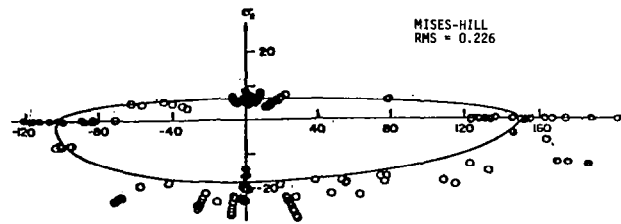
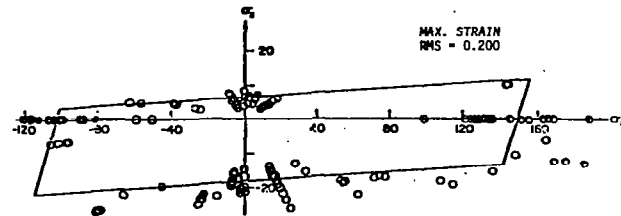
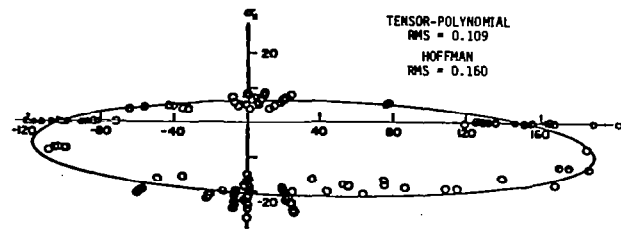
- Block: Compression σ_2 applied vertically.
- Element: Principal stress σ_2 and shear stress τ at 45° .
- Mohr's Circle: Circle in the third quadrant with center on the σ_2 axis. Failure point is at $(-\sigma_2/2, \tau)$.
- Equations: $\frac{-\sigma_2}{\tau} = 1$, $|- \sigma_2| \geq \sigma_6$.
- Label: **Hopefully not combined failure mode**

Bottom Diagram (Tension Failure):

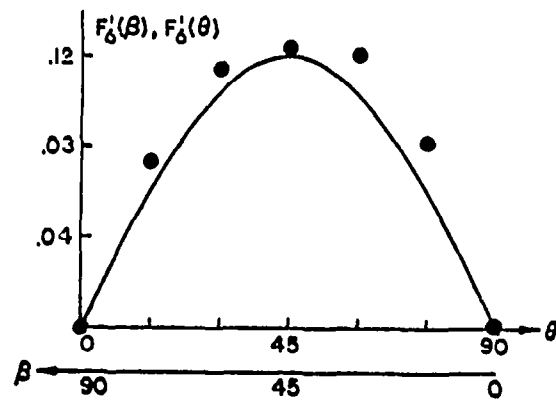
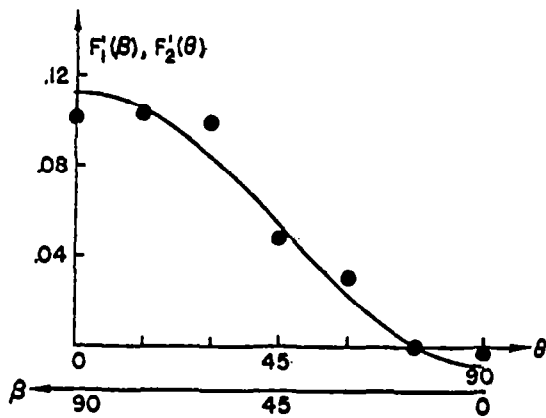
- Block: Tension σ_1 applied vertically.
- Element: Principal stress σ_1 and shear stress τ at 10° .
- Mohr's Circle: Circle in the first quadrant with center on the σ_1 axis. Failure point is at $(\sigma_1/2, \tau)$.
- Equation: $\frac{\tau}{\sigma_1} \geq \frac{\sigma_6}{\sigma_2}$.

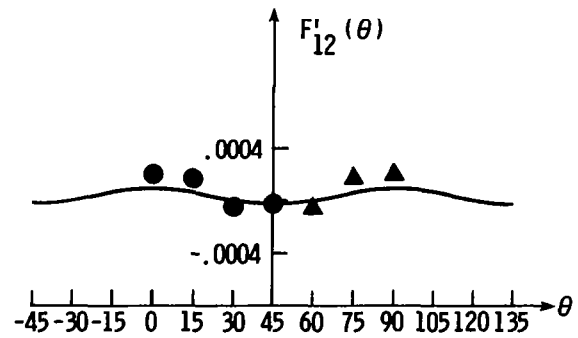
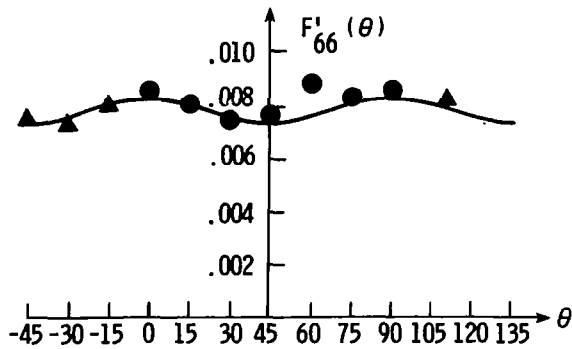
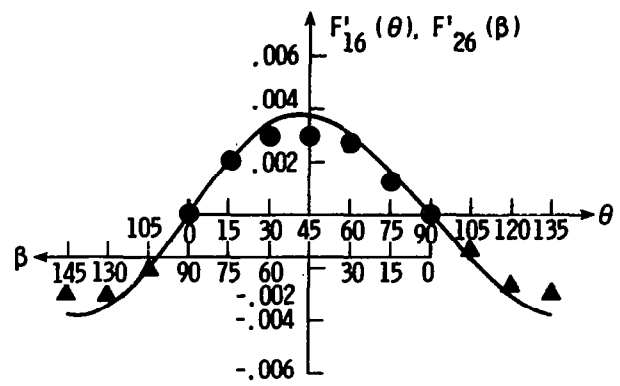
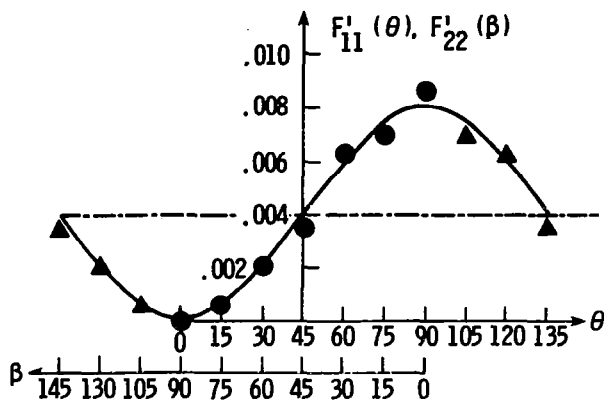






DATA INDICATES STRENGTH COUPLING

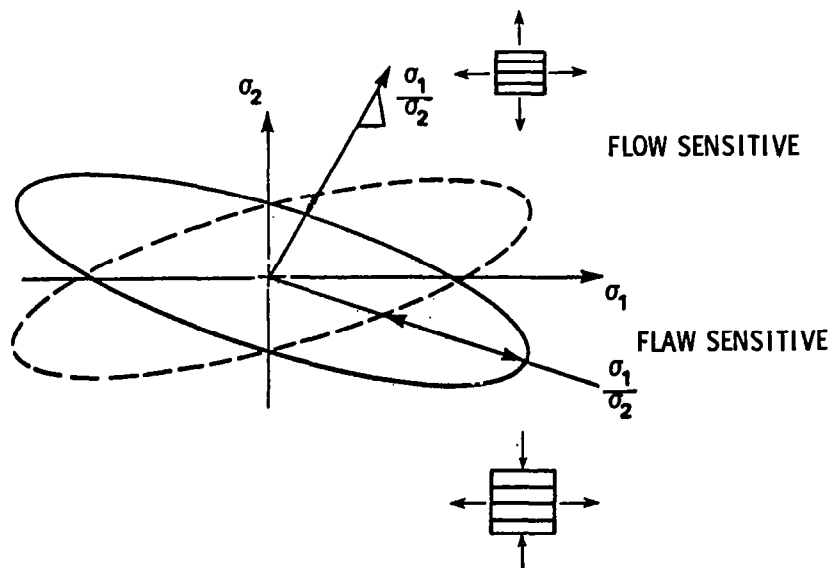




SENSITIVITY OF COMBINED STRESS EXPERIMENTS

$$F_{12} = (1 - F_1 \tilde{\sigma}_1 - F_2 \tilde{\sigma}_2 - F_{11} \tilde{\sigma}_1^2 - F_{22} \tilde{\sigma}_2^2) (1/2 \tilde{\sigma}_1 \tilde{\sigma}_2)$$

$$F_{23} = (1 - F_2 \tilde{\sigma}_2 - F_3 \tilde{\sigma}_3 - F_{22} \tilde{\sigma}_2^2 - F_{33} \tilde{\sigma}_3^2) (1/2 \tilde{\sigma}_2 \tilde{\sigma}_3)$$



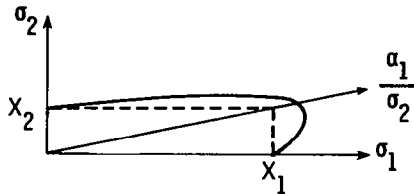
DETERMINATION OF COUPLING COEFFICIENTS

- EXPERIMENTAL MEASUREMENT AT OPTIMIZED STRESS RATIO $\frac{\sigma_1}{\sigma_2}$ (REF. 5)

- SIMPLIFIED STRESS RATIO:

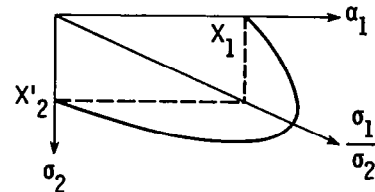
FOR DUCTILE MATRIX

MEASURE AT $\frac{\sigma_1}{\sigma_2} \sim \frac{X_1}{X_2}$



FOR BRITTLE MATRIX

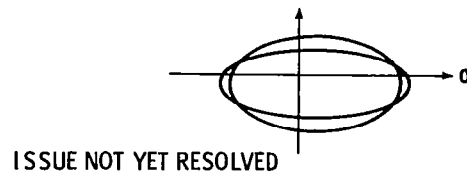
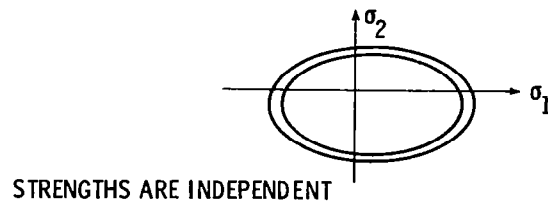
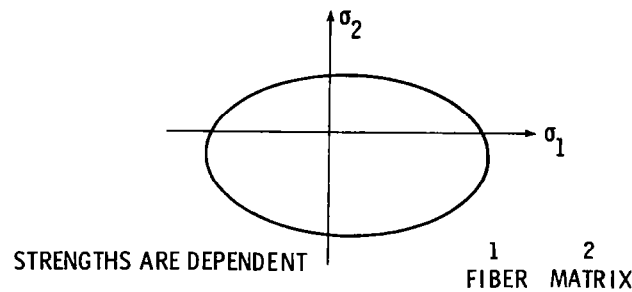
MEASURE AT $\frac{\sigma_1}{\sigma_2} \sim \frac{X_1}{-X'_2}$



- HEURISTIC ESTIMATION - BOUND $F_{12}^2 \leq F_{11} F_{22}$

IF X_1 HAS SMALL SCATTER THEN $F_{12} \rightarrow$ SMALL $\rightarrow 0$ } WITHIN BOUND
 IF X_1 HAS LARGE SCATTER THEN $F_{12} \rightarrow$ LARGE

COMBINED STRESS, ANISOTROPIC STRENGTH



SUMMARY

- MODELING OF SEQUENTIAL FAILURE - RECENT PROGRESS
- SHAPE OF COMBINED STRESS FAILURE SURFACE - LONGITUDINAL AND TRANSVERSE COUPLING EXPECTED AND OBSERVED
- FOR STRENGTH-COUPLED FAILURE SURFACE, TENSOR POLYNOMIAL IS OPERATIONALLY ATTRACTIVE:
 - COUPLING COEFFICIENTS (F_{12}) CAN BE MEASURED OR HEURISTICALLY ESTIMATED
 - READILY EXTENDABLE TO 3-D AND HIGHER ORDER
 - MOST ISSUES IN PROPER ORDER
- PROBABLISTIC REPRESENTATION OF FAILURE SURFACE NOT YET RESOLVED

REFERENCES

1. Rosen, B. W.: Tensile Failure of Fibrous Composites. AIAA Journal, vol. 2, no. 11, November 1964, pp. 1985-1991.
2. Zweben, C.; and Rosen, B. W.: A Statistical Theory of Material Strength With Application to Composite Materials. J. Mech. Physics of Solids, vol. 18, 1970, pp. 189-206.
3. Harlow, E. G., and Phoenix, L.: The Chain-of-Bundles Probability Model for the Strength of Fibrous Materials. Part I and II. J. of Composite Materials, vol. 12, April 1978, pp. 195-214.
4. Chamis, C. C.; and Sinclair, J. H.: Ten-Deg. Off-Axis Test for Shear Properties in Fiber Composites. Experimental Mechanics, vol. 17, no. 9, September 1977, pp. 339-346.
5. Wu, E. M.: Phenomenological Anisotropic Failure Criterion. Composite Materials, vol. 2 (edited by G. P. Sendeckyj), Academic Press, New York, 1974, pp. 354-431.
6. Malmeister, A. K.: Geometry of Endurance Theory. Mekhanika Polimerov, vol. 2, no. 4, 1966, pp. 519-534.
7. Puck, A.: Calculating the Strength of Glass-Fibre Plastic Laminates Under Combined Load. Kunststoffe, vol. 59, no. 11, pp. 780-787.

ANALYSIS OF DELAMINATION

**Frank W. Crossman
Lockheed Palo Alto Research Laboratory
Lockheed Missiles and Space Company, Inc.
Palo Alto, California**

INTRODUCTION

This paper reviews our understanding of the influence of delamination on the fracture sequence and final fracture of graphite-epoxy laminates. The emphasis here is on tensile fracture.

The paper is organized as follows:

- (1) Review of the common fracture modes in laminates and their interaction (based on Lockheed and NASA studies)
- (2) Review of free-edge stress analysis and prediction of delamination sites (based on studies by Lockheed Palo Alto Research Laboratory and Drexel University)
- (3) Consideration of the problem of predicting delamination fracture in regions containing a high stress gradient (based on studies by Lockheed for NASA)
- (4) Analysis of delamination fracture by calculation of strain energy release rate (based on studies by Drexel University and Lockheed)
- (5) Consideration of the interaction of interlaminar and intralaminar fracture (based on studies by Drexel University and Lockheed for the Air Force Office of Scientific Research)
- (6) Analysis of the interrelationship between strength and stiffness (based on studies by Lockheed for NASA)
- (7) Consideration of the correlation between strain energy analysis and statistical analysis approaches in predicting the criticality of a laminate crack (based on studies by Lockheed, Cornell University, and Drexel University)

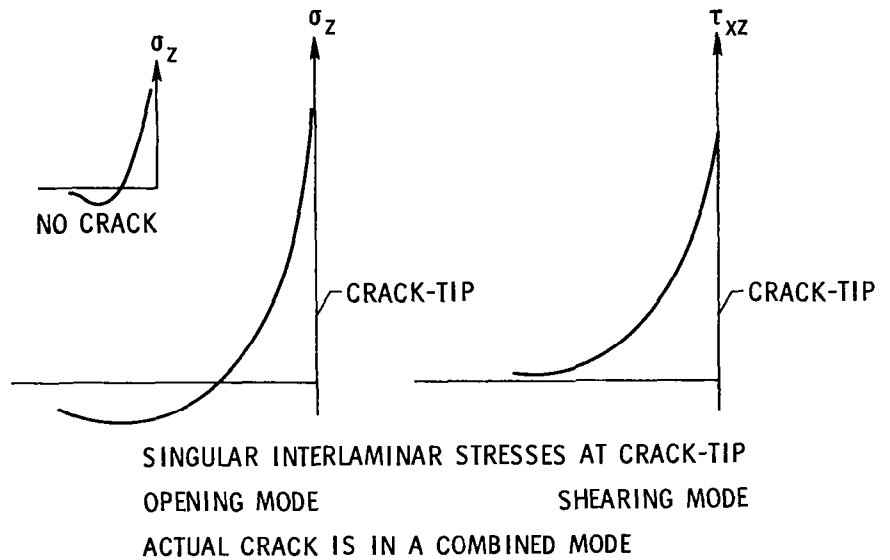
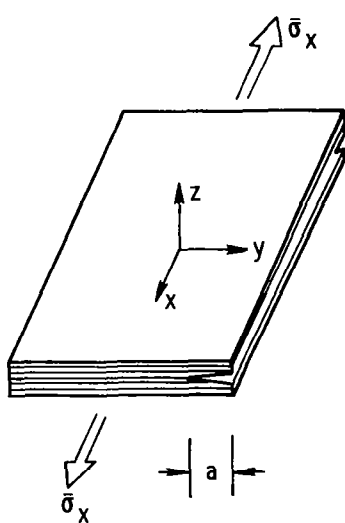
The following people contributed to the observations, analysis methods, and methodology of delamination fracture analysis described in this paper: J. G. Bjeletich and W. J. Warren (Lockheed Palo Alto), A. S. D. Wang and G. E. Law (Drexel University), T. K. O'Brien (NASA Langley), and J. T. Ryder (Lockheed Rye Canyon). Finally, many researchers have contributed to the understanding of delamination and its influence on laminate fracture. These people are acknowledged in the partial bibliography at the end of this paper.

Five cases that involve delamination fracture are presented. These are:

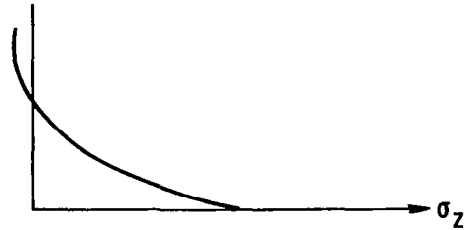
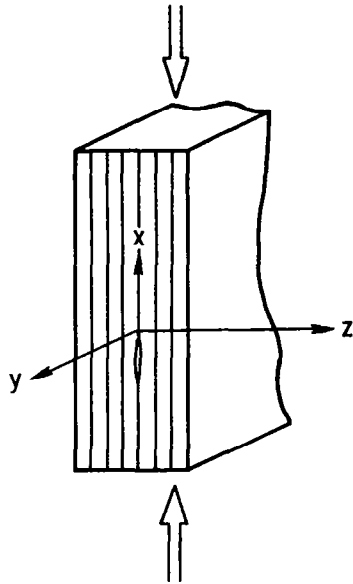
- (1) Free-edge delamination
- (2) Compression delamination
- (3) Delamination interaction with intralaminar cracking
 - (a) Ply peeling
 - (b) Delamination after transverse cracking
 - (c) Simultaneous delamination/transverse cracking

These cases are illustrated in the five figures which follow.

INTERLAMINAR FRACTURE - CASE 1: FREE EDGE PLY DELAMINATION



INTERLAMINAR FRACTURE - CASE 2: COMPRESSIVE LAMINATE FAILURE MECHANISMS



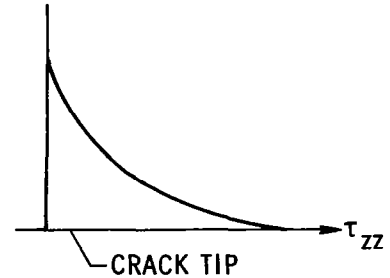
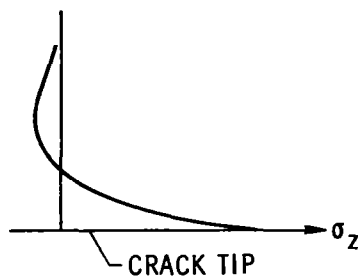
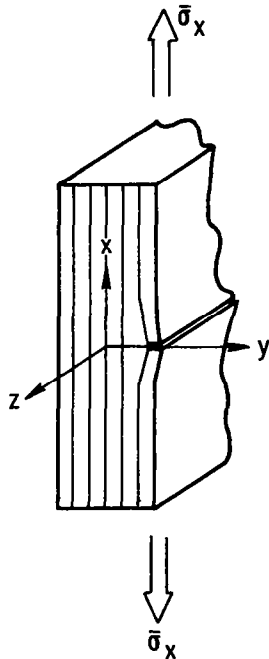
CRACK TIP

SINGULAR INTERLAMINAR CRACK TIP
NORMAL STRESS

CRACK GROWTH IS PRECIPITATED BY
STRUCTURAL BUCKLING ACTION

UNSTABLE CRACK GROWTH DETERMINES
THE COMPRESSIVE STRENGTH OF LAMINATE

INTERLAMINAR FRACTURE - CASE 3 (a): PLY-PEELING (ALSO A CASE OF PLY DELAMINATION) (SURFACE DELAMINATION)

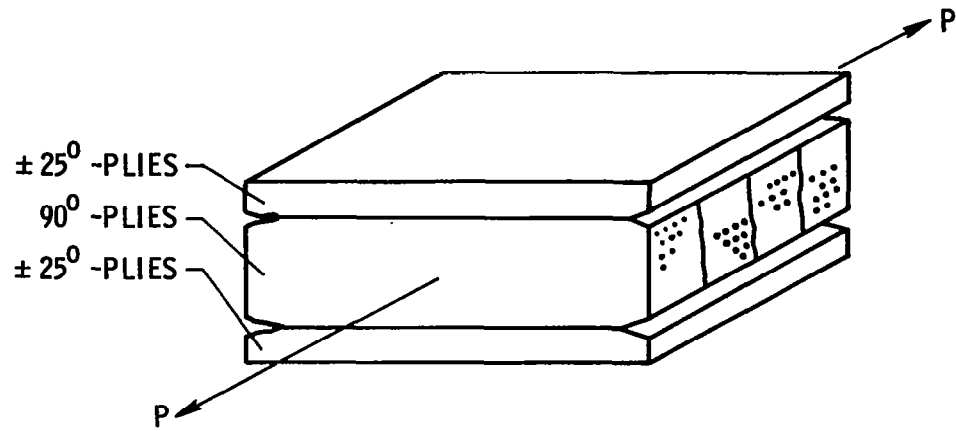


SINGULAR INTERLAMINAR STRESSES AT CRACK TIP
OPENING MODE SHEARING MODE

ACTUAL CRACK IS IN A COMBINED MODE

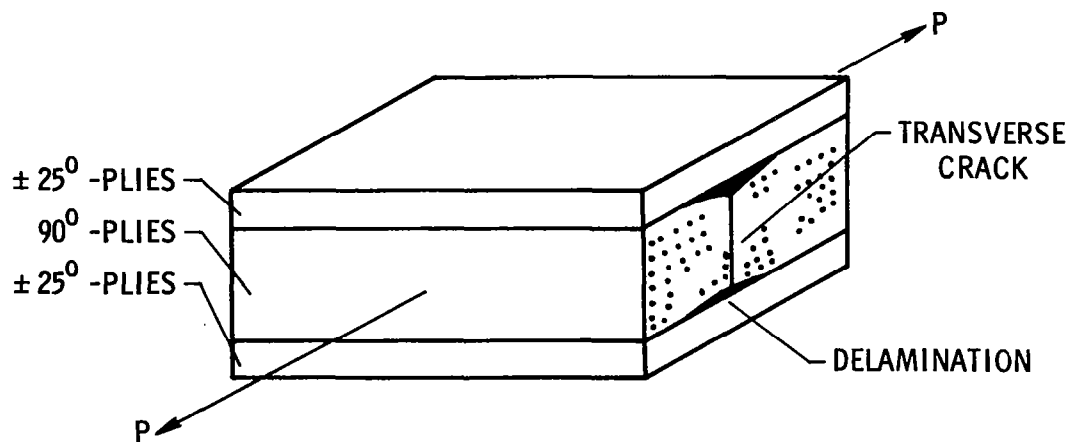
INTERLAMINAR FRACTURE - CASE 3(b):

* FREE EDGE DELAMINATION (ALONG 25/90 PLANE, MIXED MODE)



INTERLAMINAR FRACTURE - CASE 3(c):

* DELAMINATION EMANATING FROM THE ROOT OF A TRANSVERSE CRACK (MIXED MODE)

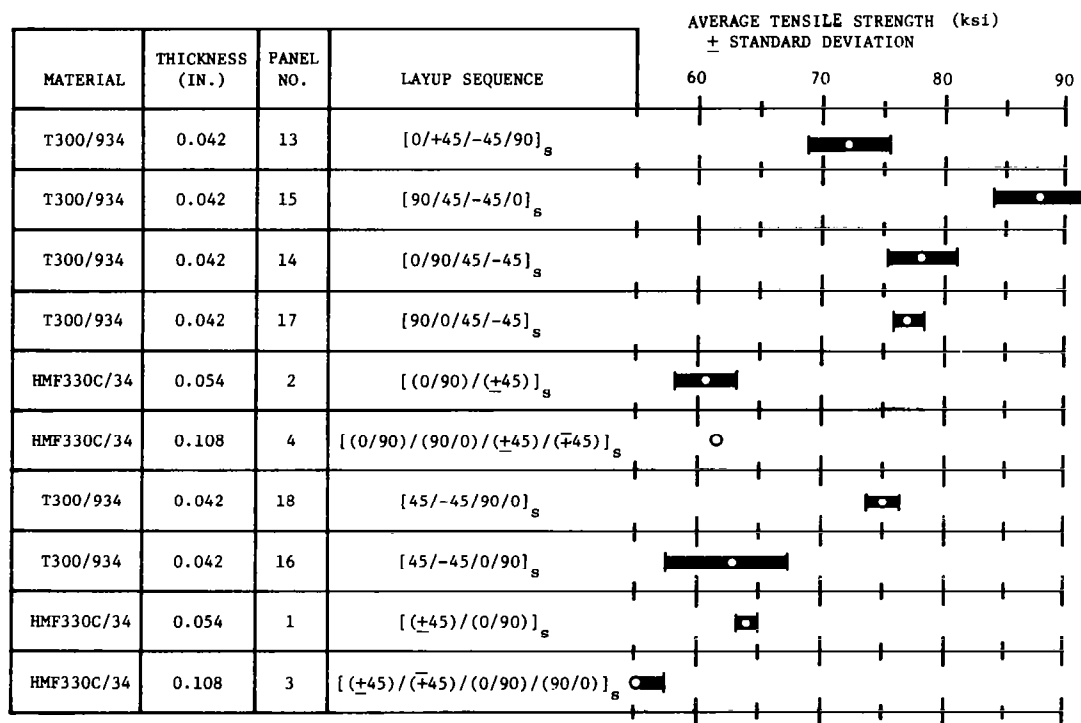


ULTIMATE TENSILE STRENGTH VERSUS STACKING SEQUENCE

Studies were conducted in the mid-1970's to examine the influence of laminate stacking sequence on the tensile properties. The results shown below and in the next figure compare the ultimate strengths of a number of quasi-isotropic laminates constructed of T300/934 tape and fabric (ref. 1). A large variation in strength was found. This variation was not predicted from laminated plate analysis where stacking sequence does not alter the in-plane ply stresses when the specimen is loaded under tension.

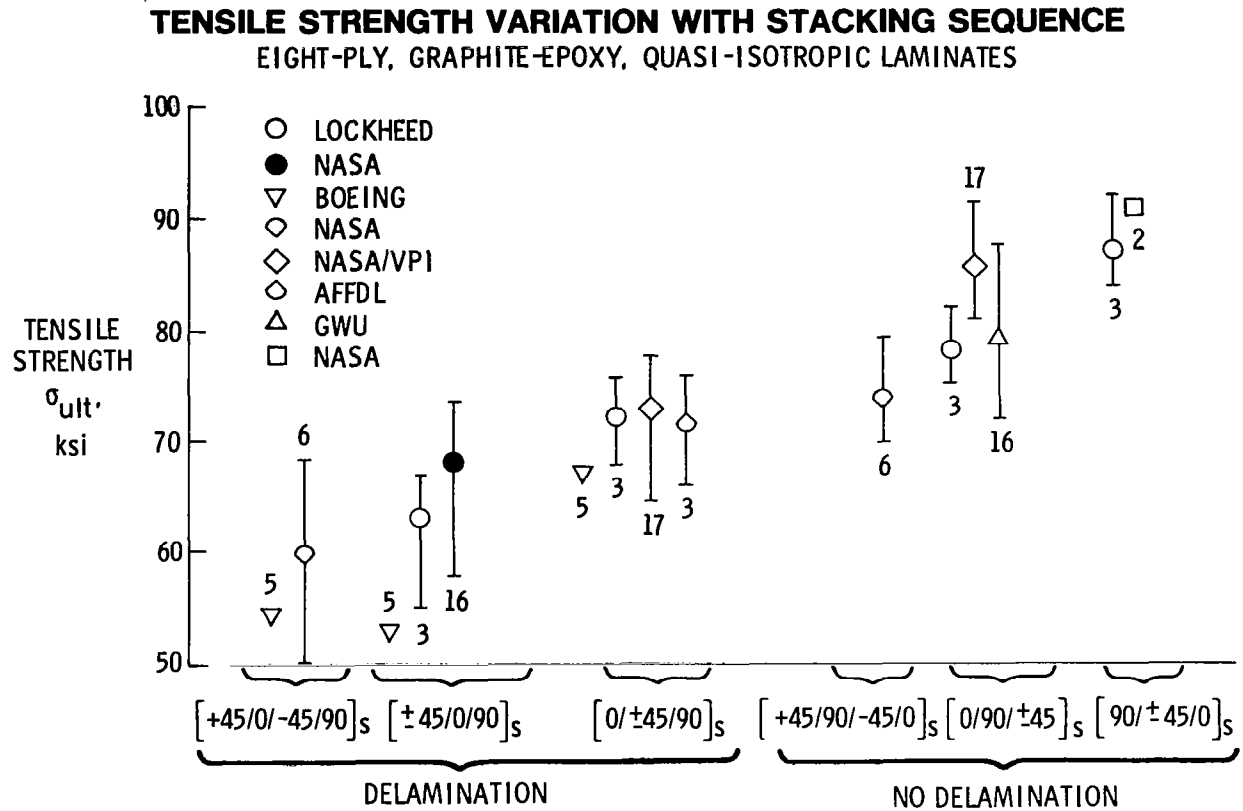
TENSILE STRENGTH OF QUASI-ISOTROPIC T300/ 934 LAMINATES AS A FUNCTION OF PLY STACKING SEQUENCE (LAMINATES DESIGNATED HMF WERE FABRICATED FROM WOVEN GRAPHITE FABRIC)

{From ref. 1}



DELAMINATION AND TENSILE STRENGTH

An examination of several independent studies confirms the observation that stacking sequences that are prone to delamination exhibit generally lower ultimate strengths.

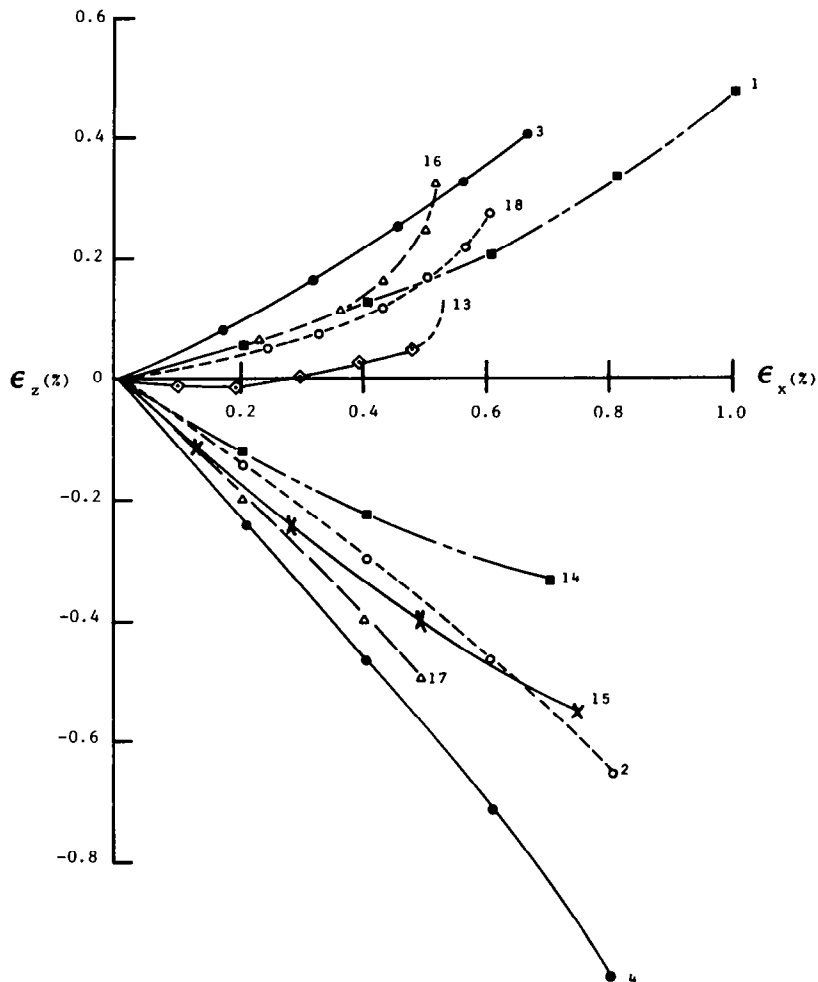


WHAT CAUSES DELAMINATION

Strain gages placed on tensile specimen edges to measure the "through-the-thickness" normal strain (z-strain) as a function of tensile strain (x-strain) showed that the delamination-prone laminates developed a negative Poisson ratio (e.g., the z-strain was positive during tensile loading). Thus interlaminar interaction that was unaccounted for in laminated plate analysis was providing a driving force for delamination.

THROUGH-THICKNESS NORMAL STRAIN ϵ_z VERSUS APPLIED TENSILE STRAIN ϵ_x AS A FUNCTION OF T300/934 PANEL TYPE DESCRIBED IN PREVIOUS FIGURE

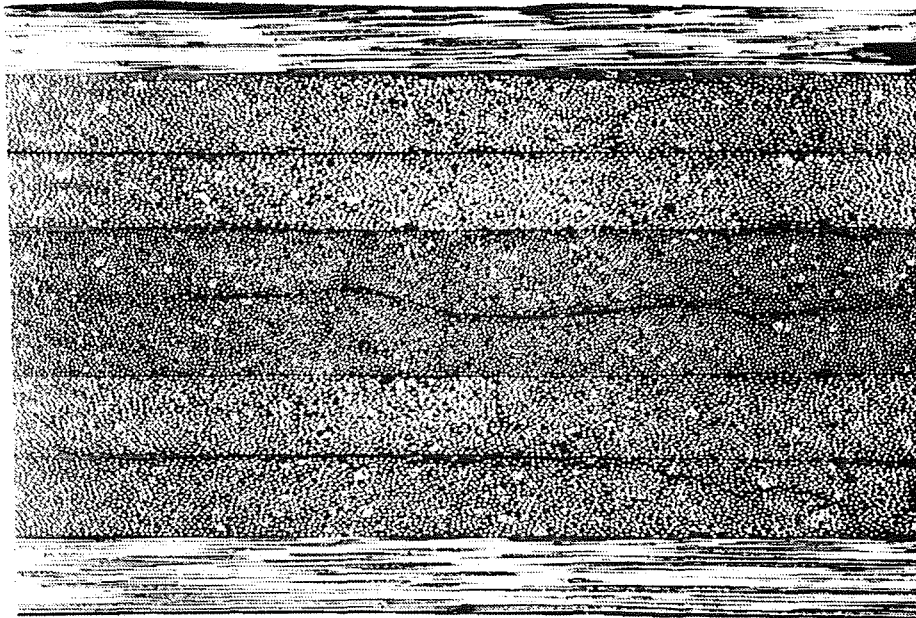
{From ref. 1}



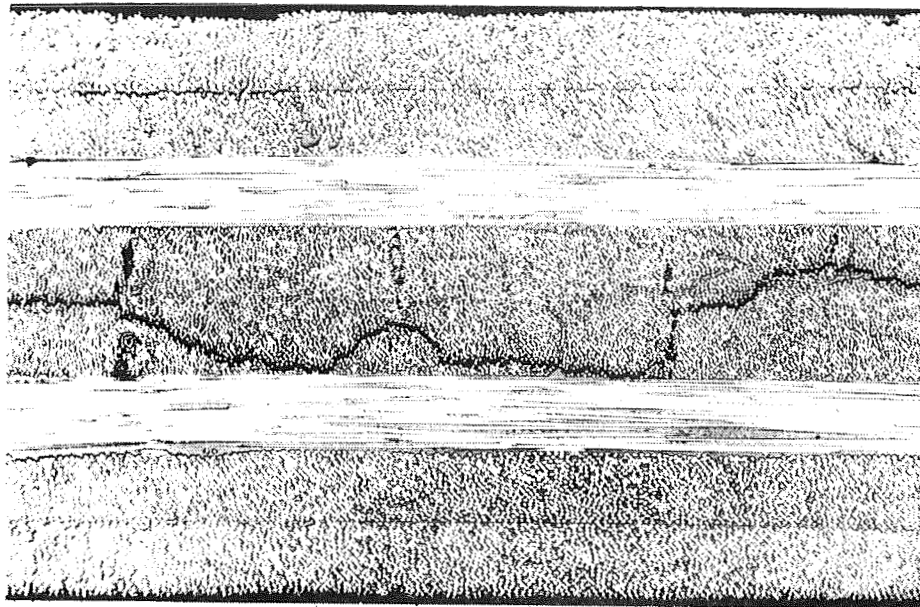
WHERE DOES DELAMINATION OCCUR

Examination of the edges of tensile specimens before and after failure revealed that the location of delamination depended on the particular stacking sequence and in some cases involved multiple delamination at several locations through the ply thickness. Transverse cracks were seen to initiate both before and after delamination, depending on stacking sequence. The extent of delamination was found to be greater at the edges than in the interior of the specimen.

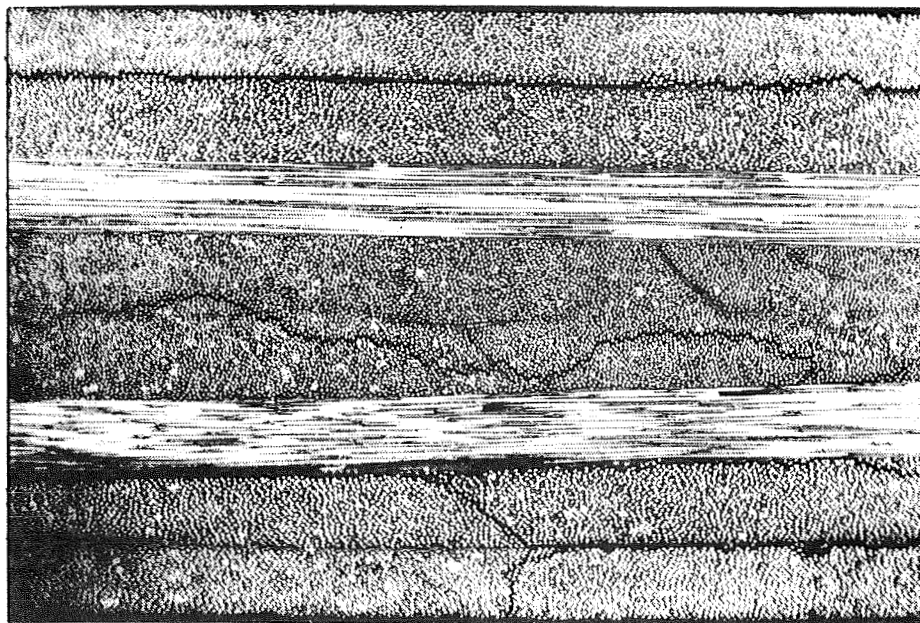
x-z EDGE VIEW OF $(0/45/-45/90)_S$ LAMINATE AFTER LOADING TO 95% UTS
(From ref. 1)



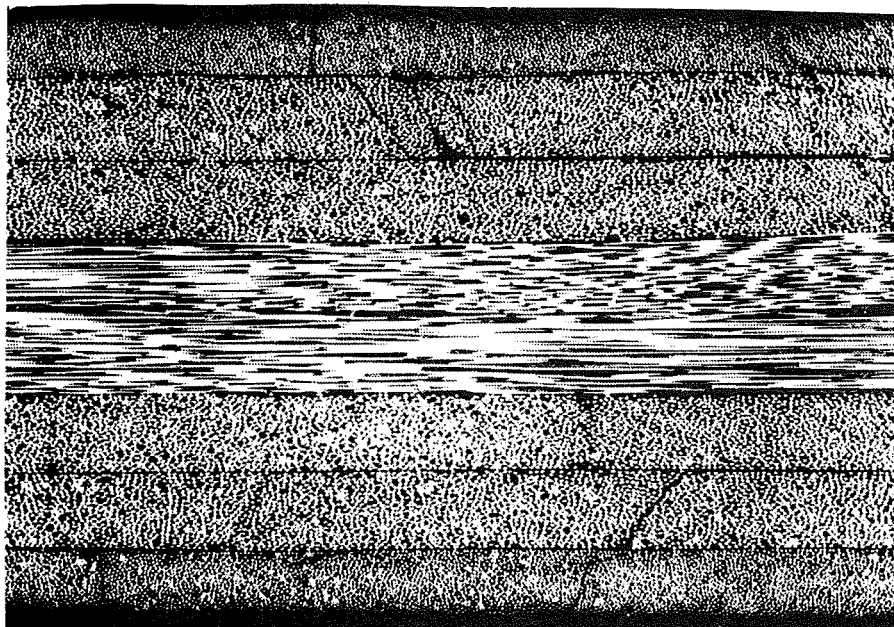
EDGE VIEW OF (45/-45/0/90)_s LAMINATE AFTER LOADING TO 95% UTS
(From ref. 1)



LONGITUDINAL x-z SECTION OF (45/-45/0/90)_s TAKEN NEAR MIDPLANE
BY SECTIONING AND POLISHING
(From ref. 1)



EDGE VIEW OF $(90/45/-45/0)_s$ LAMINATE AFTER LOADING TO 95% UTS
(From ref. 1)



ANALYSIS OF INTERLAMINAR STRESSES

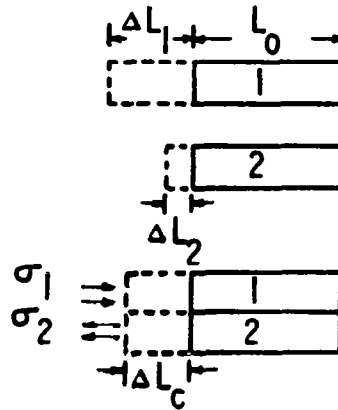
Consideration of stress equilibrium and conservation of angular momentum led to an understanding of how interlaminar stresses arise and the development of simple models to approximate the level and sign of these stresses.

ANISOTROPY IN STIFFNESS OR EXPANSION COEFFICIENTS CAUSES PLY OR LAYER STRESSES

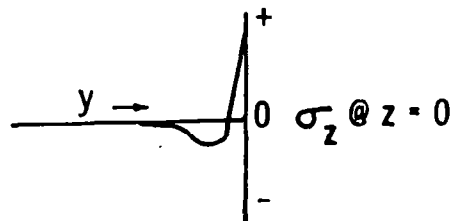
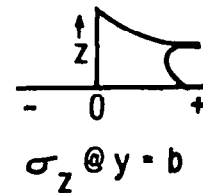
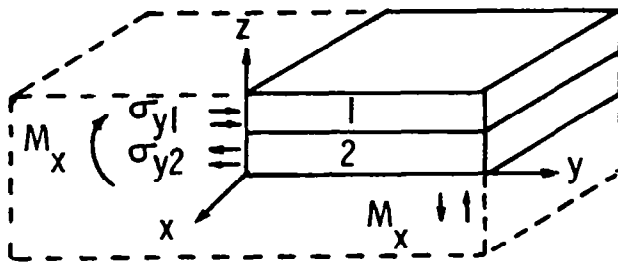
$$\Delta L_c = \frac{V_1 E_1 \Delta L_1 + V_2 E_2 \Delta L_2}{V_1 E_1 + V_2 E_2}$$

$$\sigma_1 = \frac{E_1}{L_0} (\Delta L_c - \Delta L_1)$$

$$\sigma_2 = \frac{E_2}{L_0} (\Delta L_c - \Delta L_2)$$

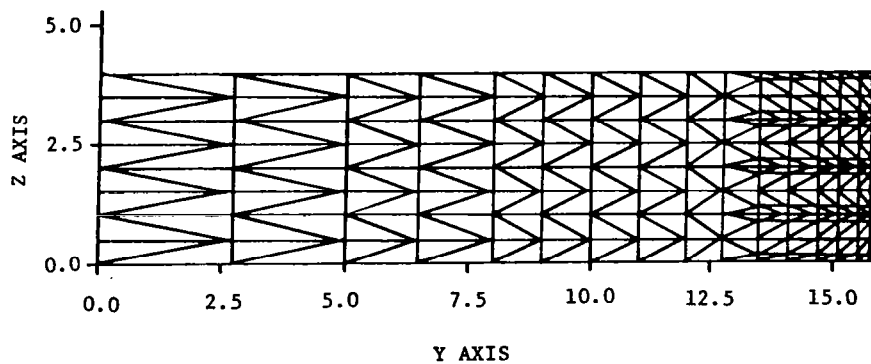
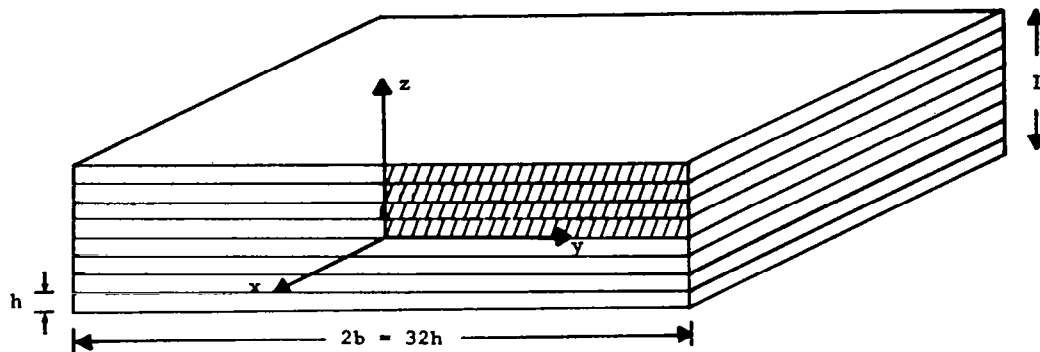


IN-PLANE PLY STRESSES RESULT IN FREE-EDGE STRESSES



NUMERICAL ANALYSIS OF INTERLAMINAR STRESSES

Finite-element and finite-difference analyses have been applied to models of an y-z section of a laminate under uniaxial loading in the x direction. The through-the-thickness Poisson ratio predicted from the analyses agreed well with experimentally measured values.

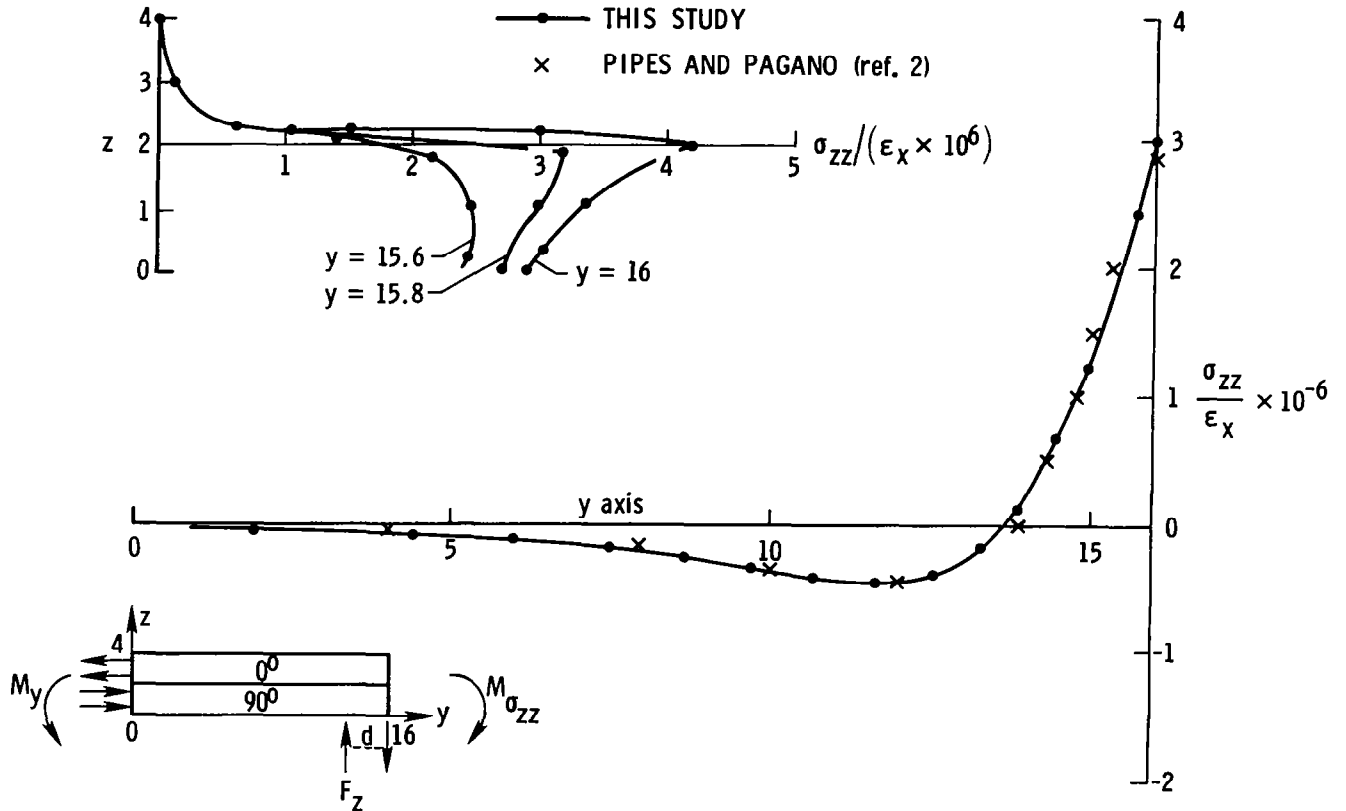


STACKING SEQUENCE DEPENDENCE OF THROUGH THICKNESS
CONTRACTION v_{xz} IN T300/934 QUASI-ISOTROPIC
LAMINATES (ref. 1)

Panel No.	Stacking Sequence	v_{xz}		Ultimate Tensile Strength (ksi)
		Experimental	Calculated	
15	$[90/45/-45/0]_s$	0.80	0.72	87
13	$[0/45/-45/90]_s$	-0.05	-0.02	72
16	$[45/-45/0/90]_s$	-0.30	-0.34	63

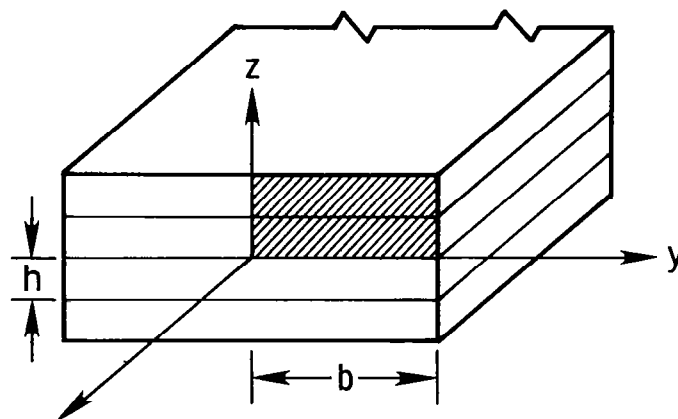
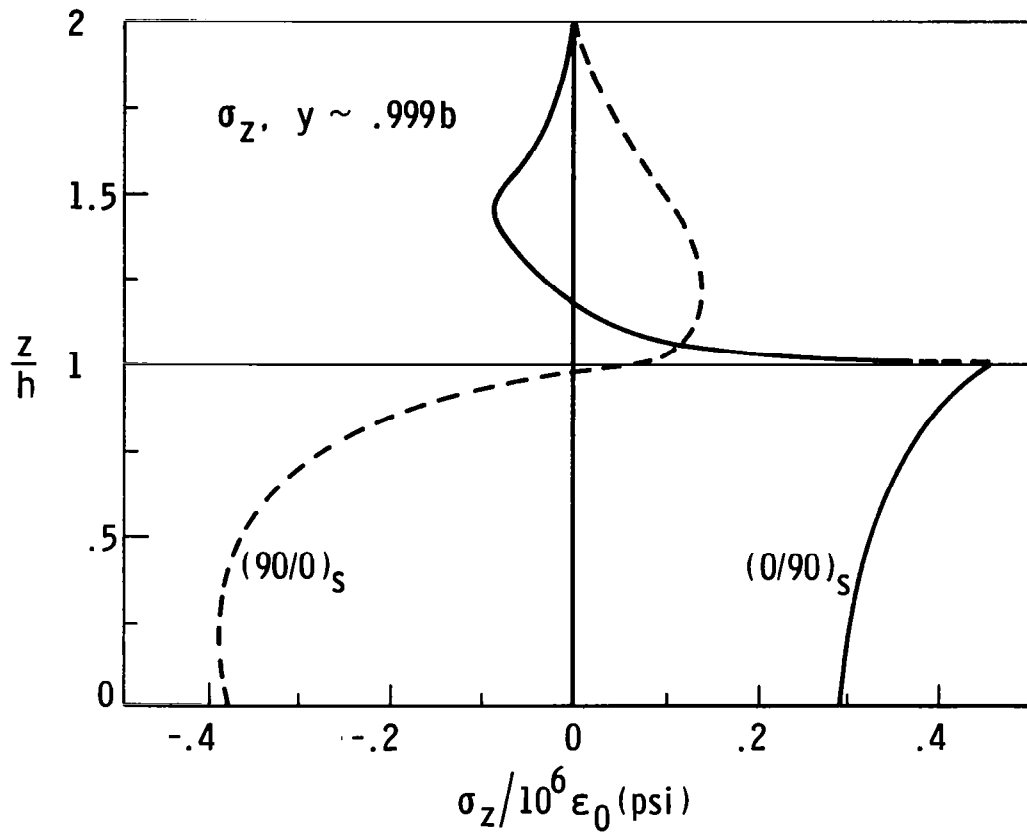
COMPARISON OF NUMERICAL METHODS

The detailed stress analysis was found to depend somewhat on the fineness of the model discretization and the order of the assumed variation of displacement or stress field in the case of finite-element analysis. Stress gradients in both the y and z directions were found in these analyses, as shown in the figures that follow.



FREE EDGE STRESSES IN $[0, 90, 90, 0]_T$ T 300/934

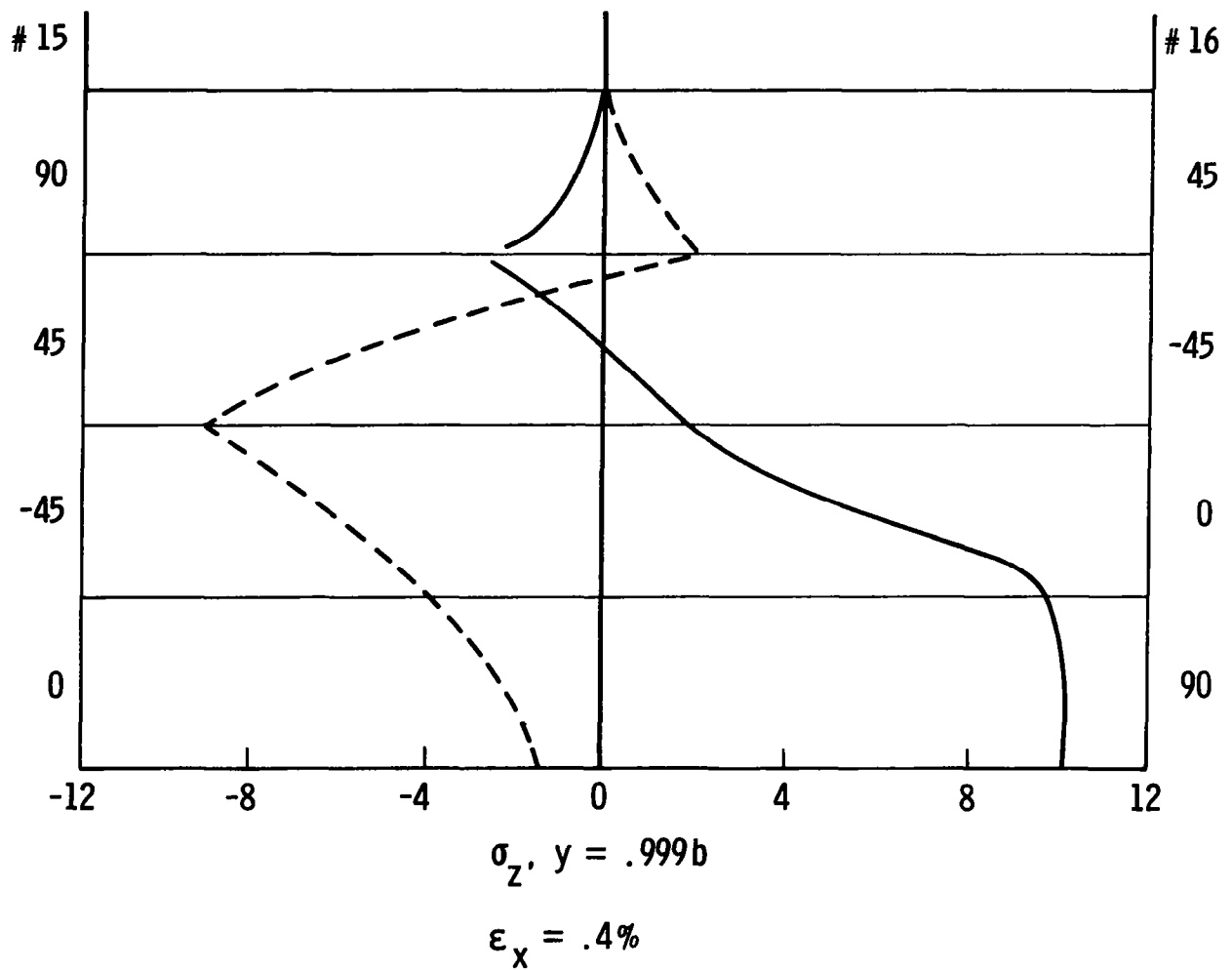
THROUGH-THICKNESS DISTRIBUTION OF σ_2 NEAR FREE EDGE



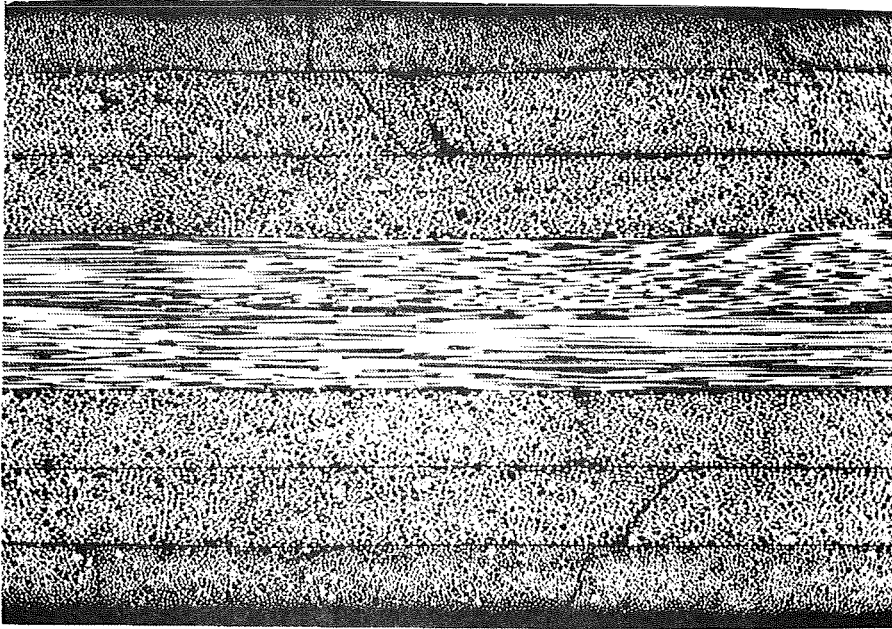
PREDICTION OF DELAMINATION LOCATION

As shown in the figures, the location of peak tensile stress in the analysis often agreed with the experimentally observed delamination location.

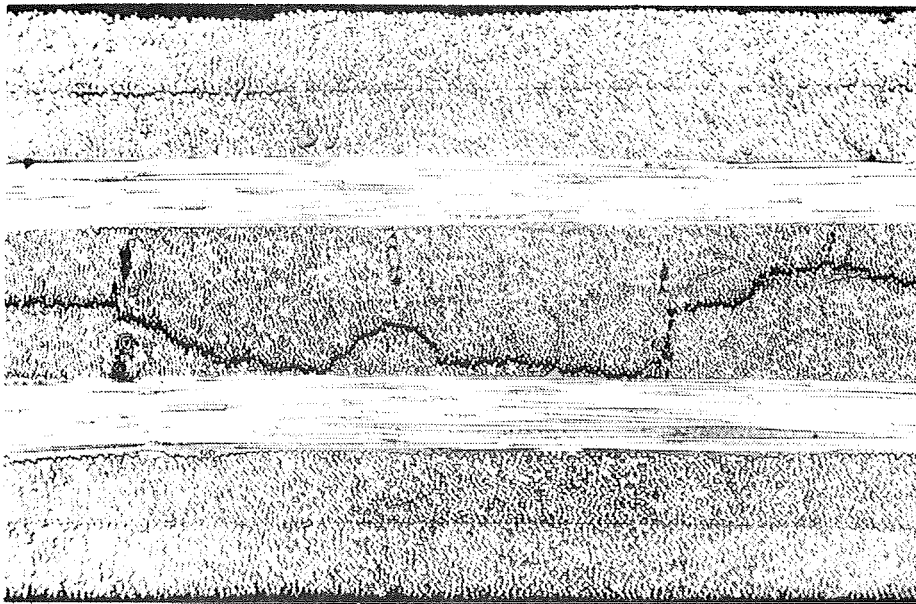
DISTRIBUTION OF σ_z NEAR FREE EDGE UNDER TENSILE LOAD IN x DIRECTION



LONGITUDINAL x-z PLANE SECTION AT FREE EDGE OF $(90/\pm 45/0)_S$ SPECIMEN
(From ref. 1)



LONGITUDINAL x-z PLANE SECTION NEAR CENTER LINE OF $(\pm 45/0/90)_S$ SPECIMEN
(From ref. 1)

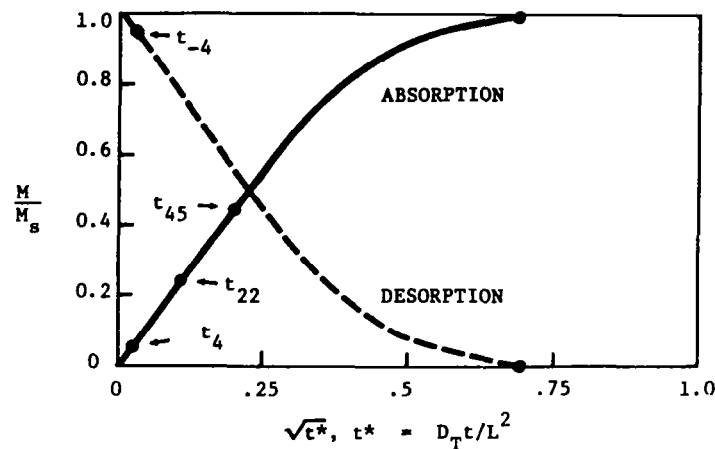


THE PROBLEM OF STRESS GRADIENTS

A problem arose, however, when the numerical analysis of interlaminar stresses associated with moisture gradients was considered. The figures show the moisture concentration as a function of y, z position at two different times during the moisture absorption process. At a time that was small with respect to the equilibrium time, the gradient of concentration is very steep near the free edge. In the limit of very small times, this gradient is infinitely steep. Since absorbed moisture is known to swell the composite locally, a gradient of hygroscopically induced stresses is introduced.

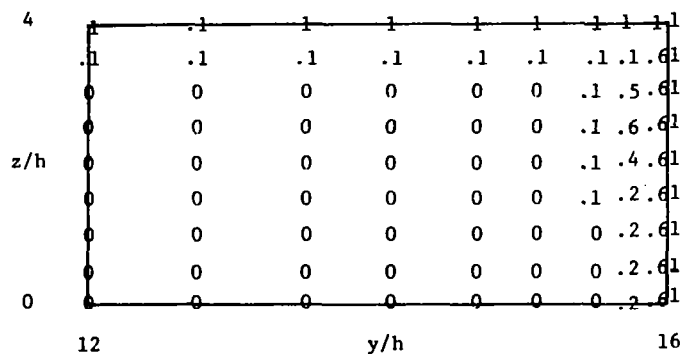
AVERAGE WEIGHT GAIN (LOSS) DURING ABSORPTION (DESORPTION)
RELATIVE TO EQUILIBRIUM MOISTURE CONTENT M_s

{From ref. 3}

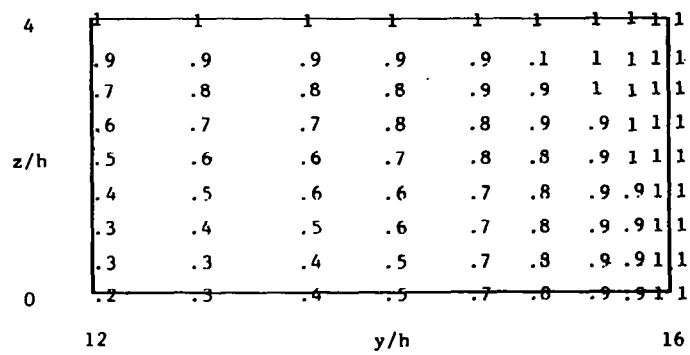


MOISTURE CONCENTRATION C/C_s AFTER ABSORPTION TIME t_4
($M/M_s \approx 4\%$)

{From ref. 3}



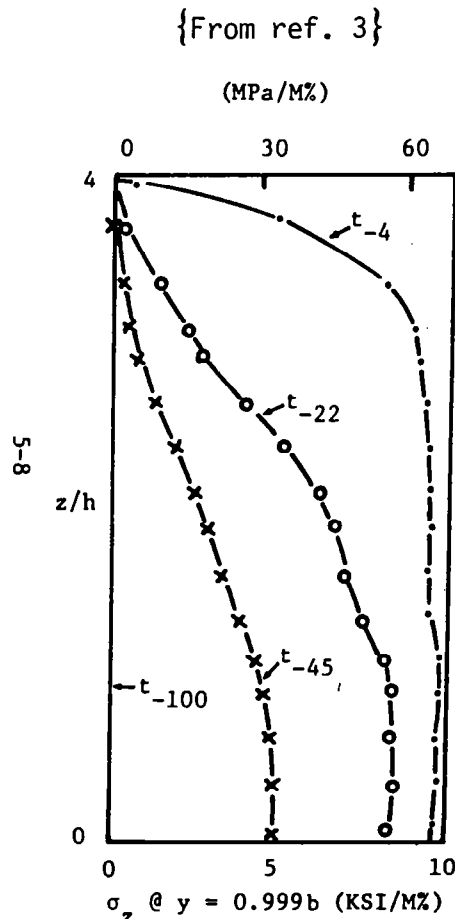
{From ref. 3}



PREDICTION OF DELAMINATION UNDER A STRESS GRADIENT

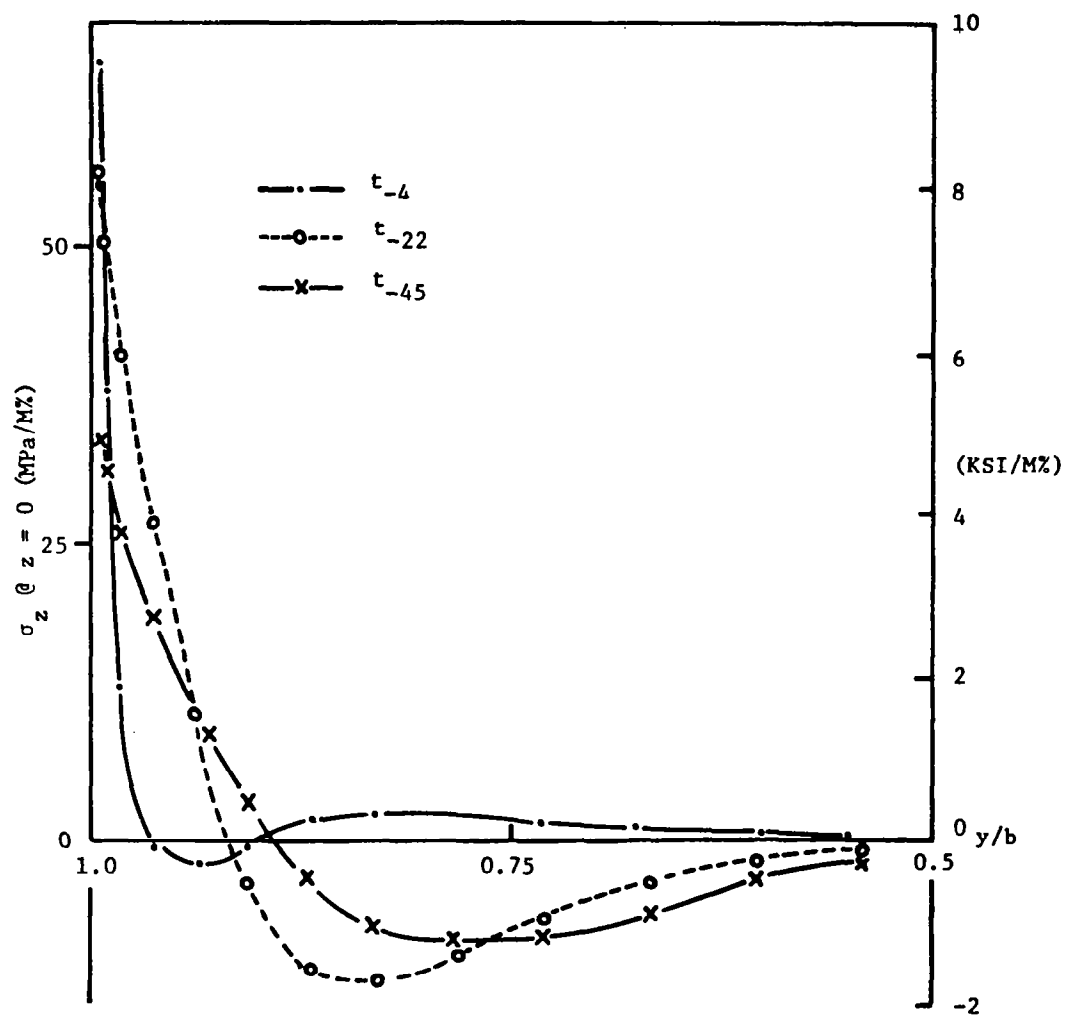
The results of stress analysis in a unidirectional laminate during desorption of moisture from an initially saturated condition show that a transverse normal stress greater than the transverse tensile strength of the material is present during the first part of the desorption period, but gradually reduces to zero upon drying out. Although strength theories based on these local stresses predict delamination during desorption, no experimental evidence of delamination was found in a series of experiments conducted under a NASA Ames contract (ref. 3). It was recognized during the analysis of these results that stresses calculated at a distance from the free edge or interlaminar region which is on the order of the fiber diameter cannot be physically real. The analysis is based on the assumption that fiber and matrix phases are smeared together at the lamina level. That assumption is not appropriate on the microstructural scale. At this level, the interaction of individual fibers and intervening matrix must be considered. Thus the analysis of interlaminar stresses is inherently limited to a cross-sectional area which contains on the order of 10 fibers. In graphite-epoxy laminates this results in a minimum finite-element size of approximately 0.001×0.001 in.

σ_z THROUGH-THICKNESS DISTRIBUTION NEAR
FREE EDGE OF UNIDIRECTIONAL 8-PLY
LAMINATE DURING DESORPTION FROM
EQUILIBRIUM MOISTURE CONTENT M_s



σ_z DISTRIBUTION ALONG MIDPLANE OF UNIDIRECTIONAL
8-PLY LAMINATE DURING DESORPTION

{From ref. 3}



PLY THICKNESS AFFECTS DELAMINATION ONSET STRESS

Rodini and Eisenmann (ref. 4) found that the onset stress in a series of quasi-isotropic laminates varied with ply thickness as approximately 1 over the square root of laminate thickness. Delamination stress analysis based on continuum theory is independent of the scale of the structure and was unable to predict the experimental results. Rodini et al. proposed that Weibull strength theory which is dependent on specimen volume could be used to explain the results.

A second approach, based on fracture mechanics, was taken at Drexel and Lockheed to account for the observed size dependence of delamination and transverse cracking onset in a series of tensile-loaded (25/-25/90_n)_s laminates where n ranged from 1/2 to 8 (ref. 5).

PLY THICKNESS EFFECTS

<u>T 300/5208 LAMINATES</u>	<u>AT ONSET OF DELAMINATION</u>	
	<u>EXPERIMENT</u>	<u>PREDICTION</u>
$(\pm 45/0/90)_s$	45.3 ksi	
	45.3	49.0 ksi
	45.5	
$(\pm 45_2/0_2/90_2)_s$	38.3	
	38.6	36.0
	37.8	
$(\pm 45_3/0_3/90_3)_s$	28.7	
	30.7	29.0

CASE STUDY USING T300/934 GRAPHITE-EPOXY LAMINATES

Laminate configuration:

$$(\pm 25/90_n)_s \quad n = \frac{1}{2}, 1, 2, 3, 4, 6, 8$$

Loading condition:

Uniaxial laminate tension $\bar{\sigma}_x$ or $\bar{\epsilon}_x$

Uniform curing temperature $\Delta T = T_o - T_{r,t}$

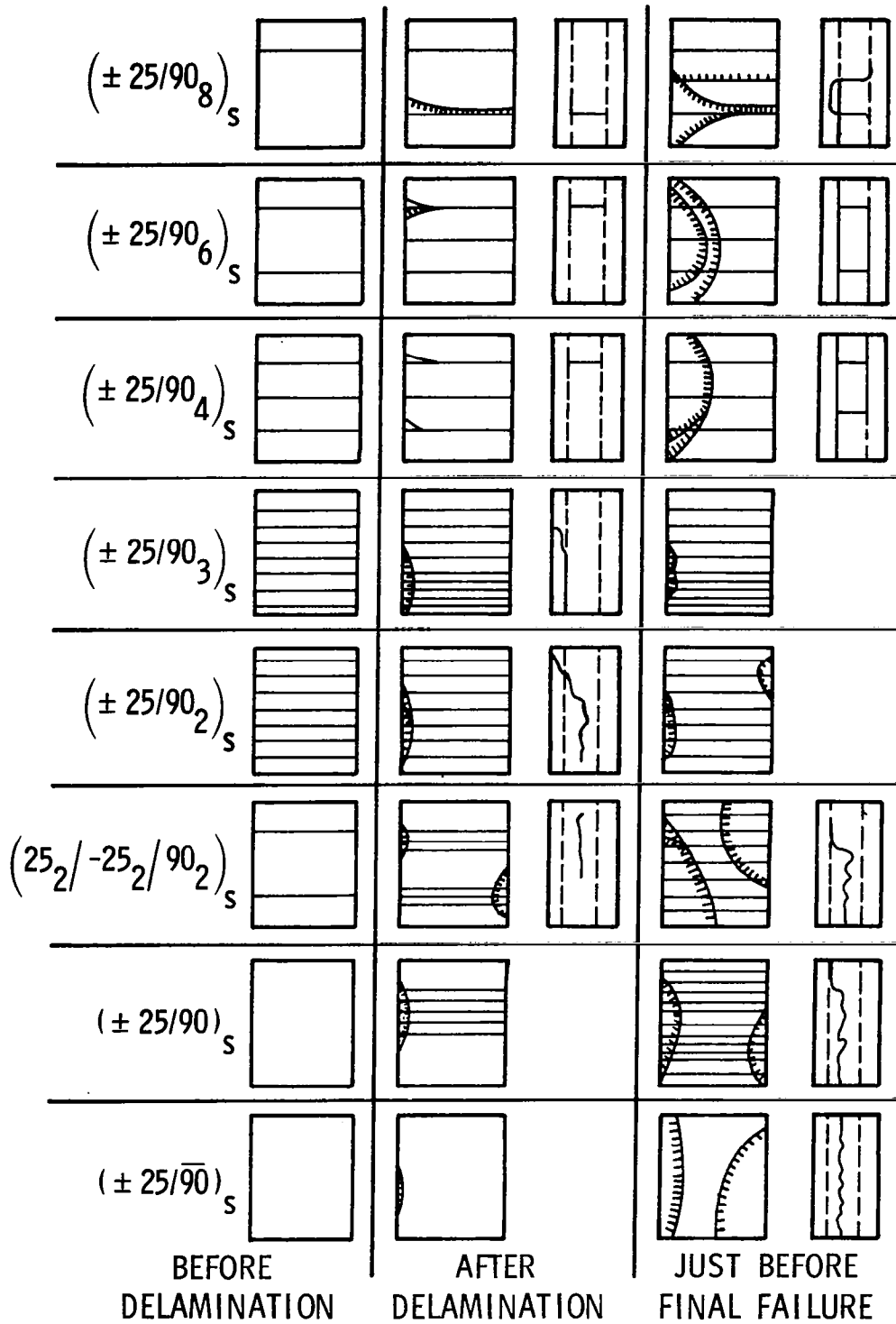
Types of cracking studied:

1. Transverse cracks in 90° layer
2. Edge delamination along $90/90$ interface (mode I) and $25/90$ interface (mixed mode), and transverse-crack-induced delamination
3. Edge-delamination-induced transverse cracks

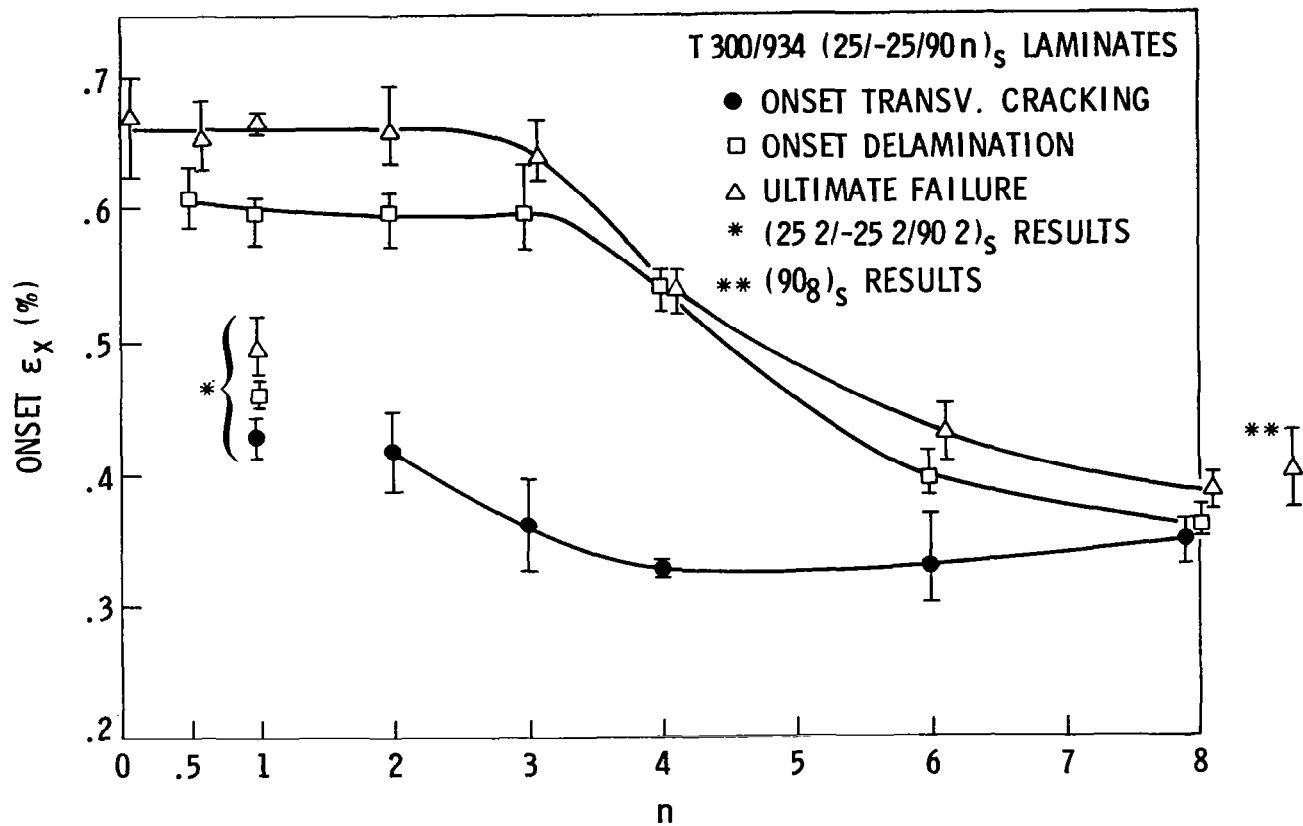
Objectives of study:

1. Onset and growth behavior of various modes of damage
2. Their interrelations
3. Physical and/or geometrical parameters influencing these behaviors
4. Whether minimechanics approach is viable tool in studying damages in composite laminates
5. How to bridge gap between micromechanics and macromechanics

SCHEMATIC OF FRACTURE SEQUENCE IN $(25/-25/90_n)_s$ LAMINATES (ref. 5)

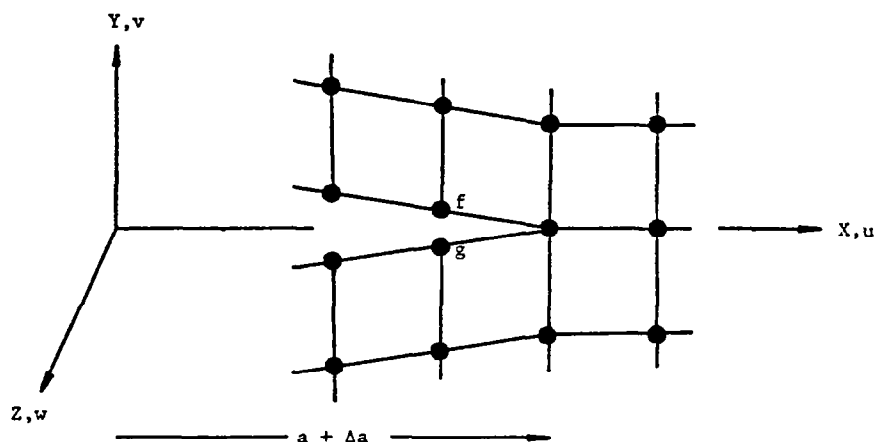
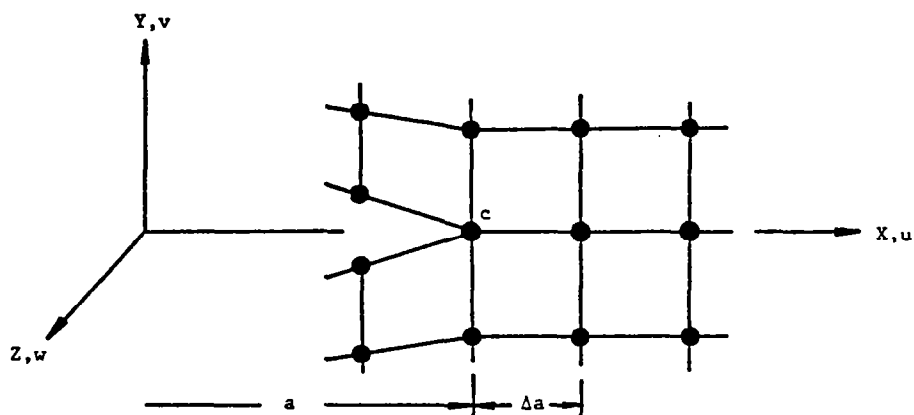


OBSERVED TENSILE STRAIN ϵ_x FOR TRANSVERSE CRACKING, DELAMINATION, AND ULTIMATE FAILURE VERSUS NUMBER OF 90° PLIES IN T300/934



ANALYSIS OF DELAMINATION STRAIN ENERGY RELEASE BY CRACK CLOSURE

The crack closure method pioneered for delamination analysis by Rybicki et al. (ref. 6) was applied to the analysis of strain energy release rate associated with both delamination and transverse cracking. The analysis accounted for the contribution of thermal stresses to the total energy release rate. The crack closure method also allows the determination of the G values associated with each crack opening mode.



The work required to close the crack extension is approximated by

$$\Delta W \sim [F_x(u_f - u_g) + F_y(v_f - v_g) + F_z(w_f - w_g)]/2$$

where F_x, F_y, F_z are the components of the nodal forces required to close nodes f and g together. Thus, the energy release rates for the three crack extension modes are approximated by:

$$G_I \sim F_y(v_f - v_g)/2\Delta a$$

$$G_{II} \sim F_x(u_f - u_g)/2\Delta a$$

$$G_{III} \sim F_z(w_f - w_g)/2\Delta a$$

ENERGY ANALYSIS

$$G = - \frac{du}{da} \approx - \frac{\Delta u}{\Delta a}$$

Energy released in crack opening equals work required to close crack:

$$-\Delta u = \frac{1}{2} \tilde{F} \cdot \tilde{D}$$

Let \tilde{F}_e, \tilde{D}_e be the elastic solution for a loading of $\epsilon_x = 10^{-6}$ and let \tilde{F}_T, \tilde{D}_T be the elastic solution for a loading of $\Delta T = -1^\circ F$.

Then

$$G = \frac{1}{2\Delta a} \{ \tilde{F}_e(\epsilon_x) + \tilde{F}_T(\Delta T) \} \cdot \{ \tilde{D}_e(\epsilon_x) + \tilde{D}_T(\Delta T) \}$$

This may be rewritten as

$$G = t \{ C_e(\epsilon_x)^2 + C_{eT}(\epsilon_x)(\Delta T) + C_T(\Delta T)^2 \}$$

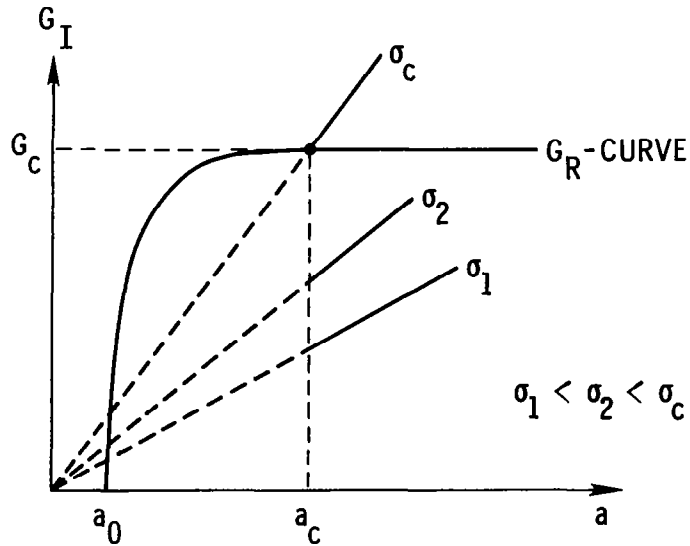
THE CRITICAL FLAW CONCEPT

The next figure below introduces the concept of an effective flaw which preexists in a material prior to loading or one which grows subcritically in the sense of satisfying the Griffith critical stress criterion based on independently measured stiffness and toughness.

If a critical flaw is not assumed to exist, then the analysis of transverse cracking of progressively thicker 90° layers in the (25/-25/90n)s laminate predicts that the energy release rate goes to infinity as the ply thickness is increased without limit. The consequence of this is that the predicted stress level for transverse cracking approaches zero for very thick 90° layers. This is inconsistent with the finite strength of transversely loaded unidirectional composites.

METHOD OF LINEAR FRACTURE MECHANICS

- CONCEPT OF ENERGY RELEASE RATE
- G-CURVES AS FUNCTIONS OF CRACK EXTENSION



FOR MODE-I COLLINEAR CRACKING IN ISOTROPIC ELASTIC SOLIDS,

$$G_I = (\pi/E) a \sigma^2$$

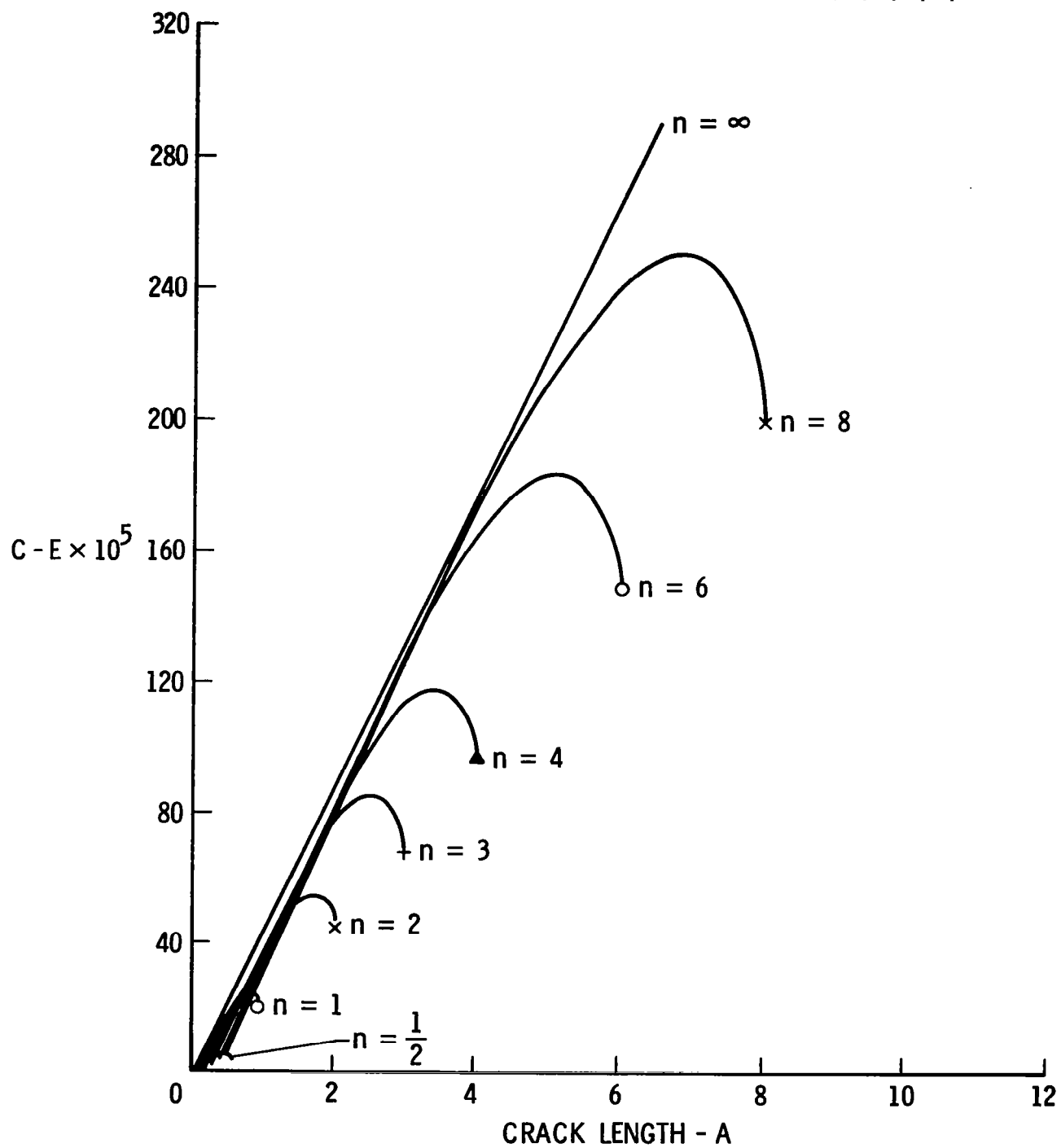
CRITERION FOR CRACK GROWTH:

$$G_I \Big|_{a_c} \rightarrow G_c$$

HENCE

$$\sigma_c = \sqrt{(G_c E) / (\pi a_c)}$$

$(\pm 25/90_n)_s$; TRANSVERSE CRACKING; $N = 0.5, 1, 2, 3, 4, 6, 8$



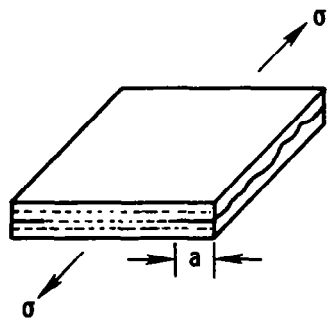
DETERMINATION OF THE CRITICAL FLAW SIZE

To determine the critical flaw size a_c , we postulate that it can be calculated by knowledge of the independently measured elastic modulus E the fracture toughness G_{Ic} and the unnotched tensile strength in the longitudinal and transverse directions. For T300/934 composites, the substitution of these quantities into the Griffith equation

$$a_c = \left(\frac{EG_{Ic}}{\pi} \right) / \sigma^2$$

gives $a_c(\text{transverse}) = 0.010$ in. and $a_c(\text{longitudinal}) = 0.020$ in. Since these are both much larger than the fiber diameter, our assumption of homogeneous ply properties in deriving the effective flaw size is consistent with the absolute size of the flaw. The transverse critical flaw size was applied to the analysis of transverse and delamination crack initiation in the analysis. The relative sizes of a_c and a_m are important in assessing the stability of delamination growth, which is found to depend on the 90° ply thickness in the (25/-25/90n)s experiments.

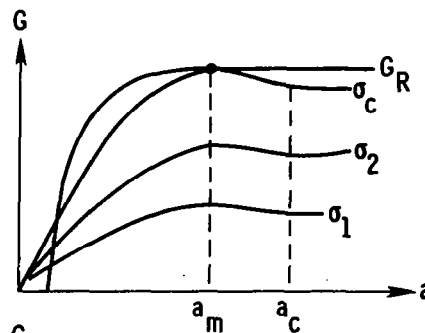
BEHAVIOR OF G-CURVES IN FREE-EDGE DELAMINATION



CONSIDER $(\pm \theta/90)_d$

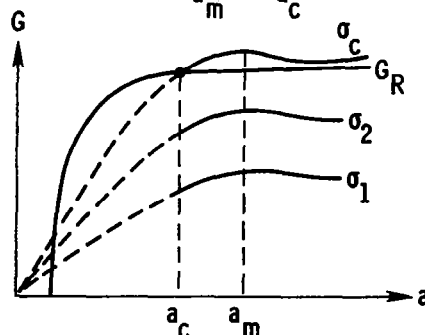
EDGE DELAMINATION MAY OCCUR

1. ALONG $90/90$ INTERFACE
(MODE I, OPENING)
2. ALONG $- \theta/90$ INTERFACE
(MODES I, III MIXED)



CRACK GROWTH STABLE

$$a_m \sim d$$



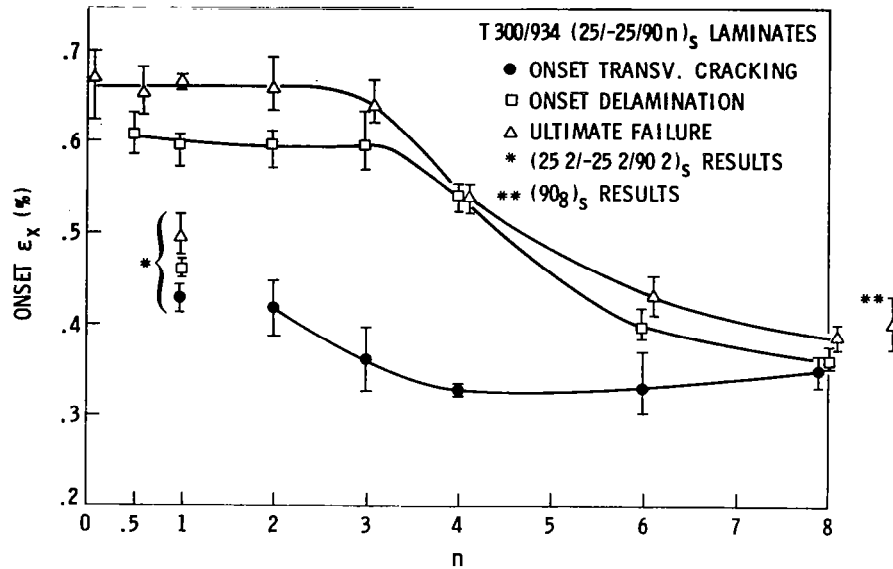
CRACK GROWTH UNSTABLE

$$a_m \sim d$$

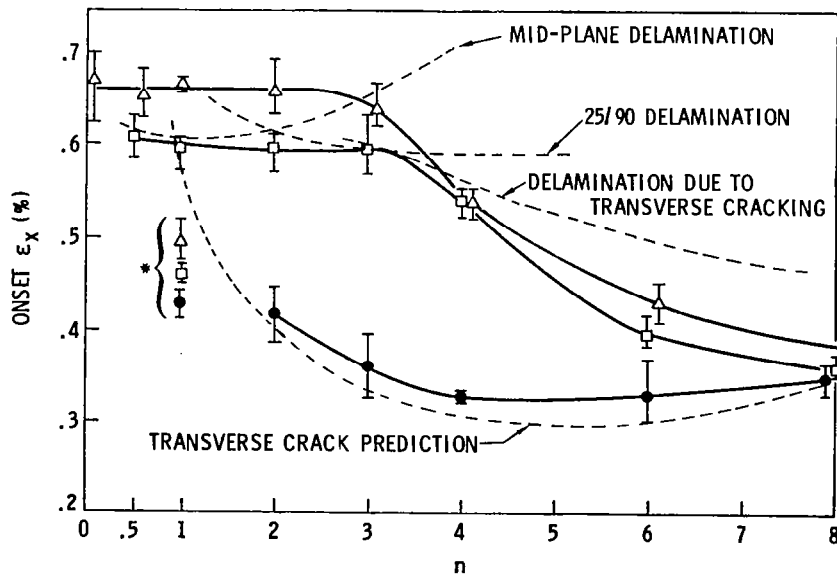
FRACTURE MODE AND SEQUENCE PREDICTION

Energy release rate analysis is qualitatively and quantitatively successful in predicting experimental behavior.

OBSERVED TENSILE STRAIN ϵ_x FOR TRANSVERSE CRACKING, DELAMINATION, AND ULTIMATE FAILURE VERSUS NUMBER OF 90° PLIES IN T300/934



COMPARISON BETWEEN THEORY (DOTTED LINES) AND EXPERIMENT
(PREDICTION BASED ON $G_c = 1.4$; $a_c = 0.008''$ AND $\Delta T = 225^\circ F$)



IMPROVING THE RESISTANCE TO DELAMINATION

From the fracture mechanics analysis of delamination onset, it is clear that the onset stress for delamination can be raised if the critical energy release rate (or delamination toughness) of the material can be improved. The table given below shows (1) that order-of-magnitude improvements in matrix toughness do not translate into large improvements in the composite prepregged from tape, and (2) that composites fabricated from cloth prepreg show greater improvement in toughness than do the tape materials. The references presented emphasize the importance of microstructural factors in controlling (and limiting) improvements in delamination toughness.

FRACTURE ENERGIES OF GRAPHITE-EPOXY MATRIX COMPOSITES

Material	Ref.	Resin or Interlaminar Fracture Energy (K J/m ²)	Comments
5208	7	0.076	TGMA / DDS Matrix
Code 69/HTS Graphite Tape	8	0.076	"
5206/Morg II Graphite Tape	9	0.17	"
F263/T200 Graphite Cloth	7	0.36	"
5206/Morg II Tape			
UD Cross Fiber	9	20.4	
(+ 45) _s Cross Fiber	9	7.8	
Q1 Cross Fiber	9	9.6	
A	10	0.16	MY750 / NMA / BDMA
A/HMS Tape	10	0.24	
B	10	0.33	MY750 / Piperidine
B/HMS Tape	10	0.28	
C	10	1.40	MY750 / 3.2% CTBN
C/HMS Tape	10	0.37	
D	10	2.2	MY750 / 6.2% CTBN
D/HMS Tape	10	0.36	
E	10	3.20	MY750 / 9% CTBN
E/HMS Tape	10	0.49	
205	7	0.27	Diglycidyl ether bisphenol A/
205/T300 Graphite Cloth	7	0.60	Novolac/Dicyandiamine Catalyst
205+CTBN	7	5.1	13x12 3000 tow T300 cloth
205+CTBN/T300 Graphite Cloth	7	4.6	CTBN + HYCAR additives

STIFFNESS/STRENGTH RELATIONSHIPS

A current Lockheed/NASA study is emphasizing the development of a structural analysis approach to assess the influence of transverse cracking and delamination on the resulting laminate stiffness and strength properties.

OBJECTIVE

- DEVELOP "STRUCTURAL" ANALYSIS FOR LAMINATES WITH ARBITRARY LAYUPS
- PREDICT RELATIONSHIP OF MATRIX CRACKING AND DELAMINATION TO LAMINATE STIFFNESS AND TENSILE STRENGTH

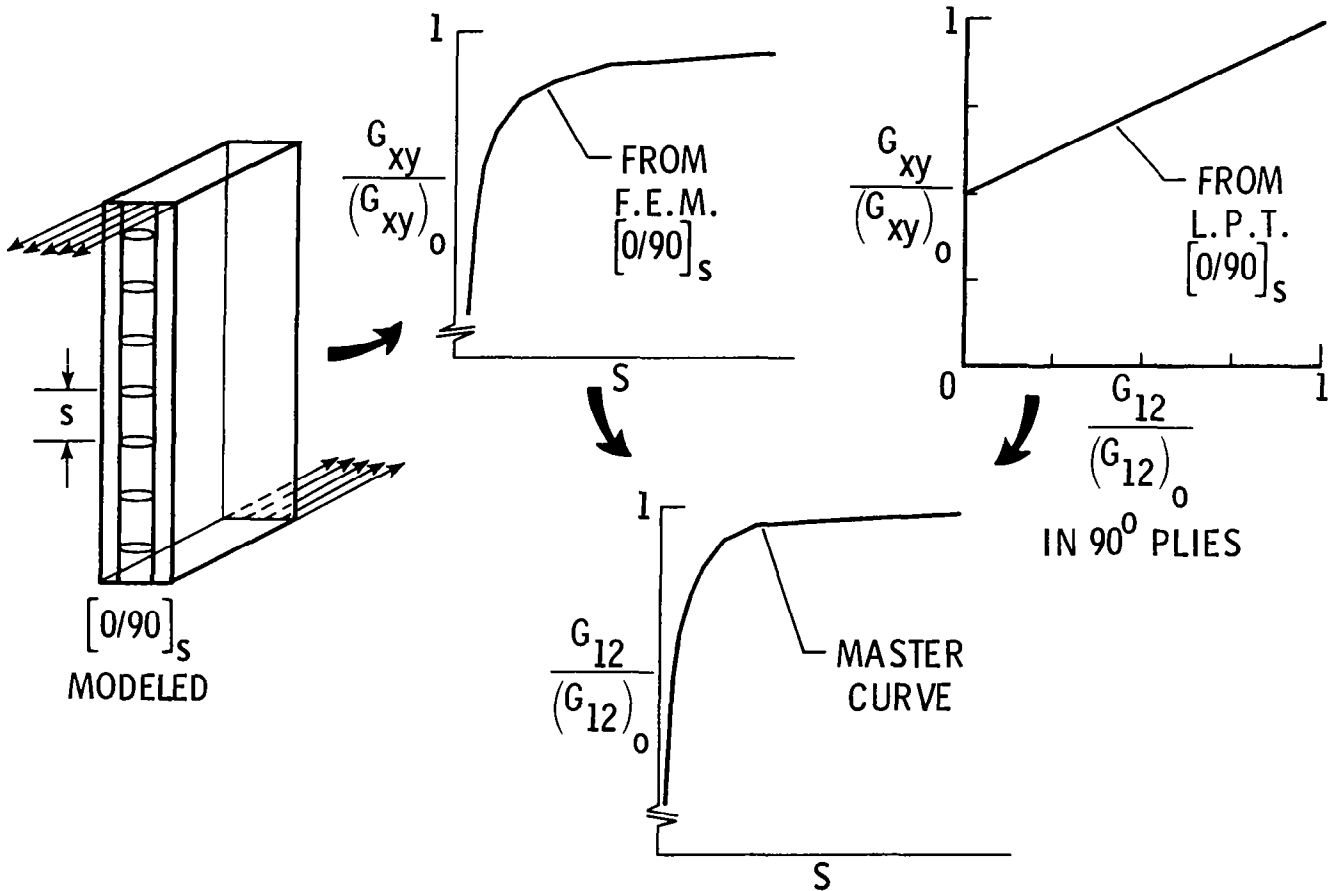
PREMISE

- A LAMINATE IS A STRUCTURE
- MATRIX CRACKS AND DELAMINATIONS MAY OR MAY NOT BE DAMAGE
- A "STRUCTURAL" ANALYSIS OF ARBITRARY LAYUPS IS NEEDED

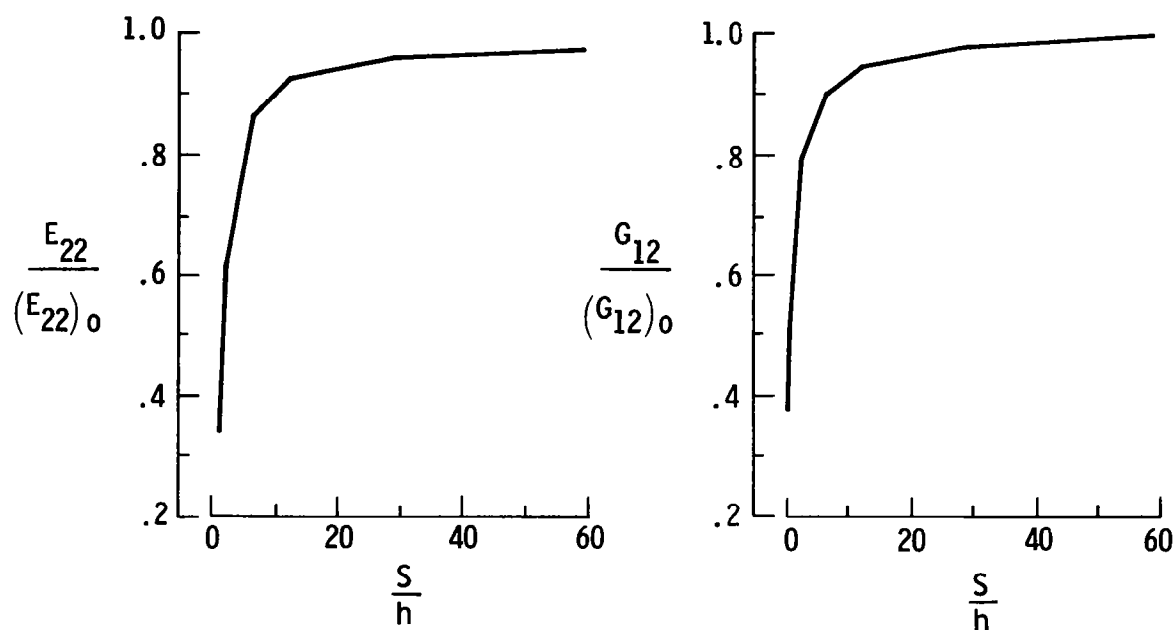
SHEAR STIFFNESS REDUCTION

Finite-element analysis was used to determine the effective in-plane transverse and shear moduli as a function of transverse crack density. The results indicate that for the experimentally determined crack densities, the loss of in-plane stiffness due to transverse cracking is very small.

SHEAR STIFFNESS REDUCTION AS A FUNCTION OF CRACK SPACING



LAMINA STIFFNESS LOSS AS A FUNCTION OF CRACK SPACING **MASTER CURVES**



STIFFNESS LOSS DUE TO MATRIX PLY CRACKING

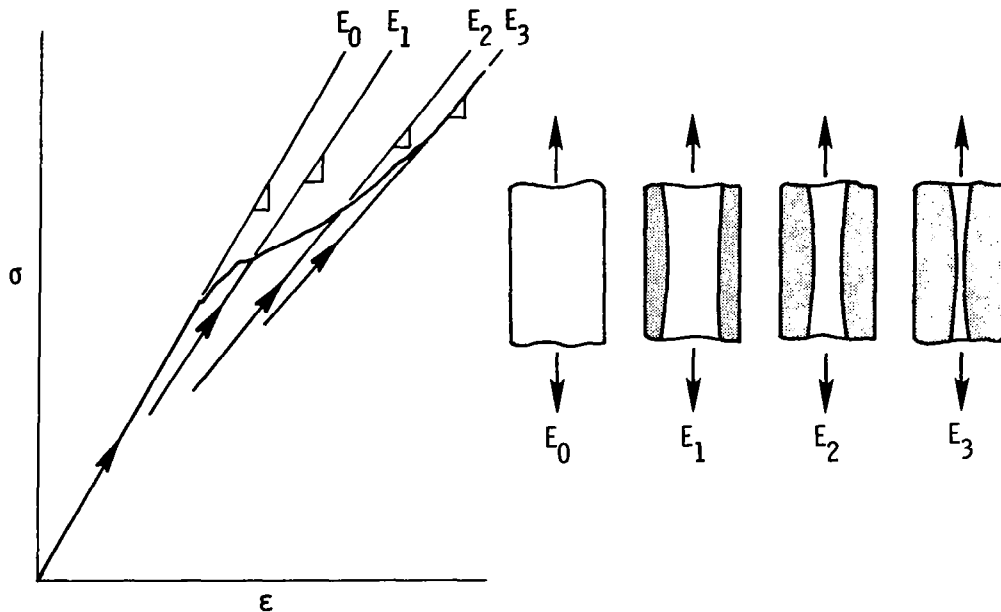
T300 - 5208 GRAPHITE EPOXY

LAYUP	90° PLIES		+45° PLIES		-45° PLIES		$\Delta E_{xx}, \%$
	$\frac{S}{h}$	$\frac{E_{22}}{(E_{22})_0}$	$\frac{S}{h}$	$\frac{G_{12}}{(G_{12})_0}$	$\frac{S}{h}$	$\frac{G_{12}}{(G_{12})_0}$	
$[0/90]_s$	3.33	65	—	—	—	—	1.2
$[0/\pm 45]_s$	—	—	14.6	95	14.2	95	0.9
$[0/90/\pm 45]_s$	2.37	52	13.6	95	—	—	2.2

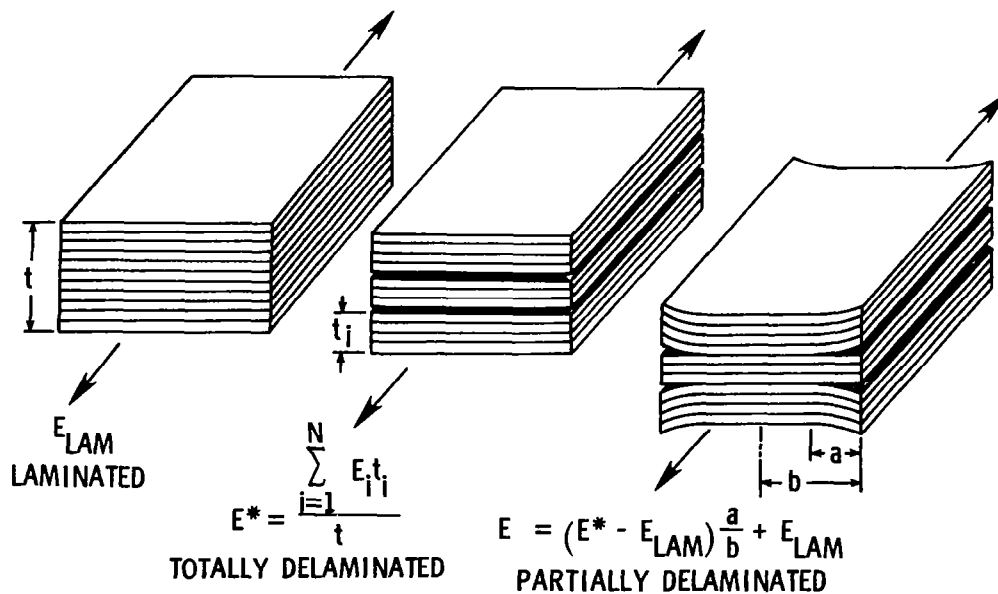
STIFFNESS CHANGE WITH DELAMINATION GROWTH

Correlation of delamination size and stiffness shows a much more significant effect on stiffness associated with delamination, which can be rather simply calculated from a modified laminate analysis.

MEASUREMENT OF STIFFNESS CHANGE WITH DELAMINATION GROWTH



RULE OF MIXTURES ANALYSIS OF STIFFNESS LOSS

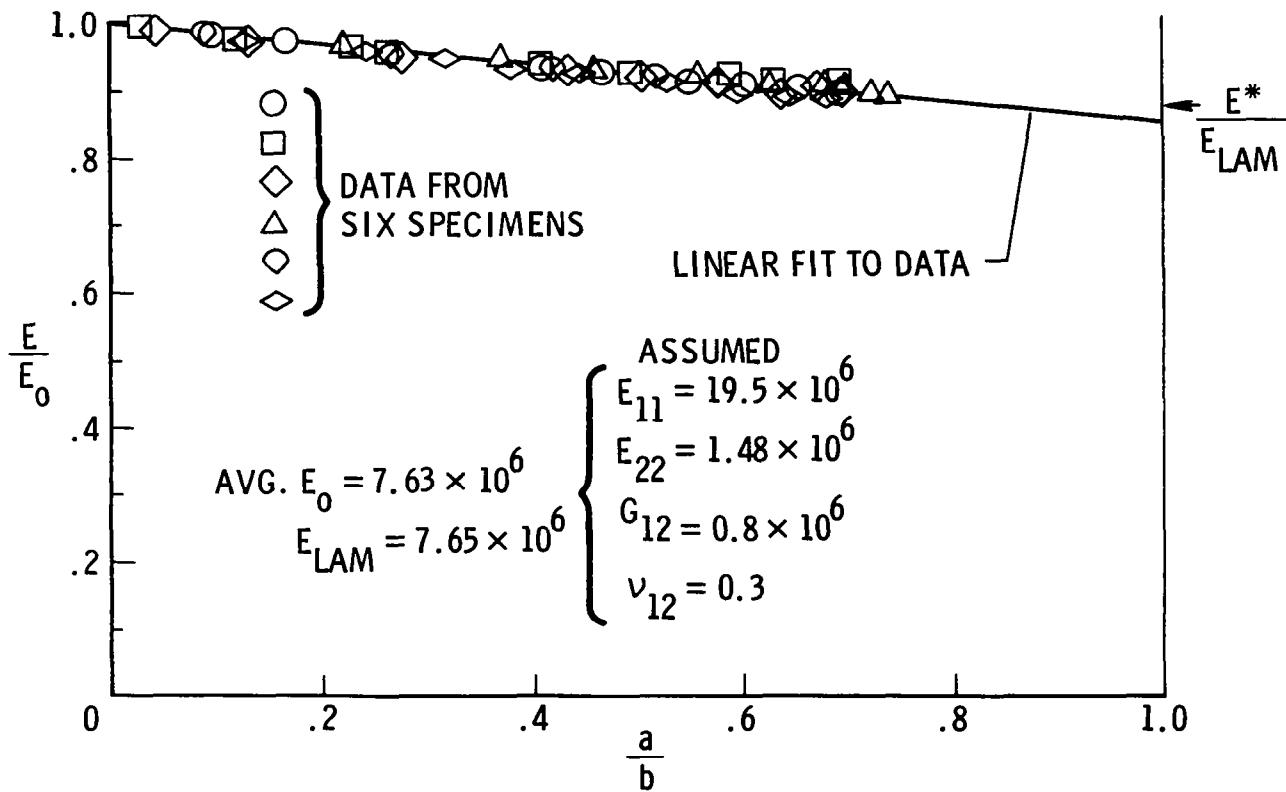


STIFFNESS LOSS AND DELAMINATION SIZE

A comparison between model prediction of stiffness loss and experimental data is given below.

STIFFNESS LOSS AS A FUNCTION OF DELAMINATION SIZE

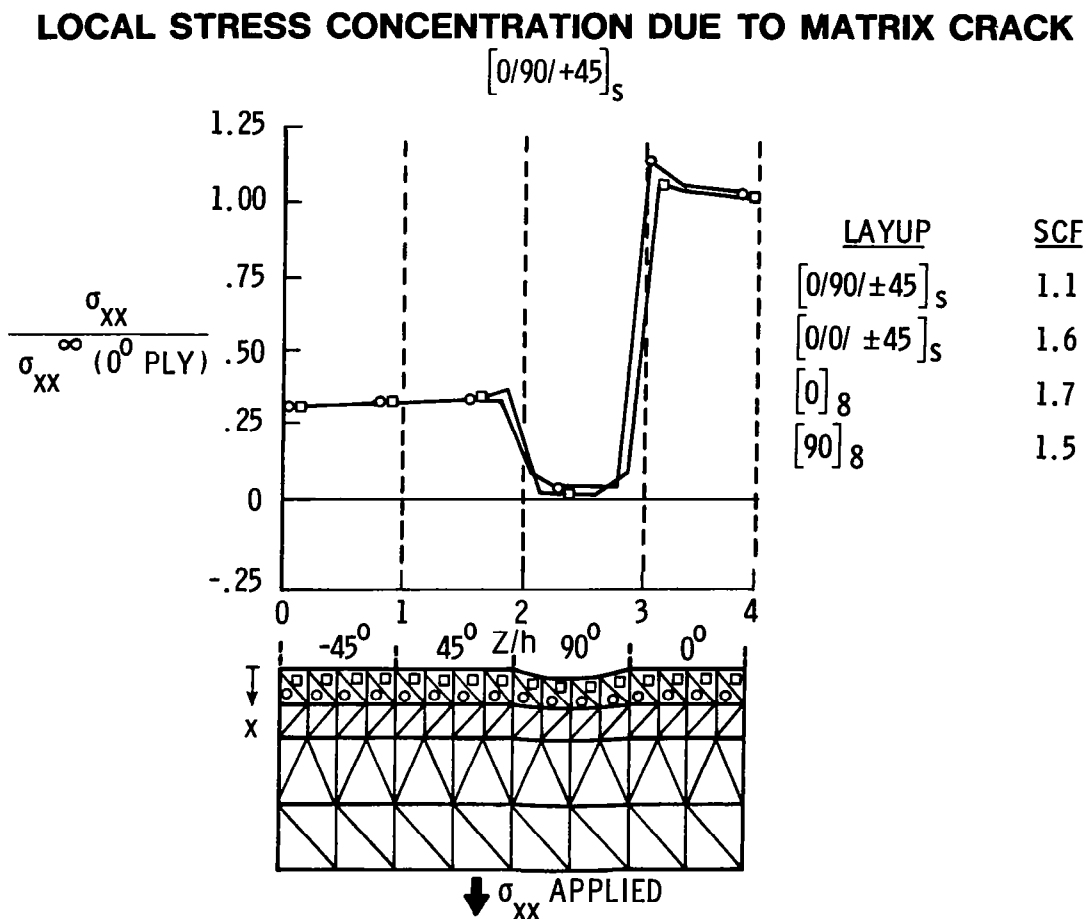
$[\pm 45/0/90]_S$ T300-5208 GRAPHITE EPOXY



TRANSVERSE-CRACK EXTENSION

Transverse cracking of a ply typically terminates at the interface of a ply of differing orientation. Microscopic and X-ray examination of the crack tip by researchers at VPI&SU and Lockheed, among others, has failed to reveal significant damage to the fibers in the neighboring ply, at least when the specimen has been subjected to only static loading (private communication, K. L. Reifsnider). Recent analysis of the stress concentration and energy release rate associated with the tip of the transverse crack has confirmed the lack of damage potential associated with a transverse ply crack.

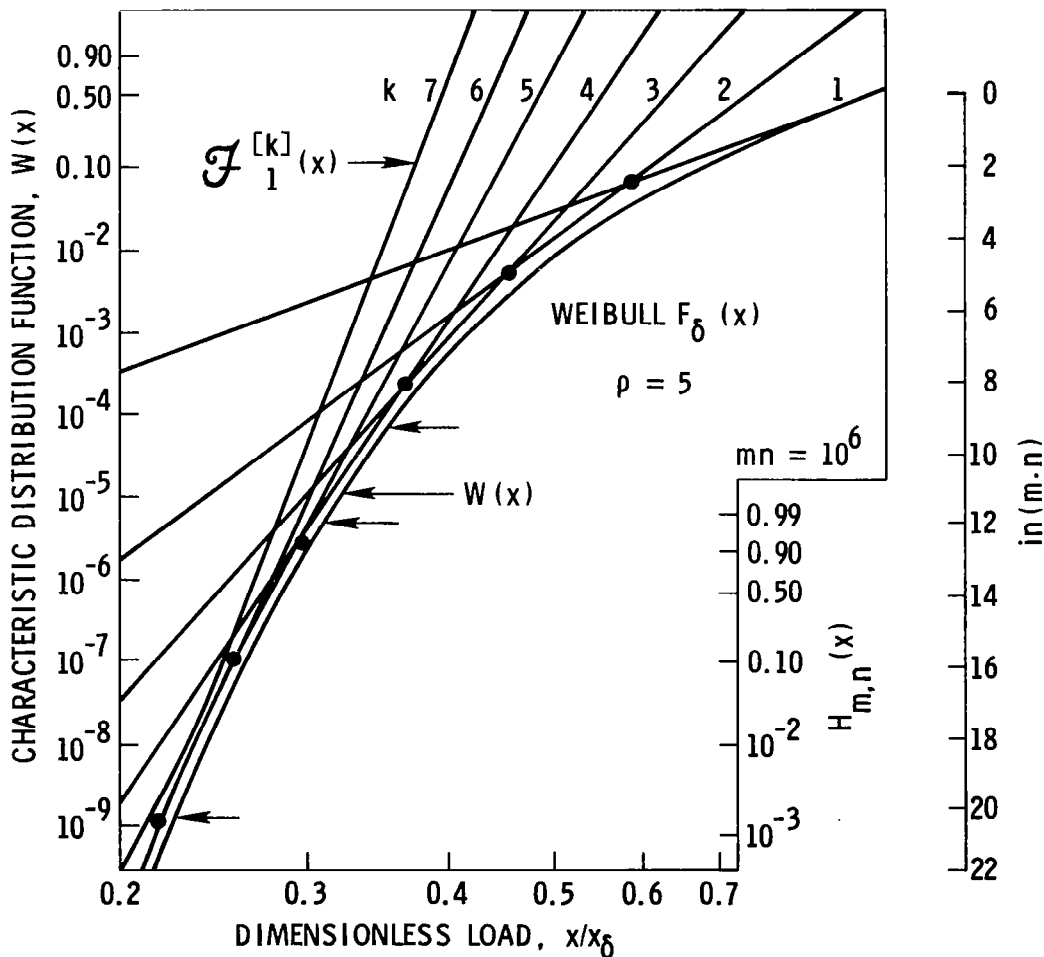
The figure below shows the finite-element model discretization of a transverse-ply crack. The ply arrangement for the quasi-isotropic configuration is shown, but three other layups were examined with the same element model. The stress concentration associated with a transverse 90°-ply crack is much less in the quasi-isotropic case than in the transverse (90)₈ laminate. This is a result of the relatively small load carried by the cracked ply in the quasi-isotropic laminate. The minimum element size used in this analysis contains approximately 10 fibers. Analysis of stresses with elements on a fiber scale would lose physical meaning, given the homogeneous-ply-stiffness assumptions of the analysis.



WEIBULL STRENGTH ANALYSIS

Phoenix (ref. 11) has derived a model which can be used to obtain the mean strength of a unidirectional composite as a function of its volume. The volume is given by the product of the number of fibers in cross section (n) and the length divided by the critical length (m). For a typical unidirectional tensile specimen, nm is on the order of 10^6 . The figure below shows the characteristic strength distribution function of a single critical length of fiber and the shift of that function associated with a volume of $nm = 10^6$. Taking $W(x) = 0.5$ as the mean strength of a given volume, one can construct a table of strength normalized to a single fiber strength or that of a typical tensile specimen.

CHARACTERISTIC DISTRIBUTION FUNCTION $W(x)$ FOR BUNDLE STRENGTH AND ASSOCIATED WEIBULL APPROXIMATIONS (ref. 11). (ALSO SHOWN IS STRENGTH DISTRIBUTION FOR A BUNDLE WITH 10^6 FIBER ELEMENTS)



TENSILE STRENGTH VERSUS VOLUME

Given that the stress concentration factor for a transverse crack in a quasi-isotropic laminate is approximately 1.1 and the volume associated with the finite element nearest the transverse crack tip is approximately 5×10^3 in mm units, we can see from the volume dependence of strength derived in the previous table that "failure" of that element is not expected on the basis of the Phoenix theory (ref. 11).

UNDIRECTIONAL TENSILE STRENGTH VS SPECIMEN VOLUME**

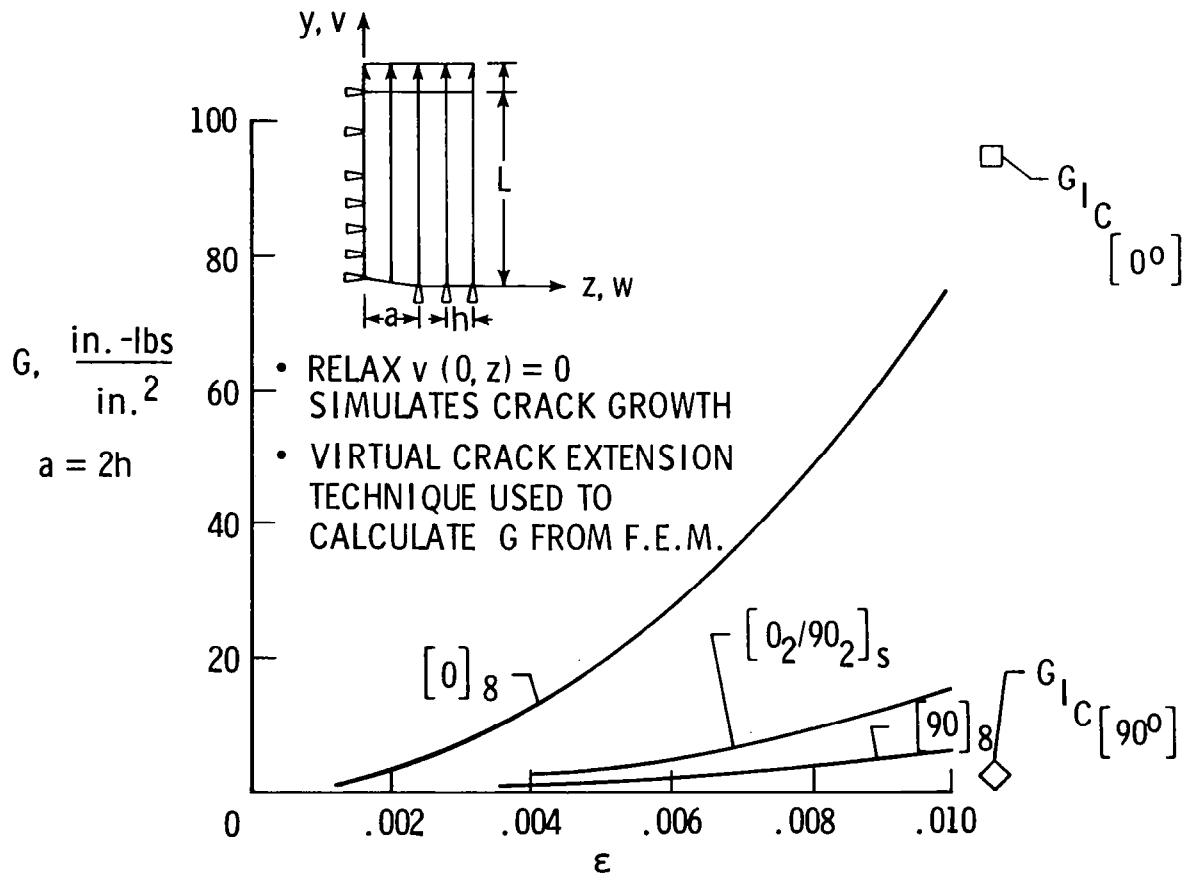
CASE	Ln (nxn)	X/X(CASE A)	X/X(CASE B)
A. A single fiber of the critical length	0.0	1.0	4.0
B. A tensile specimen of .080 x .5 x 10. in.	17.9	.25	1.0
C. A single ply .005 in. thick of length .04 in. near tip of transverse crack	9.65	.35	1.4
D. A single layer of fibers of length .04 in. at the tip of the transverse crack	7.13	.41	1.6

** A fiber spacing of .0004 in. and a critical length of .04 in. were assumed.

STRAIN ENERGY RELEASE RATE ANALYSIS

The figure presented below shows the results of strain energy release rate analysis at the tip of a transverse crack for the geometry shown in the inset. Several types of laminates were analyzed. The energy release rate is plotted as a function of tensile strain. The longitudinal fracture toughness of graphite-epoxy is on the order of 80 to 90 ft-lb/in². A transverse crack in a (0₂/90₂)_s laminate does not release enough energy to allow the transverse crack to propagate across the 0° ply. Thus the energy release rate analysis approach provides the same prediction of transverse crack stability as the Weibull strength analysis.

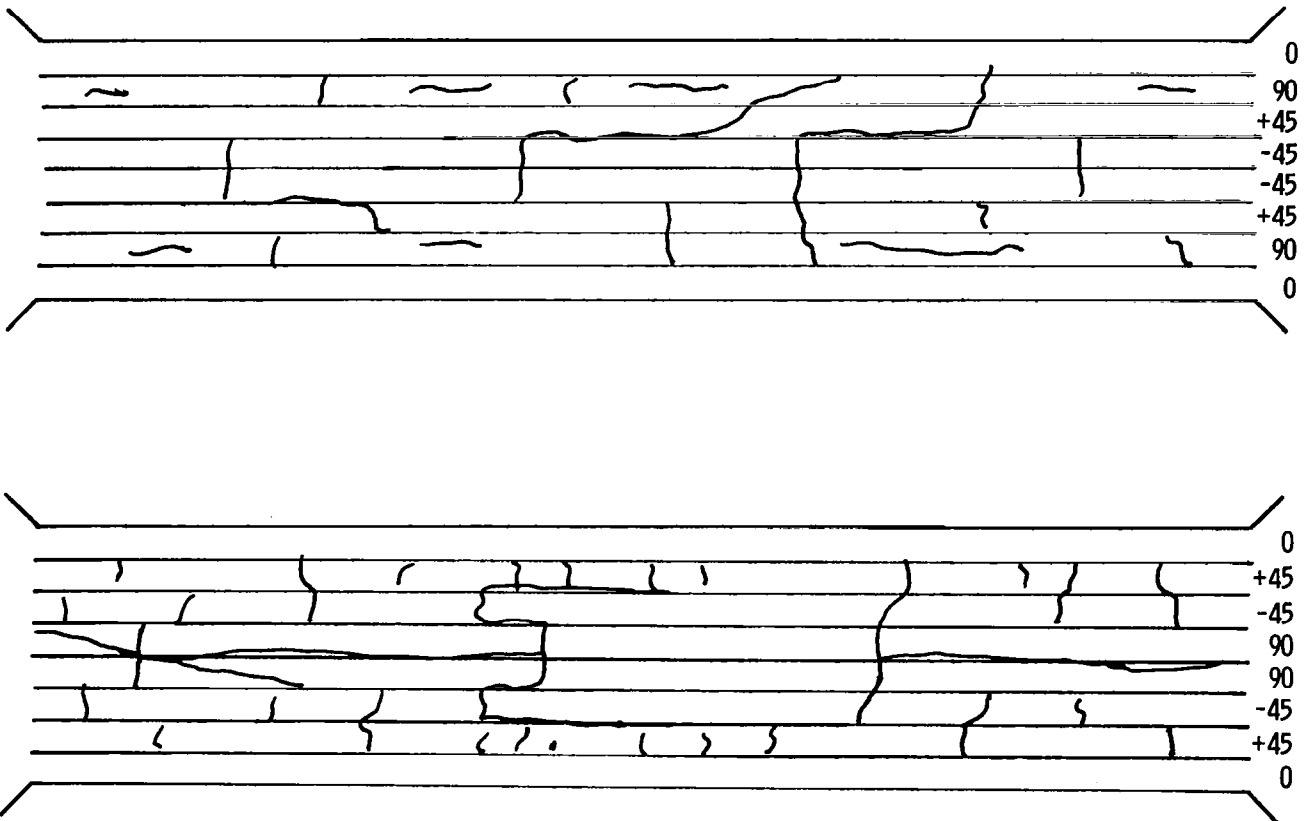
STRAIN ENERGY RELEASE RATE ANALYSIS OF MATRIX CRACKS IN EIGHT PLY GRAPHITE EPOXY LAMINATES



FAILURE BY STRUCTURAL LOAD TRANSFER

The analysis of the final fracture event for tensile-loaded laminates does not appear to depend on the details of ply microcracking. As experimental observations of laminate damage growth under tension have accumulated, the importance of local delaminations in transferring a local load increase to the major load-carrying plies had been postulated by Reifsnider and colleagues (ref. 12). The schematic edge section of laminate damage under static (top) and fatigue (bottom) loading shows regions of the fatigued specimen where essentially all of the applied load must be routed into the 0° plies around regions of extensively delaminated and transverse-cracked 90° and 45° plies. Prediction of these loads will require more detailed structural modeling.

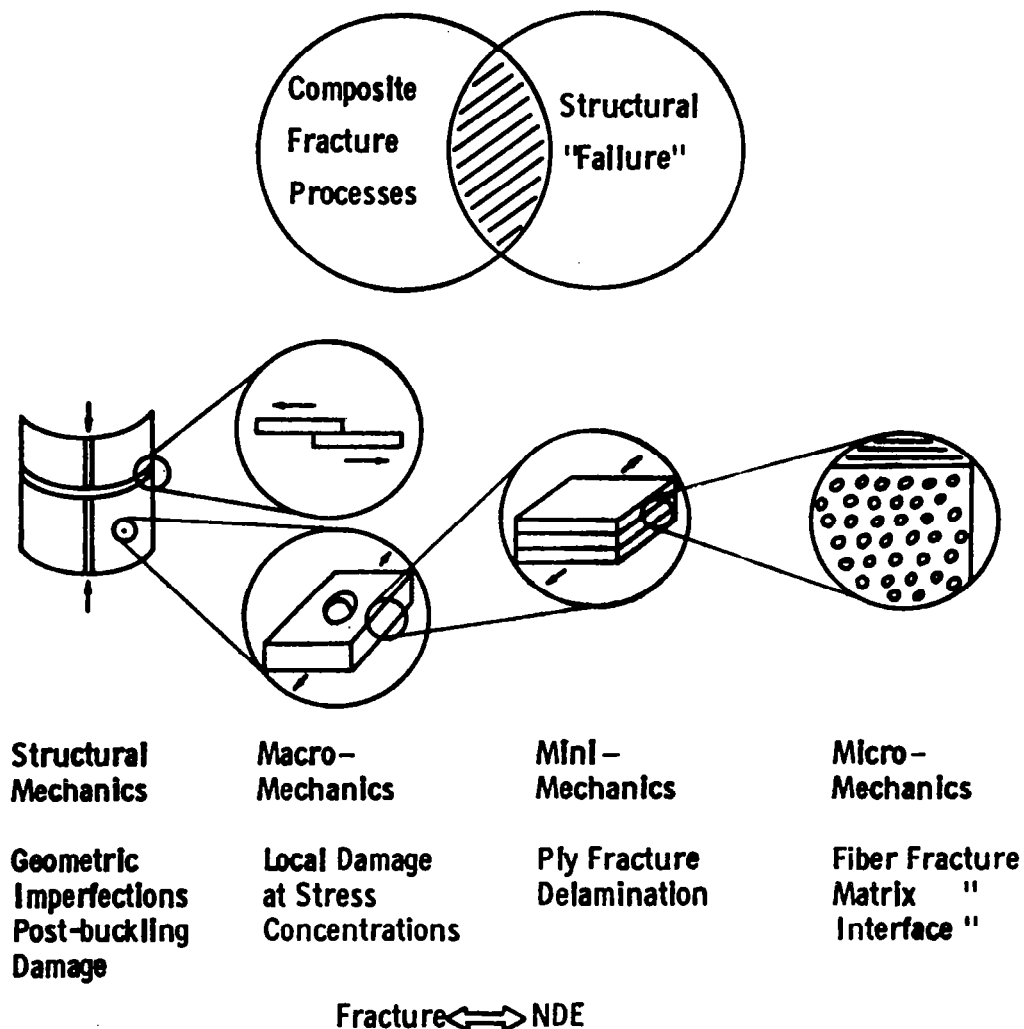
PREFRACTURE PATTERNS NEAR FRACTURE SITE (ref. 13)



"STRUCTURAL" FAILURE ANALYSIS

The degree to which the details of crack interaction must be modeled to predict tensile failure are being investigated in several ongoing research programs. Structural analysis of composite response can be carried out routinely with numerical methods like finite-element analysis at several different structural levels: microstructural, laminate structural, and macrostructural. However, this does not provide the total solution to fracture analysis of composites. Our understanding of the structural implications of cracking at each level must be improved to provide the proper failure criteria for the structural analysis.

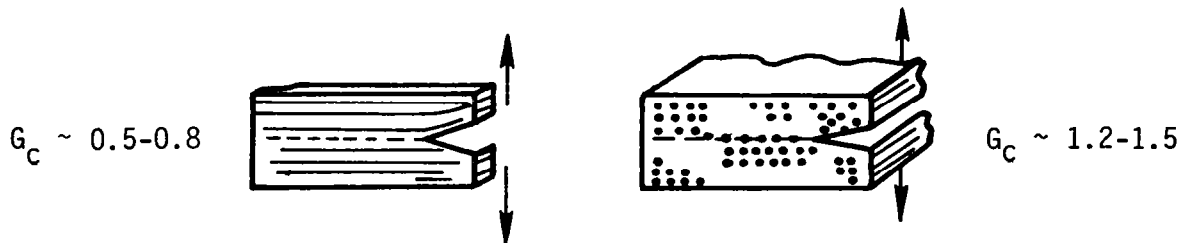
FRACTURE OF STRUCTURAL COMPOSITES



What is the significance of damage or defect on the structural integrity?

CONCLUSION AND DISCUSSION

1. Methods of classical fracture mechanics can be viable crack growth criteria for matrix-dominated sublaminar cracks, such as transverse cracking and ply delamination.
2. The energy release rate increases (generally) with the size of crack, which is constrained by the physical dimension of the laminate's ply structure, such as the thickness of the plies. Thus, ply thickness has a profound influence on the growth process of sublaminar cracking, and even on the final failure of the laminate.
3. The finite-element/crack-closure technique is a useful computational tool to simulate sublaminar crack growth, provided the crack paths are relatively simple.
4. The DIB (diiodobutane) enhanced X-radiography is a useful NDE tool for monitoring the growth of sublaminar cracks.
5. For T300/934, the value of G_C is in the range 1.2 to 1.5 in-lb/in², but other experiments found it in the range 0.5 to 0.8 (refs. 3 and 6). (See sketch.)



This difference should be verified by additional experimentation.

6. For the best fit of data, the critical material crack size a_c is taken as 0.008 in. This should be verified by micromechanical investigation. Generally, a_c is a function of the size of inhomogeneity (fiber), the stiffness property surrounding the crack, and other processing variables. However, it is not known whether a_c might also depend on the ply structure of the laminate.
7. In the study of delamination, all predictions were based on the total energy release rate $G = G_I + G_{II} + G_{III}$ for both mode-I and mixed-mode cracks. Experimental correlation indicates a need for a mixed-mode crack criterion, such as

$$G_I/G_{Ic} + G_{II}/G_{IIc} + G_{III}/G_{IIIc} = 1$$

There is no firm evidence that G_{IIc} and G_{IIIc} actually exist, and experimental means to measure them independently has not been developed.

8. Some of the observed cracks were actually 'planar cracks'. In the case of a crack front with a complicated contour, the degree to which a 2-D crack growth criterion is readily applicable is not known.

REFERENCES

1. Bjeletich, J. G.; Crossman, F. W.; and Warren, W. J.: The Influence of Stacking Sequence on Failure Modes in Quasi-Isotropic Graphite-Epoxy Laminates. Failure Modes in Composites IV, AIME, 1977, p. 118.
2. Pipes, R. B.; and Pagano, N. J.: Interlaminar Stresses in Composite Laminates Under Uniform Axial Extension. J. Comp. Mater., vol. 4, 1970, p. 538.
3. Crossman, F. W.; Mauri, R. E.; and Warren, W. J.: Hygrothermal Damage Mechanisms in Graphite-Epoxy Composites. NASA CR-3189, 1979.
4. Rodini, B. T.; and Eisenmann, J. R.: An Analytical and Experimental Investigation of Edge Delamination in Composite Laminates. Proc. Fibrous Composites in Structural Design, 1978, p. 441.
5. Reifsnider, K. L. (ed.): Damage in Composite Materials. ASTM STP 775, 1982.
6. Rybicki, E. F.; Schmueser, D. W.; and Fox, J.: An Energy Release Rate Approach for Stable Crack Growth in the Free-Edge Delamination Problem. J. Comp. Mater., vol. 11, 1977, p. 470.
7. Bascom, W. D.; Bitner, J. L.; Moulton, R. J.; and Siebert, A. R.: The Interlaminar Fracture of Organic-Matrix, Woven-Reinforcement Composites. Composites, Jan. 1980, p. 9.
8. Bader, M. G.; and Curtis, P. T.: The Micromechanics of Fibre Composites - Carbon Fibre Programme. Dept. of Metallurgy and Materials Technology, Univ. of Surrey, UK, 1977.
9. Konish, H. J.; Swedlow, J. L.; and Cruse, T. A.: Experimental Investigation of Fracture in an Advanced Fiber Composite. J. Comp. Mater., vol. 6, 1972, p. 114.
10. Scott, J. M.; and Phillips, D. C.: Carbon Fibre Composites With Rubber Toughened Matrices. J. Mater. Sci., vol. 10, 1975, p. 551.
11. Phoenix, S. L.: Statistics for the Strength of Bundles of Fibers in a Matrix. Encyclopedia of Materials Science and Engineering, Pergamon Press, 1981.
12. Reifsnider, K. L.; Stinchcomb, W. W.; Henneke, E. G.; Duke, J., Jr.; and Jamison, R.: Fatigue Damage Strength Relationships in Composite Laminate. Mechanics of Composite Review, 8th Annual (Dayton, Ohio), Air Force Materials Laboratory, 1982.
13. Reifsnider, K. L.; Henneke, E. G.; and Stinchcomb, W. W.: Defect-Property Relationships in a Composite Material. AFML-TR-76-81, Air Force Materials Laboratory, June 1981.

BIBLIOGRAPHY

FREE-EDGE STRESSES

- Pipes, R. B., and N. J. Pagano, Interlaminar Stresses in Composite Laminates Under Uniform Axial Extension, *J. Comp. Mat.*, vol. 4, 1970, p. 538.
- Pagano, N. J., and R. B. Pipes, The Influence of Stacking Sequence on Laminate Strength, *J. Comp. Mat.*, vol. 5, 1971, p. 50.
- Pipes, R. B., and I. M. Daniel, Moire Analysis of the Interlaminar Shear Edge Effect in Laminated Composites, *J. Comp. Mat.*, vol. 6, 1972, p. 62.
- Whitney, J. M., and C. E. Browning, Free-Edge Delamination of Tensile Coupons, *J. Comp. Mat.*, vol. 7, 1973, p. 29.
- Pagano, N. J., and R. B. Pipes, Some Observations on the Interlaminar Strength of Composite Laminates, *Int. J. Mech. Sci.*, vol. 15, 1973, p. 670.
- Pipes, R. B., B. E. Kaminski, and N. J. Pagano, Influence of the Free Edge Upon the Strength of Angle-Ply Laminates, *ASTM STP 521*, 1973, p. 218.
- Whitney, J. M., Free-Edge Effects in the Characterization of Composite Materials, *ASTM STP 521*, 1973, p. 167.
- Pagano, N. J., On the Calculation of Interlaminar Normal Stress in Composite Laminate, *J. Comp. Mat.*, vol. 8, 1974, p. 65.
- Barker, R. M., J. R. Dana, and C. W. Pryor, Stress Concentrations Near Holes in Laminates, *J. Engineering Mechanics Div.*, June 1974, p. 477.
- Oplinger, D. W., B. S. Parker, and F. P. Chiang, Edge-Effect Studies in Fiber-Reinforced Laminates, *Exp. Mech.*, vol. 14, 1974, p. 347.
- Chang, F. H., D. E. Gordon, B. T. Rodini, and R. H. McDaniel, Real-Time Characterization of Damage Growth in Graphite/Epoxy Laminates, *J. Comp. Mat.*, vol. 10, 1976, p. 182.
- Renieri, G. D., and C. T. Herakovich, Nonlinear Analysis of Laminated Fibrous Composites, Report No. VPI-E-76-10, Virginia Polytechnic Institute & State University, 1976.
- Wang, A. S. D., and F. W. Crossman, Some New Results on Edge Effect in Symmetric Composite Laminates, *J. Comp. Mat.*, vol. 11, 1977, p. 92.
- Hsu, P. W., and C. T. Herakovich, Edge Effects in Angle-Ply Composite Laminates, *J. Comp. Mat.*, vol. 11, 1977, p. 422.
- Bjeletich, J. G., F. W. Crossman, and W. J. Warren, The Influence of Stacking Sequence on Failure Modes in Quasi-Isotropic Graphite-Epoxy Laminates, Failure Modes in Composites IV, *AIIME*, 1977, p. 118.

- Harris, A., and O. Orringer, Investigation of Angle-Ply Delamination Specimen for Interlaminar Strength Test, J. Comp. Mat., vol. 12, 1978, p. 285.
- Rybicki, E. F., and D. W. Schmueser, Effect of Stacking Sequence and Lay-up Angle on Free-Edge Stresses Around a Hole in a Laminated Plate Under Tension, J. Comp. Mat., vol. 12, 1978, p. 301.
- Wang, S. S., Delamination Fracture From Surface Notch in (45/-45/90/0)s Graphite Epoxy Composites, ICCM2, 1978, p. 277.
- Spilker, R. L., and S. C. Chou, Edge Effects in Symmetric Composite Laminates: Importance of Satisfying the Traction-Free-Edge Condition, J. Comp. Mat., vol. 14, 1980, p. 2.
- Raju, I. S., J. D. Whitcomb, and J. B. Goree, A New Look at Numerical Analysis of Free-Edge Stresses in Composite Laminates, NASA TN-1751, 1980.

DELAMINATION AND STRAIN ENERGY RELEASE RATE

- Rybicki, E. F., D. W. Schmueser, and J. Fox, An Energy Release Rate Approach for Stable Crack Growth in the Free-Edge Delamination Problem, J. Comp. Mat., vol. 11, 1977, p. 470.
- Crossman, F. W., R. E. Mauri, and W. J. Warren, Hygrothermal Damage Mechanisms in Graphite-Epoxy Composites, NASA CR-3189, 1979.
- Rodini, B. T., and J. R. Eisenmann, An Analytical and Experimental Investigation of Edge Delamination in Composite Laminates, Proc. Fibrous Composites in Structural Design, 1978, p. 441.
- Wang, A. S., and F. W. Crossman, Initiation and Growth of Transverse Cracks and Edge Delamination in Composite Laminates, Parts 1 and 2, J. Comp. Mat., Supplemental vol. 14, 1980, p. 72.
- Wang, A. S. D., Growth Mechanisms of Transverse Cracks and Ply Delamination in Composite Laminates, ICCM3, 1980, p. 170.
- Crossman, R. W., and A. S. D. Wang, The Dependence of Transverse Cracking and Delamination on Ply Thickness in Graphite/Epoxy Laminates, ASTM STP 775, 1982, pp. 118-139.
- Law, G. E., Fracture Analysis of (25/-25/90n)s Graphite-Epoxy Composite Laminates, Ph. D. Dissertation, Drexel University, June 1981.
- Wilkins, D. J., J. R. Eisenmann, R. A. Camin, W. S. Margolis, and R. A. Benson, Characterizing Delamination Growth in Graphite Epoxy, ASTM STP 775, 1982, pp. 168-183.
- O'Brien, T. K., Characterization of Delamination Onset and Growth in a Composite Laminate, ASTM STP 775, 1982, pp. 140-167.
- Williams, D. R., Mode I Transverse Cracking in an Epoxy and Graphite Fiber Reinforced Epoxy, M. S. Thesis, Texas A&M University, Report No. MM 3724-81-16, Dec. 1981.

Cullen, J. S., Mode I Delamination of Unidirectional Graphite/Epoxy Composite Under Complex Load Histories, M. S. Thesis, Texas A&M Univ., report no. MM 3724-81-13, Dec. 1981.

Vanderkley, P. S., Mode I-Mode II Delamination Fracture Toughness of a Unidirectional Graphite/Epoxy Composite, M. S. Thesis, Texas A&M Univ., report no. MM 3724-81-15, Dec. 1981.

Early, J. W., Compression Induced Delamination in a Unidirectional Graphite/Epoxy Composite, M. S. Thesis, Texas A&M Univ., report no. MM 3724-81-14, Dec. 1981.

IMPROVING THE INTERLAMINAR TOUGHNESS OF COMPOSITES

Scott, J. M., and D. C. Phillips, Carbon Fibre Composites With Rubber Toughened Matrices, J. Mat. Sci., vol. 10, 1975, p. 551.

Bascom, W. D., R. L. Cottingham, and C. O. Timmons, Fracture Design Criteria for Structural Adhesive Bonding: Promise and Problems, Naval Engineers J., Aug. 1976, p. 73.

Bascom, W. D., J. L. Bitner, R. J. Moulton, and A. R. Siebert, The Interlaminar Fracture of Organic-Matrix, Woven Reinforcement Composites, Composites, Jan. 1980, p. 9.

Miller, A. G., P. E. Hertzberg, and V. W. Rantala, Toughness Testing of Composite Materials, SAMPE Quarterly, Jan. 1981, p. 36.

THE INFLUENCE OF DELAMINATION OF COMPOSITE FAILURE

Mulville, D. R., and I. Wollock, Failure of Polymer Composites, in Developments in Polymer Fracture I, E. H. Andrews, ed., chapter 8, Applied Science Pub., London, 1979.

Reifsnider, K. L., E. G. Henneke, and W. W. Stinchcomb, Defect-Property Relationships in Composite Materials, AFML-TR-76-81, Air Force Materials Laboratory, June 1981.

Reifsnider, K. L., Mechanics of Failure of Composite Materials, presented at Fracture Mechanics Symposium, Charlottesville, NC, 1978 (Navy Structural Mechanics Series).

O'Brien, T. K., The Effect of Delamination on the Tensile Strength of Unnotched, Quasi-Isotropic, Graphite/Epoxy Laminates, Proc. SESA/JSME Conf., Hawaii, May 1982.

Stinchcomb, W. W., K. L. Reifsnider, P. Young, and M. N. Gibbons, Investigation and Characterization of Constraint Effects on Flaw Growth During Fatigue Loading of Composite Materials, Final Report on NASA Grant NSG-1364, June 1979.

Kim, R. Y., Experimental Assessment of Static and Fatigue Damage of Graphite/Epoxy Laminates, ICCM3, 1980, p. 1015.

Reifsnider, K. L., and A. Tulag, Analysis of Fatigue Damage in Composite Laminates, Int. J. Fatigue, Jan. 1980, p. 3.

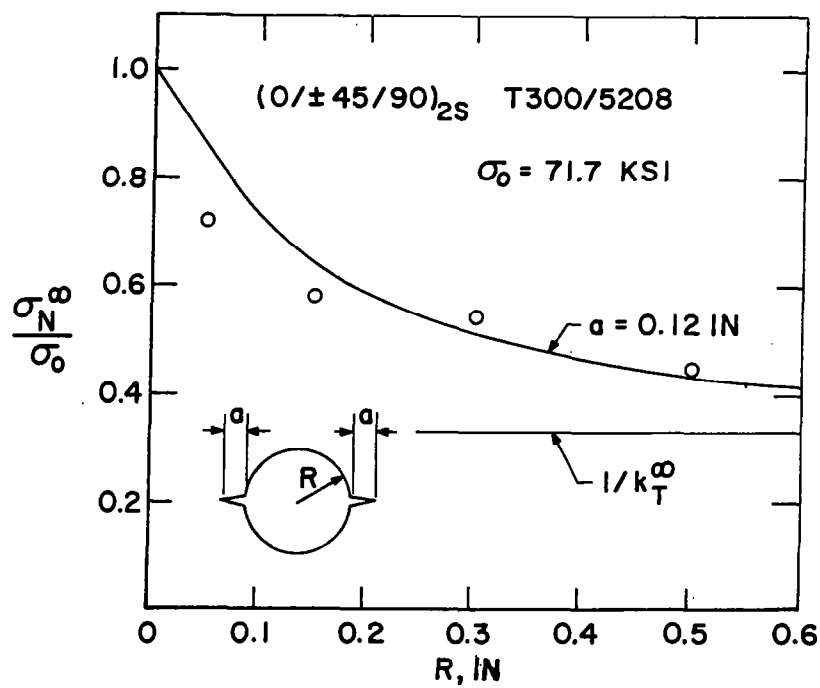
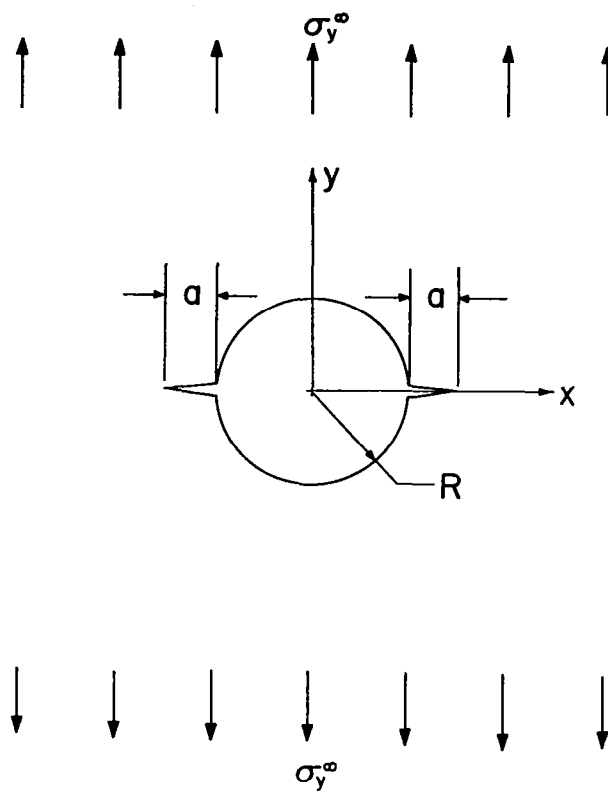
- Reifsnider, K. L., The Effect of Lamination-Induced Stresses on Fatigue Damage Development at Internal Flaws, *Comp. Tech. Rev.*, vol. 3, 1981, p. 17.
- Batdorf, S. B., Tensile Strength of Unidirectionally Reinforced Composites, Part I, *J. Reinforced Plast. & Comp.*, To be published in 1982.
- Phoenix, S. L., Statistics for the Strength of Bundles of Fibers in a Matrix, *Encyclopedia of Materials Science and Engineering*, Pergamon Press, 1981.
- Smith, R. L., A Probability Model for Fibrous Composites with Local Load-Sharing, *Proc. Roy. Soc. London Ser. A*-372, p. 539.

FRACTURE MECHANICS

- Zweben, C., Fracture Mechanics and Composite Materials: A Critical Analysis, *ASTM STP 521*, 1973, p. 65.
- Kanninen, M. F., E. F. Rybicki, and H. F. Brinson, A Critical Look at Current Applications of Fracture Mechanics to the Failure of Fibre-Reinforced Composites, *Composites*, Jan. 1977, p. 17.
- Waddoups, M. E., J. R. Eisenmann, and B. E. Kaminski, Macroscopic Fracture Mechanics of Advanced Composite Materials, *J. Comp. Mat.*, vol. 5, 1971, p. 164.
- Konish, H. J., J. L. Swedlow, and T. A. Cruse, Experimental Investigation of Fracture in an Advanced Fiber Composite, *J. Comp. Mat.*, vol. 6, 1972, p. 114.
- Cruse, T. A., and M. G. Stout, Fractographic Study of Graphite-Epoxy Laminated Fracture Specimens, *J. Comp. Mat.*, vol. 7, 1973, p. 200.
- Mandell, J. F., S. S. Wang, and F. J. McGarry, The Extension of Crack Tip Damage Zones in Fiber Reinforced Plastic Laminates, *J. Comp. Mat.*, vol. 9, 1975, p. 266.
- Altus, E., and A. Rotem, A 3-D Fracture Mechanics Approach to the Strength of Composite Materials, *Eng. Fracture Mech.*, vol. 14, 1981, p. 637.

NOTCH STRENGTH OF COMPOSITES

**James M. Whitney
Air Force Wright Aeronautical Laboratories
Wright Patterson Air Force Base, Ohio 45433**



STATISTICAL BEHAVIOR OF COMPOSITES

WEIBULL STATISTICAL STRENGTH THEORY

$$R(S) = \exp \left[-B(S) \right]$$

$B(S)$ = RISK - TO - BREAK

TWO PARAMETER WEIBULL DISTRIBUTION

$$B(S) = \int_V \left(\frac{S}{S_0} \right)^\alpha dV$$

TENSION: $B_t = V_t \left(\frac{S}{S_0} \right)^\alpha$

$$R(S) = \exp \left[- \left(\frac{S}{S_t} \right)^\alpha \right]$$

$$S_t = \frac{S_0}{(V_t)^{1/\alpha}}$$

BENDING

$$R(S) = \text{EXP} \left[\left(-\frac{S}{S_b} \right)^\alpha \right]$$

$$\begin{aligned} \underline{4 \text{ PT:}} \quad B_b &= \frac{(\alpha + 2) V_b}{4(\alpha + 1)^2} \left(\frac{S}{S_0} \right)^\alpha \\ S_b &= S_0 \left[\frac{4(\alpha + 1)^2}{(\alpha + 2) V_b} \right]^{1/\alpha} \end{aligned}$$

$$\begin{aligned} \underline{3 \text{ PT:}} \quad B_b &= \frac{V_b}{2(\alpha + 1)^2} \left(\frac{S}{S_0} \right)^\alpha \\ S_b &= S_0 \left[\frac{2(\alpha + 1)^2}{V_b} \right]^{1/\alpha} \end{aligned}$$

BENDING (3 PT):

$$\frac{S_b}{S_t} = \left[2(\alpha + 1)^2 \left(\frac{V_t}{V_b} \right) \right]^{1/\alpha} = \begin{cases} 1.52, & \alpha = 15 \\ 1.33, & \alpha = 25 \end{cases}$$

BENDING (4 PT):

$$\frac{S_b}{S_t} = \left[\frac{4(\alpha + 1)^2}{(\alpha + 2)} \left(\frac{V_t}{V_b} \right) \right]^{1/\alpha} = \begin{cases} 1.31, & \alpha = 15 \\ 1.20, & \alpha = 25 \end{cases}$$

THICKNESS EFFECTS

TENSION:

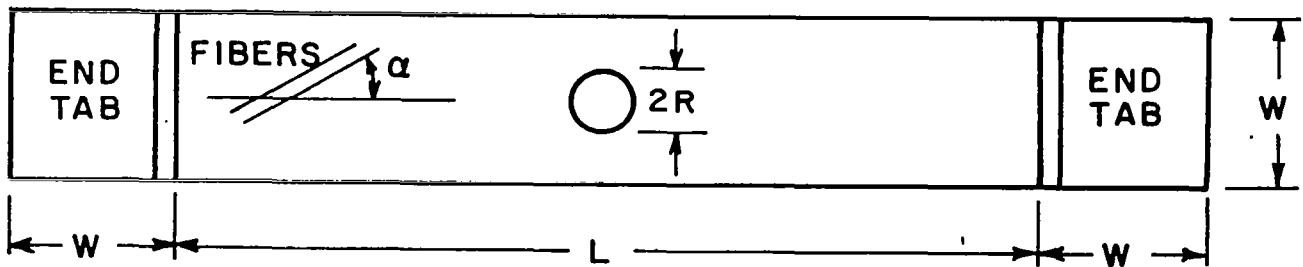
$$S_t = S_0 \left(\frac{1}{L_b h} \right)^{1/\alpha}$$

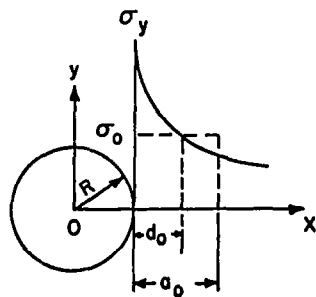
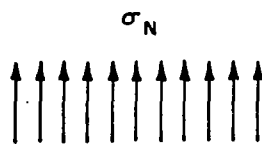
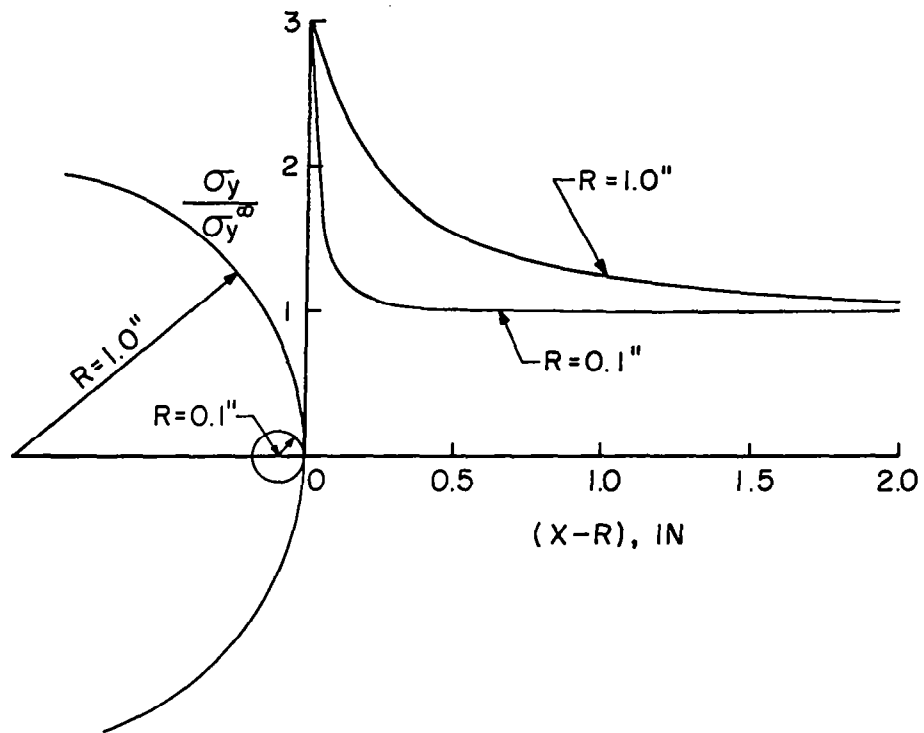
$$\frac{S_{t1}}{S_{t2}} = \left(\frac{h_2}{h_1} \right)^{1/\alpha}, \quad h_2 > h_1$$

BENDING:
(3 PT)

$$S_b = \left[S_0 \frac{(\alpha + 1)^2 h}{L_b h^2} \right]^{1/\alpha}$$

$$\frac{S_{b1}}{S_{b2}} = \left(\frac{h_2}{h_1} \right)^{2/\alpha}, \quad h_2 > h_1$$



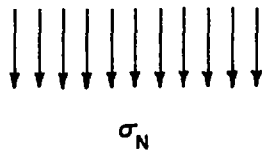


POINT STRESS CRITERION

$$\sigma_y (R + d_0, 0) = \sigma_0$$

AVERAGE STRESS CRITERION

$$\frac{1}{a_0} \int_R^{R+d_0} \sigma_y (X, 0) dx = \sigma_0$$



CIRCULAR HOLE APPROXIMATE STRESSES

$$\sigma_y(x,0) = \frac{\sigma_y^\infty}{2} \left\{ 1 + \left(\frac{R}{X}\right)^2 + 3\left(\frac{R}{X}\right)^4 - (K_T - 3) \left[5\left(\frac{R}{X}\right)^6 - 7\left(\frac{R}{X}\right)^8 \right] \right\}$$

$X > R$

$$K_T^\infty = 1 + \sqrt{2 \left(\sqrt{\frac{\bar{E}_2}{\bar{E}_1}} - \nu_{12} \right) + \frac{\bar{E}_2}{\bar{G}_{12}}}$$

CIRCULAR HOLE

POINT STRESS CRITERION

$$\frac{\sigma_N^\infty}{\sigma_0} = \frac{2}{\left[2 + \xi_1^2 + 3\xi_1^4 - (K_T^\infty - 3)(5\xi_1^6 - 7\xi_1^8) \right]}$$

$$\xi_1 = \frac{R}{R + d_0}$$

AVERAGE STRESS CRITERION

$$\frac{\sigma_N^\infty}{\sigma_0} = \frac{2(1 - \xi_2)}{\left[2 - \xi_2^2 - \xi_2^4 + (K_T^\infty - 3)(\xi_2^6 - \xi_2^8) \right]}$$

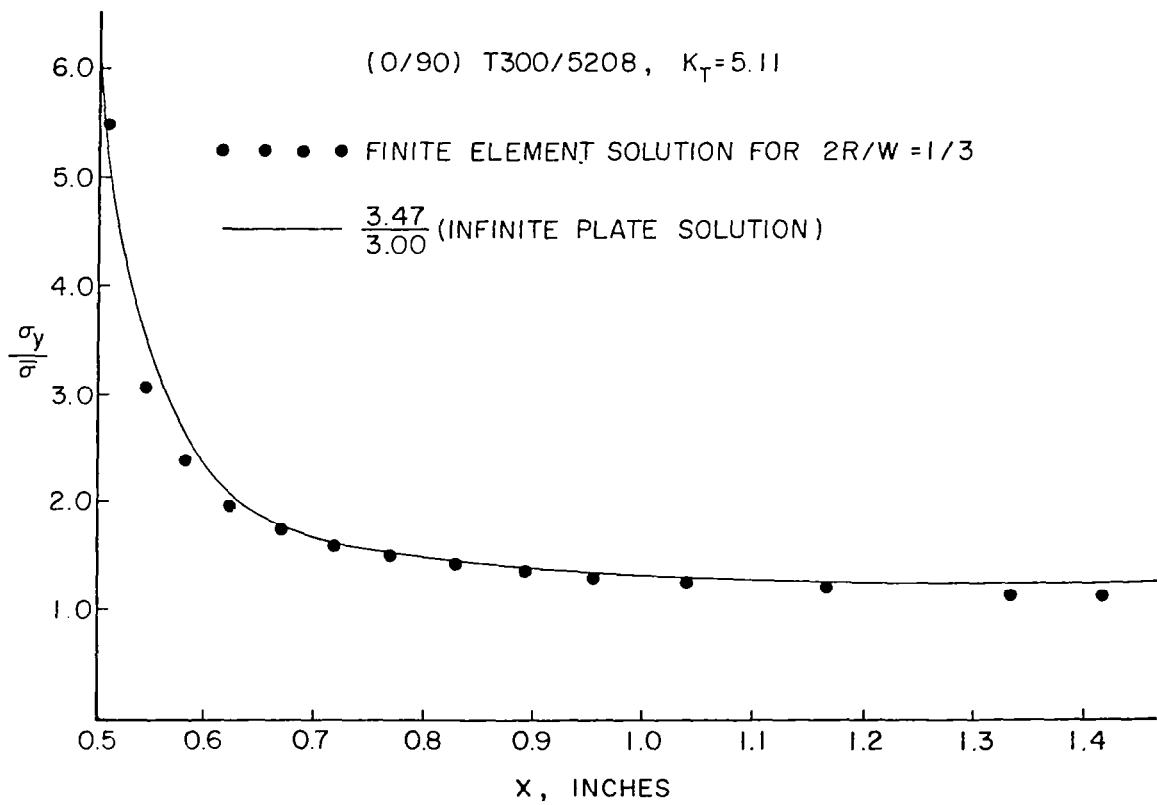
$$\xi_2 = \frac{R}{R + a_0}$$

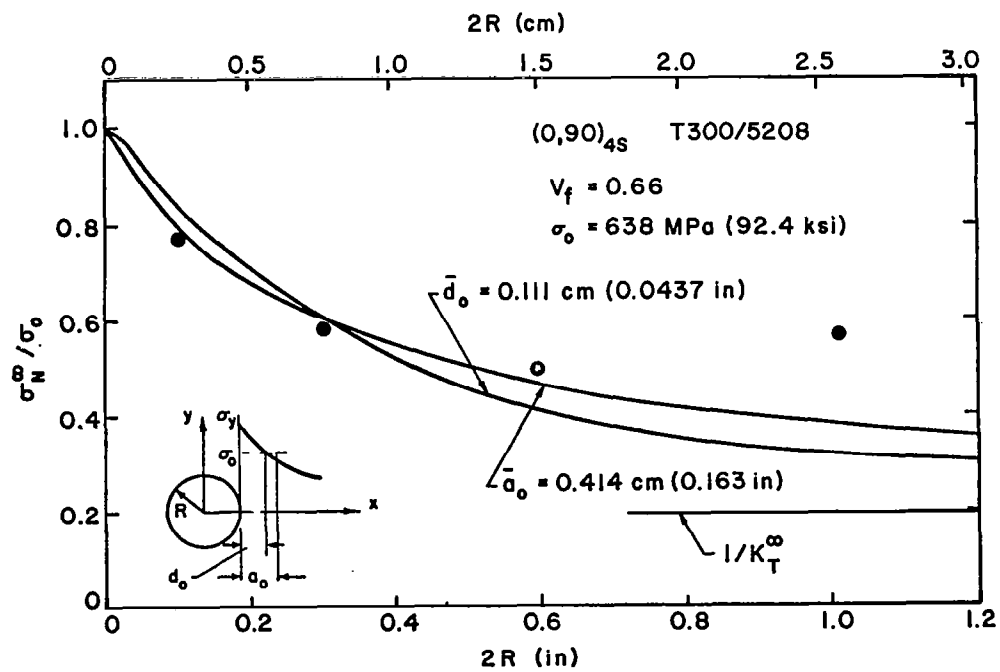
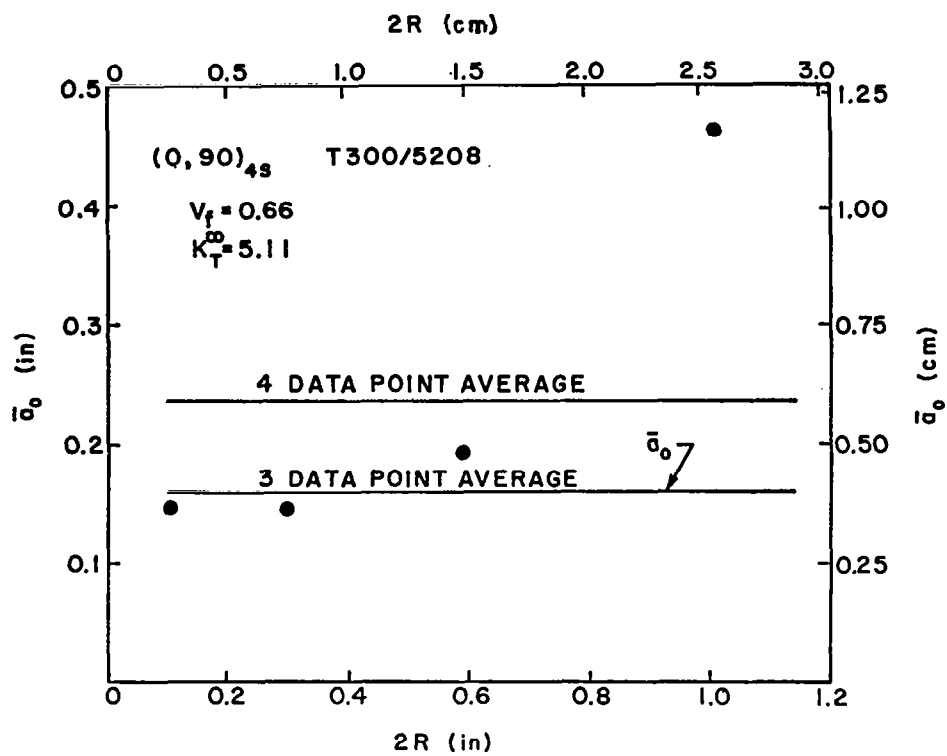
FINITE WIDTH CORRECTION -

CIRCULAR HOLE

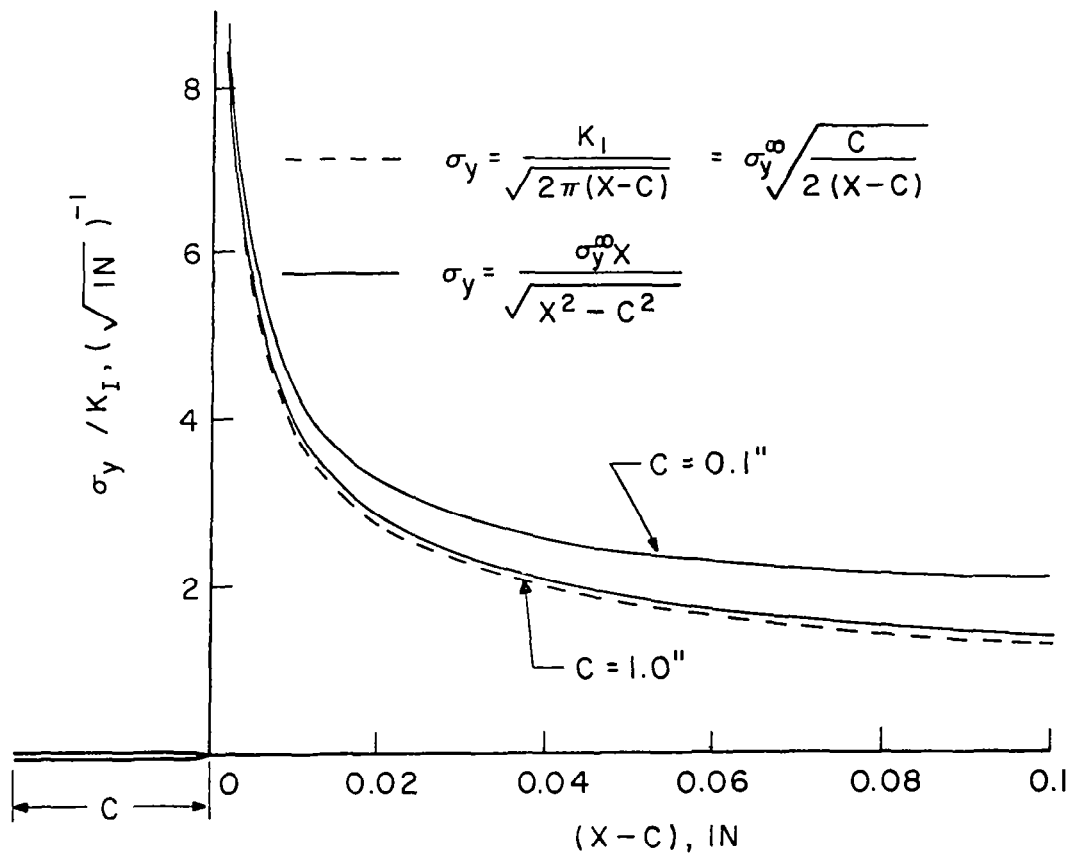
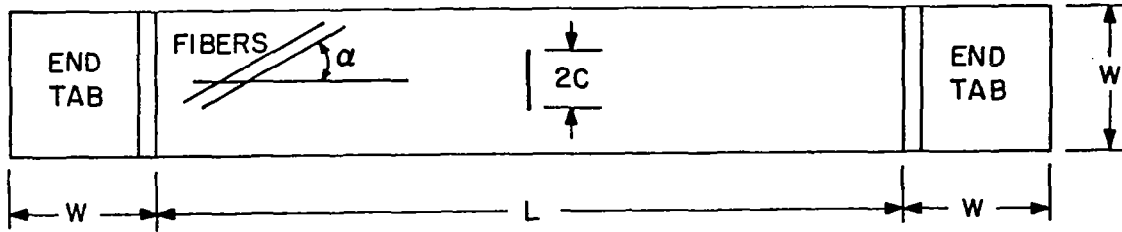
$$\sigma_N^{\infty} = Y_3 (2R/W) \sigma_N$$

$$Y_3(2R/W) = \frac{2 + (1 - 2R/W)^3}{3(1 - 2R/W)}$$





CENTER-CRACKED SPECIMEN



CENTER CRACK

$$\sigma_y(X,0) = \frac{\sigma_y^\infty X}{\sqrt{X^2 - c^2}} = \frac{K_I X}{\sqrt{\pi c (X^2 - c^2)}} , X > c$$

POINT STRESS CRITERION

$$\frac{\sigma_N^\infty}{\sigma_0} = \sqrt{1 - \xi_3^2} , \quad \xi_3 = \frac{c}{c + d_0}$$

AVERAGE STRESS CRITERION

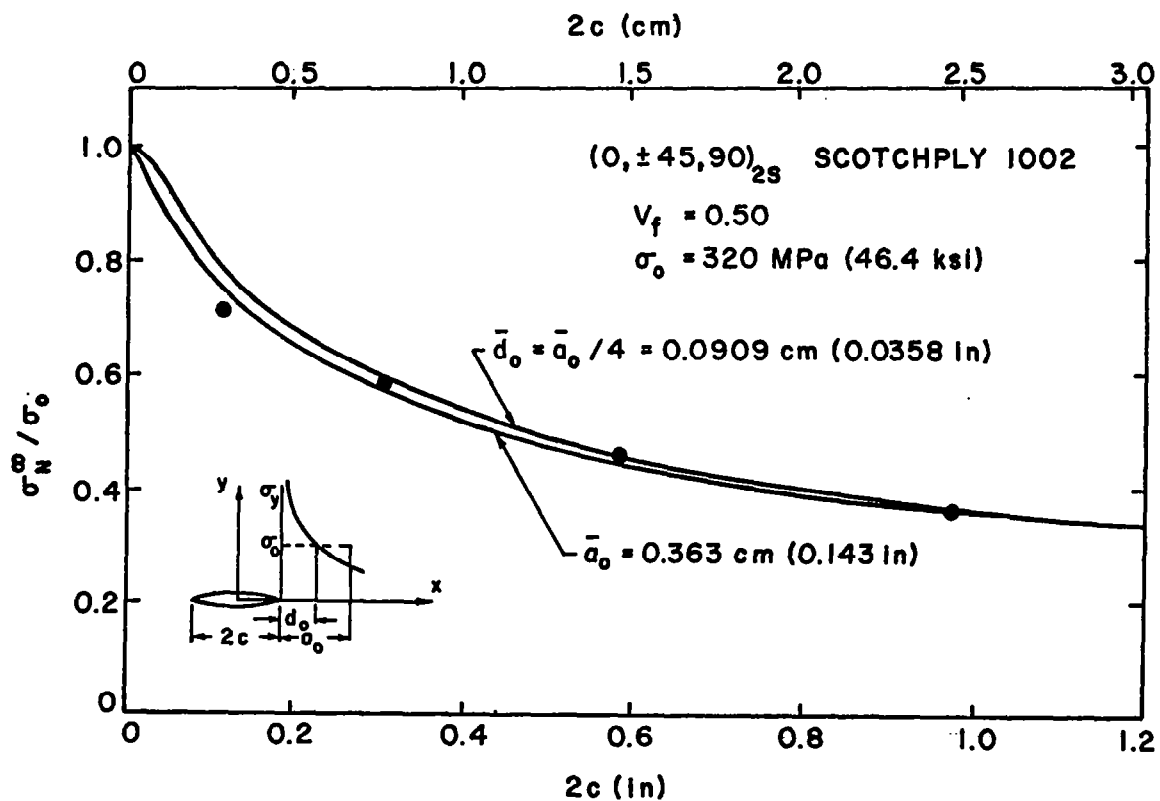
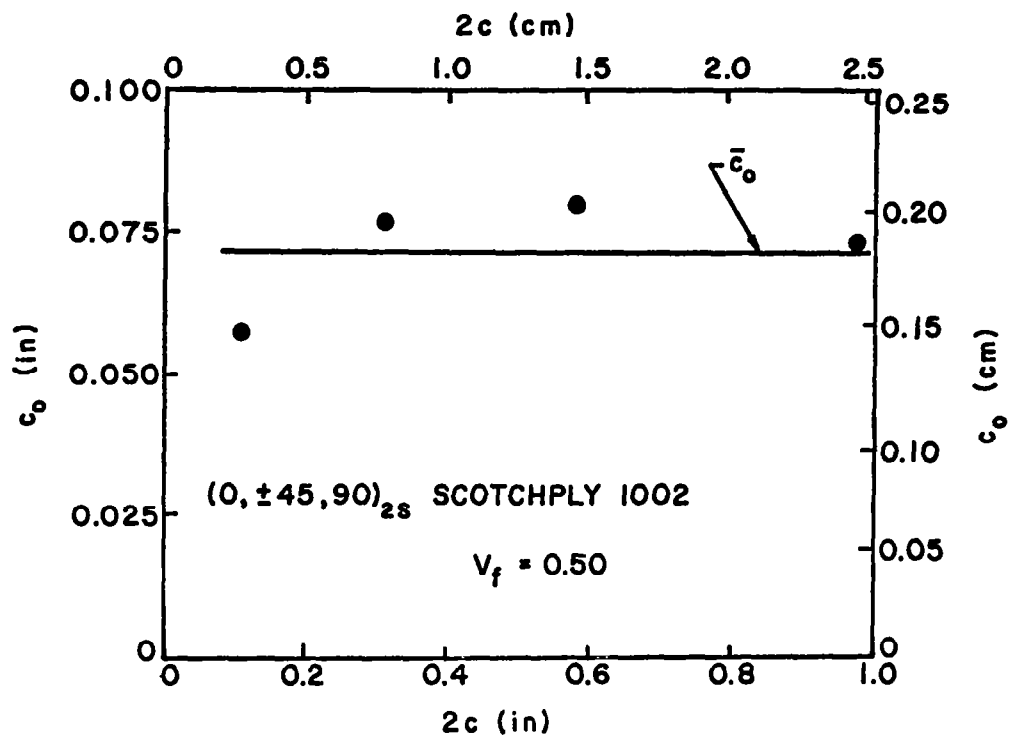
$$\frac{\sigma_N^\infty}{\sigma_0} = \sqrt{\frac{1 - \xi_4}{1 + \xi_4}} , \quad \xi_4 = \frac{c}{c + a_0}$$

FINITE WIDTH CORRECTION - CENTER CRACK

$$\sigma_N^\infty = Y_1 (2c/w) \sigma_N$$

$$Y_1 (2c/w) = 1 + 0.128 (2c/w) - 0.288 (2c/w)^2 \\ + 1.52 (2c/w)^3$$

$$2c/w \leq 0.7, \text{ ERROR} < 0.5\%$$



FRACTURE TOUGHNESS

POINT STRESS CRITERION

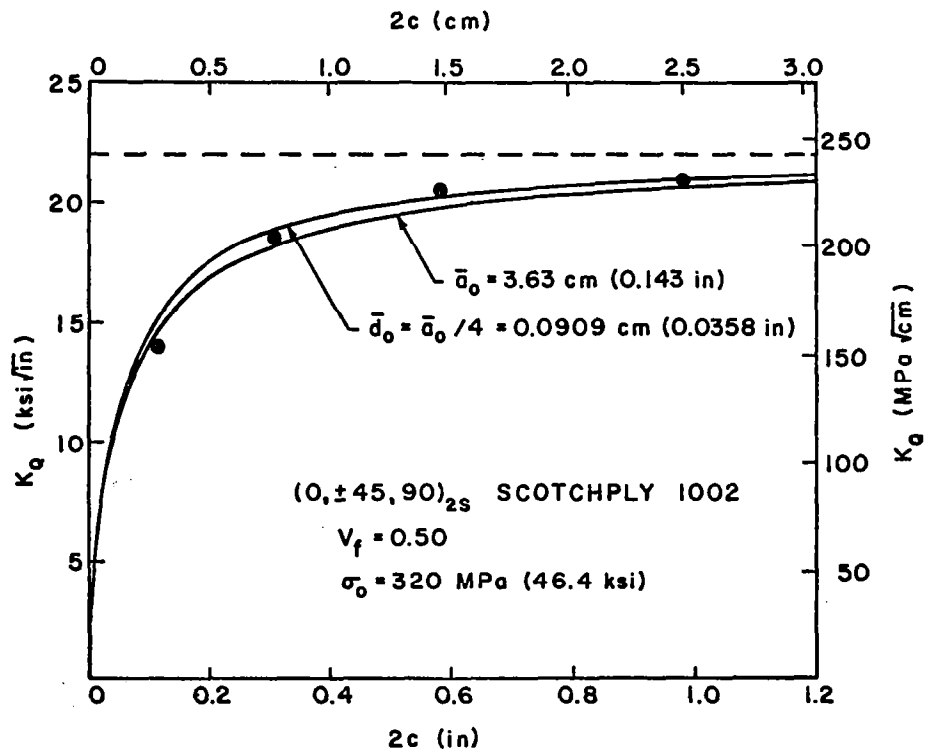
$$K_Q = \sigma_0 \sqrt{\pi c (1 - \xi_3^2)}$$

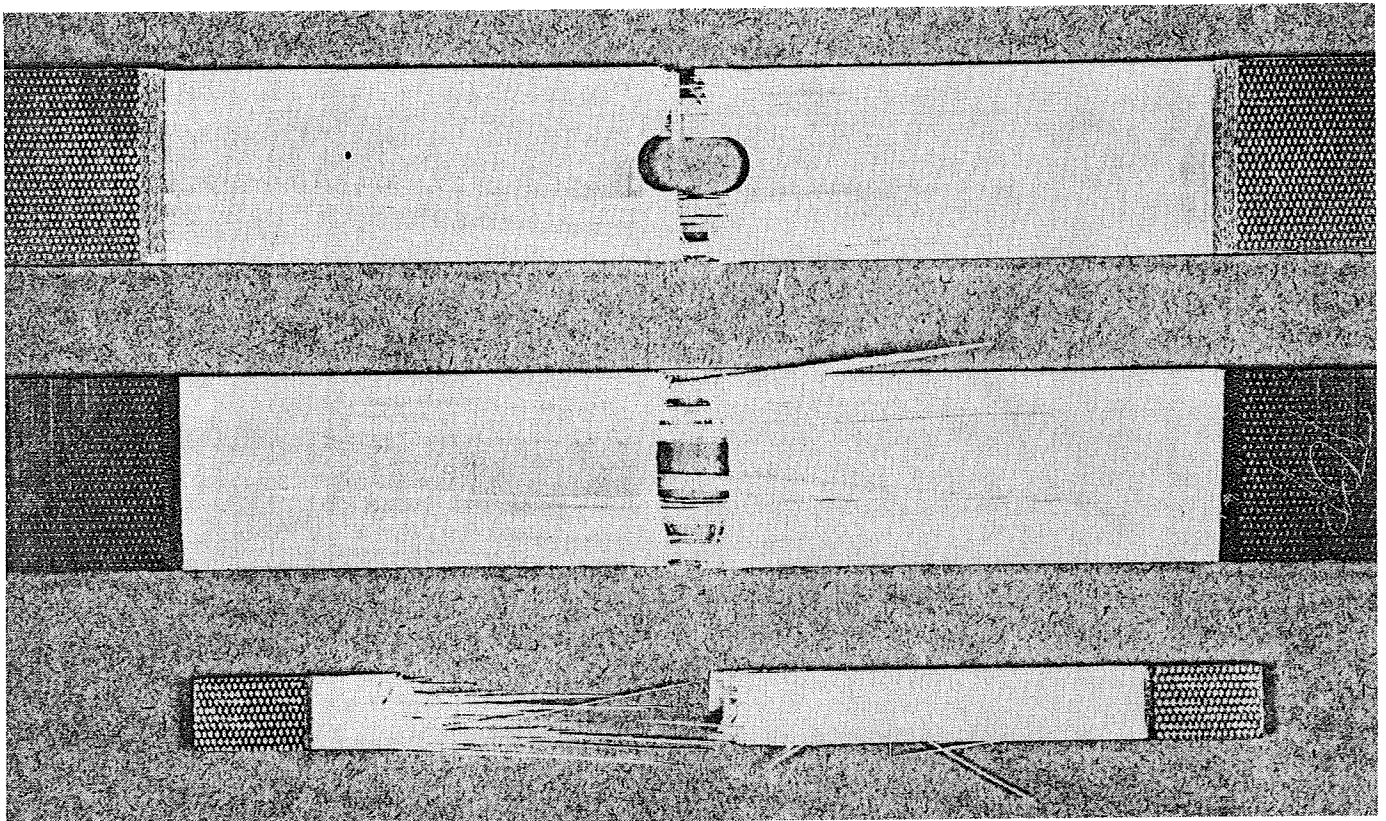
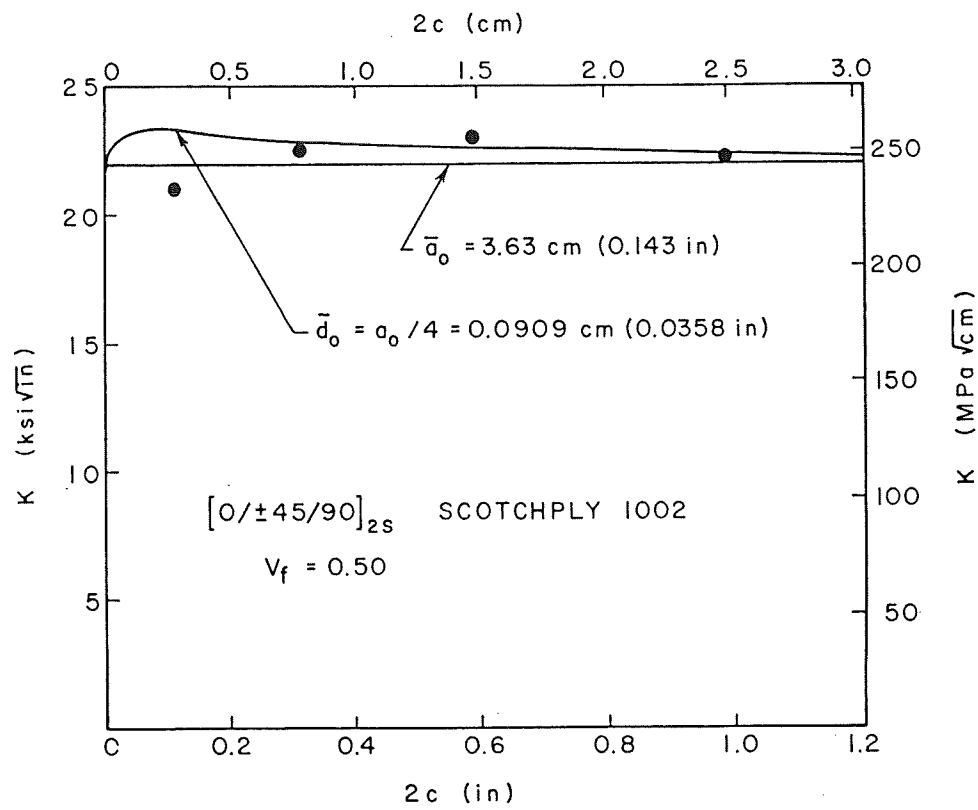
$$c \rightarrow \infty, K_Q \rightarrow \sigma_0 \sqrt{2\pi d_0}$$

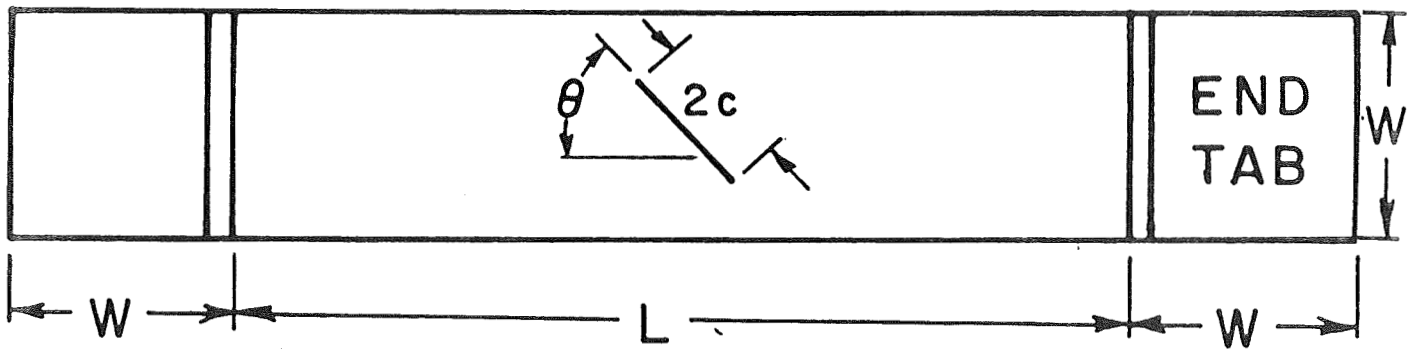
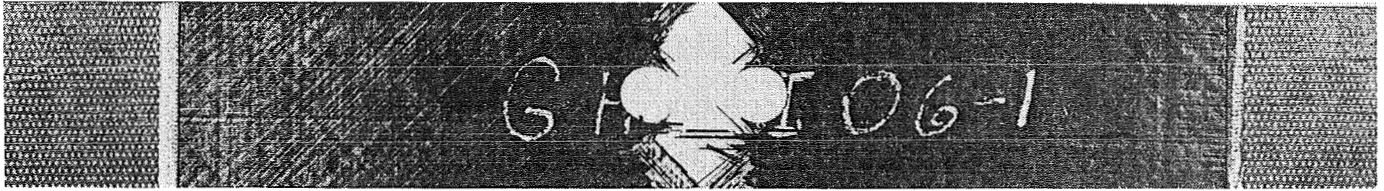
AVERAGE STRESS CRITERION

$$K_Q = \sigma_0 \sqrt{\frac{\pi c (1 - \xi_4)}{(1 + \xi_4)}}$$

$$c \rightarrow \infty, K_Q \rightarrow \sigma_0 \sqrt{\frac{\pi d_0}{2}}$$







MODIFIED THEORY

$$d_0 = R^m / R_0^{m-1} C$$

R = HOLE RADIUS

R_0 = NORMALIZING FACTOR = UNIT LENGTH

m = EXPONENTIAL PARAMETER

C = NOTCH SENSITIVITY FACTOR

$$\frac{\sigma_N}{\sigma_0} = \frac{2}{[(2 + \lambda^2 + 3\lambda^4) - (K_T^\infty - 3)(5\lambda^6 - 7\lambda^8)]}$$

$$\lambda = \frac{C}{\left[C + \left(\frac{R}{R_0} \right)^{m-1} \right]}$$

CASE 1: $m = 0$

$d_0 = \text{CONSTANT}$: ORIGINAL THEORY RECOVERED

CASE 2: $0 < m < 1$

$$R \longrightarrow \infty, \lambda \longrightarrow 1, \frac{\sigma_N}{\sigma_0} \longrightarrow \frac{1}{K_T^\infty}$$

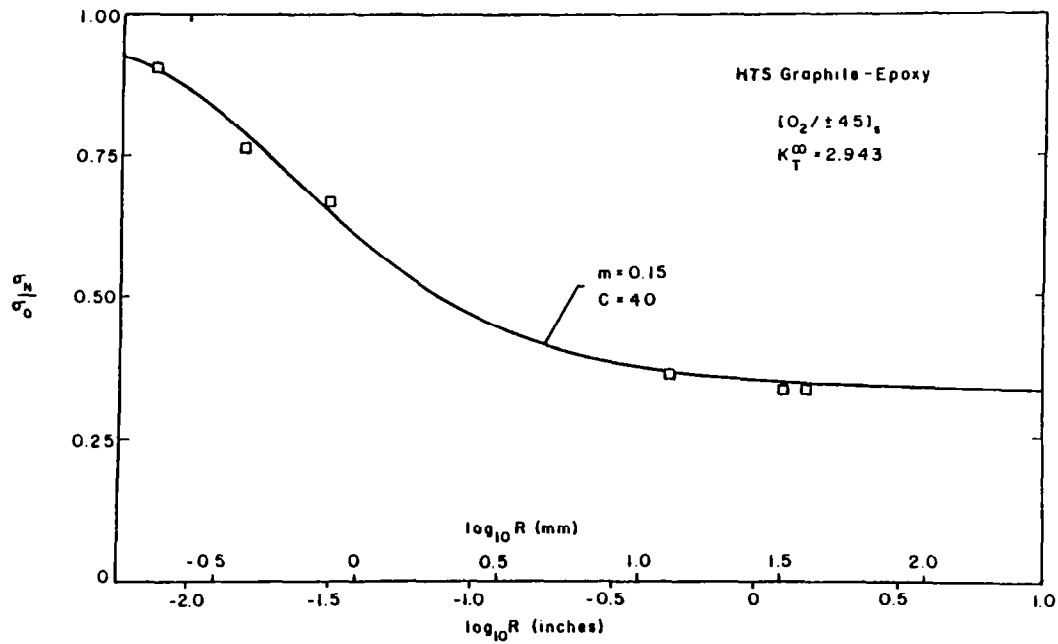
CASE 3: $m = 1$

$$\lambda = \frac{C}{C+1}, \frac{\sigma_N}{\sigma_0} \text{ INDEPENDENT OF } R$$

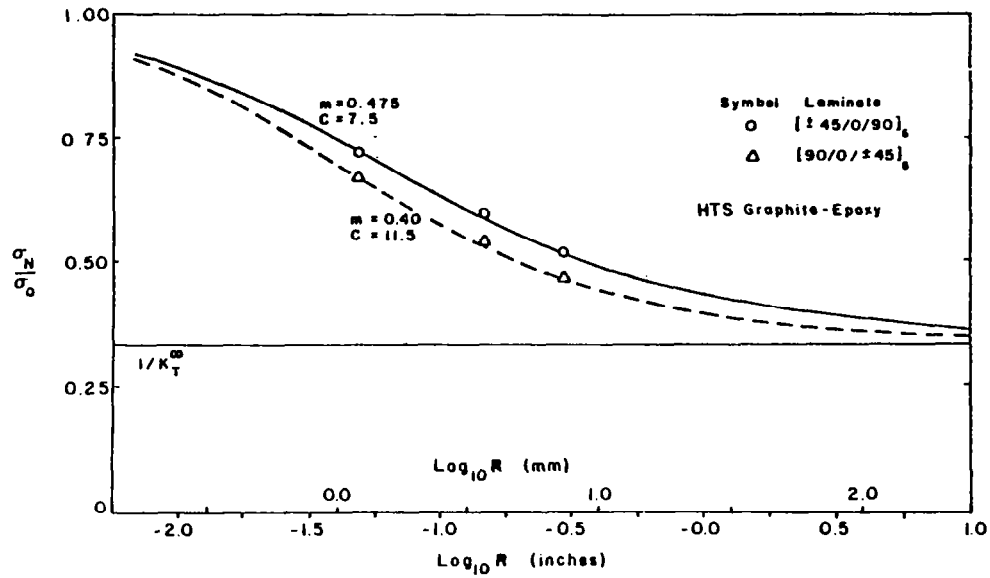
CASE 4: $m > 1$

$$R \longrightarrow \infty, \lambda \longrightarrow 0, \frac{\sigma_N}{\sigma_0} \longrightarrow 1$$

$$0 \leq m < 1$$



INFLUENCE OF STACKING SEQUENCE ON NOTCHED STRENGTH



SUPERIMPOSING NOTCHED STRENGTH

MATERIAL 1 AND MATERIAL 2

$$\left(\frac{\sigma_N}{\sigma_0}\right)_1 = \left(\frac{\sigma_N}{\sigma_0}\right)_2 \quad \text{IF } \lambda_2 = \lambda_1 \quad \text{AND } (K_T^{\infty})_2 = (K_T^{\infty})_1$$

R = ARBITRARY RADIUS FOR MATERIAL 1

R_e = RADIUS IN MATERIAL 2 PRODUCING SAME PERCENT STRENGTH REDUCTION

$$\frac{1}{C_1} \left(\frac{R_e}{R_0}\right)^{m_1-1} = \frac{1}{C_2} \left(\frac{R}{R_0}\right)^{m_2-1}$$

$$\text{LET } R_e = a_{cm} R$$

$$a_{cm} = \left(\frac{C_2}{C_1}\right)^{1/(m_2-1)} \left(\frac{R}{R_0}\right)^{\left(\frac{m_1-m_2}{m_2-1}\right)}$$

FOR CONSTANT m:

$$a_c = \left(\frac{C_1}{C_2} \right)^{1/(1-m)}$$

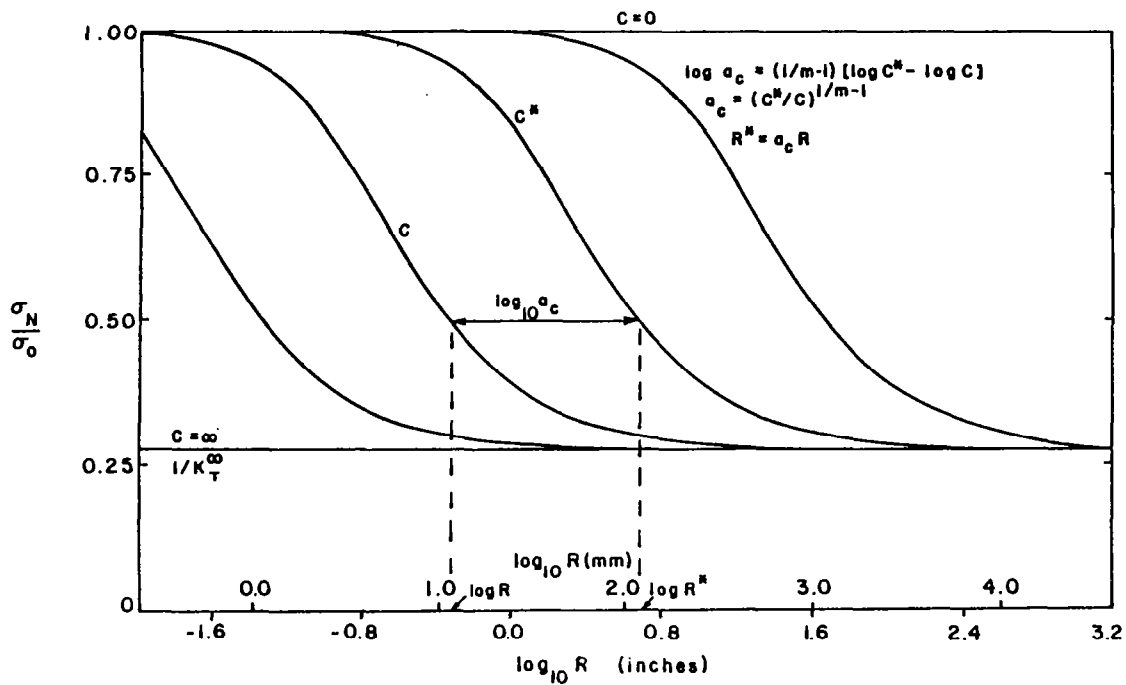
$$\text{LOG } a_c = \frac{1}{(1-m)} (\text{LOG } C_1 - \text{LOG } C_2)$$

FOR MOST COMPOSITES:

$$2 \leq K_T^\infty < 4$$

$$\frac{\sigma_N}{\sigma_0} \text{ INSENSITIVE FOR } R \leq 1.0$$

RADIUS-NOTCH SENSITIVITY FACTOR SUPERPOSITION



DEFINE EXPONENTIAL SHIFT PARAMETER

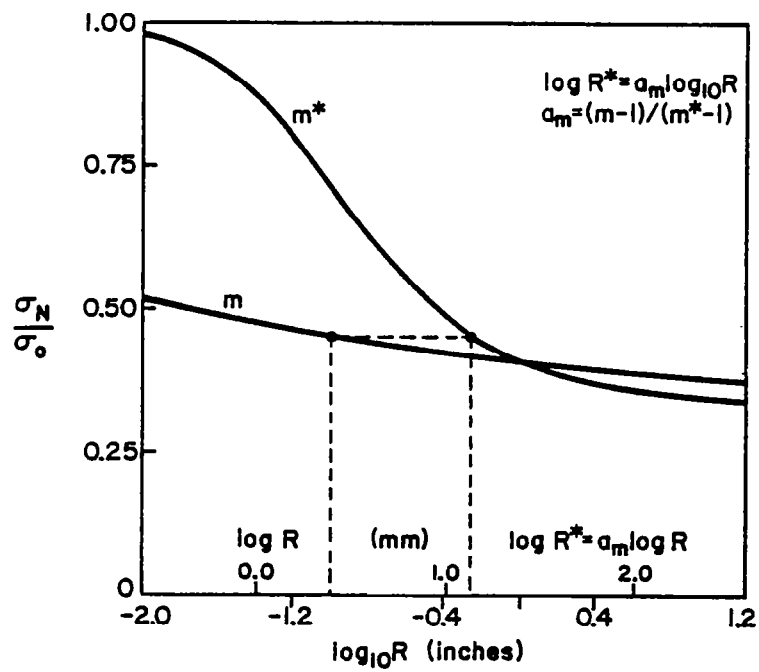
$$(K_T^\infty)_2 = (K_T^\infty)_1 ; C_2 = C_1$$

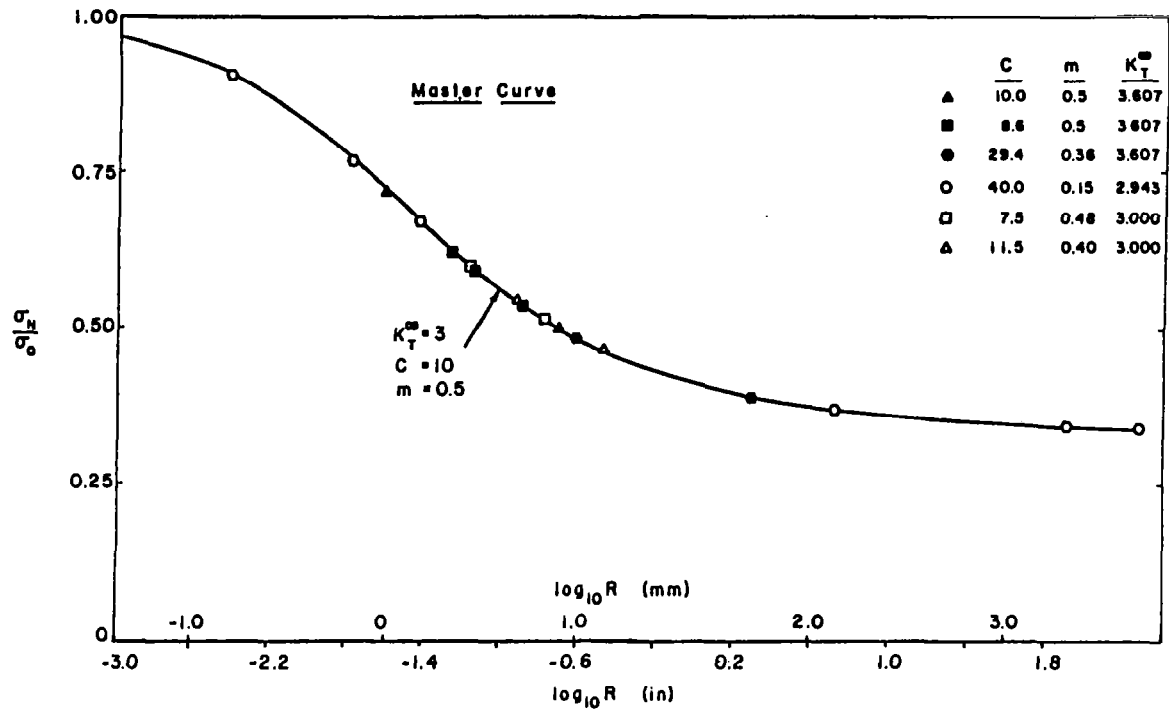
$$\frac{R_e}{R_0} = \left(\frac{R}{R_0} \right)^{a_m}$$

$$\text{LOG } R_e = a_m \text{ LOG } R$$

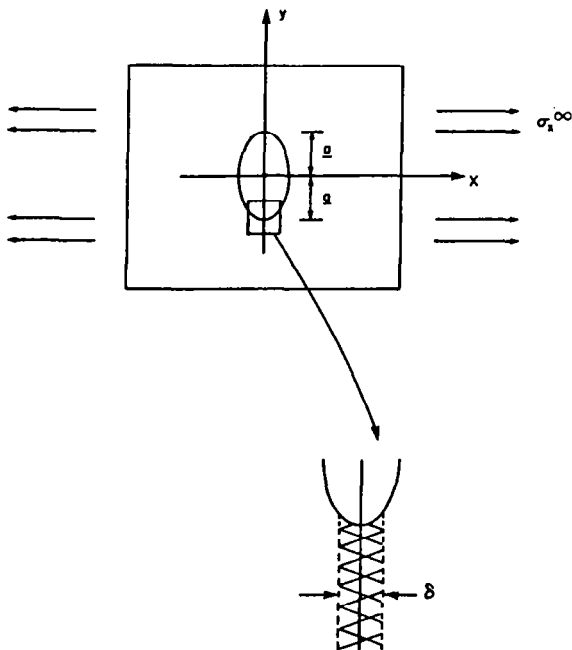
$$a_m = \left(\frac{m_1 - 1}{m_2 - 1} \right)$$

EXPONENTIAL SHIFT PARAMETER





COMPARISON BETWEEN WEIBULL THEORY AND MODIFIED THEORY



$$-\delta/2 \leq x \leq \delta/2$$

$$a \leq y \leq L$$

$$-h/2 \leq z \leq h/2$$

$$\frac{\sigma_N}{\sigma_0} = \left(\frac{L}{\int_a^L [t(0, y)]^\alpha dy} \right)^{1/\alpha}$$

$$t(0, y) = 1 + 1/2\rho^2 + 3/2\rho^4$$

$$- (K_T^m - 3)(5/2\rho^6 - 7/2\rho^8)$$

$$\text{where } \rho = R/y$$

$$\sigma_N/\sigma_0 = [1 + 1/2\xi^2 + 3/2\xi^4$$

$$- (K_T^m - 3)(5/2\xi^6 - 7/2\xi^8)]^{-1}$$

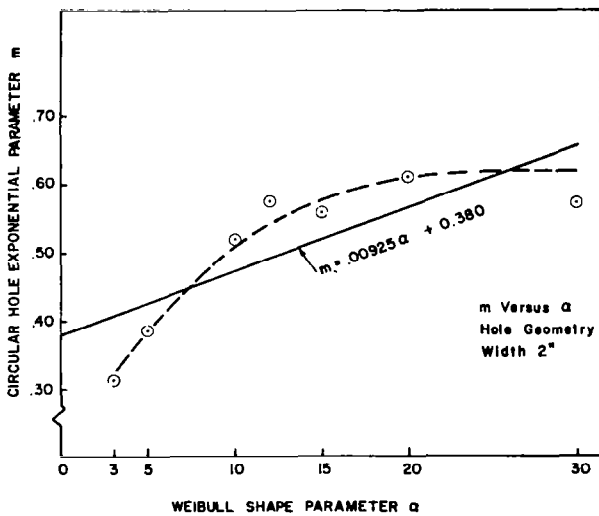
$$\text{where } \xi = R/(R + d_0) \text{ and } d_0 = R^m/K$$

Loading geometry - volume of numerical integration.

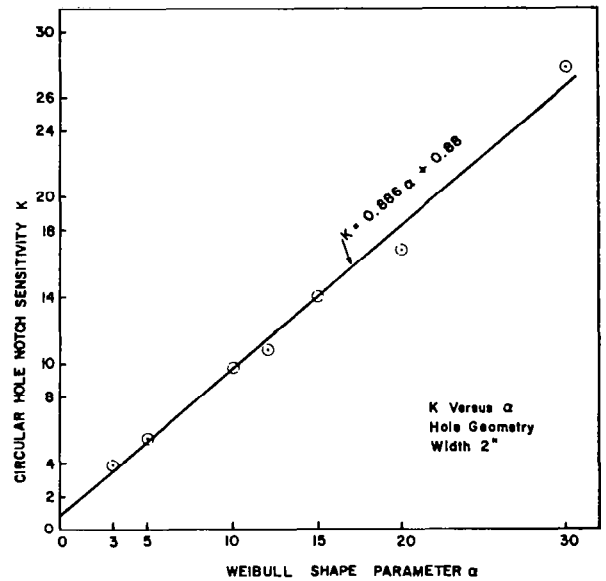
$$\ln d_0 = m \ln R - \ln K$$

Shape parameter α	Exponential parameter m	Notch sensitivity K	Correlation coefficient* r
3	0.31	3.9	0.985
5	0.39	5.5	0.987
10	0.52	9.7	0.990
12	0.57	10.8	0.986
15	0.56	14.0	0.983
20	0.61	16.8	0.996
30	0.57	27.8	0.977

* Correlation coefficient from the least squares fit of linear equation,
 $\ln d_s = m \ln R - \ln K$; minimum three points (radii) used for each given α .



Exponential parameter m as a function of shape parameter α .



Notch sensitivity K as a function of shape parameter α .

COMMENT

An interesting observation has been made (ref. 1) concerning the Whitney "point stress" or "average stress" criterion. In particular, the center-notched unidirectional laminate with no notch tip damage is shown to have a square root type stress distribution with an equivalent notch length which differs from the actual number of broken fibers by a small but constant amount, independent of the number of broken fibers. This is consistent with the assumptions leading to the "point stress" and "average stress" criterion. This is not the case if notch tip damage (in the form of matrix yielding or transverse broken fibers) is present, and it is shown that the damage produces stresses in the unbroken fibers which are less severe than a square root behavior, and also that an analogous equivalent notch length does not exist.

REFERENCE

1. Goree, J. G.; Dharani, L. R.; and Jones, W. F.: Mathematical Modeling of Damage in Unidirectional Laminates. NASA CR-3453, 1981.

James G. Goree
Clemson University

COMMENT

The Weibull distribution function is based on a weakest link concept of failure, which in general is not applicable to composites. This concept underlies the size effect which would account for the difference between bending and uniform tensile strength in purely brittle materials. The difference between tensile and bending strengths in composites is more likely related to the "gradient" effect, which allows localized failure and stress redistribution, as in the case of elastic-plastic materials.

I. M. Daniel
Illinois Institute of Technology

COMMENT

The present point stress and average stress criteria relate the notched strength of a laminate to the average strength of a relatively long tensile coupon. Tests of notched specimens in which microstrain gages have been placed at or near the edges of the holes have measured strains much larger than those measured in an unnotched tensile coupon. Furthermore, orthotropic stress concentration analyses of failed notched laminates have also indicated that failure occurred at strains much larger than those experienced on tensile coupons with normal gage lengths. Earlier, both Hahn (ref. 1) and Wu (ref. 2) presented data that related fiber strength to gage length. This suggests that the high strains at the edge of a hole can be related to the very short length of fiber subjected to these strains. Since the length of fiber that is highly strained is proportional to the hole size, this would explain the higher strains to failure measured at the edge of smaller holes.

Lockheed has attempted to correlate a series of tests of several laminates with holes ranging from 0.19 to 0.50 in. Although the average stress criterion correlated well with test results for hole sizes equal to or greater than 0.50 in., it overestimated the laminate strength in the range of hole sizes from 0.19 to 0.38 in. It thus appears that we need a theory that is based on the mechanics of failure and is more generally applicable to the range of hole sizes and the varieties of laminates found in aircraft construction.

REFERENCES

1. Hahn, H. T.: Failure Mechanisms. Failure Analysis and Mechanisms of Failure of Fibrous Composite Structures, NASA CP-2278, August 1983, pp. 153-171.
2. Wu, Edward M.: Strength Theories of Composites: Status and Issues. Failure Analysis and Mechanisms of Failure of Fibrous Composite Structures, NASA CP-2278, August 1983, pp. 173-189.

Larry Fogg
Lockheed-California Company

**COMPRESSION FAILURE OF
COMPOSITE LAMINATES**

**R. B. Pipes
Center for Composite Materials
College of Engineering
University of Delaware
Newark, Delaware**

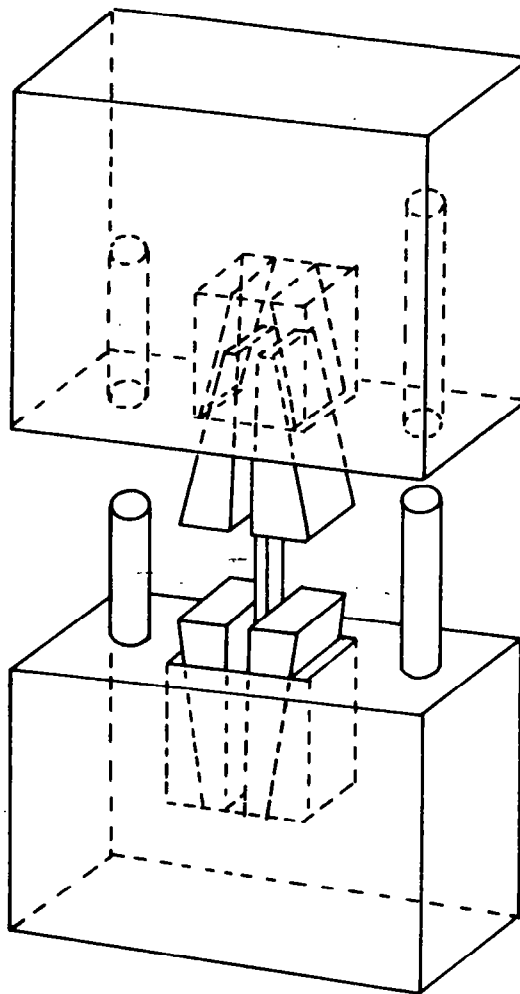
This presentation will attempt to characterize the compressive behavior of Hercules AS-1/3501-6 graphite-epoxy composite. This involves:

Studying the effect of varying specimen geometry on test results

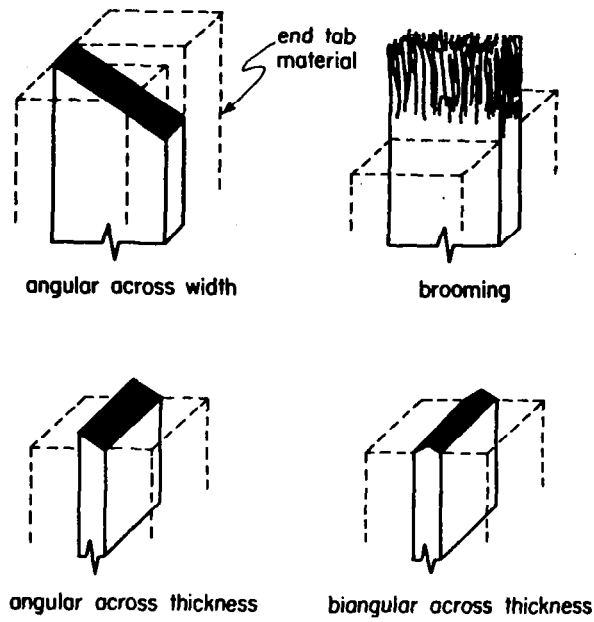
Determining end condition factors for IITRI fixture

Determining transition region between buckling and compressive failure

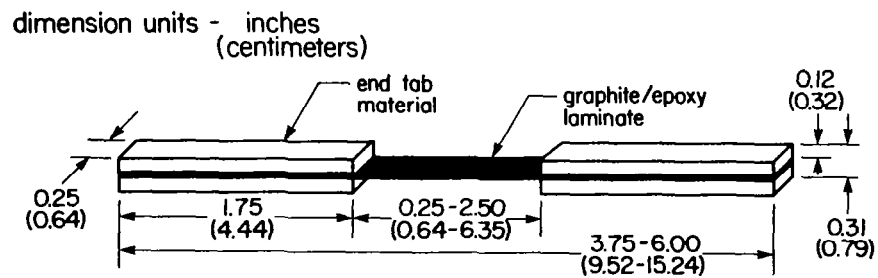
Defining failure modes and developing analytical models to describe and/or predict these modes



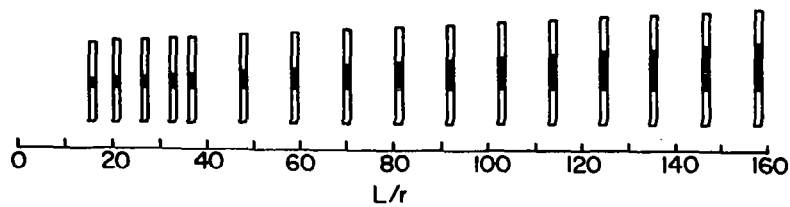
Modified IITRI compression fixture.



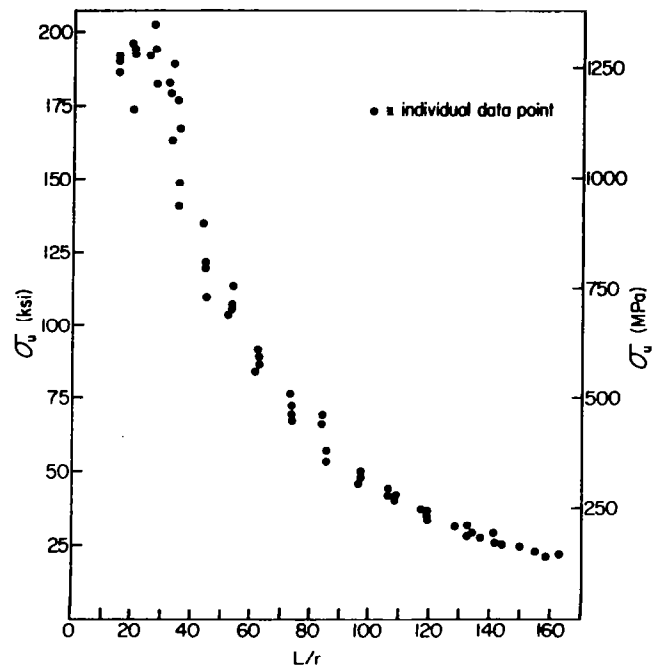
Failure modes



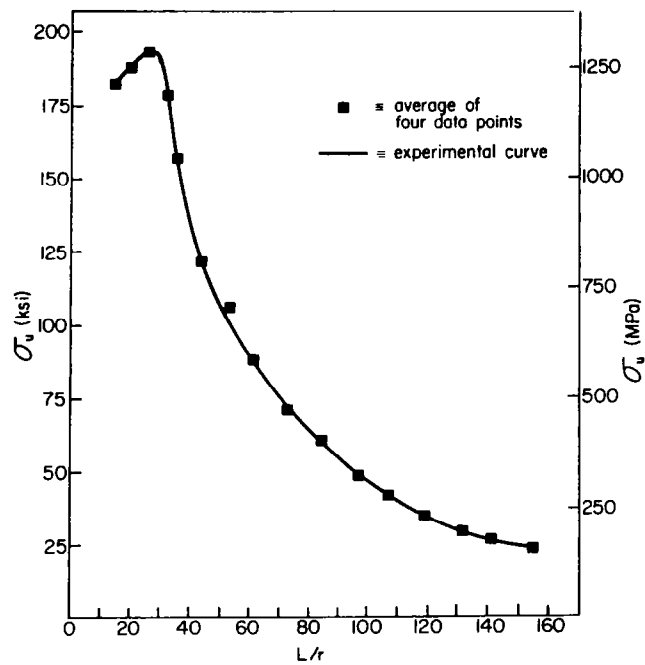
four specimens tested at each L/r ratio



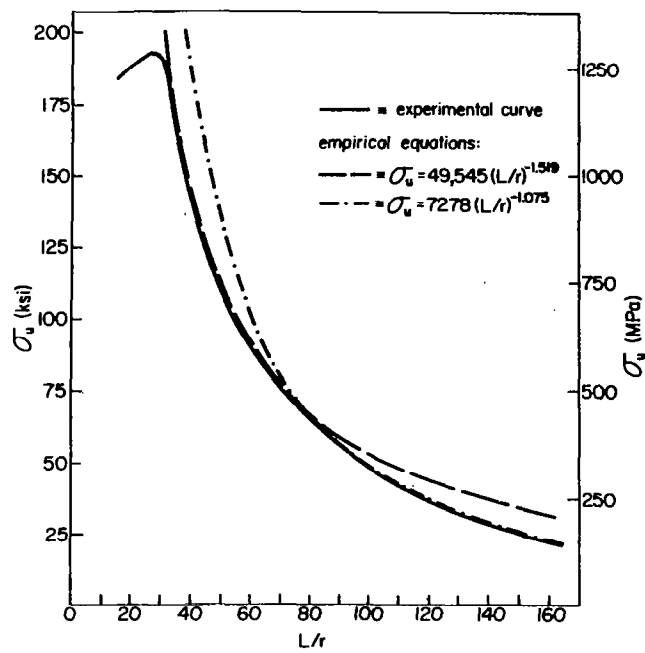
Test coupons



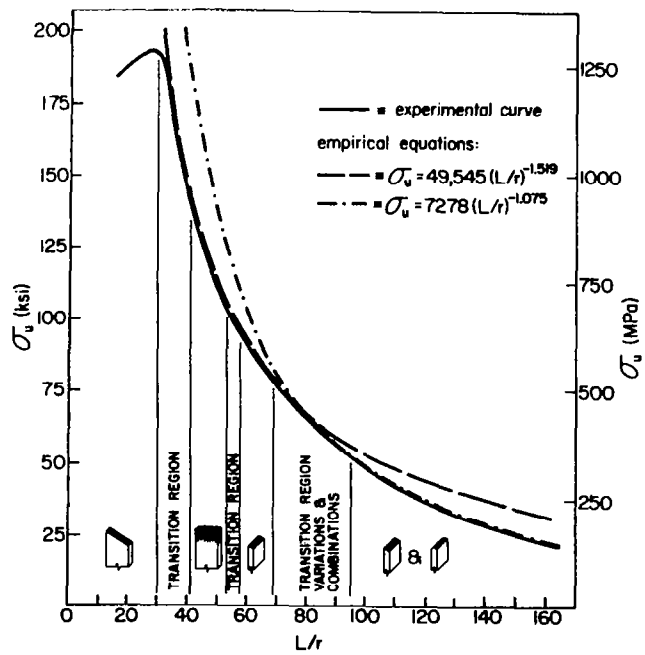
Ultimate stress (σ_u) versus
slenderness ratio (L/r)



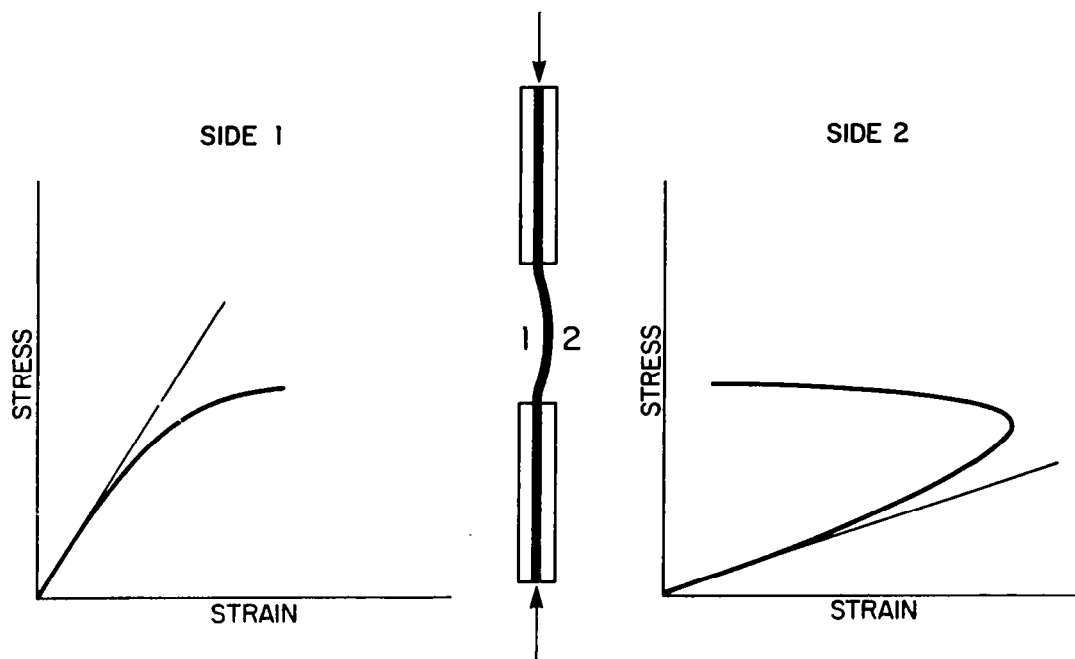
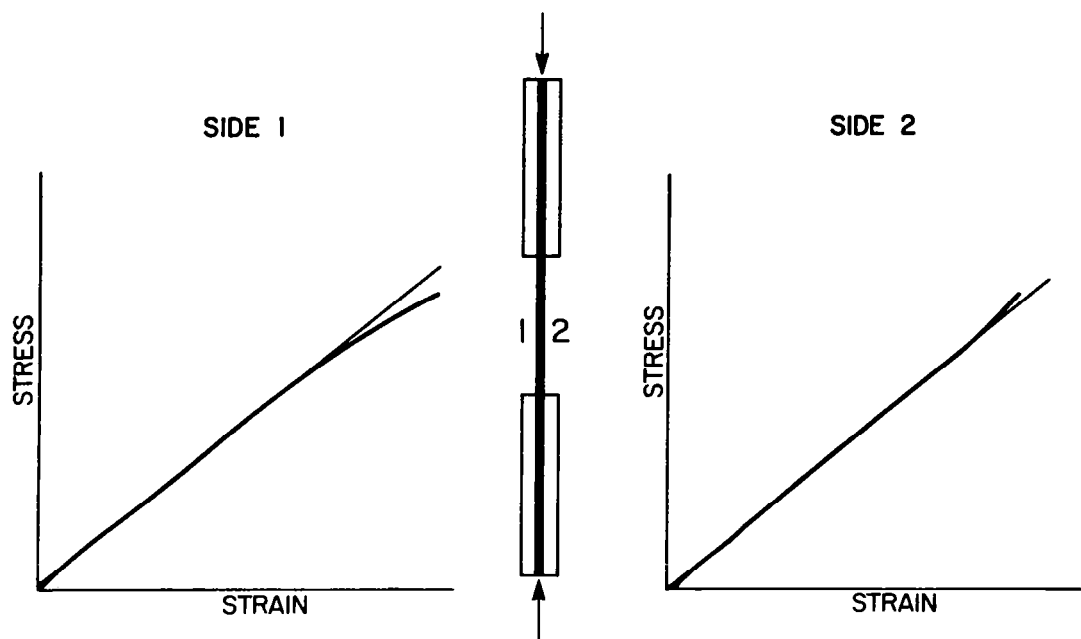
Ultimate stress (σ_u) versus
slenderness ratio (L/r)



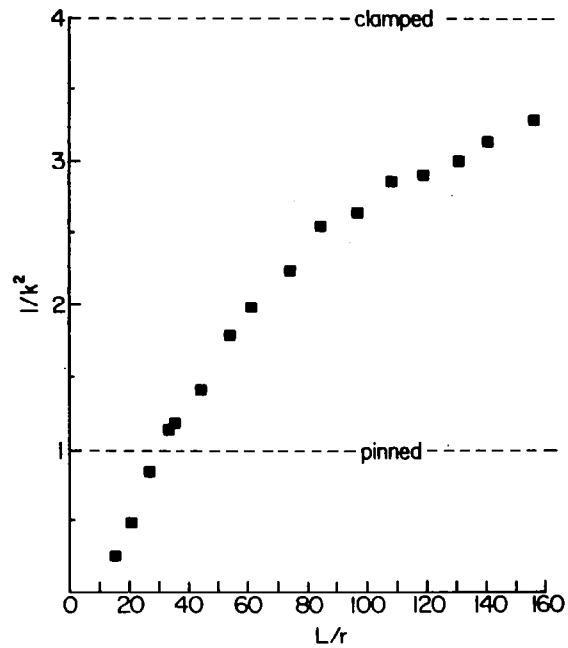
Ultimate stress (σ_u) versus slenderness ratio (L/r)



Ultimate stress (σ_u) versus slenderness ratio (L/r)



Strain gage output



End condition factor ($1/k^2$) versus
slenderness ratio (L/r)

Maximum compressive strength occurred at $25 < L/r < 30$

End condition factor increased as L/r increased

Failure modes change with varying L/r

Conclusions

Induce fatigue damage in the vicinity of a circular hole in a composite laminate through compressive loading

Observe and characterize the nature and extent of damage

Determine the influence of induced damage upon residual compressive failure

Objectives

(R=0.1, frequency of 10 Hertz,
ambient conditions)

Specimen	S-Level	Cycles
1	(Static)	--
2	(Static)	--
3	(Static)	--
4	0.50	1×10^6
5	0.50	1×10^6
6	0.50	1×10^6
7	0.60	1×10^6
8	0.60	1×10^6
9	0.60	1×10^6
10	0.60	5×10^6
11	0.60	5×10^6
12	0.60	5×10^6

Fatigue program

A: $[0_2/\pm 45]_{5s} \quad \Leftrightarrow$

$[0/0/45/-45/0/0/45/-45/0/0/45/-45/0/0/45/-45]_s$

B: $[0/45/0/-45]_{5s} \quad \Leftrightarrow$

$[0/45/0/-45/0/45/0/-45/0/45/0/-45/0/45/0/-45]_s$

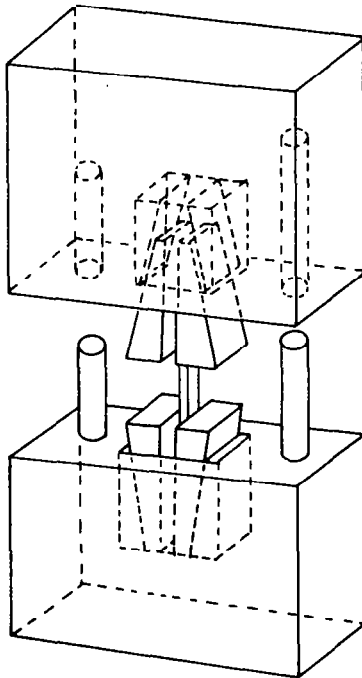
C: $[0/\pm 45/90]_{5s} \quad \Leftrightarrow$

$[0/45/-45/90/0/45/-45/90/0/45/-45/90/0/45/-45/90]_s$

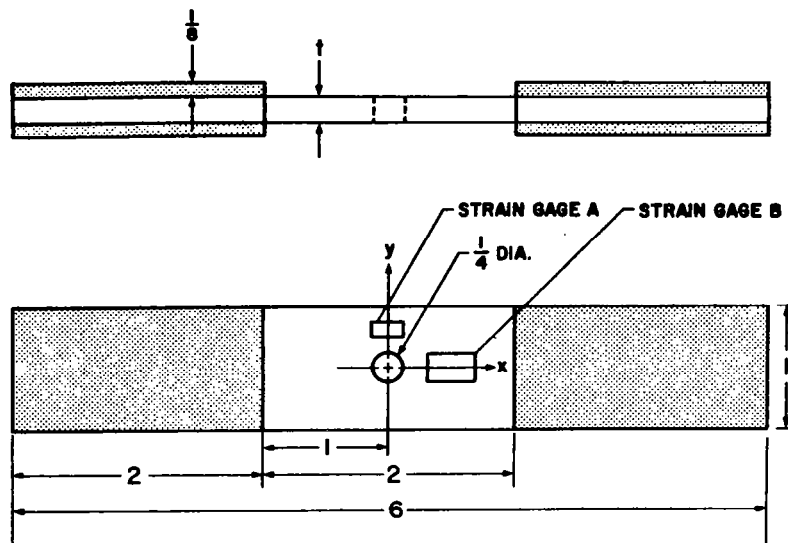
D: $[90/0/\pm 45]_{5s} \quad \Leftrightarrow$

$[90/0/45/-45/90/0/45/-45/90/0/45/-45/90/0/45/-45]_s$

Laminate configurations



Modified IITRI compression fixture

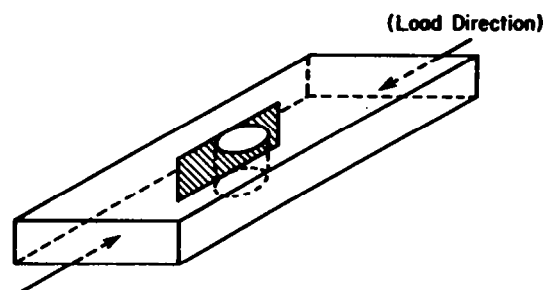


MICRO-MEASUREMENTS

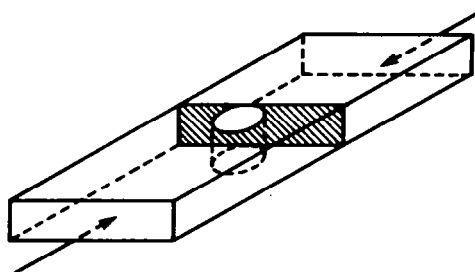
STRAIN GAGE A: EA-06-125BZ-350

STRAIN GAGE B: EA-06-125AC-350

Notched fatigue specimen

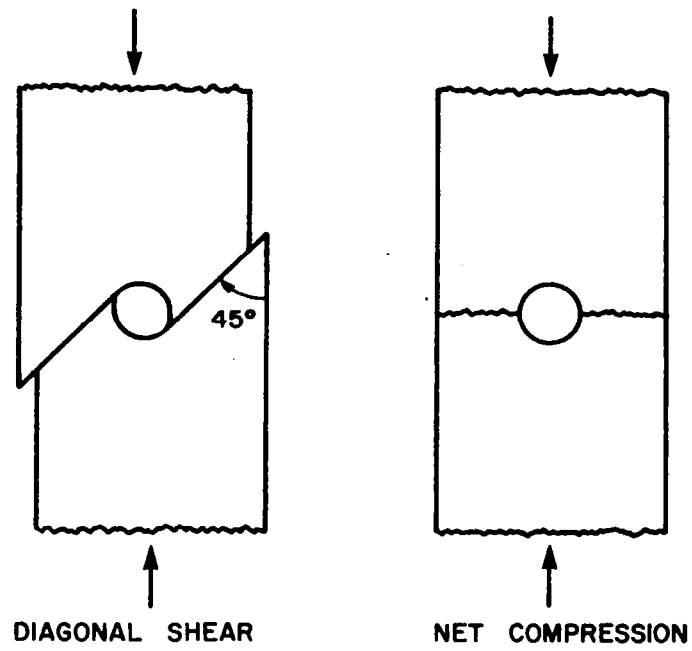


AXIAL SECTION

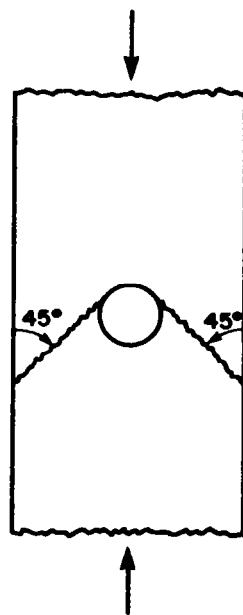


TRANSVERSE SECTION

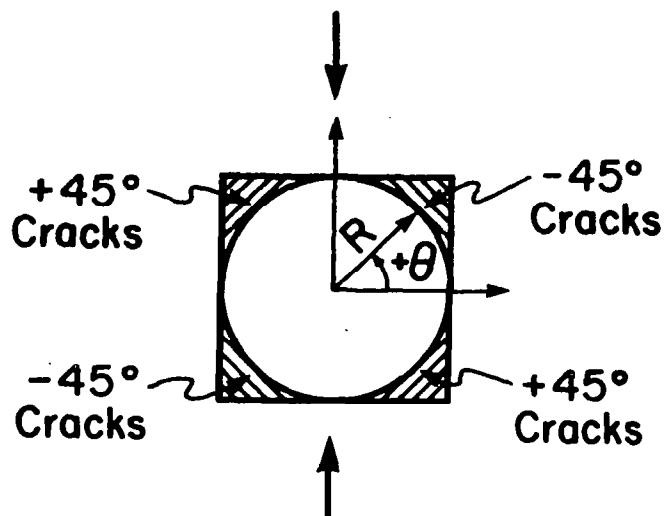
Micrograph section orientations



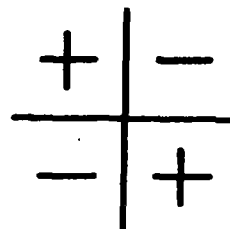
Notched compression failure modes



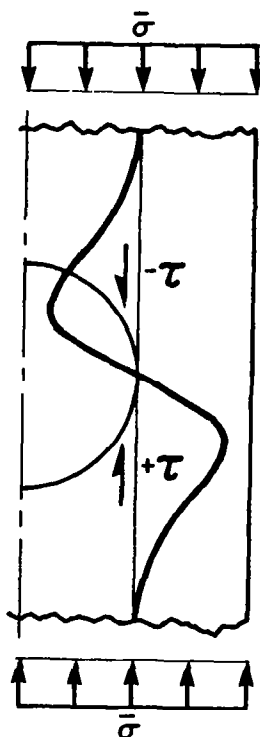
Dual shear compression failure mode



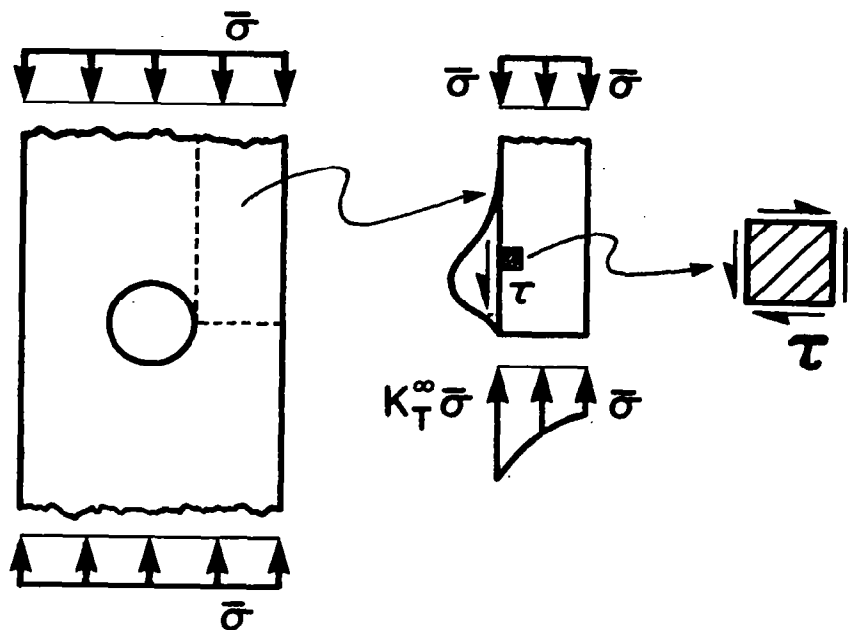
Fatigue crack pattern



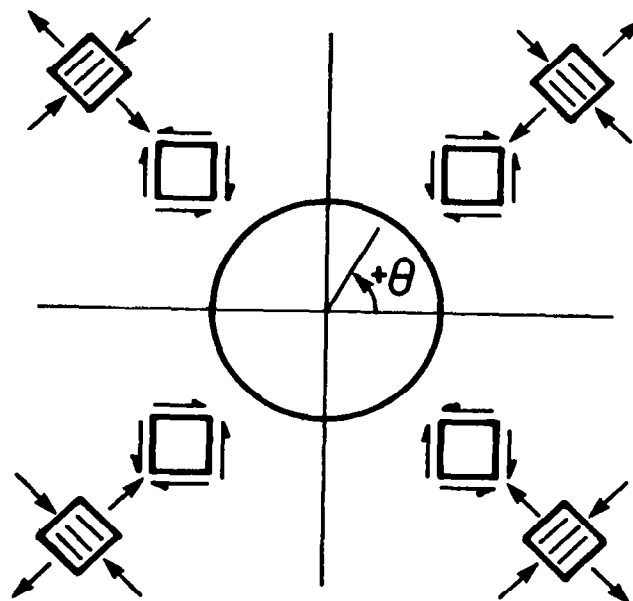
Cracked laminae by quadrant



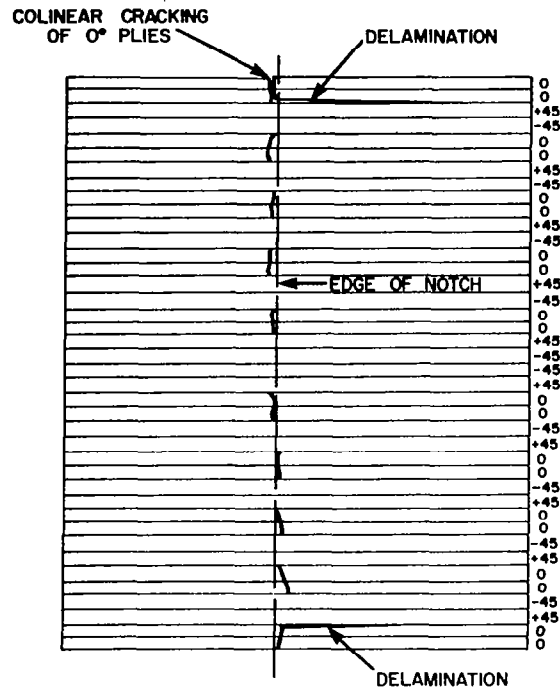
Antisymmetric distribution of shearing stress τ



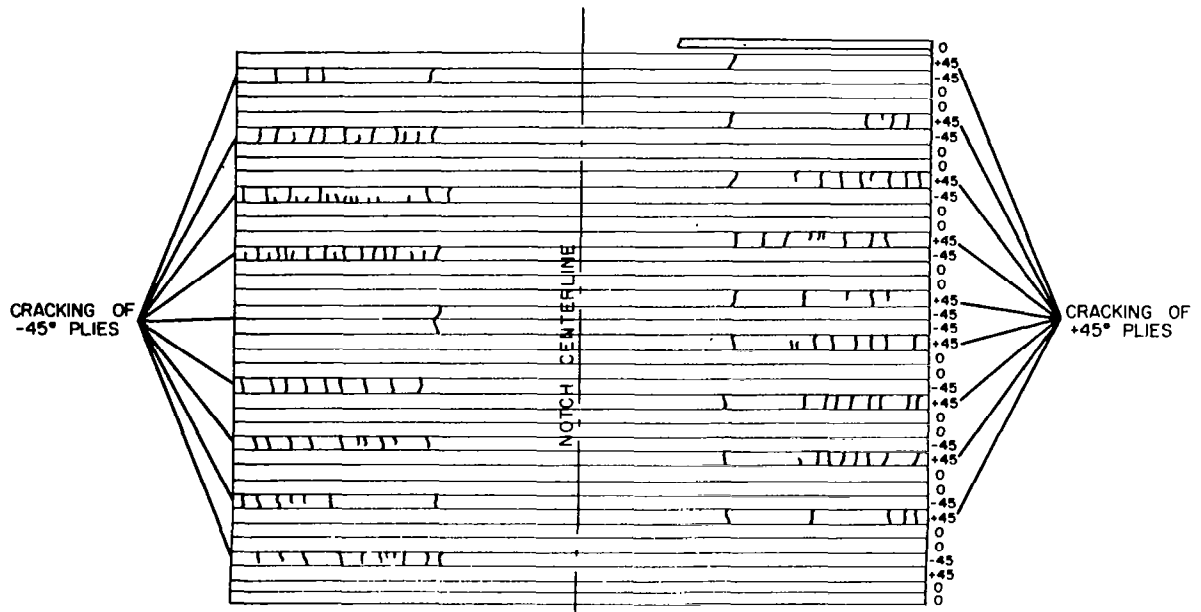
Direction of shearing stress τ



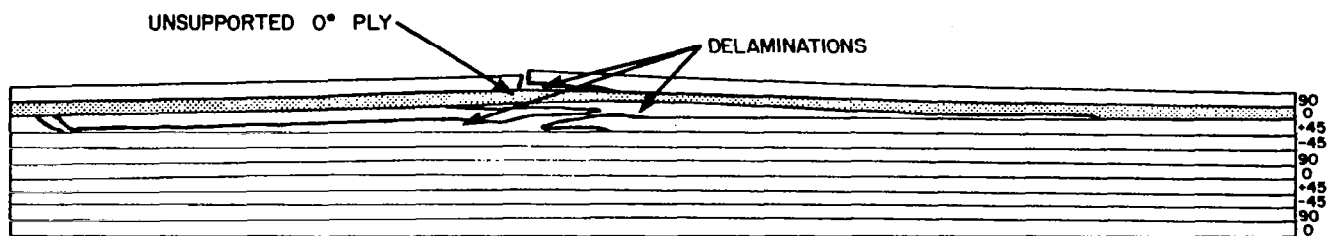
Shear-induced transverse tensile stresses



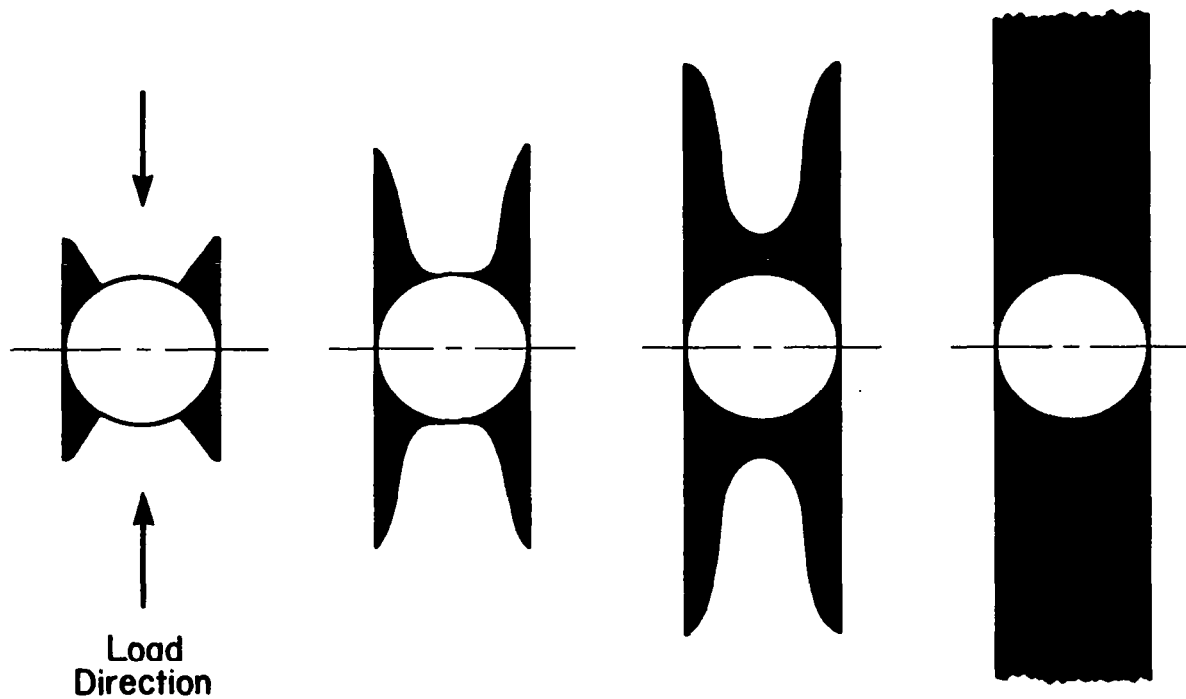
Laminate "A"; $[0_2/\pm 45]_{5S}$; transverse section (50 \times)



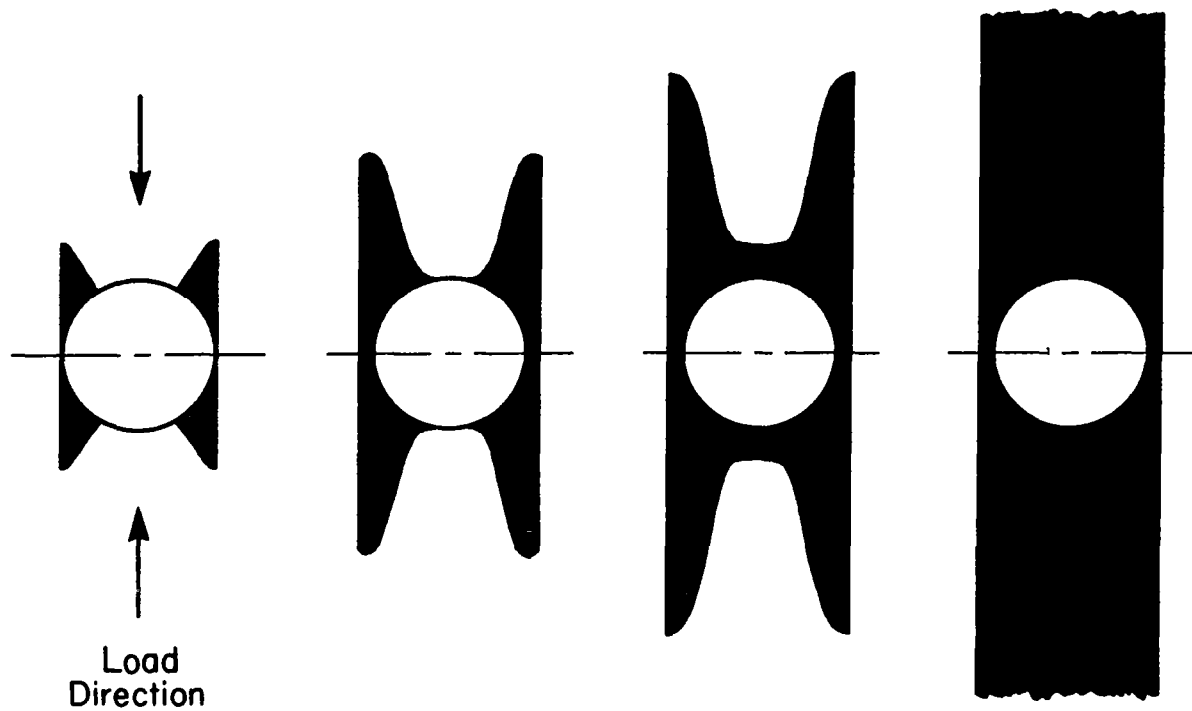
Laminate "A"; $[0_2/\pm 45]_{5S}$; axial section (50 \times)



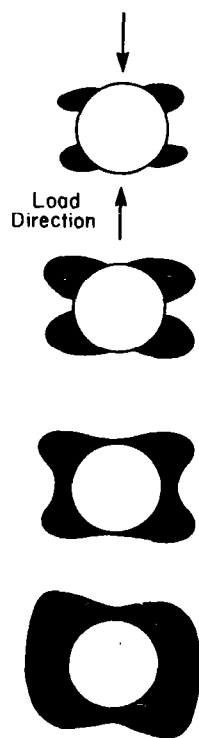
Laminate "D"; $[90/0/\pm 45]_{5S}$; axial section (50 \times)



Near-surface delamination growth - laminate "A"



Near-surface delamination growth - laminate "C"



Near-surface delamination growth - laminate "D"

Two modes of compressive failure observed:

Diagonal shear - predominant mode in fiber-dominated laminates

Net compression - predominant mode in quasi-isotropic laminates

Both failure modes are characterized by local instability of individual lamina or small lamina subgroupings

Mode of failure is related to the nature of the specimen delamination and the fatigue-induced cracking

Angle plies crack in transverse tension during fatigue cycling with the cracked layers determined by quadrant location about the hole

Primary direction of near-surface delamination progression is dependent upon the fiber direction of the laminate surface ply

Laminate stacking sequence affects the nature of cracking as well as the predominant failure mode

Failure mechanisms are not significantly different for the two resin systems

Conclusions

- DEVELOPMENT OF AN EXPRESSION FOR THE BUCKLING OF THE DEBONDED REGION ABOVE AN IMPLANTED FLAW.
- VERIFICATION OF THE BUCKLING ANALYSIS THROUGH THE USE OF EXPERIMENTAL TESTING.
- DEVELOPMENT OF AN UNDERSTANDING, THROUGH EXPERIMENTAL TESTING, OF THE INFLUENCE OF IMPLANTED FLAWS ON THE COMPRESSIVE PERFORMANCE OF SEVERAL GRAPHITE/EPOXY LAMINATES.

Objectives

- DEBOND DEFECTS MAY ALLOW FOR PREMATURE COMPRESSIVE FAILURE OF LAMINATES.
- INSTABILITY ANALYSIS MUST TREAT ASYMMETRIC LAMINATES AND CONSIDER TRANSVERSE SHEAR DEFORMATIONS.
- BOUNDARY GEOMETRY INFLUENCES BUCKLING LOAD MORE THAN LAMINATE ASYMMETRY.
- LAMINATE GEOMETRY (FIBER ORIENTATION AND STACKING SEQUENCY) STRONGLY INFLUENCES DEFECT CRITICALITY.
- DEFECT INSTABILITY PRECEDES INTERLAMINAR CRACK PROPAGATION AND ULTIMATE FAILURE.
- SIMPLIFIED BUCKLING ANALYSES MODEL INSTABILITY INITIATION.
- STRENGTH LOSSES OF 50 PERCENT WERE OBSERVED.

Debond defect studies.

FOR AN ISOTROPIC MATERIAL

$$D = \frac{Eh^3}{12(1-\nu^2)}$$

THE POTENTIAL ENERGY FOR A PLATE WITH A SINGLE IN-PLANE LOAD IS

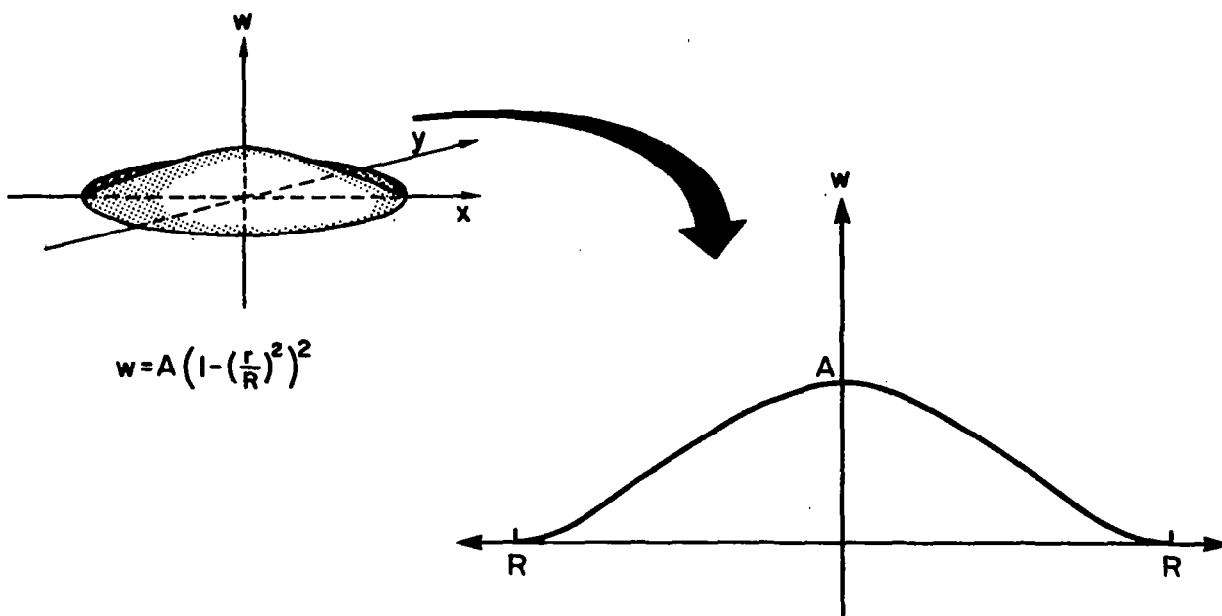
$$\frac{1}{2} \int_S \left\{ D[(w_{xx} + w_{yy})^2 - 2(1-\nu)(w_{xx}w_{yy} - w_{xy}^2)] + [N_x w_x^2] \right\} dS = \text{Constant}$$

INSERTING OUR ASSUMED DEFLECTION SHAPE

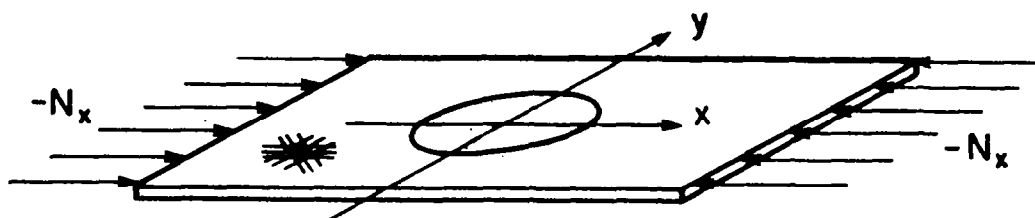
$$w(r) = A \left[1 - \left(\frac{r}{R} \right)^2 \right]^2$$

PERFORMING THE INTEGRATION AND THE VARIATION YIELDS THE BUCKLING CONDITION FOR THE ISOTROPIC CASE

$$N_{x_{crit}} = \frac{-32D}{R^2}$$



Approximate buckling strength for Rayleigh-Ritz approximation



Disbond load geometry

INSERTING THE DEFLECTION SHAPE AND PERFORMING THE INTEGRATION YIELDS

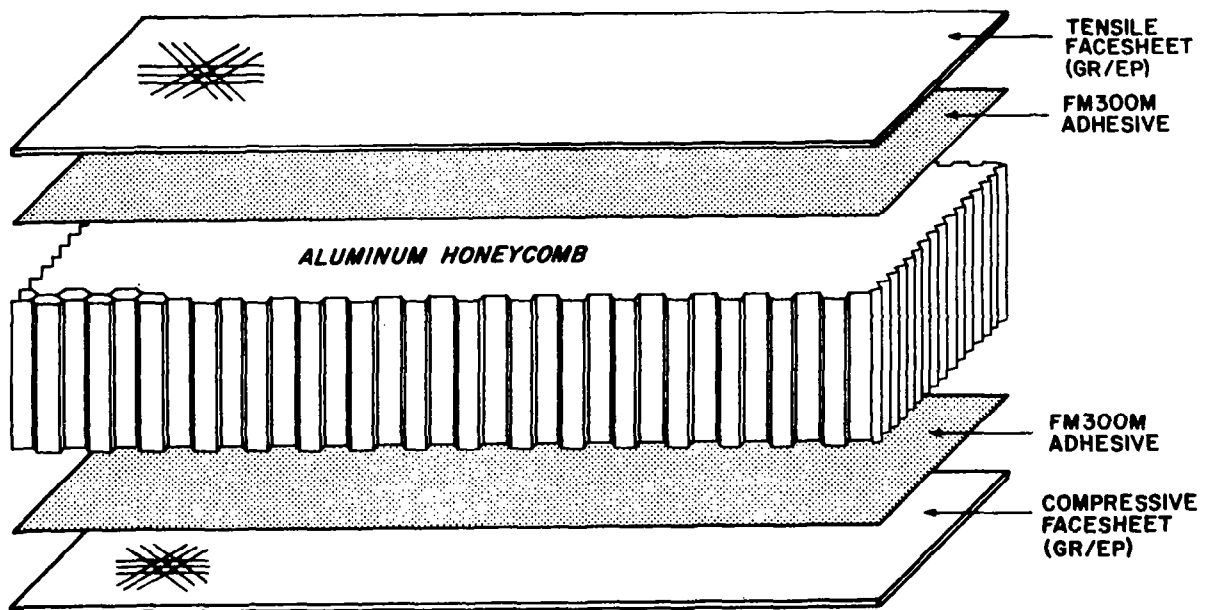
$$N_{x_{crit}} = \frac{-24}{R^2} \left(\frac{D_{11}^* + D_{22}^*}{2} + \frac{D_{12}^* + 2D_{66}^*}{3} \right)$$

BY COMPARING ELEMENTS OF THE BENDING STIFFNESS MATRIX WE SEE THAT FOR AN ISOTROPIC MATERIAL

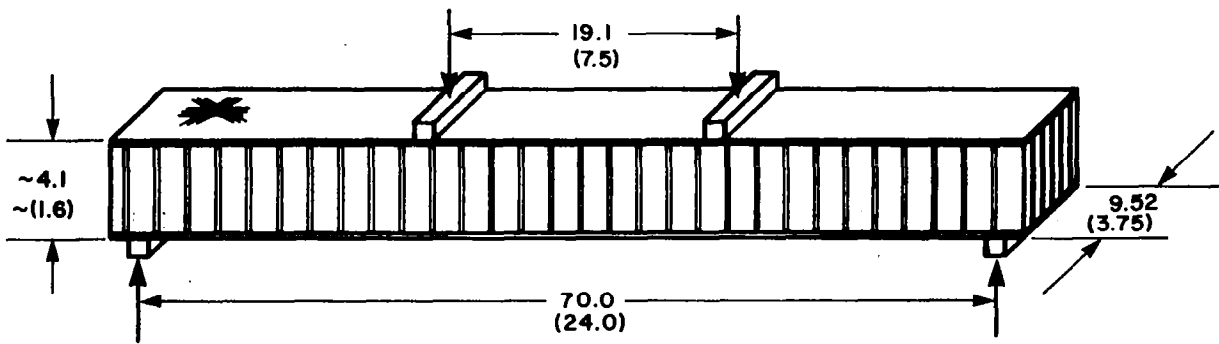
$$\begin{aligned} D_{12} &= \nu D \\ D_{11} &= D_{22} = D \\ D_{66} &= \frac{(1-\nu)}{2} D \end{aligned}$$

INSERTING THESE INTO THE ORTHOTROPIC RESULT PRODUCES THE ISOTROPIC CASE.

$$N_{x_{crit}} = \frac{-24}{R^2} \left(\frac{D + D}{2} + \frac{\nu D + 2(1-\nu)/2D}{3} \right) = \frac{-32D}{R^2}$$



Sandwich construction



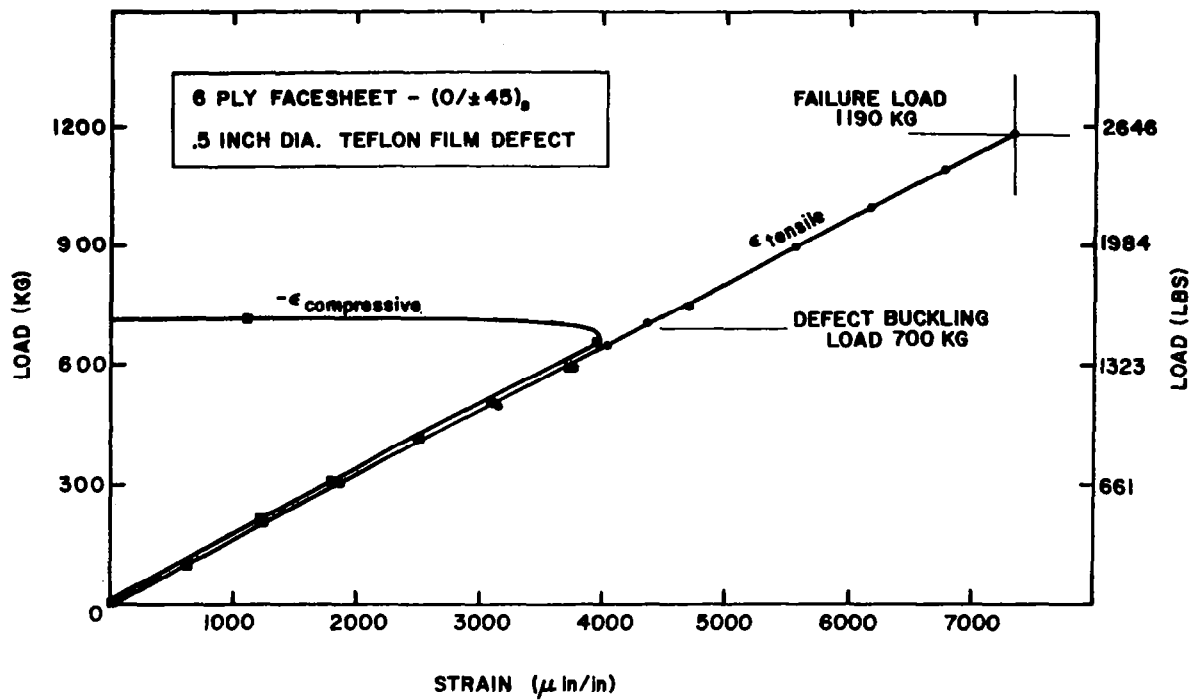
- NOTES: 1. LOADING PADS ARE 1.905cm (.75 in) WIDE ALUMINUM
 2. ACTUAL HEIGHT IS DETERMINED BY FACE THICKNESS
 3. OVERALL BEAM LENGTH (PLUS OVERHANG) IS 66.0cm (26.0 in)

Sample geometry

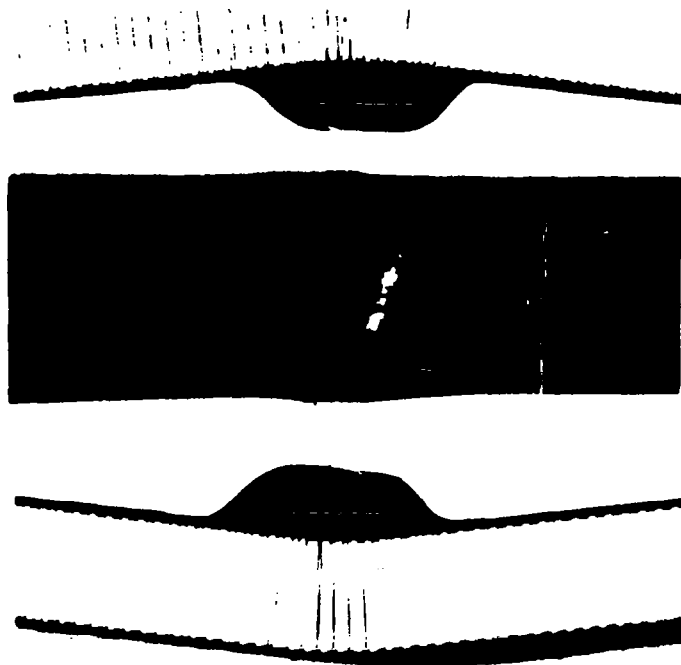
	Teflon Film Defect			Kapton Bag Defect			No Defect
	2.0 in. Dia.	1.0 in. Dia.	0.5 in. Dia.	2.0 in. Dia.	1.0 in. Dia.	0.5 in. Dia.	
[0/±45] _{2s} (12 ply)	F ₁₂ -1-1*	F ₁₂ -2-1	F ₁₂ -3-1	F ₁₂ -6-1	F ₁₂ -5-1	F ₁₂ -4-1	F ₁₂ -0-1
	F ₁₂ -1-2	F ₁₂ -2-2	F ₁₂ -3-2	F ₁₂ -6-2	F ₁₂ -5-2	F ₁₂ -4-2	F ₁₂ -0-2 F ₁₂ -0-3
[±45] _{2s} (8 ply)	F ₈ -3-1	F ₈ -2-1	F ₈ -1-1	F ₈ -6-1	F ₈ -5-1	F ₈ -4-1	F ₈ -0-1
	F ₈ -3-2	F ₈ -2-2	F ₈ -1-2	F ₈ -6-2	F ₈ -5-2	F ₈ -4-2	F ₈ -0-2 F ₈ -0-3
[0/±45] _s (6 ply)	F ₆ -3-1	F ₆ -2-1	F ₆ -1-1	--	--	--	F ₆ -0-4
	F ₆ -3-2	F ₆ -2-2	F ₆ -1-2				F ₆ -0-5 F ₆ -0-6
[90/±45] _s (6 ply)	--	--	--	F ₆ -6-1	F ₆ -5-1	F ₆ -4-1	F ₆ -0-1
				F ₆ -6-2	F ₆ -5-2	F ₆ -4-2	F ₆ -0-2 F ₆ -0-3

*Specimen Identification Number

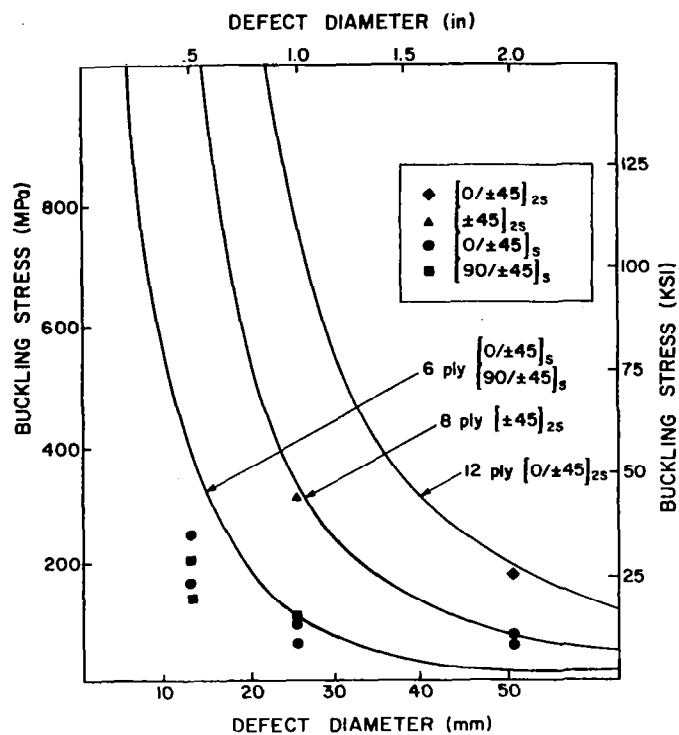
Experimental test program



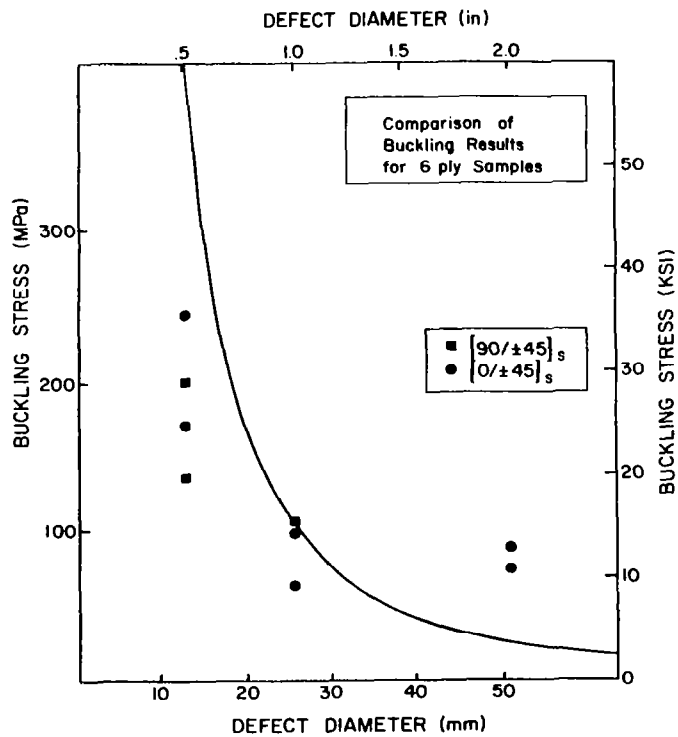
Load/strain data for sample F₆-1-2



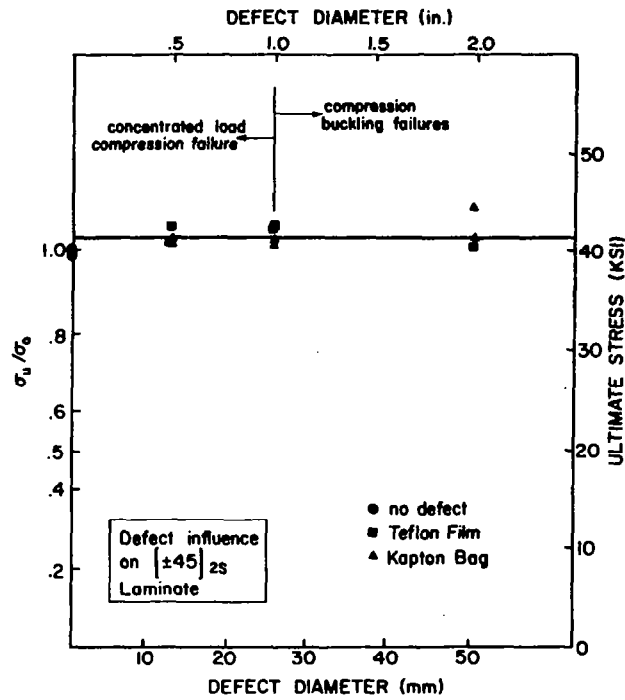
Failure of a sandwich beam composite
with a 1.5-in. circular defect located
at the near surface



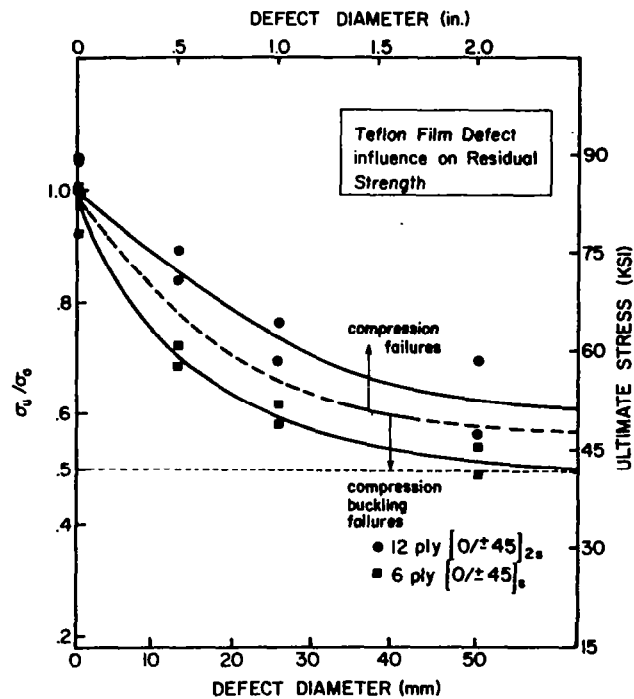
Buckling stress versus defect diameter
for all laminates



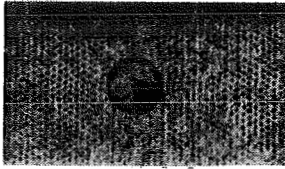
Buckling results for 6-ply laminates



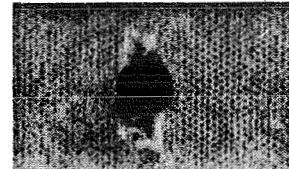
Influence of Kapton bag and Teflon film defects on residual strength of the $[\pm 45]_{2s}$ laminate



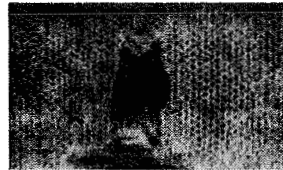
Effect of laminate thickness on residual strength of the $[0/\pm 45]_{ns}$ laminate



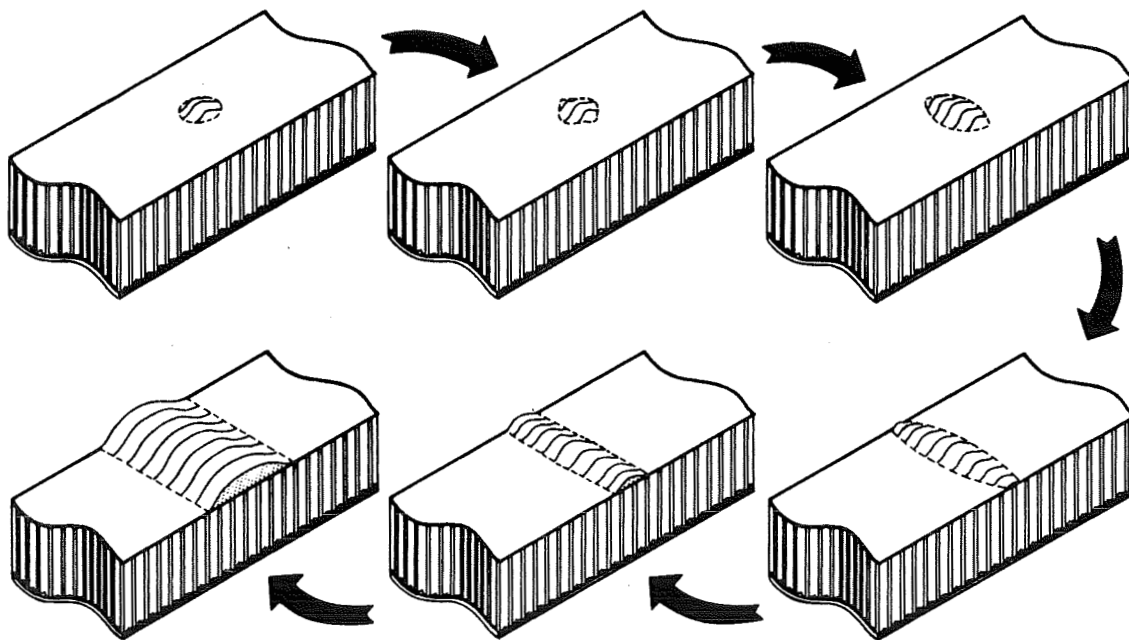
1.0-in. circular near-surface
delamination prior to testing



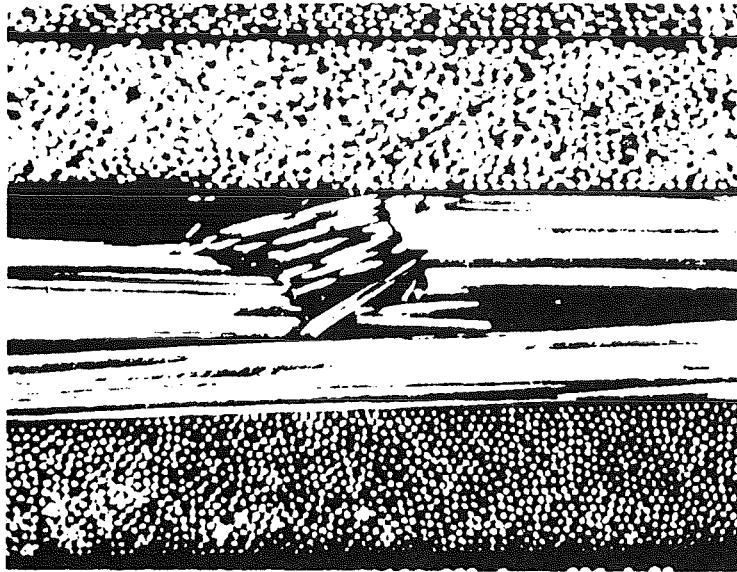
1.0-in. circular near-surface
delamination after buckling



1.0-in. circular near-surface
delamination after 2000-kg
applied load



Disbond propagation sequence



Load compressive failure in graphite/epoxy (200x)

- STUDY VARIOUS DEFECT CONFIGURATIONS TO EVALUATE THE SENSITIVITY OF THE LAMINATE TO DEFECT MATERIALS AND CONSTRUCTION.
- EXTEND THE WORK TO DEFECTS LOCATED AT OTHER POSITIONS THROUGHOUT THE LAMINATE THICKNESS.
- CONDUCT TESTING DESIGNED TO PRODUCE BUCKLING IN AN EFFORT TO VERIFY THE BUCKLING RESULT.
- PRODUCE A SOLUTION TO THE TWO-DIMENSIONAL FRACTURE PROBLEM WHICH STEMS FROM THE BUCKLED GEOMETRY.

Recommendations for future work

- LAMINATE RESIDUAL STRENGTH IS A FUNCTION OF FAILURE MODE FOR THE HIGH STRENGTH CONFIGURATIONS BUT NO INFLUENCE ON STRENGTH WAS SEEN FOR THE LOW STRENGTH LAMINATES.
- CERTAIN LAMINATES FAIL BY A CHARACTERISTIC MECHANISM AND THIS MECHANISM MAY BE INDEPENDANT OF THE PRESENCE OF DELAMINATION FLAWS.
- IMPLANTED FLAW CONSTRUCTION CAN HAVE A SUBSTANTIAL INFLUENCE ON COMPRESSIVE PERFORMANCE. THIS HIGHLIGHTS THE NECESSITY OF SELECTING AN APPROPRIATE DEFECT CONSTRUCTION WHEN MODELING A DELAMINATION.
- THE OCCURRENCE OF BUCKLING PLAYS AN IMPORTANT ROLE IN THE FAILURE PROCESS BECAUSE DELAMINATION GROWTH OCCURS WITH THE ONSET OF DEFECT INSTABILITY.
- THE BUCKLING ANALYSIS IS USEFUL IN PREDICTING THE DEFECT BUCKLING LOAD FOR THE THICKER LAMINATES BUT THE ACCURACY OF THE APPROXIMATION IS LOST FOR THE THIN 6 PLY RESULTS.

Summary

COMMENT

The fact that it is difficult to measure compressive strength in composites does not mean that there is no such property. Even if it were impossible to measure it, we would have to define it in order to deal with structures subjected to combined states of stress. It can be defined macroscopically as a structural failure of the particular lamina or laminate.

I. M. Daniel
Illinois Institute of Technology

THE IN SITU TRANSVERSE LAMINA STRENGTH
OF COMPOSITE LAMINATES

Donald L. Flaggs
Applied Mechanics Laboratory
Lockheed Palo Alto Research Laboratory
Palo Alto, California

The objective of the work reported in this presentation is to determine the in situ transverse strength of a lamina within a composite laminate. From a fracture mechanics standpoint, in situ strength may be viewed as constrained cracking that has been shown to be a function of both lamina thickness and the stiffness of adjacent plies that serve to constrain the cracking process. From an engineering point of view, however, constrained cracking can be perceived as an apparent increase in lamina strength. With the growing need to design more highly loaded composite structures, the concept of in situ strength may prove to be a viable means of increasing the design allowables of current and future composite material systems.

As a means of introducing the current research, some earlier results for cross-plyed graphite/epoxy and glass/epoxy laminates and $[\pm 25/90_n]_s$ graphite/epoxy laminates are presented. In this work the strain at onset of transverse cracking is seen to be a strong function of 90° -laminae thickness. In the figures that follow, ϵ represents the total or measured strain and $\bar{\epsilon}$ represents the elastic strain ($\bar{\epsilon} = \epsilon - \alpha \Delta T$). Data are also presented indicating that for an off-axis loading angle greater than about 5° , matrix cracking is the initial lamina failure mode. Experimental results from this research are given, and the σ_2 stress (in situ transverse strength) in the 90° laminae of the $[\pm \theta/90_n]_s$ laminates is plotted, based on laminated plate theory predictions, at the onset of transverse cracking. The separate contributions of applied and residual thermal stresses on the predicted in situ strength are illustrated, and the effect of the different constraining $\pm \theta$ laminae on in situ strength (which has been termed an interaction effect) is examined.

A simplified one-dimensional analytical model is presented that is used to predict the strain at onset of transverse cracking. While it is accurate only for the most constrained cases, the model is important in that the predicted failure strain is seen to be a function of a lamina's thickness d and of the extensional stiffness bE_θ of the adjacent laminae that constrain crack propagation in the 90° laminae.

The possibility is investigated of using a Weibull brittle failure model, in which the probability of failure is related to the volume of stressed material, to predict the in situ strength. Using a shape parameter determined for a material system (T300/5208) similar to that used in the current investigation (T300/934), it was seen that the Weibull model underestimated the observed thickness effects. Additionally, there is no mechanism in the model to account for the interaction effect on in situ strength. However, it was interesting to note that by assuming that the shape parameter was not a material parameter, we could quite accurately fit the experimental behavior.

In closing, perhaps the most important conclusion that can be drawn from these results is that strength predictions for failure modes associated with matrix cracking in composite laminates should not be based upon the concept that strength is an intrinsic material property. Work is currently under way to investigate the possibility of integrating these results into existing strength theories.

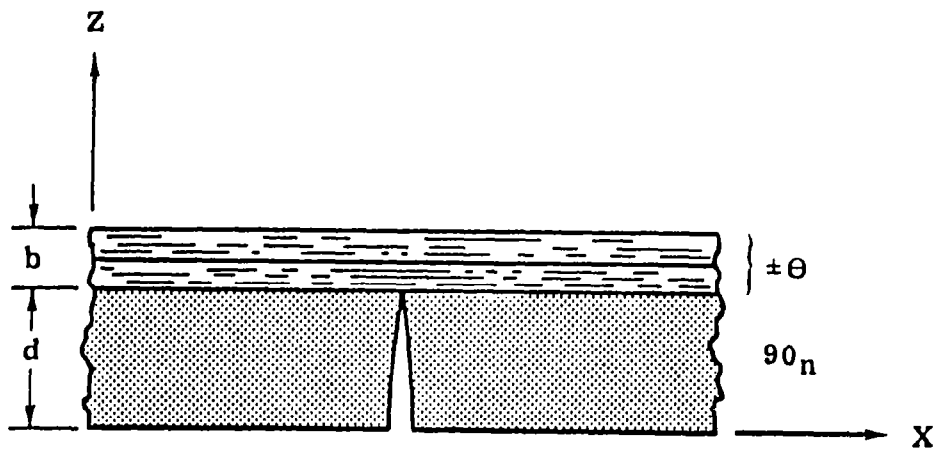
REFERENCES

1. Parvazi, A.; Garrett, K. W.; and Bailey, J. E.: constrained Cracking in Glass Fibre-Reinforced Epoxy Cross-Ply Laminates. J. Matl. Sci., vol. 13, 1978, p. 195.
2. Crossman, R. W.; and Wang, A. S. D.: The Dependence of Transverse Cracking and Delamination on Ply Thickness in Graphite/Epoxy Laminates. Damage in Composite Materials, K. L. Reifsnider, ed., ASTM STP 775, 1982.
3. Bader, M. G.; and Curtis, P. T.: The Micromechanics of Fibre Composites - Carbon Fibre Programme. Dept. of Metallurgy and Materials Technology, Univ. of Surrey, U.K., 1977.

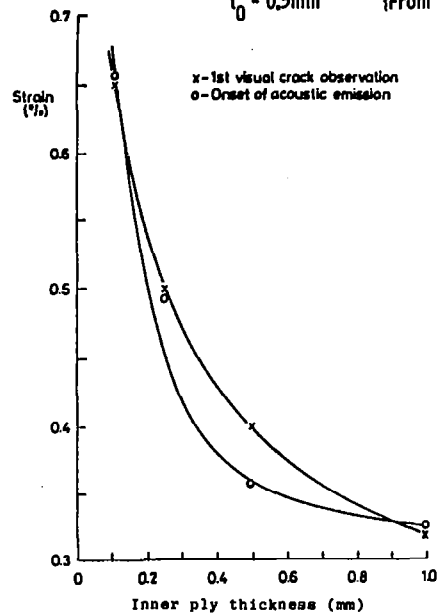
Fracture modes in off-axis tensile loading
of $(0_8)_T$ Modmor-I/epoxy laminates

<u>Mode</u>	<u>Load angle</u>
Longitudinal tension	$0 < \theta < 5^\circ$
Intralamina shear	$5 < \theta < 20^\circ$
Mixed mode	$20 < \theta < 45^\circ$
Transverse tension	$45 < \theta < 90^\circ$

Laminate geometry of $[\pm \theta / 90_n]_s$ specimens



Strain at initiation of transverse cracking in graphite/epoxy $[0/90/0]_t$ laminates;
 $t_0 = 0.5\text{mm}$ {From ref. 1}



t_{90} (mm)	\bar{E}_2
0.125	.798
0.25	.627
0.50	.495
1.00	.461

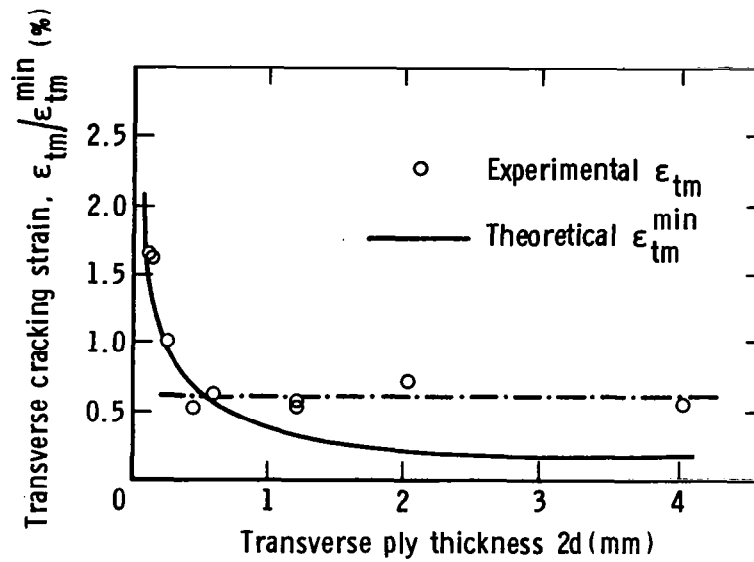
Calculated transverse stress in 90° plies of $[\pm 25/90_n]_s$
T300/934 laminates at transverse cracking onset
{From ref. 2}

N	Y_T^*	$\epsilon_x(\%)$
.5	106 (15,370)	.650**
1	111 (16,095)	.665**
2	83.9 (12,165)	.415
3	76.5 (11,092)	.360
4	71.2 (10,324)	.325
6	69.4 (10,063)	.330
8	69.2 (10,034)	.345

* MPA (Psi)

** ULTIMATE FAILURE STRAIN

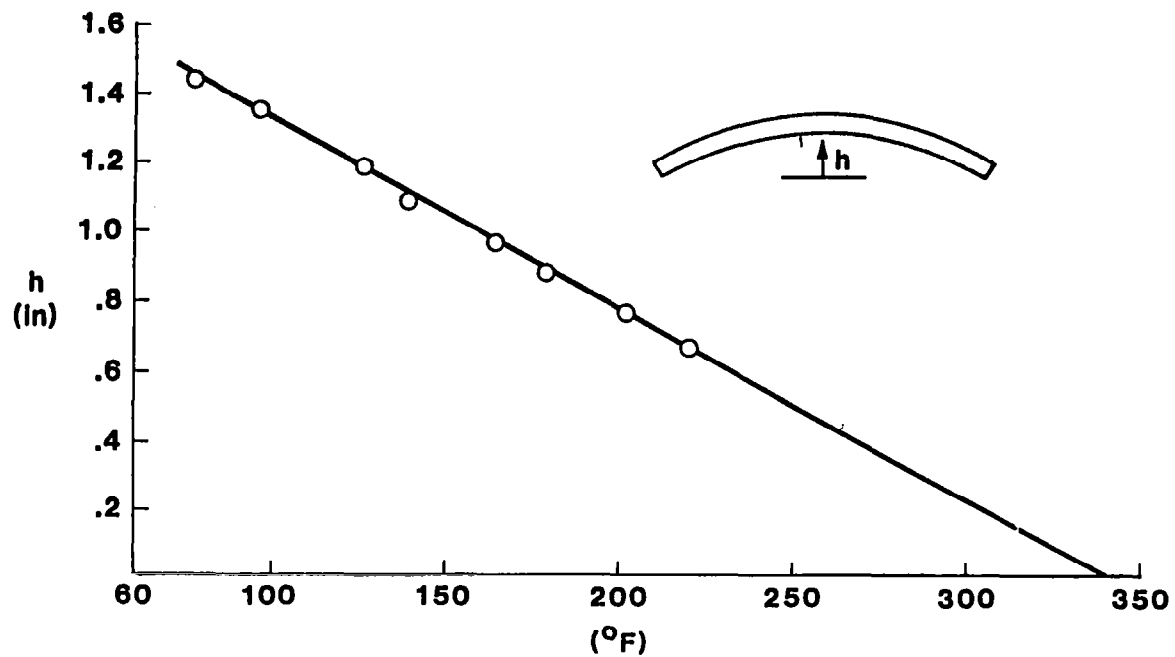
Mechanical strain at onset of transverse cracking in $[0/90/0]_t$
glass fiber/epoxy laminates; $t_0 = 0.5\text{mm}$ {From ref. 3}



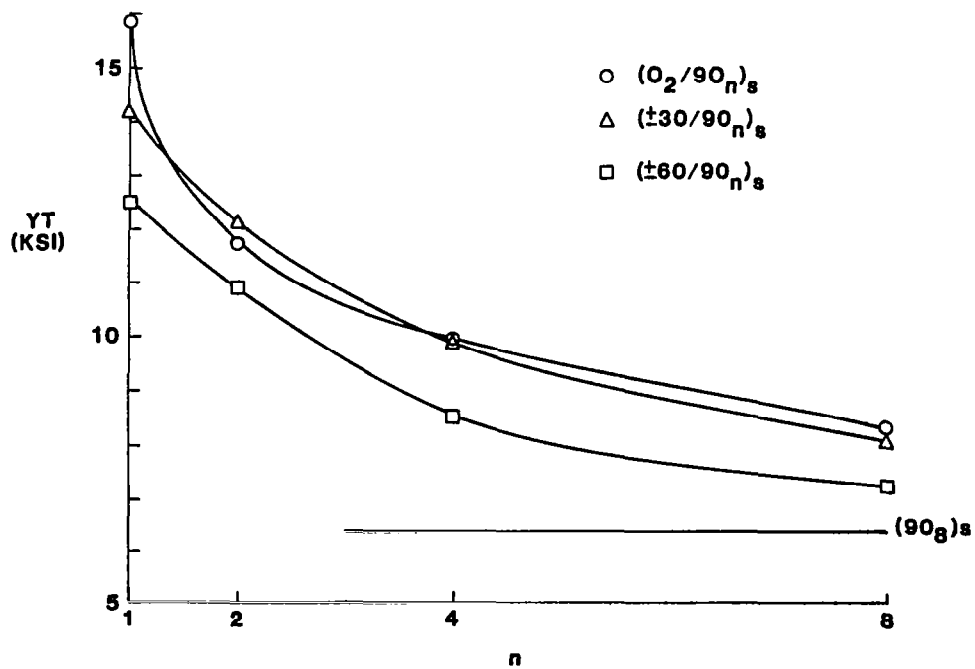
Experimental results

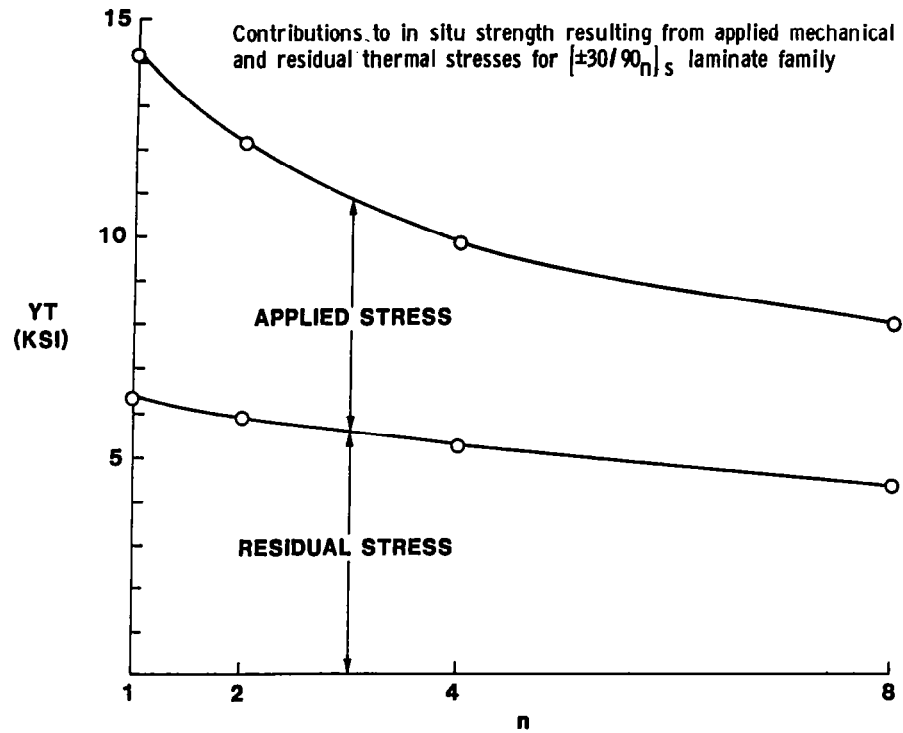
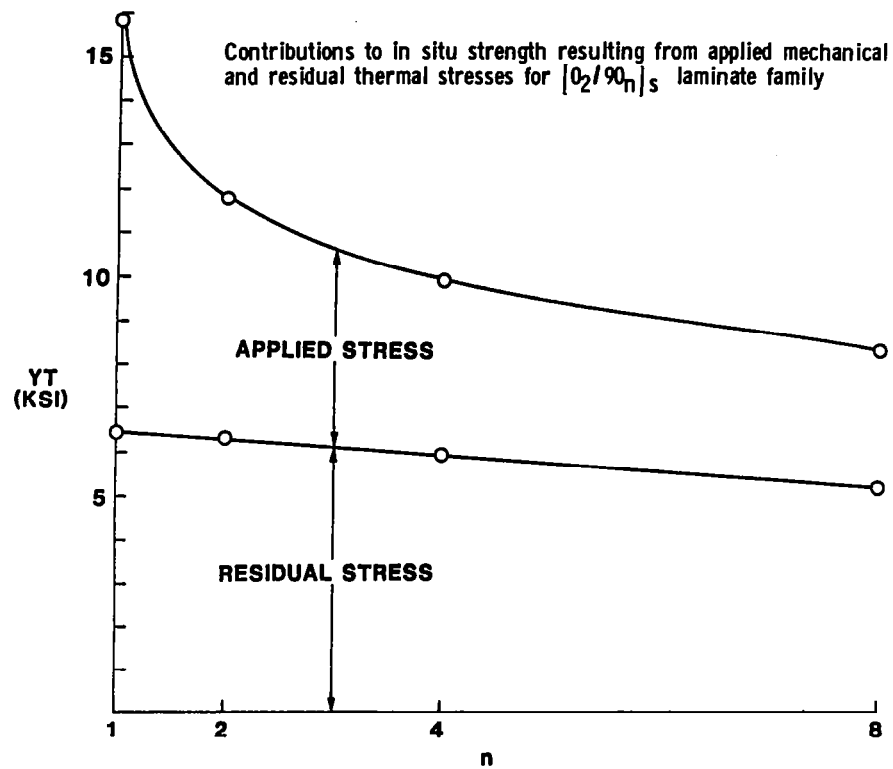
Specimen Family	n	Number of Specimens	E_x (Msi)	ϵ_x (%)	N_x (lb/in)
$(0_2/90_n)_s$	1	4	13.73	.555 (.549-.562)	2428.9 (2390.4-2491.0)
	2	4	10.92	.319 (.287-.378)	1456.3 (1381.5-1676.5)
	4	4	7.51	.236 (.221-.242)	1158.4 (1083.7-1184.6)
	8	5	5.29	.188 (.173-.225)	1034.7 (894.8-1289.9)
$(+30/90_n)_s$	1	4	7.73	.498 (.489-.506)	1219.9 (1206.3-1259.8)
	2	4	6.41	.386 (.371-.431)	1036.3 (995.5-1150)
	4	3	4.82	.293 (.267-.338)	865.4 (799.2- 997.5)
	8	4	3.43	.242 (.231-.254)	860.5 (796.9- 898.8)
$(+60/90_n)_s$	1	2	2.08	.592 (.568-.615)	387.1 (374.4- 399.7)
	2	4	1.95	.553 (.475-.596)	449.5 (399.8- 474.5)
	4	4	1.86	.453 (.405-.503)	511.1 (471.7- 524.3)
	8	4	1.73	.405 (.387-.416)	717.2 (701.8- 742.2)

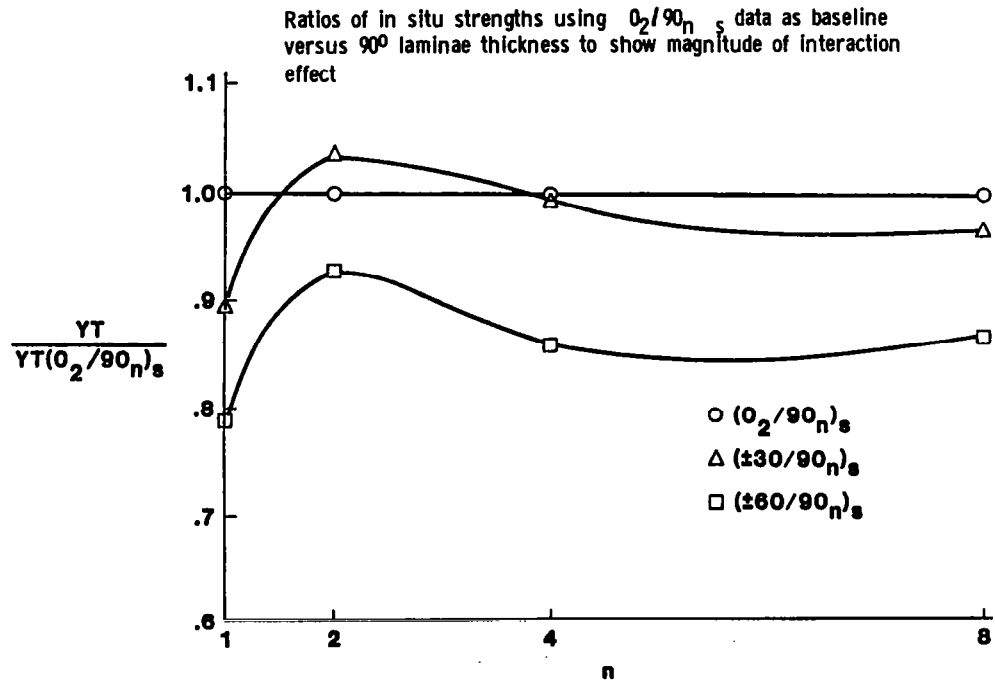
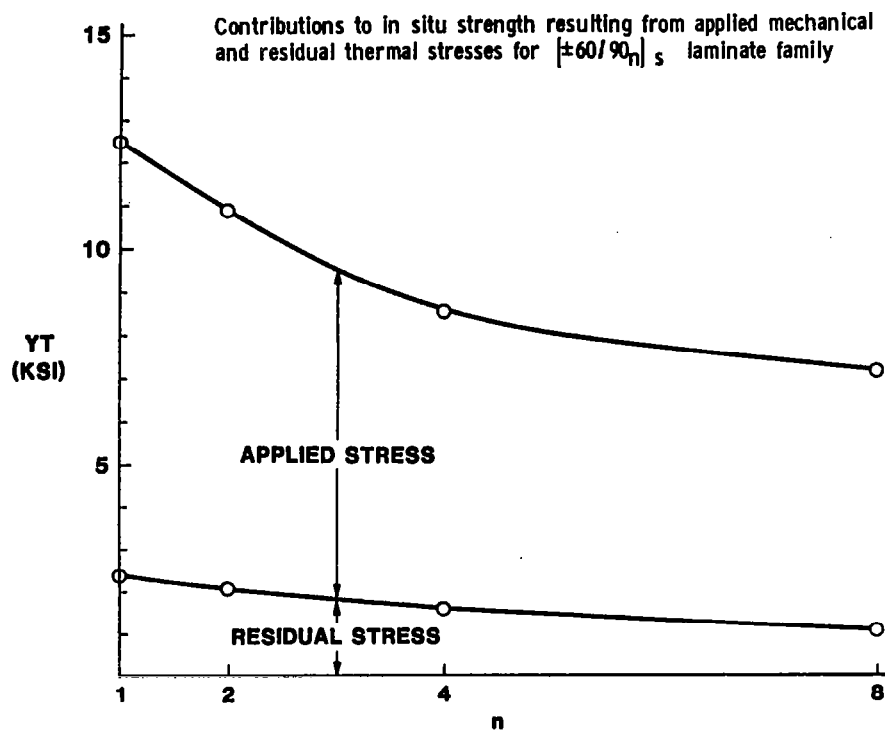
Cord height of nonsymmetric $[0_4/90_4]_t$ T300/934 laminate as a function of temperature



In situ transverse lamina strengths as a function of thickness and orientation of adjacent $\pm\theta$ laminae.







Analytical model for predicting onset of transverse cracking

Griffith energy balance used in conjunction with a one-dimensional shear lag model to account for load transfer resulting from a Mode I crack spanning the 90 laminae

$$\text{Griffith energy balance: } \Delta W - \Delta U = 2\gamma_{90} V_{90} \quad (\text{per unit area})$$

$$\text{One-dimensional shear lag model: } \Delta \sigma = \frac{d}{b} E_2 \bar{\epsilon}_2^{\text{TC}} \text{EXP}(-\phi^{\frac{1}{2}} X)$$

Resulting expression for in situ transverse strength:

$$\bar{\epsilon}_2^{\text{TC}} = \left[\frac{b E_{\theta m}}{(b+d) d^2 E_X} \right]^{\frac{1}{k}} ; \quad m = \frac{G_{23} G_{1c}^2}{E_2^3}$$

Weibull material (?)

$$P_s(v) = \exp \left\{ -v \left(\frac{\sigma - \sigma_U}{\sigma_0} \right)^\alpha \right\} \quad \text{where } \begin{array}{l} \alpha \equiv \text{shape parameter} \\ \sigma_U \equiv \text{strength cut-off} \\ \sigma_0 \equiv \text{scale parameter} \end{array}$$

$$P_s(v_1) = P_s(v_2) \Rightarrow \left(\frac{v_2}{v_1} \right)^{1/\alpha} = \frac{\sigma_1 - \sigma_U}{\sigma_2 - \sigma_U}$$

$$\text{For T300/5208, } \alpha = 7.68; \quad \left(\frac{v_{n=8}}{v_{n=1}} \right)^{1/\alpha} = 8^{1/7.68} \approx 1.31$$

Now, consider the $[0_2/90_n]_s$ family (assuming $\sigma_U = 0$):

$$\frac{\sigma_1}{\sigma_8} = \frac{15,847}{8,350} = 1.89 ?$$

Summary of in situ transverse strengths

Specimen Family	n	$\frac{\text{exp.}}{\epsilon_2(\%)}$	$\frac{\text{pred.}}{\epsilon_2(\%)}$	YT(psi)
(0 ₂ /90 _n) _s	1	.953	.950	15,847
	2	.700	.662	11,751
	4	.590	.465	9,944
	8	.497	.316	8,350
(±30/90 _n) _s	1	.879	.839	14,154
	2	.739	.579	12,140
	4	.604	.397	9,869
	8	.496	.269	8,063
(±60/90 _n) _s	1	.721	.815	12,503
	2	.666	.545	10,909
	4	.540	.352	8,540
	8	.463	.223	7,234

Experimental versus predicted in situ strength ratios

$$\frac{Y_{T_n}}{Y_{T_1}} = \left(\frac{V_1}{V_n} \right)^{1/\alpha}$$

Specimen Family	α	Vol. Ratio, $\frac{V_n}{V_1}$	Experimental, $\frac{Y_{T_1}}{Y_{T_n}}$	Predicted, $\frac{Y_{T_1}}{Y_{T_n}}$
(0 ₂ /90 _n) _s	3.245	2:1	1.349	1.238
		4:1	1.594	1.533
		8:1	1.898	1.898
(±30/90 _n) _s	3.697	2:1	1.166	1.206
		4:1	1.434	1.455
		8:1	1.755	1.755
(±60/90 _n) _s	3.802	2:1	1.146	1.200
		4:1	1.464	1.440
		8:1	1.728	1.728

Summary

DESIGN IMPLICATIONS:

- O INDIVIDUAL PLIES SHOULD BE DISPERSED RATHER THAN STACKED WHEN PRACTICAL
- O LAMINATE FAILURE ANALYSES SHOULD INCLUDE THESE IN SITU STRENGTH EFFECTS AS SOON AS A METHODOLOGY HAS BEEN ESTABLISHED FOR QUANTIFYING THEM FOR GENERAL LOADING CONDITIONS

WORK IN PROGRESS:

- O EXPERIMENTAL DETERMINATION OF EFFECT OF τ_{12} ON ONSET OF TRANSVERSE CRACKING
- O ANALYTICAL SIMULATION OF TRANSVERSE CRACKING USING A GENERALIZED PLANE STRAIN FE MODEL
 - 1) BETTER ANALYTICAL REPRESENTATION OF CRACKING PHENOMENON
 - 2) CAN ACCOUNT FOR MIXED MODE EFFECTS
 - 3) ANALYTICAL DERIVE DESIGN CURVES

EFFECTS OF DEFECTS IN COMPOSITE
STRUCTURES

G. P. Sendeckyj
Structural Integrity Branch
Flight Dynamics Laboratory
Air Force Wright Aeronautical Laboratories
Wright-Patterson Air Force Base, Ohio

DESIGN CRITERIA

FIRST PLY FAILURE

- DESIGN ULTIMATE STRAIN (DUS) IS STRAIN FOR FIRST PLY FAILURE

STATE OF THE ART

- DUS IS FAILURE STRAIN OF LAMINATE WITH 0.25-in. HOLE

POSSIBLE

- DUS IS FAILURE STRAIN OF LAMINATE WITH LOW-ENERGY IMPACT DAMAGE
- BUFFER AND SOFTENING STRIPS USED

UPPER BOUND

- DUS IS FAILURE STRAIN OF LAMINATE
- STRESS CONCENTRATIONS DESIGNED AROUND LEAST CONSERVATIVE

PREPREG DEFECTS

HOLLOW FIBERS

EXCESSIVE VARIABILITY IN FIBER PROPERTIES

RESIN-STARVED OR FIBER-STARVED AREAS

WRINKLES, WAVINESS, MISCOLLIMATION

FOREIGN PARTICLES, CONTAMINATION

PILLS AND FUZZ BALLS

NONUNIFORM AGGLOMERATION OF HARDENER

PREPREG OUT OF SPECS.

DEFECTS IN LAMINATES

HOLLOW FIBERS
FIBER BREAKS
EXCESSIVE POROSITY, VOIDS
RESIN-RICH AND RESIN-STARVED AREAS
FIBER WAVINESS, WRINKLES, MISCOLLIMATION
FOREIGN PARTICLES, CONTAMINATION, INCLUSIONS
INCOMPLETE AND/OR VARIABLE CURE
WRONG STACKING SEQUENCE
DENTS, TOOL IMPRESSIONS, SCRATCHES

DELAMINATIONS
PLY GAPS

LAMINATE POROSITY

STUDIED EXTENSIVELY

MATRIX DOMINATED PROPERTIES DEGRADED (DELAMINATION NOT INCLUDED)

5% STRENGTH REDUCTION FOR 1% POROSITY
50% LIFE REDUCTION FOR 1% POROSITY

FIBER-DOMINATED PROPERTIES NOT AFFECTED

DELAMINATION GROWTH AFFECTED - NOT WELL DOCUMENTED

MOISTURE ABSORPTION

EQUILIBRIUM MOISTURE LEVELS INCREASED
AGGRAVATES THERMAL SPIKE PHENOMENON

EFFECT OF PLY GAP DEFECT

(REF. 1)

$[(0/45/90/-45)_S]_2$ LAMINATE

- 16.9% STRENGTH REDUCTION FOR GAP(S) IN 90 PLIES
- 8.7% REDUCTION FOR GAP(S) IN 0 PLIES

$[(0/45/0/-45/0)_S]_2$ LAMINATE

- 6.5% STRENGTH REDUCTION FOR GAPS IN 0 PLIES

(REF. 2)

$[(0/\pm 45/90)_S]_2$ LAMINATE

- 12.8% STRENGTH REDUCTION FOR GAPS IN OUTER 45 PLIES

$[(0/-/45/0)_S]_2$ LAMINATE

- 6.2% STRENGTH REDUCTION FOR GAPS IN OUTER 45 PLIES

DEFECT CRITICALITY - BENIGN FOR DESIGN ULTIMATE STRAIN 0.7%

EFFECT OF PLY WAVINESS DEFECT

(REF. 3)

SURFACE 0 PLY WAVINESS IN $[(0/45/90/-45)_S]_2$ LAMINATE

STATIC TENSILE STRENGTH REDUCTION

- 10% FOR SLIGHT WAVINESS
- 25% FOR EXTREME WAVINESS

FATIGUE LIFE REDUCTION

- AT LEAST A FACTOR OF 10
- CONSISTENT WITH STATIC STRENGTH REDUCTION

DEFECT CANNOT BE FOUND BY STANDARD NDE

STRENGTH LOSS CAN BE PREDICTED BY ASSUMING LOSS OF
LOAD CARRYING CAPACITY DUE TO THE WAVINESS

DEFECT CRITICALITY - INSUFFICIENT DATA FOR ACCURATE ASSESSMENT

- SHOULD BE BENIGN FOR DESIGN ULTIMATE STRAINS 0.7%

MACHINING DEFECTS

EDGE DELAMINATIONS	EDGE NOTCHES AND SURFACE NOTCHES
OVERSIZE HOLES	HEAT-DAMAGED MACHINED EDGES
UNDERSIZE HOLES	FIBER BREAK-OUT ON HOLE EXIT SIDE
TILTED HOLES	OUT-OF-ROUND HOLES
TILTED COUNTERSINKS	IMPROPER DEPTH OF COUNTERSINKS

DENTS, FIBER BREAKING FROM IMPACT

TEAROUT OR PULL-THROUGH IN COUNTERSINKS

EFFECT OF SURFACE NOTCHES

EXPERIMENTAL DATA

STATIC STRENGTH REDUCED UP TO 50%

LOCAL DELAMINATION AT NOTCH

FATIGUE LOADING REDUCES STRESS CONCENTRATION

RESIDUAL STRENGTH HIGHER THAN STATIC STRENGTH

DATA AVAILABLE FOR VARIOUS STACKING SEQUENCES

ANALYSIS

ECCENTRIC BEAM MODEL PREDICTS STRENGTH REDUCTION

STRENGTH REDUCTION IS SMALL FOR SIZES EXPECTED
IN SERVICE

DEFECT CRITICALITY

NOT CRITICAL FOR $DUS < 0.7$

BOLTED ASSEMBLY DEFECTS

OVERTORQUED FASTENERS IMPROPER FASTENER SEATING
MISSING FASTENERS FASTENER INSTALLATION DAMAGE
OVERSIZED AND UNDERSIZED FASTENER

BONDING DEFECTS

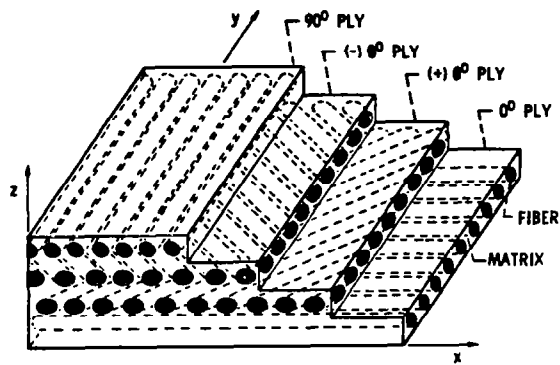
ADHESIVE POROSITY
MISCURE
ADHESIVE-STARVED AREAS
IMPROPER SURFACE PREPARATION

REFERENCES

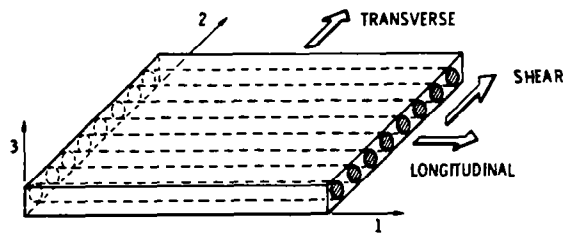
1. Ryder, J. T.; and Walker, E. K.: The Effect of Compressive Loading on the Fatigue Lifetime of Graphite/Epoxy Laminates. AFML-TR-79-4128, U. S. Air Force, January 1979.
2. Hunsziker, R.; Konishi, D.; Burroughs, B. A.; Altman, J. M.; and Costanza, L.: Advanced Composites Serviceability Program. AFWAL-TR-80-4092, U. S. Air Force, July 1980.
3. Ryder, J. T.: Effect of Load History on Fatigue Life. AFWAL-TR-80-4044, U. S. Air Force, June 1980.

**EXPERIMENTAL METHODS FOR
IDENTIFYING FAILURE MECHANISMS**

**I. M. Daniel
Illinois Institute of Technology
Chicago, Illinois**



Fiber composite



Single ply

MICROSCOPIC

MATRIX FAILURE (TENSILE, COMPRESSIVE, SHEAR)
 BOND FAILURE
 FIBER FAILURE

MINISCOPIC

FIRST-PLY FAILURE
 LAMINA FAILURE CRITERIA

MACROSCOPIC

LAMINATE FAILURE CRITERIA

Scales of observation of failure

1. PHOTOELASTIC (2-D, 3-D, MICROPHOTOELASTIC, DYNAMIC, BIREFRINGENT COMPOSITES, BIREFRINGENT COATINGS)
2. MOIRÉ
3. STRAIN GAGES
4. INTERFEROMETRIC AND HOLOGRAPHIC METHODS
5. NONDESTRUCTIVE EVALUATION (ULTRASONICS, ACOUSTIC EMISSION, X-RAY, THERMOGRAPHY)
6. FRACTOGRAPHY

Experimental methods

STRESS-OPTIC LAW

$$\sigma_1 - \sigma_2 = 2nf/t$$

where

$$\sigma_1 - \sigma_2 = \text{difference of "secondary" principal stresses}$$

$$n = \text{fringe order}$$

$$f = \text{material fringe value (constant for material)}$$

$$t = \text{specimen thickness}$$

Photoelastic method

$$\epsilon = \frac{1}{S_g} \left(\frac{\Delta R}{R} \right)$$

where

S_g = gage factor (function of alloy and backing of gage)

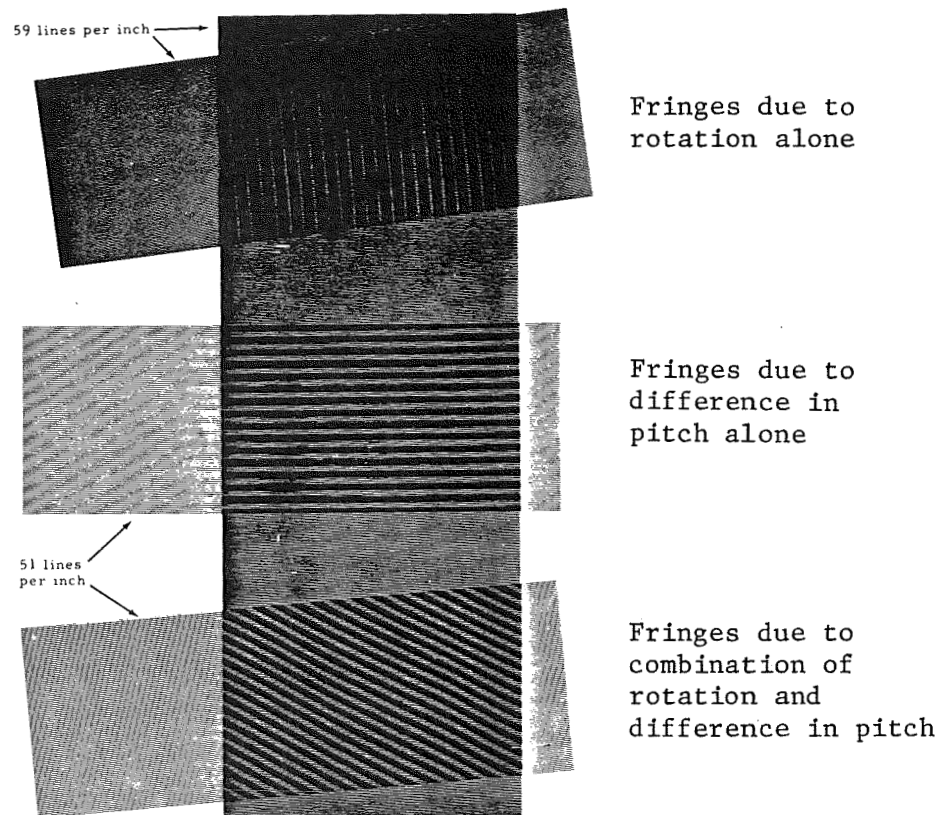
$$\left(\frac{\Delta R}{R} \right)_{\Delta T} = (\beta - \alpha) S_g \Delta T + \gamma \Delta T$$

α = thermal coefficient of expansion of gage material

β = thermal coefficient of expansion of base material

γ = coefficient of resistivity of gage material

Electrical resistance strain gages



Mechanism of formation of Moire fringes

Strain-optic law:

$$\epsilon_1^c - \epsilon_2^c = \epsilon_1^s - \epsilon_2^s = \frac{Nf_\epsilon}{2h} = NF_\epsilon$$

where

f_ϵ = strain fringe value

N = fringe order

h = coating thickness

c, s = refer to coating and specimen, respectively.

Conditions at boundary:

At interface between coating and specimen,

$$\epsilon_{22}^c = \epsilon_{22}^s = -\nu_{12}^s \epsilon_{11}^s$$

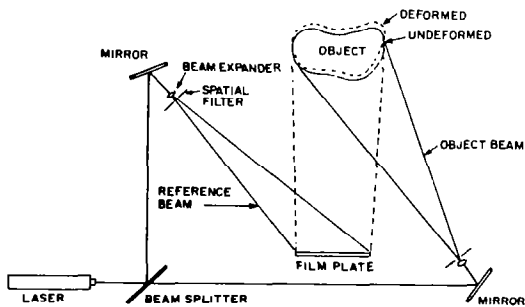
At top surface of coating,

$$\epsilon_{22}^c = -\nu^c \epsilon_{11}^c = -\nu^c \epsilon_{11}^s$$

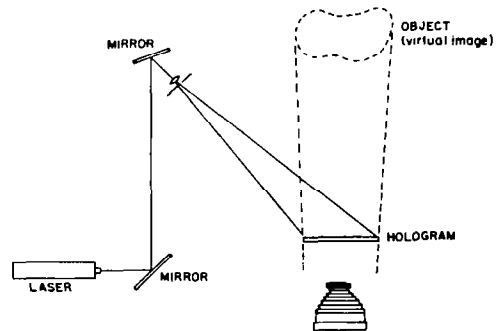
Principal strain along boundary,

$$\epsilon_{11}^s = \frac{Nf_\epsilon}{2h} \cdot \frac{1}{1 + \nu^c}$$

Photoelastic coating method (refs. 1 to 4)

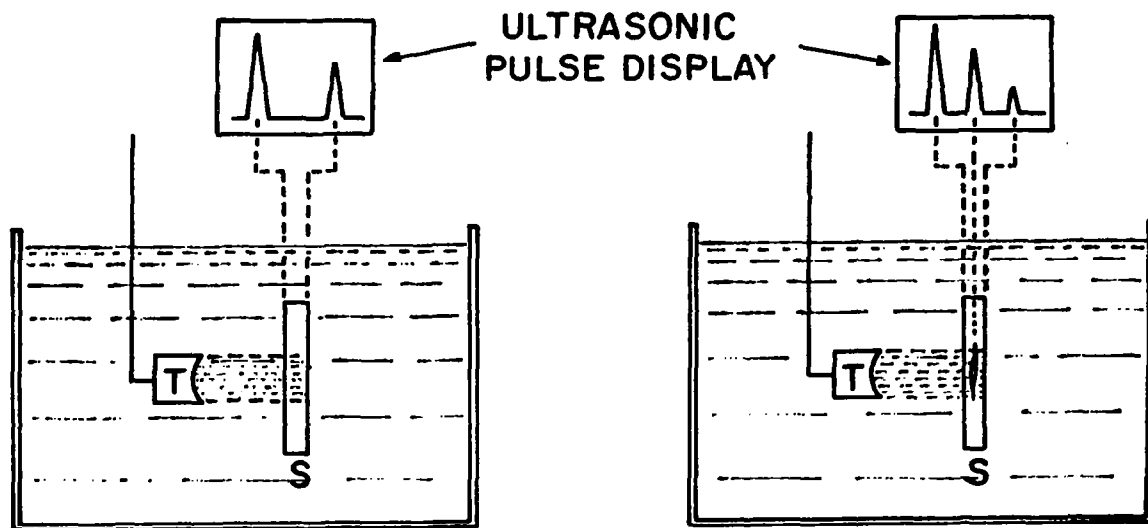


Hologram recording

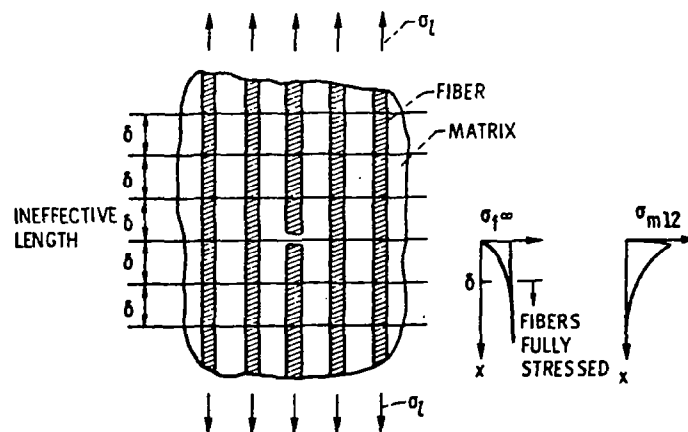


Reconstruction

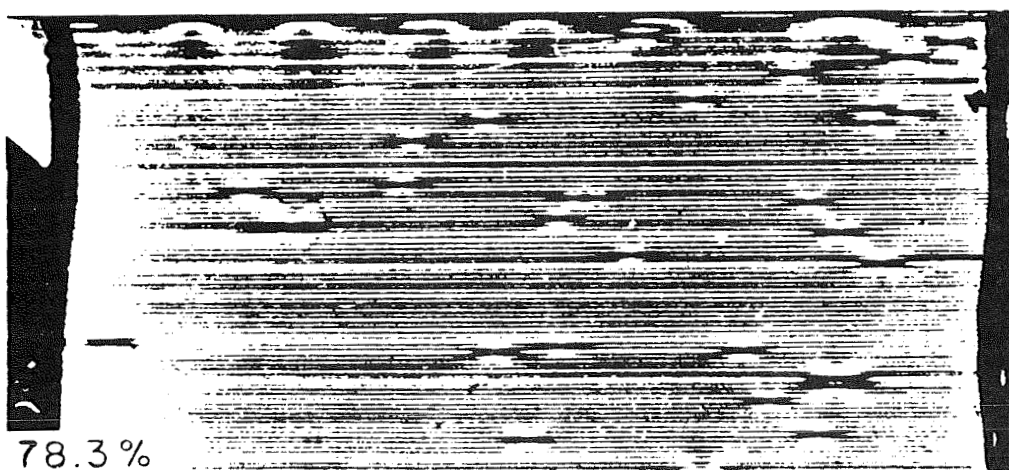
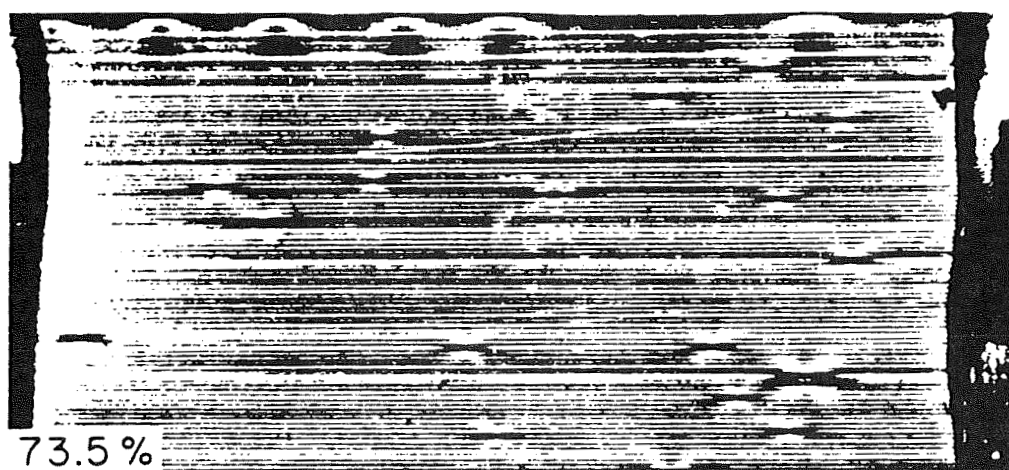
Holographic processes



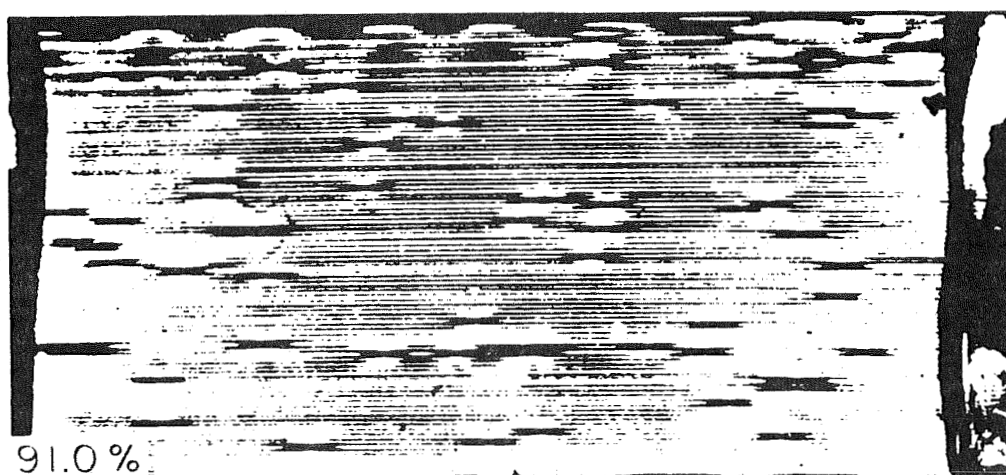
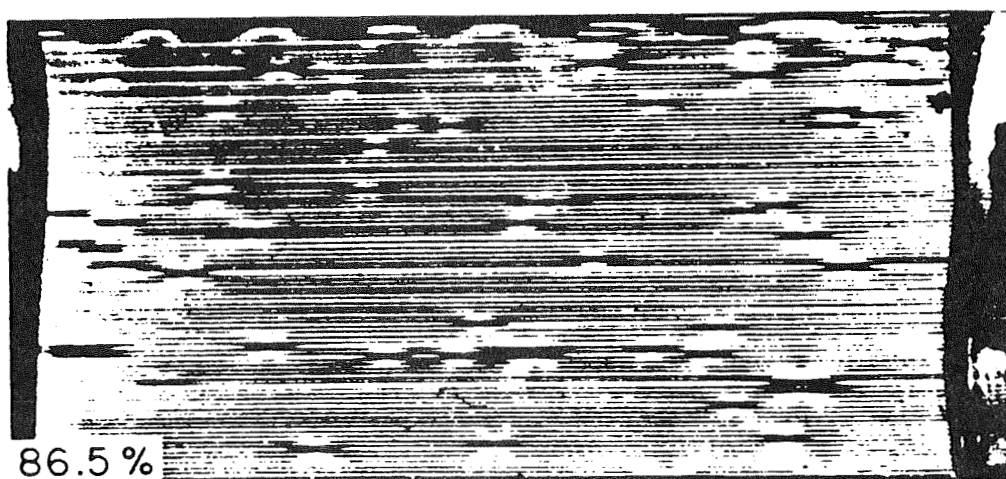
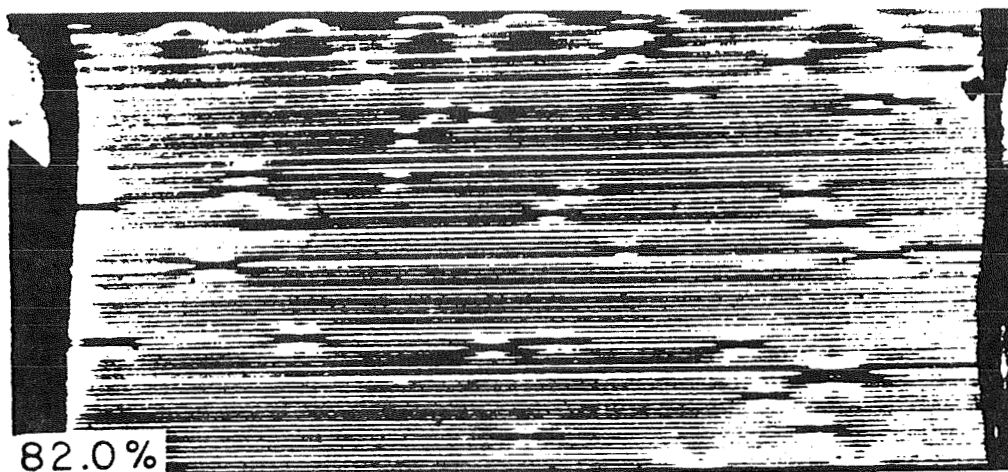
Ultrasonic pulse echo method



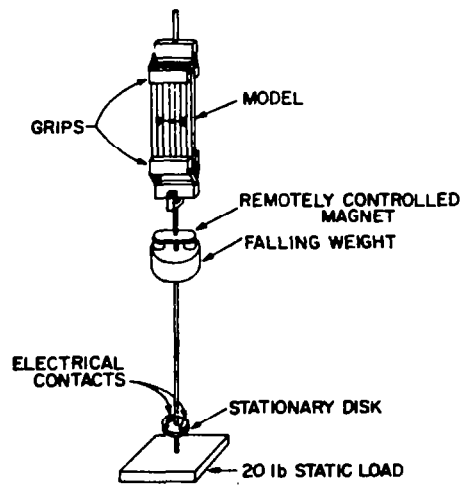
Failure model of unidirectional composite under longitudinal tension (ref. 5)



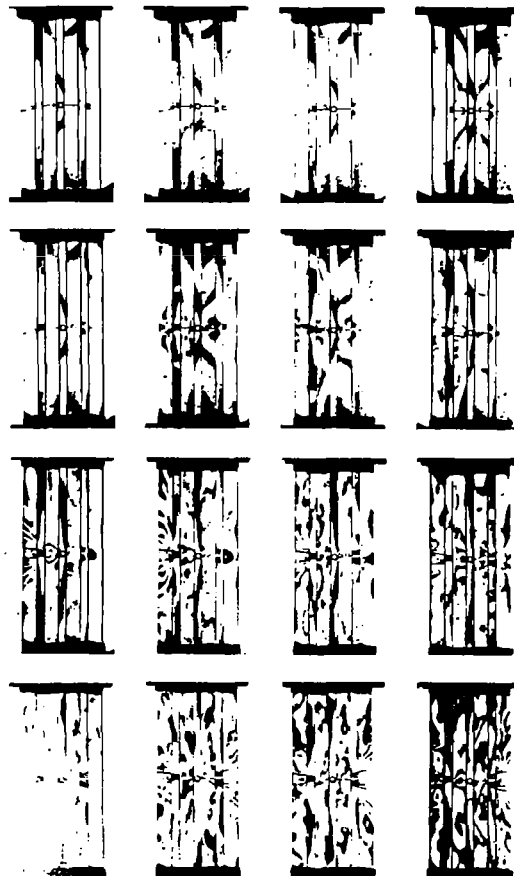
Sequence of photographs showing distribution of fiber breaks
in unidirectional composite under longitudinal tension



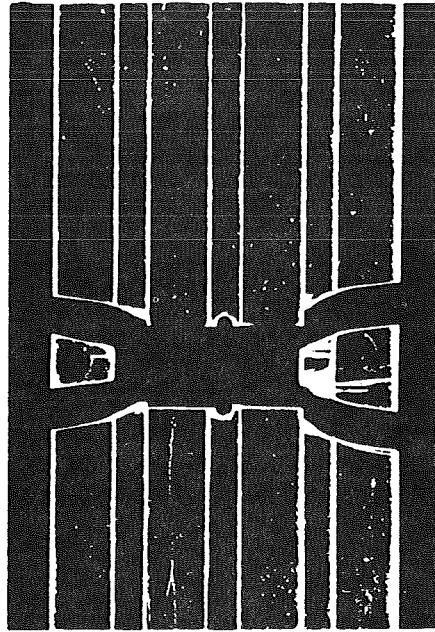
Sequence of photographs showing distribution of fiber breaks
in unidirectional composite under longitudinal tension



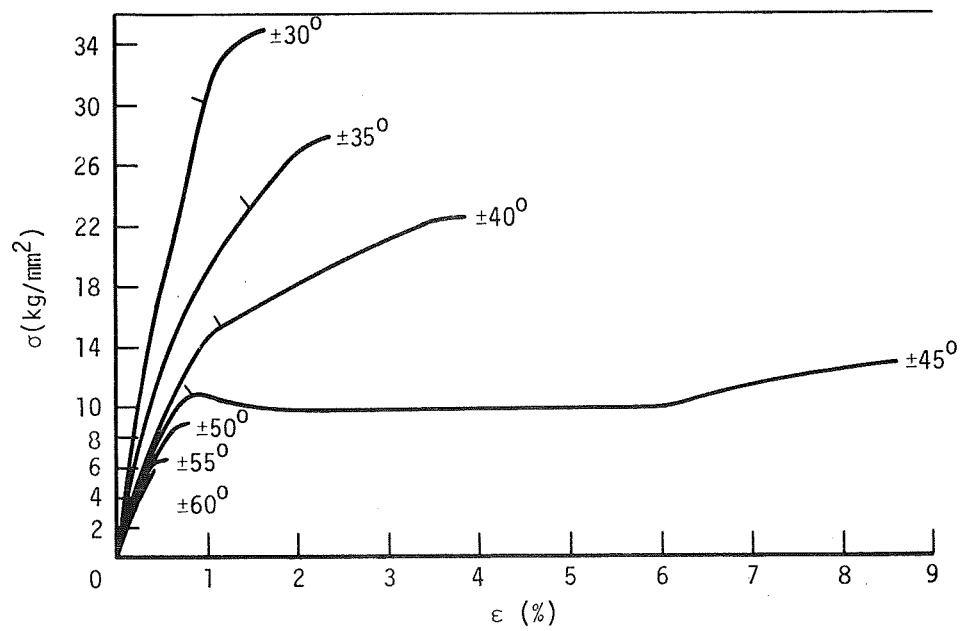
Fixture for dynamic tensile loading of composite models



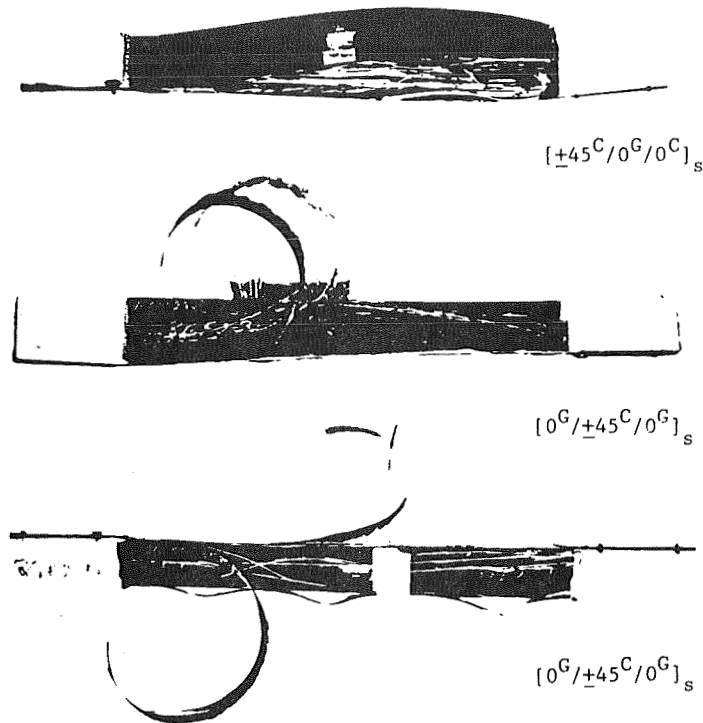
Transient isochromatic fringe patterns in a glass-plastic composite model under dynamic tension (Camera speed: 200,000 frames per second)



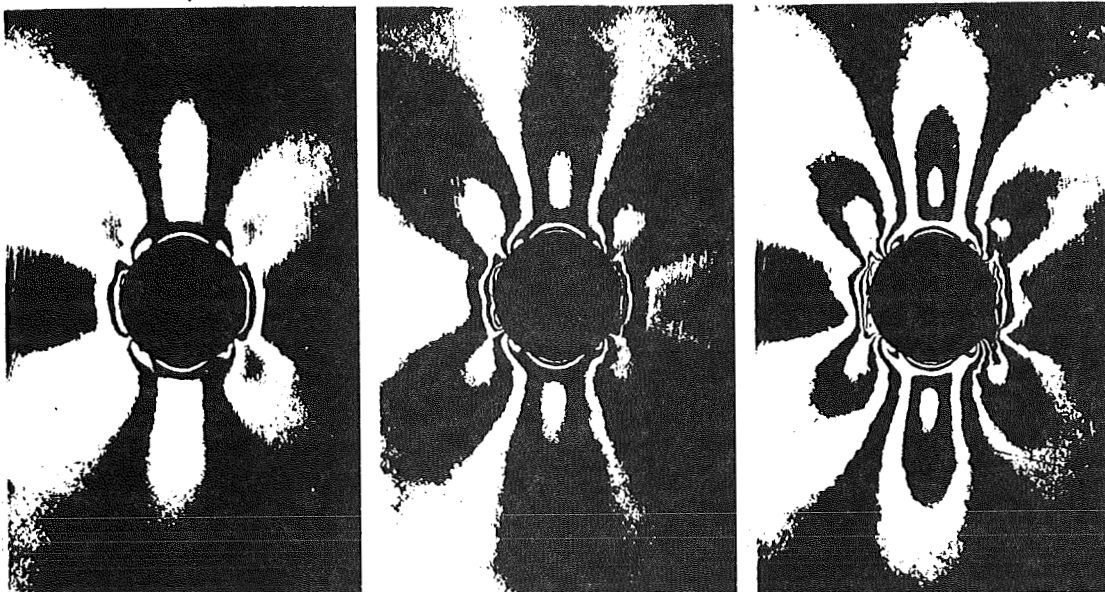
Failure pattern in model of preceding figure



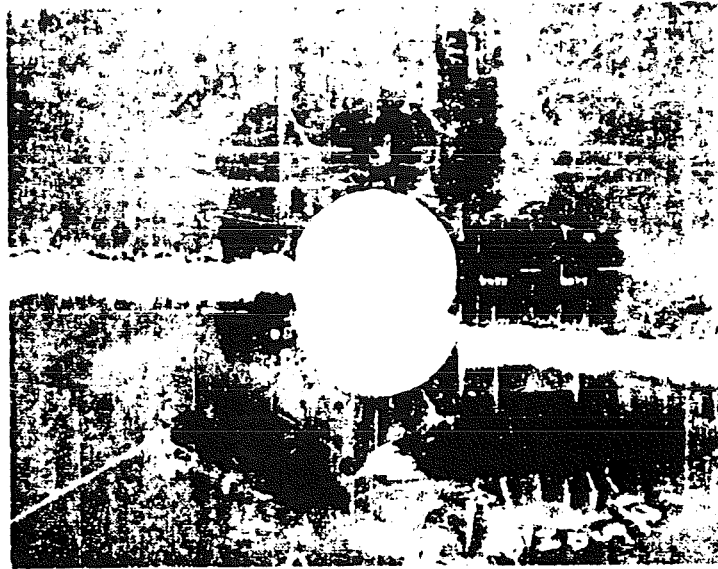
Stress-strain curves of $(\pm\theta)$ angle-ply glass/epoxy laminates



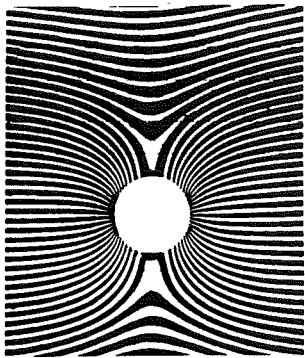
Characteristic failure patterns of three graphite/S-glass/high-modulus epoxy specimens under uniaxial tensile loading



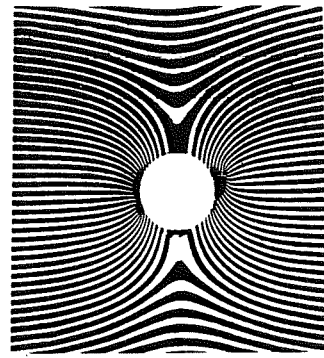
Isochromatic fringe patterns around hole in $[0/\pm 45/0/\bar{90}]$ boron/epoxy specimen for applied uniaxial stresses of 166 MPa (24.0 ksi), 225 MPa (32.6 ksi), and 293 MPa (42.4 ksi)



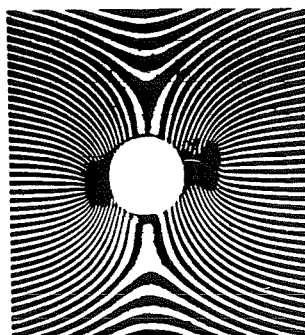
Typical failure pattern around hole in $[0/\pm 45/0/\bar{90}]_s$ boron/epoxy specimen under uniaxial tensile loading



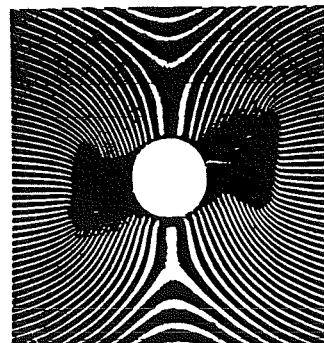
198 MPa (28.7 ksi)



206 MPa (29.9 ksi)

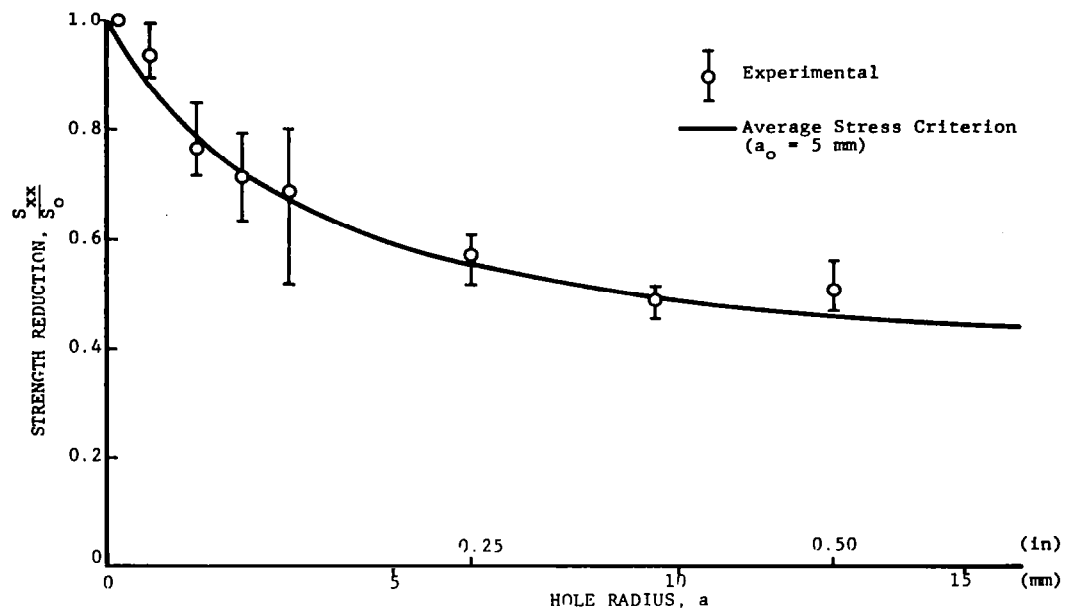


206 MPa (29.9 ksi)

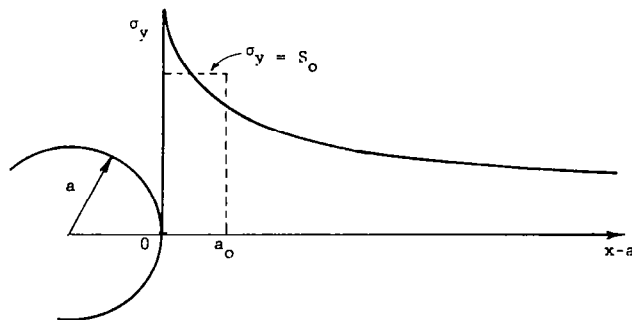


210 MPa (30.4 ksi)

Sequence of Moiré fringe patterns corresponding to vertical displacements in $[0/\pm 45/0/\bar{90}]_s$ glass/epoxy specimen at various applied uniaxial stresses



Strength reduction as a function of hole radius for $[0_2/\pm 45]_2$ graphite/epoxy plates with circular holes under uniaxial tensile loading



Approximate Stress Distribution

$$\sigma_y(x, 0) = \sigma_0 \left[1 + \frac{1}{2} \rho^{-2} + \frac{3}{2} \rho^{-4} + \frac{1}{2} (k_\sigma - 3) (5\rho^{-6} - 7\rho^{-8}) \right]$$

σ_0 = far field stress

$\rho = x/a$

k_σ = anisotropic stress concentration factor

Strength Reduction Ratio

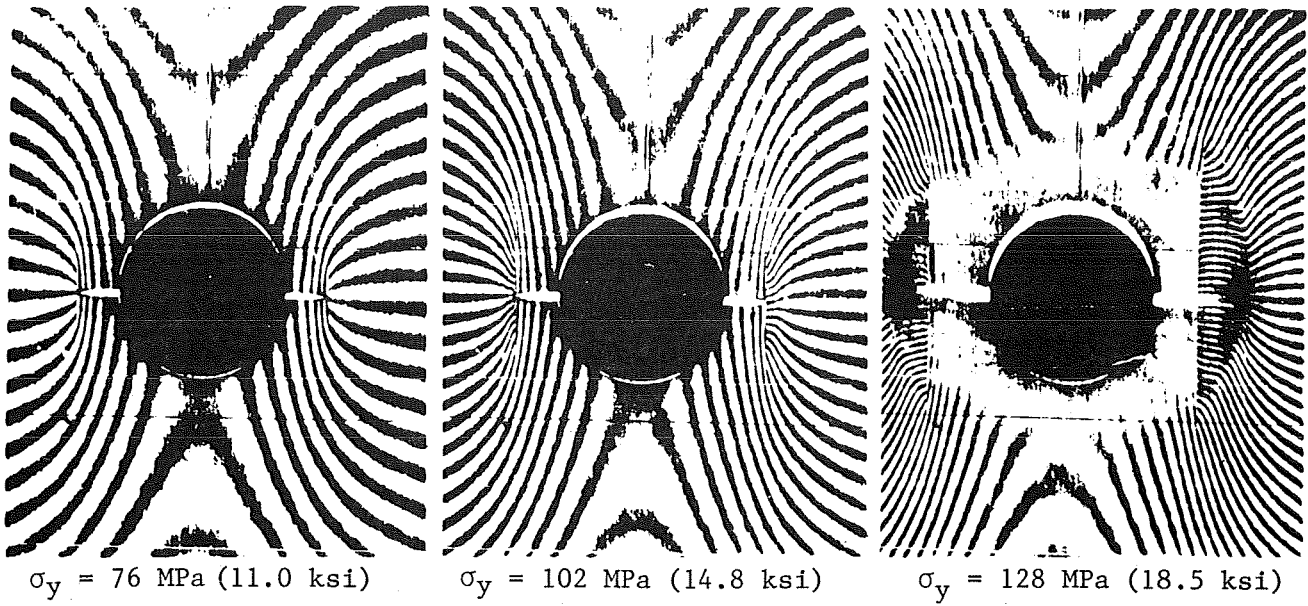
$$\frac{S_{yy}}{S_0} = \frac{2}{(1+\xi) [2 + \xi^2 + (k_\sigma - 3) \xi^6]}$$

$$\xi = \frac{a}{a_0}$$

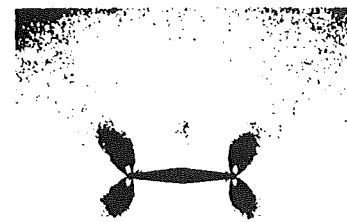
a_0 = characteristic length dimension

S_{yy}, S_0 = strengths of notched and unnotched laminates, respectively.

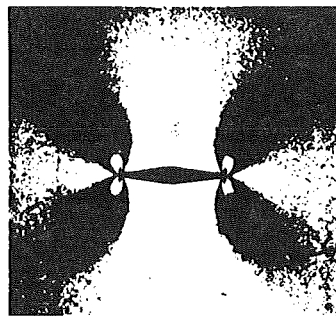
Strength reduction of uniaxially loaded composite plate with hole according to average stress criterion



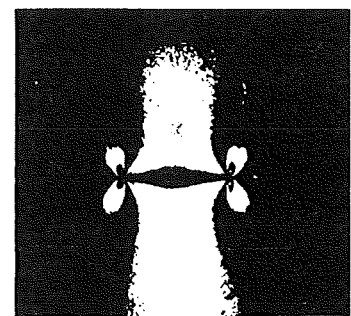
Moiré fringe patterns around crack in glass/epoxy composites $[0/90/0/\bar{90}]_s$ at three levels of applied stress



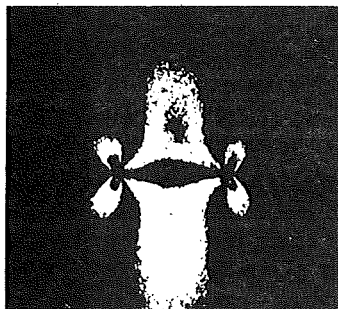
121 MPa (18 ksi)



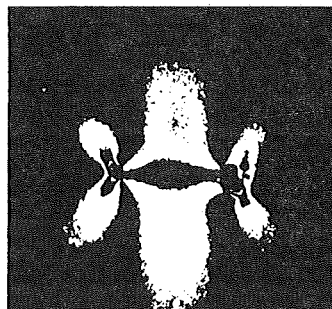
162 MPa (23 ksi)



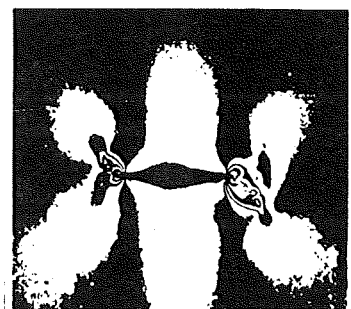
202 MPa (29 ksi)



222 MPa (32 ksi)

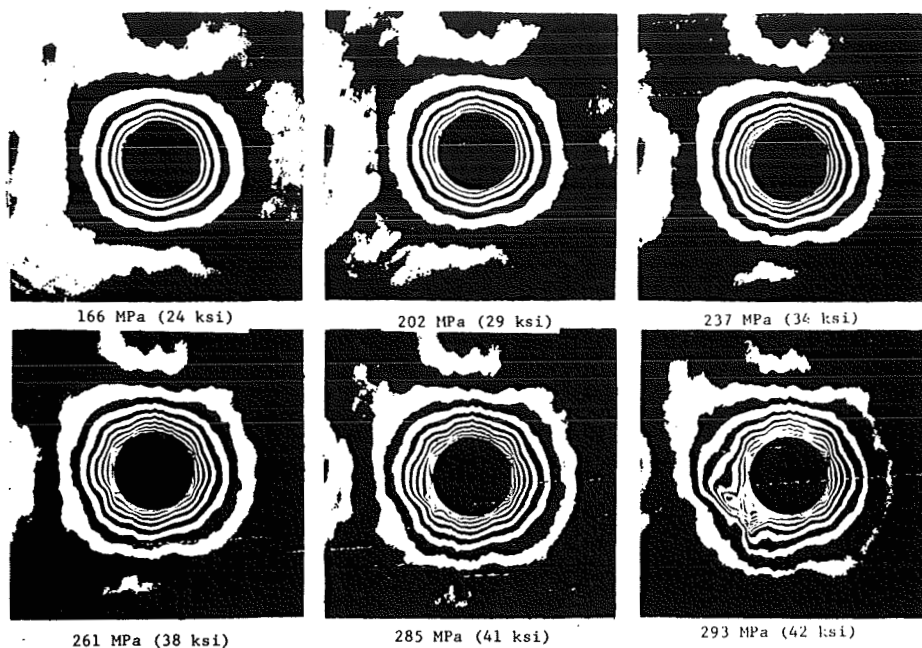


243 MPa (35 ksi)

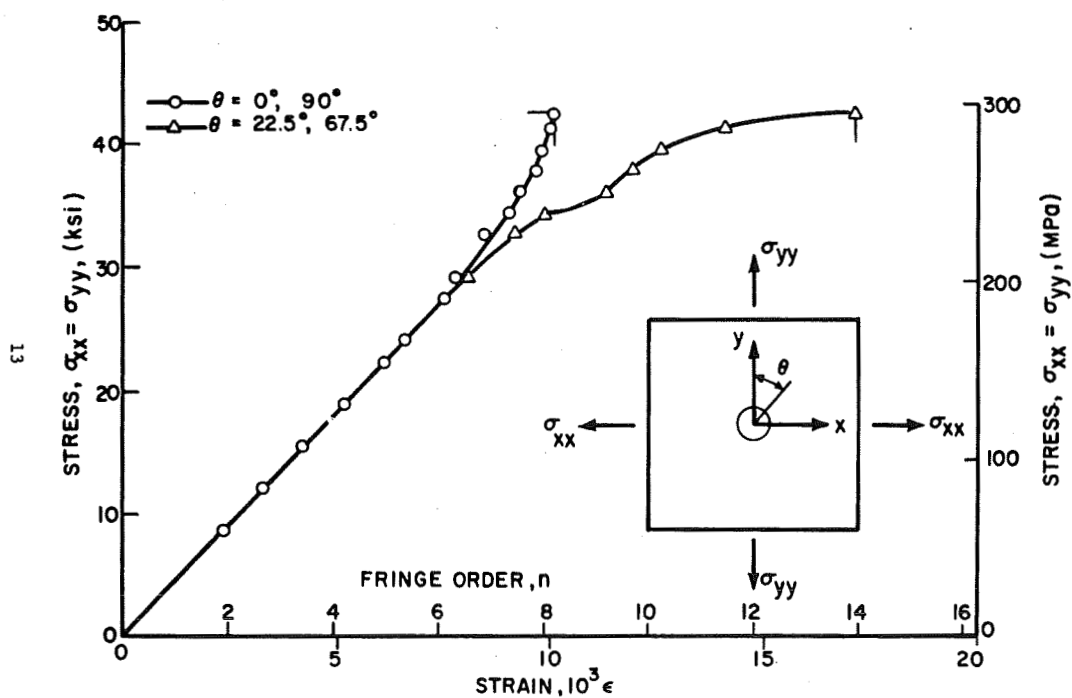


273 MPa (40 ksi)

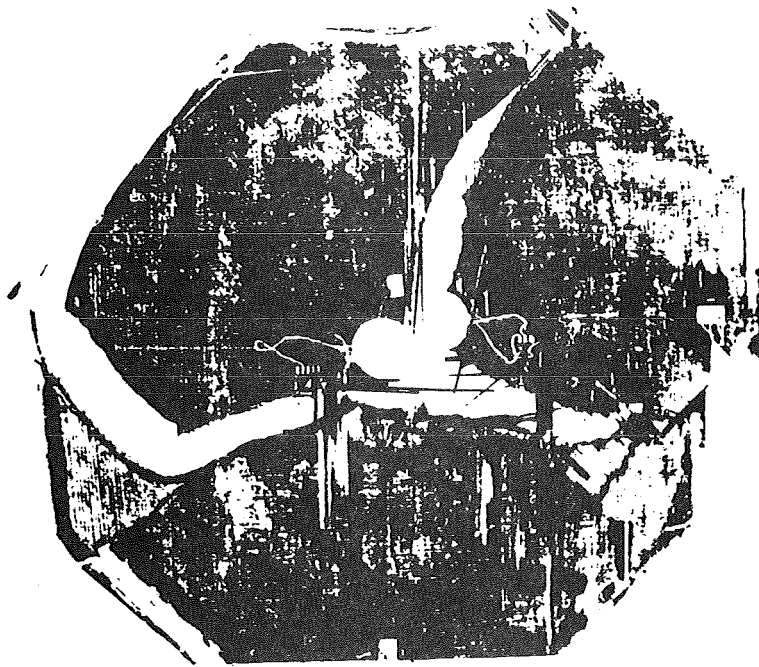
Isochromatic fringe patterns in photoelastic coating around 1.27-cm (0.50 in.) crack of $[0/\pm 45/90]_s$ graphite/epoxy specimen at various levels of applied stress



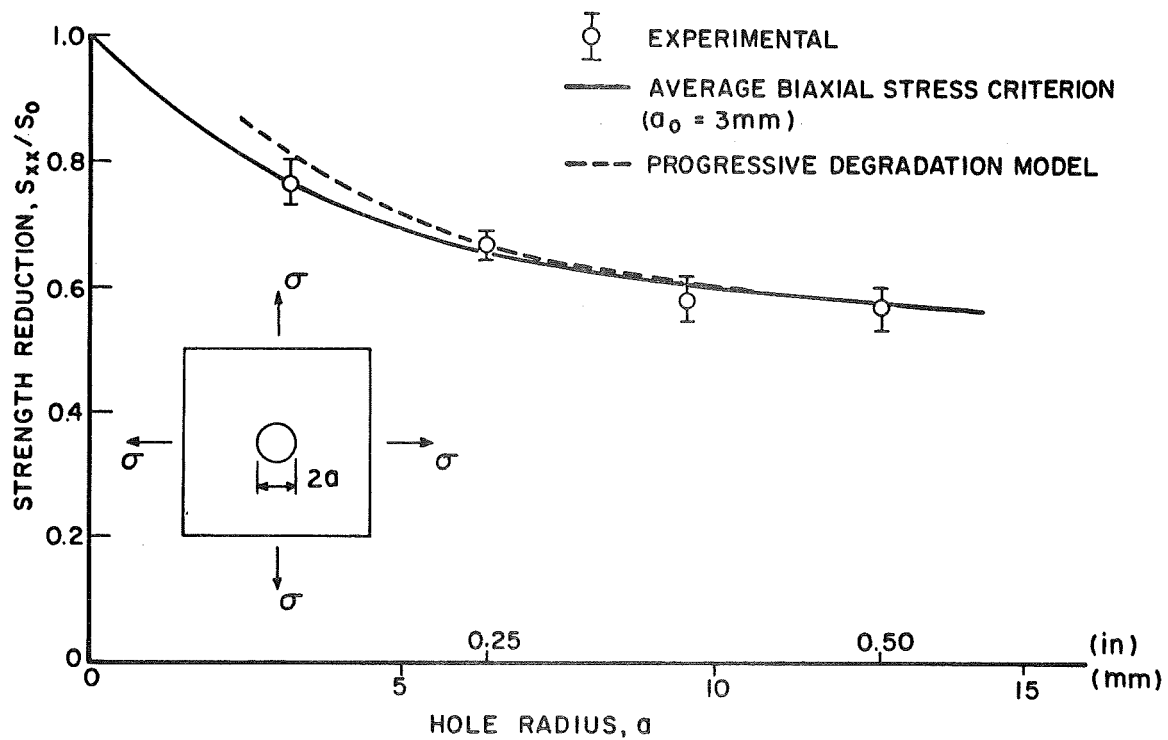
Isochromatic fringe patterns in photoelastic coating of $[0/\pm 45/90]_S$ graphite/epoxy specimen with 2.54-cm-diameter (1 in.) hole under equal biaxial tensile loading (Far-field biaxial stress marked)



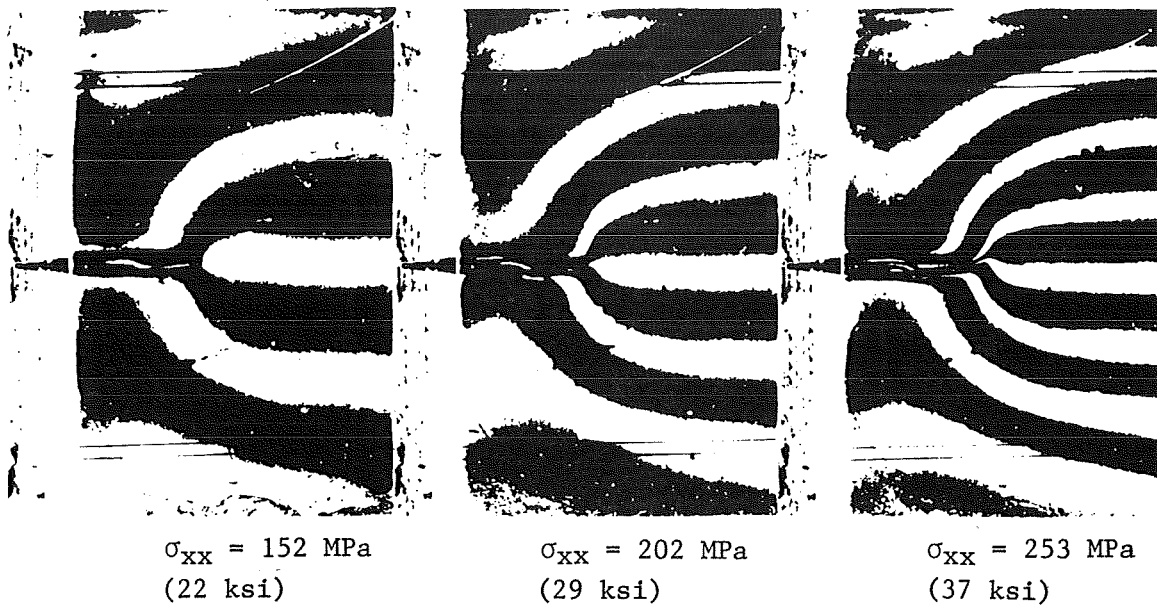
Fringe order and circumferential strain at two locations on the hole boundary for $[0/\pm 45/90]_S$ graphite/epoxy specimen with 2.54-cm-diameter (1 in.) hole under equal biaxial loading



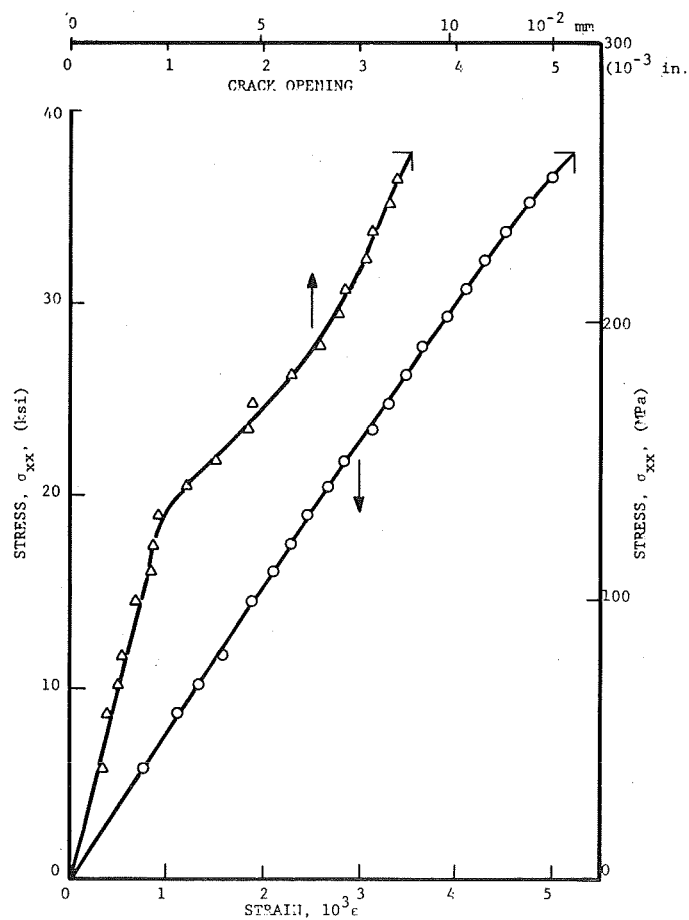
Failure pattern in $[0/\pm 45/90]_s$ graphite/epoxy specimen with 1.91-cm-diameter (0.75 in.) hole under equal biaxial tensile loading



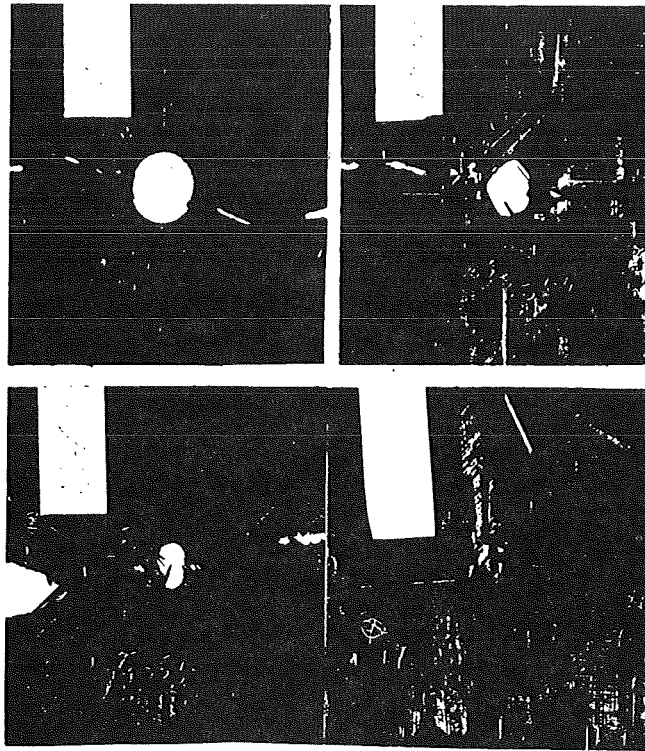
Strength reduction as a function of hole radius for $[0/\pm 45/90]_s$ graphite/epoxy plates with circular holes under 1:1 biaxial tensile loading



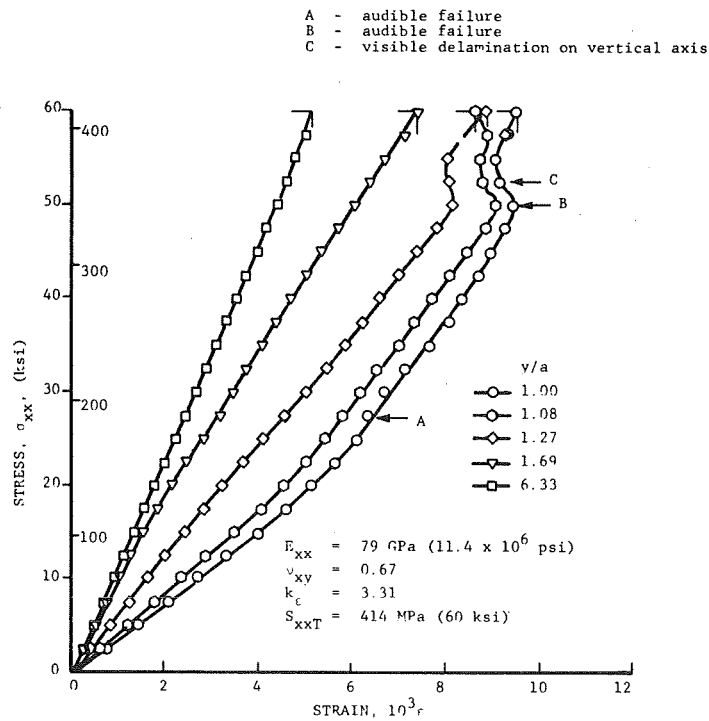
Moiré fringe patterns around crack in uniaxially loaded $[0/\pm 45/90]_s$ graphite/epoxy specimen for three levels of applied stress.



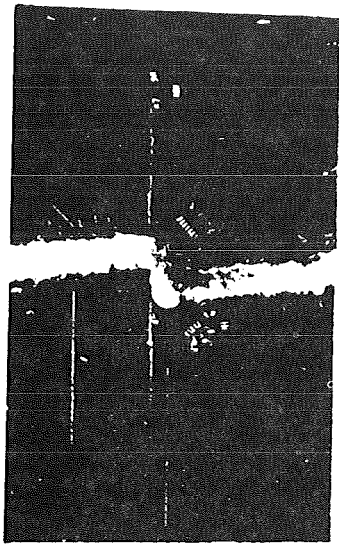
Crack opening displacement and far-field strain for $[0/\pm 45/90]_s$ graphite/epoxy specimen with a 1.27-cm (0.50 in.) horizontal crack



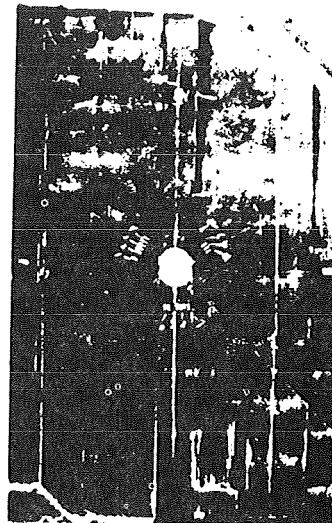
Failure patterns in $[0_2/\pm 45]_s$ graphite/epoxy specimens with holes of various sizes under uniaxial tension (Hole diameters are 2.54 cm (1 in.), 1.91 cm (0.75 in.), 1.27 cm (0.50 in.), and 0.64 cm (0.25 in.))



Vertical strains along horizontal axis of $[0_2/\pm 45]_s$ graphite/epoxy specimen with 1.91-cm-diameter (0.75 in.) hole under uniaxial tensile loading

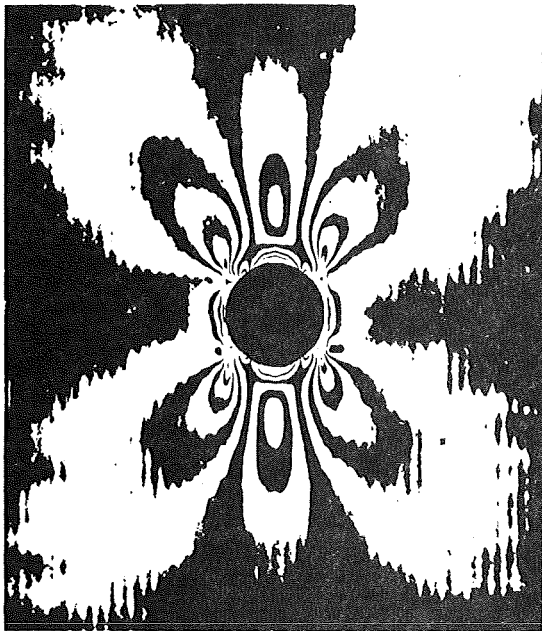


Specimen no. 43; Bo/E;
 $[\pm 45/0_2/\bar{0}]_s$

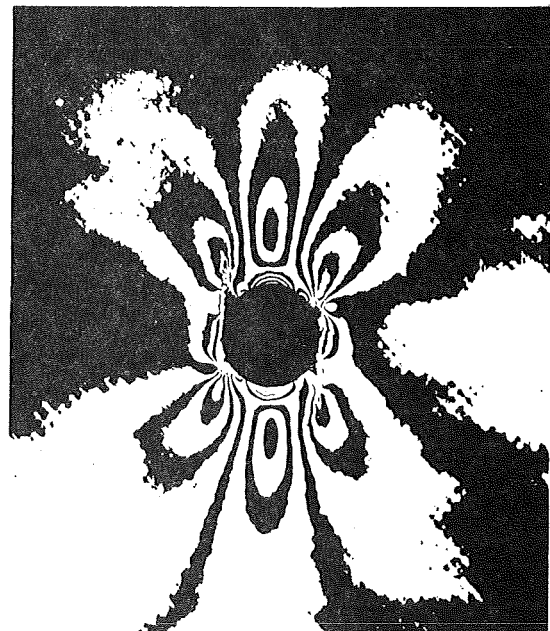


Specimen no. 45; Bo/E;
 $[0_2/\pm 45/\bar{0}]_s$

Failure patterns of boron-epoxy tensile panels with holes

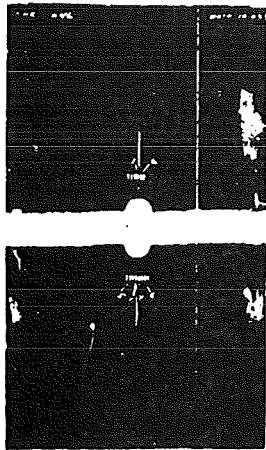


$[0_2/\pm 45/\bar{0}]_s$



$[\pm 45/0_2/\bar{0}]_s$

Isochromatic fringe patterns in photoelastic coating around hole in boron/epoxy specimens of two different stacking sequences ($\sigma_y = 392 \text{ MPa}$ (56.8 ksi))



$[0/90/0/90]_s$



$[45/90/0/-45]_s$



$[\pm 45/0/\pm 45]_s$

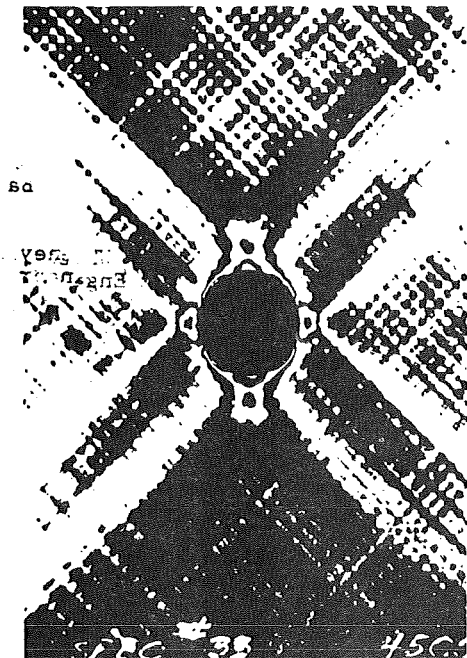


$[\pm 45/\pm 45]_s$

Failure patterns of boron-epoxy panels with holes of various laminate constructions

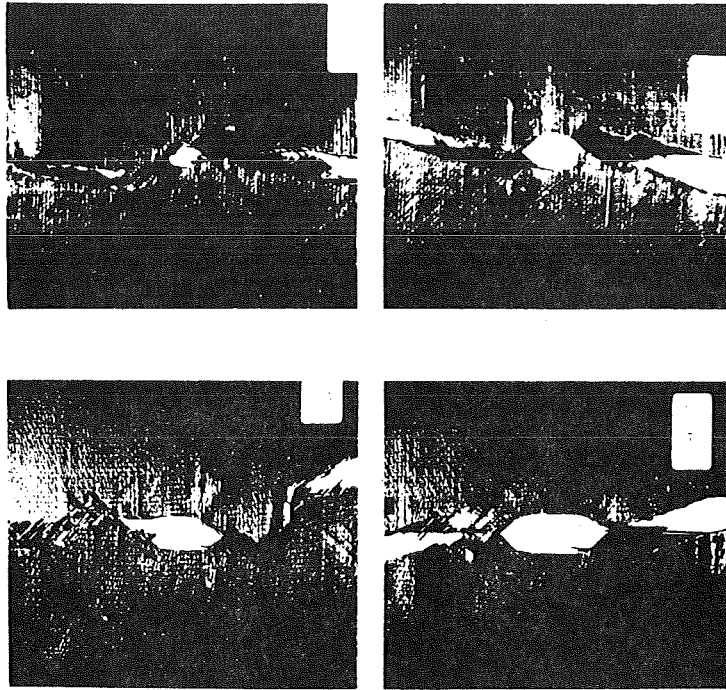


$[0/90/0/90]_s$; $\sigma_y = 170 \text{ MPa (24.6 ksi)}$

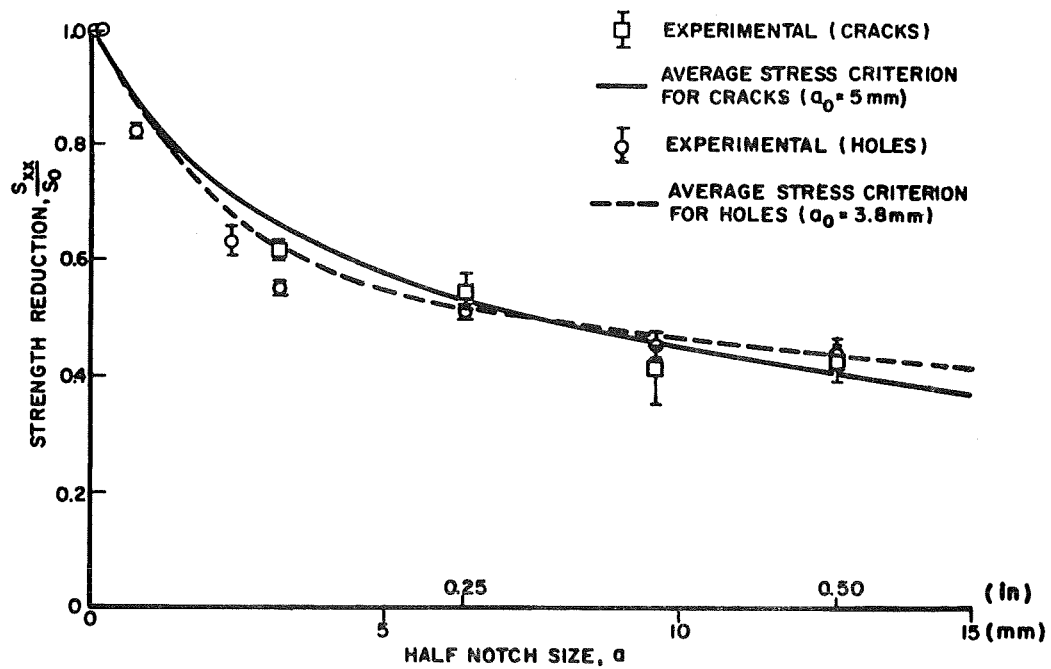


$[\pm 45/\pm 45]_s$; $\sigma_y = 77 \text{ MPa (11.1 ksi)}$

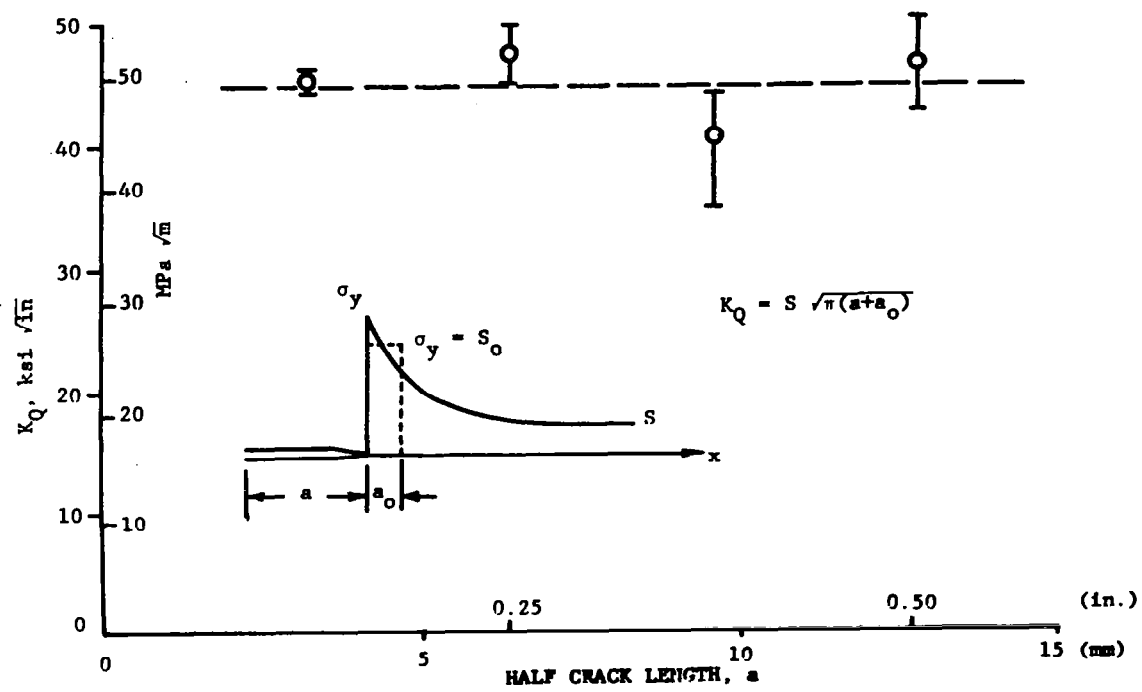
Isochromatic fringe patterns in photoelastic coating around hole in boron/epoxy specimens



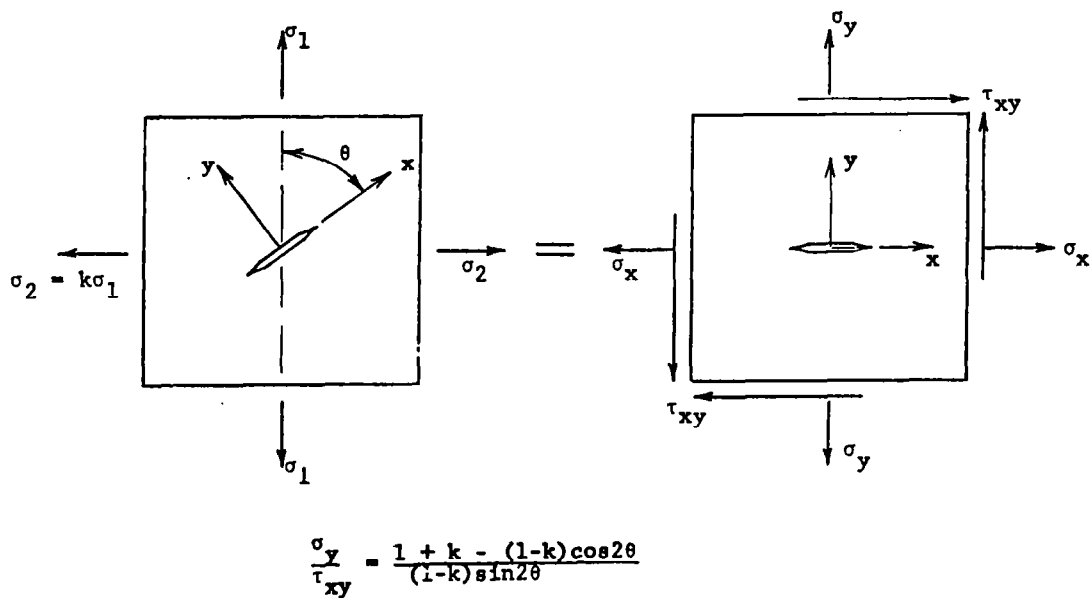
Failure patterns in uniaxially loaded $[0/\pm 45/90]_s$ graphite/epoxy plates with cracks of various lengths (Crack lengths are 0.64 cm (0.35 in.), 1.27 cm (0.50 in.), 1.91 cm (0.75 in.), and 2.54 cm (1.00 in.))



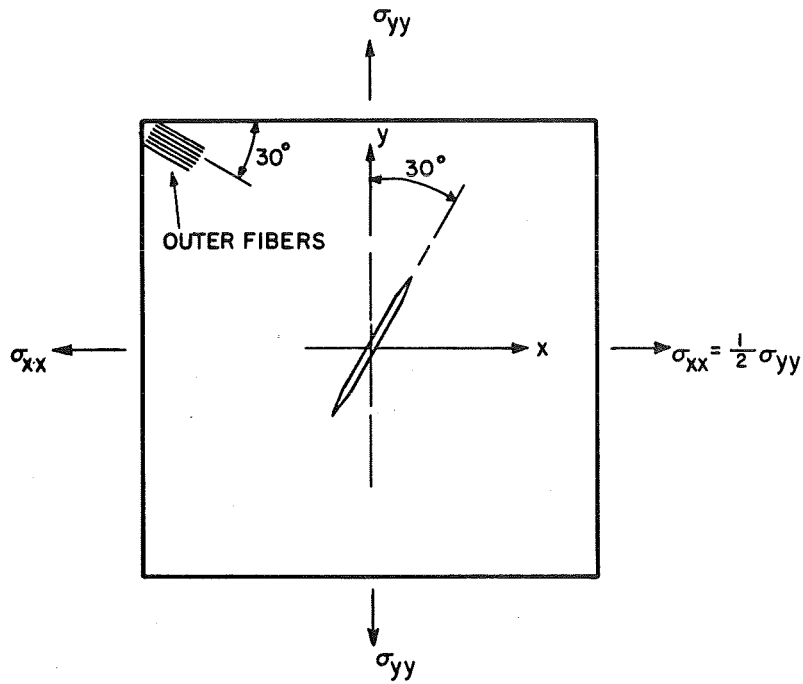
Strength reduction as a function of notch size for $[0/\pm 45/90]_s$ graphite/epoxy plates with circular holes and horizontal cracks under uniaxial tensile loading



Critical stress intensity factor as a function of crack length for $[0/\pm 45/90]_s$ graphite/epoxy plates with horizontal cracks under uniaxial tensile loading



Stress transformations of the far-field biaxial state of stress around a crack.



Biaxial loading of $[0/\pm 45/90]_s$ graphite/epoxy specimens with cracks



$\sigma_{yy} = 392 \text{ MPa (42.4 ksi)}$



$\sigma_{yy} = 303 \text{ MPa (43.9 ksi)}$



$\sigma_{yy} = 260 \text{ MPa (37.7 ksi)}$

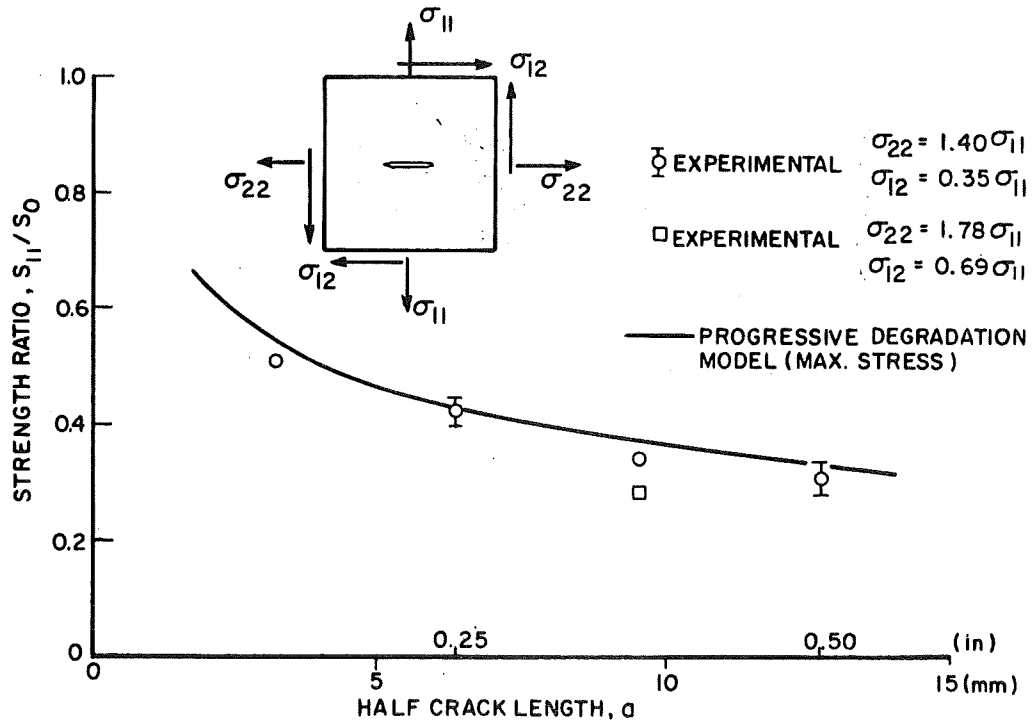


$\sigma_{yy} = 278 \text{ MPa (40.3 ksi)}$

Isochromatic fringe patterns in photoelastic coating around 1.27-cm (0.5 in.) crack in $(0/\pm 45/90)_s$ graphite/epoxy specimen under biaxial loading - $\sigma_{yy} = 2.03\sigma_{xx}$ at 30 deg with crack direction



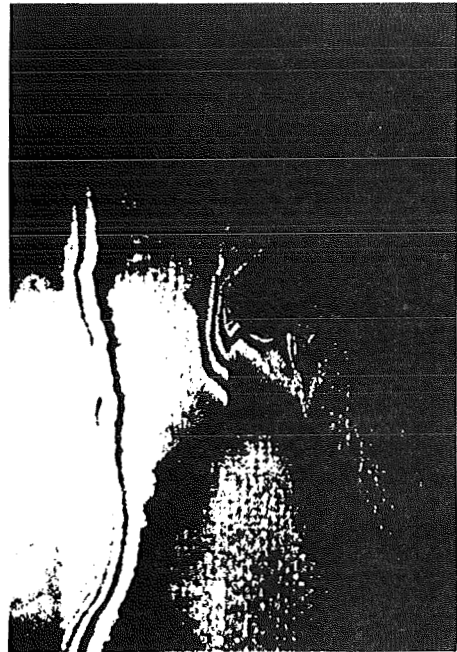
Biaxial specimen with 1.91-cm-long (0.75 in.) crack after failure



Comparison of experimental and theoretical results for strength ratio for $[0/\pm 45/90]_S$ graphite/epoxy plates with cracks under biaxial loading

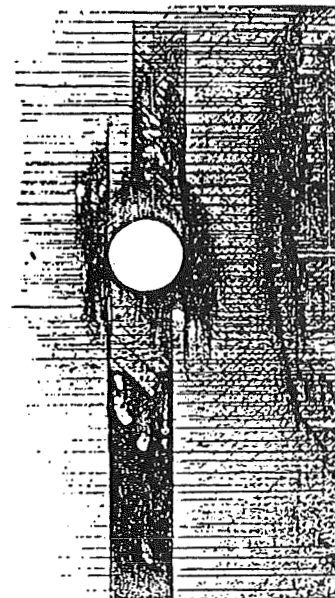
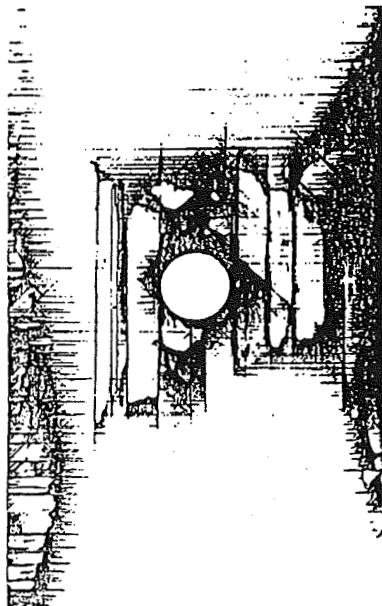


Front surface

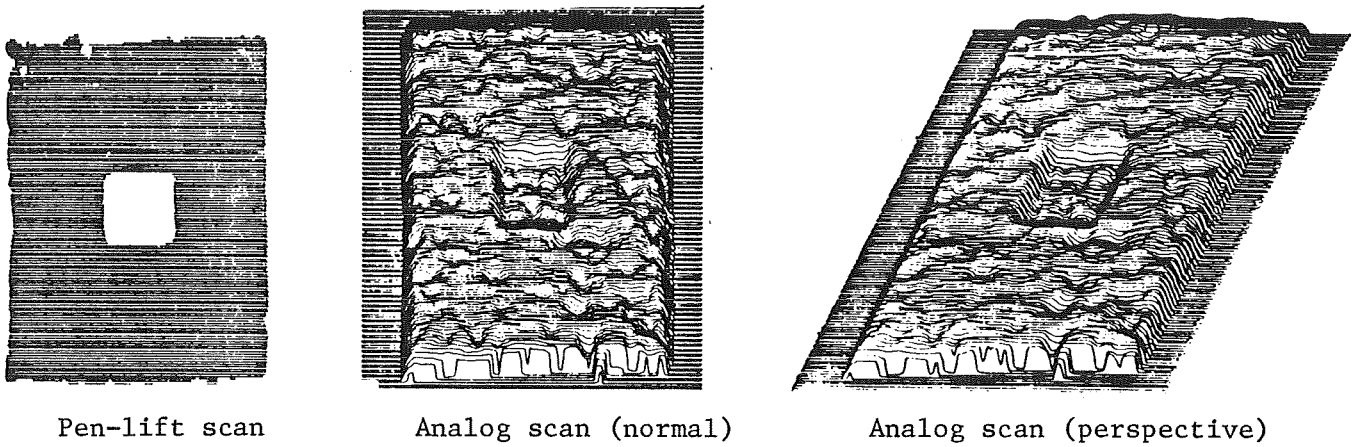


Back surface as viewed from the front through the specimen (ref. 6)

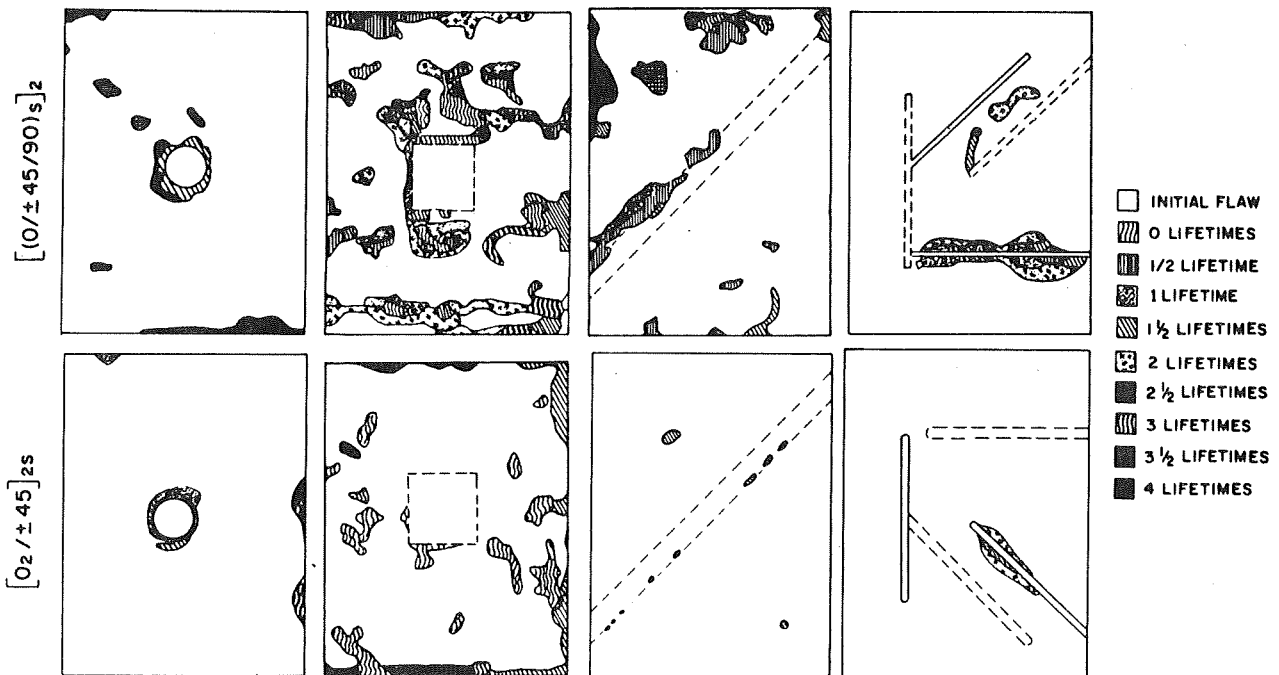
Thermally induced holographic fringe patterns in fatigue-loaded $[0/\pm 45/90]_s$ graphite/epoxy specimen with circular hole



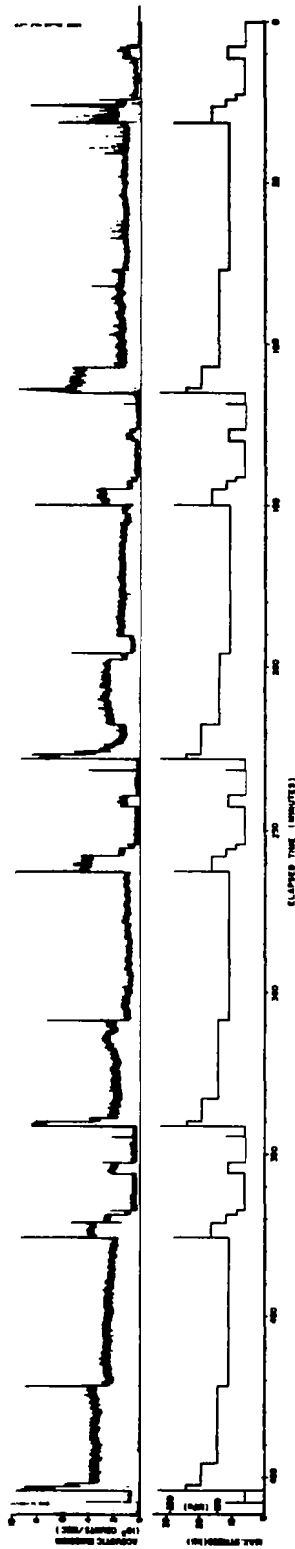
TBE enhanced X-ray photographs showing fatigue-induced damage in $[(0/\pm 45/90)_s]_2$ graphite/epoxy specimens



Ultrasonic C-scans of $[0/\pm 45/90]_s]_2$ graphite/epoxy specimen with a film patch



Flaw growth under spectrum fatigue loading in $[(0/\pm 45/90)_s]_2$ and $[0_2/\pm 45]_2s$ graphite/epoxy specimens with four types of initial flaws (Ambient environment)



Acoustic emission and corresponding load spectrum as a function of elapsed time for
 $[O_2/\pm 45]_2s$ graphite/epoxy specimens with holes (Time increases from right to left)

REFERENCES

1. Daniel, I. M.; and Rowlands, R. E.: Experimental Stress Analysis of Composite Materials. ASME paper no. 72-DE-6, 1972.
2. Daniel, I. M.: Optical Methods for Testing Composite Materials - Stress Analysis and Fracture Mechanics. Failure Models of Composite Materials With Organic Matrices and Their Consequences on Design, AGARD Conference Proceedings no. 163, 1975.
3. Whitney, J. M.; Daniel, I. M.; and Pipes, R. B.: Experimental Mechanics of Fiber-Reinforced Composite Materials. SESA monograph no. 4, Society for Experimental Stress Analysis, 1982.
4. Dally, J. W.; and Alfievich, I.: Application of Birefringent Coatings to Glass-Fiber-Reinforced Plastics. Exper. Mech., vol. 9, 1969, pp. 97-102.
5. Rosen, B. Walter: Mechanics of Composite Strengthening. Fiber Composite Materials, American Society for Metals, 1965, pp. 37-75.
6. Krautkraemer, J.; and Krautkraemer, H.: Ultrasonic Testing of Materials. Springer-Verlag, New York, 1977.

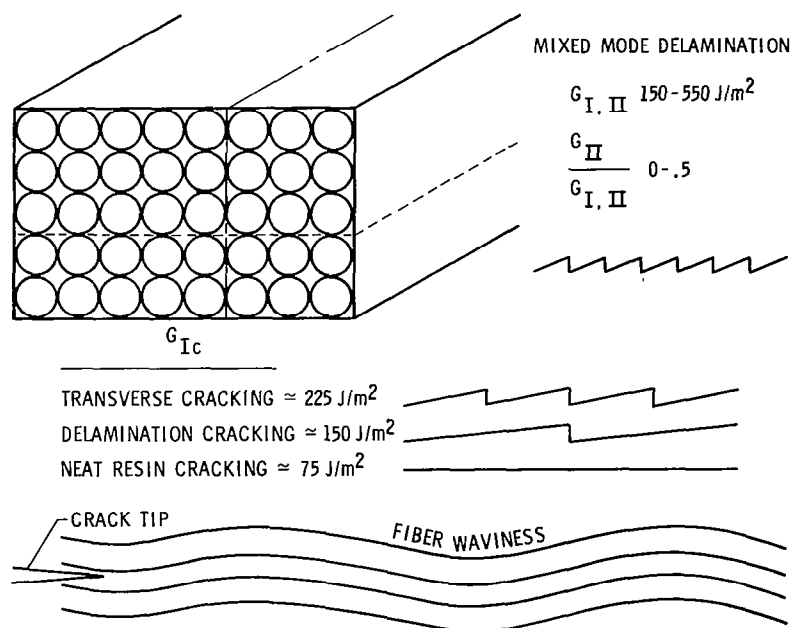
GENERAL
DISCUSSION

DISCUSSION OF MATRIX CRACKING IN GRAPHITE/EPOXY COMPOSITE MATERIALS

Walter L. Bradley
Texas A&M University

Recent work on the epoxy 3502 with and without carbon fiber reinforcement has demonstrated that reinforcement of a weak brittle material with a strong brittle material enhances the fracture toughness, even when cracking is parallel to the fibers. Neat material compact tension coupons indicated that $G_{IC} = 75 \text{ J/m}^2$. Delamination cracking of ASI/3502 gave a toughness of 150 J/m^2 , whereas transverse cracking parallel to the fibers gave a toughness of 225 J/m^2 . In delamination cracking, occasional crack tip interaction with the fibers results in either fiber breakage or crack arrest, requiring renucleation in the adjacent matrix material. Coalescence of the existing crack and the new crack gives a serrated or scalloped appearance to the fracture surface. For transverse cracking in a 90° compact tension specimen, the resin path through which the cracking occurs is quite "lean" compared to the resin-"rich" region between plies which is cracked during delamination. Thus, the incidence of crack tip interaction with the fiber is enhanced and the energy required to propagate the crack increases accordingly.

Finally, mixed-mode delamination fracture appears to occur microscopically on the plane of principal normal stress, thus increasing the angle between the delamination plane and the plane of principal normal stress. The result is that crack propagation is continually being redirected into the fibers, resulting in either fiber breakage or crack arrest, with the need for renucleation in adjacent matrix material. As was discussed previously, this has the effect of increasing the energy required to propagate the crack. For $G_{II}/(G_I + G_{II})$ increasing from 0 to 0.35, $G_{I,II} = G_I + G_{II}$ was observed to increase from 150 J/m^2 to 550 J/m^2 .



DISCUSSION OF COMPOSITE STRUCTURES

John N. Dickson
Lockheed-Georgia Company

Composite Structures , Are We Ready ?

SECONDARY STRUCTURE

OH SURE!

CONTROL SURFACES

O. K.!

HORIZONTAL OR VERTICAL TAIL

MAYBE!

WING OR PRESSURIZED FUSELAGE

OH NO!

Composite Primary Structure

PRINCIPAL DESIGN DRIVERS

- DAMAGE TOLERANCE
- OUT-OF-PLANE DEFORMATIONS
- JOINTS AND ATTACHMENTS

Damage Tolerance Requirements Metallic Airplanes

MILITARY

REQUIREMENTS PER MIL-A-83444
(AIRPLANE DAMAGE TOLERANCE REQUIREMENTS, JULY 1974)

COMMERCIAL

MANUFACTURER/FAA

Damage Tolerance Requirements Composite Structures

- NO SPECIFIC REQUIREMENTS ESTABLISHED YET
- WILL NOT ACCEPT COMPOSITE STRUCTURES THAT ARE LESS DAMAGE TOLERANT THAN METALS

Composite Structures

DAMAGE CAUSES

- MANUFACTURING
- MAINTENANCE AND REPAIR
- IN-SERVICE IMPACT
- STRUCTURAL OVERLOAD

Damage Tolerance Metallic vs Composites

METALLIC

FLAWS, CRACKS; TENSION CRITICAL
METHODOLOGY FAIRLY WELL ESTABLISHED

COMPOSITES

MULTIPLE DELAMINATIONS, DISBONDS;
COMPRESSION CRITICAL
METHODOLOGY VIRTUALLY NON EXISTENT

Composite Structures

DO WE DESIGN STRUCTURE FOR UNLIMITED LIFE
IN THE PRESENCE OF NONVISIBLE DAMAGE?

Composite Structures In-Service Impact

DEGREE OF DAMAGE / INSPECTION

- NONVISIBLE / ?
- VISIBLE, BACK SURFACE ONLY / DEPOT
- VISIBLE, BOTH SURFACES / FLIGHT EVIDENT
GROUND EVIDENT
SPECIAL VISUAL, ETC.

Composite Structure Out-of-Plane Deformations

PRESSURIZATION, POST-BUCKLING

SKIN/STRINGERS

SKIN/SUBSTRUCTURE

SPAR WEB/STIFFENERS



ATTACHMENT?

CO-CURE; ADHESIVE BONDING; MECHANICAL FASTENERS;
STITCHING; STAPLING; COMBINATIONS

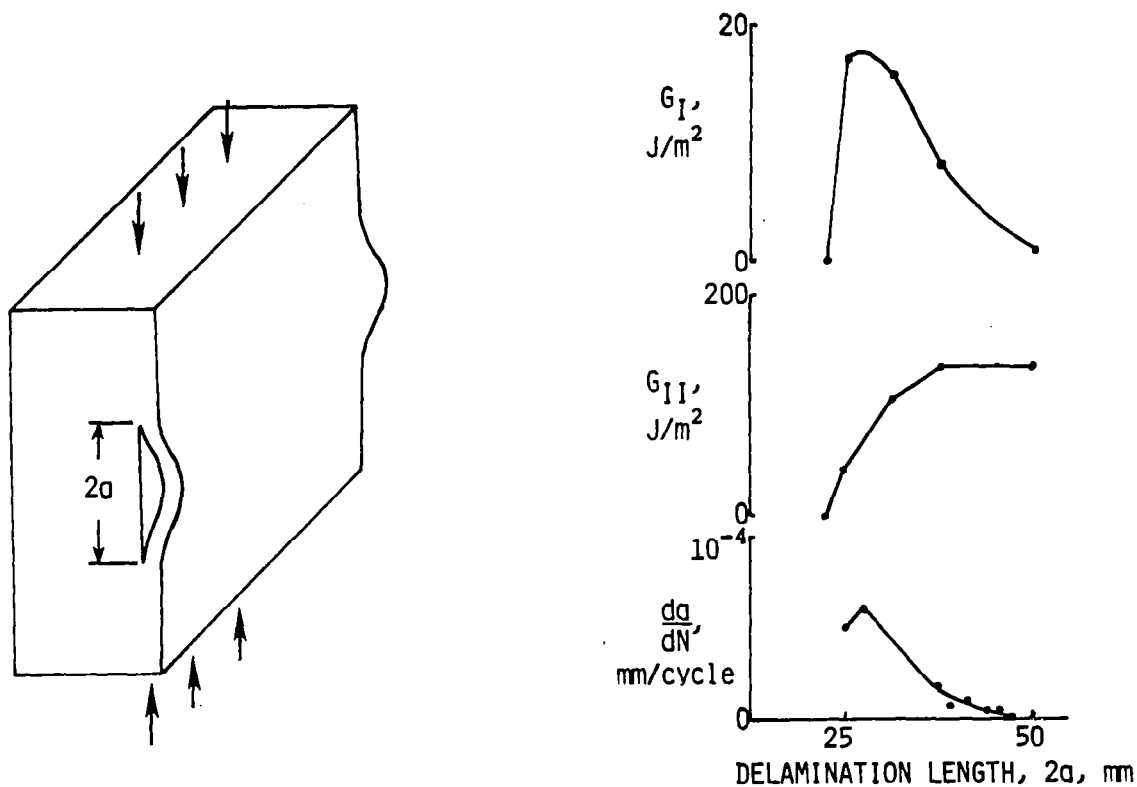
ANALYSIS EXPLAINS VARIABLE RATE OF INSTABILITY-RELATED DELAMINATION GROWTH

John D. Whitcomb
NASA Langley Research Center

Under compression fatigue, delaminations in composites sometimes induce localized buckling, causing high interlaminar stresses at the ends of the delamination. Rapid delamination growth and loss of structural stability often ensue. Because delamination growth can lead to structural instability, the growth process must be understood.

To improve our understanding, through-width delaminations (see figure) were studied experimentally and analytically. The figure shows a comparison of measured growth rates and calculated strain energy release rates, which are a measure of the intensity of stresses at the crack tip. In the figure, G_I and G_{II} are the energy release rates related to peel and shear stresses, respectively. Note that both G_I and the growth rate first increase then decrease rapidly with crack extension, whereas G_{II} increases monotonically and does not reflect the change in growth rate. Apparently the rate of delamination growth is governed by the intensity of the peel stress field. Hence, prediction of growth depends on an accurate assessment of the peel stress field around the crack tip.

COMPARISON OF STRAIN-ENERGY RELEASE RATES AND DELAMINATION GROWTH RATES



THE APPROACH TO FAILURE ANALYSIS OF COMPOSITES

Kenneth Reifsnider
Materials Response Group
Virginia Polytechnic Institute and State University

Much of the philosophy of failure analysis expressed at this workshop took the general direction of damage tolerance concepts. This is certainly a reasonable approach for structures, since, for example, a structure such as an airplane must be periodically inspected and the service of that structure continued (or discontinued) based on an interpretation of the residual strength and serviceability of the component. Such an approach requires nondestructive examination methods that can identify and quantitatively measure observables that are precisely and reliably related to engineering response. It is also essential that failure induced by long-term loading be sufficiently well understood and represented so that accurate anticipations of residual strength, stiffness, and life (the materials response) can be made based on the observables.

The experience of our Materials Response Group at VPI&SU and our perception of the results of other investigators suggest that the failure of composite laminates after long periods of loading at engineering levels can be typified by three rather distinct aspects. One of these aspects, which was highlighted at this workshop, and is the primary component of most current efforts to discuss damage tolerance. That aspect is stress redistribution. Currently it is typical, for example, to try to use nondestructive methods to find a major delamination, introduce the geometry of that defect into an approximate stress analysis of the component, and attempt to predict the residual strength of the component by typifying the failure resistance of the material using, say, a critical strain energy release rate or toughness determined from quasi-static laboratory tests.

However, such an approach neglects the other two major aspects of long-term failure which we believe must be addressed. In addition to stress redistribution, we believe that material degradation and localization of damage are critical aspects of long-term damage development and consequent failure. Even under uniaxial uniform stress states, unnotched coupons (not dominated by edge effects) eventually fail under load levels which may be only 60 to 70 percent of the static ultimate (tensile) strength (i.e., the residual strength is reduced by 30 to 40 percent). As a result of recent work in our laboratory, we know that a very complex, widely distributed, and dense array of microdamage develops under such circumstances, and that there is a distinct localization process that precedes the final failure event. We also know that strength reductions of as much as 30 to 40 percent can result from these damage aspects, as we have mentioned. While we have made some preliminary efforts (and other investigators are undoubtedly making similar attempts), a philosophy and (appropriate) analysis have not yet been established such that these aspects can be described and anticipated by a rational and rigorous model. Our efforts continue in this direction. We believe that the ultimate success of failure analysis efforts, especially those based on a damage tolerance approach, will depend on the degree to which all three of the basic aspects of long-term damage development (stress redistribution, material degradation, and localization) are successfully investigated and characterized.

Finally, we also believe that there is a need for investigative and developmental efforts directed towards the mechanics of nondestructive testing and evaluation. We illustrate this opinion by mentioning two examples which emphasize an important contrast. The contrast is between methods which present analog or strictly geometric information (the most typical schemes) and methods which function based on the actual mechanical response of the material component. One example of the latter is a technique developed in our laboratory at Virginia Tech called vibrothermography. That technique, simply put, uses variable-frequency mechanical excitation to generate hysteresis energy heat patterns which are directly related to the stress distributions and the disturbances in mechanical response produced by internal damage. The sensitivity and, indeed, the physical basis of this technique are primarily mechanical, and therein lie the contrast and strength of this technique for the prediction of subsequent strength and life of a damaged laminate. The second example is the use of stiffness change as a method of detecting and interpreting damage. As micro-damage develops in composite laminates, stiffness components change in precise and significant amounts which reflect the nature and severity of damage. For long-term load histories, the engineering Young's modulus, for example, typically changes by the same order of magnitude as the residual strength (i.e., by as much as 30 to 40 percent) even for fiber-dominated laminates. These stiffness changes enter the constitutive equations and, therefore, the analytical mechanics and modeling quite naturally. The measurement and interpretation of stiffness and stiffness changes are familiar exercises.

We feel strongly that there is a great need for a research and development effort that addresses the need for better understanding and exploitation of the mechanics of nondestructive testing and evaluation. In summary, we believe that a proper failure analysis must consider the distribution of damage, the consequent local state of stress, and local state of the material. The analysis should be based on a sound rational mechanics development, which in turn is based on physical observables directly related to the mechanical response that is to be anticipated. If such a body of philosophy is to be successfully and completely developed, it will require that specialists in mechanics, materials, and structures work closely and effectively together.

DISCUSSION OF INTERLAMINAR STRENGTH EFFECTS ON AIRCRAFT DESIGN

D. J. Watts
Douglas Aircraft Co.

A primary issue in the design of high-load-intensity primary aircraft structures is the identification and determination of small out-of-plane forces due to externally applied or deflection-induced loads which produce interlaminar forces within the laminate. Interlaminar shear forces from in-plane loadings can also be significant in high-load-intensity structural designs in the vicinity of discontinuities. These interlaminar forces can initiate and propagate delaminations which can drastically reduce the residual compressive strength of structural elements. Methodology and data are required to establish interlaminar static strength, delamination initiation and growth characteristics, the effect of flaws on these characteristics, and the residual compressive strength of delaminated structures. Resolution of these issues not only affects the design but is important in guiding manufacturing technology development to avoid developing methods and processes which cannot be applied to designs that strive to minimize interlaminar forces.

BIBLIOGRAPHY

I. DAMAGE DEFINITION, DEFECT IDENTIFICATION AND FAILURE MECHANISMS

Damage Definition

1. Chatterjee, S. N., Hashin, Z., and Pipes, R. B., "Definition and Modeling of Critical Flaws in Graphite Fiber Reinforced Resin Matrix Composite Materials," Materials Sciences Corporation Report TFR-1105/1008, Blue Bell, Pennsylvania, 1979.
2. Greszczuk, L. B., "Microbuckling of Lamina-Reinforced Composites," Third Conference on Composite Materials: Testing and Design, ASTM STP 546, 1974, pp. 5-29.
3. Mast, P. W., Beaubien, L. A., Clifford, M. A., Mulville, D. R., Sutton, S. A., Thomas, R. W., Tirosh, J., and Wolock, I., "Predicting the Onset of Fracture in Composites," Mekhanika Kompozitnykh Materialov, March-April 1979, pp. 313-316 (in Russian).
4. Olsen, G. C., "Degradation Mechanisms in Aluminum Matrix Composites: Alumina/Aluminum and Boron/Aluminum," Ph.D. Thesis, North Carolina State University at Raleigh, 1981.
5. Pagano, N. J., "Failure Mechanisms and Criteria in Composite Materials," Mechanics of Composites Review, USAF, October 1976, pp. 183-198.
6. Rose, J. L. and Shelton, W., "Damage Analysis in Composite Materials," Composite Reliability, ASTM STP 580, 1975, pp. 215-226.
7. Reifsnider, K. L. and Highsmith, A., "Characteristic Damage States: A New Approach to Representing Fatigue Damage in Composite Laminates," in Materials, Experimentation and Design in Fatigue, F. Sherratt and J. B. Sturgeon, eds., Westbury House, 1981, pp. 246-260.

Defect Identification

1. Cawley, P. and Adams, R. D., "Defect Location in Structures by a Vibration Technique," Design Engineering Technical Conference, ASME, St. Louis, Missouri, September 10-12, 1979.
2. Chatterjee, S. N., "On Interlaminar Defects in Laminated Composites," in Modern Developments in Composite Materials and Structures; Proceedings of the Winter Annual Meeting, New York, Dec. 2-7, 1979, ASME, pp. 1-15.
3. Chung, W. Y. and Testa, R. B., "The Elastic Stability of Fibers in a Composite Plate," Journal of Composite Materials, Vol. 3, Jan. 1969, pp. 58-62.
4. Claus, W. D., Jr., "Filament Misalignment and Composite Strength," Second Conference on Composite Materials: Testing and Design, ASTM STP 497, 1972, pp. 564-574.

5. Frye, E. R. and Rayner, R. M., "Observations of Failure Modes in Composite Materials," *Journal of Composite Materials*, Vol. 6, April 1972, pp. 286-292.
6. Hennecke, E. G., II, Reifsnider, K. L. and Stinchcomb, W. W., "Defect-Property Relationships in Composite Materials," *Mechanics of Composites Review*, USAF, October 1976, pp. 159-175.

Failure Mechanisms

1. Aoki, R. and Stellbrink, K., "The Influence of Defects on the Behavior of Composites," Deutsche Forschungs- und Versuchsanstalt fuer Luft- und Raumfahrt, Stuttgart, West Germany. In AGARD - Effect of Serv. Environ. on Composite Material, August 1980.
2. Bader, M. G., Bailey, J. E., Curtis, P. T. and Parvizi, A., "The Mechanisms of Initiation and Development of Damage in Multi-Axial Fibre-Reinforced Plastic Laminates," *Proceedings of the Third International Symposium on Mechanical Behavior of Materials*, Cambridge, United Kingdom, Vol. 3, 1979, p. 227.
3. Bailey, J. E. and Parvizi, A., "On Fibre Debonding Effects and the Mechanism of Transverse-Ply Failure in Cross-Ply Laminates of Glass Fibre/Thermoset Composites," *Journal of Materials Science*, Vol. 16, March 1981, pp. 649-659.
4. Drzal, L. T., Rich, M. J., Camping, J. D., and Park, W. J., "Interfacial Shear Strength and Failure Mechanisms in Graphite Fiber Composites," in *Rising to the Challenge of the '80s; Annual Conference and Exhibit*, 35th, New Orleans, Louisiana, Feb. 4-8, 1980, Society of the Plastics Industry, Inc., pp. 20-C1 to 20-C7.
5. Eselun, S. A., Neubert, H. D. and Wolff, E. G., "Microcracking Effects on Dimensional Stability," *Proceedings of the 24th National SAMPE Symposium*, San Francisco, California, May 1979, p. 1299.
6. Henneke, E. G., II and Reifsnider, K. L., "Observation of Fatigue Damage in Graphite Epoxy Composite Laminates," *Proceedings of the 15th Annual Meeting of the Society of Engineering Science*, 1978, pp. 303-308.
7. Lovell, E. G., "Shear Buckling of an Elastically Supported Fiber," *Journal of Composite Materials*, Vol. 6, April 1972, pp. 296-299.
8. McLaughlin, P. V., Huang, S. N. and Rosen, B. W., "Investigations of Failure Mechanisms in Fiber Composite Laminates," *Materials Sciences Corporation Report TFR/7508*, Blue Bell, PA, June 1975.
9. Morgan, R. J., Mones, E., Steele, W. J. and Deutscher, S. B., "Failure Modes and Durability of Kevlar/Epoxy Composites," presented at the 12th National SAMPE Technical Conference, Seattle, Washington, October 7-9, 1980.
10. Parvizi, A., Garrett, K. W. and Bailey, J. E., "Constrained Cracking in Glass Fibre-Reinforced Epoxy Cross-Ply Laminates," *Journal of Materials Science*, Vol. 13, 1978, p. 195.

11. Reifsnider, K. L., "Mechanics of Failure of Composite Materials," in Fracture Mechanics: Proceedings of the Tenth Symposium on Naval Structural Mechanics, Washington, D.C., Sept. 11-13, 1978, University of Virginia Press, 1978, pp. 317-331.
12. Reifsnider, K. L. and Talug, A., "Characteristic Damage States in Composite Laminates," Duke University Research Workshop on Mechanics of Composite Materials, 1978, pp. 147-178.
13. Rotem, A. and Hashin, Z., "Failure Modes of Angle-Ply Laminates," Journal of Composite Materials, Vol. 9, 1975, pp. 191-206.
14. Walrath, D. E. and Adams, D. F., "Damage Mechanisms/Failure Mechanics of Carbon-Carbon Composite Materials," Department of Mechanical Engineering, University of Wyoming, Laramie, September 1979.
15. Waring, G., Hofer, K. E., Jr., Vadala, E., and Trabocco, R., "Failure Mechanisms for Advanced Composite Sandwich Construction in Hostile Environments - Naval Aircraft Structures," in Advanced Composites - Special Topics; Proceedings of the Conference, 1979, pp. 83-122.
16. Rosen, B. W., "Failure of Fiber Composite Laminates," IUTAM Symposium on Mechanics of Composite Materials, Z. Hashin and C. T. Herakovich, eds., Pergamon Press (to be published).
17. Dharoni, L. R. and Goree, J. G., "Analysis of a Hybrid, Unidirectional Laminate with Damage," IUTAM Symposium on Mechanics of Composite Materials, Z. Hashin and C. T. Herakovich, eds., Pergamon Press (to be published).
18. Starnes, J. H., Jr. and Williams, J. G., "Failure Characteristics of Graphite-Epoxy Structural Components Loaded in Compression," IUTAM Symposium on Mechanics of Composite Materials, Z. Hashin and C. T. Herakovich, eds., Pergamon Press (to be published).
19. Nuismer, R. J. and Tan, S. C., "The Role of Matrix Cracking in the Continuum Constitutive Behavior of a Damaged Composite Ply," IUTAM Symposium on Mechanics of Composite Materials, Z. Hashin and C. T. Herakovich, eds., Pergamon Press (to be published).
20. Dow, N. F. and Gruntfest, I. J., "Determination of Most-Needed, Potentially Possible Improvements in Materials for Ballistic and Space Vehicles," Technical Information Series, R60SD369, General Electric, 1960.
21. Rosen, B. W., "Mechanics of Composite Strengthening. Fiber Composite Materials." American Society for Metals, 1965, pp. 37-75.
22. Schuerch, H., "Prediction of Compressive Strength in Uniaxial Boron Fiber-Metal Matrix Composite Materials," AIAA Journal, Vol. 4, No. 1, January 1966, pp. 102-106.
23. Foye, R. L., "Compression Strength of Unidirectional Composites," AIAA Paper 66-143, January 1966.

24. Herrmann, L. R., Mason, W. E., and Chan, S. T. K., "Response of Reinforcing Wires to Compressive States of Stress," *Journal of Composite Materials*, Vol. 1, 1967, pp. 212-226.
25. Sadowsky, M. A., Pu, S. L., and Hussain, M. A., "Buckling of Microfibers," *Journal of Applied Mechanics*, Vol. 34, December 1967, pp. 1011-1016.
26. Lanir, Y. and Fung, Y. C. B., "Fiber Composite Columns Under Compression," *Journal of Composite Materials*, Vol. 6, 1972, pp. 387-401.
27. Kiusalaas, J. and Juanzemis, W., "Internal Buckling of a Laminated Medium," *Fifth Southeastern Conference on Theoretical and Applied Mechanics*, G. L. Rodgers (Editor), University of North Carolina Press, 1970, pp. 151-173.
28. Lager, J. R. and June, R. R., "Compressive Strength of Boron-Epoxy Composites," *Journal of Composite Materials*, Vol. 3, 1969, pp. 48-56.
29. De Ferran, E. M. and Harris, B., "Compression Strength of Polyester Resin Reinforced with Steel Wires," *Journal of Composite Materials*, Vol. 4, 1970, pp. 62-72.
30. Greszczuk, L. B., "Compressive Strength and Failure Modes of Unidirectional Composites," *Analysis of the Test Methods for High Modulus Fibers and Composites*, ASTM STP 521, ASTM, 1973, pp. 192-217.
31. Greszczuk, L. B., "Microbuckling Failure of Circular Fiber-Reinforced Composites," *AIAA Paper No. 74-354*, April 1974.
32. Davis, J. G., Jr., "Compressive Strength of Fiber-Reinforced Composite Materials," *Composite Reliability*, ASTM STP 580, ASTM, 1975, pp. 364-377.
33. Suarez, J. A., Whiteside, J. B., and Hadcock, R. N., "The Influence of Local Failure Modes on the Compressive Strength of Boron-Epoxy Composites," *Composite Materials: Testing and Design (Second Conference)*, ASTM STP 497, ASTM, 1972, pp. 237-256.
34. Williams, J. G., and Rhodes, M. D., "The Effect of Resin on the Impact Damage Tolerance of Graphite-Epoxy Laminates," *NASA TM-83213*, October 1981.

II. DAMAGE PROPAGATION

Tension

1. Adams, D. F., "Longitudinal Tensile Behavior of Unidirectional Carbon-Carbon Composites," *Journal of Composite Materials*, Vol. 8, Oct. 1974, pp. 320-332.
2. Aveston, J. and Kelly, A., "Tensile First Cracking Strain and Strength of Hybrid Composites and Laminates," *Royal Society, Discussion on New Fibers and Their Composites*, London, England, May 18-19, 1978. *Royal Society, Philosophical Transactions, Series A*, Vol. 294, No. 1411, Jan. 21, 1980, pp. 519-534.
3. Bader, M. G., Bailey, J. E., Parvizi, A., Curtis, P. T., "The Mechanisms of Initiation and Development of Damage in Multi-Axial Fibre-Reinforced Plastics Laminates," in *Mechanical Behavior of Materials; Proceedings of the Third International Conference*, Cambridge, England, Aug. 20-24, 1979, Vol. 3, Oxford, Pergamon Press, 1980, pp. 227-239.
4. Barry, P. W., "The Longitudinal Tensile Strength of Unidirectional Fibrous Composites," *Journal of Materials Science*, Vol. 13, Oct. 1978, pp. 2177-2187.
5. Henriksen, M. and Thornton, H. R., "Material Damage of Graphite/Epoxy Composites Under Tensile Loading," *SAMPE Quarterly*, Vol. 10, Jan. 1979, pp. 15-20.
6. Herakovich, C. T., "On Failure Modes in Finite Width Angle Ply Laminates," in *Advances in Composite Materials: Proceedings of the Third International Conference on Composite Materials*, Paris, France, Aug. 26-29, 1980, Vol. 1, Oxford, Pergamon Press, 1980, pp. 425-435.
7. Herakovich, C. T., Davis, J. G., Jr. and Viswanathan, C. N., "Tensile and Compressive Behavior of Borsic/Aluminum," *Fourth Conference on Composite Materials: Testing and Design*, ASTM STP 617, 1977, pp. 344-357.
8. Kim, R. Y., "On the Off-Axis and Angle-Ply Strength of Composites," in *Test Methods and Design Allowables for Fibrous Composites; Proceedings of the Symposium*, Dearborn, Michigan, Oct. 2-3, 1979, ASTM, 1981, pp. 91-108.
9. Lifshitz, J. M. and Rotem, A., "An Observation on the Strength of Unidirectional Fibrous Composites," *Journal of Composite Materials*, Vol. 4, January 1970, pp. 133-135.
10. Pagano, N. J., "Analysis of the Flexure Test of Bidirectional Composites," *Journal of Composite Materials*, Vol. 1, Oct. 1967, pp. 336-343.
11. Riggs, D., "Prediction of the Transverse Strength of Graphite/Aluminum Composites," in *New Developments and Applications in Composites: Proceedings of the Symposium*, St. Louis, Missouri, Oct. 16-17, 1978, *Metallurgical Society of AIME*, 1979, pp. 252-260.
12. Rosen, B. W., "Tensile Failure of Fibrous Composites," *AIAA Journal*, Vol. 2, 1964, p. 1985.

13. Yeow, Y. T. and Brinson, M. F., "An Experimental Investigation of the Tensile Moduli and Strengths of Graphite Epoxy Laminates," *Experimental Mechanics*, Vol. 17, No. 11, Nov. 1977.
14. Sandhu, R. S., "Analytical-Experimental Correlation of the Behavior of 0° , $\pm 45^\circ$, 90° Family of AS/3501-5 Graphite Epoxy Composite Laminates Under Uniaxial Tensile Loading," Air Force Flight Dynamics Laboratory, AFFDL-TR-79-3064, May 1979.
15. Sandhu, R. S., Gallo, R. L., and Sendeckyj, G. P., "Initiation and Accumulation of Damage in Composite Laminates," ASTM Sixth Conference on Composite Materials: Testing and Design, May 12-13, 1981.

Compression

1. Card, M. F. and Rhodes, M. D., "Graphite Epoxy Panel Compression Strength Reduction Due to Local Impact," presented at the AGARD 50th Meeting of the Structures and Materials Panel Specialists Meeting on the Effect of Service Environment on Composite Materials, Athens, Greece, April 13-18, 1980.
2. Chang, M. and Scala, E., "Plastic Deformation Processing and Compressive Failure Mechanism in Aluminum Composite Materials," Third Conference on Composite Materials: Testing and Design, ASTM STP 546, pp. 561-579.
3. Chou, T. W. and Kelly, A., "The Effect of Transverse Shear on the Longitudinal Compressive Strength of Fibre Composites," *Journal of Materials Science*, Vol. 15, Feb. 1980, pp. 327-331.
4. Chou, T. W., Stewart, W. B., Bader, M. G., "On the Compression Strength of Glass-Epoxy Composites," in *New Developments and Applications in Composites: Proceedings of the Symposium*, St. Louis, Missouri, Oct. 16-17, 1978, Metallurgical Society of AIME, 1979, pp. 331-346.
5. Clark, R. K. and Lisagor, W. B., "Compression Testing of Graphite/Epoxy Composite Materials," in *Test Methods and Design Allowables for Fibrous Composites: Proceedings of the Symposium*, Dearborn, Michigan, Oct. 2-3, 1979, American Society for Testing and Materials, 1981, pp. 34-53.
6. Davis, J. G., Jr., "Compressive Strength of Fiber-Reinforced Composite Materials," *Composite Reliability*, ASTM STP 580, 1975, pp. 364-377.
7. Hahn, H. T., "Effect of Constituent Properties on Composite Strength," presented at the 24th Annual SAMPE Symposium, San Francisco, California, May 8-10, 1979.
8. Hanasaki, S. and Hasegawa, Y., "Compressive Strength of Unidirectional Fibrous Composites," *Journal of Composite Materials*, Vol. 8, July 1974, pp. 306-309.

9. Lager, J. R. and June, R., "Compressive Strength of Boron-Epoxy Composites," *Journal of Composite Materials*, Vol. 3, Jan. 1969, pp. 48-57.
10. Lanir, Y. and Fung, Y. C. B., "Fiber Composite Columns Under Compression," *Journal of Composite Materials*, Vol. 6, July 1972, pp. 387-402.
11. Mikulas, M. M., Jr., "Failure Prediction Techniques for Compression Loaded Composite Laminates with Holes," in *Selected NASA Research in Composite Materials and Structures*, 1980, pp. 1-33.
12. Nuismer, R. J. and Labor, J. D., "Applications of the Average Stress Failure Criterion II - Compression," *Journal of Composite Materials*, Vol. 13, Jan. 1979, pp. 49-60.
13. Ryder, J. T. and Black, E. D., "Compression Testing of Large Gauge Length Composite Coupons," *Fourth Conference on Composite Materials: Testing and Design*, ASTM STP 617, 1977, pp. 170-189.
14. Starnes, J. H., Jr., Rhodes, M. D., and Williams, J. G., "Effect of Impact Damage and Holes on the Compressive Strength of a Graphite/Epoxy Laminate," in *Nondestructive Evaluation and Flaw Criticality for Composite Materials; Proceedings of the Symposium*, Philadelphia, Pennsylvania, Oct. 10-11, 1978, ASTM, 1979, pp. 145-171.
15. Weller, T., "Analytical and Experimental Studies of Graphite-Epoxy and Boron-Epoxy Angle-Ply Laminates in Compression," NASA CR-145234, 1977.
16. Weller, T., "Experimental Studies of Graphite-Epoxy and Boron-Epoxy Angle-Ply Laminates in Compression," NASA CR-145233, 1977.
17. Knauss, J. F., "The Compressive Failure of Graphite/Epoxy Plates with Circular Holes," *Composites Technology Review*, Vol. 3, Summer, 1981.

Shear

1. Adams, D. F. and Doner, D. R., "Longitudinal Shear Loading of a Unidirectional Composite," *Journal of Composite Materials*, Vol. 1, Jan. 1967, pp. 4-17.
2. Hayford, D. T., Hennecke, E. G., II and Stinchcomb, W. W., "The Correlation of Ultrasonic Attenuation and Shear Strength in Graphite-Polyimide Composites," *Journal of Composite Materials*, Vol. 11, Oct. 1977, pp. 429-444.
3. Johnson, J. W., "Fracture Mechanisms and Crack Propagation in Cross-Ply Laminates Tested by the Short Beam Shear Technique," *Plastics and Rubber Institute, Interfaces in Composite Materials*, University of Liverpool, England, April 1-2, 1981.
4. Kaminski, B. E. and Ashton, J. E., "Diagonal Tension Behavior of Boron-Epoxy Shear Panels," *Journal of Composite Materials*, Vol. 5, Oct. 1971, p. 553.
5. Sayers, K. H. and Harris, B., "Interlaminar Shear Strength of a Carbon Fibre Reinforced Composite Material Under Impact Conditions," *Journal of Composite Materials*, Vol. 7, Jan. 1973, pp. 129-133.

6. Sims, D. F., "In-Plane Shear Stress Strain Response of Unidirectional Composite Materials," Journal of Composite Materials, Vol. 7, Jan. 1973, pp. 124-128.
7. Slepetz, J. M., Zagaeski, T. F. and Novello, R. F., "In-Plane Shear Test for Composite Materials," Army Materials and Mechanics Research Center, AMMRC-TR-78-30, 1978.
8. Weller, T., "Analytical and Experimental Studies of Graphite-Epoxy and Boron-Epoxy Angle Ply Laminates in Shear," NASA CR-145232, 1977.
9. Weller, T., "Experimental Studies of Graphite-Epoxy and Boron-Epoxy Angle Ply Laminates in Shear," NASA CR-145231, 1977.

Combined Loads

1. Daniel, I. M., "Deformation and Failure of Composite Laminates with Cracks in Biaxial Stress Fields," Verein Deutscher Ingenieure, Internationale Konferenz ueber experimentelle Spannungsanalyse, 6th, Munich, West Germany, Sept. 18-22, 1978. VDI-Berichte, No. 313, 1978, pp. 705-710.
2. Francis, P. H., "Biaxial Fatigue of Composites," Mechanics of Composites Review, USAF, October 1976, pp. 209-220.
3. Francis, P. H., Walrath, D. E. and Weed, D. N., "Investigation of First Ply Failure in Graphite/Epoxy Laminates Subjected to Biaxial Static and Fatigue Loadings," Air Force Materials Laboratory, AFML-TR-77-62, June 1977.
4. McLaughlin, P. V., Jr. and Rosen, B. W., "Combined Stress Effects Upon Failure of Fiber Composites," Materials Sciences Corporation Report TFR/7404, Blue Bell, PA, April 1974.
5. Parry, T. V. and Wronski, A. S., "Kinking and Tensile, Compressive and Interlaminar Shear Failure in Carbon-Fibre-Reinforced Plastic Beams Tested in Flexure," Journal of Materials Science, Vol. 16, Feb. 1981, pp. 439-450.
6. Saint-John, C. F. and Streets, K. N., "B-Al Composite Failure Under Combined Torsion and Tension Loading," Journal of Composite Materials, Vol. 8, July 1974, pp. 266-274.

III. DELAMINATION AND STRESS CONCENTRATIONS

1. Baillie, J. A., Duggan, M. F. and Fisher, L. M., "The Influence of Holes on the Compression Strength of Graphite Epoxy Cloth and Tape Laminate at Temperatures Up to 430 K," in *Advances in Composite Materials; Proceedings of the Third International Conference on Composite Materials*, Paris, France, Aug. 26-29, 1980, Vol. 1, Oxford, Pergamon Press, 1980, pp. 198-211.
2. Beaumont, P. W. R. and Phillips, D. C., "Tensile Strengths of Notched Composites," *Journal of Composite Materials*, Vol. 6, January 1972, pp. 32-47.
3. Chai, H., Babcock, C. D. and Knauss, W. G., "One-Dimensional Modeling of Failure in Laminated Plates by Delamination Buckling," *International Journal of Solids and Mechanics*, Vol. 17, No. 11, 1981, pp. 1069-1083.
4. Chou, S. C., Orringer, O. and Rainey, J. H., "Post-Failure Behavior of Laminates: II - Stress Concentration," *Journal of Composite Materials*, Vol. 11, January 1977, pp. 71-78.
5. Crossman, F. W., "Analysis of Free Edge Induced Failure of Composite Laminates," in *Proceedings of the First USA-USSR Symposium on Fracture of Composite Materials*, Riga, Latvian SSR, Sept. 4-7, 1978. Alphen aan den Rijn, Netherlands, Sijthoff and Noordhoff International Publishers, 1979, pp. 291-302.
6. Crossman, F. W. and Wang, A. S. D., "The Dependence of Transverse Cracking and Delamination on Ply Thickness in Graphite/Epoxy Laminates," *Proceedings of the ASTM Symposium "Damage in Composite Materials: Basic Mechanisms, Accumulation, Tolerance and Characterization"*, Bal Harbour, Florida, November 1980.
7. Crossman, F. W., Warren, W. J., Wang, A. S. D. and Law, G. E., Jr., "Initiation and Growth in Transverse Cracks and Edge Delamination in Composite Laminates. II - Experimental Correlation," *Journal of Composite Materials Supplement*, Vol. 14, No. 1, 1980, pp. 88-108.
8. Cruse, T. A., "Tensile Strength of Notched Composites," *Journal of Composite Materials*, Vol. 7, April 1973, p. 218.
9. de Charentenay, F. X. and Benzeggagh, M., "Fracture Mechanics of Mode I Delamination in Composite Materials," in *Advances in Composite Materials; Proceedings of the Third International Conference on Composite Materials*, Paris, France, Aug. 26-29, 1980, Vol. 1, Oxford, Pergamon Press, 1980, pp. 186-197.
10. Devitt, D. F., Schapery, R. A., and Bradley, W. L., "A Method for Determining the Mode I Delamination Fracture Toughness of Elastic and Viscoelastic Composite Materials," *Journal of Composite Materials*, Vol. 14, Oct. 1980, pp. 270-285.
11. Herakovich, C. T., "On the Relationship Between Engineering Properties and Delamination of Composite Laminates," NASA CR-163956, February 1981. Also in *Journal of Composite Materials*, Vol. 15, July 1981, pp. 336-348.

12. Konishi, D. Y. and Johnston, W. R., "Fatigue Effects on Delamination and Strength Degradation in Graphite/Epoxy Laminates," in Proceedings of the Fifth Conference on Composite Materials: Testing and Design, New Orleans, Louisiana, March 20-22, 1978, ASTM, 1979, pp. 597-619.
13. Richards, R. J., Buck, O. and Morris, W. I., "Effects of Flaws on Delamination of Composites," Report No. SC5255.8FR, Rockwell International Science Center, Thousand Oaks, California, April 1981.
14. Salamon, N. J., "An Assessment of the Interlaminar Stress Problem in Laminated Composites," Journal of Composite Materials Supplement, Vol. 14, No. 1, 1980, pp. 177-194.
15. Takeda, N., "Experimental Studies of the Delamination Mechanisms in Impacted Fiber-Reinforced Composite Plates," Ph.D. Thesis, Florida University, Gainesville, 1980.
16. Tarnopolskii, Iu. M., "A Delamination Failure Mode of Composite Bars in Compression," in Proceedings of the First USA-USSR Symposium on Fracture of Composite Materials, Riga, Latvian SSR, Sept. 4-7, 1978. Alphen aan den Rijn, Netherlands, Sijthoff and Noordhoff International Publishers, 1979, pp. 159-169.
17. Troshin, V. P., "Stability of Cylindrical Shells with Delaminations," Mekhanika Kompozitnykh Materialov, July-Aug. 1981, pp. 729-731 (in Russian).
18. Updike, D. P. and Yuceoglu, U., "Delamination of Layered Cylindrical Shells Under Internal Pressure," Winter Annual Meeting of Americal Society of Mechanical Engineers, Chicago, Illinois, Nov. 16-21, 1980.
19. Wang, A. S. D., "Growth Mechanisms of Transverse Cracks and Ply Delaminations in Composite Laminates," Proceedings of the Third International Conference on Composite Materials, Paris, France, August 1980, p. 170.
20. Wang, A. S. D. and Crossman, F. W., "Initiation and Growth of Transverse Cracks and Edge Delamination in Composite Laminates. I - An Energy Method," Journal of Composite Materials Supplement, Vol. 14, No. 1, 1980, pp. 71-87.
21. Wang, S. S., "An Analysis of Delamination in Angle-Ply Fiber Reinforced Composites," Winter Annual Meeting of American Society of Mechanical Engineers, San Francisco, California, Dec. 12-15, 1978. ASME, Transactions, Journal of Applied Mechanics, Vol. 47, March 1980, pp. 64-70.
22. Wang, S. S., "Delamination Crack Growth in Unidirectional Fiber-Reinforced Composites Under Static and Cyclic Loading," in Composite Materials: Testing and Design; Proceedings of the Fifth Conference, New Orleans, Louisiana, March 20-22, 1978, ASTM, 1979, pp. 642-663.
23. Wang, S. S., "Edge Delamination in Angle-Ply Composite Laminates," in 22nd Structures, Structural Dynamics and Materials Conference, Atlanta, Georgia, April 6-8, 1981, Technical Papers, Part I, New York, AIAA, 1981, pp. 473-484.

24. Whitcomb, J. D., "Finite Element Analysis of Instability-Related Delamination Growth," NASA TM-81964, 1981.
25. Garbo, S. P. and Ogonowski, J. M., "Design Strength and Life of Mechanically Fastened Composite Joints - Literature Survey," Air Force Flight Dynamics Laboratory, AFFDL-TR-78-179, 1978.
26. Garbo, S. P. and Ogonowski, J. M., "Strength Predictions of Composite Laminates with Unloaded Fastener Holes," AIAA Journal, May 1980 (presented at 20th SDM Conference, April 1979).
27. Garbo, S. P., "Compression Strength of Laminates with Unloaded Fastener Holes," presented at 21st SDM Conference, AIAA, May 12-14, 1980.
28. Garbo, S. P. and Ogonowski, J. M., "Effect of Variances and Manufacturing Tolerances on the Design Strength and Life of Mechanically Fastened Composite Joints," Air Force Wright Aeronautical Laboratory, AFWAL-TR-81-3041, three volumes, April 1981.
29. Garbo, S. P. and Gallo, R. L., "Strength of Laminates with Loaded Holes," presented at Fifth DOD/NASA Conference on Fibrous Composites in Structural Design, January 27-29, 1981.
30. Garbo, S. P., "Effect of Bearing/Bypass Load Interaction on Laminate Strength," Air Force Wright Aeronautical Laboratory, AFWAL-TR-81-3114, September 1981.
31. Garbo, S. P. and Buchanan, D., "Design of Highly Loaded Composite Joints and Attachments for Wing Structures," Naval Air Development Command, NADC-81194-60, August 1981.
32. Hedgepeth, J. M., "Stress Concentrations for Filamentary Structures," NASA TN-D-882, 1961.
33. Hedgepeth, J. M. and Van Dyke, P., "Local Stress Concentrations in Imperfect Filamentary Composite Materials," Journal of Comp. Mater., Vol. 1, 1967, pp. 294-309.
34. Van Dyke, P. and Hedgepeth, J. M., "Stress Concentrations from Single Filament Failures in Composite Materials," Textile Research, Vol. 39, 1969, pp. 613-626.
35. Zweben, C., "Fracture Mechanics and Composite Materials: A Critical Analysis," Special Technical Publication 521, ASTM, 1973, pp. 63-97.
36. Zweben, C., "An Approximate Method of Analysis for Notched Unidirectional Composites," Engineering Fracture Mechanics, Vol. 6, 1974, pp. 1-10.
37. Goree, J. G. and Gross, R. S., "Analysis of a Unidirectional Composite Containing Broken Fibers and Matrix Damage," Engineering Fracture Mechanics, Vol. 13, 1979, pp. 563-578.

38. Goree, J. G. and Gross, R. S., "Stresses in a Three-Dimensional Unidirectional Composite Containing Broken Fibers," *Engineering Fracture Mechanics*, Vol. 13, 1979, pp. 395-405.
39. Goree, J. G. and Wilson, E. B., Jr., "Transverse Shear Loading in an Elastic Matrix Containing Two Elastic Circular Cylindrical Inclusions," *Journal of Applied Mechanics*, Vol. 34, 1967, pp. 511-513.
40. Sova, J. A. and Poe, C. C., Jr., "Tensile Stress-Strain Behavior of Boron/Aluminum Laminates," NASA TP-1117, 1978.
41. Poe, C. C., Jr., "A Single Fracture Toughness Parameter for Fibrous Composite Laminates," NASA TM-81911, 1981.
42. Goree, J. G., Dharani, L. R. and Jones, W. F., "Mathematical Modeling of Damage in Unidirectional Composites," NASA CR-3453, August 1981. (Also in press in *Engineering Fracture Mechanics*.)

Delamination

1. Altus, E., Rotem, A. and Shmueli, M., "Free Edge Effect in Angle Ply Laminates - A New Three-Dimensional Finite Difference Solution," *Journal of Composite Materials*, Vol. 14, January 1980, pp. 21-30.
2. Crossman, F. W., "Analysis of Free Edge Induced Failure of Composite Laminates," in *Proceedings of the First USA-USSR Symposium on Fracture of Composite Materials*, Riga, Latvian SSR, Sept. 4-7, 1978. Alphen aan den Rijn, Netherlands, Sijthoff and Noordhoff International Publishers, 1979, pp. 291-302.
3. Harris, A. and Orringer, O., "Investigation of Angle Ply Delamination Specimen for Interlaminar Strength Test," *Journal of Composite Materials*, Vol. 12, July 1978, pp. 285-299.
4. Herakovich, C. T., Nagarkar, A. and O'Brien, D. A., "Failure Analysis of Composite Laminates with Free Edges," in *Modern Developments in Composite Materials and Structures; Proceedings of the Winter Annual Meeting*, New York, Dec. 2-7, 1979, ASME, 1979, pp. 53-66.
5. Hsu, P. W. and Herakovich, C. T., "Edge Effects in Angle Ply Composite Laminates," *Journal of Composite Materials*, Vol. 11, Oct. 1977, pp. 422-428.
6. Isakson, G. and Levy, A., "Finite Element Analysis of Interlaminar Shear in Fibrous Composites," *Journal of Composite Materials*, Vol. 5, April 1971, pp. 273-276.
7. Konishi, D. Y. and Johnston, W. R., "Fatigue Effects on Delaminations and Strength Degradation in Graphite/Epoxy Laminates," in *Composite Materials: Testing and Design; Proceedings of the Fifth Conference*, New Orleans, Louisiana, March 20-22, 1978, ASTM, 1979, pp. 597-619.
8. Pagano, N. J., "Free Edge Stress Fields in Composite Laminates," *International Journal of Solids and Structures*, Vol. 14, 1978, pp. 401-406.

9. Peters, P. W. M., "The Interlaminar Shear Strength of Unidirectional Boron/Aluminum Composites," *Journal of Composite Materials*, Vol. 12, January 1978, pp. 53-62.
10. Reifsnider, K. L., Hennecke, E. G., II and Stinchcomb, W. W., "Delamination in Quasi-Isotropic Graphite-Epoxy Laminates," *Fourth Conference on Composite Materials: Testing and Design*, ASTM STP 617, 1977, pp. 93-105.
11. Stalnaker, D. O. and Stinchcomb, W. W., "Load History - Edge Damage Studies in Two Quasi-Isotropic Graphite Epoxy Laminates," in *Composite Materials: Testing and Design; Proceedings of the Fifth Conference*, New Orleans, Louisiana, March 20-22, 1978, ASTM, 1979, pp. 620-641.
12. Tarnopolskii, Iu. M., "A Delamination Failure Mode of Composite Bars in Compression," in *Proceedings of the First USA-USSR Symposium on Fracture of Composite Materials*, Riga, Latvian SSR, Sept. 4-7, 1978. Alphen aan den Rijn, Netherlands, Sijthoff and Noordhoff International Publishers, 1979, pp. 159-169.
13. Wang, A. S. D. and Crossman, F. W., "Some New Results on Edge Effect in Symmetric Composite Laminates," *Journal of Composite Materials*, Vol. 11, January 1977, pp. 92-106.
14. Wang, A. S. D. and Crossman, F. W., "Edge Effects on Thermally Induced Stresses in Composite Laminates," *Journal of Composite Materials*, Vol. 11, July 1977, pp. 300-312.
15. Wang, A. S. D. and Crossman, F. W., "Calculation of Edge Stresses in Multi-Layer Laminates by Sub-Structuring," *Journal of Composite Materials*, Vol. 12, January 1978, pp. 76-83.
16. Wang, S. S., "An Analysis of Delamination in Angle Ply Fiber Reinforced Composites," *ASME, Transactions, Journal of Applied Mechanics*, Vol. 47, March 1980, pp. 64-70.
17. Wang, S. S., "Delamination Crack Growth in Unidirectional Fiber-Reinforced Composites Under Static and Cyclic Loading," in *Composite Materials: Testing and Design; Proceedings of the Fifth Conference*, New Orleans, Louisiana, March 20-22, 1978, ASTM, 1979, pp. 642-663.
18. Whitney, J. M. and Browning, C. E., "Free Edge Delamination of Tensile Coupons," *Journal of Composite Materials*, Vol. 6, April 1972, pp. 300-303.
19. Whitcomb, J. D., Raju, J. S. and Goree, J. G., "Reliability of the Finite Element Method for Calculating Free Edge Stresses in Composite Laminates," *Computers and Structures*, Vol. 15, No. 1, 1982, pp. 23-37.
20. Raju, J. S. and Crews, J. H., Jr., "Interlaminar Stress Singularities at a Straight Free Edge in Composite Laminates," *Computers and Structures*, Vol. 14, No. 1-2, 1981, pp. 21-28.
21. Pipes, R. Byron, and Pagano, N. J., "Interlaminar Stresses in Composite Laminates Under Uniform Axial Extension," *Journal of Composite Materials*, Vol. 4, October 1970, pp. 538-548.

22. Pagano, N. J. and Pipes, R. Byron, "The Influence of Stacking Sequence on Laminate Strength," *Journal of Composite Materials*, Vol. 5, January 1971, pp. 50-57.
23. Pipes, R. B., Kaminski, B. E. and Pagano, N. J., "Influence of the Free Edge Upon the Strength of Angle-Ply Laminates," *Analysis of the Test Methods for High Modulus Fibers and Composites*, ASTM STP 521, ASTM, 1973, pp. 218-228.
24. Pipes, R. Byron, and Pagano, N. J., "Interlaminar Stresses in Composite Laminates - An Approximate Elasticity Solution," *Journal of Applied Mechanics*, Vol. 41, No. 3, September 1974, pp. 668-672.

Stress Concentrations

1. Bailie, J. A., Duggan, M. F., Fisher, L. M., Dickson, J. N., "The Influence of Holes on the Compression Strength of Graphite Epoxy Cloth and Tape Laminate at Temperatures up to 430 K," in *Advances in Composite Materials: Proceedings of the Third International Conference on Composite Materials*, Paris, France, Aug. 26-29, 1980, Vol. 1, Oxford, Pergamon Press, 1980, pp. 198-211.
2. Barker, R. M. and MacLaughlin, T. F., "Stress Concentrations Near a Discontinuity in Fibrous Composites," *Journal of Composite Materials*, Vol. 5, Oct. 1971, pp. 492-503.
3. Gerstner, R. W. and Dundurs, J., "Representation of Stress Concentration Factors for a Composite in Plane Strain," *Journal of Composite Materials*, Vol. 3, Jan. 1969, pp. 108-115.
4. Greszczuk, L. B., "Stress Concentrations and Failure Criteria for Orthotropic and Anisotropic Plates with Circular Openings," *Second Conference on Composite Materials: Testing and Design*, ASTM STP 497, 1972, pp. 363-381.
5. Knauss, J. F. and Henneke, E. G., "The Compressive Failure of Graphite/Epoxy Plates with Circular Holes," *Composites Technology Review*, Vol. 3, 1981, pp. 64-75.
6. Kulkarni, S. V., Rosen, B. W. and Zweben, C., "Load Concentration Factors for Circular Holes in Composite Laminates," *Journal of Composite Materials*, Vol. 7, July 1973, pp. 387-393.
7. Nuismer, R. J. and Whitney, J. M., "Uniaxial Failure of Composite Laminates Containing Stress Concentrations," *Fracture Mechanics of Composites*, ASTM STP 593, 1975, pp. 117-142.
8. Padawer, G. E., "The Notch Sensitivity of Boron Film Reinforced Composites," *Journal of Composite Materials*, Vol. 8, Oct. 1974, pp. 333-339.
9. Pipes, R. B., Gillespie, J. W., Jr. and Wetherhold, R. C., "Notched Strength of Composite Materials," *Journal of Composite Materials*, Vol. 13, April 1979, pp. 148-160.

10. Pipes, R. B., Gillespie, J. W., Jr. and Wetherhold, R. C., "Superposition of the Notched Strength of Composite Laminates," *Polymer Engineering and Science*, Vol. 19, No. 16, Dec. 1979, pp. 1151-1155.
11. Ueng, C. E. S., Aberson, J. A. and Lafitte, B. A., "Tensile Analysis of An Edge Notch in a Unidirectional Composite," *Journal of Composite Materials*, Vol. 11, April 1977, pp. 222-234.
12. Whitney, J. M. and Nuismer, R. J., "Stress Fracture Criteria for Laminated Composites Containing Stress Concentrations," *Journal of Composite Materials*, Vol. 8, July 1974, pp. 253-265.
13. Xing-Juan, X., "Tensile Failure Behavior of Edge Notch in Carbon Fiber Reinforced Epoxy Composite Material," in *Advances in Composite Materials: Proceedings of the Third International Conference on Composite Materials*, Paris, France, Aug. 26-29, 1980, Vol. 1, Oxford, Pergamon Press, 1980, pp. 212-222.
14. Rhodes, M. D., Mikulas, M. M., Jr., and McGowan, P. E., "Effect of Orthotropic Properties and Panel Width on the Compression Strength of Graphite-Epoxy Laminates with Holes," *AIAA Paper 82-0749*, May 1982.
15. de Jong, Th., "Stresses Around Pin-Loaded Holes in Composite Materials," *IUTAM Symposium on Mechanics of Composite Materials*, Z. Hashin and C. T. Herakovich, eds., Pergamon Press (to be published).

IV. FAILURE CRITERIA AND STRENGTH THEORIES

1. Chamis, C. C. and Sullivan, T. L., "In Situ Ply Strength: An Initial Assessment," NASA TM-73771, 1978.
2. Chou, P. C., McNamee, B. M. and Chou, D. K., "The Yield Criterion of Laminated Media," Journal of Composite Materials, Vol. 7, Jan. 1973, pp. 22-35.
3. Collins, B. R. and Crane, R. L., "A Graphical Representation of the Failure Surface of a Composite," Journal of Composite Materials, Vol. 5, July 1971, pp. 408-413.
4. Dvorak, G. J., Rao, M. S. M. and Tarn, J. Q., "Yielding in Unidirectional Composites Under External Loads and Temperature Changes," Journal of Composite Materials, Vol. 7, April 1973, pp. 194-217.
5. Eckold, G. C., Leadbetter, D., Soden, P. D. and Griggs, P. R., "Lamination Theory in the Prediction of Failure Envelopes for Filament Wound Materials Subjected to Biaxial Loading," Composites, Vol. 9, Oct. 1978, pp. 243-246.
6. Goldenblat, I. I. and Kopnov, V. A., "Strength Criteria for Anisotropic Materials," Izvestia Akademii Nauk SSR, Mekhanika, No. 6, 1965, pp. 77-83.
7. Hashin, Z., "Failure Criteria for Unidirectional Fiber Composites," ASME, Transactions, Journal of Applied Mechanics, Vol. 47, June 1980, pp. 329-334.
8. Hashin, Z. and Rotem, A., "A Fatigue Failure Criterion for Fiber Reinforced Materials," Journal of Composite Materials, Vol. 7, Oct. 1973, pp. 448-465.
9. Nagarkar, A. P. and Herakovich, C. T., "Nonlinear Temperature Dependent Failure Analysis of Finite Width Composite Laminates," NASA CR-162868, Dec. 1979.
10. Narayanaswami, R. and Adelman, H. M., "Evaluation of the Tensor Polynomial and Hoffman Strength Theories for Composite Materials," Journal of Composite Materials, Vol. 11, October 1977, pp. 366-377.
11. Sandhu, R. S., "A Survey of Theories of Failure of Isotropic and Anisotropic Materials," Air Force Flight Dynamics Laboratory, AFFDL-TR-72 71, 1972.
12. Snell, M. B., "Strength and Elastic Response of Symmetric Angle Ply Carbon Fibre Reinforced Plastics," Royal Aircraft Establishment Report RAE-TR-76091, England, 1978.
13. Sun, C. T. and Yamada, S. E., "Strength Distribution of a Unidirectional Fiber Composite," Journal of Composite Materials, Vol. 12, April 1978, p. 169.
14. Tennyson, R. C., "Application of the Cubic Strength Criterion to the Failure Analysis of Composite Structures," NASA CR-165712, May 1981.

15. Tennyson, R. C., MacDonald, D. and Nanyaro, A. P., "Evaluation of the Tensor Polynomial Failure Criterion for Composite Materials," Journal of Composite Materials," Vol. 12, Jan. 1978, p. 63.
16. Tennyson, R. C., Nanyard, A. P. and Wharram, G. E., "Application of the Cubic Polynomial Strength Criterion to the Failure Analysis of Composite Materials," Journal of Composite Materials Supplement, Vol. 14, No. 1, 1980, pp. 28-41.
17. Tsai, S. W. and Azzi, V. D., "Strength of Laminated Composite Materials," AIAA Journal, Vol. 4, No. 2, Feb. 1966, p. 296.
18. Tsai, S. W. and Wu, E. M., "A General Theory of Strength for Anisotropic Materials," Journal of Composite Materials, Vol. 5, 1971, pp. 58-80.
19. Wu, E. M. and Scheublein, G., "Laminate Strength - A Direct Characterization Procedure," ASTM STP 546, 1974, p. 188.
20. Wu, E. M., "Three-Dimensional Strength Characterization of Thick Composite Laminates," Duke University Research Workshop on Mechanics of Composite Materials, 1978, pp. 195-200.
21. Wu, E. M., "Phenomenological Anisotropic Failure Criterion," Composite Materials, Vol. 2, (edited by G. P. Sendeckyj), Academic Press, 1974, pp. 353-431.
22. Vicario, A. A., Jr. and Toland, R. H., "Failure Criteria and Failure Analysis of Composite Structural Components," Chapter 2 in Structural Design and Analysis, Part I, (edited by C. C. Chamis), Composite Materials, Vol. 7, Academic Press, 1974, pp. 51-97.
23. Sandhu, R. S., "Ultimate Strength Analysis of Symmetric Laminates," Air Force Flight Dynamics Laboratory, AFFDL-TR-73-137, February 1974.
24. Craddock, J. N. and Champagne, D. J., "A Comparison of Failure Criteria for Laminated Composite Materials," AIAA Paper No. 82-0739, 1982.
25. Hoffman, O., "The Brittle Strength of Orthotropic Materials," Journal of Composite Materials, Vol. 1, 1967.
26. Puppo, A. H. and Evensen, H. A., "Strength of Anisotropic Materials Under Combined Stresses," AIAA Journal, Vol. 10, April 1972.
27. Chamis, C. C., "Failure Criteria for Filamentary Composites," NASA TN-5367, 1969.
28. Sendeckyj, G. P., "A Brief Survey of Empirical Multiaxial Strength Criteria for Composites," Composite Materials: Testing and Design (Second Conference), ASTM STP 497, 1971, pp. 41-51.

V. POSTBUCKLING OF FIBROUS COMPOSITE STRUCTURES

1. Agarwal, B. L., "Postbuckling Behavior of Composite Shear Webs," in 21st Structures, Structural Dynamics and Materials Conference, Seattle, Washington, May 12-14, 1980, Technical Papers, Part 1, New York, AIAA, 1980, pp. 210-218.
2. Ashton, J. E. and Love, T. S., "Experimental Study of the Stability of Composite Plates," Journal of Composite Materials, Vol. 3, April 1969, pp. 230-243.
3. Bhatia, N. M., "Postbuckling Fatigue Behavior of Advanced Composite Shear Panels," Army Materials and Mechanics Research Center, AMMRC MS-76-3, 1976, p. 8.
4. Dickson, J. N., Biggers, S. B. and Wang, J. T. S., "A Preliminary Design Procedure for Composite Panels with Open-Section Stiffeners Loaded in the Postbuckling Range," in Advances in Composite Materials: Proceedings of the Third International Conference on Composite Materials, Paris, France, Aug. 26-29, 1980, Vol. 1, Oxford, Pergamon Press, 1980, pp. 812-825.
5. Knutsson, L., "Theoretical and Experimental Investigation of the Buckling and Postbuckling Characteristics of Flat CFRP Panels Subjected to Compression," Report No. FFA-TN-HU-1934, Aeronautical Research Institute of Sweden, Stockholm, 1978.
6. Noor, A. K. and Peters, J. M., "Bifurcation and Postbuckling Analysis of Laminated Composite Plates Via Reduced Basis Technique," Computer Methods in Applied Mechanics and Engineering, Vol. 29, 1981, pp. 271-295.
7. Ostrom, R. B., "Postbuckling Fatigue Behavior of Flat, Stiffened Graphite/Epoxy Panels Under Shear Loading," Report No. NADC-78137-60, Naval Air Development Command, 1981.
8. Rhodes, J. E., "Postbuckling and Membrane Structural Capability of Composite Shell Structures," in Advances in Composite Materials: Proceedings of the Third International Conference on Composite Materials, Paris, France, Aug. 26-29, 1980, Vol. 2, Oxford, Pergamon Press, 1980, pp. 1707-1720.
9. Rhodes, J. E., "Effect of Postbuckling on the Fatigue of Composite Structures," in Fatigue of Fibrous Composite Materials; Proceedings of the Symposium, San Francisco, California, May 22-23, 1979, ASTM, 1981, pp. 3-20.
10. Samuelson, L. A., Vestergren, P., Knutsson, L., Gamziukas, V., and Wangberg, K. G., "Stability and Ultimate Strength of Carbon Fiber Reinforced Plastic Panels," in Advances in Composite Materials; Proceedings of the Third International Conference on Composite Materials, Paris, France, Aug. 26-29, 1980, Vol. 1, Oxford, Pergamon Press, 1980, pp. 327-341.
11. Spier, E. E. and Wang, G., "On Buckling of Unidirectional Boron/Aluminum Stiffeners - A Caution to Designers," Journal of Composite Materials, Vol. 9, Oct. 1975, pp. 347-360.

12. Starnes, J. H., Jr. and Rouse, M., "Postbuckling and Failure Characteristics of Selected Flat Rectangular Graphite-Epoxy Plates Loaded in Compression," in 22nd Structures, Structural Dynamics and Materials Conference, Atlanta, Georgia, April 6-8, 1981, Technical Papers, Part 1, New York, AIAA, 1981, pp. 423-434.
13. Vestergren, P. and Knutsson, L., "Theoretical and Experimental Investigation of the Buckling and Postbuckling Characteristics of Flat Carbon Fibre Reinforced Plastic/CFRP/Panels Subjected to Compression on Shear Loads," in Proceedings of the 11th Congress of the International Council of the Aeronautical Sciences, Lisbon, Portugal, Sept. 10-16, 1978, Vol. 1, Cologne, International Council of the Aeronautical Sciences Secretariat, 1978, pp. 217-223.
14. Whitney, J. M., "Shear Buckling of Unsymmetrical Cross-Ply Plates," Journal of Composite Materials, Vol. 3, April 1969, pp. 359-363.
15. Williams, J. G. and Stein, M., "Buckling Behavior and Structural Efficiency of Open-Section Stiffened Composite Compression Panels," AIAA Journal, Vol. 14, No. 11, Nov. 1976, pp. 1618-1626.
16. Starnes, J. H., Knight, N. F., Jr., and Rouse, M., "Postbuckling Behavior of Selected Flat Stiffened Graphite-Epoxy Panels Loaded in Compression," AIAA Paper 82-0777, May 1982.
17. Stein, M., "Postbuckling of Orthotropic Composite Plates Loaded in Compression," AIAA Paper 82-0778, May 1982.
18. Noor, A. K. and Peters, J. M., "Recent Advances in Reduction Methods for Instability Analysis of Structures," Computers and Structures, Vol. 16, Nos. 1-4, 1983, pp. 67-80.

VI. ANALYSIS METHODOLOGY FOR PREDICTING FAILURE

1. Adams, D. F., "Inelastic Analysis of a Unidirectional Composite Subjected to Transverse Normal Loading," *Journal of Composite Materials*, Vol. 4, 1970, pp. 310-328.
2. Altus, E. and Rotem, A., "A Three-Dimensional Fracture Mechanics Approach to the Strength of Composite Materials," *Engineering Fracture Mechanics*, Vol. 14, No. 3, 1981, pp. 637-645, 647-649.
3. Chai, H., Babcock, C. D. and Knauss, W. G., "One-Dimensional Modeling of Failure in Laminated Plates by Delamination Buckling," *International Journal of Solids and Structures*, Vol. 17, No. 11, 1981, pp. 1069-1083.
4. Chamis, C. C., "Prediction of Fiber Composite Mechanical Behavior Made Simple," in *Rising to the Challenge of the 80's; Annual Conference and Exhibit*, 35th, New Orleans, Louisiana, Feb. 4-8, 1980, Society of the Plastic Industry, Inc., 1980, pp. 12-A1 to 12-A10.
5. Chou, S. C., "Methods for Predicting Failure Behavior of Composite Materials," in *First USA-USSR Symposium on Fracture of Composite Materials*, Riga, Latvian SSR, Sept. 4-7, 1978. Alphen aan den Rijn, Netherlands, Sijthoff and Noordhoff International Publishers, 1979, pp. 77-91.
6. Chou, S. C., "Methods of Predicting Failure in Composites," *Mekhanika Kompozitnykh Materialov*, March-April 1979, pp. 297-304 (in Russian).
7. Crane, D. A. and Adams, D. F., "Finite Element Microchemical Analysis of a Unidirectional Composite Including Longitudinal Shear Loading," Report No. AMMRC-TR-81-7, Army Materials and Mechanics Research Center, Watertown, Massachusetts, February 1981.
8. Hashin, Z., Bagchi, D. and Rosen, B. W., "Nonlinear Behavior of Fiber Composite Laminates," NASA CR-2313, April 1974.
9. Hegemier, G. A., "Mechanics of Composite Materials," Department of Applied Mechanics and Engineering Sciences, University of California, San Diego, December 1979.
10. Kanninen, M. F., Rybicki, E. F. and Brinson, H. F., "A Critical Look at Current Applications of F.M. to the Failure of Fibre-Reinforced Composites," *Composites*, January 1977, pp. 17-22.
11. McLaughlin, P. V., Dasgupta, A. and Chun, Y. W., "BILAM - A Composite Laminate Failure Analysis Code Using Bilinear Stress-Strain Approximations," Lawrence Livermore Laboratory, UCRL-15371, October 1980.
12. Monib, M. M., "Three-Dimensional Elastoplastic Finite Element Analysis of Laminated Composites," Ph.D. Thesis, University of Wyoming, Laramie, 1981.
13. Nuismer, R. J., "Continuum Modeling of Damage Accumulation and Ultimate Failure in Fiber Reinforced Laminated Composite Materials," *Duke University Research Workshop on Mechanics of Composite Materials*, 1978, pp. 55-77.

14. Nuismer, R. J., "Predicting the Performance and Failure of Multidirectional Polymeric Matrix Composite Laminates - A Combined Micro-Macro Approach," in *Advances in Composite Materials; Proceedings of the Third International Conference on Composite Materials*, Paris, France, Aug. 26-29, 1980, Vol. 1, Oxford, Pergamon Press, 1980, pp. 436-452.
15. Shu, L. S. and Rosen, B. W., "Strength of Fiber-Reinforced Composites by Limit Analysis Methods," *Journal of Composite Materials*, Vol. 1, Oct. 1967, pp. 366-381.
16. Sih, G. C. and Chen, E. P., *Cracks in Composite Materials: A Compilation of Stress Solutions for Composite Systems with Cracks*, Martinus Nijhoff Publishers (Mechanics of Fracture, Vol. 6), The Hague, 1981.
17. Sih, G. C. and Moyer, E. T., Jr., "Influence of Interface on Composite Failure," *Proceedings of the Conference on Advanced Composites - Special Topics*, El Segundo, California, Dec. 4-6, 1979, pp. 283-312.
18. Soni, S. R., "Failure Analysis of Composite Laminates with Fastener Hole," Wright Patterson Air Force Base, Ohio, AFWAL-TR-80-4010, 1979.
19. Turvey, G. J., "Flexural Failure Analysis of Angle Ply Laminates of GRRP and CFRP," *Journal of Strain Analysis for Engineering Design*, Vol. 15, Jan. 1980, pp. 43-49.
20. Wang, A. S. D., "A Nonlinear Microbuckling Model Predicting the Compressive Strength of Unidirectional Composites," ASME Paper No. 78-WA/Aero-1, 1978.
21. Wang, S. S., Mandell, T. F. and McGarry, F. J., "Three-Dimensional Solution for a Through-Thickness Crack in a Cross-Plied Laminate," *Fracture Mechanics of Composites*, ASTM STP 593, 1975, pp. 36-60.
22. Wang, S. S., Mandell, J. F. and McGarry, F. J., "Three-Dimensional Solution for a Through-Thickness Crack with Crack Tip Damage in a Cross-Plied Laminate," *Fracture Mechanics of Composites*, ASTM STP 593, 1975, pp. 61-85.
23. Williams, R. S. and Reifsnider, K. L., "Strain Energy Release Rate Method for Predicting Failure Modes in Composite Materials," in *Proceedings of the Eleventh National Symposium on Fracture Mechanics*, June 12-14, 1978, Blacksburg, Virginia, Part 1, ASTM, 1979, pp. 629-650.
24. Whitcomb, J. D., "Finite Element Analysis of Instability-Related Delamination Growth," NASA TM-81964, March 1981.
25. Woolstencroft, D. H. and Haresceugh, R. I., "A Comparison of Test Techniques Used for the Evaluation of the Unidirectional Compressive Strength of Carbon Fibre-Reinforced Plastic," *Composites*, Vol. 12, Oct. 1981, pp. 275-280.
26. Wu, E. M., Lo, K. H. and Christensen, R. M., "Stress Analysis and Strength Characterization of Thick Composite Laminates," Report No. AMMRC-TR-79-29, Army Materials and Mechanics Research Center, Watertown, Mass., 1979.

27. Sandhu, R. S., "Nonlinear Behavior of Unidirectional and Angle Ply Laminate," Journal of Aircraft, Vol. 13, 1976, p. 104.
28. Sandhu, R. S., "Computer Program (NOLAST) for Nonlinear Analysis of Composite Laminates," Air Force Flight Dynamics Laboratory, AFFDL-TR-76-1, February 1976.
29. Talug, A., "Analysis of Stress Fields in Composite Laminates with Interior Cracks," Journal of Fiber Science and Technology, Vol. 12, 1979, pp. 201-215.



VII. CURRENT DESIGN PRACTICES

1. Bahei-El-Din, Y. A. and Dvorak, G. J., "Plastic Deformation of a Laminated Plate with a Hole," ASME, Transactions, Journal of Applied Mechanics, Vol. 47, Dec. 1980, pp. 827-832.
2. Beaumont, P. W. R. and Anstice, P. D., "A Failure Analysis of the Micro-mechanisms of Fracture of Carbon Fibre and Glass Fibre Composites in Monotonic Loading," Journal of Materials Science, Vol. 15, Oct. 1980, pp. 2619-2635.
3. Conen, H., "The Design of Fiber Composite Structures/Carbon Composites/ for Long Life," Deutsche Gesellschaft fuer Luft- und Raumfahrt, Symposium ueber Ermuebungsfestigkeit von Flugzeugen und Modernen, Bauweisen, Darmstadt, West Germany, Sept. 22, 1978 (in German).
4. Dorey, G., "Damage Tolerance in Advanced Composite Materials," Proceedings of the Conference on Helicopter Structures Technology, Moffett Field, California, Nov. 16-18, 1977, U.S. Army Air Mobility Research and Development Laboratory, 1978.
5. Goodman, J. W., Lincoln, J. W. and Petrin, C. L., "On Certification of Composite Structures for USAF Aircraft," Aircraft Systems and Technology Conference, AIAA, Dayton, Ohio, Aug. 11-13, 1981.
6. Poe, C. C., Jr. and Kennedy, J. M., "An Assessment of Buffer Strips for Improving Damage Tolerance of Composite Laminates," Journal of Composite Materials Supplement, Vol. 14, No. 1, 1980, pp. 57-70.
7. Rosen, B. W., "Design Considerations for Composite Materials," Proceedings of the Second International Conference on Composite Materials, Toronto, Canada, April 16-20, 1978, Metallurgical Society of AIME, 1978, pp. 9-30.
8. Sharma, A. V., "Damage Tolerance of Composite Sandwich Structures Subjected to Projectile Impact - of Low Velocity Foreign Object," in New Horizons - Materials and Processes for the Eighties; Proceedings of the Eleventh National Conference, Boston, MA, Nov. 13-15, 1979, Society for the Advancement of Material and Process Engineering, Azusa, California, 1979, pp. 900-917.
9. Williams, J. G., Anderson, M. S., Rhodes, M. D., Starnes, J. H., Jr., and Stroud, W. J., "Recent Development in the Design, Testing and Impact-Damage Tolerance of Stiffened Composite Panels," presented at the Fourth Conference on Fibrous Composites in Structural Design, San Diego, California, Nov. 1978. Also: NASA TM-80077, April 1979.
10. Anderson, M. S. and Stroud, W. J., "General Panel Sizing Computer Code and Its Applications to Composite Structural Panels," AIAA Journal, Vol. 17, No. 8, August 1979, pp. 892-897.
11. Stroud, W. J., "Optimization of Composite Structures," IUTAM Symposium on Mechanics of Composite Materials, Z. Hashin and C. T. Herakovich, eds., Pergamon Press (to be published).

VIII. NONDESTRUCTIVE EVALUATION AND EXPERIMENTAL METHODS FOR IDENTIFYING FAILURE MECHANISMS

1. Chang, F. H., Couchman, J. C., Eisenmann, J. R. and Yee, B. G. W., "Application of a Special X-Ray Nondestructive Testing Technique for Monitoring Damage Zone Growth in Composite Laminates," Composite Reliability, ASTM STP 580, 1975, pp. 176-190.
2. Daniel, I. M., "Biaxial Testing of Graphite/Epoxy Composites Containing Stress Concentrations," Mechanics of Composites Review, USAF, Oct. 1976, pp. 123-151.
3. Daniel, I. M., "Biaxial Testing of Graphite/Epoxy Composites Containing Stress Concentrations," Part I, Air Force Materials Laboratory, AFML-TR-76-244, June 1977.
4. Daniel, I. M., "Strain and Failure Analysis in Graphite/Epoxy Plates with Cracks," Experimental Mechanics, Vol. 18, July 1978, pp. 246-252.
5. Daniel, I. M., "Deformation and Failure of Composite Laminates with Cracks in Biaxial Stress Fields," Proceedings of the Sixth International Conference on Experimental Stress Analysis, VDI-Berichte Nr. 313, Munich, West Germany, September 1978, pp. 705-710.
6. Daniel, I. M., "The Behavior of Uniaxially Loaded Graphite/Epoxy Plates with Holes," Proceedings of the 1978 International Conference on Composite Materials, Metallurgical Society of AIME, April 16-20, 1978, Toronto, Canada, pp. 1019-1034.
7. Daniel, I. M., "Behavior of Graphite/Epoxy Plates with Holes Under Biaxial Loading," Experimental Mechanics, Vol. 20, 1980, pp. 1-8.
8. Daniel, I. M., "Biaxial Testing of Graphite/Epoxy Laminates with Cracks," in Test Methods and Design Allowables for Fibrous Composites; Proceedings of the Symposium, Dearborn, Michigan, Oct. 2-3, 1979, ASTM, 1981, pp. 109-12.
9. Daniel, I. M. and Liber, T., "Nondestructive Evaluation Techniques for Composite Materials," presented at the Twelfth Symposium on Nondestructive Evaluation, April 24-26, 1979, San Antonio, Texas.
10. Daniel, I. M., Rowlands, R. E. and Whiteside, J. B., "Deformation and Failure of Boron Epoxy Plate with Circular Hole," Analysis of the Test Methods for High Modulus Fibers and Composites, ASTM STP 521, ASTM, 1973, pp. 143-164.
11. Daniel, I. M., Rowlands, R. E. and Whiteside, J. B., "Effects of Material and Stacking Sequence on Behavior of Composite Plates with Holes," Experimental Mechanics, Vol. 14, January 1974, pp. 1-9.
12. Daniel, I. M., Schramm, S. W. and Liber, T., "Ultrasonic Monitoring of Flaw Growth in Graphite/Epoxy Laminates Under Fatigue Loading," in Advanced Composites - Special Topics; Proceedings of the Conference, El Segundo, California, Dec. 4-6, 1979, pp. 267-282.

13. Domanus, J. C. and Lilholt, H., "Nondestructive Control of Carbon Fiber Reinforced Composites by Soft X-Ray Radiography," Proceedings of the 1978 International Conference on Composite Materials, April 16-20, 1978, Toronto, Canada, Metallurgical Society of AIME, pp. 1072-1092.
14. Green, A. T. and Landy, R. J., "Acoustic Emission NDE for Advanced Composite Structures," in Advanced Composites - Special Topics; Proceedings of the Conference, El Segundo, California, Dec. 4-6, 1979, pp. 228-245.
15. Guess, T. R., "Biaxial Testing of Composite Cylinders - Experimental-Theoretical Comparison," Composites, Vol. 11, July 1980, pp. 139-148.
16. Henneke, E. G. and Duke, J. C., Jr., "A Review of the State-of-the-Art of Nondestructive Evaluation of Advanced Composite Materials," Sept. 1979. Virginia Polytechnic Institute and State University Technical Report prepared under Union Carbide Corp. contract number 19X-13673V.
17. Krautkramer, J. and Krautkramer, H., Ultrasonic Testing of Materials, Springer-Verlag, New York, 1977.
18. Liber, T., Daniel, I. M. and Schramm, S. W., "Ultrasonic Techniques for Inspecting Flat and Cylindrical Composite Specimens," Nondestructive Evaluation and Flaw Criticality for Composite Materials, ASTM STP 696, 1979, pp. 5-25.
19. Mandell, J. F., Wang, S. S. and McGarry, F. J., "The Extension of Crack Tip Damage Zones in Fiber Reinforced Plastic Laminates," Journal of Composite Materials, Vol. 9, July 1975, pp. 266-287.
20. Matzkanin, G. A., Burkhardt, G. L. and Teller, C. M., "Nondestructive Evaluation of Fiber Reinforced Epoxy Composites - A State-of-the-Art Survey," Southwest Research Institute for U.S. Army Aviation Research and Development Command, St. Louis, Missouri (Contract No. DLA 900-77-C-3733), April 1979.
21. Mool, D. and Stephenson, R., "Ultrasonic Inspection of a Boron/Epoxy Aluminum Composite Panel," Materials Evaluation, Vol. 29, No. 7, July 1971, pp. 159-164.
22. Ramkumar, R. L., Kulkarni, S. V. and Pipes, R. B., "Analytical Modeling and ND Monitoring of Interlaminar Defects in Fiber-Reinforced Composites," in Fracture Mechanics; Proceedings of the Eleventh National Symposium, Blacksburg, Virginia, June 12-14, 1978, American Society for Testing and Materials, 1979, pp. 668-684.
23. Roderick, G. L. and Whitcomb, J. D., "X-Ray Method Show Fibers Fail During Fatigue of Boron-Epoxy Laminates," Journal of Composite Materials, Vol. 9, Oct. 1975, pp. 391-393.
24. Rotem, A., "The Discrimination of Micro-Fracture Mode of Fibrous Composite Material by Acoustic Emission Technique," Fibre Science and Technology, Vol. 10, 1977, pp. 101-121.

25. Rowlands, R. E., Daniel, I. M. and Whiteside, J. B., "Geometric and Loading Effects on Strength of Composite Plates with Cutouts," Composite Materials: Testing and Design (Third Conference), ASTM STP 546, ASTM, 1974, pp. 361-375.
26. Rowlands, R. E., Daniel, I. M. and Whiteside, J. B., "Stress and Failure Analysis of a Glass-Epoxy Plate with a Hole," Experimental Mechanics, Vol. 13, Jan. 1973, pp. 31-37.
27. Rybicki, E. F. and Hopper, A. T., "Analytical Investigation of Stress Concentrations Due to Holes in Fiber-Reinforced Plastic Laminated Plates, Three-Dimensional Models," Air Force Materials Laboratory, AFML-TR-73-100, June 1973.
28. Ryder, J. T. and Wadin, J. R., "Acoustic Emission Monitoring of a Quasi-Isotropic Graphite/Epoxy Laminate Under Fatigue Loading," in Advanced Composites - Special Topics; Proceedings of the Conference, El Segundo, California, Dec. 4-6, 1979, pp. 246-266.
29. Schuetze, R. and Hillger, W., "Recognizing Defects in Carbon-Fiber-Reinforced Plastics," Deutsche Forschungs- und Versuchsanstalt fuer Luft- und Raumfahrt, Institut fuer Strukturmechanik, Braunschweig, West Germany, Deutsche Gesellschaft fuer Luft- und Raumfahrt, Jahrestagung, Aachen, West Germany, May 11-14, 1981 (in German).
30. Sendeckyj, G. P., Maddux, G. E. and Tracy, N. A., "Comparison of Holographic, Radiographic and Ultrasonic Techniques for Damage Detection in Composite Materials," Proceedings of the 1978 International Conference on Composite Materials, April 16-20, 1978, Toronto, Canada, Metallurgical Society of AIME, pp. 1037-1056.
31. Sheldon, "Comparative Evaluation of Potential NDE Techniques for Inspection of Advanced Composite Structures," Materials Evaluation, Vol. 36, No. 2, Feb. 1978, pp. 41-46.
32. Vary, A. and Bowles, K. J., "An Ultrasonic-Acoustic Technique for Non-destructive Evaluation of Fiber Composite Strength," Proceedings of the 33rd Annual Technical Conference, 1978, Reinforced Plastics/Composites Institute, The Society of Plastics Industry, Inc., Sec. 24-A.
33. White, R. G. and Tretout, H., "Acoustic Emission Detecting Using a Piezo-electric Strain Gauge for Failure Mechanism Identification in CFRP," Composites, Vol. 10, April 1979, pp. 101-109.
34. Stinchcomb, W. W. (Editor), "The Mechanics of Vibrothermography," Mechanics of Nondestructive Testing, Plenum Press, New York, August 1980.
35. Henneke, E. G., Reifsnider, K. L. and Stinchcomb, W. W., "Thermography - An NDI Method for the Detection of Damage," Journal of Metals, September 1979.
36. Jones, G. L., "Description of Damage in Composites by Acoustic Emission," Materials Evaluation, Vol. 37, July 1979.

37. Reifsnider, K. L. and Stinchcomb, W. W., "Vibrothermography and Ultrasonic Pulse-Echo Methods Applied to the Detection of Damage in Composite Laminates," Proceedings of the ARPA/AFML Review of Progress in Quantitative NDE, AFML-TR-78-205 (Science Center, Rockwell International, Thousand Oaks, California, 1979).
38. Duke, J. C., Jr. and Henneke, E. G., II, "Acoustic Emission Monitoring of Advanced Fiber Reinforced Composite Materials - A Review," Proceedings of the Fifth Acoustic Emission Symposium, Tokyo, 1980.
39. Reifsnider, K. L., Henneke, E. G., Stinchcomb, W. W., and Duke, J. C., "Damage Mechanics and NDE of Composite Laminates," IUTAM Symposium on Mechanics of Composite Materials, Z. Hashin and C. T. Herakovich, eds., Pergamon Press (to be published).

1. Report No. NASA CP-2278		2. Government Accession No.		3. Recipient's Catalog No.	
4. Title and Subtitle FAILURE ANALYSIS AND MECHANISMS OF FAILURE OF FIBROUS COMPOSITE STRUCTURES				5. Report Date August 1983	
				6. Performing Organization Code 534-03-23-07	
7. Author(s) Ahmed K. Noor, Mark J. Shuart, James H. Starnes, Jr., and Jerry G. Williams, Compilers				8. Performing Organization Report No. L-15641	
				10. Work Unit No.	
9. Performing Organization Name and Address NASA Langley Research Center Hampton, Virginia 23665				11. Contract or Grant No.	
				13. Type of Report and Period Covered Conference Publication	
12. Sponsoring Agency Name and Address National Aeronautics and Space Administration Washington, DC 20546				14. Sponsoring Agency Code	
15. Supplementary Notes Ahmed K. Noor: The George Washington University Joint Institute for Advancement of Flight Sciences, Langley Research Center, Hampton, Virginia. Mark J. Shuart, James H. Starnes, Jr., and Jerry G. Williams: Langley Research Center.					
16. Abstract This conference publication contains the presentations and discussions from the joint NASA/George Washington University Workshop on Failure Analysis and Mechanisms of Failure of Fibrous Composite Structures held at Langley Research Center, March 23-25, 1982. Presentations were made in the following areas of composite failure analysis and design practices: failure mechanisms and failure criteria, delaminations and stress concentrations, compression failure and transverse strength, effects of defects and experimental methods, and design technology.					
17. Key Words (Suggested by Author(s)) Composite materials Composite structures Failure mechanisms Failure analysis				18. Distribution Statement Unclassified - Unlimited Subject Category 24	
19. Security Classif. (of this report) Unclassified	20. Security Classif. (of this page) Unclassified	21. No. of Pages 384	22. Price A17		